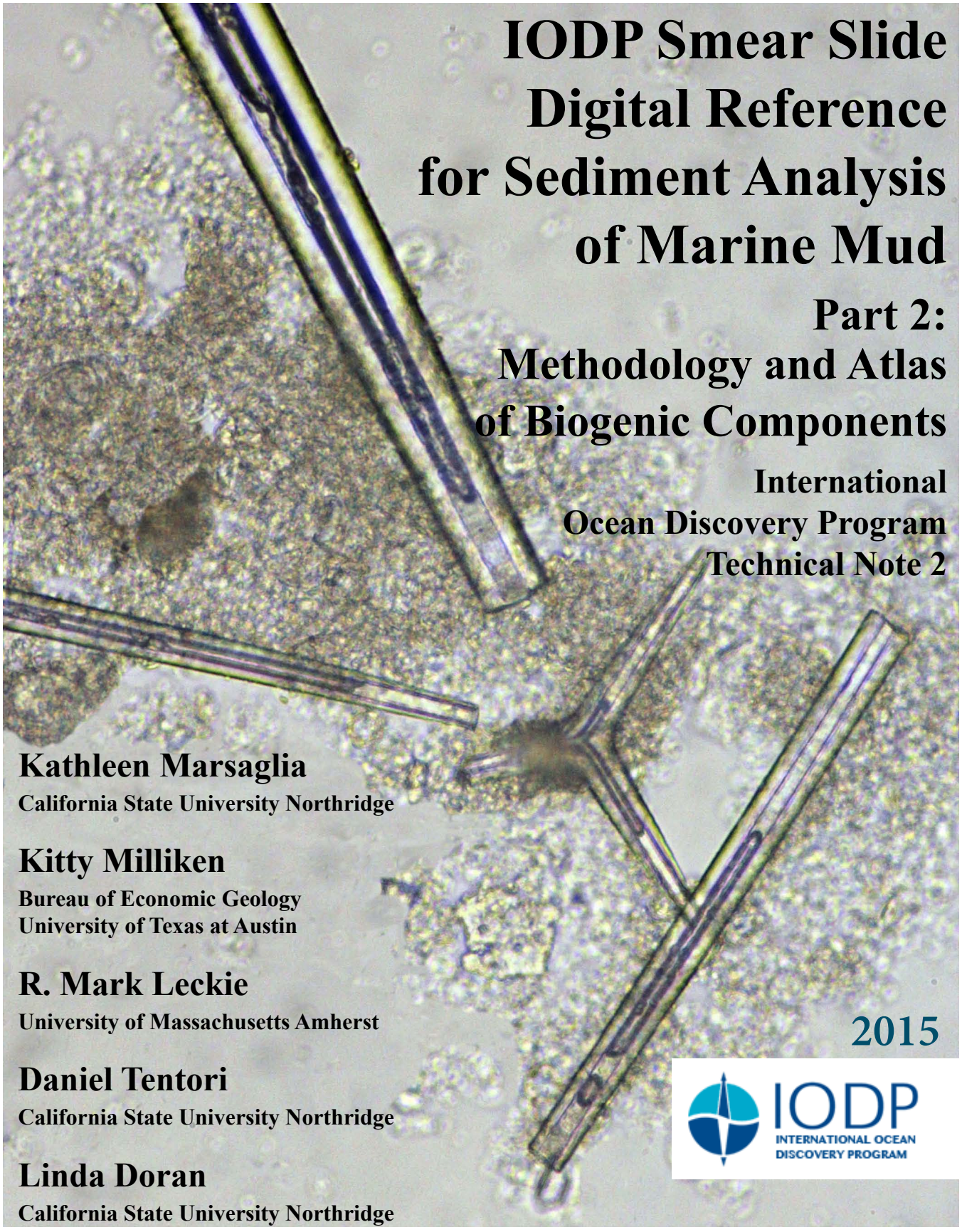

IODP Smear Slide Digital Reference for Sediment Analysis of Marine Mud

Part 2: Methodology and Atlas of Biogenic Components

International Ocean Discovery Program Technical Note 2

Kathleen Marsaglia
California State University Northridge

Kitty Milliken
Bureau of Economic Geology
University of Texas at Austin

R. Mark Leckie
University of Massachusetts Amherst

Daniel Tentori
California State University Northridge

Linda Doran
California State University Northridge

2015

IODP
INTERNATIONAL OCEAN DISCOVERY PROGRAM

To Contents

next

Publisher's Notes

Citation

Marsaglia, K., Milliken, K., Leckie, R., M., Tentori, D., Doran, L., 2015. IODP Smear Slide Digital Reference for Sediment Analysis of Marine Mud. Part 2: Methodology and Atlas of Biogenic Components. IODP Technical Note 2. doi:10.14379/iodp.tn.2.2015

Distribution

Electronic copies of this document and the previously published Part I (Marsaglia et al., 2013) may be obtained from the International Ocean Discovery Program (IODP) Scientific Publications homepage on the World Wide Web at http://iodp.tamu.edu/publications/TN.html.

Source of Funding

Funding for this publication was provided by the U.S. Science Support Program for the International Ocean Discovery Program (USSSP-IODP). USSSP-IODP is sponsored by the Consortium for Ocean leadership, Inc. and the National Science Foundation (NSF).

Disclaimer

Any opinions, findings, and conclusions or recommendations expressed in this publication are those of the author(s) and do not necessarily reflect the view of Ocean Leadership or NSF.

January 2015

Interactive Table of Contents

Introduction

Smear slide examination is an essential aspect of the description of the fine-grained material (mud) that dominates marine sedimentary successions. The goal of this tutorial is to convey the essentials of the smear slide method to sedimentologists engaged in marine core description on board International Ocean Discovery Program (IODP) drilling vessels or at IODP core repositories. Study of this tutorial will help core describers develop and apply solid skills in the identification and semiquantification of mud components that are fundamental to classifying sediment types.

The focus in this atlas is on important sediment-forming bioclasts in fine-grained deep-sea, sediments. Across vast areas of the deep sea, microfossils are the volumetrically dominant part of the sediment (e.g., calcareous and siliceous oozes). In addition, other microfossils of environmental or stratigraphic significance are included here even though they are seldom of volumetric significance. Sand-sized and larger bioclasts and bioclasts of shallow marine environments can be reviewed in a number of sources given in the references list.

The tutorial was produced in two phases, the first focusing on siliciclastic and volcanogenic components and associated authigenic components (Part 1, Marsaglia et al., 2013) and the second concentrating on biogenic and associated authigenic components (Part 2, this volume). The map on the following page (Figure 1) highlights the DSDP/ODP/IODP site locations of sample images in this Atlas. Note that these are only a subset of the total samples (325 total samples, 53 total sites; Kochi repository=79 samples, 11 sites; Tamu repository=103 samples, 14 sites; Bremen repository=143 samples, 28 sites) reviewed for consideration.

How to use this material

This document is in a layered, interactive, portable document format (PDF), created using Adobe Acrobat version 10.1.4. Buttons and text links allow flexible navigation of the contents. Additional links throughout the document, in the form of both buttons and highlighted text, allow additional options for navigation. It is possible to study the entire document sequentially, through the use of the "next" button on each page, but many other options for navigation are provided. Most images can be zoomed up to 400% to provide a higher-magnification view of sediment components.

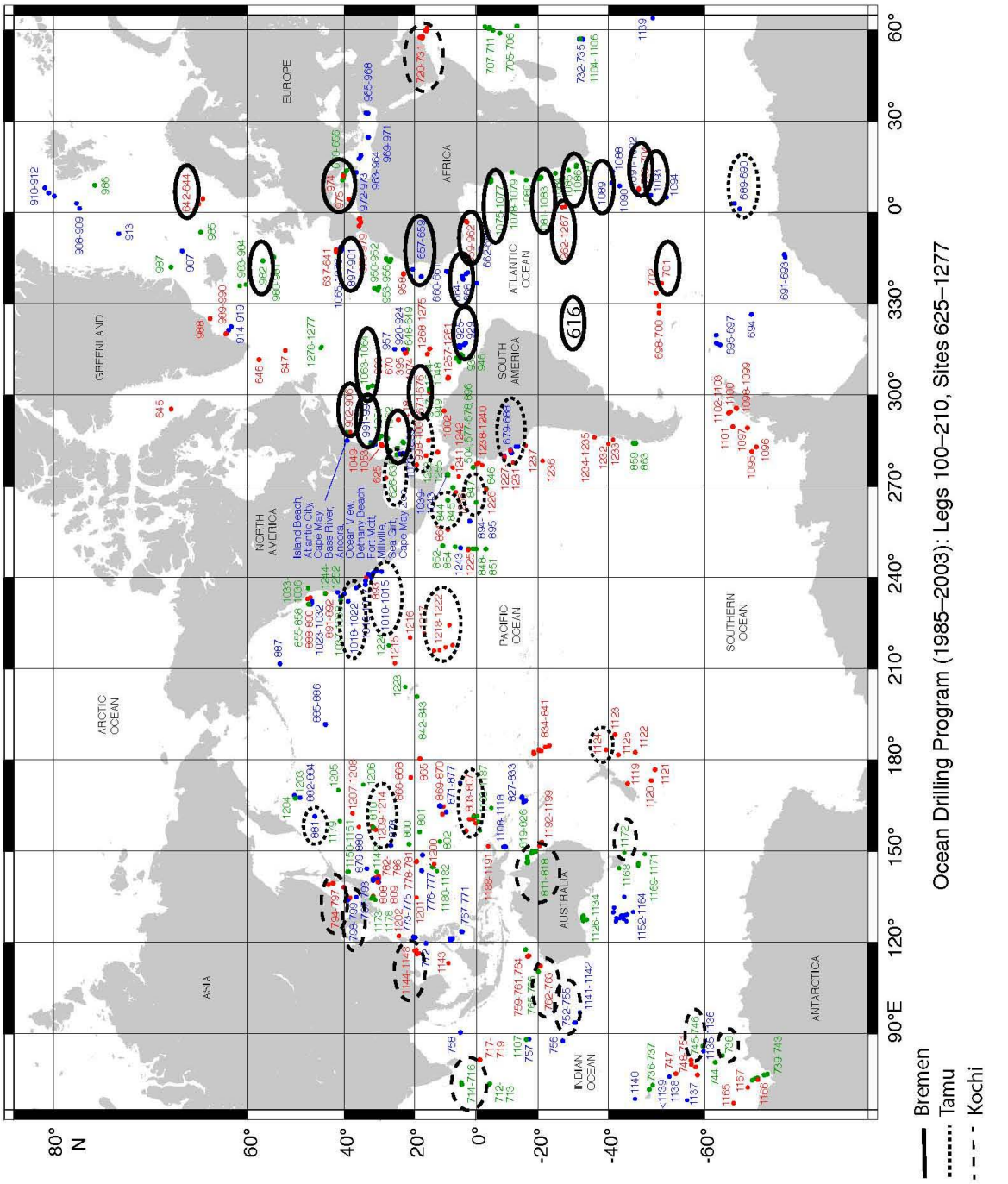

Figure 1: DSDP/ODP/IODP site locations for samples used in this Atlas.

The main areas of the tutorial include:

1. **Text** describing the smear slide method, smear slide production, and smear slide description.

2. An **atlas** of common components seen in smear slides. This section contains basic guidance for identifying common biogenic components in smear slides, a thumbnail page aiding navigation to individual atlas images, and an extensive image collection covering major categories of biogenic and diagenetic components in sediments. By fully opening the layers window in the navigation panel on the left side of the main pdf window, the viewer may toggle between plane-polarized and cross-polarized views of the atlas images and turn scale grids and information layers on and off (Figure 2).

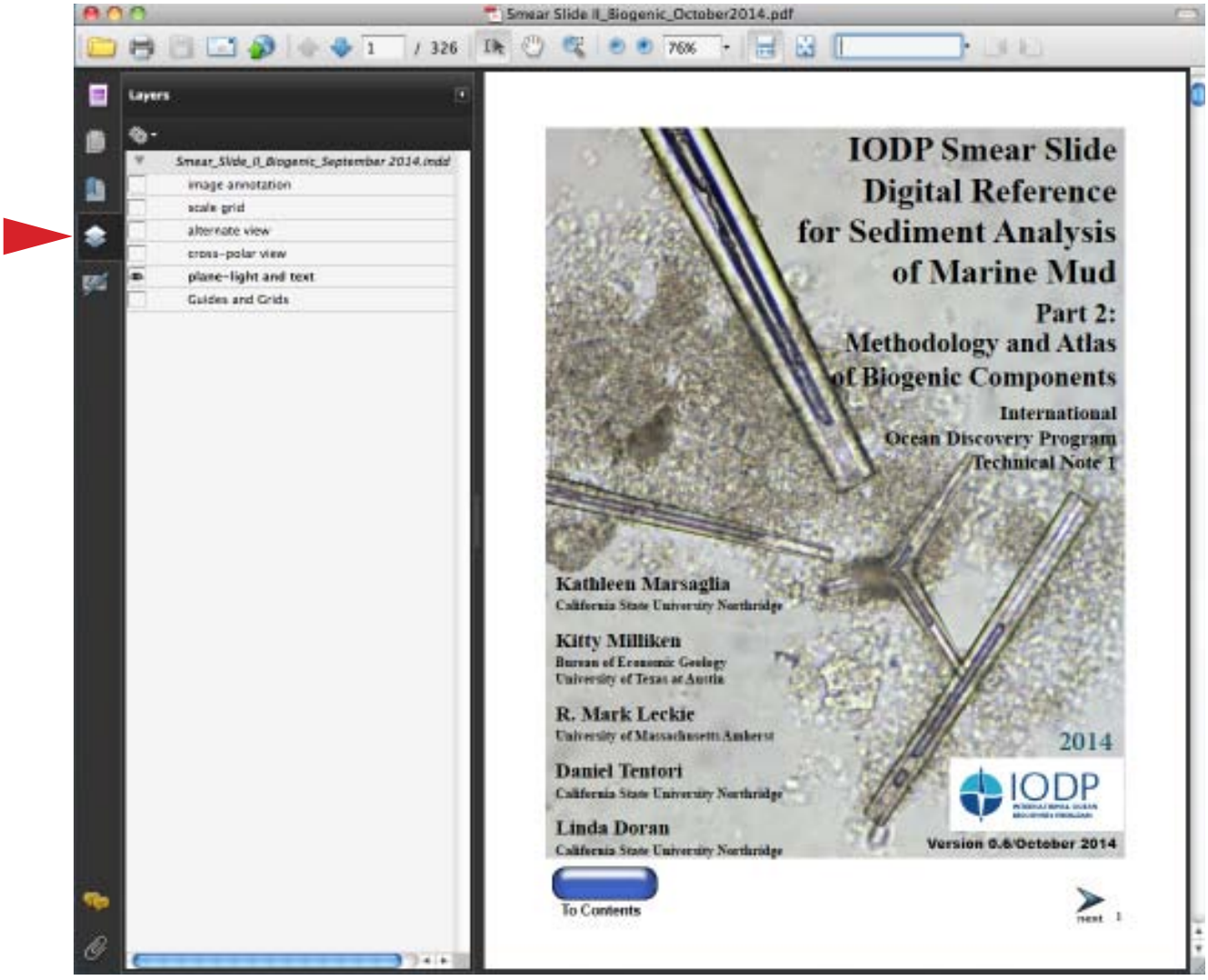

Figure 2: Screen shot of first page of this pdf document showing the location of the layers symbol (red arrow), which can be opened with a click of the mouse.

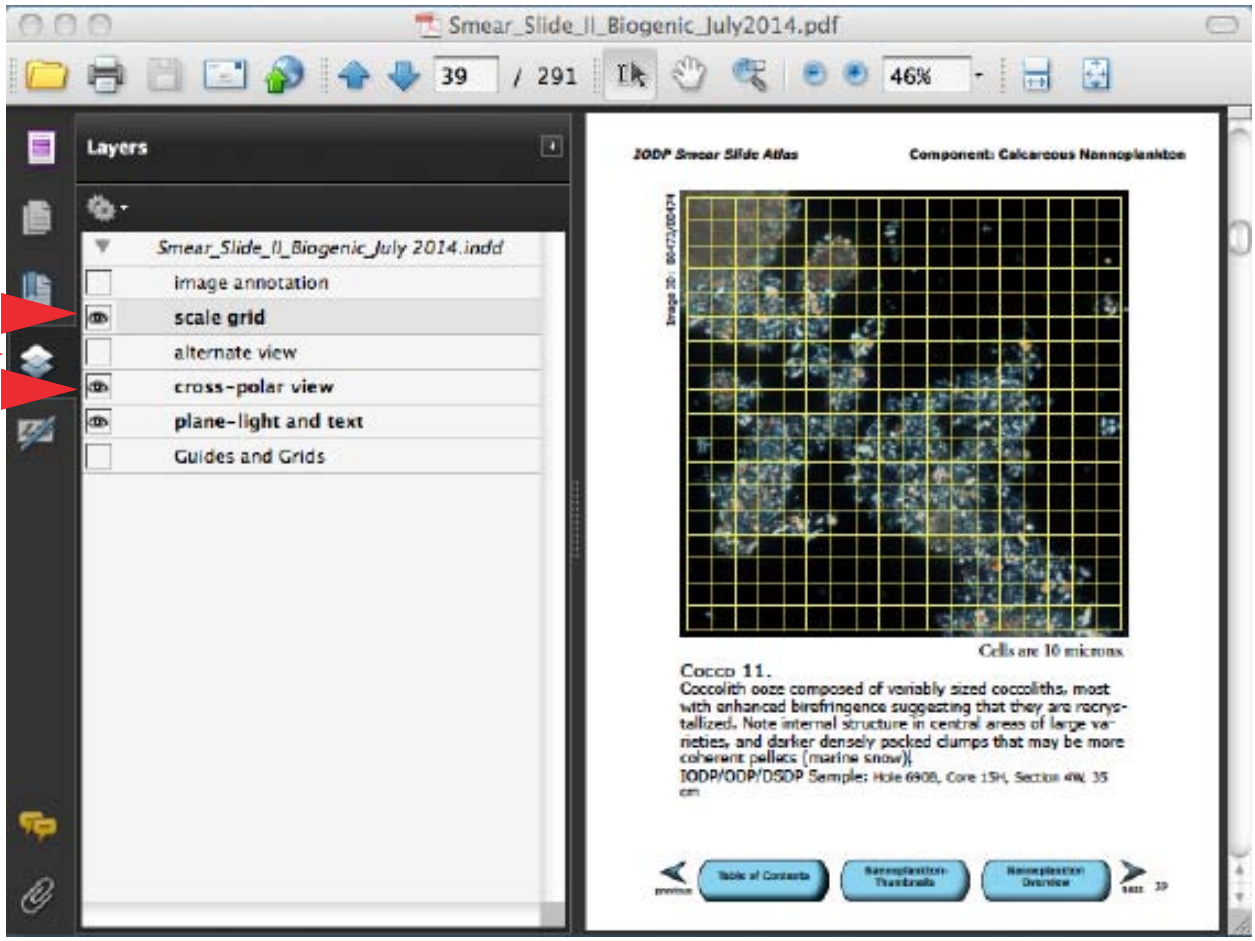

Figure 3: Screen shot of image page with the layers window opened. Black background in petrographic image on right and "eyeball" icon activated on left indicates the cross-polar view as well as the yellow scale grid have been activated.

Atlas images contain multiple layers, though not every image will contain every possible layer. The layers window may be opened by clicking on the "blue stacked paper" symbol in the navigation panel on the left side of the page (Figure 2). Layers active for a given image are indicated when the layer is shown in bold on the layers window (Figure 3).

Individual layers may be toggled on and off by clicking the "eye" symbols to reveal: a plane-light image with text, a crossed-polar image, an alternate view (such as higher magnification, reflected light, or different focus) where provided, an image annotation view, and a scale grid. The general image description is shown in a text box beneath the image.

3. A **tutorial** section (also with layered images including an additional scale grid) that allows the user to test acquired knowledge of component identification and estimation in broader fields of view that contain many biogenic grain types.

4. A **set** of 50 slides (see page 382) has been selected to provide a range of biogenic components and pelagic lithologies of Cretaceous to Holocene age from sites in each of the major ocean basins. Sets of these slides are available for study on IODP drilling vessels and at the IODP core repositories. Suites of samples from sites 628, 690, 763, 807, 1124, 1210, and 1267 provide more detailed record of sediment biogenic input and compositional change at specific sites across the globe.

Authors

Kathie Marsaglia, Ph.D.

Although her research has centered on provenance and distribution of marine sand, early in her career Kathie realized the importance of characterizing the mud fraction using the smear slide technique. She produced and described her first smear slide aboard the *JOIDES Resolution* on Leg 126 in 1989. Since then she has participated as a shipboard sedimentologist on Ocean Drilling Program (ODP Legs 141, 149, 161, 198, and 210) and IODP expeditions (317, 320T, and 351), where she enthusiastically volunteered to make and describe smear slides. With Shawn Shapiro, she produced an Atlas of Sedimentary Structures and Lithologies using ODP core photos (Marsaglia and Shapiro, 2005). She has published on petrology and diagenesis of sand and sandstone, Precambrian and Permian carbonate-to-volcaniclastic transitions, Cretaceous oceanic anoxic layers and chert, the Messinian evaporite-to-carbonate transition, and Pliocene cyclic sedimentation. She is a Professor of Geology at California State University Northridge.

Kitty Milliken, Ph.D.

A research focus on the chemical and mechanical evolution of rocks in the subsurface has led Kitty to an interest in petrographic methods. Her previous projects in petrographic education include Sandstone Petrology: A Tutorial Petrographic Image Atlas (v. 1.0 and 2.0; 2003, 2007) and Carbonate Petrology v. 1.0: An Interactive Petrography Tutorial (2011). She first encountered the smear slide technique under the tutelage of Kathie Marsaglia on ODP Leg 149 to the Iberia Abyssal Plain. Subsequently, she sailed as a sedimentologist on the *Chikyu* (IODP Expeditions 316 and 338) and on the *JOIDES Resolution* (IODP Expedition 320T). Her published papers examine the diagenesis of sandstone, mudrock, limestone, dolomite, chert, and serpentinite. She is a Senior Research Scientist at the Bureau of Economic Geology and a member of the Graduate Studies Committee in the Jackson School of Geosciences at The University of Texas at Austin.

R. Mark Leckie, Ph.D.

Mark Leckie is a Professor of Geology at the University of Massachusetts Amherst. He co-led the scientific instruction of the IODP 'School of Rock' expedition in 2005 and subsequently co-taught numerous shore-based short-courses and workshops. These efforts culminated in the publication of Reconstructing Earth's Climate History, Inquiry-Based Exercises for Lab and Class (St. John et al., 2011; Wiley-Blackwell). Leckie is a marine micropaleontologist, specializing in paleoceanography and ocean-climate history of the past 120 million years. He has participated in six Deep Sea Drilling Project and Ocean Drilling Program scientific expeditions (DSDP Leg 79 and ODP Legs 101, 130, 165, 198, and 210), and served as Co-Chief Scientist of ODP Leg 165. He is a co-author of a classroom activity book: Investigating the Oceans, Illustrated Concepts and Classroom Inquiry (Leckie and Yuretich, 2012; McGraw-Hill, 4th ed.). He has been an instructor at the Urbino Summer School on Paleoclimatology (2008-2012). His teaching responsibilities at UMass include: Introductory Oceanography; History of the Earth; Introductory Field Methods; Paleoceanography; and Marine Micropaleontology.

Daniel Tentori, M.S.

Daniel Tentori earned a bachelor's degree in Geology at the University of Rome "La Sapienza" and is currently completing his master's degree program at California State University of Northridge working with Kathie Marsaglia. His Master's thesis research focusses on the provenance of the Roman Basin sediments and aims to integrate petrographic signatures with the sequence-stratigraphic intepretation of Quaternary Tiber River coastal and deltaic successions. Daniel was aknowledged for his help in producing the Smear Atlas Phase I publication and for helping to reformat and transfer Marsaglia and Shapiro (2005) into a pdf format.

Linda Doran, M.S.

After earning a bachelor's degree in Geology at the University of New Mexico and spending many years as a science writer, most recently in education outreach at NASA's Jet Propulsion Laboratory, Linda entered a master's degree program working with Kathie Marsaglia at California State University Northridge. Her Master's Thesis research (Doran, 2013) focused on the provenance of Taranaki Basin sediments off of South Island, New Zealand. Previous stints have included working in corporate communications at Sandia National Laboratories in Albuquerque, New Mexico, and in science reporting for the San Gabriel Valley Tribune in West Covina, California. Linda is aknowledged for helping to reformat and transfer Marsaglia and Shapiro (2005) into a pdf format.

Acknowledgments

Construction of this tutorial atlas was funded under a grant from Ocean Leadership (Marsaglia, PI) with the Support of Jeff Schuffert and Charna Meth. The Part II tutorial is modeled after Part I which was funded by IODP Management International, Inc. Hiroshi Kawamura and Jamus Collier (IODP-MI) provided essential enthusiasm and support at the project's inception. We are grateful to Ivano Aiello, Tim Bralower, Martin Crundwell, John Firth, David Harwood, Chris Hollis and David Lazarus for their efforts to review and comment on early versions of this product. We also thank geology student Shawna Couplin at California State University Northridge for her assistance in preparing this document. Some of the concepts for digital tutorial construction implemented here were developed in collaboration with Suk-joo Choh (Korea University) under previous grants from the Course, Curriculum, and Laboratory Improvement program of the Division of Undergraduate Education at the National Science Foundation (Milliken, PI; award numbers 0088763, 0230578, and 0536085). Thanks also go to the curatorial staffs at the IODP Core repositories in Bremen, College Station and Kochi for sampling the cores.

Dedication

This tutorial is dedicated to the memory of Dr. Albert V. Carozzi, sedimentary petrographer extraordinaire.

The Smear Slide Method

Introduction

As outlined in the "Handbook for Shipboard Sedimentologists" by Mazzullo and Graham (1988; http://www-odp.tamu.edu/publications/tnotes/digital/tnote_08.pdf), the two major aspects of core description by shipboard and shore-based sedimentologists are direct visual observation of the core (supported by hand lens observation and low-magnification stereo microscopy) and microscopic observation via smear slides or thin sections viewed with a petrographic microscope. Image-based aids have been developed through the Joint Oceanographic Institutions (JOI) for core description (Marsaglia and Shapiro, 2005) and independently for identification of generally sand-sized components in sediments and lithified sedimentary rocks (Milliken and Choh, 2011; Bolli et al., 1985; Carozzi, 1993; Lipps, 1993; Scholle, 1978; Scholle and Ulmer-Scholle, 2003), but there is no similar guide for smear slide analysis of unlithified fine-grained sediment.

Most of the cores recovered by Deep Sea Drilling Project (DSDP), ODP, and IODP are unlithified, and fine-grained, so the smear slide technique is critical to sediment characterization and the determination of lithologic names assigned to cored materials. Mastery of the technique requires that sedimentologists have sufficient training in optical mineralogy, sedimentary petrography, and micropaleontology to identify individual sediment components. Unfortunately, microscopy training in many academic programs is on the decline or has been dropped from the curriculum entirely. This tutorial fills a distinct need for a self-instructive module on smear slide preparation, description, and interpretation for use by shipboard sedimentologists who have not previously benefited from petrographic training in describing sediments and sedimentary rocks. Even trained petrographers who have not worked previously with smear slides will benefit from using these tutorial resources and reference materials.

Throughout this tutorial we assume a basic understanding of the components and operation of a petrographic microscope. If you have no such training, then we recommend that you first look at basic texts such as Kerr (1977) or Nesse (2004) to get information on the petrographic microscope, as well as basic mineral attributes in thin section such as color, relief, cleavage, birefringence (or alternatively isotropism), pleochroism, twinning, and zoning that we will discuss in the course of this tutorial.

The Reference Slide Set consists of 100 smear slides (50 in Part 1---Marsaglia et al., 2013, and 50 in Part 2) showing examples of components in various proportions. The samples used for images and smear slides come from archived ODP and IODP cores. Effort was made to cover a variety of oceanographic and tectonic settings to make the sample array globally relevant.

Rationale for selection of smear slide samples during core description

The smear slide method is mainly used for description of cores obtained with the Hydraulic Piston Corer (HPC) in soft sediments, and Extended Core Barrel (XCB) in the sediment-to-sedimentary-rock transition zone where recovered materials can be most easily disaggregated. It can also provide some information on more lithified rocks (e.g., cement mineralogy, amygdule filling, mineralogy of phenocrysts or grains) at depths where Rotary Core Barrel (RCB) coring is necessary.

HPC cores are generally the first type of samples encountered in the borehole. Once the HPC cores are processed, sliced with a wire, and separated into archive and sampling halves, the description process can begin on the archive half. It is common practice to lay out the fully split core, with the working half on the sampling table and archive half on the description table. This enables the sedimentary description (archive half) and physical properties groups (working half) to quickly review and discuss the core prior to analysis. At this point, broad variations in lithology are noted, and physical property measurements/sampling, carbonate/total organic carbon (TOC) sampling, and smear slide sampling are coordinated. Smear slides are not taken until after the archive core is digitally color-imaged and scanned with a spectrophotometer.

Smear slides can be made to identify fine-grained major and minor lithologies as well as isolated components (e.g., burrow fills, pods, fossil fills). The tendency at the first site in an Expedition is to make smear slides of all major and minor fine-grained lithologies in the first cores. As discussed below, coarser lithologies with sand-sized grains are better determined using hand-lens and binocular microscope observations, or alternatively by examining thin sections of loose grain mounts or semilithified bits. Lithological variation determines the distribution and number of smear slides needed. Only in situations where a core is completely visually homogenous is a single smear slide sufficient. Generally a minimum of two smear slides (major and minor lithology) are needed per core, with three to four being more common.

Smear slides are not only meant to facilitate shipboard description but also to serve as archives of information for future scientific study. For this reason, they are boxed and returned to core repositories along with the cores. Like thin sections, the smear slides may be requested by shipboard and shore-based scientists to clarify shipboard descriptions and/or help define sampling intervals of cores. Thus, it is the duty of the shipboard sedimentologists to document core lithology in smear slides and thin sections as a legacy of the Expedition.

How to make a smear slide

Smear slide production is generally quick and easy, requiring minimal equipment (highlighted in discussion below) and bench space (Figure 4). Our favored technique is outlined below (steps 1-7) and pictured in Figures 5 through 8. An alternate technique, favored by biostratigraphers, is also described, in which the sample slurry is prepared on the coverslip rather than the slide (see step 8).

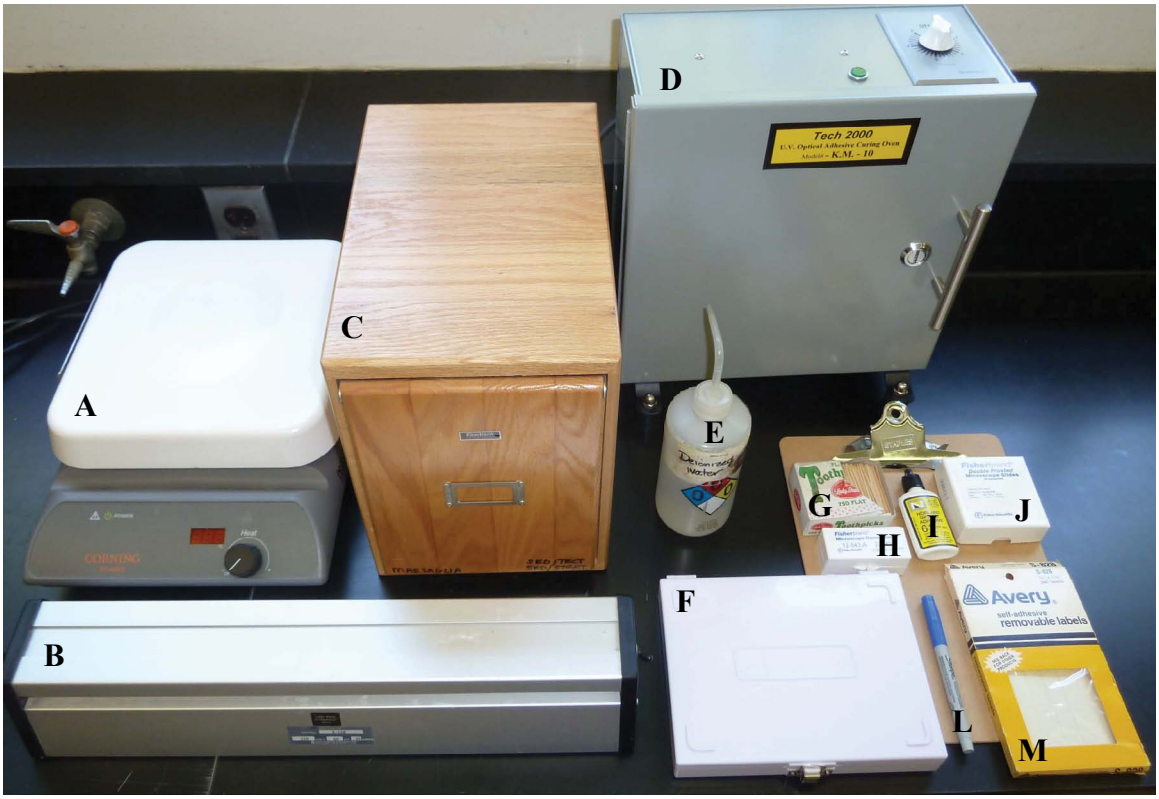

Figure 4. The equipment needed for smear slide preparation includes a hot plate (A); UV curing apparatus, either a UV light (B) or specially manufactured box (D); slide storage, such as wood benchtop box with trays (C) or plastic portable box (F); water bottle (E), preferably with nanopure water if available; flat toothpicks (G); slide coverslips (H); optical adhesive (I), such as Norland 61; glass slides (J); slide labels (M); and a permanent fine-point marker (L). Note that shipboard slide labels are automatically generated with barcodes. Shore-based slides can be marked with adhesive labels, but these may ultimately deteriorate. If glass slides with frosted ends are used, slide information can be written directly on the slide with a permanent fine-point marker.

1. Pick intervals for smear slide analysis and create slide labels using a computer and label printer (alternatively, information can be written directly on frosted slide ends). Slide labels should include Expedition, Site, Hole,

Core, Section, and Interval information as well as information as to whether the slide is made from a minor or major lithology and a unique barcode.

2. Affix slide labels to ends of long (25 × 75 mm) glass slides (note that slides may need to be cleaned depending on quality of manufacture). We prefer to lay these slides out on a clipboard, essentially using it as a tray to carry them to and from the core description table (Figure 5).

Figure 5. With muddy sediments the amount of material needed is small, just covering the end of a toothpick. Two amounts are shown, one smaller (c) and one larger (d), with the latter wetted and in the process of disaggregation. The amount of material determines the consistency of the slurry, whether it is more dilute (C) or more dense (D), which in turn affects the petrographic analysis. The material can be too thinly or too thickly spread. See Slide Tutorials for examples.

3. At the core description table, use flat wooden toothpicks to sample the core (note that pointed toothpicks will not work!). At each interval, use the flat end of a toothpick to scoop approximately 1-2 mm^3 of sediment from the cut and cleaned core surface. Next, stick the muddy toothpick end to its

labeled slide (Figure 6). An alternative technique is to use a long pin to sample and smear, but care must be taken to thoroughly clean the pin if used for multiple samples and a steel implement may be more likely to crush delicate grains. Once all intervals are sampled, carry the clipboard with toothpick-laden slides to the preparation bench. With consolidated and well-lithified cores it is best to not scrape the sawn flat core surface, but to sample the curved drilled surface in contact with the core liner. Generally such cores occur in pieces that can be manipulated in the core liner. First rotate the core piece in the core liner to expose the rounded outer edge of the core. Clean the core surface by scraping it with a metal spatula. Next, place a slide close to the core surface and scrape a representative amount of material onto the slide. Of course, this method tends to pulverize grains and minerals and only serves to provide minimal information for core description while the core is on the description table. Representative thin section billets should always be requested for thorough description of lithified units, but these take time to produce and a quick smear slide may be useful in determining lithology as the core is being described.

4. At the preparation bench, moisten the sample with a few drops of water (preferably nanopure) from a squeeze bottle, making sure not to wet the label (Figure 5). Use the toothpick to break up and create a diluted slurry of sediment on the slide. Note that if the sediment is cohesive and/or semilithified, it helps to let the sample soak a bit before attempting disaggregation. Rather than use the toothpick to disaggregate harder samples, it is best to crush the sample with a metal spatula rather than grind it vigorously with a toothpick, as the latter approach adds wood fragments to the slurry. Once crushed with the spatula, a toothpick can be used to create the slurry. Lightly tamping the flat toothpick lengthwise across the slide helps to spread the slurry across the slide surface (Figure 5). The slurry should be semitranslucent rather than densely packed, but a variable density across the slide is preferable, ranging from more closely packed grains (darker) to more thinly disseminated material at the other end. If the sediment is spread too thin, it is difficult to estimate percentages, but if it is too dense, it is difficult to identify constituent grains.

5. The preparation bench equipment should include a large hot plate where slides are placed to dry once the desired consistency of slurry is reached (Figure 6). To facilitate easy removal, only the end of the slide with the slurry is placed on the hot plate and left for a few minutes until completely dry. The label end of the slide extends off the edge of the hot plate so that the slide can be easily removed by hand without burning your fingers. A moderate hot-plate temperature (150 °C) is best.

Figure 6. Smear slides are placed on a moderately heated hot plate to dry. It is important to leave the labeled end off the plate surface to facilitate removal of the hot dried slide.

6. Once the slurry is dried, a coverslip (22 × 40 mm) is affixed to the slide using an optical adhesive such as Norland 61, which has a refractive index of 1.56. Drops of the adhesive are placed on the coverslip and then the coverslip is quickly turned over and placed on the slide (Figure 7). An alternative technique is to put a few drops of adhesive in the middle of the slide and tilt the coverslip onto it, thus minimizing capture of bubbles. Then, gentle pressure is applied with a fingernail or a pencil eraser to force any bubbles to the edge of the glass. The slide is then put in a tray in the ultra-violet curing oven where ultraviolet light quickly cures the adhesive within a few minutes (Figure 8). In using the curing agent, one must be warned that if expired, the agent may start to crystallize. Also, as the bottle empties, there is a tendency for air bubbles to be produced with excessive squeezing.

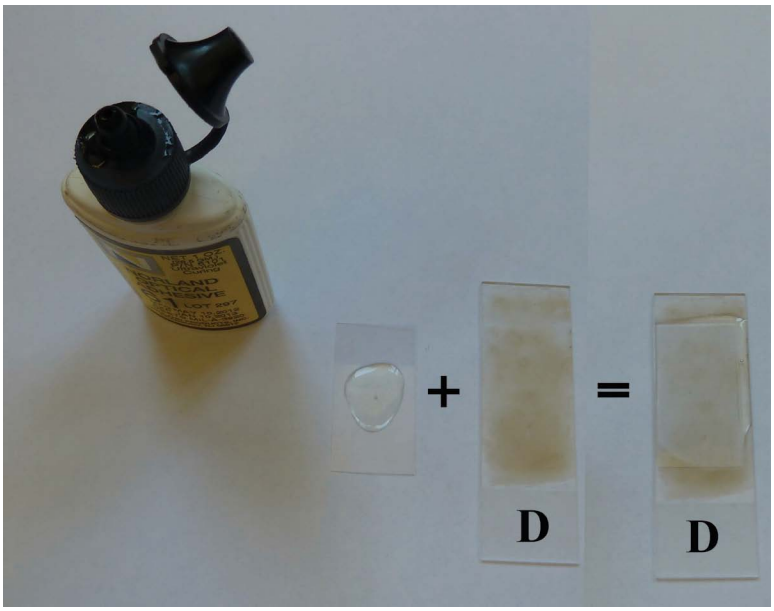

Figure 7. Let slides cool after removal from the hot plate. Squeeze optical adhesive onto the coverslip and place on the slide. Note that the adhesive will automatically flow out to the coverslip edges. If you have too much adhesive it will extrude out from the coverslip, like that shown in the top left corner of the example pictured here; if you have the right amount, it will just fill the area under the coverslip (lower part of covered slide). The latter effect was achieved where the bleb of adhesive was narrower. Note that the single large bubble originally in the middle of the adhesive bleb on the coverslip migrates to the edge and into the extruded epoxy in upper right. An alternative cover method is to put the adhesive directly on the dried slide and then tilt and progressively place the coverslip on the slide. If adhesive extrudes out onto the edge of the slide, you run the risk of adhering the slide to the underlying surface when exposed to UV light. If excess adhesive is inadvertently used, try to wipe excess off the sides prior to curing in UV light, as the excess, if insufficiently curred, can sometime be smeared off onto the objective lens of the microscope which, in turn, is difficult to clean.

Figure 8. UV light curing apparatuses also pictured in Figure 3. Purple to bluish glow signals the lamps are switched on (note that you should avoid directly viewing UV light). Slides are placed on a tray or piece of paper to cure either under a UV lamp or within a specially made curing oven. The UV lamp, a less expensive option, can simply be placed over the slides as pictured here. The length of time needed to fully cure is normally less than 10 minutes but may vary. A simple touch of the finger can test whether extruded adhesive is tacky (partly cured) or fully solidified (cured).

7. Once slides are made, they are temporarily placed in trays in the wooden slide storage box next to the microscope. The trays are generally numbered for easy reference, and slides are ordered by Site, Hole, Core, Section, and Interval. After a site is completed, the slides are shifted to permanent white storage boxes and officially curated.

8. In an alternate method preferred by micropaleontologists (pers. commun., David Harwood), the sediment slurry is created directly on the coverslip, which is then heated on the hotplate until dry. Adhesive is then added to the labeled glass slide, which is turned upside down with mounting medium suspended over the sediment-laden coverglass lying on the hotplate. The slide is then lowered onto the coverslip, adhering to it, and then quickly flipped over. The glass slide can then be placed on the hotplate for a few minutes to decrease adhesive viscosity so that micropores in fossils are completely filled. This alternate method places the smaller microfossils just below the cover slip and above the mounting medium, which allows for better focusing on specimens when using very high magnifications (63x and 100x objectives).

Selection of shipboard petrographer(s)

The shipboard duties of the sedimentary description group generally include scanning the archive halves; describing cores, including sedimentary structures and features in the cores; and doing smear slide petrography. The latter task usually falls to those individuals who have the most petrographic training or are the most willing to learn. Uniformity of methods between shifts is best accomplished by having a designated individual responsible for acquiring these data on each shift (this should be considered in making shift assignments). In situations where only one petrographer is available, this person should consider straddling shifts (e.g., 6 a.m. - 6 p.m). Once criteria are established for the first site, alternate petrographers may be trained and designated as needed later in the cruise. Note that haphazard assignment or minimal attention to this responsibility may result in the need for painful revisions later in the cruise or at the first post-cruise meeting, especially in the event that lithologic names have been inconsistently determined and reported on visual core description (VCD) sheets and in smear slide reports. It is not uncommon for sedimentologists to make significant revisions to the report from the first site later in the cruise!

Smear slide description and data collection

The petrographic microscope in the sedimentology description area should be equipped with a range of objectives, optimally a 40×, 20×, 10×, and 5×, and an eyepiece with reticule. It is important that the highest magnification objective be clean and centered. If not already indicated on the microscope, an optical micrometer should be used to determine the scale of reticule subdivisions, particularly the size cutoffs for clay- and silt-sized particles (4 and 63 µm, respectively).

There is a tendency to be paperless on the *JOIDES Resolution*, but we have found that smear slide description sheets (see example in Figure 9) are useful means of documenting components and percentages. Shipboard computers have been known to be problematic (erase data) and these sheets serve as a needed backup. They also provide a handy place to take notes on specific components and other corroborating data sets, such as carbonate measurements, TOC, and X-ray diffracton (XRD). As there can be uneven concentration of certain components across a slide, it is common practice to estimate percentages at several places in a slide, then average those, and adjust to 100% of the sample. Later these data need to be calibrated using shipboard analytical measurements (e.g., calcite weight percent, total organic carbon, and XRD determinations of mineral abundance) on the intervals (see note about coordinated sampling above and about calibration below). As these calibrations often result in the need to adjust percentage totals, we recommend not putting the data into the computer database until this calibration process is complete. These sheets should ultimately be scanned and archived as part of the shipboard database for the Expedition.

The major components of marine sediments are listed on the smear slide description sheet with space for additional components or name modification. Review of Shipboard Results from previous DSDP, ODP, and IODP cruises in the region may help provide information on what components are likely to be encountered in a smear slide. It is often helpful to organize the database entry table in the same order as the components are listed on the sheet to minimize time needed for input into the shipboard database. This list also serves as a reminder for the operator to specifically look for certain components in each smear slide. Even documenting trace amounts of certain components may be helpful to other shipboard scientists (for example, it may help biostratigraphers focus on key intervals for dating or alert physical properties scientists to minor diagenetic features that have strong effects on bulk rock properties).

Sediment Smear Slide / Thin Section Description Sheet

Date:

Expedition: Observer:

Site: Hole: Core: Sect.: Interval:

Sediment Name:

Smear Slide	Thin Section	Coarse Fraction	Grain Mount	Dominant Grain Composition: Siliciclastic	Volcaniclastic	Biogenic	Other material	Percent Texture: Sand	Silt	Clay
		Check one.				Check one.				

Percent	Composition
	Major Siliciclastic Grain Types
	Quartz
	Feldspar
	Clay mineral (matrix)
	Lithic Grains
	Sedimentary Lithics
	Chert
	Mudstone
	Siltstone/sandstone
	Limestone
	Metamorphic lithic
	Plutonic lithic
	Volcaniclastic Grains
	Vitric fragments
	Clear glass
	Colored glass
	Pumice
	Volcanic lithics
	Felsitic
	Microlitic
	Lathwork
	Altered volcanic(palagonite)

Percent	Composition
	Planktic Grains
	Calcareous
	Nannofossils
	Foraminifers
	Siliceous
	Diatoms
	Radiolaria
	Sillicoflagellates
	Unknown bioclast
	Other Bioclasts
	Mollusks
	Benthic foraminifers
	Ostracods
	Echinoderms
	Sponge spicules
	Other bioclast (specify)
	Other carbonate allochems
	Peloid
	Intraclast
	Silt or sand-size carbonate allochem fragment (unspecified)
	Clay-size carbonate (< 4 microns; apart from nannos)

Percent	Composition
	Minor Grain Types
	Dense minerals[1]
	Micas (biotite, musc, chl)[1]
	Glauconite
	Phosphate (bones, teeth, etc)
	Opaque grains
	Marine organic matter
	Terrestrial organic matter
	Other (specify):
	Authigenic Components
	Pyrite (framboids)
	Pyrite (euhedra)
	Pyrite (grain coating)
	Calcite
	Dolomite
	Glauconite
	Phosphate
	Zeolite
	Fe/Mn oxide
	Other (specify):

[1] List under remarks if possible

Fill percentage (Total must be 100).

Remarks:

* This form is not designed for shallow water (neritic) carbonate sediments

Figure 9: Example of smear slide description sheet.

Estimating percentages of components

Comparator charts (Figure 16 on p. 41 in: http://www-odp.tamu.edu/publications/tnotes/digital/tnote_08.pdf) are the best method for estimating silt/clay proportions.

Estimating the abundance of the clay-size (<4-micron) fraction is challenging. With this in mind, we have created a series of reference slides with known proportions of clay-size vs. silt-size minerals (slide sets stored on ship and at core repositories; see Marsaglia et al. (2013) tutorial for details). Specific techniques for seeing the clay fraction include viewing at high magnification (40× or 60×). Note that where sand grains are present in a slide, this may preclude the investigator from focusing on the fines at high magnification because the separation between the cover glass and the slide onto which the fines have settled is too great. That is why we suggest segregating the coarse material at one end of the slide so that the coverslip rests at an angle, allowing for closer magnification on the fine end of the slide or using the alternate method of making the sediment slurry on the coverslip. The clay- to fine-silt fraction is best seen when the polars are semicrossed, providing an oblique illumination.

Estimated proportions of clay and silt may be corroborated by tactile tests on core material (e.g., ability to create a ribbon between thumb and forefinger indicates clay, grittiness on the teeth indicates silt). Another test is to suspend the sediment in water in a translucent glass vial (paleosample vial) and observe how rapidly the sediment settles (sand and silt) or remains suspended for a long period (clay). Again, the proportion of sand, silt, and clay determines the sediment name, and terminology must be consistently applied between smear slide and core describers.

Unfortunately, the term “clay” has both a textural and mineralogical connotation. Most clay mineral grains are, indeed, of clay-size and estimating the proportion of clay in biogenic-dominated sediments can be more challenging, but important in naming the sediment/rock (e.g. hemipelagic vs. pelagic). Often sediment core color can be linked to proportions of biogenic versus terrigeneous components. For example see color-lithology correlation discussions in Taylor and Fujioka et al. (1990) for Leg 126, and Bralower, Premoli Silva, and Malone et al. (2002) for Leg 198.

Calibration of smear estimates using other data

Chemical determination of bulk carbonate and XRD mineralogical data should be used to help calibrate smear slide estimates of components. This is possible only if sampling is coordinated for these analyses (in the same exact intervals), as noted above.

The proportion of carbonate is significant in naming the sediment lithology in that it determines the classification scheme used (see Handbook for Shipboard Sedimentologists: http://www-odp.tamu.edu/publications/tnotes/digital/tnote_08.pdf). The percentage of clay minerals versus carbonate in the clay-sized fraction can be a difficult call, especially in finer-grained Pleistocene sediments where nannofossils are very small and exhibit low birefringence, making them less easily quantified even at high (40×) magnification. Recognition of very small Pleistocene nannofossils is usually a problem starting with the very first cores described on the expedition, so coordination with carbonate analyses is best begun immediately at the start of core description. In some instances where the microscope lacked a 40× objective, carbonate content has been completely missed!

X-ray diffraction analyses can be used to clarify identification of major and (to some extent) minor mineral components in smear slides. We have used such data to provide semiquantitative ratios of quartz and feldspar, as well as to identify carbonate mineral components and authigenic minerals such as clays, zeolites, and Fe sulfides. Amorphous material (volcanic glass and opal) also may be identified using this method, though these components are usually easily discerned optically.

References Cited and Petrography Resources

Bolli, H.M., Saunders, J.B., and Perch-Nielsen, 1985, Plankton Stratigraphy, K. (Eds.), Cambridge (Cambridge Univ. Press), 1032 p.

Bralower, T.J., Premoli Silva, I., Malone, M.J., et al., 2002. Proc. ODP, Init. Repts., 198: College Station, TX (Ocean Drilling Program). doi:10.2973/odp.proc.ir.198.2002

Carozzi, A. V., 1993, Sedimentary Petrography, Englewood Cliffs, NJ, 263 p.

Garrison, R.E., and Kastner, M., 1990, Phosphatic sediments and rocks recovered from the Peru margin during ODP Leg 112: Proceedings of the Ocean Drilling Program, Scientific results, v. 112, p.

Haq , B.U., and Boersma, A., 1976 and 1998, Introduction to marine micropaleontology, Elsevier, 376 p.

Kerr, P.F., 1977, Optical Mineralogy, McGraw-Hill, New York, 492 p.

Lipps, J. H., 1993, Fossil Prokaryotes and Protists, Blackwell Scientific Publications, Oxford, 342 p.

Mange, M.A., and Maurer, H.F.W., 1992, Heavy minerals in colour, Chapman and Hall, London, 147 p.

Marsaglia, K.M., and Shapiro, S., 2005, ODP Core Photo Atlas, CD format (submitted report/project -- publication status pending).

Mazzullo, J., and Graham, A.G., 1988, Handbook for shipboard sedimentologists, Ocean Drilling Program, Technical Note No. 8, 70 p.

Milliken, K. L., and S.-J. Choh, 2011, Carbonate Petrology: An Interactive Petrography Tutorial, v. 1.0, Discovery Series, Tulsa, Oklahoma, Ameri can Association of Petroleum Geologists.

Nesse, W.D. 2004, Introduction to Optical Mineralogy, Oxford University Press, New York, 348 p.

Rothwell, R.G., 1989, Minerals and mineraloids in marine sediments, Elsevier, 279 p.

Scholle, P. A., 1978, A Color Illustrated Guide to Carbonate Rock Constituents, Textures, Cements, and Porosities, Memoir, v. 27, Tulsa, Oklahoma, American Association of Petroleum Geologists, 241 p.

Scholle, P. A., and D. S. Ulmer-Scholle, 2003, A Color Guide to the Petrography of Carbonate Rocks: Grains, Textures, Porosity, Diagenesis, Memoir, v. 77, Tulsa, Oklahoma, American Association of Petroleum Geologists, 474 p.

Taylor, B., Fujioka, K., et al., 1990. Proc. ODP, Init. Repts., 126: College Station, TX (Ocean Drilling Program). doi:10.2973/odp.proc.ir.126.1990

Biogenic Sediments in the World Ocean

Biogenic sediment is composed primarily of the mineralized or amorphous microscopic shells/hard parts of marine **plankton**, typically single-celled protists, including the calcareous coccolithophorids, other calcareous nannoplankton, and foraminifera (less common: calcareous dinoflagellates and bolboforma), and the siliceous diatoms and radiolarians (less common: silicoflagellates and ebridians). Organic walled marine dinoflagellates and terrestrial pollen and spores are most common along continental margins. Small metazoans also contribute to biogenic sediments, including the aragonitic pteropods (gastropods), calcareous ostracods (arthropods) and the spines of echinoderms, phosphatic teeth, bone, and otoliths of fish, the spicules of sponges, holothurians, and tunicates, as well as the agglutinated tests of tintinnids (Choreotrich ciliates). This atlas focuses mostly on the microscopic organisms that are likely to be observed in smear slides.

The microscopic plankton are grazed and preyed upon by a variety of animals in the photic zone and upper thermocline where their shells/hard parts are packaged into **fecal pellets**. Fecal pellets are an important mode of transport to the deep seafloor. Passive settling through the water column or incorporation into organic detritus (**marine snow**) are other modes of deposition. **Pelagic sediment** refers to those sedimentary particles that settle through the water column, such as shells/hard parts of plankton and wind-blown silt and clay. **Biogenic ooze** and **red clay** are examples of pelagic sediments. **Hemipelagic sediment** is a mix of terrigenous or volcaniclastic sediments and biogenic sediments, such as terrigenous mud and calcareous microfossils, or red clay and siliceous microfossils. **Periplatform ooze** is calcareous sediment, rich in shallow water biogenic shell debris that accumulates in an apron around carbonate platforms, reefs, and atolls.

Calcareous Ooze. The near-surface ocean is generally saturated with respect to calcite. Plankton with shells of calcium carbonate ($CaCO_3$) are found throughout the world ocean, although their abundance and diversity are greater in the low to mid-latitudes. By contrast, the deep ocean is undersaturated with respect to calcite and the **lysocline** represents the depth where the rate of dissolution and fragmentation of calcareous shells begins. The **Calcite Compensation Depth (CCD)** is the depth where the supply of calcite from above equals the rate of dissolution caused by low temperature, high pressure, and relatively high concentration of dissolved CO_2. Today the CCD is ~5000 m in the North Atlantic and ~4000 m in the North Pacific, although the level of the CCD has changed significantly through geologic time due to changes in sea level, ocean circulation, and global climate change. As a result, calcareous ooze accumulates on bathymetric highs above the CCD. Along continental margins, calcareous (and siliceous) microfossils are diluted by terrigenous sediment. Burial compaction of pure calcareous ooze yields **chalk** and eventually **limestone** at greater depths below the seafloor.

Siliceous Ooze. The ocean is undersaturated with respect to silica, even in

regions where deeper, nutrient-rich waters are returned to the surface by upwelling. Despite this, plankton with shells of opaline silica ($SiO_2.H_2O$) are found throughout the world ocean. Their abundance and diversity is greater in areas of upwelling, in part because of the greater preservation potential in areas of higher burial rates and/or higher saturation of silicic acid in the sediment pore water. Radiolarian-rich siliceous ooze is characteristic of equatorial or tropical upwelling regions, while diatom-rich siliceous ooze is typical of the oceanic divergence and the Polar Front around the Southern Ocean and subarctic-arctic regions (Figure 10). Siliceous microfossils are also found in abyssal red clays deposited below the CCD. Dissolution of siliceous microfossils, including sponge spicules, is the typical source of **chert** nodules and beds in older deep-sea sediments.

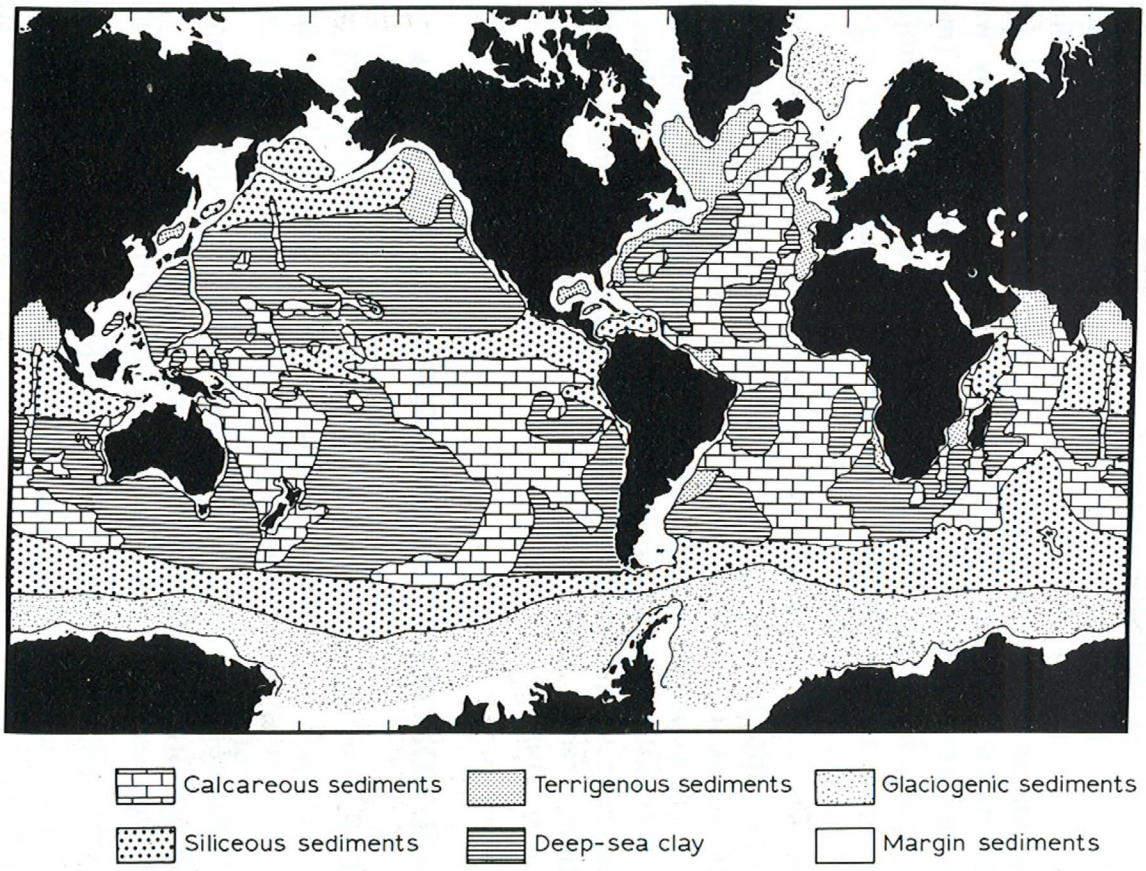

Figure 10: Distribution of the primary sediment types on the seafloor (from Davies and Gorsline, 1976; Rothwell, 1989).

Microfossils as Paleoceanographic Proxies

Beyond the continents, the shells/hard parts and tough organic remains of **microfossils are the sediments**. These include **autotrophs** (coccolithophorids, diatoms, silicoflagellates, bolboforma, and dinoflagellates) and **heterotrophs** (foraminifera, radiolarians, ebridians, some dinoflagellates, as well as sponges, echinoderms, pteropods, ostracods, and tintinnids), useful in reconstructing community structure and biodiversity through time. Many of these groups have long geologic records that extend back through the Jurassic. They are studied as **biological communities** and provide a **wide**

range of organic and inorganic geochemical proxies of temperature, ice volume, productivity, and ocean circulation. For example,

- Assemblages and fluxes of pelagic shells are proxies for **upper water column structure, seasonality, and productivity**.
- **Paleobiogeography** of microfossil assemblages yield information about **ocean circulation**.
- Freshwater diatoms and terrestrial spores, pollen, and phytoliths provide paleoclimatic information about the adjacent land masses.
- Benthic organisms (benthic foraminifera, ostracods, sponges, echino derms) can provide information about **hypoxia**.
- Geochemical proxies of planktic and benthic foram shells are used to reconstruct **sea surface and deep-sea paleotemperatures** ($\partial^{18}O_p$, Mg/Ca), **ice volume** ($\partial^{18}Ob$), **water column structure and gradients** ($\partial^{18}O_{b\text{-}p}$, $\partial^{18}O_{t\text{-}m}$), **productivity** ($\partial^{13}C_{p\text{-}b}$, $\partial^{13}C_{m\text{-}t}$), and **deep-water circulation** ($\partial^{13}C_b$, ε_{Nd} – Neodymium isotopes from fish teeth and Mn crusts).
- Organic biomarkers provide **additional paleotemperature proxies** (alkenones, TEX86).
- Importantly, these marine protists provide a record of the **biotic response to global change**.
- They also are used to study the **processes and rates of evolution**.

Taxonomic Classification of Microfossils in this Atlas

The Taxonomic Classification of Margulis and Chapman (2010) is followed here. All the organisms presented and discussed here belong to the Superkingdom (or Domain) Eukarya, and include representatives of the Kingdoms Protoctista and Animalia. No representatives of the Kingdoms Fungi or Plantae are discussed here.

Margulis, L., and Chapman, M.J., 2010. Kingdoms and Domains: An Illustrated Guide to the Phyla of Life on Earth. Elsevier, 731 p.

Web Resources for Microfossil Images and Information

Publications of the Deep Sea Drilling Project (DSDP Initial Reports volumes) and the Ocean Drilling Program (ODP Initial Reports and Scientific Results volumes) are rich sources for micropaleontological data and images. All images used in the plates presented here for each group have come DSDP and ODP publications, which are available online. Key references and examples are provided for each of the microfossil groups described here. For additional images and more detailed descriptions of microfossils, refer to University College London's MIRACLE image database:

1. Deep Sea Drilling Project Initial Reports: http://www.deepseadrilling.org/i_reports.htm
2. Ocean Drilling Program Initial Reports and Scientific Results: http://odplegacy.org/samples_data/publications.html
3. University College London's 'Microfossil Image Recovery and Circulation for Learning and Education' (MIRACLE) website: http://www.ucl.ac.uk/GeolSci/micropal/index.html

Summary of common marine microfossils. Major marine **microfossil groups** in bold.

Calcareous Microfossils	Hard Parts	Size	Geologic Range
Coccolithophorids and other **Calcareous Nannofossils**	Individual plates, discs, scales (coccoliths, nannoliths), or spherical coccosphere	3-20 µm, up to 50 µm	Late Triassic – present
Calcareous Dinoflagellates ('Calcispheres')	Single spherical or ovoid calcareous chamber; may have an aperture visible	10-80 µm, up to 180 µm	Late Triassic – present (especially Cretaceous – present)
Planktic Foraminifera and Smaller Benthic Forams	Most are multi-chambered (many species are coiled), perforated shell/test of calcite or agglutinated particles	~20-1000 µm (1 mm), up to 2000 µm (2 mm)	Cambrian – present (planktics: early Jurassic – present)
Bolboforma	Typically single-chambered (sub)spherical, smooth to strongly ornamented test with terminal aperture	50-150 µm, up to 250 µm	Early Eocene – late Pliocene
Ostracods	Ovate or kidney-shaped bivalved shells; smooth to ornamented	100 µm to >2000 µm	Ordovician – present
Pteropods	Coiled to uncoiled 'snail' shells of aragonite	>5 mm (whole)	Late Paleocene – present
Echinoderm Spines	Porous calcite rods	>200 µm	Jurassic - present
Siliceous	**Microfossils**		
Diatoms	Frustules generally flat, perforated, circular (centric), triangular, or elongated (pennate)	20-200 µm, up to 2000 µm long (2 mm)	Aptian/Albian – present
Radiolarians	Perforated cones (nassellarian), spherical shells with spines, or discoidal delicate lattices (spumellarian)	~30-2000 µm (2 mm)	Cambrian – present
Silicoflagellates	Simple skeleton of connected hollow rods forming a basal ring (and apical structure: Cenozoic)	10-100 µm, up to 500 µm	Aptian/Albian – present
Ebridians	Simple skeleton of solid elements (bars, rings, spines) with angular (sometimes jagged) edges	15-65 µm, generally <25 µm	Paleocene – present
Sponge Spicules	Solid or hollow rods, barbed rods; siliceous and calcareous	10-2000 µm	Neoproterozoic – present
Organic	**Microfossils**		
Dinoflagellates (Dinocysts)	Theca-like shape, or body with spine-like processes; may have opening (archeopyle)	15-100 µm, up to 2000 µm (2 mm)	Silurian? Late Triassic – present
Tintinnids	Agglutinated vase-shaped loricae	20-200 µm	Jurassic – present
Spores and Pollen	Brown-colored, compressed, ovate to circular shaped	10-100 µm ('megaspores' >200 µm)	Devonian – present
Phosphatic	**Microfossils**		
Fish teeth and bone	Amber to brown-colored teeth and bone fragments	Generally >200 µm	Devonian – present

Calcareous Nannofossils

INTRODUCTION TO CALCAREOUS NANNOFOSSILS

Overview – Calcareous nannofossils are the fossil remains of a diverse group of single-celled planktic algae, including the Coccolithophorids, that produce calcareous disk-like scales (coccoliths) or other non-circular, non-elliptical calcareous elements (nannoliths) of varying shapes. These protists are responsible for thick deposits of deep-sea calcareous ooze and chalk since the latest Jurassic. Calcareous nannofossils are very useful for establishing relative age (biostratigraphy), correlation, and paleoenvironmental reconstructions.

Diagnostic Features – Tiny nannofossils; typically 3 to 20 µm, up to 50 µm across. **Coccoliths** (Jurassic to Recent) are circular to elliptical in shape, with a proximal and distal shield joined by a central tube; the shields consist of one or more cycles of crystal elements; the central area may be closed or have a bridge, bar, cross, grill, porous plate, or other structures. These various crystal elements and ornament yield distinctive optic extinction patterns under crossed nicols of a polarizing microscope. Examples of other calcareous nannofossil groups: **Discoasters** (asteroliths) are of great biostratigraphic value in the Cenozoic; Paleocene-Eocene forms are characteristically rosette-shaped (short free rays) while Oligocene-Neogene forms are star-shaped (long free rays); the discoasters went extinct at the end of the Pliocene. ***Braarudosphaera*** (Early Cretaceous to present) is an enigmatic group consisting of 5-sided pentaliths; known to occur in abundance following the K/Pg boundary and in the Oligocene of the South Atlantic. **Ceratoliths** (late Miocene to present) are horseshoe- or wishbone-shaped nannoliths. **Sphenoliths** (Paleocene to Pliocene) are pointed nannoliths with multiple tiers of radiating elements (e.g., blades and apical spine). **Rhabdoliths** (Paleocene to Recent) have a single shield with a long stem. ***Helicosphaera*** (early Eocene to present) have distorted, asymmetrical oval shapes. **Fasciculithid** (Paleogene) are ornamented cylindrical nannoliths. **Nannoconids** (latest Jurassic-Early Cretaceous) were a group of heavily calcified nannoliths with a conical shape and axial canal.

Biology – Kingdom Protoctista, Subkingdom Isokonta, Phylum Haptomonada, Class Prymnesiophyceae. **Coccolithophorids** are haptophyte algae that contain golden brown chloroplasts and secrete three types of cell coverings: organic scales, holococcoliths, and heterococcoliths. A coccosphere surrounds the cell and is composed of individual coccoliths, which typically disarticulate after death. Coccoliths are made of low Mg-calcite; holococcoliths are rarely preserved. Other forms of calcareous nannofossils were also likely produced by single-celled algae, but are of unknown origins.

Ecology – Autotrophs. These phytoplankton have been among the most abundant primary producers of the Mesozoic and Cenozoic. Typical of warm, stratified, oligotrophic near-surface waters, although they occur throughout the world ocean. Some species experience seasonal blooms in cooler, mesotrophic to eutrophic waters (e.g., *Emiliania huxleyi*).

Paleobiogeography – Most abundant in oligotrophic, tropical to warm temperate waters.

Stratigraphic Range – Late Triassic to Recent.

Key References and Examples:

Bown, P.R., 2005a. Cenozoic calcareous nannofossil biostratigraphy, ODP Leg 198 Site 1208 (Shatsky Rise, Northwest Pacific Ocean). In, Bralower, T.J., Premoli Silva, I., and Malone, M.J. (Eds.), Proceedings of the ODP, Scientific Results, 198:44 p.

Bown, P.R., 2005b. Early to mid-Cretaceous calcareous nannoplankton from the North west Pacific Ocean, Leg 198, Shatsky Rise. In, Bralower, T.J., Premoli Silva, I., Malone, M.J., et al., Proceedings of the ODP, Scientific Results, 198:82 p.

Bown, P.R., and Cooper, J.R. 1998. Jurassic. In Bown, P.R. (Ed.), Calcareous Nanno fossil Biostratigraphy: London (Chapman and Hall), 34-85.

Bown, P.R., and Young, J.R., 1998. Introduction. In Bown, P.R. (Ed.), Calcareous Nannofossil Biostratigraphy: London (Chapman and Hall), 1-15.

Bown, P.R., Rutledge, D.C., Crux, J.A., and Gallagher, L.T., 1998. Lower Cretaceous. In Bown, P.R. (Ed.), Calcareous Nannofossil Biostratigraphy: London (Chapman and Hall), 86-102.

Bralower, T.J., Bown, P.R., and Siesser, W.G., 1992. Upper Triassic calcareous nannoplankton biostratigraphy, Wombat Plateau, northwest Australia. In, von Rad, U., Haq, B.U., et al., Proceedings of the ODP, Scientific Results, 120:437-451.

Burnett, J.A., 1999. Upper Cretaceous. In Bown, P.R. (Ed.), Calcareous Nannofossil Biostratigraphy: London (Chapman and Hall), 132-199.

Erba, E., 2006. The first 150 million years history of calcareous nannoplankton: Biosphere-geosphere interactions. Palaeogeography, Palaeoclimatology, Palaeoecology, 232: 237-250.

Haq, B.U., 1978. 3: Calcareous Nannoplankton. In Haq, B.U., and Boersma, A. (Eds.), Introduction to Marine Micropaleontology: Elsevier, 79-107.

Katz, M.E., Finkel, Z.V., Grzebyk, D., Knoll, A.H., and Falkowski, P.G., 2004. Evolutionary trajectories and biogeochemical impacts of marine eukaryotic phytoplankton. Annual Reviews of Ecology and Evolutionary Systems, 35:523-556.

Katz, M.E., Wright, J.D., Miller, K.G., Cramer, B.S., Fennel, K., and Falkowski, P.G., 2005. Biological overprint of the geological carbon cycle. Marine Geology, 217: 323-338.

Lees, J.A., and Bown, P.R., 2005. Upper Cretaceous calcareous nannofossil biostratigraphy, ODP Leg 198 (Shatsky Rise, Northwest Pacific Ocean). In, Bralower, T.J., Premoli Silva, I., and Malone, M.J. (Eds.), Proceedings of the ODP, Scientific Results, 198:60 p.

Mutterlose, J., Bornemann, A., Herrle, J.O., 2005 Mesozoic calcareous nannofossils – state of the art. Paläontologische Zeitschrift, 79(1):113-133.

Perch-Nielsen, K., 1985. 10: Mesozoic calcareous nannofossils. In Bolli, H.M., Saunders, J.B., and Perch-Nielsen, K. (Eds.), Plankton Stratigraphy: Cambridge (Cambridge Univ. Press): 329- 426.

Perch-Nielsen, K., 1985. 11: Cenozoic calcareous nannofossils. In Bolli, H.M., Saunders, J.B., and Perch-Nielsen, K. (Eds.), Plankton Stratigraphy: Cambridge (Cambridge Univ. Press): 427- 554.

Raffi, I., Backman, J., Fornaciari, E., Pälike, H., Rio,D., Lourens, L., and Hilgen, F.,

2006. A review of calcareous nannofossil astrobiochronology encompassing the past 25 million years. Quaternary Science Reviews, 3113-3137.
Siesser, W.G., 1993. 11: Calcareous Nannoplankton. In Lipps, J.H. (Ed.), Fossil Prokaryotes and Protists: Blackwell Scientific Publications, 169-201.
Watkins, D.K., 1992. Upper Cretaceous nannofossils from Leg 120, Kerguelen Plateau, Southern Ocean. In, Wise, S.W., Jr., Schlich, R. et al., Proceedings of the ODP, Scientific Results, 120:343-370.
Wise, S.W., Jr., 1983. Mesozoic and Cenozoic calcareous nannofossils recovered by DSDP Leg 71 in the Falkland Plateau region, southwest Atlantic Ocean. In, Ludwig, W.J., Krasheninnikov, V.A., et al., Initial Reports of the DSDP, 71:481-550.
Young, J.R., Geisen, M., Cros, L., Kleijne, A., Probert, I. & Ostergaard, J.B., 2003. A guide to extant coccolithophore taxonomy. Journal of Nannoplankton Research, Special Issue, 1: 1-132.

Web Resources:

http://www.ucl.ac.uk/GeolSci/micropal/calcnanno.html
http://ina.tmsoc.org/Nannotax3/index.php?dir=Coccolithophores
http://ina.tmsoc.org/terminology/index.htm

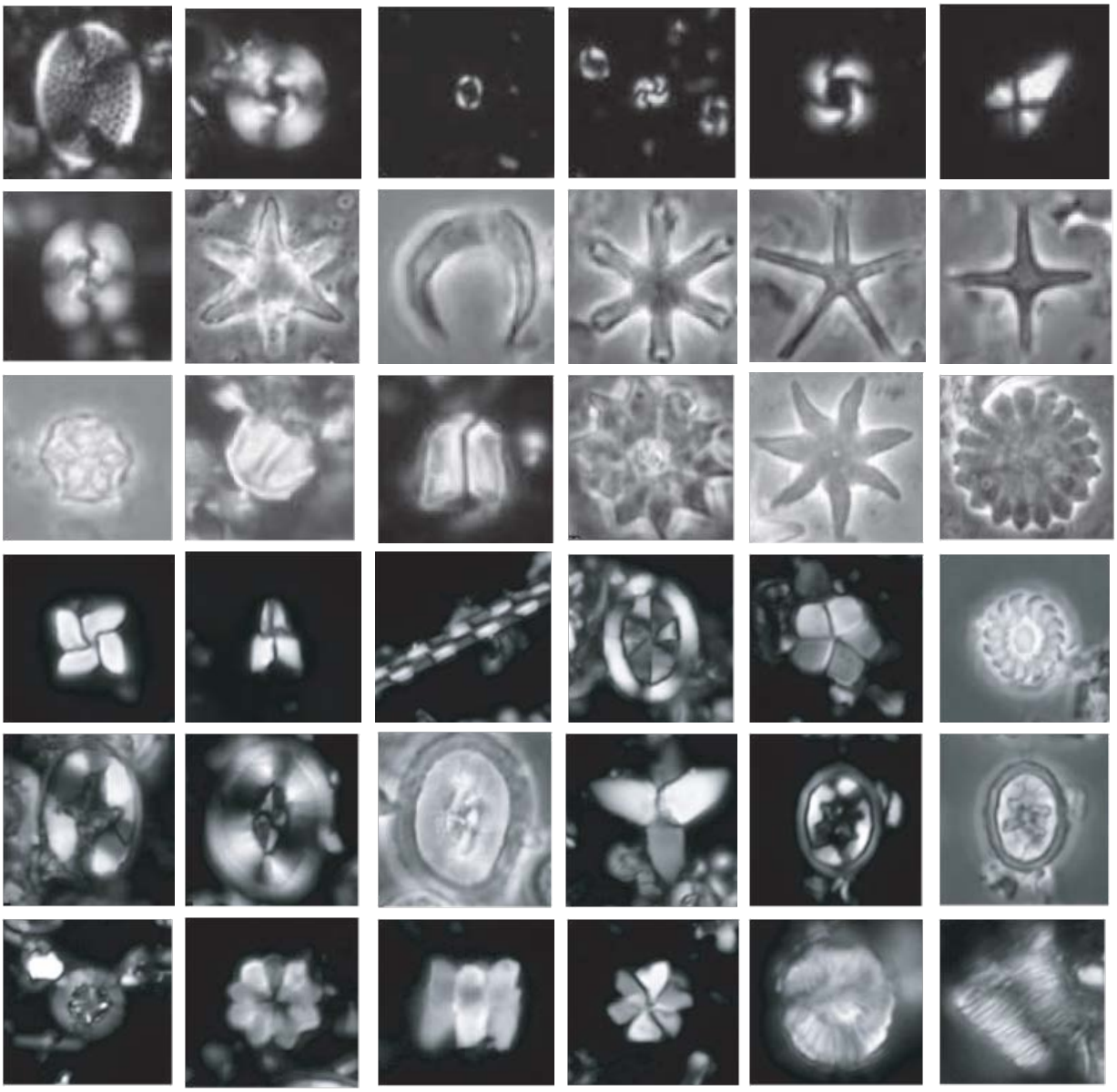

Representative Cretaceous and Cenozoic calcareous nannofossils; LM = light microscope, XPL = cross-polarized light. Top row: *Pontosphaera discopora, Cyclicargolithus floridanus, Emiliania huxleyi, Gephyrocapsa small, Reticulofenestra haqii, Sphenolithus heteromorphus*. Second row: *Reticulofenestra bisecta, Rhomboaster bramlettei, Amaurolithus primus, Discoaster surculus, Discoaster hamatus, Discoaster tamalis*. Third row: *Catinaster coalitus, Catinaster coalitus, Fasciculithus bobii, Discoaster diastypus, Discoaster lodoensis, Discoaster multiradiatus*. Fourth row: *Micula murus, Ceratolithoides sagittatus, Microrhabdulus decoratus, Arkhangelskiella cymbiformis, Baarudosphaera africana, Cribrocorona gallica*. Fifth row: *Eiffellithus eximius, Broinsonia parca constricta (LM, XPL), Uniplanarius trifidus, Eiffellithus turriseiffelii* (LM, XPL). Bottom row: *Prediscosphaera columnata, Eprolithus floralis, Eprolithus floralis, Rucinolithus wisei, Nannoconus sp., Nannoconus abundans*?. Photomicrographs from Bown, 2005a, b; Lees and Bown, 2005.

Calcareous Nannofossils

Coccoliths


Cocco 1


Cocco 2


Cocco 3


Cocco 4


Cocco 5


Cocco 6


Cocco 7


Cocco 8


Cocco 9


Cocco 10


Cocco 11


Cocco 12


Cocco 13


Cocco 14


Cocco 15


Cocco 16


Cocco 17

Discoasters


Disco 1


Disco 2


Disco 3


Disco 4


Disco 5


Disco 6

Other Nannoliths


Nanno 1


Nanno 2


Nanno 3


Nanno 4


Nanno 5


Nanno 6


Nanno 7


Nanno 8


Nanno 9


Nanno 10

Image ID: 0450/0451

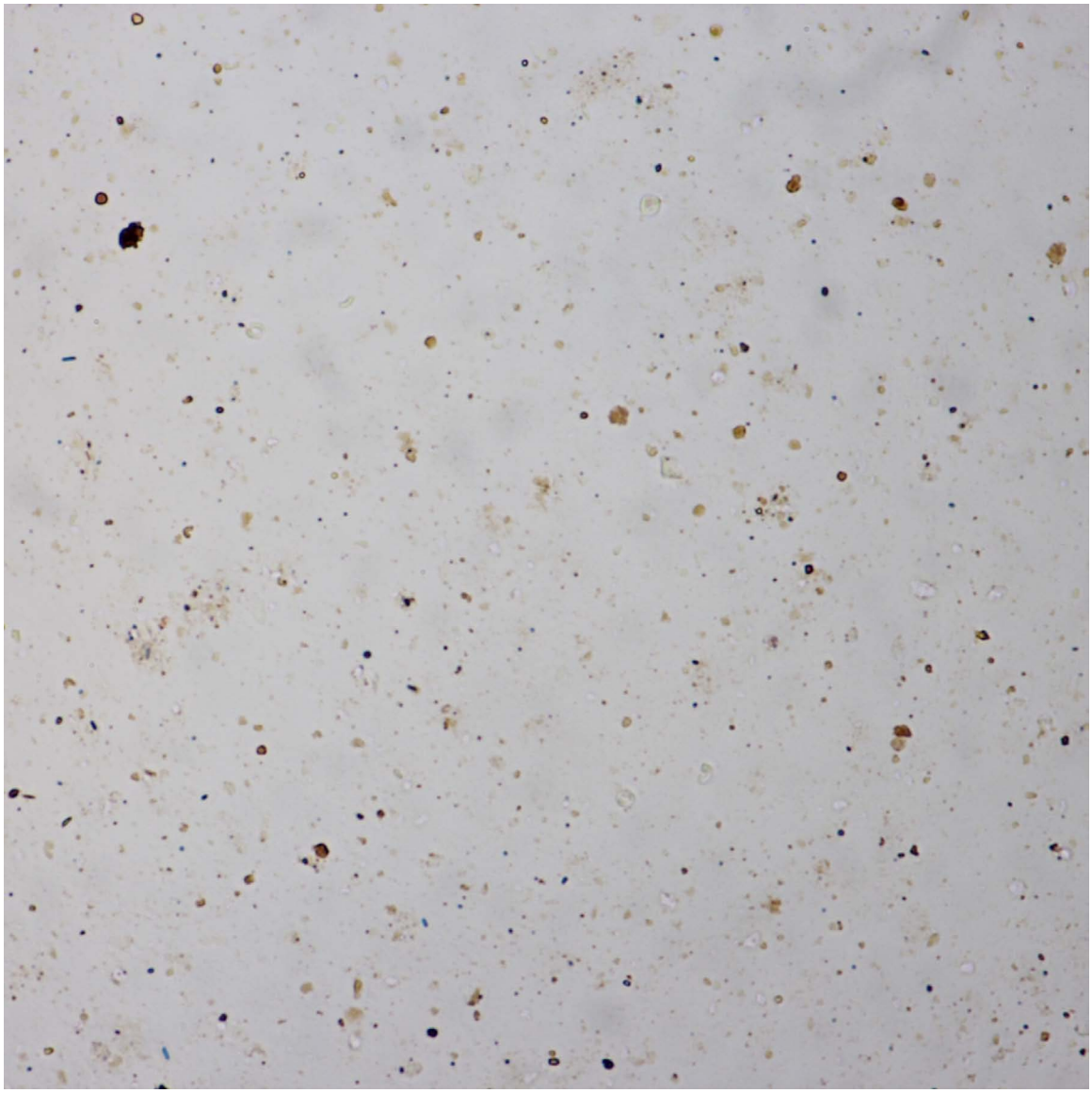

Cocco 1.

Sparse (<1%) coccoliths in well dispersed clay are recognizable only when polars are crossed to show their characteristic first-order white birefringence with an internal "x" resulting from the radial arrangement of their calcite crystals, their <30 micron size, and their shield morphology.

DSDP Sample (Late Cretaceous/Campanian): Leg 86, Hole 576B, Core 7H, Section 6W, 36 cm

Image ID: B0013/B0014

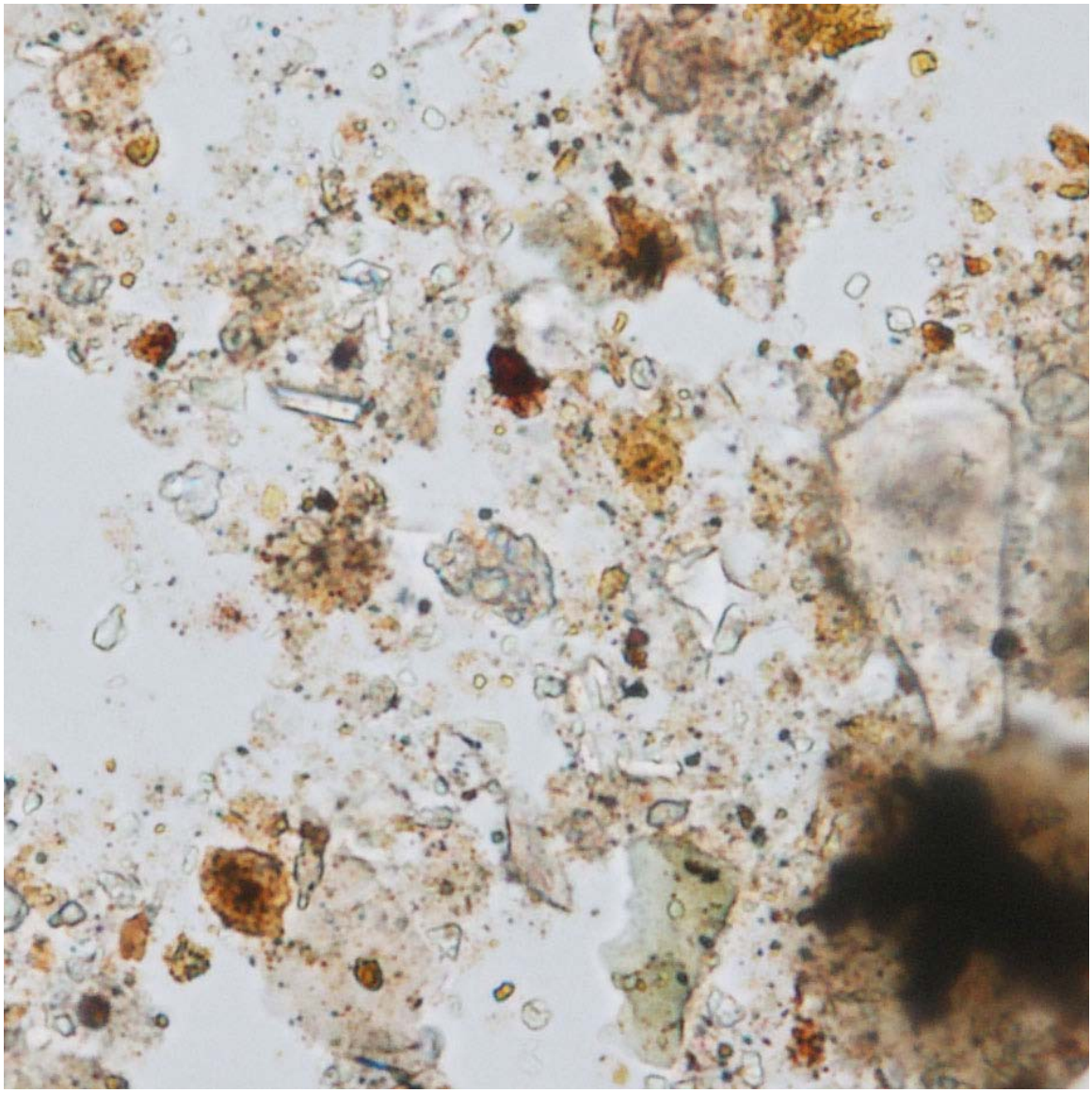

Cocco 2.

In this view of calcareous mixed terrigenous sediment with detrital brownish (organic?) clay and silt (mica), the higher-relief grains are carbonate (micrite) of uncertain affinity, best seen with polars crossed. Sparse coccoliths are not discernible in plane light, but can be seen with polars crossed as white/grey/black circular pinwheels. Note mica grains show no birefringence because they lie flat with their c-axes perpendicular to the field of view.

DSDP Sample (late Miocene/Messinian): Leg 13, Hole 132, Core 22, Section 1, 12 cm

Image ID: 00472/00473

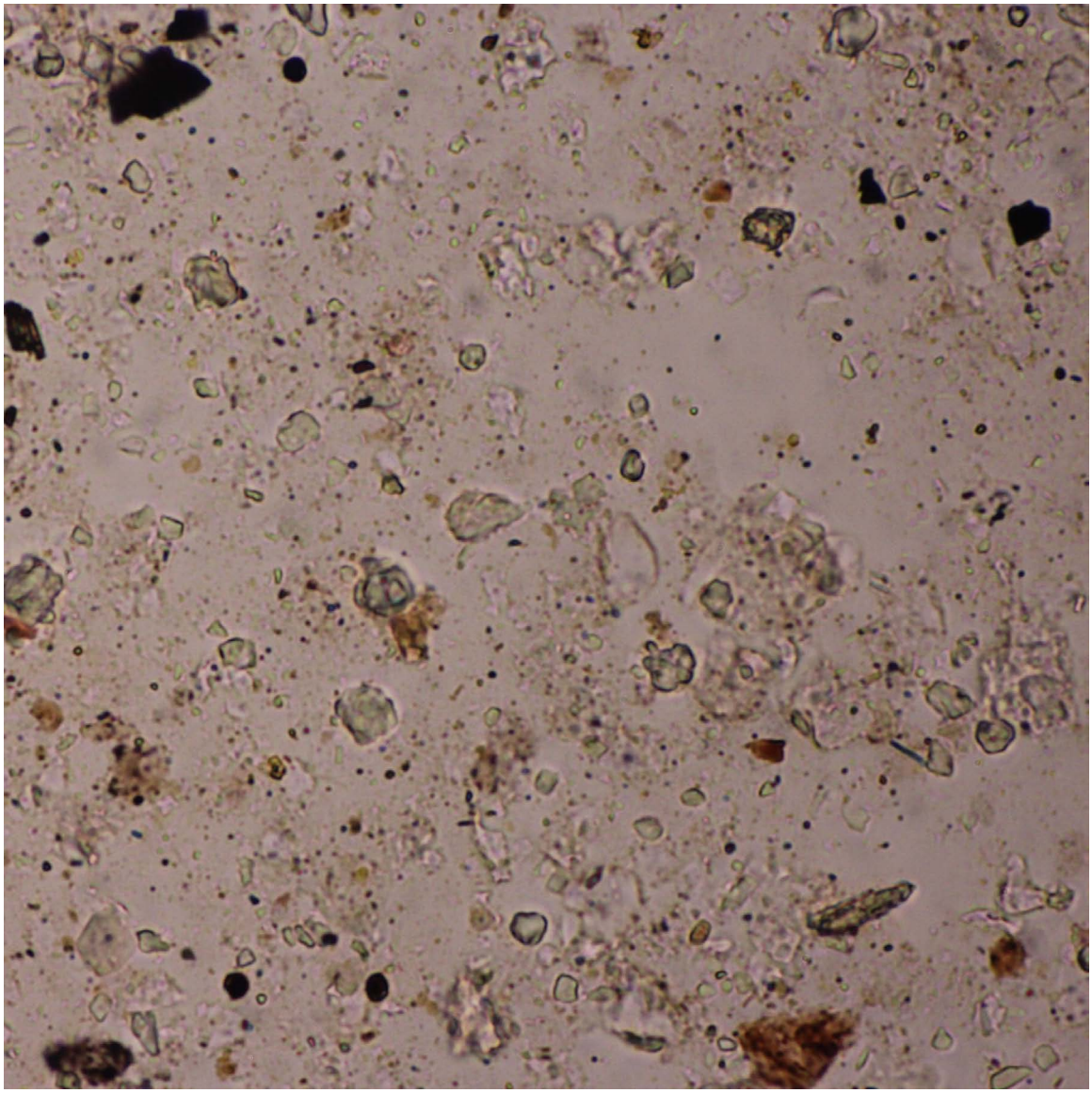

Cocco 3.

In this view of calcareous, mixed terrigenous sediment, silty clay to clayey silt with brownish (organic?) matter and opaque minerals, the higher relief grains are carbonate (micrite) of uncertain affinity, best seen with polars crossed. Sparse, large coccoliths are not discernible in plane light, but can be seen with polars crossed as white/grey/black circular pinwheels.

DSDP Sample (Pleistocene): Leg 96, Hole 614*, Core 2H, Section 1W, 22 cm

Image ID: B0375/B0376

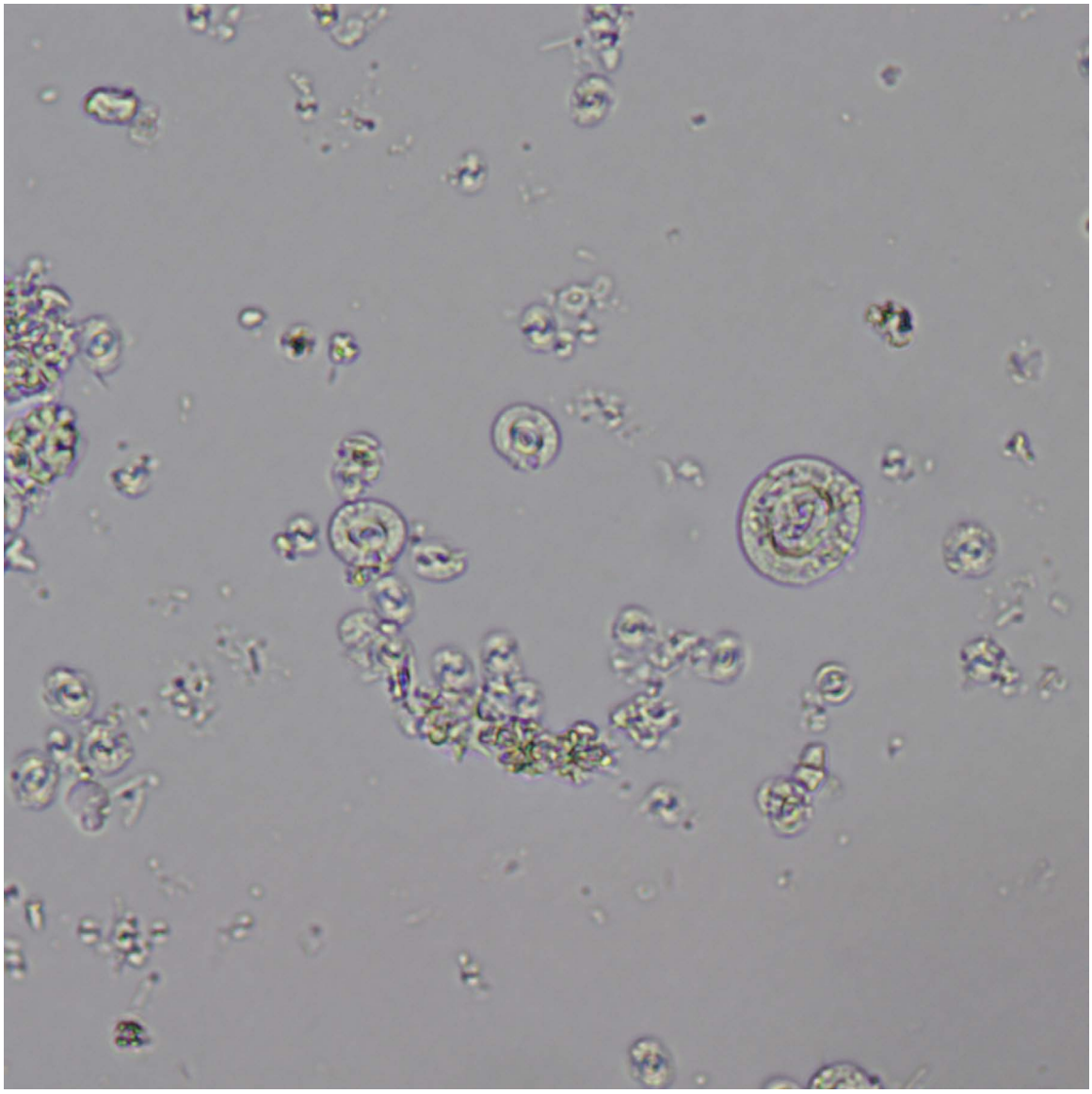

Cocco 4.

The largest coccoliths in this ooze show distal and proximal rings, whereas the remainder exhibit characteristic low birefringence with pinwheel extinction pattern. Some show up to first-order red birefringence, perhaps as a result of incipient recrystallyzation.

ODP Sample (late Oligocene): Leg 101, Hole 628A, Core 21H, Section 1, 52 cm

Image ID: B0496/B0497

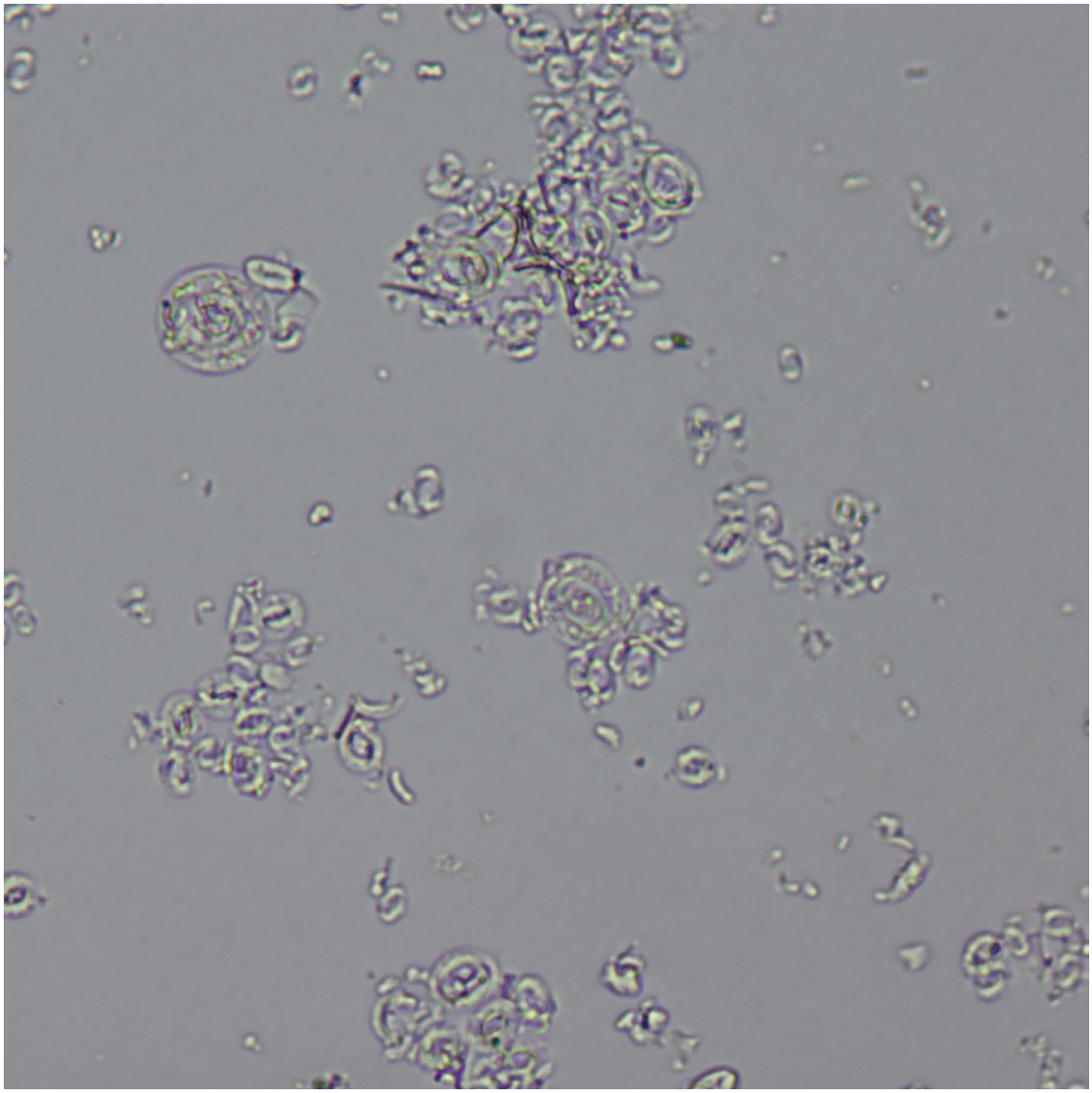

Cocco 5.

This image shows various views of coccoliths, with the large varieties showing distal and proximal rings and possible evidence of recrystallization including higher first-order birefringence. The smaller varieties exhibit characteristic low birefringence with pinwheel extinction pattern.

ODP Sample (early Oligocene): Leg 119, Hole 738B, Core 3H, Section 4W, 10 cm

Image ID: B0385/B0386

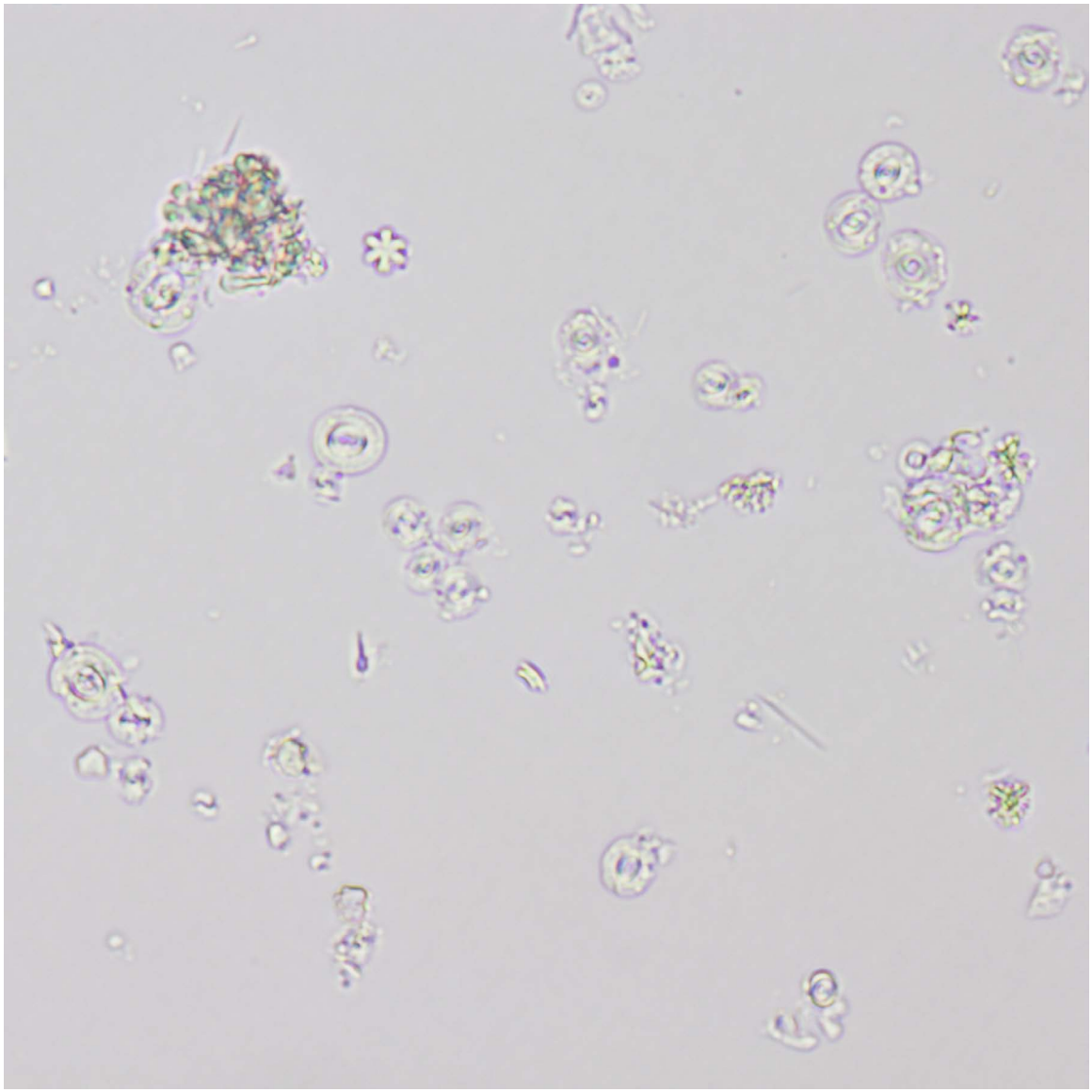

Cocco 6.

Coccoliths are highly dispersed across this field of view. The larger varieties showing evidence of recrystallization including higher first-order birefringence. The smaller varieties exhibit characteristic low birefringence with pinwheel extinction pattern. Clumps may be partly intact coccospheres.

ODP Sample (late Oligocene): Leg 101, Hole 628A, Core 21H, Section 1, 52 cm

Image ID: B0498/B0499

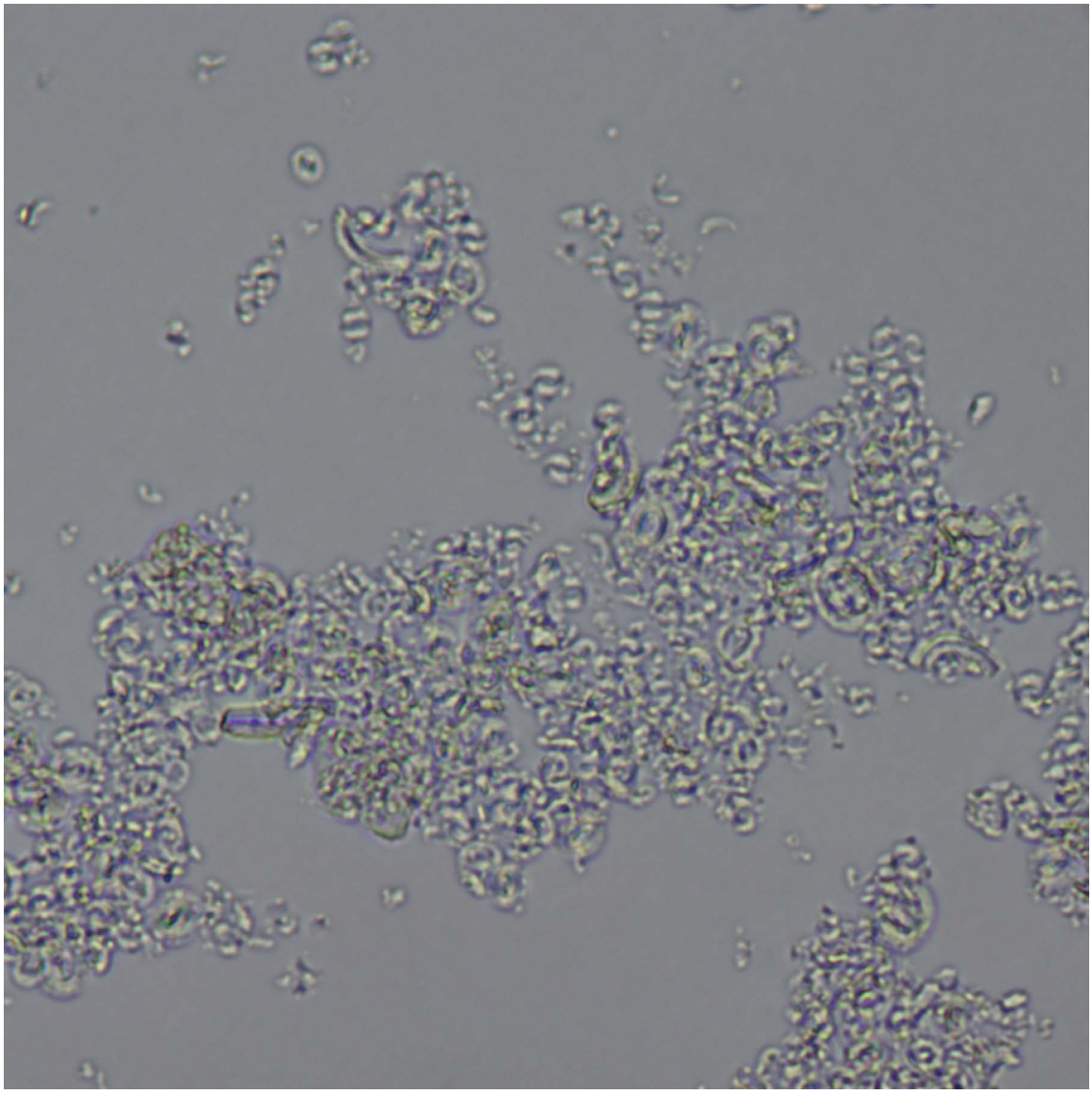

Cocco 7.

This ooze consists of a variably-sized coccoliths thinly spread across the slide.

ODP Sample (early Oligocene): Leg 119, Hole 738B, Core 3H, Section 4W, 10 cm

Image ID: B0465/B0466

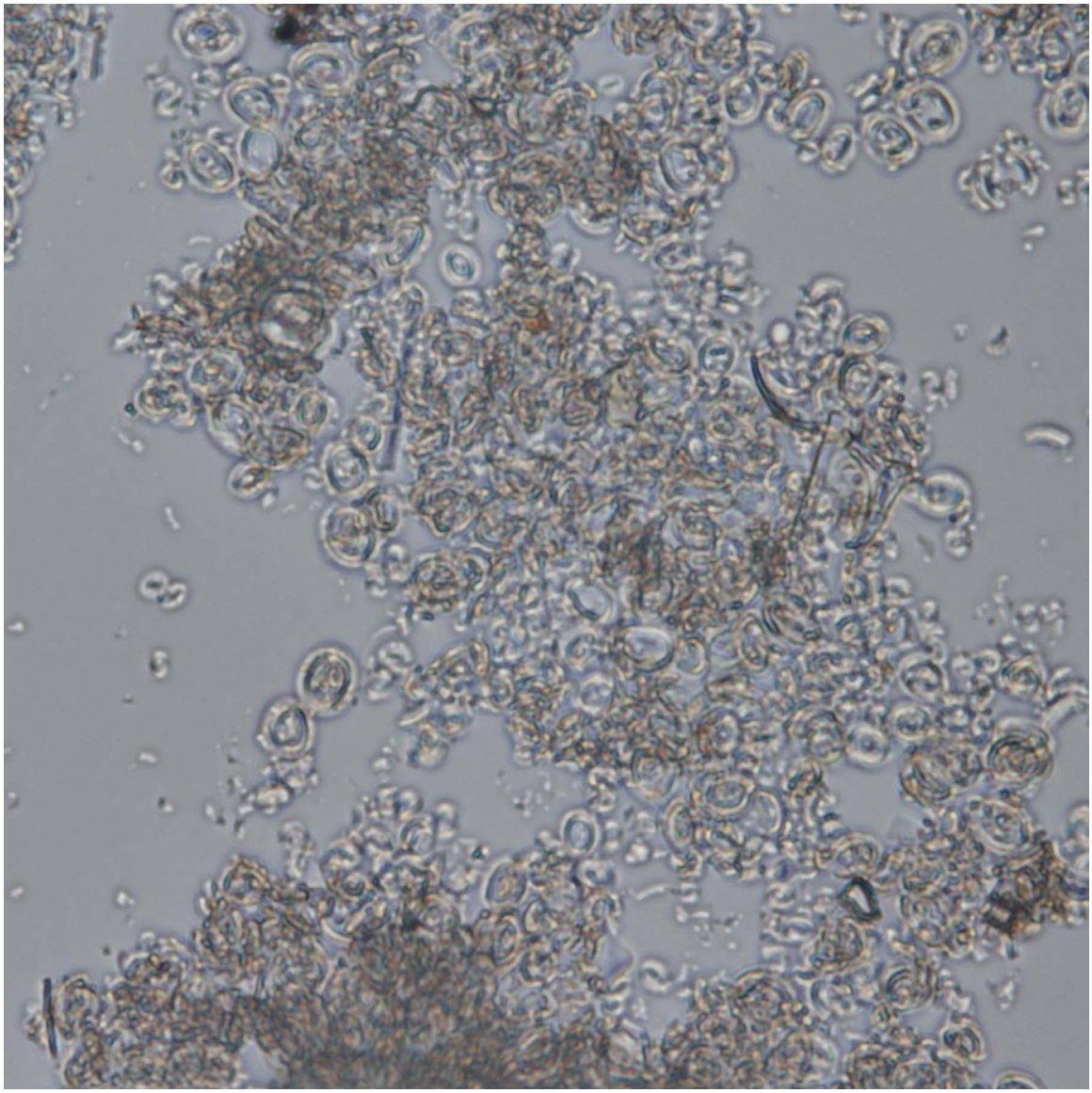

Cocco 8.

This coccolith ooze is composed of variably sized and distributed coccoliths with a trace of isotropic biogenic siliceous debris. Enhanced birefringence in some coccoliths suggests that they may be starting to recrystallize.

ODP Sample (late Oligocene): Leg 113, Hole 690B, Core 7H, Section 5W, 78 cm

Image ID: B0477/B0478

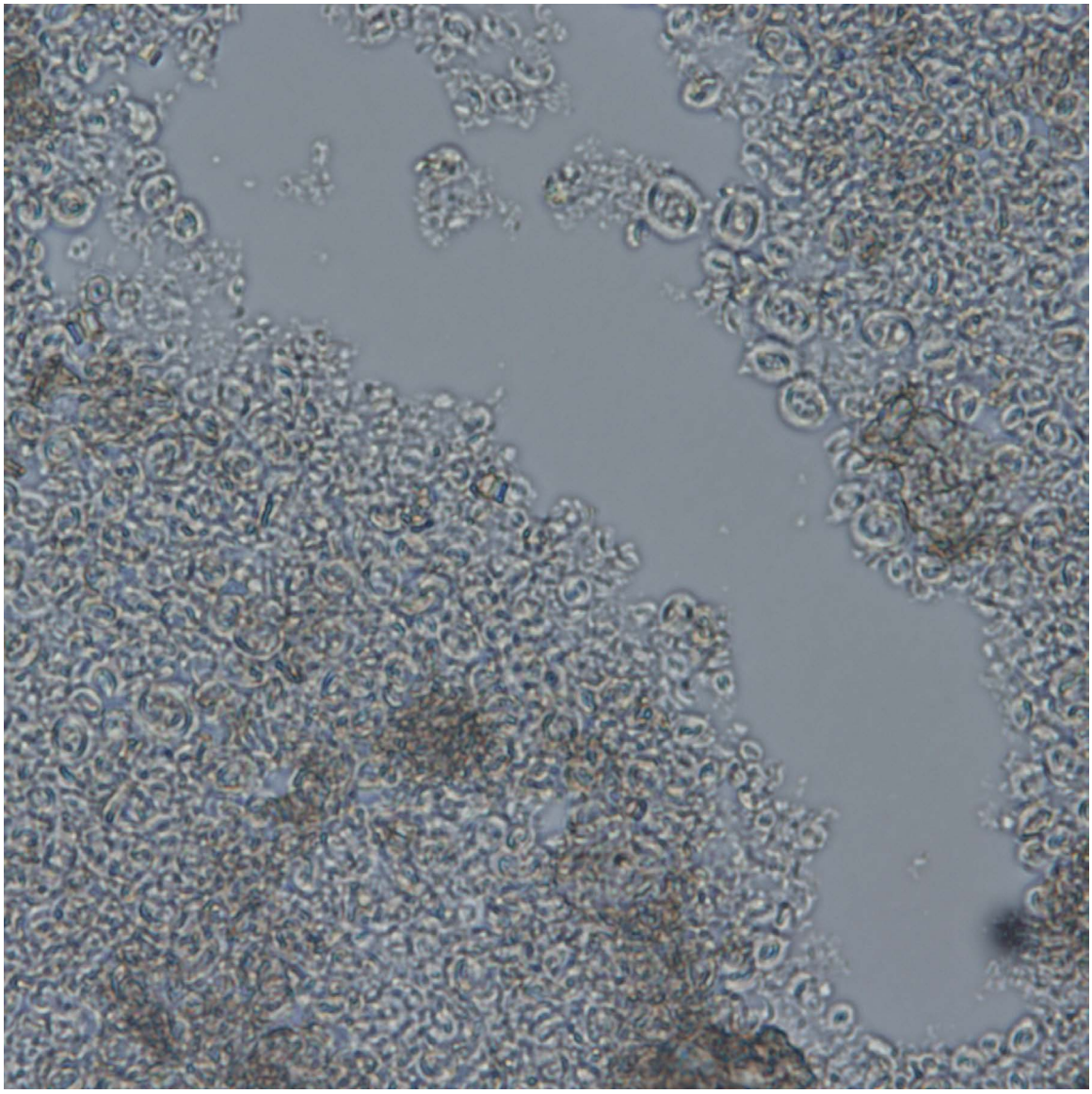

Cocco 9.

In this coccolith ooze composed of variably sized coccoliths, most have enhanced birefringence suggesting that they have recrystallized. Note the internal structure in central areas of the larger species.

ODP Sample (late Paleocene): Leg 113, Hole 690B, Core 25H, Section 3W, 60 cm

Image ID: B0473/B0474

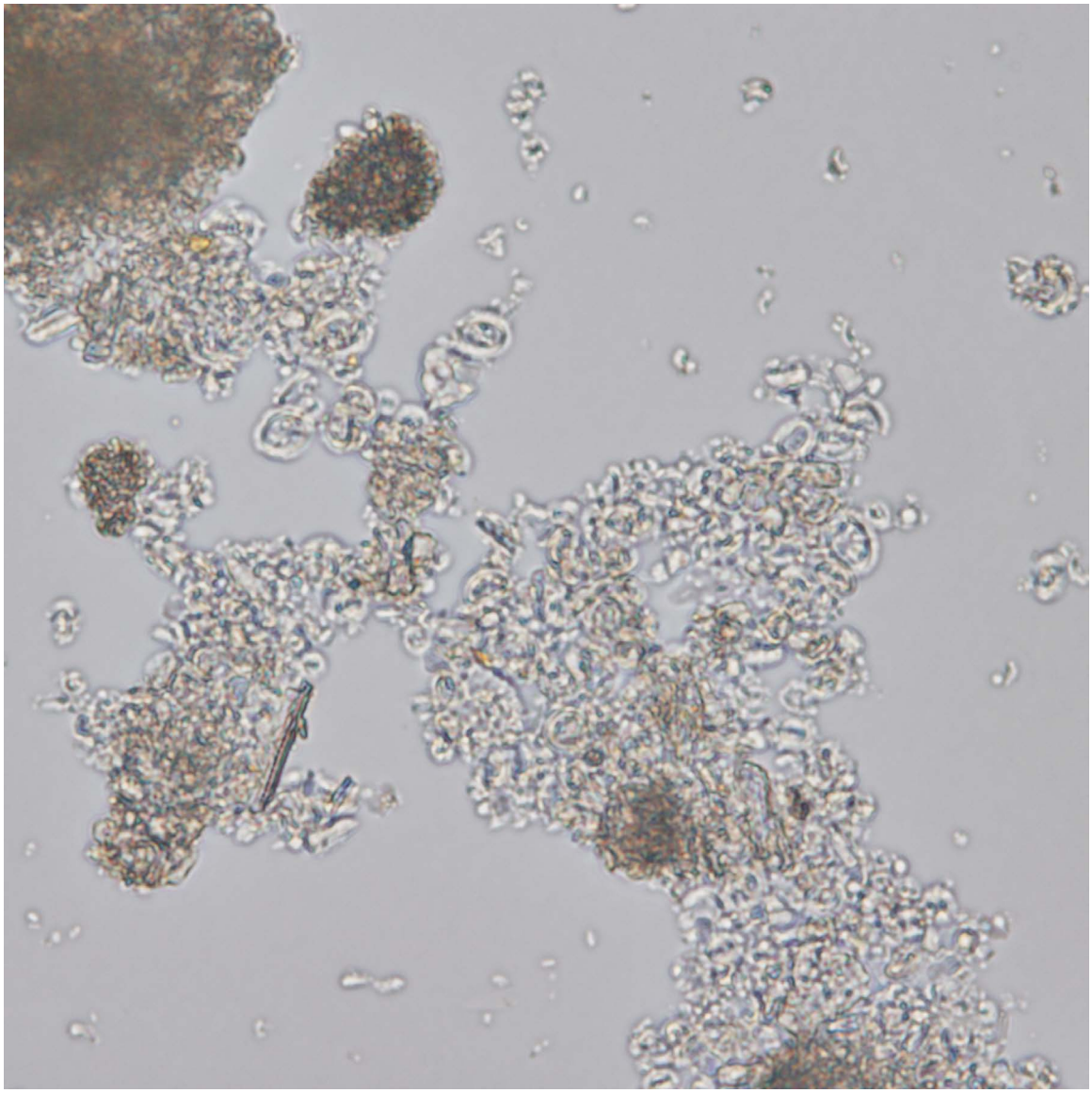

Cocco 10.

This coccolith ooze is composed of variably-sized coccoliths. Note the internal structure in the central areas of large varieties, and darker, densely packed clumps that may be more coherent pellets or marine snow.

ODP Sample (early Eocene to late Paleocene): Leg 113, Hole 690B, Core 15H, Section 4W, 35 cm

Image ID: B0471/B0472

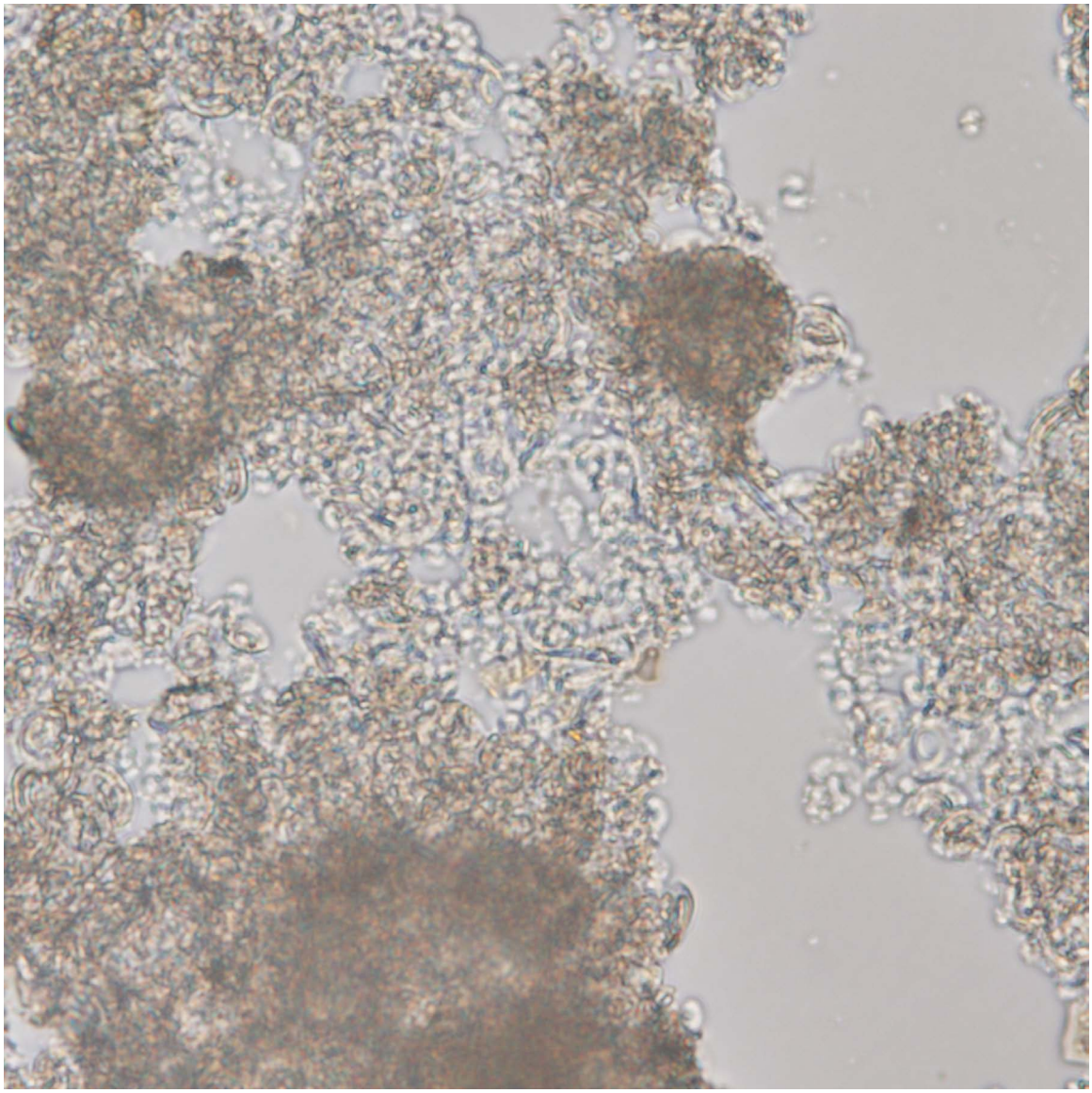

Cocco 11.

In this coccolith ooze of variably sized coccoliths, note darker, densely packed clumps that may be remnants of more coherent pellets or marine snow. In such densely packed zones, it is more difficult to recognize individual components.
ODP Sample (late Eocene): Leg 113, Hole 690B, Core 11H, Section 5W, 90 cm

Image ID: B0500/B0501

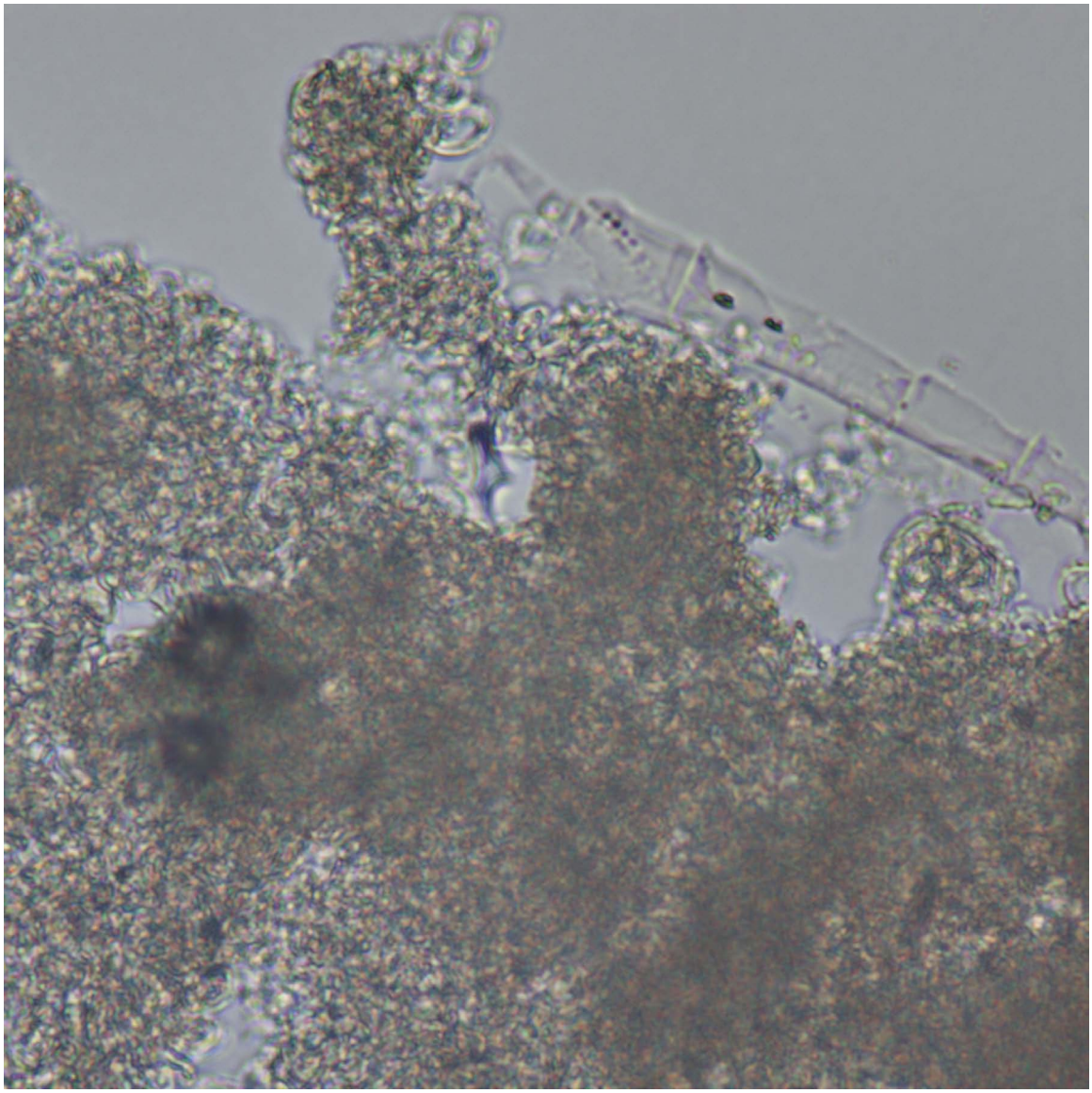

Cocco 12.

This view of dark sediment consisting of densely packed coccoliths shows what a thin section of nannofossil chalk might look like, with discrete coccoliths best distinguished along the thinner edges. A large low-birefringent toothpick fragment (?) dominates the upper right corner. One rounded clump below the fragment may be a semi-intact coccosphere, best seen with polars crossed.

ODP Sample (early Oligocene): Leg 119, Hole 738B, Core 3H, Section 4W, 10 cm

Image ID: B0463/B0464

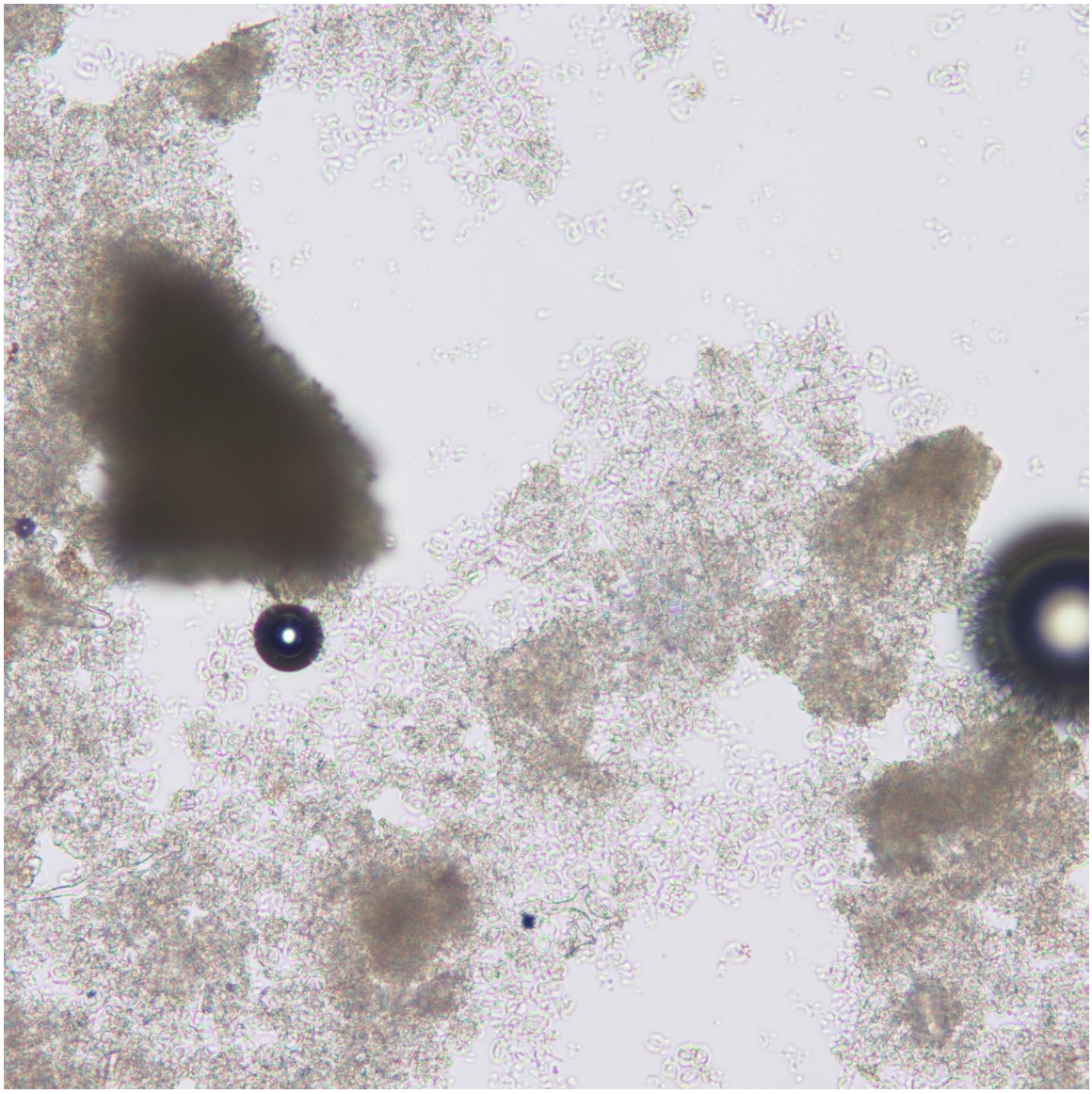

Cocco 13.

In this low-magnification view of an unevenly distributed coccolith ooze, coccolith texture is best seen where coccoliths are thinly spread on the slide. The dark, opaque sand-sized fragment (upper left) may be a bioclast. Dark round circular features are bubbles in the mounting medium.

ODP Sample (late Oligocene): Leg 113, Hole 690B, Core 7H, Section 5W, 78 cm

Image ID: B0475/B0476

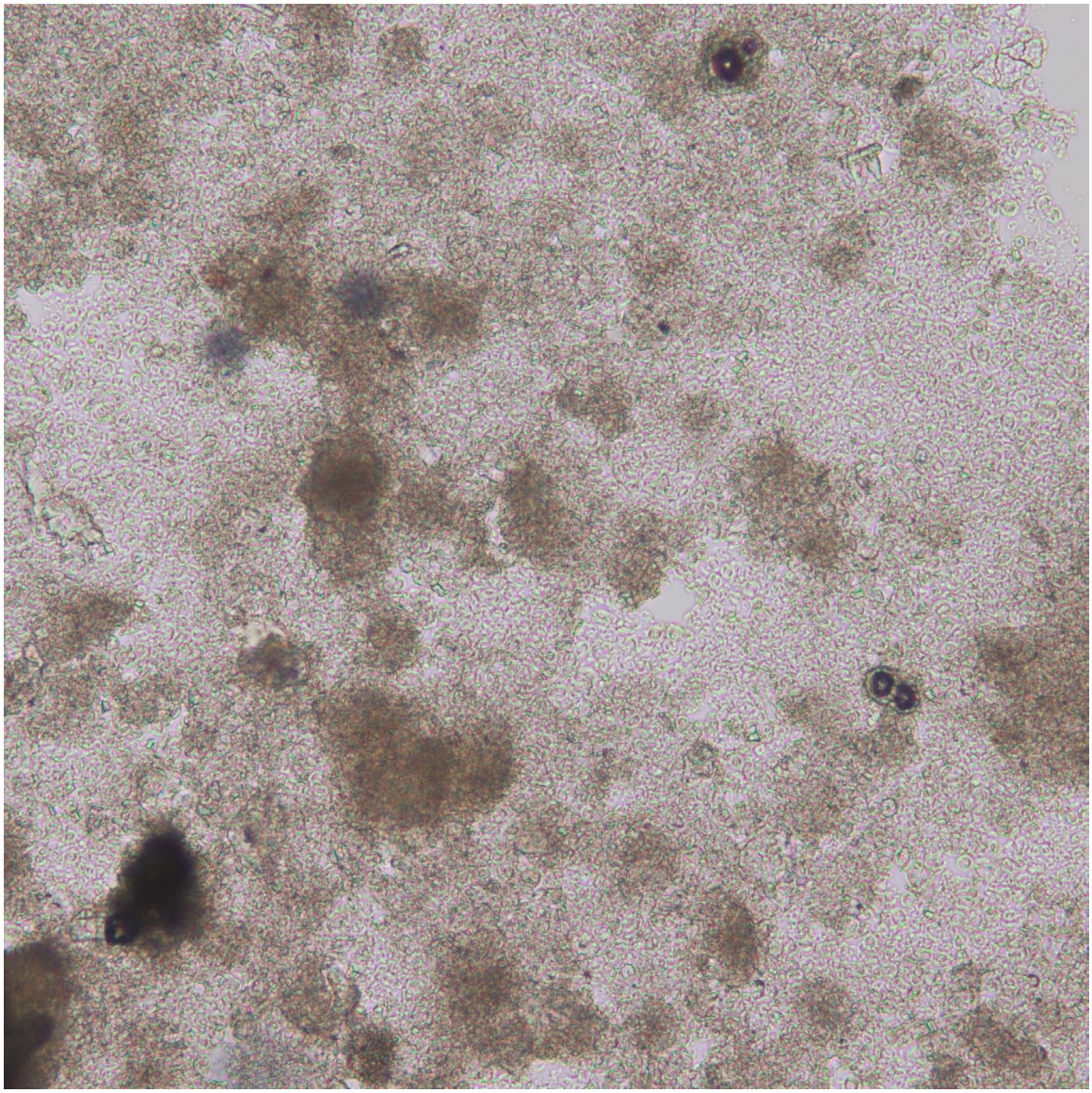

Cocco 14.

Low magnification view of more densely packed coccolith ooze, darker brown patches may be pellets. Sand-size foraminifera (circled) appear dark gray to black because of air bubbles in their chambers. These foraminifera constitute ~2% of the sample.

ODP Sample (late Paleocene): Leg 113, Hole 690B, Core 25H, Section 3W, 60 cm

Image ID: B0568/B0569

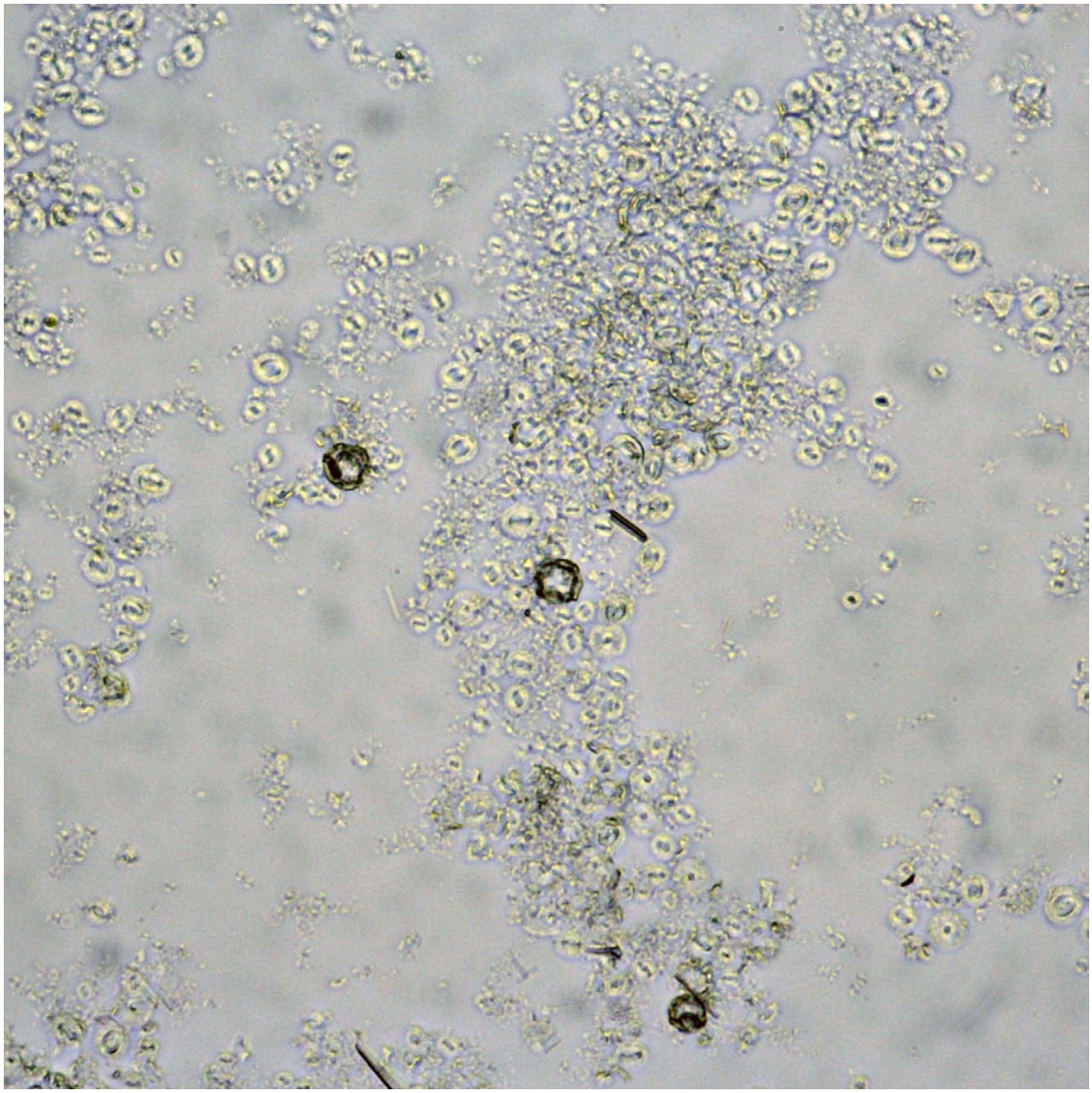

Cocco 15.

The coccoliths in this nannofossil ooze are variably dispersed across the slide and include several intact coccospheres (darker circles). These have higher birefringence.

ODP Sample (early Pliocene): Leg 162, Hole 982A, Core 10H, Section 4W, 50 cm

Image ID: B559/B0560

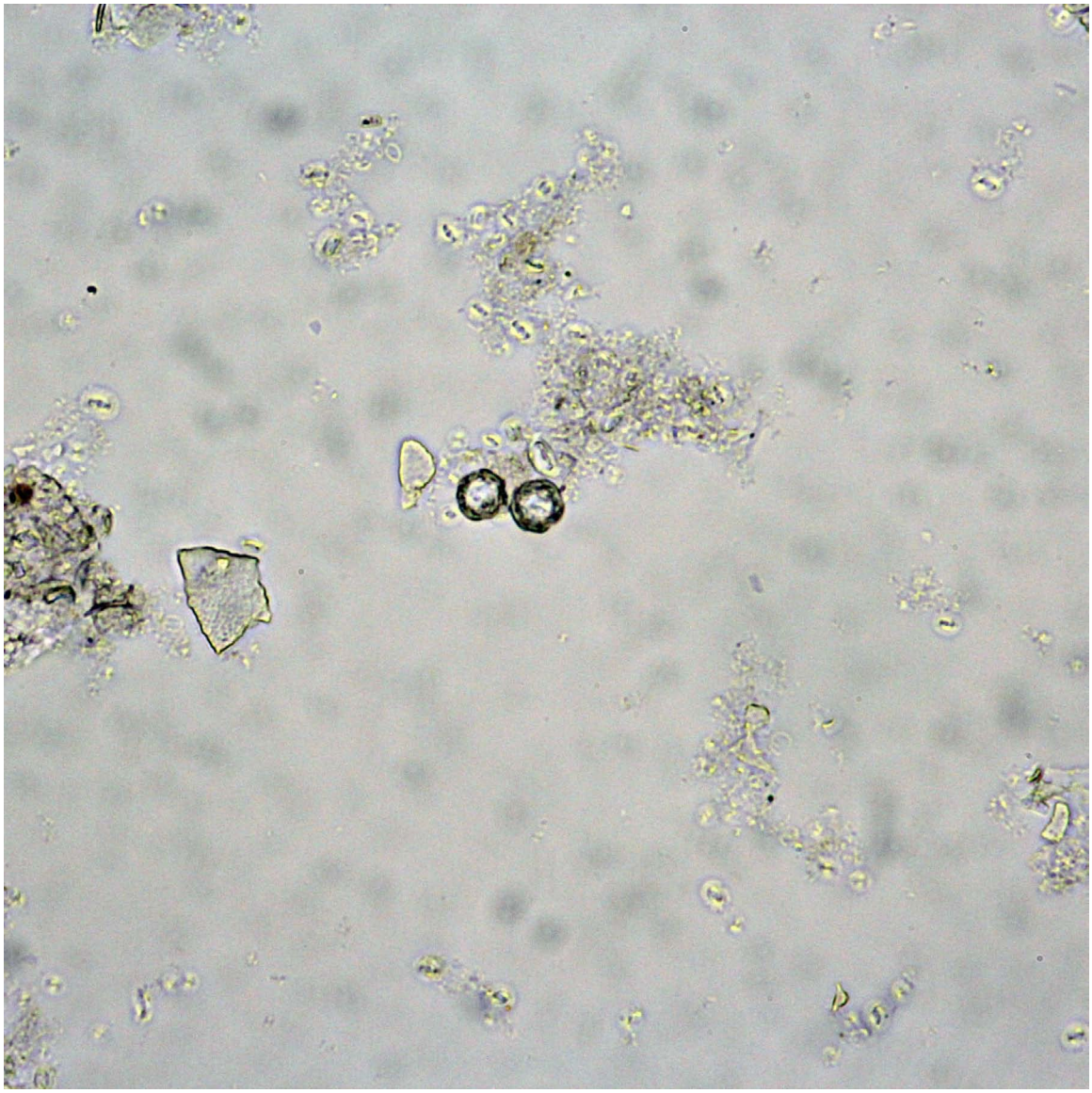

Cocco 16.

This ooze sample consists of nannofossils and bioclasts variably dispersed across the slide. Several intact coccospheres (darker circles) are present in the center of the field of view. These have higher birefringence.

ODP Sample (Pleistocene): Leg 162, Hole 982A, Core 1H, Section 1W, 9 cm

Image ID: B0674/B0675

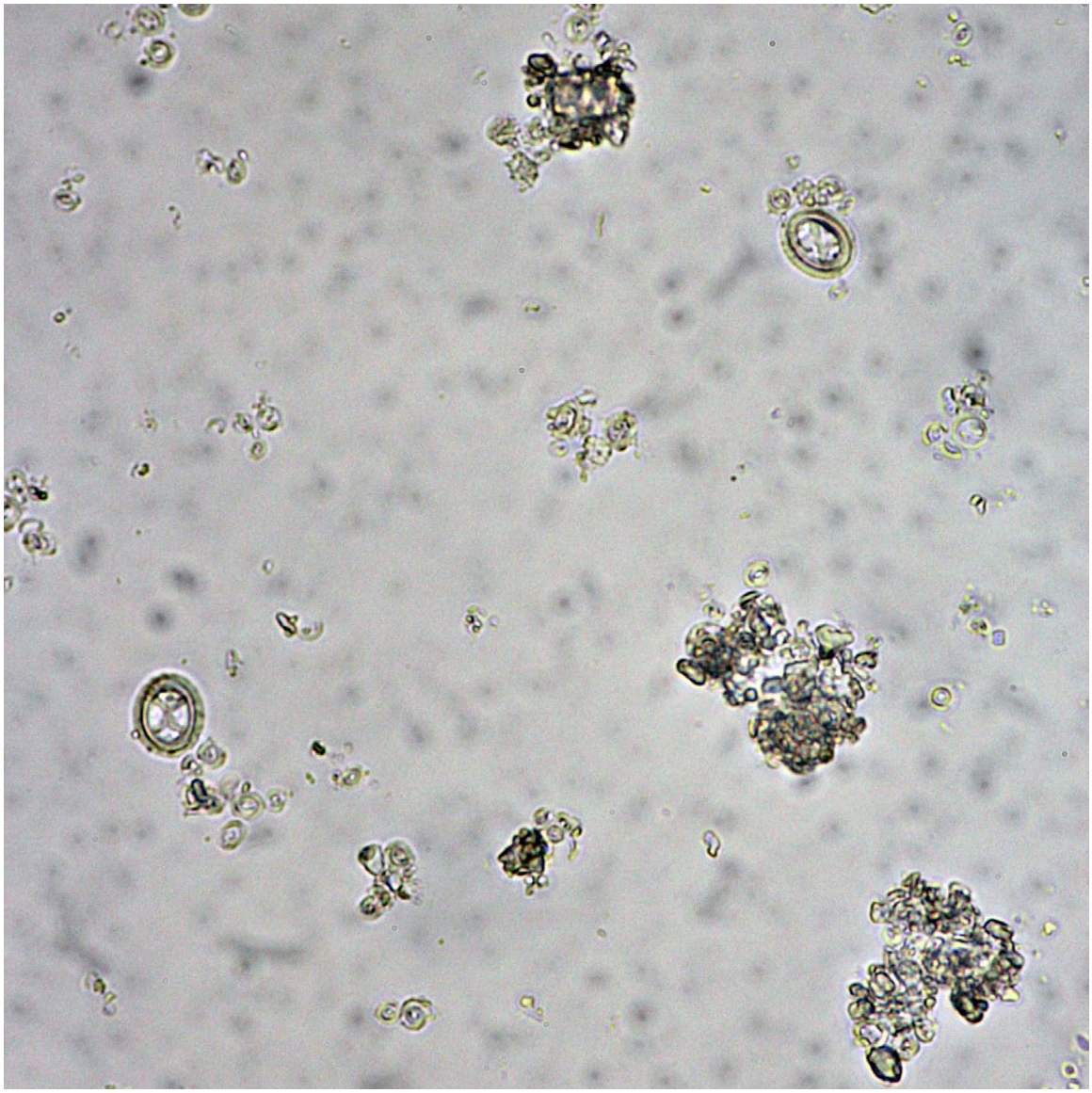

Cocco 17.

In the upper right and lower left quadrants, there are large coccoliths with internal bridges/bars. These show higher carbonate birefringence than the other smaller coccoliths.

ODP Sample (middle Eocene): Leg 122, Hole 763B, Core 6X, Section 4W, 31 cm

Image ID: B0516/B0517

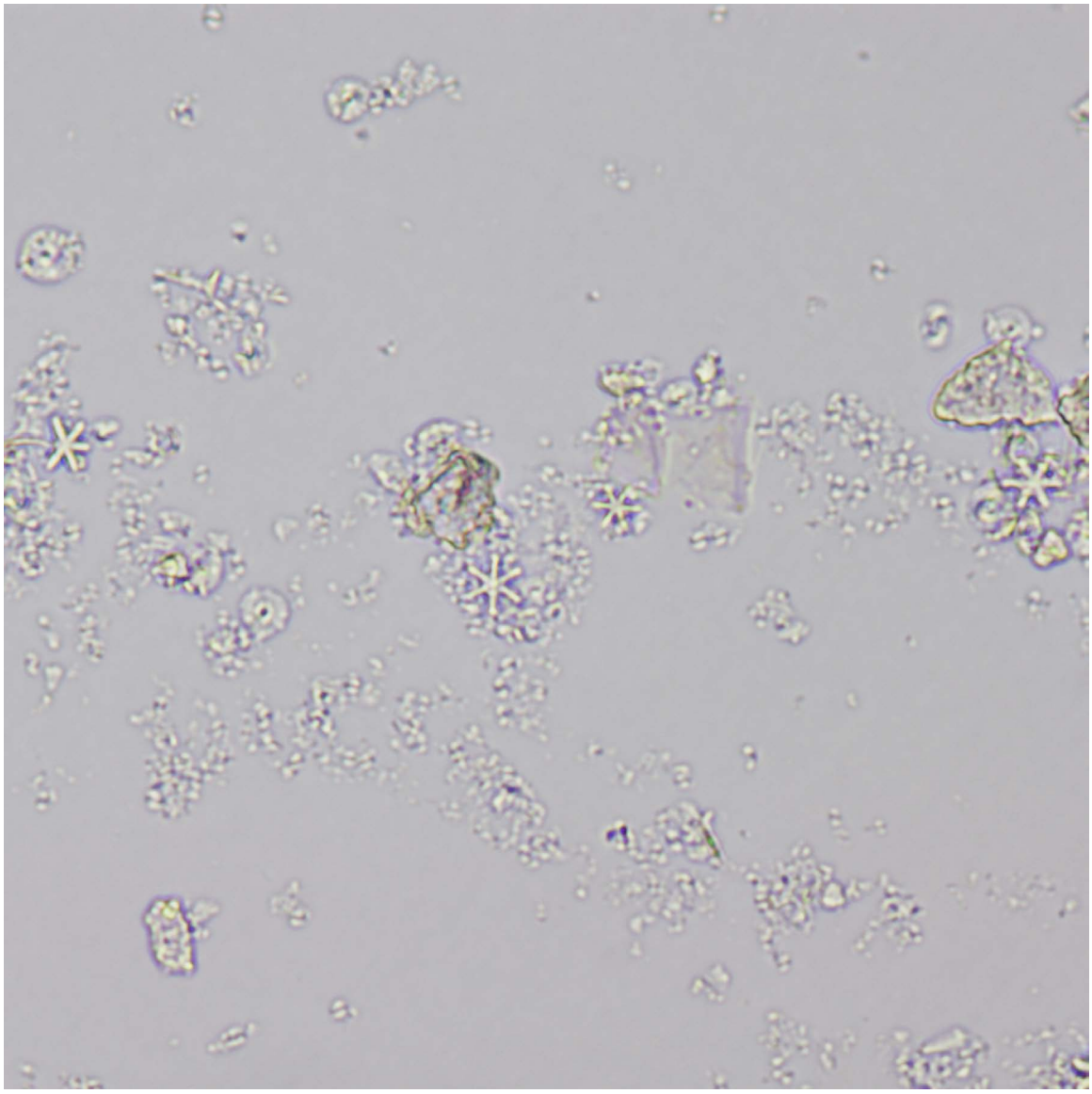

Disco 1.

A mix of coccoliths and star-shaped discoasters make up this nannofossil ooze. Note the T-shaped rhabdolith in the upper left corner (circled). Note that the discoasters are essentially nonbirefringent, whereas one carbonate fragment (bioclast?) has the highest birefringence.

ODP Sample (early Pliocene): Leg 121, Hole 752A, Core 2H, Section 5W, 20 cm

Image ID: B0377/B0378

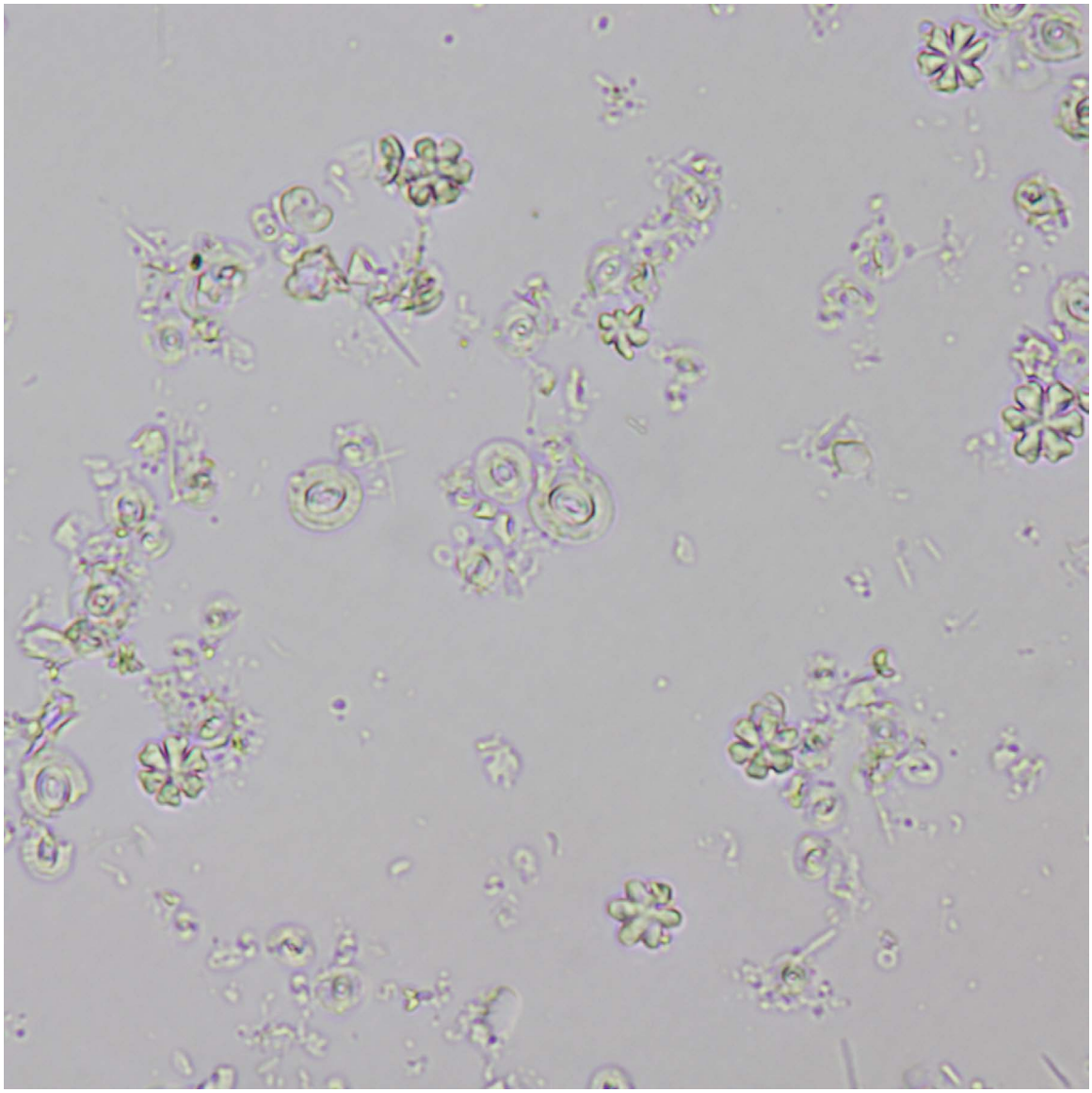

Disco 2.

This sample has a diverse assemblage of nannofossils, including coccoliths, discoasters, and sphenoliths. The latter are small spearhead-shaped, and best seen with polars crossed (circled). The rays on some discoasters show poorly developed branches. The coccoliths exhibit higher birefringence than the discoasters, which are just barely visible with polars crossed.

ODP Sample (late Oligocene): Leg 101, Hole 628A, Core 21H, Section 1, 52 cm

Image ID: B0278/B0279

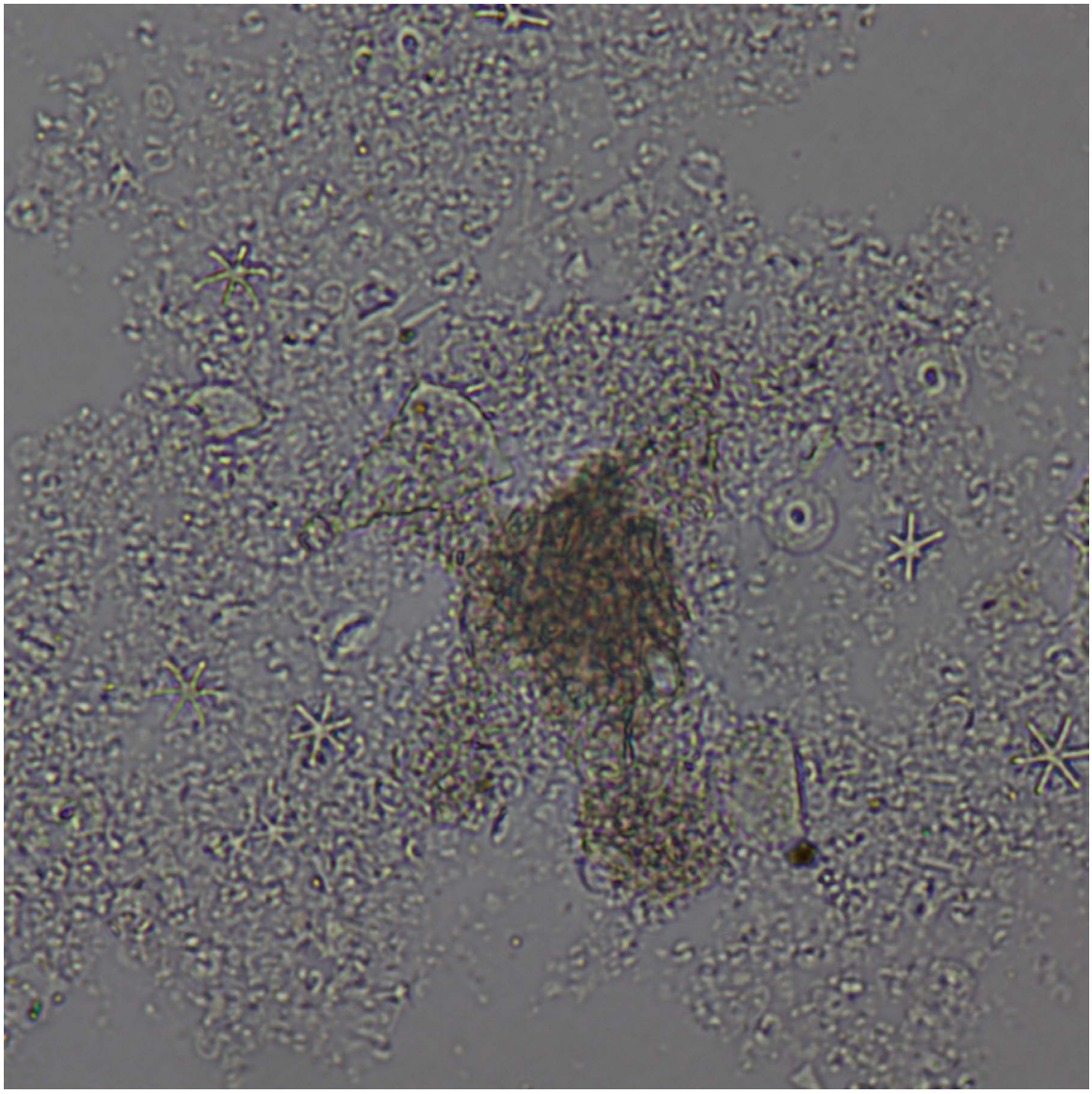

Disco 3.

Several types of coccoliths and discoasters comprise this nannofossil ooze. The variably-sized, doughnut-shaped coccoliths are dominant, and include larger, lower birefringent zoned varieties (inner and outer shields?). The discoasters are nonbirefringent, simple and star shaped, with some exhibiting “curved” rays (circled). The brownish clump in the center could be a pellet.

ODP Sample (late Pliocene): Leg 122, Hole 763A, Core 6H, Section 1W, 41 cm

Image ID: B0365/B0366

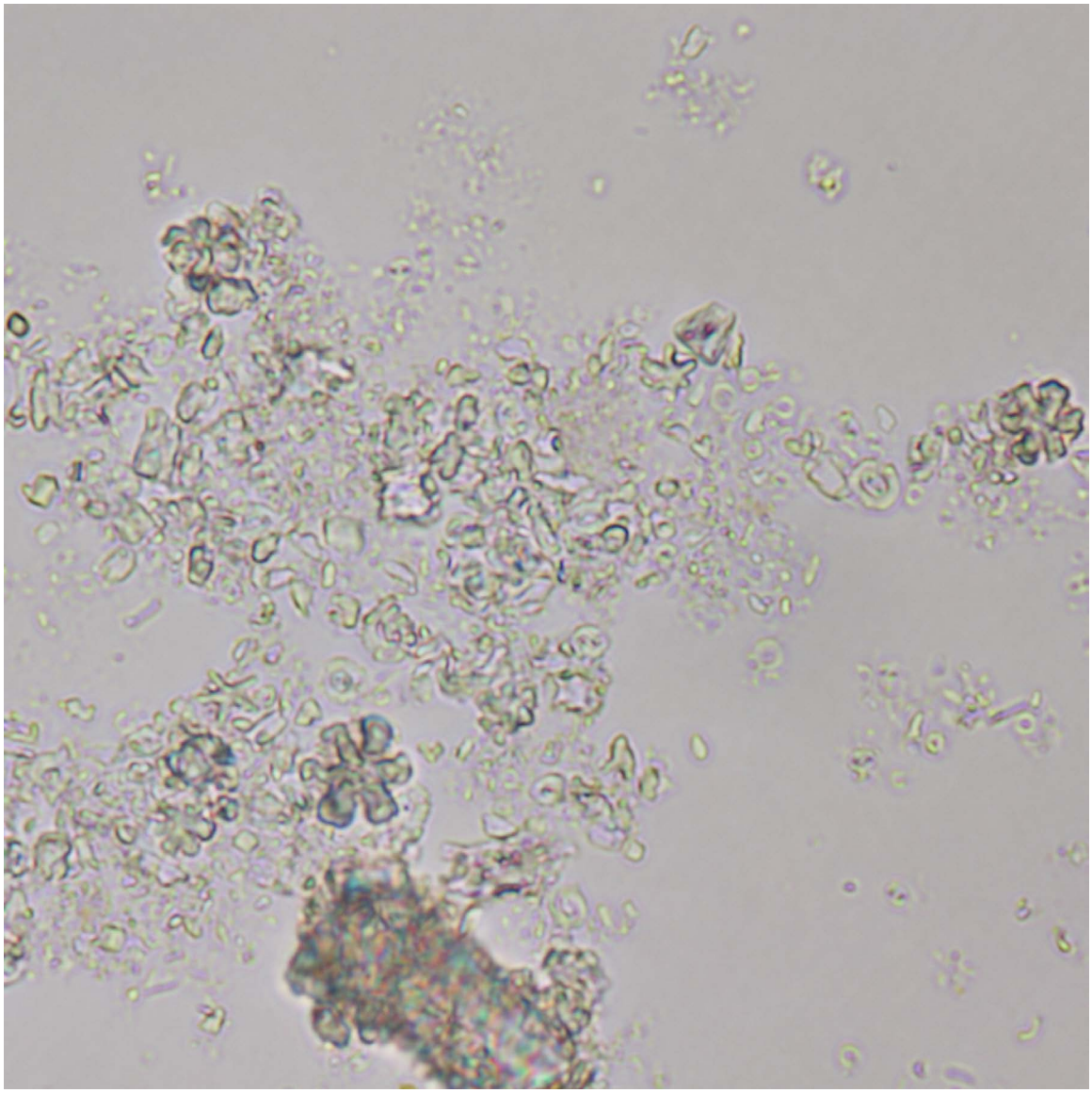

Disco 4.

The high relief and bulky, petal-like rays of the discoasters in this field of view make them stand out in plane light among the other more common components of this calcareous ooze: doughnut-shaped, low-birefringent coccoliths and micrite with higher birefringence potentially of biogenic origin. The discoaster morphology may be exagerated by calcite overgrowths. The large bioclast in the lower center may be a echinoderm fragment with uniaxial extiction.

ODP Sample (middle Miocene): Leg 101, Hole 628A, Core 15H, Section 2, 52 cm

Image ID: B0270/B271

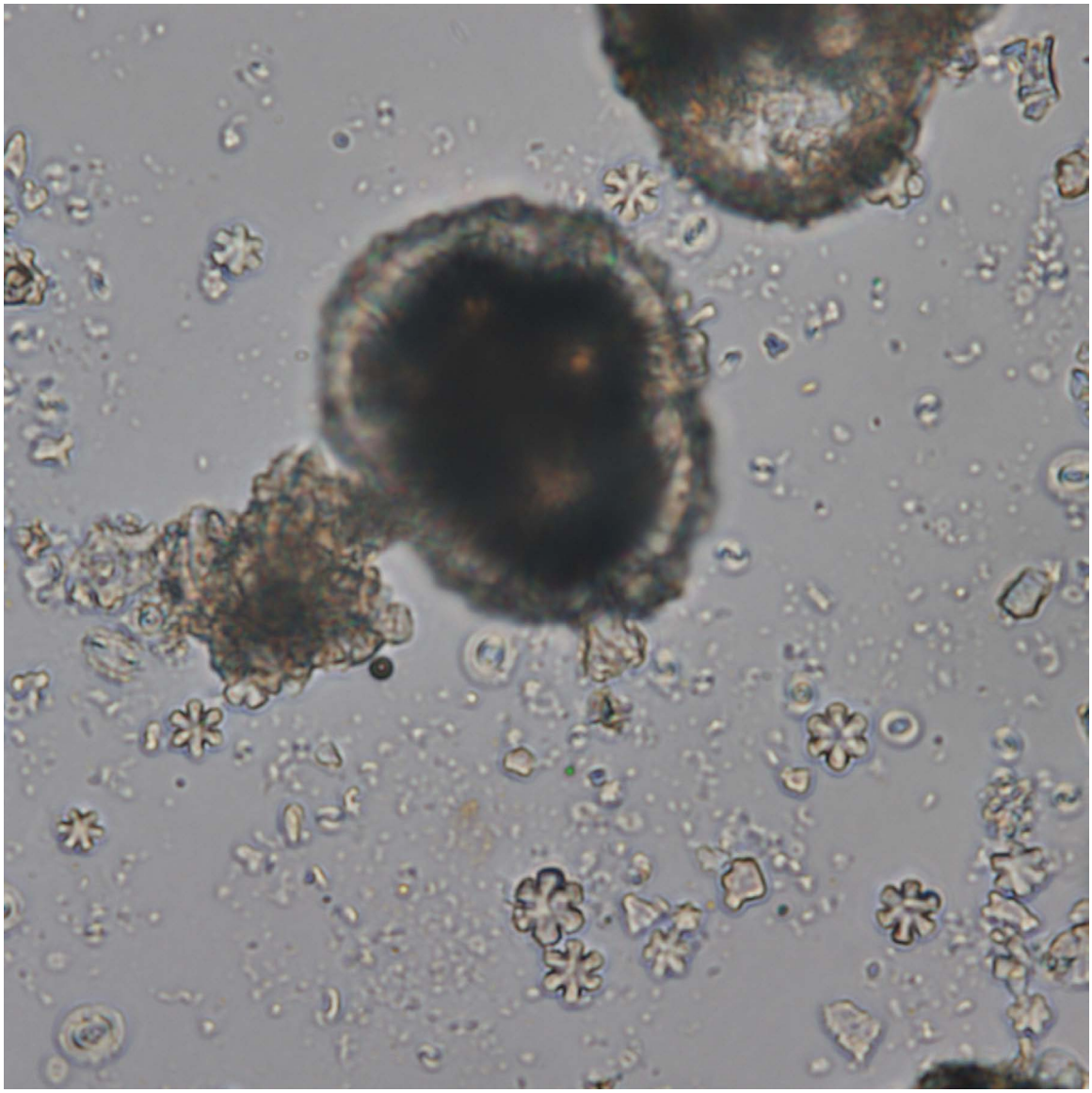

Disco 5.

Larger, darker, out-of-focus grains in this field of view are planktic foraminifera. Dispersed nannofossils include slightly birefringent star-shaped discoasters, some of which, in the lower right corner, exhibit central nodes.

ODP Sample (early Miocene): Leg 122, Hole 763A, Core 17H, Section 5W, 22 cm

Image ID: B0652/B0653

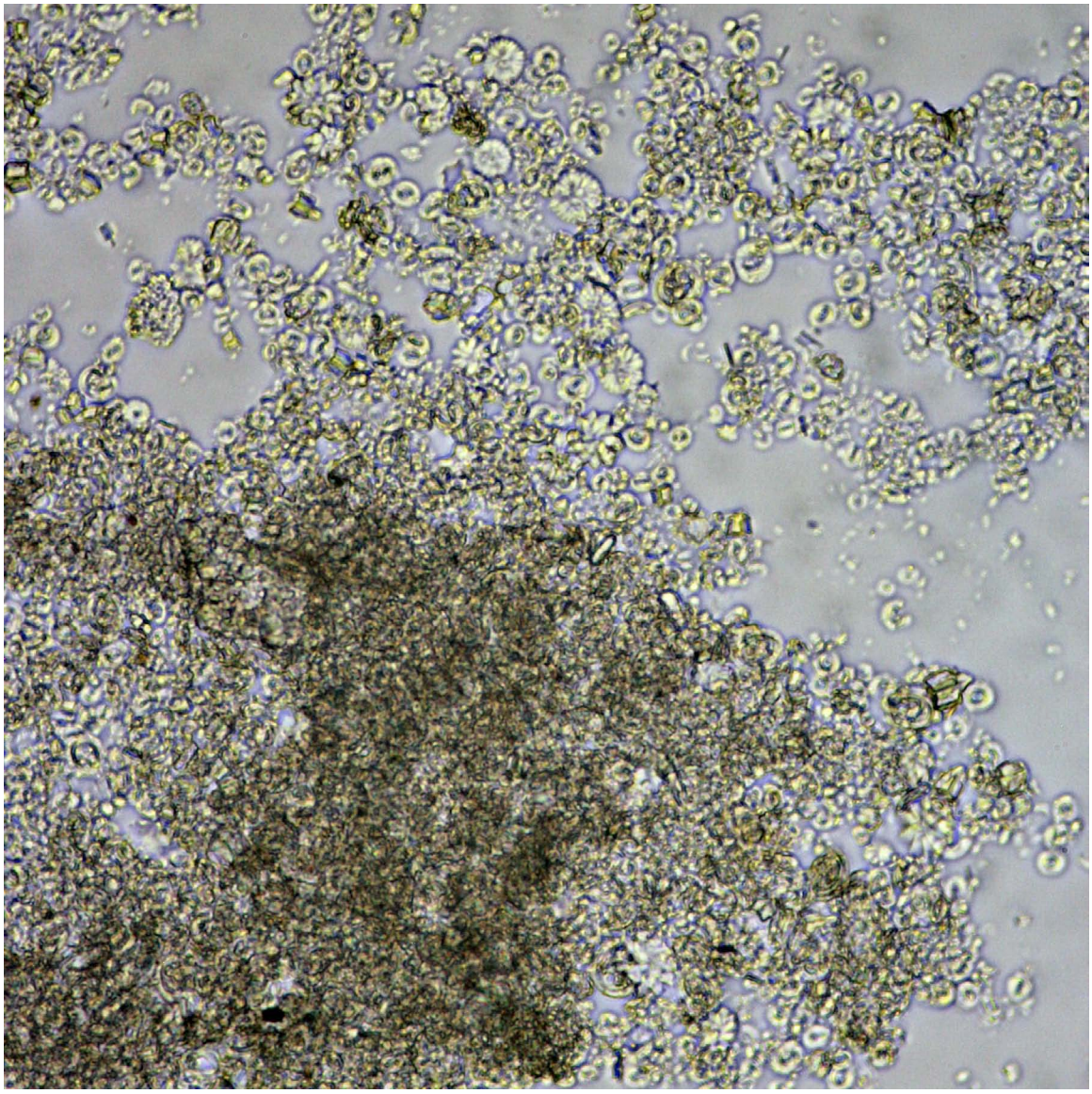

Disco 6.

This well-dispersed nannofossil ooze includes rosette discoasters (large circle) and a cylindrical *Fasciculithus* (small circle) with a fin-like ornament.

ODP Sample (late Paleocene): Leg 208, Hole 1267A, Core 23H, Section 1W, 60 cm

Image ID: B0379/B0380

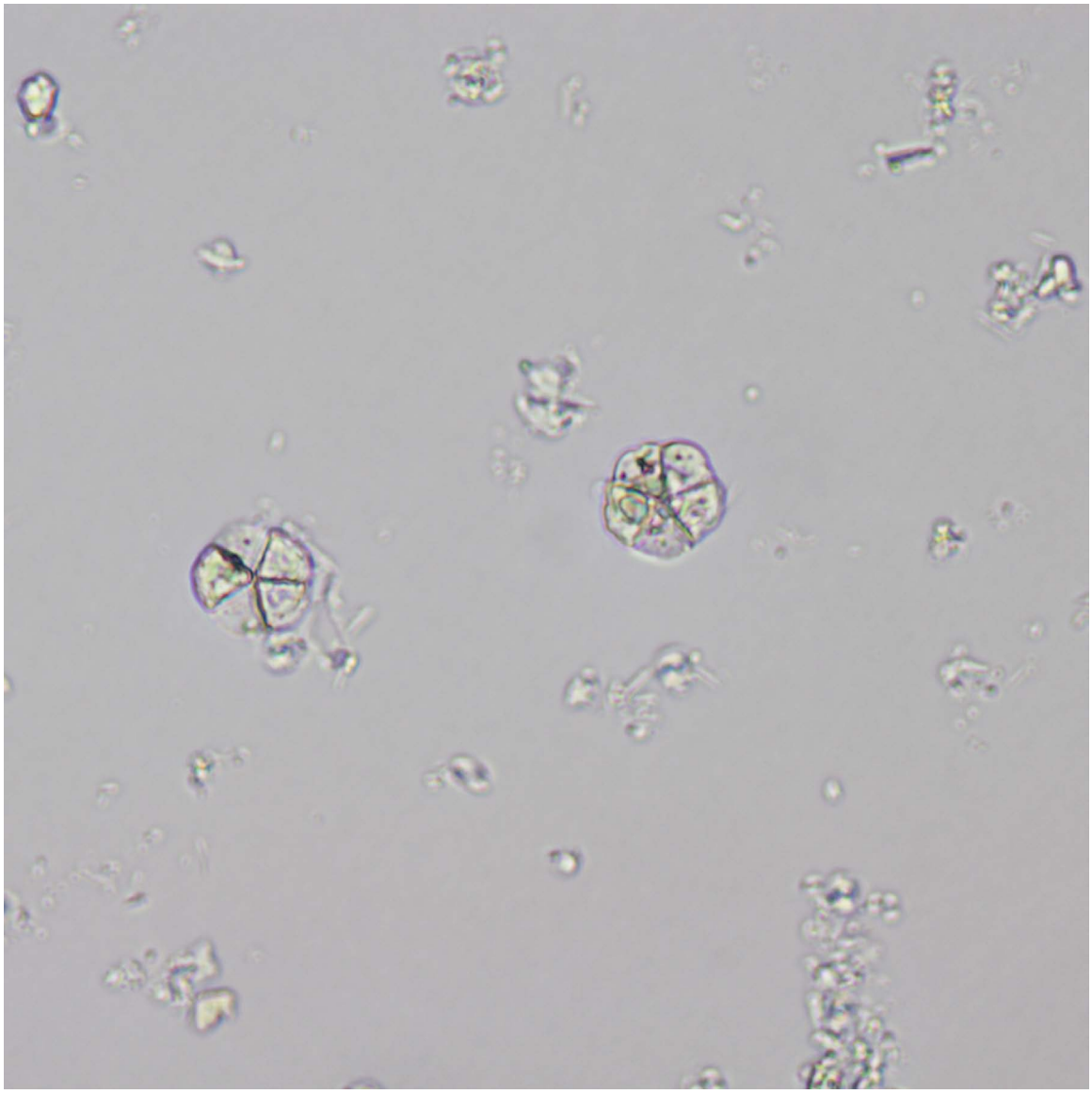

Nanno 1.

Braarudosphaerids showing their characteristic pentalith form composed of five carbonate crystal units. The pentalith on the left has three components with similar optical orientation, two of which are nearly extinct. The pentalith on the right shows variable optical orientation (different colors) under polarized light. Other components in the field of view are coccoliths.

ODP Sample (late Oligocene): Leg 101, Hole 628A, Core 21H, Section 1, 52 cm

Image ID: B0389/B0390

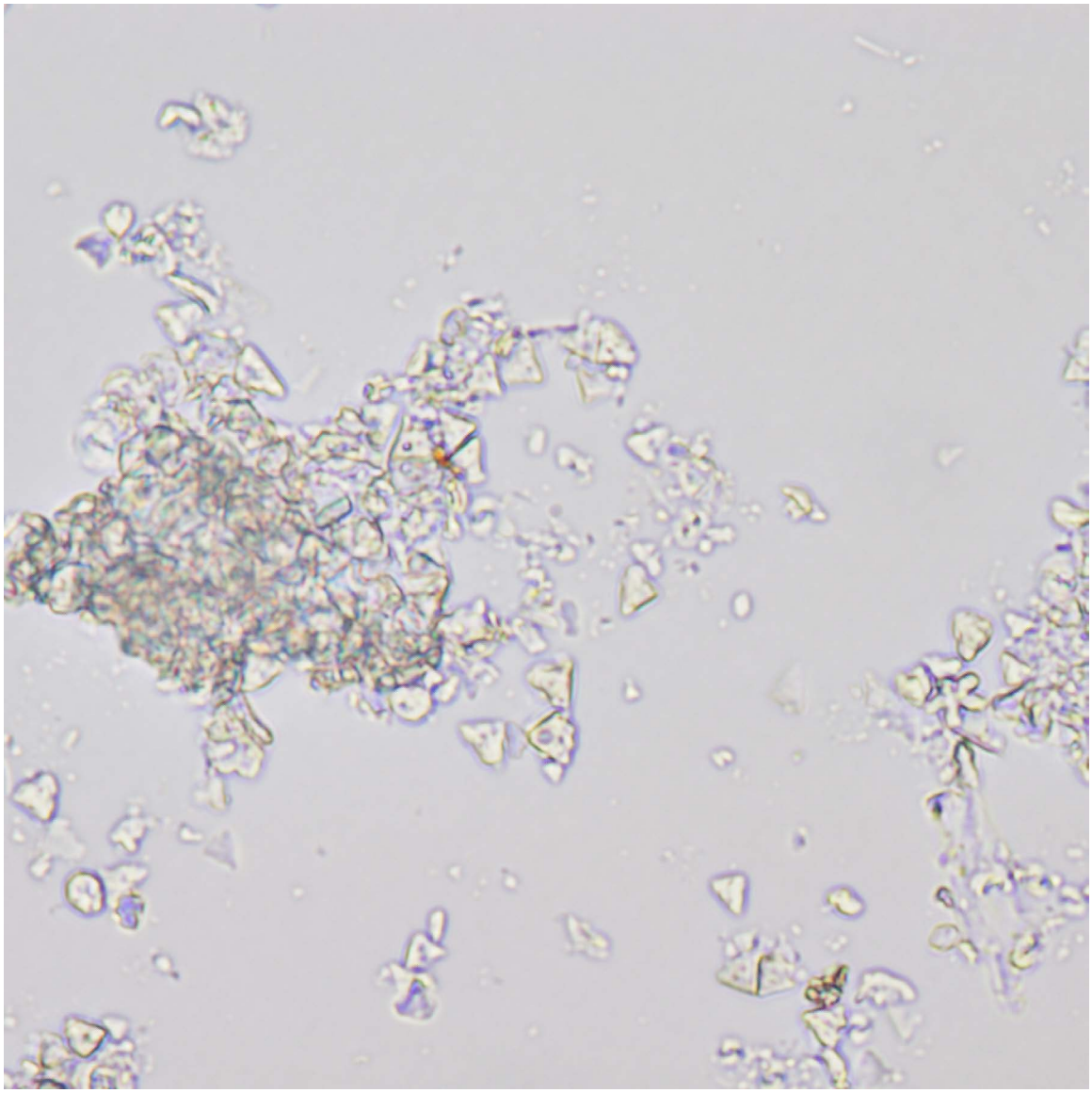

Nanno 2.

Triangular, birefringent carbonate bits in this field of view are disarticulated braarudosphaerid units. Some partially articulated units are also visible under polarized light.

ODP Sample (early Oligocene to latest Eocene): Leg 101, Hole 628A, Core 29X, Section 1, 52cm

Image ID: B0395/B0396

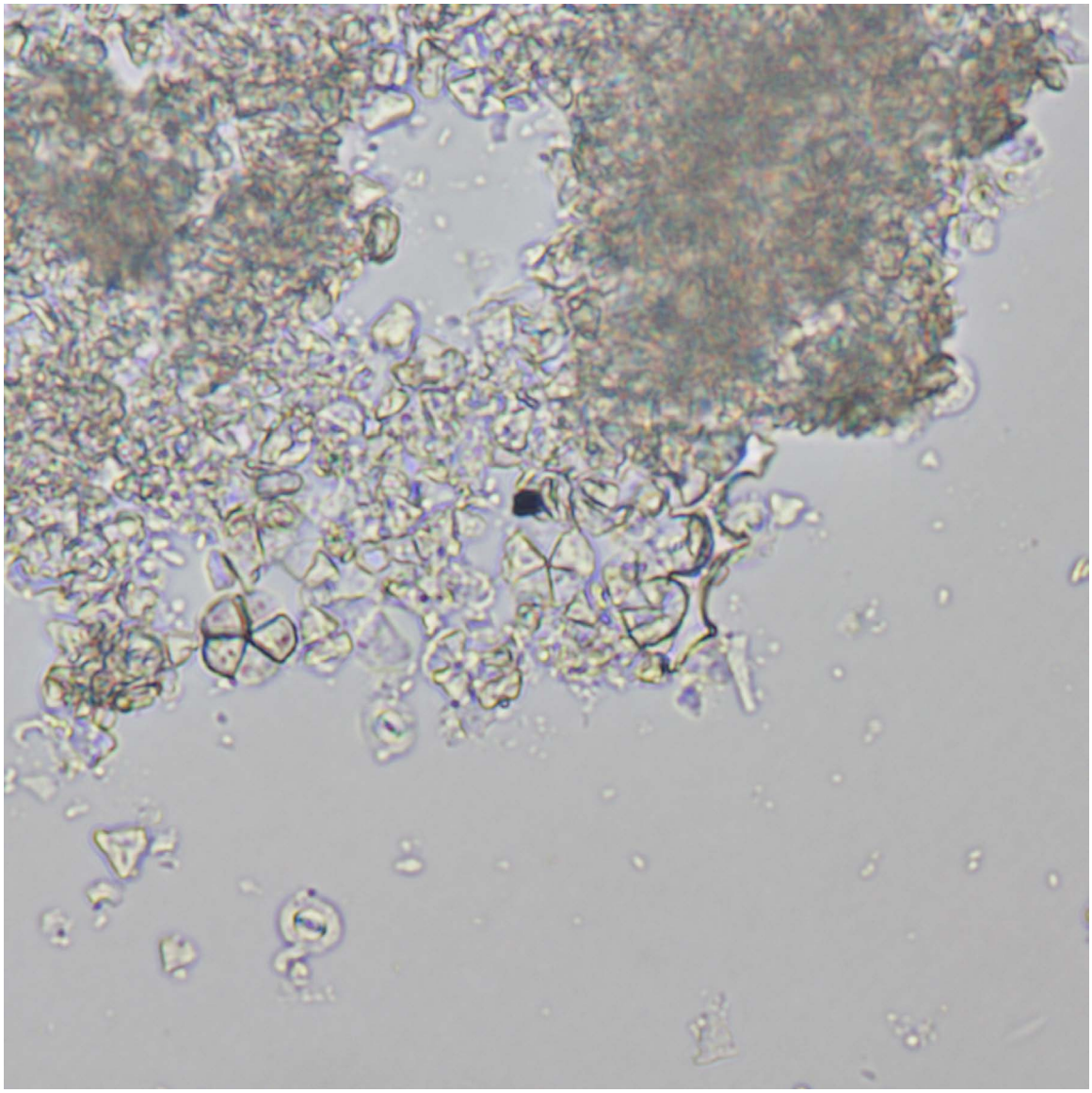

Nanno 3.

Calcareous ooze that is a mixture of coccoliths and braarudosphaerids, with some of the latter being distinctly intact and others fragmented (triangular shaped bits). Note that the higher birefringence of the braarudosphaerids vs. the coccoliths implies that the darker clumps of ooze/chalk are mixtures of both components. There is one siliceous microfossil fragment (isotropic) at the right edge of the clump.

ODP Sample (early Oligocene to latest Eocene): Leg 101, Hole 628A, Core 29X, Section 1, 52 cm

Image ID: B0254/B0255

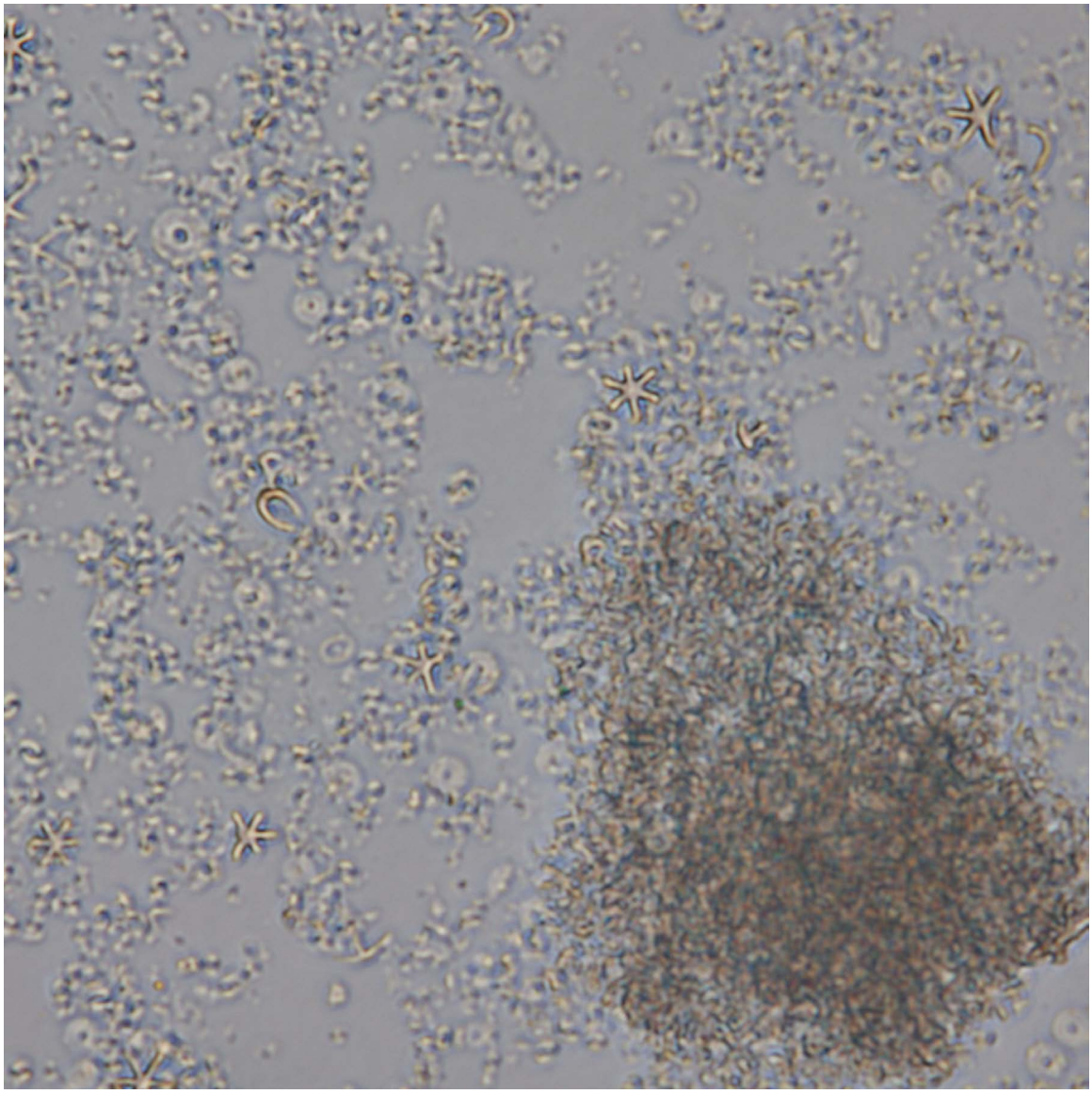

Nanno 4.

Several types of coccoliths and discoasters comprise this nannofossil ooze. For the most part, they are evenly spread across the slide except in the lower right corner where they are clumped in a darker tan mass, potentially a pellet that was less easily disaggregated during slide preparation. The discoasters are simple star shaped and the few ceratoliths are U-shaped (circled). Coccoliths are dominant, and appear to include lower birefringent, zoned varieties (inner and outer shields?).

ODP Sample (Miocene): Leg 208, Hole 1267A, Core 9H, Section 2W, 50 cm

Image ID: B0237/B0238

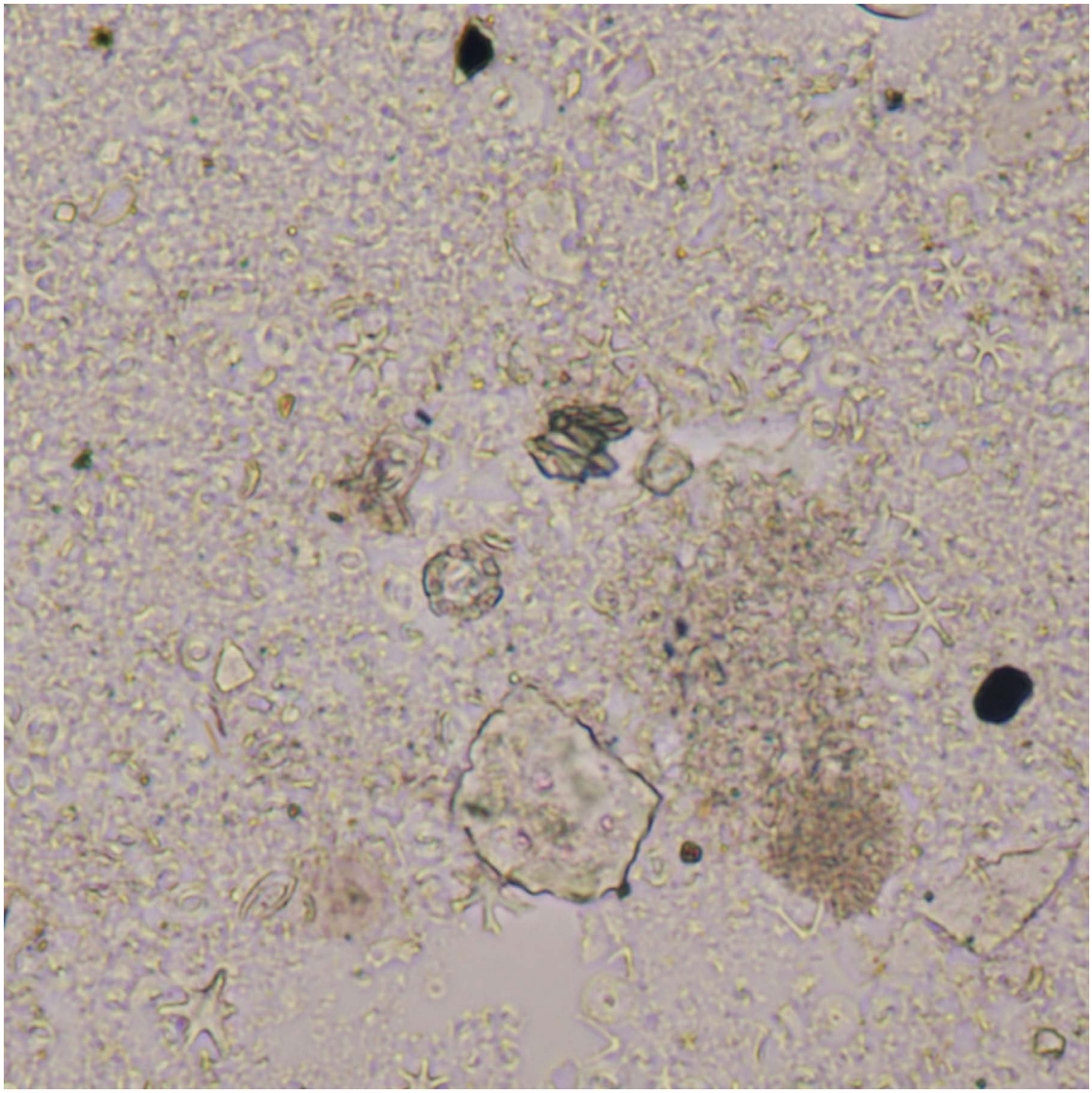

Nanno 5.

The nannofossils in this slide are densely packed, making it hard to differentiate nannofossil types and to estimate the percentage of terrigenous components, except where obvious, like the greenish, irregular shaped amphibole(?) grain in the center. Note the dramatically birefringent, oblique, U-shaped ceratolith in the lower left corner and the larger coccolith in the center of the field of view, the outer rim of which has higher relief and higher birefringence, suggesting diagenetic overgrowth by carbonate. Other components include platy fragments of foraminifera and discoasters.

ODP Sample (early Pliocene): Leg 157, Hole 950A, Core 20X, Section 4W, 23 cm

Image ID: B0235/B0236

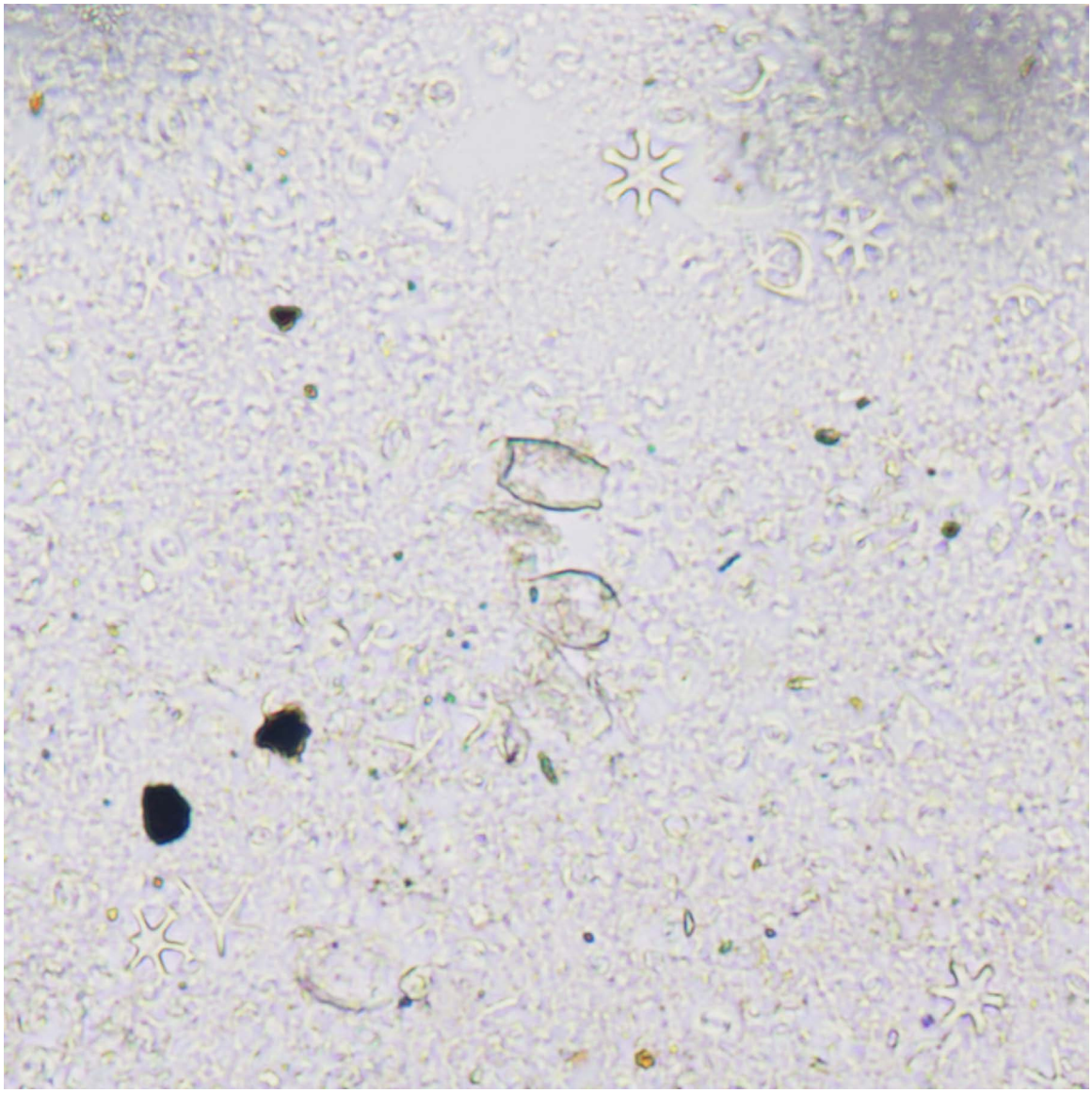

Nanno 6.

Closely-packed, circular coccoliths dominate the nannofossil ooze shown here. A few vase-shaped microfossils with higher birefringence (Scyphosphaera) are visible in the center, as well as several essentially nonbirefringent discoasters. Note that the one star-like discoaster in the upper right has rays that branch at the tips and is adjacent to a ceratolith. There are some dispersed opaque minerals.

ODP Sample (early Pliocene): Leg 157, Hole 950A, Core 20X, Section 4W, 23 cm

Image ID: B0762/B0763

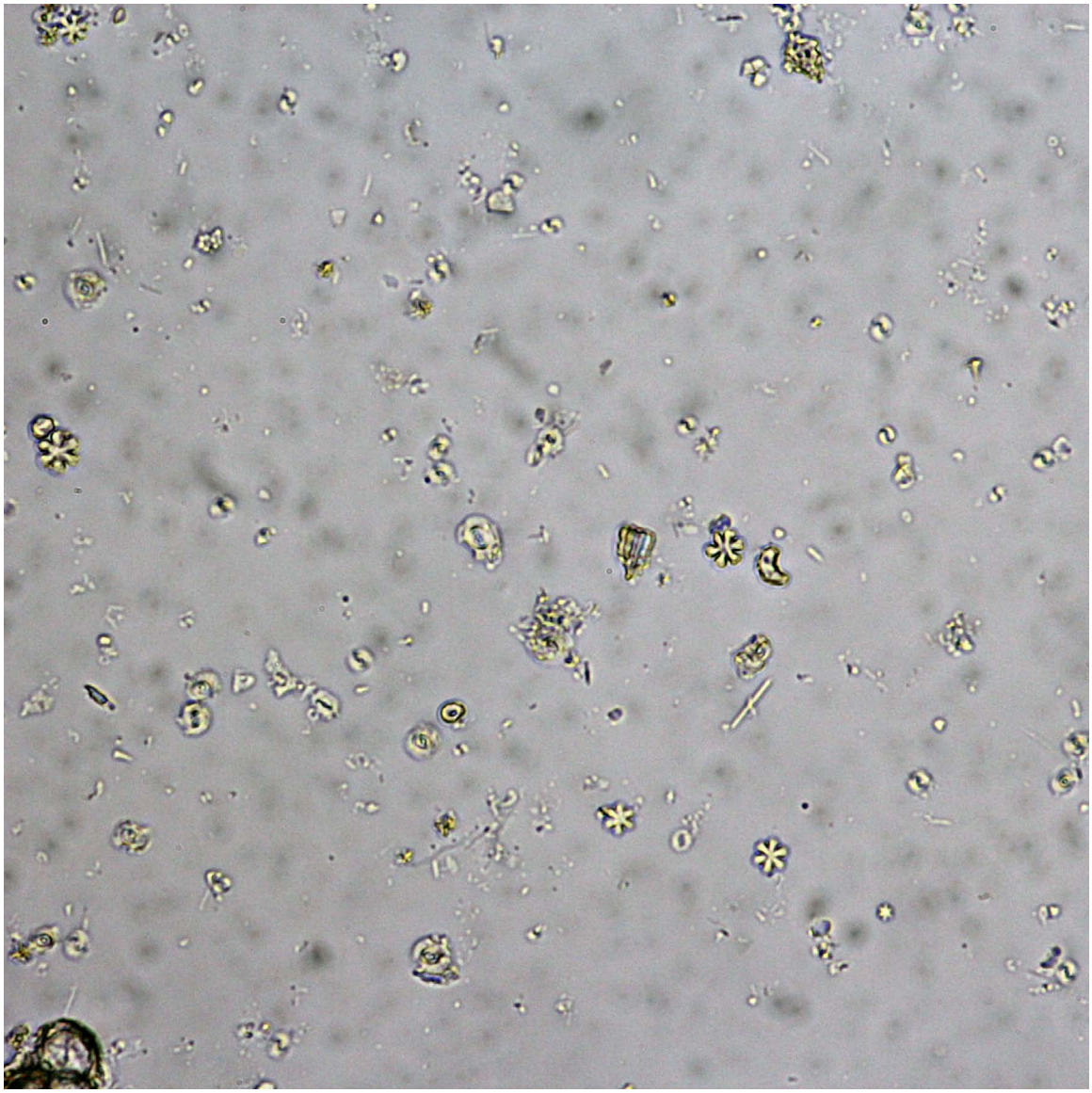

Nanno 7.

This nannofossil ooze contains a variety of nannoliths, discoasters, coccoliths and an excellent example of a sphenolith in the center of the field of view.

ODP Sample (late Oligocene): Leg 101, Hole 628A, Core 21H, Section , 52 cm

Image ID: B0629/B0630

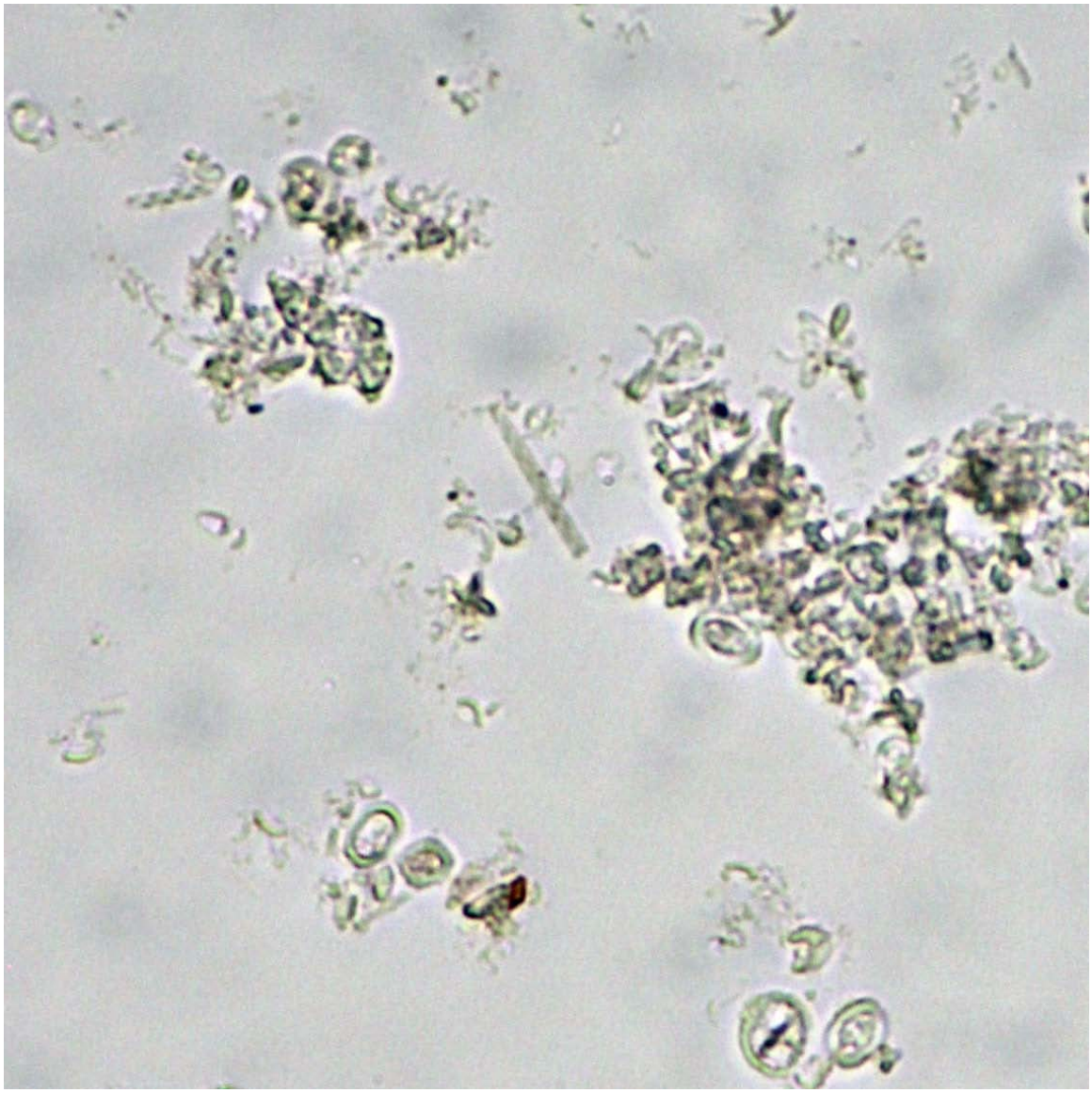

Nanno 8.

The thin rod in the upper center of the field of view exhibits a checkerboard pattern with polars crossed that indicates it is a *Microrhabdulus* nannofossil.

ODP Sample (Late Cretaceous): Leg 208, Hole 1267A, Core 33X, Section 1, 30 cm

Image ID: B0654/B0655

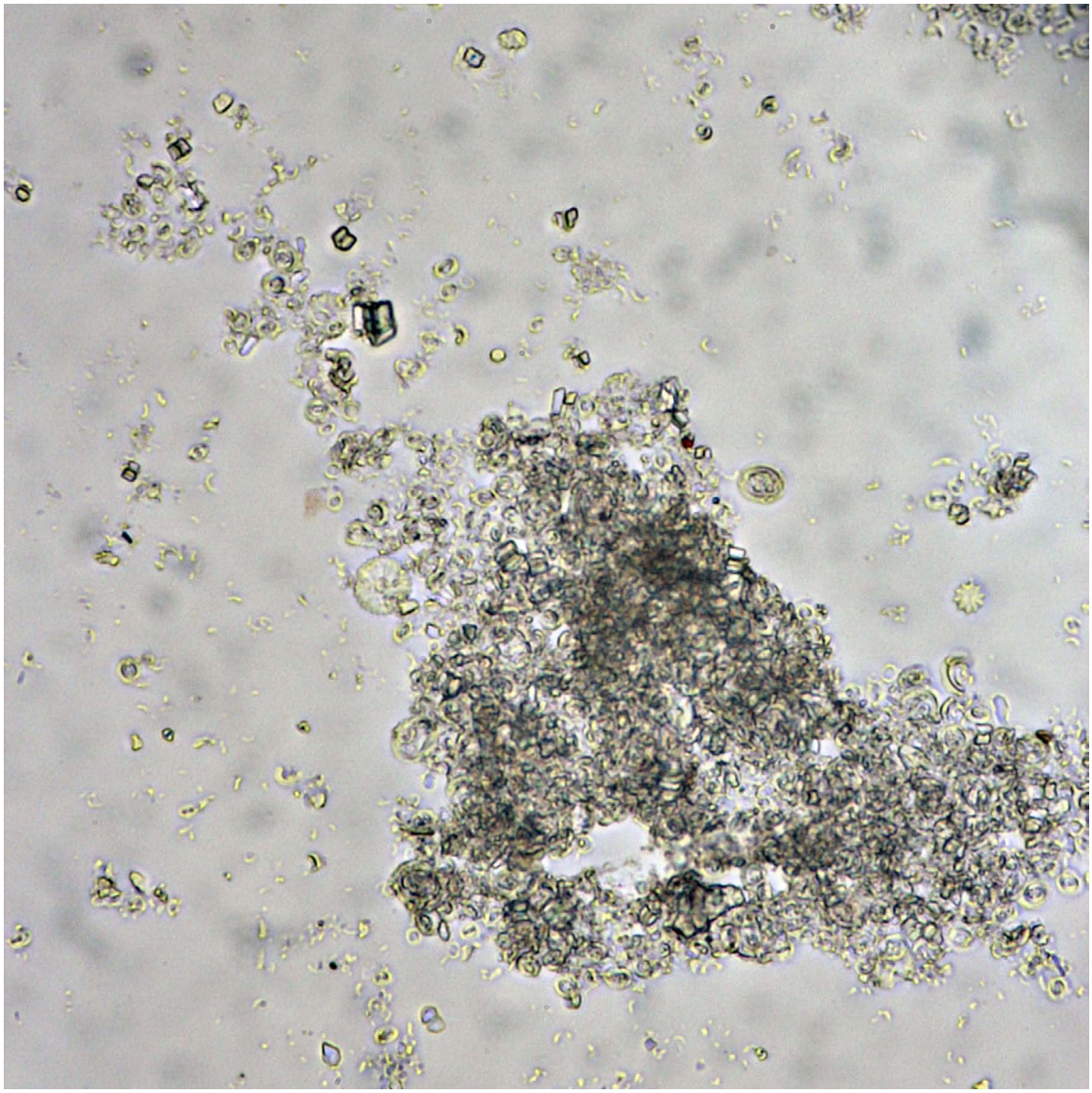

Nanno 9.

This nannofossil ooze includes *Fasciculithus* which is cylindrical in some views. They show a range of sizes and are best identified by their higher relief.

ODP Sample (late Paleocene): Leg 208, Hole 1267A, Core 23H, Section 1W, 60 cm

Image ID: B0760/B0761

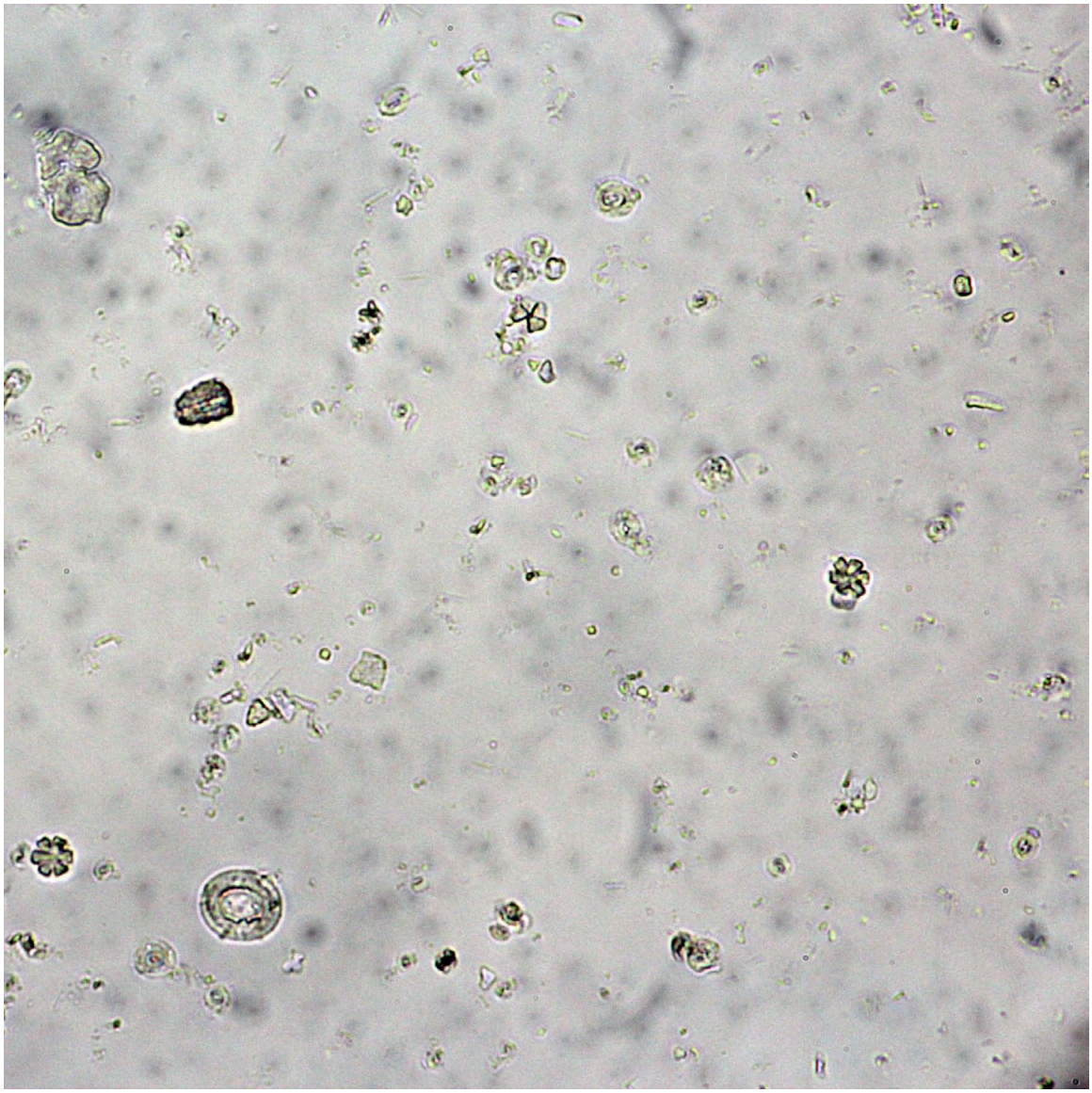

Nanno 10.

This nannofossil ooze contains a variety of nannoliths, discoasters, coccoliths and an in the upper center of the field of view a *Braarudosphaera* (pentalith), and a specimen on its side to the left (high relief grain).

ODP Sample (late Oligocene): Leg 101, Hole 628A, Core 21H, Section 1W, 52 cm

Foraminifera

INTRODUCTION TO Foraminifera

Overview – Foraminifera are single-celled testate protists. They have a long geologic record that extends back at least to the Cambrian Period (>500 Ma). “Forams” are silt and sand-size microfossils (~20 to >1000 µm, or ~0.020 to >1.0 mm), which have a shell (**test**) composed of calcium carbonate or agglutinated particles. There are a diverse number of species, modern and ancient, that are larger than 1 mm and are typical of tropical reef environments. There are forms that live in the plankton and passively drift with ocean currents (**planktic foraminifera**), and there are forms that live on or within the top 10 cm of the sediment (**benthic foraminifera**). Most species have tests composed of multiple chambers that increase in size during growth. There are ~50 living planktic species and many thousands of extant benthic species. Forams are ubiquitous in marine and marginal marine environments; they range from the tropics to the polar seas, from the surface ocean to the deepest seafloor, to salt marshes and estuaries. Together with the remains of other mineralized plankton such as coccolithophorids and other calcareous nannofossils, diatoms, radiolarians, and pteropods, foram tests comprise the calcareous sediment (calcareous ooze) that covers vast areas of the seafloor beyond the continental margins and above the calcite compensation depth (CCD) in the deep sea.

Biology – Kingdom Protoctista, Subkingdom Amoebamorpha, Phylum Granuloreticulosa, Order Foraminiferida. Foraminifera are testate amoeboid cells that have granuloreticulate pseudopodia; thin, branching strands of cytoplasm that are used to collect organic matter, snare prey, deploy photosymbionts, remove wastes, and provide mobility by way of bidirectional streaming. The primary aperture (foramen) acts as the principle access portal for the cytoplasm. **Symbioses** are common in both planktic and benthic forams, including phototrophic algae in near-surface dwelling planktic species and in larger reef-dwelling benthic species, as well as chemoautotrophic bacteria in some low oxygen dwelling benthics.

Planktic Foraminifera

Overview – Planktic foraminifera live at various depths in the upper water column from the surface mixed layer down through the thermocline, with the greatest concentration of species and individuals in the upper 100-150 m. Highest diversity is in subtropical to temperate waters.

Diagnostic Features – Planktic forams have silt and sand size tests ranging in size from ~20 µm (juveniles) to >1000 µm (>1 mm). Pores range in diameter from <1 micron to >2.5 µm, although they may be enlarged by dissolution or narrowed by secondary calcification. Shell texture varies as a function of pore size and surface ornament. Planktic foraminifera have a wide variety of shapes and chamber arrangement from trochospiral and planispiral coiling, to elongate biserial and triserial chamber arrangements. In smear slides, small juveniles and broken chamber fragments of adults

are likely to be observed. The planktic foram test differs from a radiolarian skeleton in being calcareous, rather than siliceous, and in having true circular pores through the test wall, rather than a skeleton consisting of a structural framework.

Biology – Planktic forams reproduce sexually. Cenozoic planktic foraminifera have spinose and non-spinose forms (no spinose forms are known from the Mesozoic). Most spinose forms host photosymbionts, typically dinoflagellates or chrysophyte algae.

Ecology – Heterotrophs. Modern spinose species are generally carnivorous, feeding on metazoans such as copepod, pteropods, and planktic ostracodes. Non-spinose species are primarily herbivorous grazers or detritus feeders, feeding on phytoplankton such as diatoms and dinoflagellates, as well as bacteria, and particulate organic matter (marine snow).

Paleobiogeography – They occur throughout the world ocean but are most diverse in the low to mid-latitudes.

Stratigraphic Range – Late Early Jurassic (Toarcian) to Present.

Key References and Examples:

Bé, A.W.H., 1977. An ecological, zoogeographic and taxonomic review of Recent planktonic foraminifera. In Ramsey, A.T.S. (Ed.), Oceanic Micropaleontology, 1: 1-100.

Bolli, H.M., and Saunders, J.B., 1985. 6: Oligocene to Holocene low latitude planktic foraminifera. In Bolli, H.M., Saunders, J.B., and Perch-Nielsen, K. (Eds.), Plankton Stratigraphy: Cambridge (Cambridge Univ. Press), 155– 262.

Caron, M., 1985. 4: Cretaceous planktic foraminifera. In Bolli, H.M., Saunders, J.B., and Perch Nielsen, K. (Eds.), Plankton Stratigraphy: Cambridge (Cambridge Univ. Press), 17– 86.

Chaisson, W.P., and Leckie, R.M., 1993. High-resolution Neogene planktonic foraminifer biostratigraphy of Site 806, Ontong Java Plateau (western equatorial Pacific). In, Berger, W.H., Kroenke, L.W., Mayer, L.A., et al., Proceedings of the ODP, Scientific Results, 130:137-178.

Hemleben, C., Spindler, M., and Anderson, O.R., 1989. Modern Planktonic Foraminifera. Springer (New York), 363 p.

Iaccarino, S., 1985. 8: Mediterranean Miocene and Pliocene planktic foraminifera. In Bolli, H.M., Saunders, J.B., and Perch Nielsen, K. (Eds.), Plankton Stratigraphy: Cambridge (Cambridge Univ. Press), 283-314.

Jenkins, D.G., 1985. 7: Southern mid-latitude Paleocene to Holocene planktic foraminifera. In Bolli, H.M., Saunders, J.B., and Perch Nielsen, K. (Eds.), Plankton Stratigraphy: Cambridge (Cambridge Univ. Press), 263-282.

Kennett, J.P., and Srinivasan, M.S., 1983. Neogene Planktonic Foraminifera: A Phylogenetic Atlas: Stroudsberg, PA (Hutchinson Ross).

Kucera, M., 2007. Planktonic foraminifera as tracers of past oceanic environments. In Developments in Marine Geology: Elsevier, 213-262.

Leckie, R.M., Farnham, C., and Schmidt, M.G., 1993. Oligocene planktonic foraminifer biostratigraphy of Hole 803D (Ontong Java Plateau) and Hole 628A (Little Bahama Bank), and comparison with the southern high latitudes. In, Berger, W.H., Kroenke, L.W., Mayer, L.A., et al., Proceedings of the ODP,

Scientific Results, 130:113-136.
Olsson, R.K., Hemleben, C., Berggren, W.A., and Huber, B.T. (Eds.), 1999. Atlas of Paleocene Planktonic Foraminifera. Smithsonian Contrib. Paleobiol., 85.
Postuma, J.A., 1971. Manual of Planktonic Foraminifera: Amsterdam (Elsevier).
Robaszynski, F., Caron, M. (Coord.), and the European Working Group on Planktonic Foraminifera, 1979. Atlas de Foraminifères Planctoniques du Crétacé Moyen (Vols. 1 and 2). Cah. Micropaleontol.
Robaszynski, F., Caron, M., Gonzalez-Donoso, J.-M., Wonders, A.A.H., and the European Working Group on Planktonic Foraminifera, 1984. Atlas of Late Cretaceous Globotruncanids. Rev. Micropaleontol., 26:145– 305.
Schiebel, R., and Hemleben, C., 2005. Extant planktic foraminifera: A brief review. Paläontologische Zeitschrift, 79(1): 135-148.
Toumarkine, M., and Luterbacher, H., 1985. 5: Paleocene and Eocene planktic foraminifera. In Bolli, H.M., Saunders, J.B., and Perch-Nielsen, K. (Eds.), Plankton Stratigraphy: Cambridge (Cambridge Univ. Press), 87– 154.

Smaller Benthic Foraminifera

Overview – 'Smaller' benthic foraminifera is a general term for those species smaller than ~2 mm. So-called 'larger' foraminifera are typical of shallow, tropical-subtropical carbonate-dominated environments of reefs and carbonate platforms where warm water and algal symbioses foster rapid growth and large-size in the benthic forams. Smaller benthic forams occur in all marginal marine to open marine environments.

Diagnostic Features – Benthic forams display a wider range of variability in wall structure and composition than the planktics, ranging from agglutinated, hyaline (glassy) calcite, porcellaneous calcite, to aragonite and opaline silica. Most hyaline benthics are composed of low Mg-calcite; the principle exception are the porcellanous miliolids, which are composed of high-Mg calcite. The chamber number, shape and arrangement, aperture style, and test ornament are highly variable accounting for the much higher diversity of benthic forams compared with planktics. For example, chamber arrangement and coiling includes a single chamber, uniserial, biserial, and triserial arrangements to trochospiral, planispiral, milioline, and streptospiral coiling, as well as various combinations of coiling such as planispiral to biserial, and triserial to uniserial.

Biology – Benthic foraminifera have an alteration of generations, between a haploid megalospheric generation and a diploid microspheric generation. Forams have a variety of feeding strategies including predation, suspension feeding, and detritus feeding.

Ecology – Benthic foraminifera from salt marshes to the deep-sea are stratified from the sediment-water interface (epifaunal species) to within the upper 10 cm of sediments (infaunal species).

Paleobiogeography – Benthic forams are found in all marginal marine to marine environments, from salt marshes and estuaries to all depths of the world ocean. Below the calcite compensation depth, the assemblages are dominated by agglutinated taxa.

Stratigraphic Range – Cambrian to present.

Key References and Examples:

Boersma, A., 1978. 2: Foraminifera. In Haq, B.U., and Boersma, A. (Eds.), Introduction to Marine Micropaleontology: Elsevier, 19-77.

Boersma, A., 1990. Late Oligocene to late Pliocene benthic foraminifera from depth traverses in the central Indian Ocean. In., Duncan, R.A., Backman, J., Peterson, L.C., et al., Proceedings of the ODP, Scientific Results, 115:315-379.

Culver, S.J., 1993. 12: Foraminifera. In Lipps, J.H. (Ed.), Fossil Prokaryotes and Protists: Blackwell Scientific Publications, 203-247.

Dailey, D.H., 1983. Late Cretaceous and Paleocene benthic foraminifera from DSDP Site 516, Rio Grande Rise, western South Atlantic. In., Carlson, P.F., Johnson, D.A., et al., Initial Reports DSDP, 72:757-782.

Douglas, R.G., and Woodruff, F., 1981. Deep-sea benthic foraminifera. In Emiliani, C. (Ed.), The Sea, The Oceanic Lithosphere. Wiley-Interscience, 1233-1327.

Gooday, A.J., 2003. Benthic foraminifera (Protista) as tools in deep-water palaeoceanography: Environmental influences on faunal characteristics. Advances in Marine Biology, 46: 1-90.

Jorissen, F.J., Fontanier, C., and Thomas, E., 2007. Paleoceanographical proxies based on deep-sea benthic foraminiferal assemblage characteristics. In Developments in Marine Geology: Elsevier, 263-325.

Leckie, R.M., and Olson, H., 2003. Foraminifera as proxies of sea-level change on silici clastic margins. In Olson, H.C., and Leckie, R.M. (Eds.), Micropaleontologic Proxies of Sea-Level Change and Stratigraphic Discontinuities: Tulsa, SEPM (Society of Sedimentary Geology), Special Publication 75: 5-19.

Murray, J.W., 2006. Ecology and Applications of Benthic Foraminifera. Cambridge Univ. Press, 426 p.

Sen Gupta, B.K. (Ed.), 2003. Modern Foraminifera. Dordrecht, Kluwer Academic Publ., 371 p. – Contains many excellent papers on both benthic and planktic forams.

Thomas, E., 2007. Cenozoic mass extinctions in the deep sea: What perturbs the largest habitat on Earth? In Monechi, S., Coccioni, R., and Rampino, M.R. (Eds.), Large Ecosystem Perturbations: Causes and Consequences. GSA Special Paper, 424: 1-23.

Tjalsma, R.C., and Lohmann, G.P., 1983. Paleocene–Eocene bathyal and abyssal benthic foraminifera from the Atlantic Ocean. Micropaleontol. Spec. Publ., 4.

Van Morkhoven, F.P.C.M., Berggren, W.A., and Edwards, A.S., 1986. Cenozoic cosmopolitan deep-water benthic foraminifera. Bull. Cent. Rech. Explor.—Prod. Elf-Aquitaine, 11.

Web Resources:

http://www.ucl.ac.uk/GeolSci/micropal/foram.html
http://www.ucmp.berkeley.edu/fosrec/Wetmore.html
http://www.geo.umass.edu/faculty/leckie/Utility%20of%20forams_Leckie.pdf
CHRONOS Portal with access to the taxonomic databases for Mesozoic, Paleocene, and Eocene planktic forams – http://portal.chronos.org/gridsphere/gridsphere?cid=resources
http://ethomas.web.wesleyan.edu/BFhandout.htm

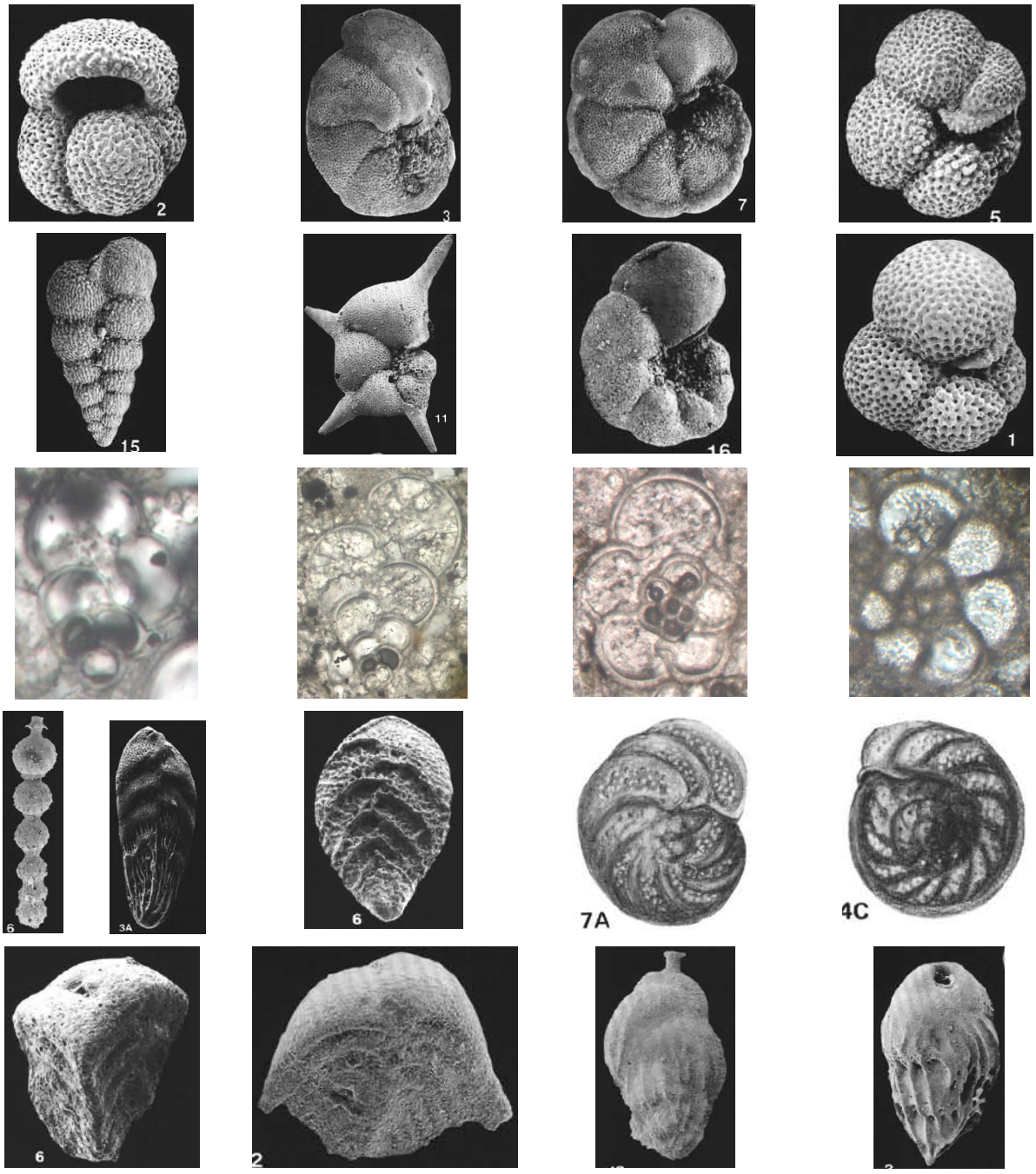

Representative Cretaceous and Cenozoic planktic foraminifera (top three rows) and benthic forams (bottom two rows). Top row: *Globigerinoides obliquus* (trochospiral), *Globorotalia fohsi* (trochospiral, keeled), *Globorotalia menardii* (trochospiral, keeled), Neogloboquadrina acostaensis (trochospiral). Second row: *Chiloguembelina cubensis* (biserial), *Hantkenina alabamensis* (planispiral), *Pseudohastigerina micra* (planispiral), *Paragloborotalia nana* (trochospiral). Third row: *Guembelitria cretacea* (triserial), *Heterohelix globulosa* (biserial), *Muricohedbergella delrioensis* (trochospiral), *Muricohedbergella planispira* (trochospiral). Fourth row: *Stilostomella lepidula* (uniserial), *Bolivina tectiformis* (biserial), *Aragonia velascoensis* (biserial), *Planulina renzi* (trochospiral), *Cibicidoides ungerianus* (trochospiral). Bottom row: *Gaudryina pyramidata* (triserial, agglutinated), *Vulvulina spinosa* (biserial, agglutinated), *Uvigerina schwageri* (triserial), *Bulimina alazanensis* (triserial). SEM photomicrographs from Boersma, 1990; Chaisson and Leckie, 1993; Dailey, 1983; Leckie et al., 1993. Thin section photomicrographs from R.M. Leckie, unpublished, ODP Site 1276. Line drawings from Tjalsma, 1983.

Foraminifera


Foram 1


Foram 2


Foram 3

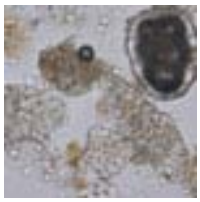
Foram 4


Foram 5


Foram 6


Foram 7


Foram 8


Foram 9


Foram 10


Foram 11


Foram 12


Foram 13


Foram 14


Foram 15


Foram 16


Foram 17


Foram 18


Foram 19


Foram 20

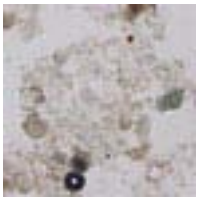
Foram 21

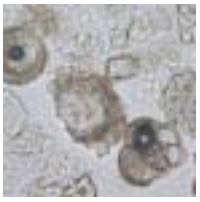
Foram 22

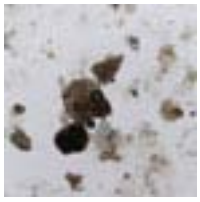
Foram 23

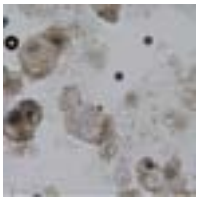
Foram 24


Foram 25

Foraminifera

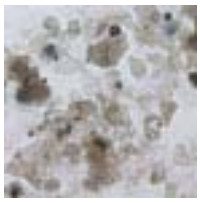
Foram 26

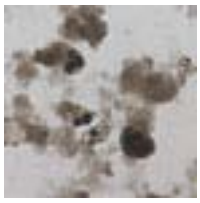
Foram 27

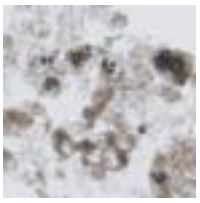
Foram 28

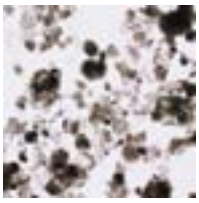
Foram 29

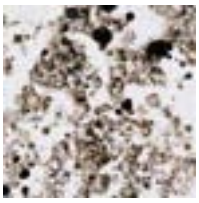
Foram 30


Foram 31


Foram 32


Foram 33


Foram 34

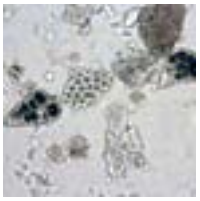
Foram 35


Foram 36


Foram 37

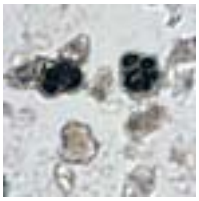
Foram 38


Foram 39


Foram 40

Image ID: B0166/B0167

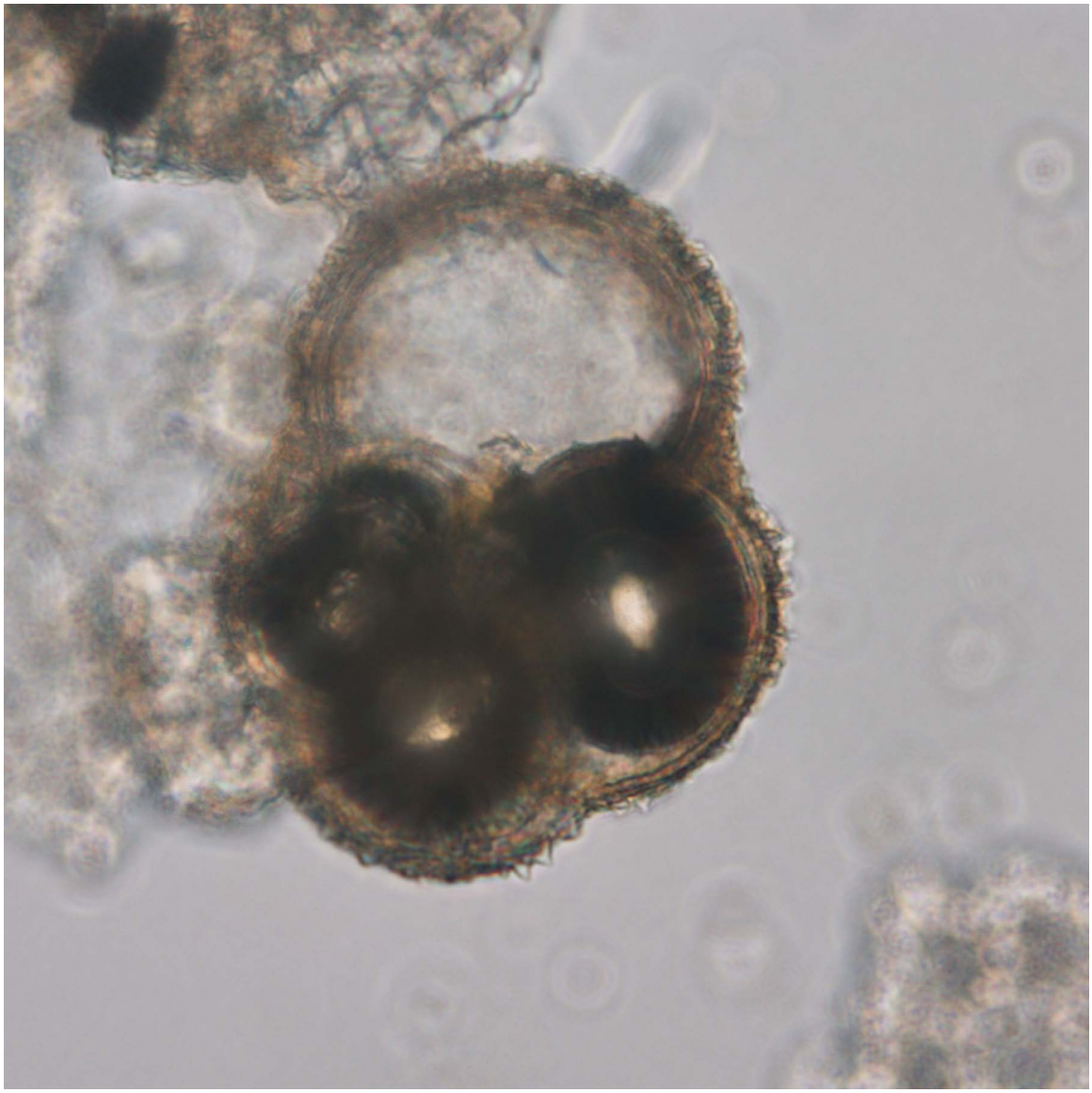

Foram 1.

Air bubbles (dark) in all but one of the spherical chambers of this trochospirally coiled, planktic foraminifer cause them to be dark. Under crossed polars, the chamber that is not dark has a distinct, characteristic pseudo-uniaxial cross owing to the arrangement of carbonate crystals in the foraminifer test perpendicular to the outer curved surface of the chamber. The air bubbles in the other chambers impede this effect. Small, birefringent triangular carbonate crystals at the bottom of the test are ornamentation.

ODP Sample (Pleistocene): Leg 130, Hole 807A, Core 1H, Section 2W, 93 cm

Image ID: B0159/B0160

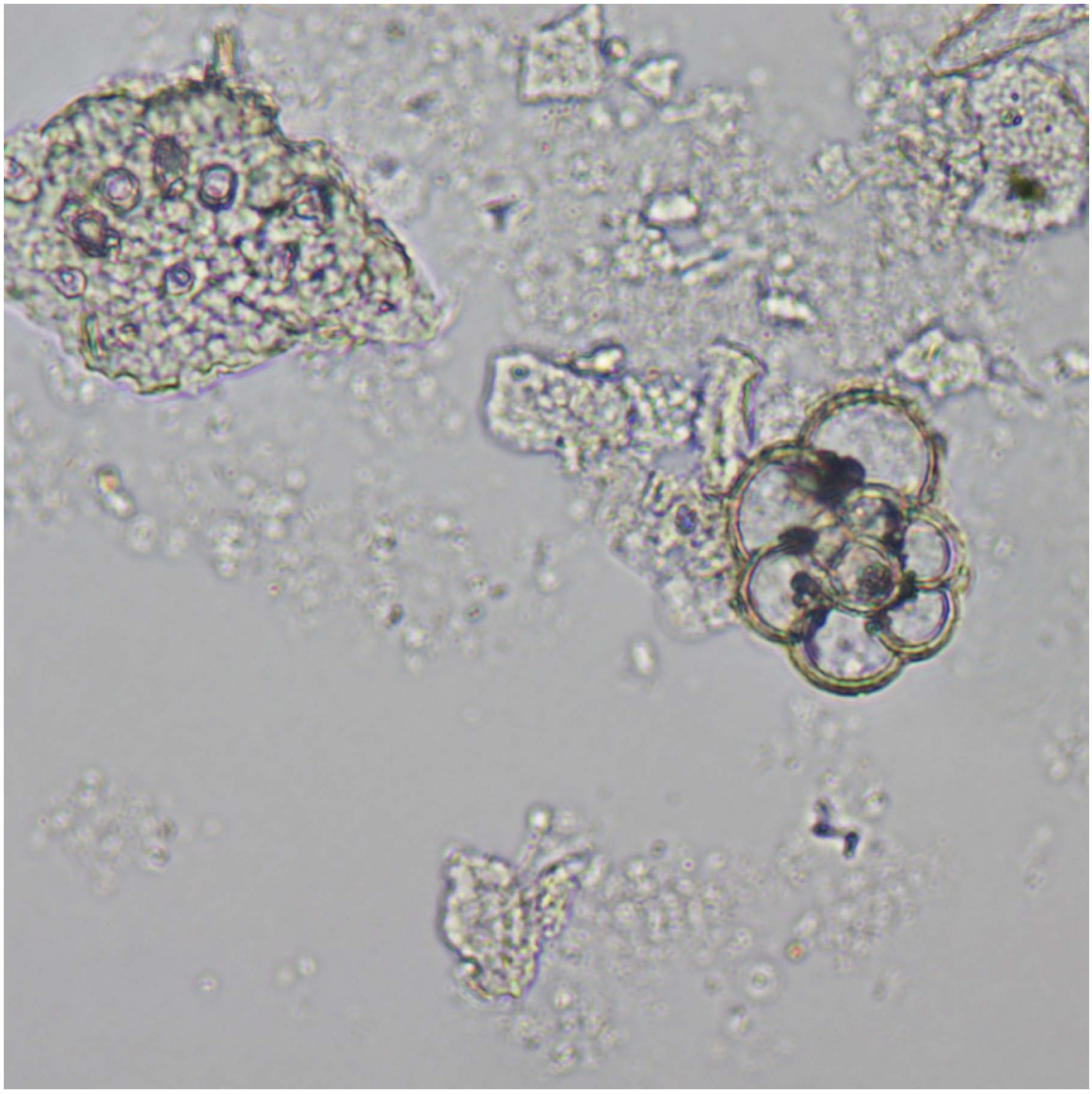

Foram 2.

This view highlights a thin-walled trochospiral planktic foraminifer in a calcareoues ooze of foraminifer fragments and calcareous nannofossils. As a result, the nannofossils are out of focus and appear as gray hazy areas in plane light. Individual chambers exhibit some opaque (pyrite?) inclusions and show pseudo-uniaxial crosses with polars crossed. Note that higher-relief, porous foraminifer chamber fragments lie relatively flat on the slide, so that the c-axes of calcite crystals forming the tests are perpendicular to the field of view and thus show uncharacteristically low, first-order, gray to white birefringence.
ODP Sample (Pleistocene): Leg 130, Hole 807A, Core 1H, Section 2W, 93 cm

Image ID: B0173/B0174

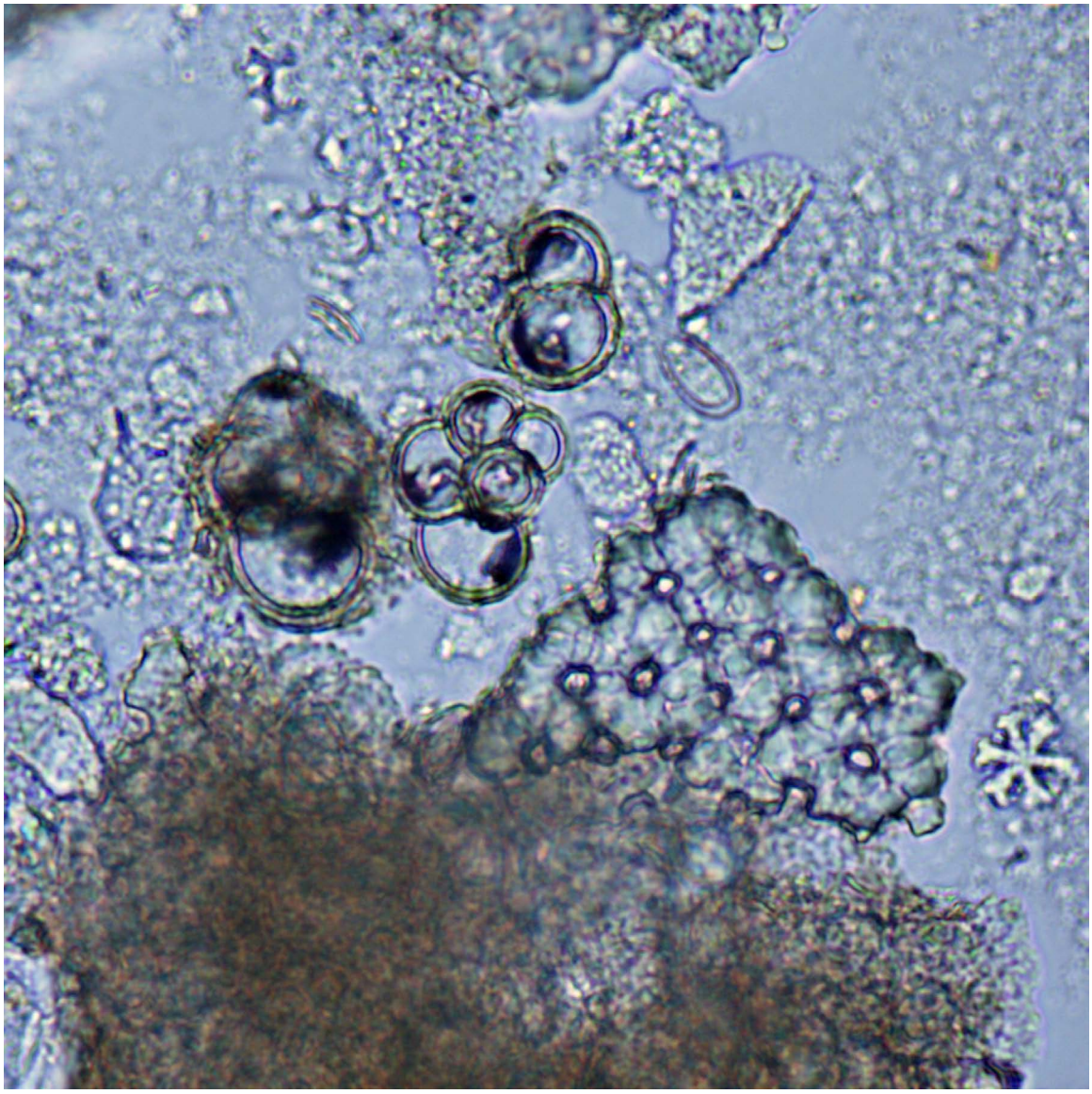

Foram 3.

A cluster of three juvenile, trochospiral, planktic foraminifera, and a large triangular-shaped porous foraminifer fragment fill the center of this image. Nannofossils include a large discoaster with branched rays and a ceratolith. See tutorial for more information.

ODP Sample (Pleistocene): Leg 130, Hole 807A, Core 1H, Section 2W, 93 cm

Image ID: B0007/B0008

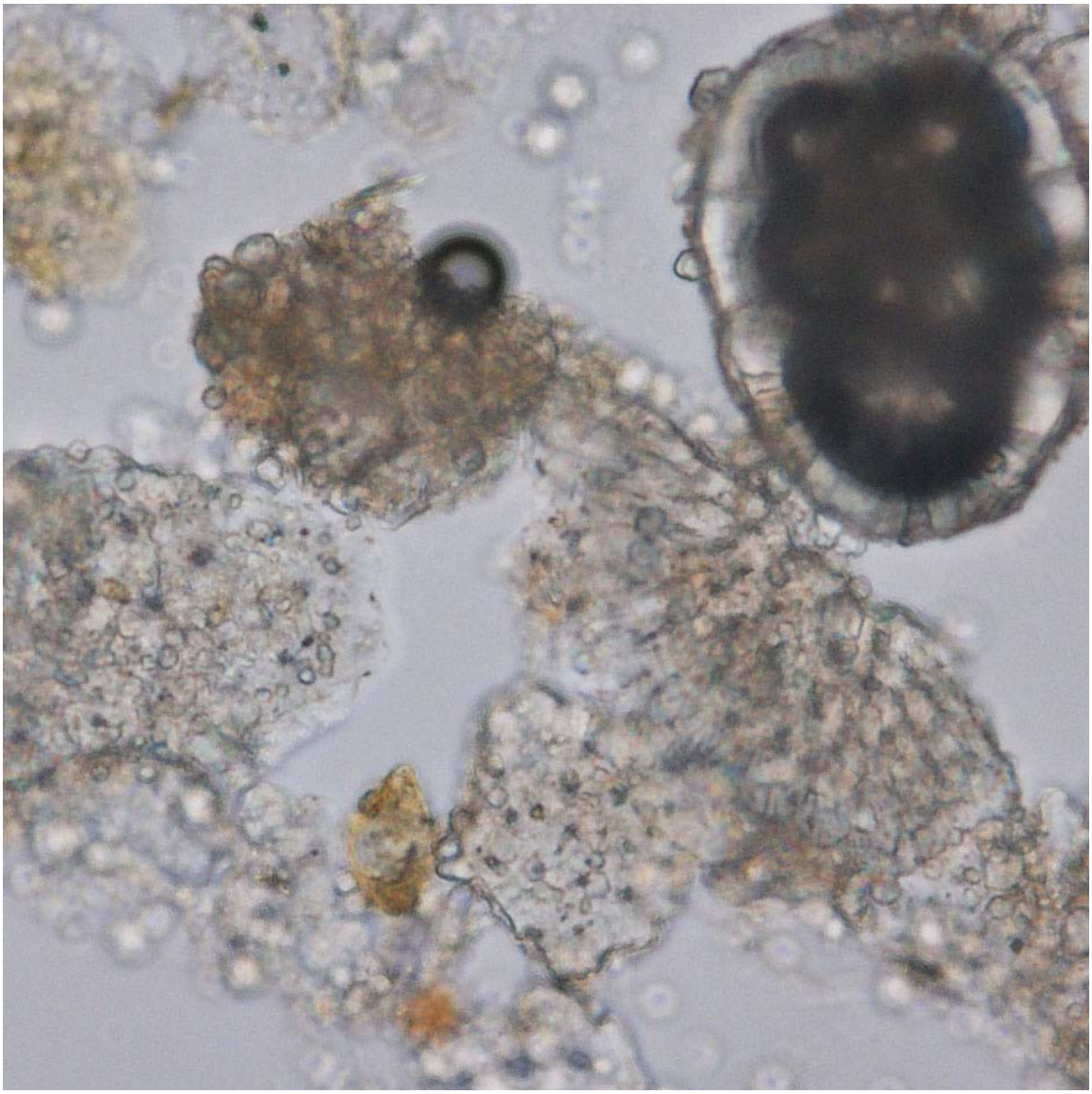

Foram 4.

A juvenile planktic foraminifer is visible in the upper right, above angular, porous foraminifer fragments.

ODP Sample (early Pleistocene): Leg 13, Hole 126, Core 2, Section 4, 12 cm

Image ID: B0508/B0509

Foram 5.

The last chamber of this juvenile planktic foraminifer has been broken off. The remaining chambers are dark because they contain air bubbles.

ODP Sample (Pleistocene): Leg 121, Hole 752A, Core 1H, Section 1W, 55 cm

Image ID: B0189/B0190

Foram 6.

The inflated chambers of this biserial planktic foraminifer are dark because they contain air bubbles.

ODP Sample (late Miocene): Leg 130, Hole 807A, Core 21H, Section 3W, 80 cm

Image ID: B0183/B0184

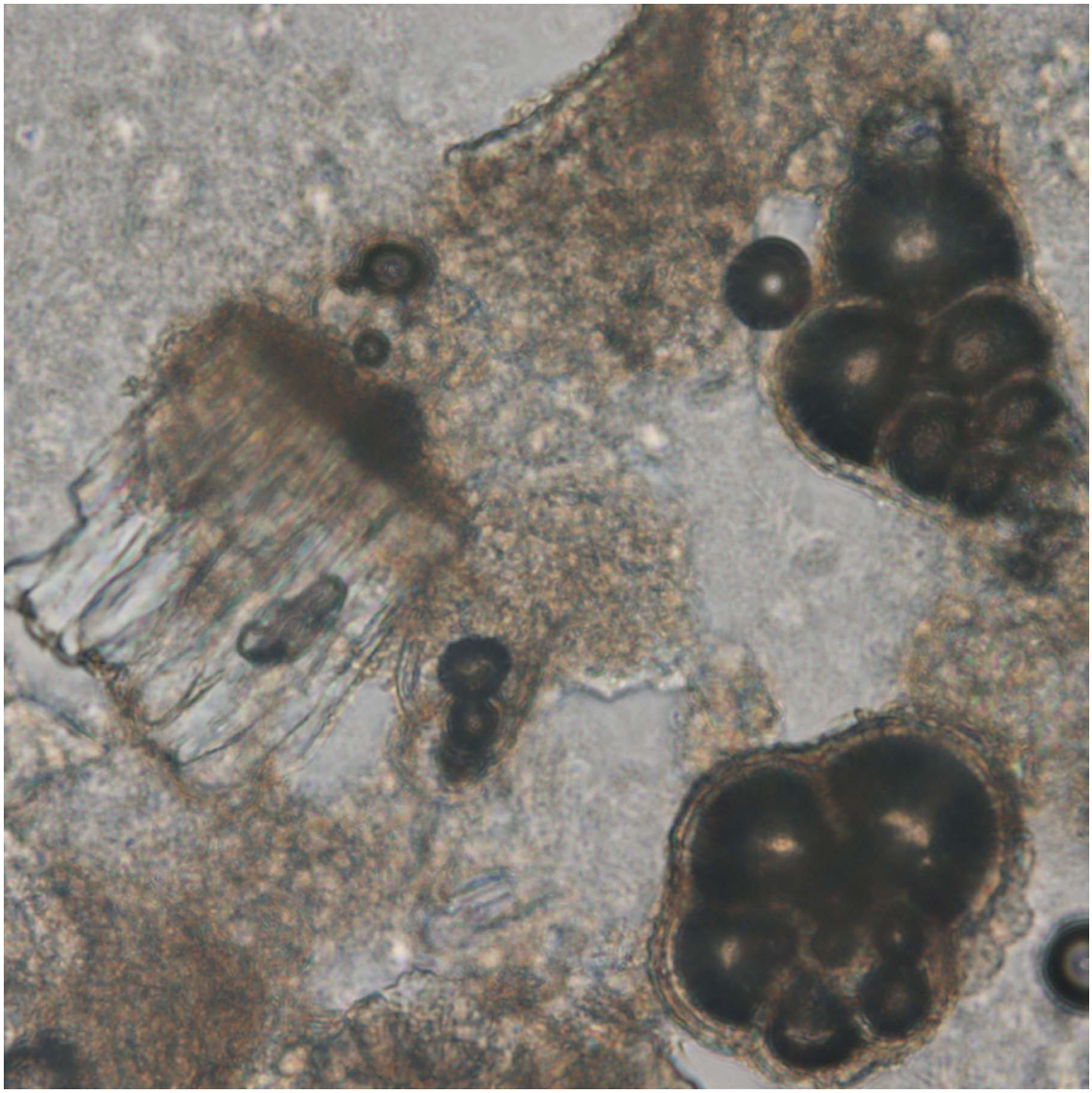

Foram 7.

One biserial (upper right) and one trochospiral, coiled (lower right) planktic foraminifer are visible in this mixed foraminifer-nannofossil ooze. Foraminifer fragments include a thick, crystalline cross section (center left) of a wall fragment of a much larger foraminifer adult.

ODP Sample (late Miocene): Leg 130, Hole 807A, Core 21H, Section 3W, 80 cm

Image ID: B0349/B0350

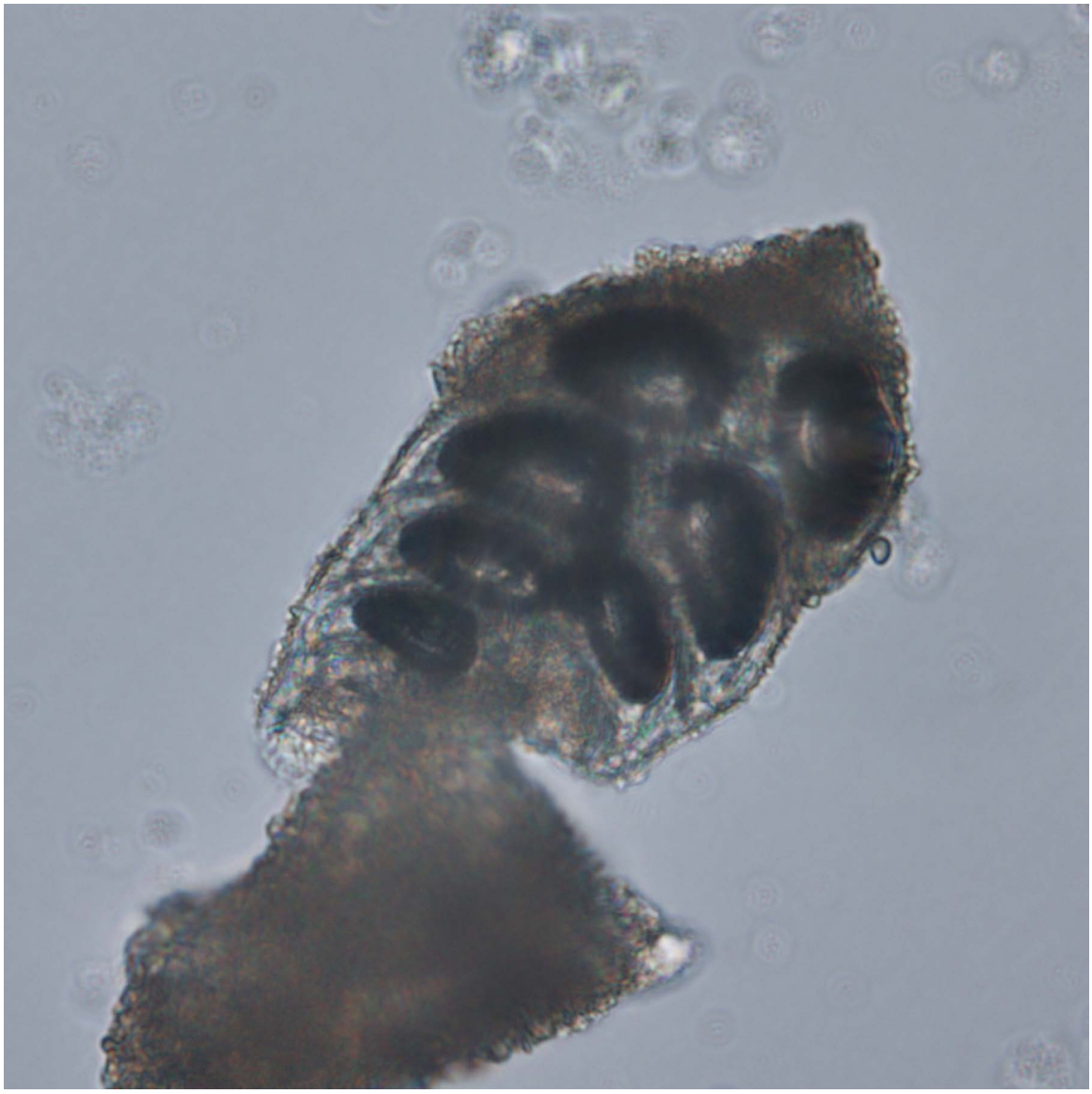

Foram 8.

A broken test of biserial benthic foraminifer with dark, air-bubbled-filled chambers lies above an angular micritic bioclast that has no distinguishing features.

ODP Sample (Pleistocene): Leg 101, Hole 628A, Core 1H, Section 1, 51 cm

Image ID: B0504/B0505

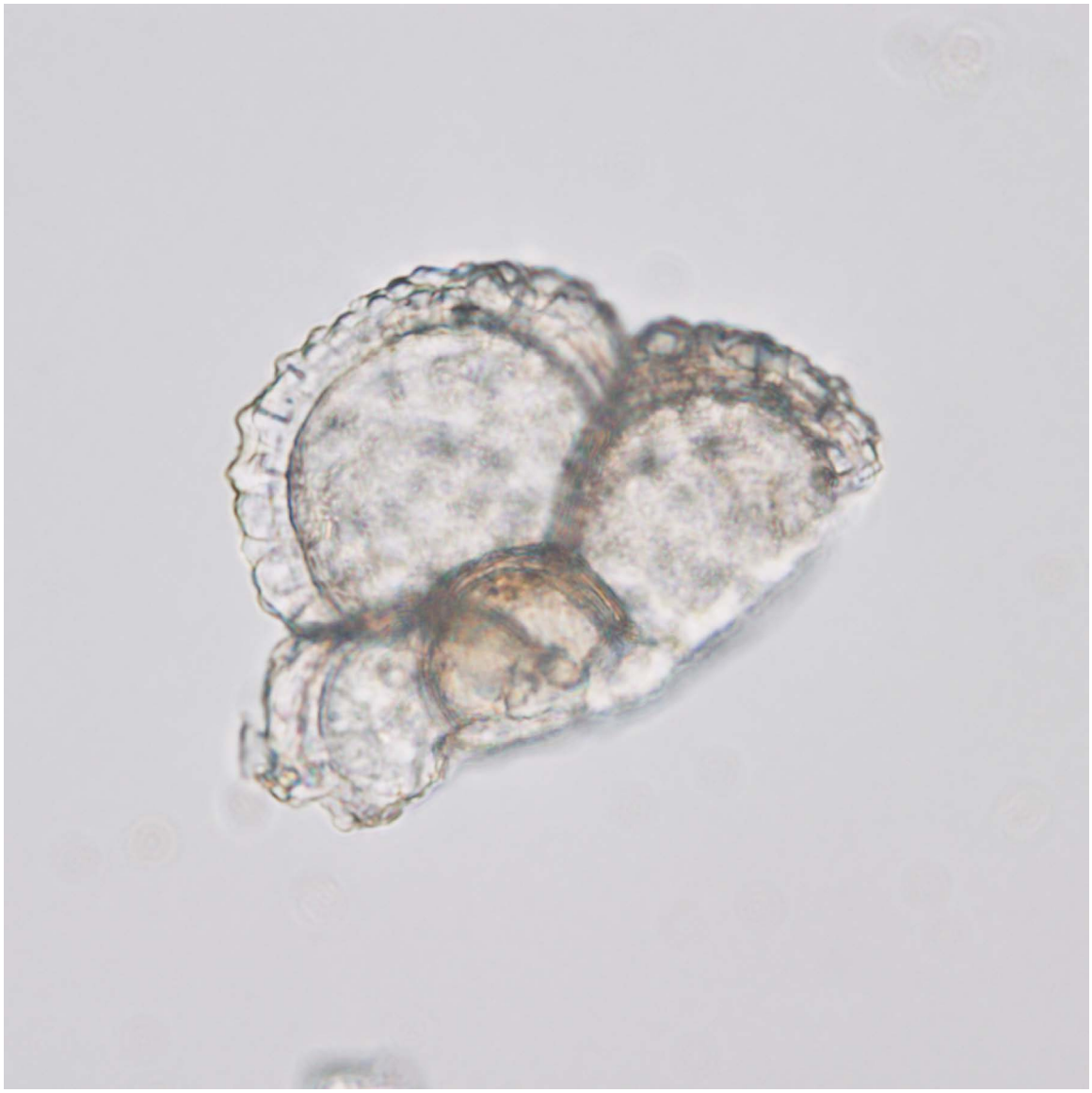

Foram 9.

This is a broken planktic foraminifer with chambers exhibiting characteristic pseudo-uniaxial cross extinction patterns owing to the alignment of crystals perpendicular to the test chamber walls.

ODP Sample (Pleistocene): Leg 121, Hole 752A, Core 1H, Section 1W, 55 cm

Image ID: 0289/0290

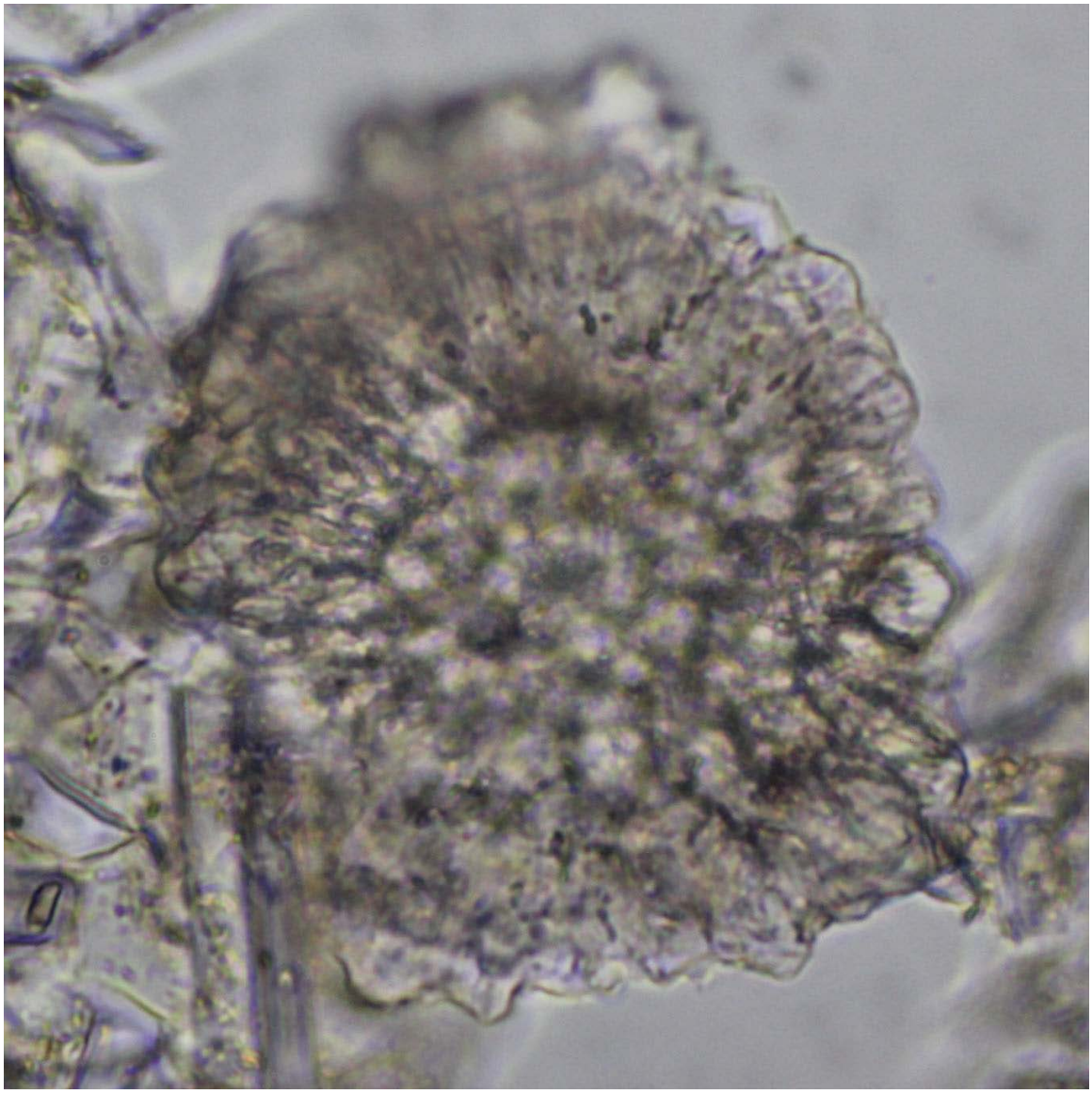

Foram 10.

This fragment of a curved foraminifer chamber is porous, heavily calcified, and exhibits a pseudo-uniaxial cross extinction.

ODP Sample (Quaternary): Leg 126, Hole 791A, Core 16H, Section 5, 73 cm

Image ID: 0064

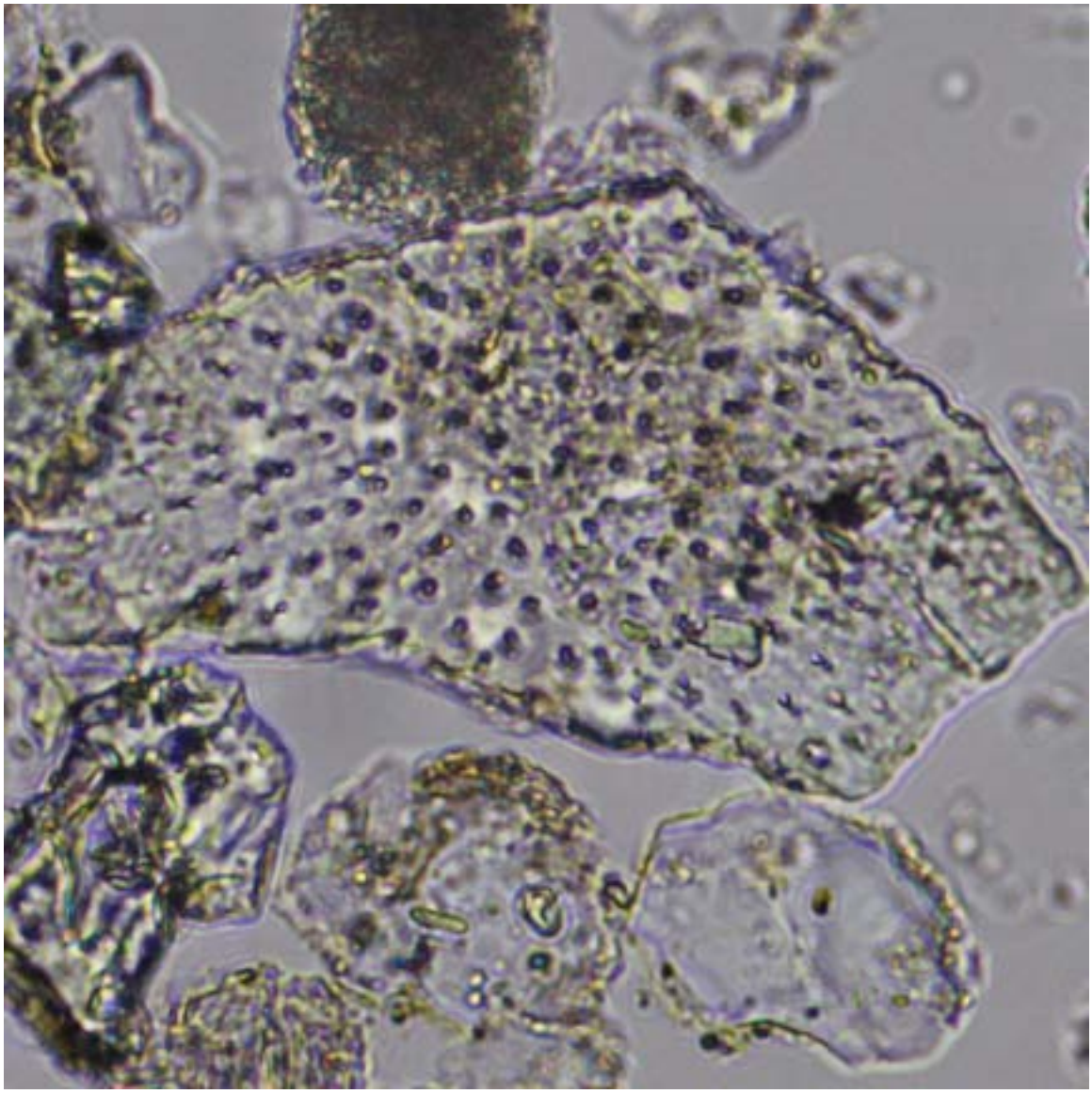

Foram 11.

Dominant in this image is an angular porous, fragment of a planktic foraminifer test surrounded by terrigenous silt grains. Note that no cross-polar view is provided.

ODP Sample (Pleistocene): Leg 130, Hole 1119C, Core 10A, Section 2W, 125 cm

Image ID: B0005/B0006

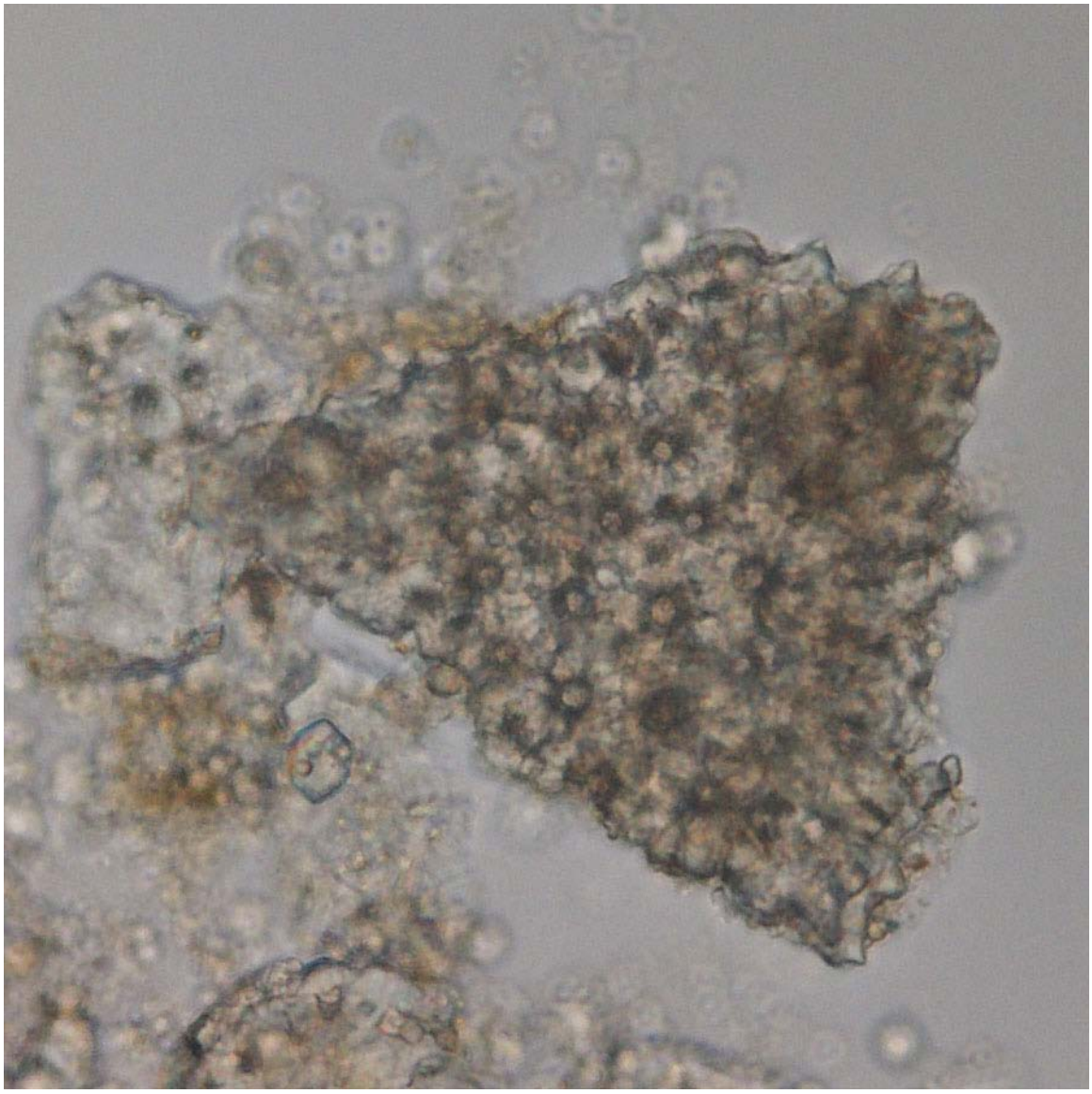

Foram 12.

This is a triangular porous fragment of a planktic foraminifer test. Other smaller pelagic foraminifer fragments are out of focus, but still identifiable by their pseudo-uniaxial cross extinction when polars are crossed.

ODP Sample (early Pleistocene): Leg 13, Hole 126, Core 2, Section 4, 12 cm

Image ID: B0479/B0480

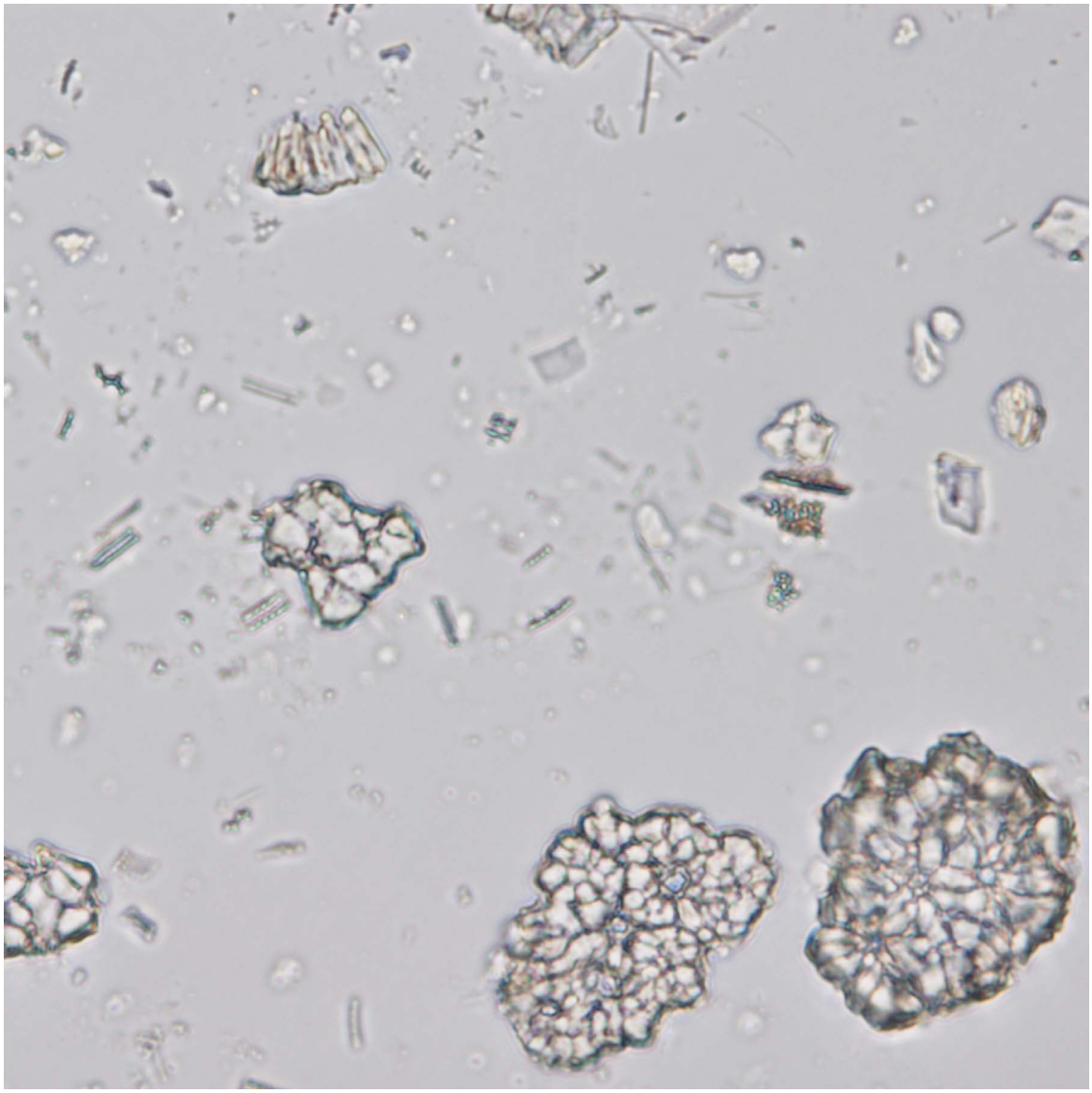

Foram 13.

These planktic foraminifer fragments have pores surrounded by crystalline mosaics that dictate the geometrical shape of the fragments. These test fragments are lying flat on the slide with c-axes approximately perpendicular to the field of view, causing them to have very low birefringence. A cross-sectional fragment in the upper left, in contrast, is birefringent.

ODP Sample (Quaternary): Leg 119, Hole 738B, Core 1H, Section 2W, 69 cm

Image ID: B0171/B0172

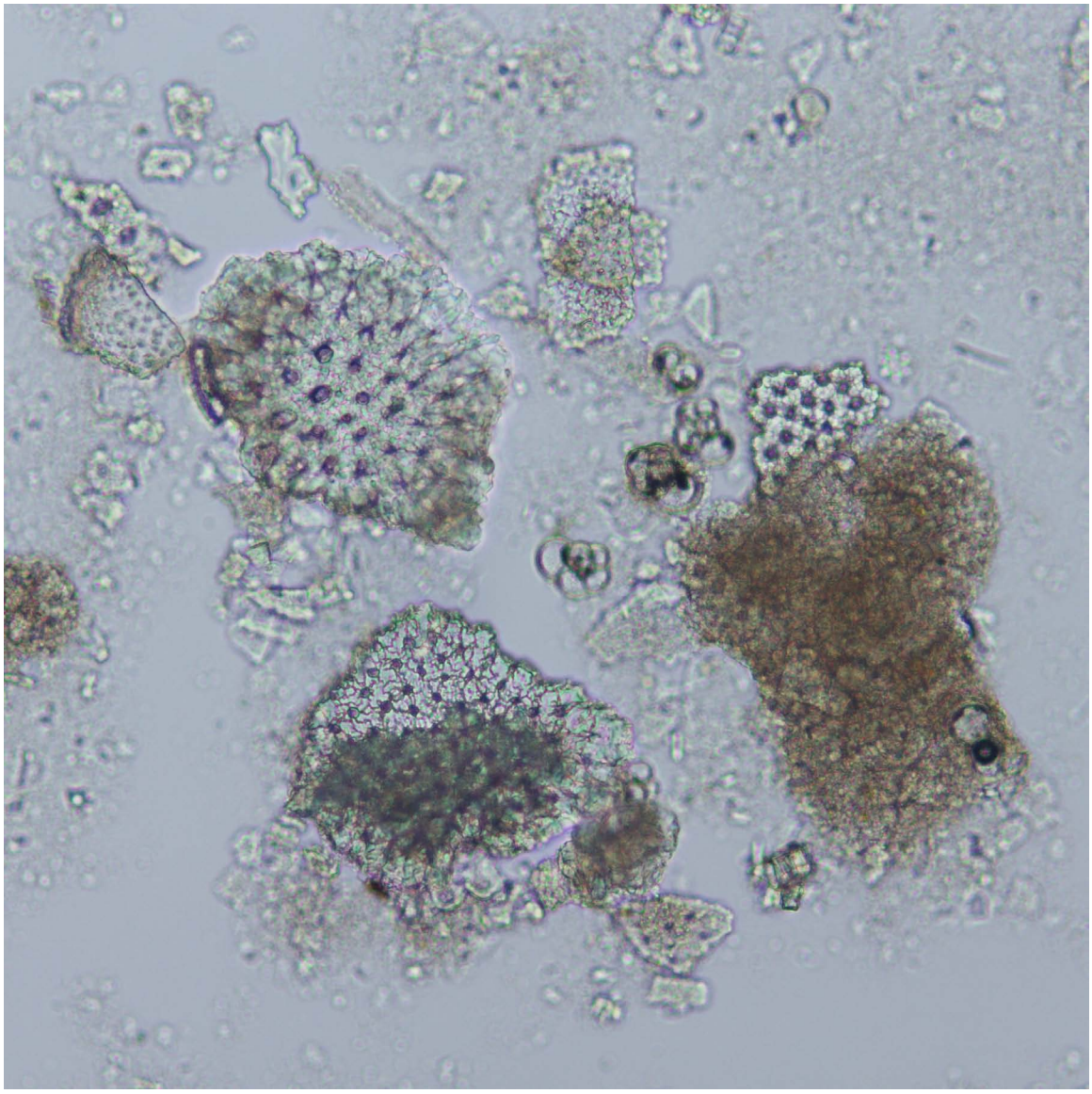

Foram 14.

In this general view of a foraminifer-nannofossil ooze, planktic foraminifer fragments exhibit pores surrounded by crystalline mosaics that dictate fragment geometrical shape. These test fragments are lying flat on the slide with c-axes approximately perpendicular to the field of view, so they have very low birefringence. Note the cluster of smaller juvenile planktic foraminifera in center of the field of view.

ODP Sample (Pleistocene): Leg 130, Hole 807A, Core 1H, Section 2W, 93 cm

Image ID: 0142/0143

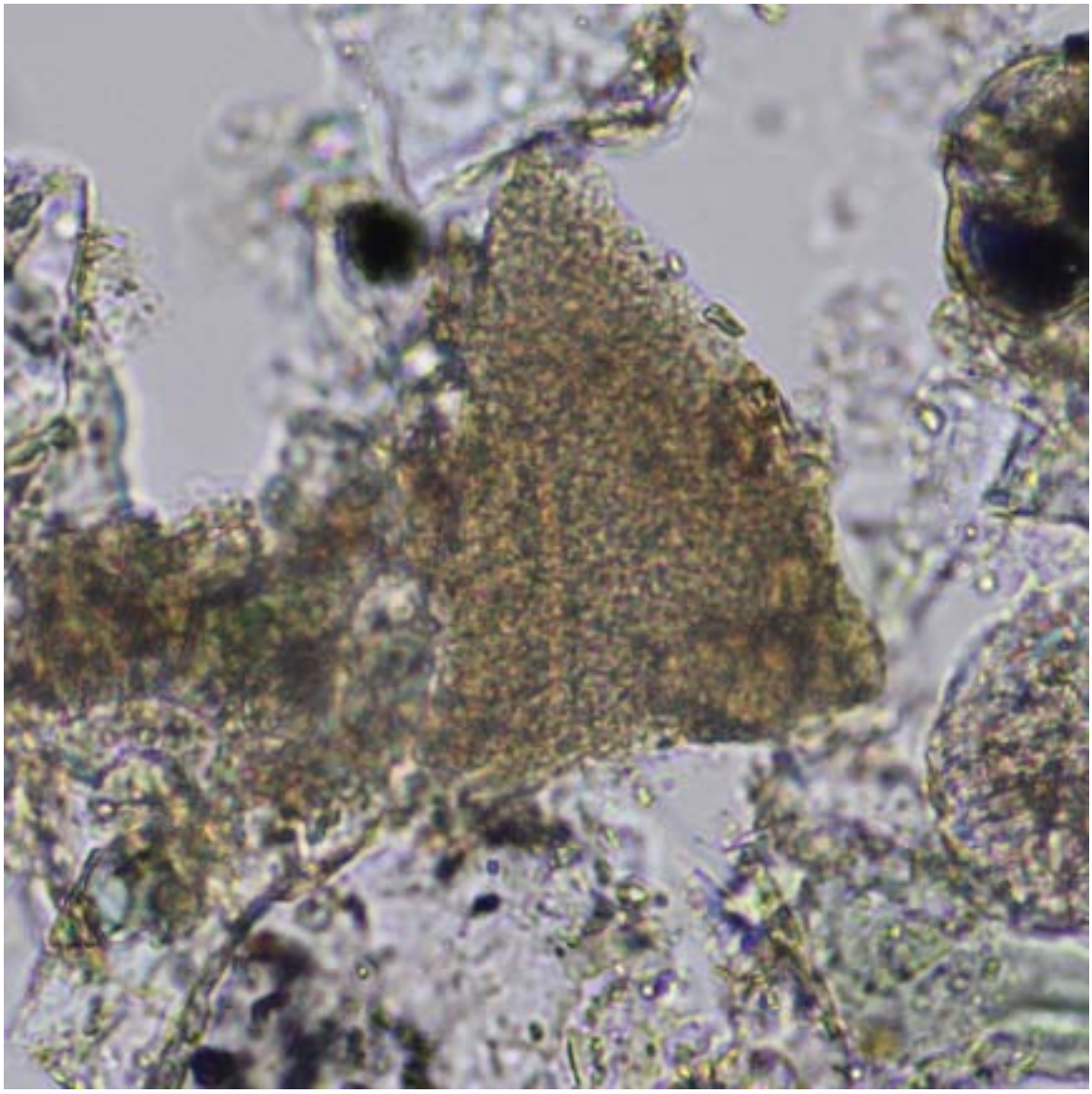

Foram 15.

Shown here is a large, nonporous triangular, porcellaneous benthic foraminifer (miliolid) fragment that is brownish in plane light and exhibits microcrystalline texture under crossed polars.

IODP Sample (Pleistocene): Leg 317, Hole 1352B, Core 11H, Section 2W, 21 cm

Image ID: B0514/B0515

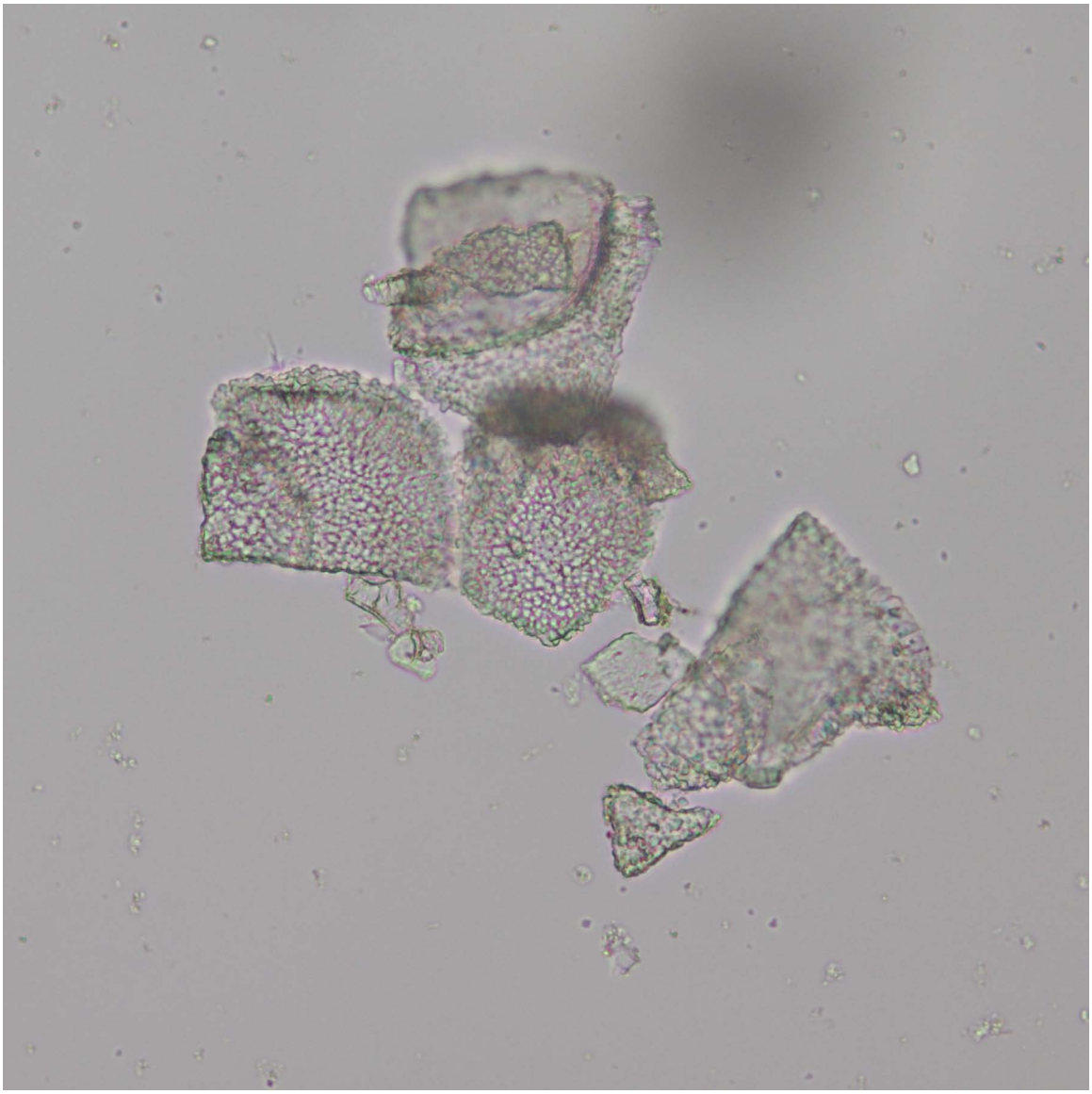

Foram 16.

A cluster of calcareous bioclasts which are recognizable as foraminifer fragments because of their porous texture and pseudo-uniaxial cross extinction. Clasts are oriented in such a way that they display internal chamber surfaces.

ODP Sample (Pleistocene): Leg 121, Hole 752A, Core 1H, Section 1W, 55 cm

Image ID: B0181/B0182

Foram 17.

Set within a mixture of nannofossils and smaller foraminifer fragments, the sub-rectangular fragment of planktic foraminifer wall in cross section shows radial crystalline ultrastructure.

ODP Sample (late Miocene): Leg 130, Hole 807A, Core 21H, Section 3W, 80 cm

Image ID: B0185/B0186

Foram 18.

Set within a mixture of nannofossils and planktic foraminifer fragments, this sub-rectangular fragment of a planktic foraminifer wall shows slight curvature, zonation, and radial porous (dark) crystalline ultrastructure. The arrow indicates a primary organic layer near inner edge.

ODP Sample (late Miocene): Leg 130, Hole 807A, Core 21H, Section 3W, 80 cm

Image ID: B0177/B0178

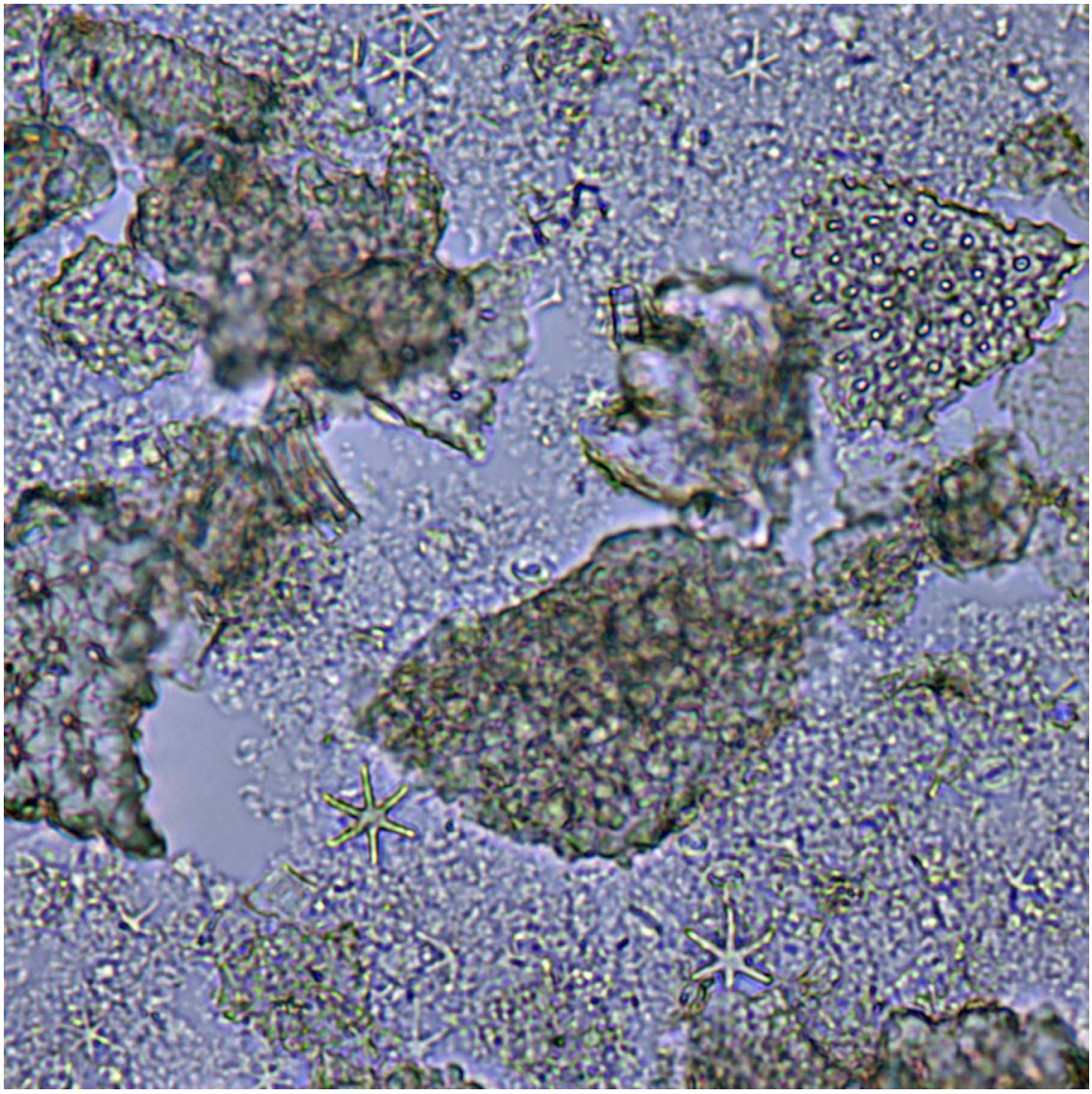

Foram 19.

Multiple planktic foraminifer fragments in a matrix of nanno-fossils that includes star-shaped discoasters.

ODP Sample (late Miocene): Leg 130, Hole 807A, Core 21H, Section 3W, 80 cm

Image ID: B0209/B0210

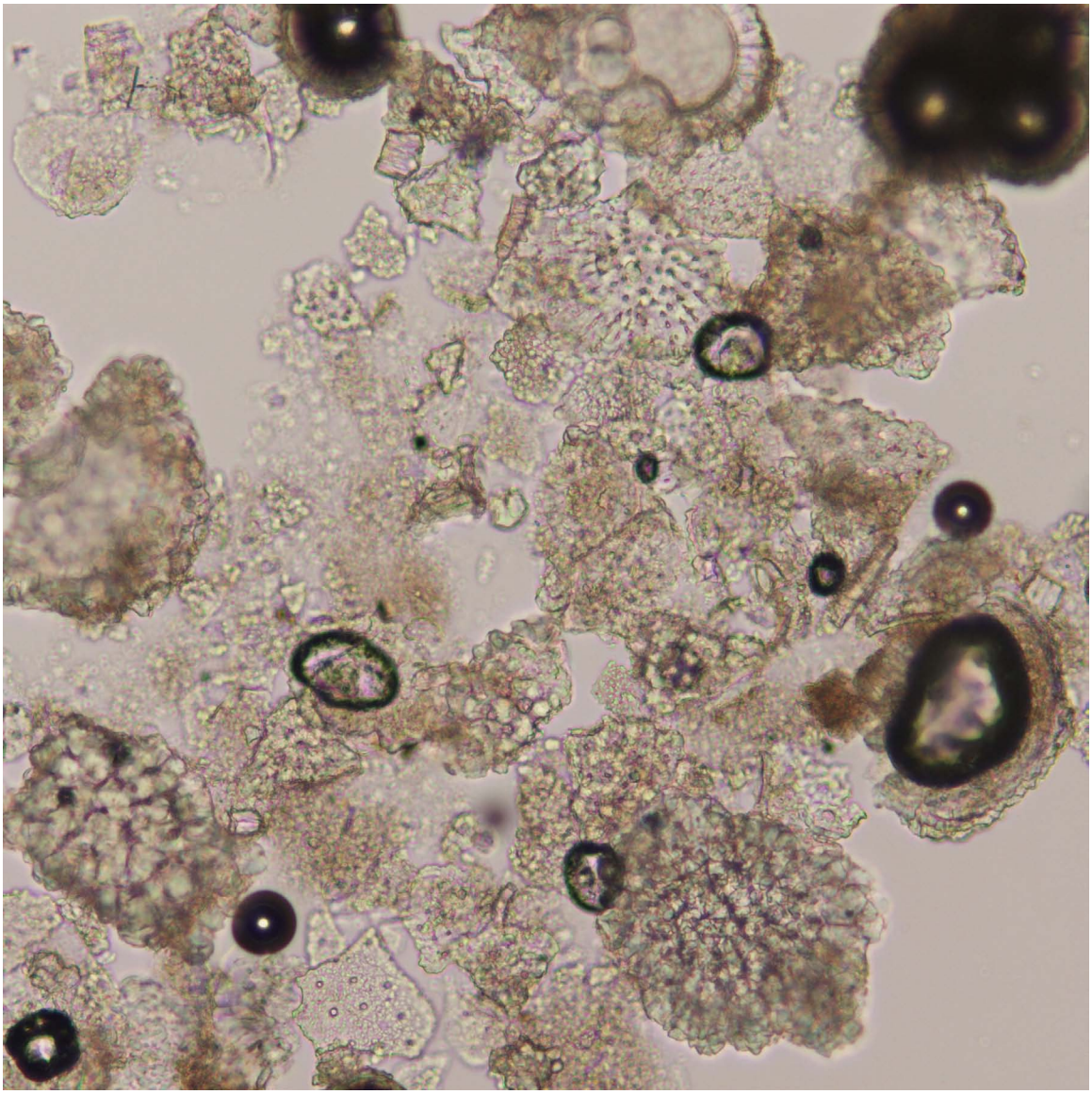

Foram 20.

In this foraminifer ooze consisting mainly of porous fragments with pseudo-uniaxial cross-extinction patterns, multiple species are indicated by varying pore densities and sizes. Dark circles are bubbles in epoxy and in foraminifer chambers.

ODP Sample (early Pleistocene): Leg 103, Hole 637A, Core 7R, Section 2W, 79 cm

Image ID: B0003/B0004

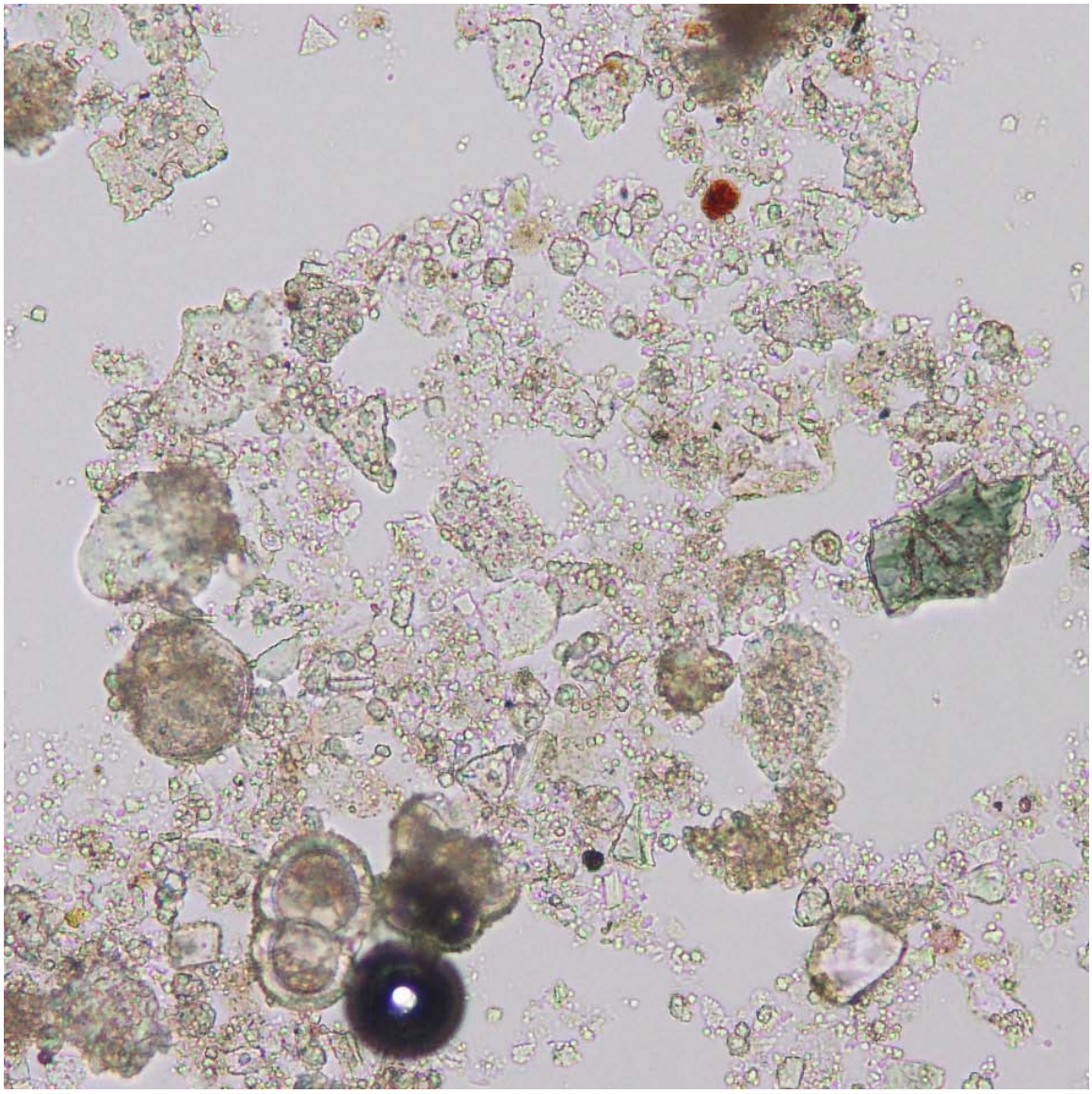

Foram 21.

Under plane light, this image appears to show mainly micrite and terrigenous debris with a few semi-intact foraminifera. When the polars are crossed, however,many fragments exhibit pseudo-uniaxial cross extinction, revealing them to be planktic foraminifer fragments.

ODP Sample (early Pleistocene): Leg 13, Hole 126, Core 2, Section 4, 12 cm

Image ID: B0156/B0157/B0158

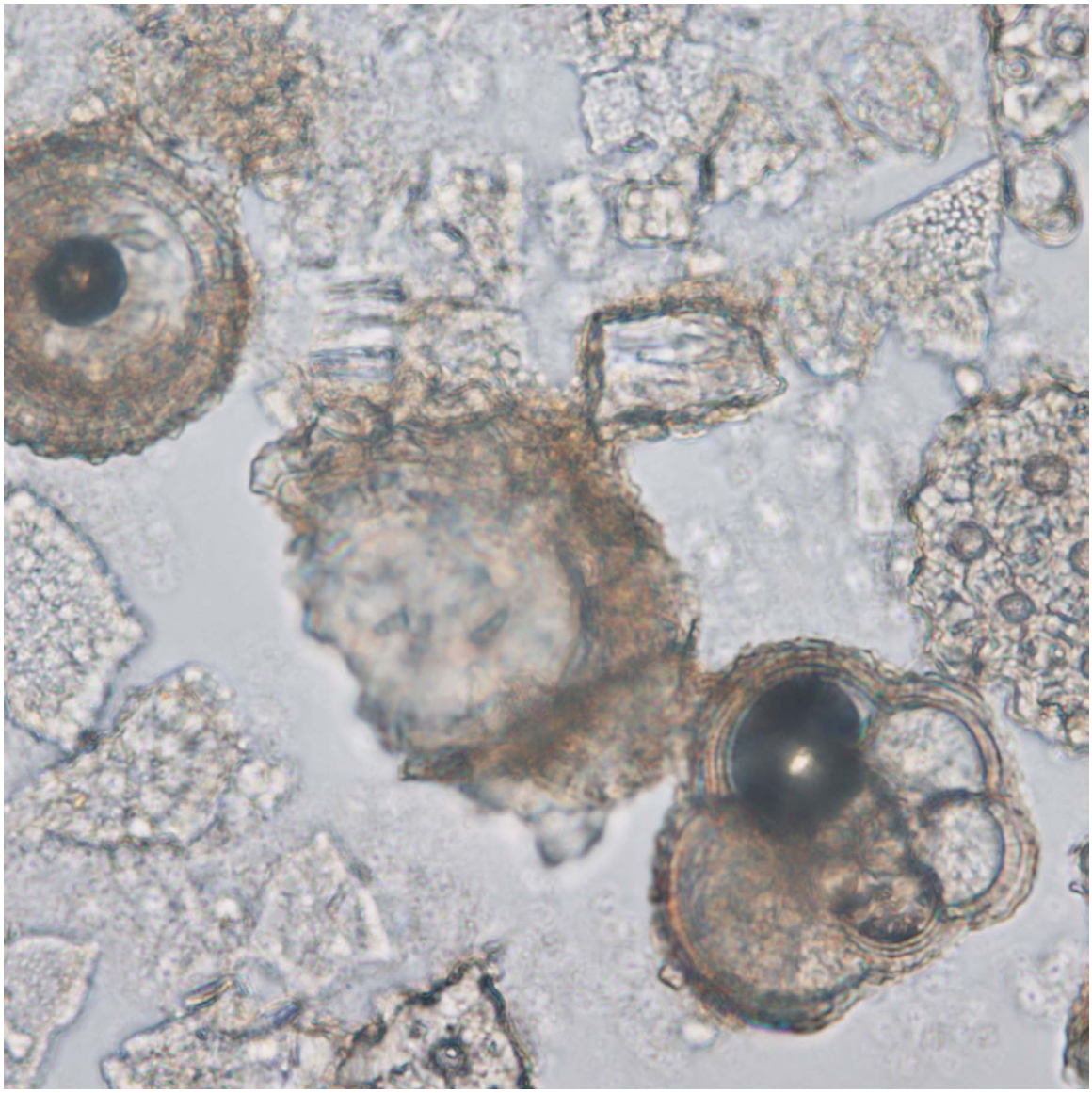

Foram 22.

This diverse suite of planktic foraminifer debris comprises mainly fragments along with one trochospirally coiled juvenile.

ODP Sample (Pleistocene): Leg 130, Hole 807A, Core 1H, Section 2W, 93 cm

Image ID: B0161/B0162/B0163

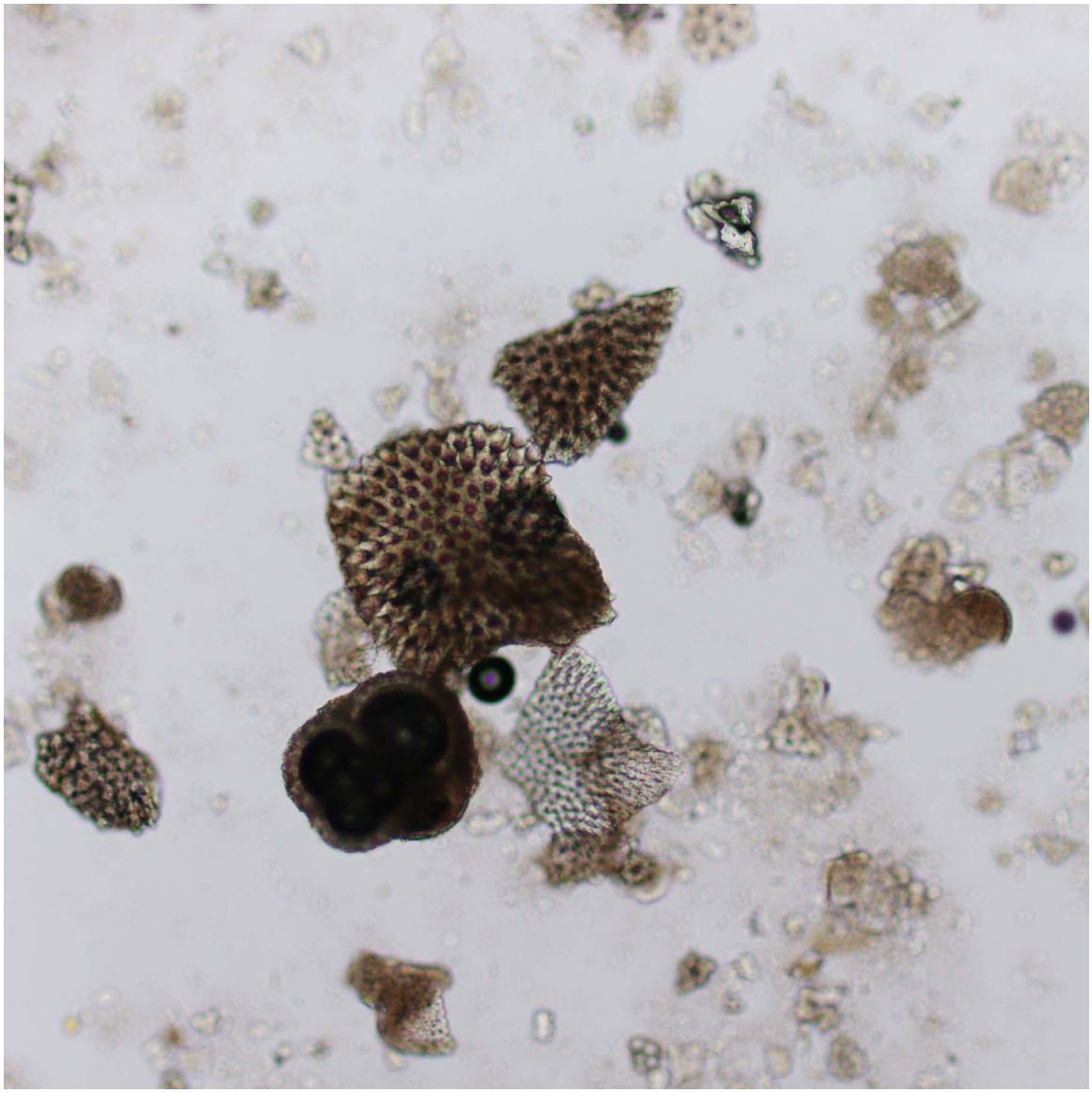

Foram 23.

Larger sand-sized grains in this general view of foraminifer-nannofossil ooze are porous foraminifer fragments together with one dark, intact juvenile. When the polars are crossed, many smaller fragments exhibit pseudo-uniaxial cross extinction indicating that they are also foraminifer fragments set in a matrix of slightly birefringent nannofossils. See tutorial for more information.

ODP Sample (Pleistocene): Leg 130, Hole 807A, Core 1H, Section 2W, 93 cm

Image ID: B0400/B0401

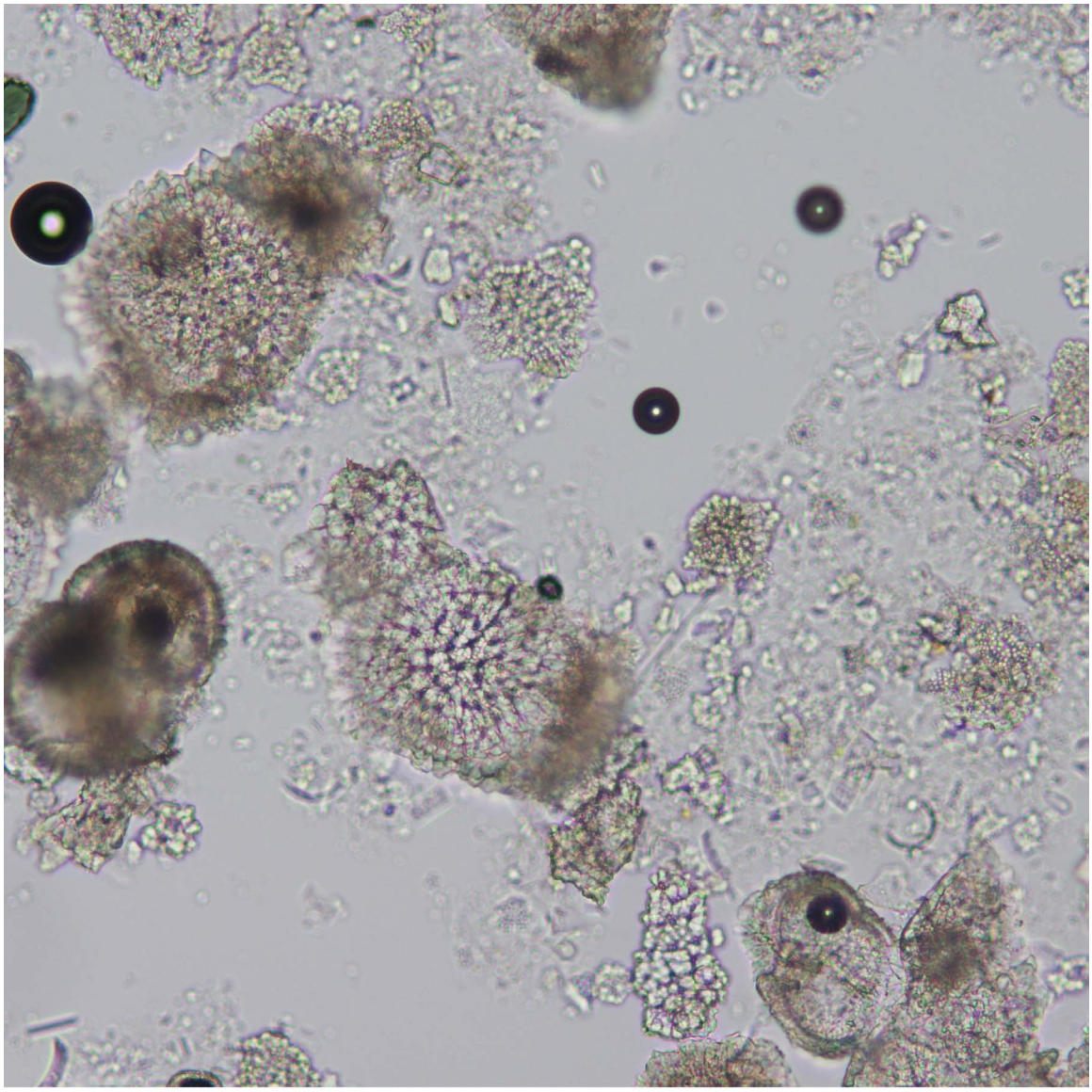

Foram 24.

Whole specimens and fragments of planktic varieties of foraminifera are visible in this general view of a foraminifer-nannofossil ooze.

ODP Sample (late Pliocene): Leg 113, Hole 690A, Core 1H, Section 1, 110 cm

Image ID: B0207/B0208

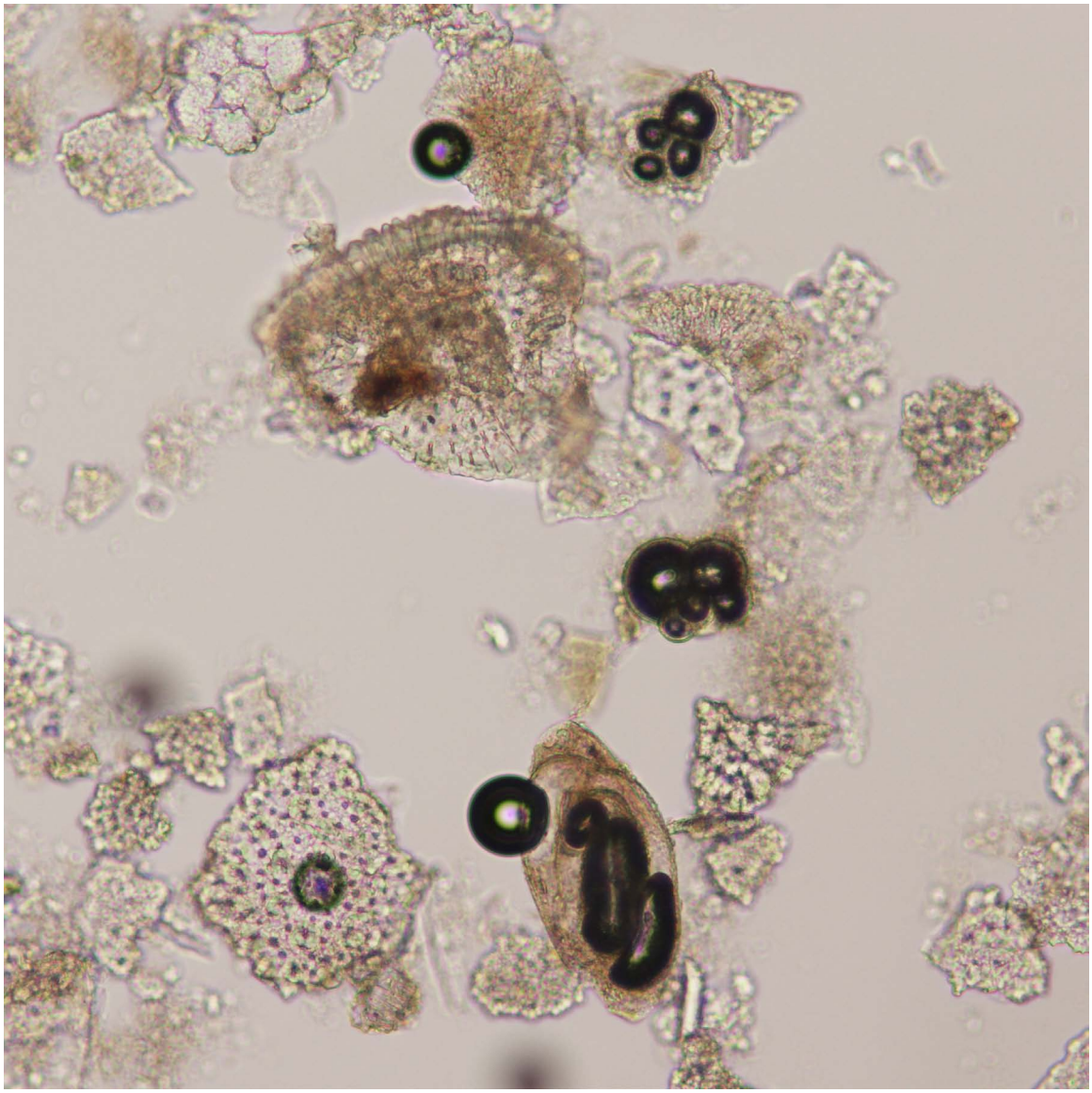

Foram 25.

This is a general view of foraminifer ooze consisting mainly of porous fragments, several intact chambered foraminifera are easily identified by the cluster of air bubbles in their chambers. An elongate foraminifer at bottom center with bubble-filled oval chambers may be a benthic foraminifer.

ODP Sample (early Pleistocene): Leg 103, Hole 637A, Core 7R, Section 2W, 79 cm

Image ID: B0175/B0176

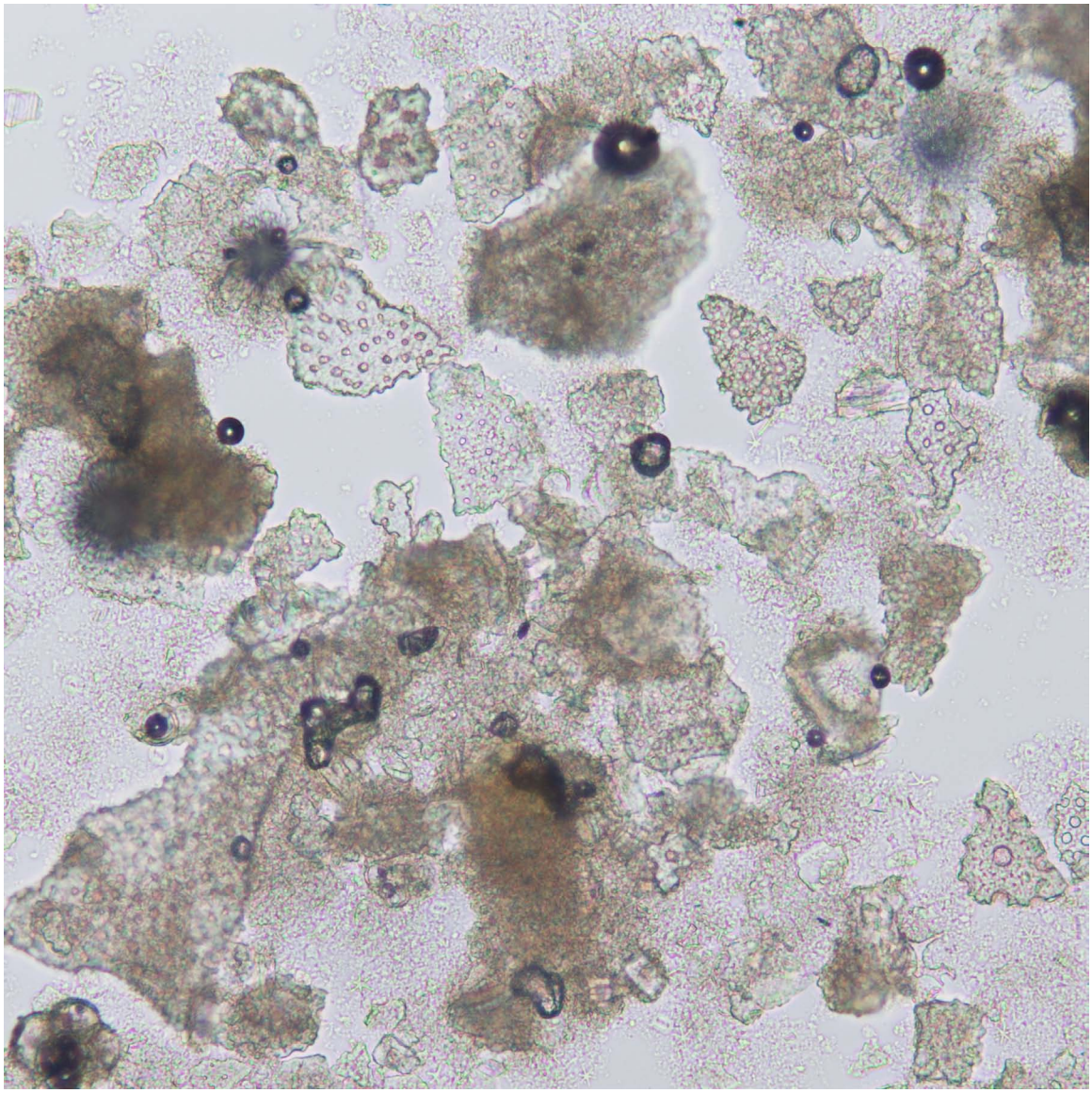

Foram 26.

Variably shaped foraminifer fragments admixed with fine nannofossils are identifiable in this foraminifer-nannofossil ooze.

ODP Sample (late Miocene): Leg 130, Hole 807A, Core 21H, Section 3W, 80 cm

Image ID: B0191/B0192

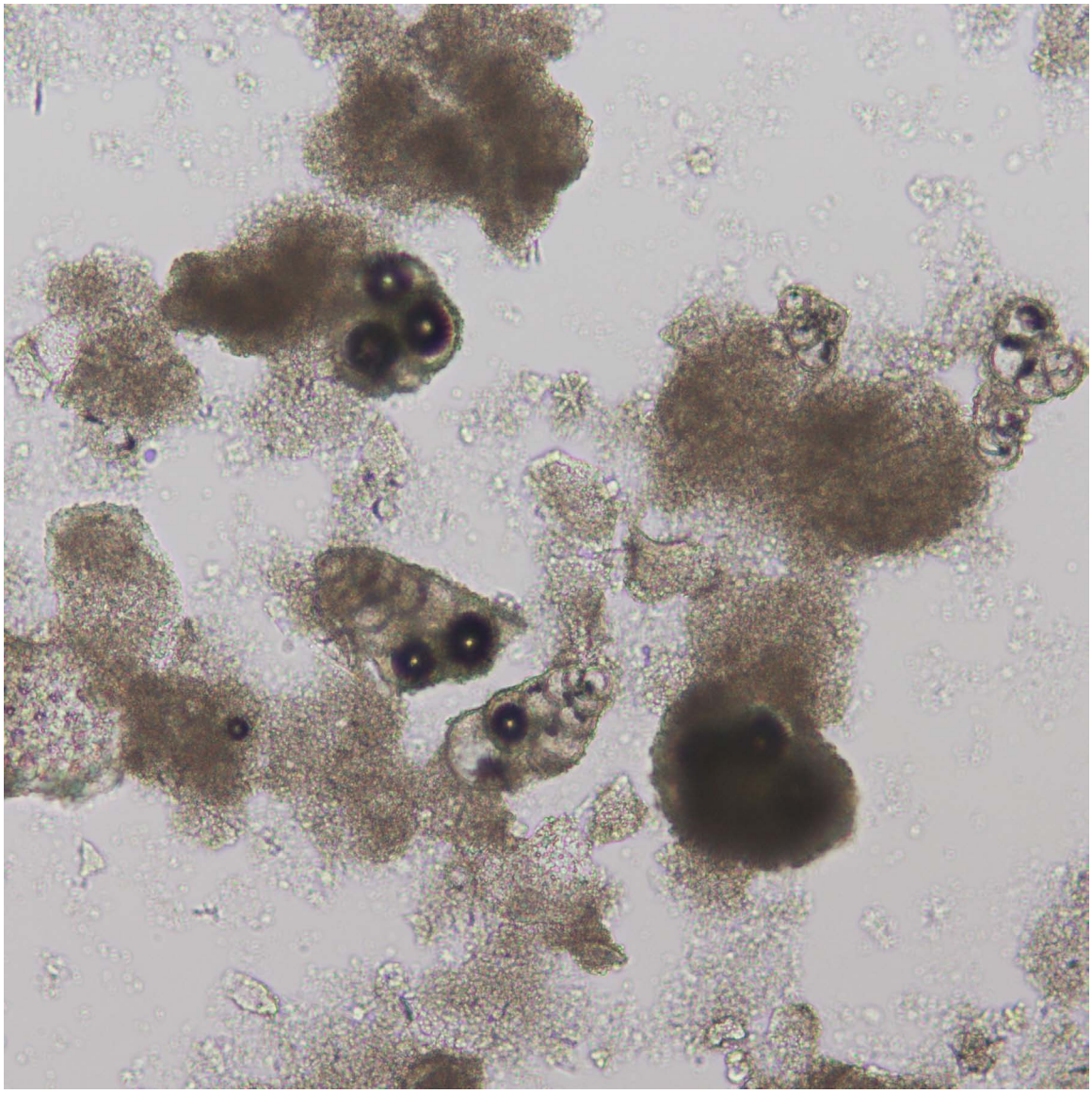

Foram 27.

A variety of biserial and trochospiral and other foraminifer types are visible in this nannofossil-foraminifer ooze. The largest foraminifer appears semi-opaque. The nannofossil matrix appears darker tan to brown where more concentrated.

ODP Sample (late Miocene): Leg 130, Hole 807A, Core 21H, Section 3W, 80 cm

Image ID: B0323/B0324

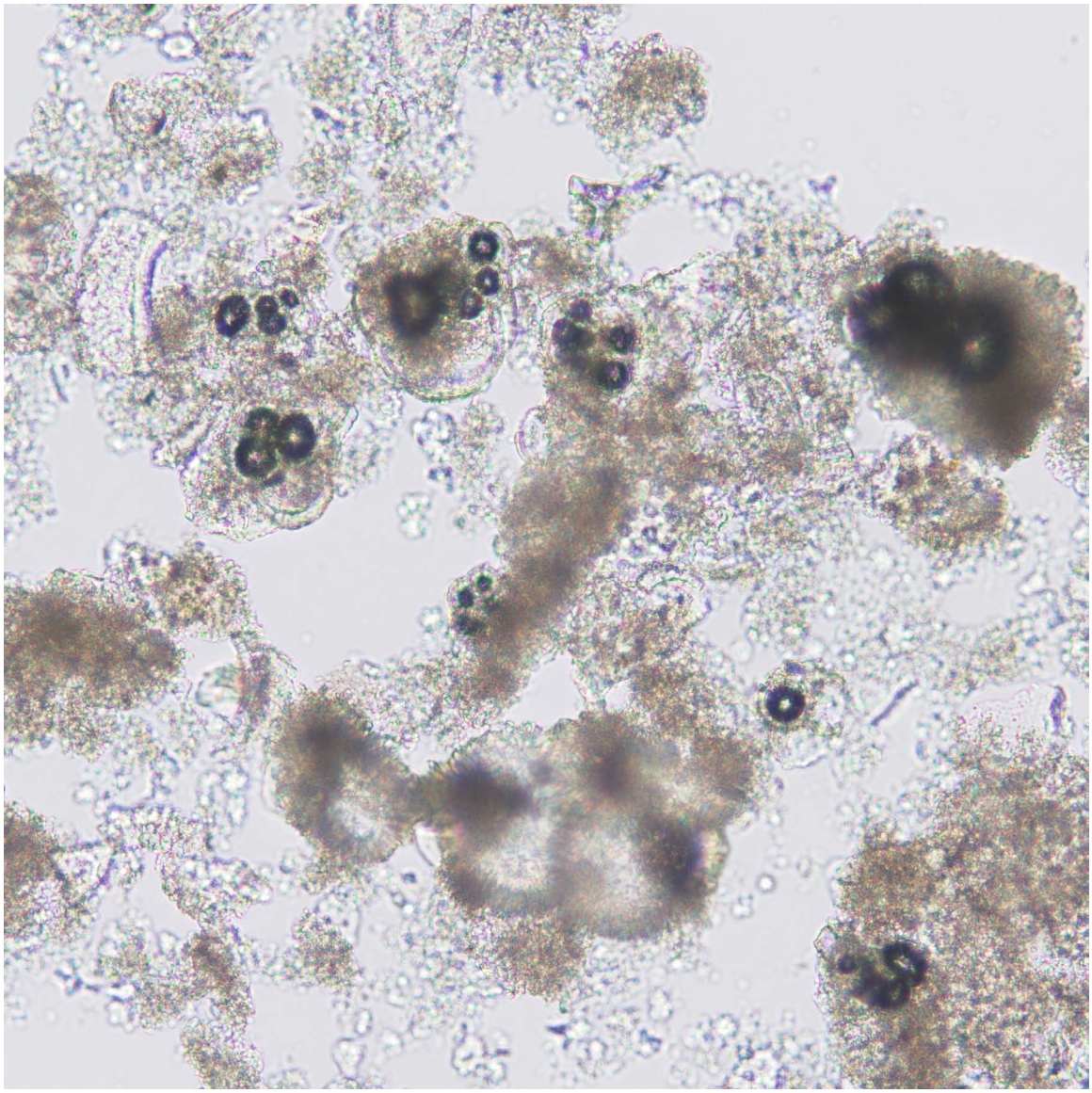

Foram 28.

Areas that appear to be out of focus in this general view of foraminifer nannofossil ooze are large, sand-size foraminifera. Smaller foraminifera can be identified by the black-rimmed air bubbles that fill their chambers. The matrix is less distinct because of the highly variable grain size affects the ability to focus on it.

ODP Sample (early Miocene): Leg 165, Hole 999A, Core 47X, Section 5W, 80 cm

Image ID: B0325/B0326

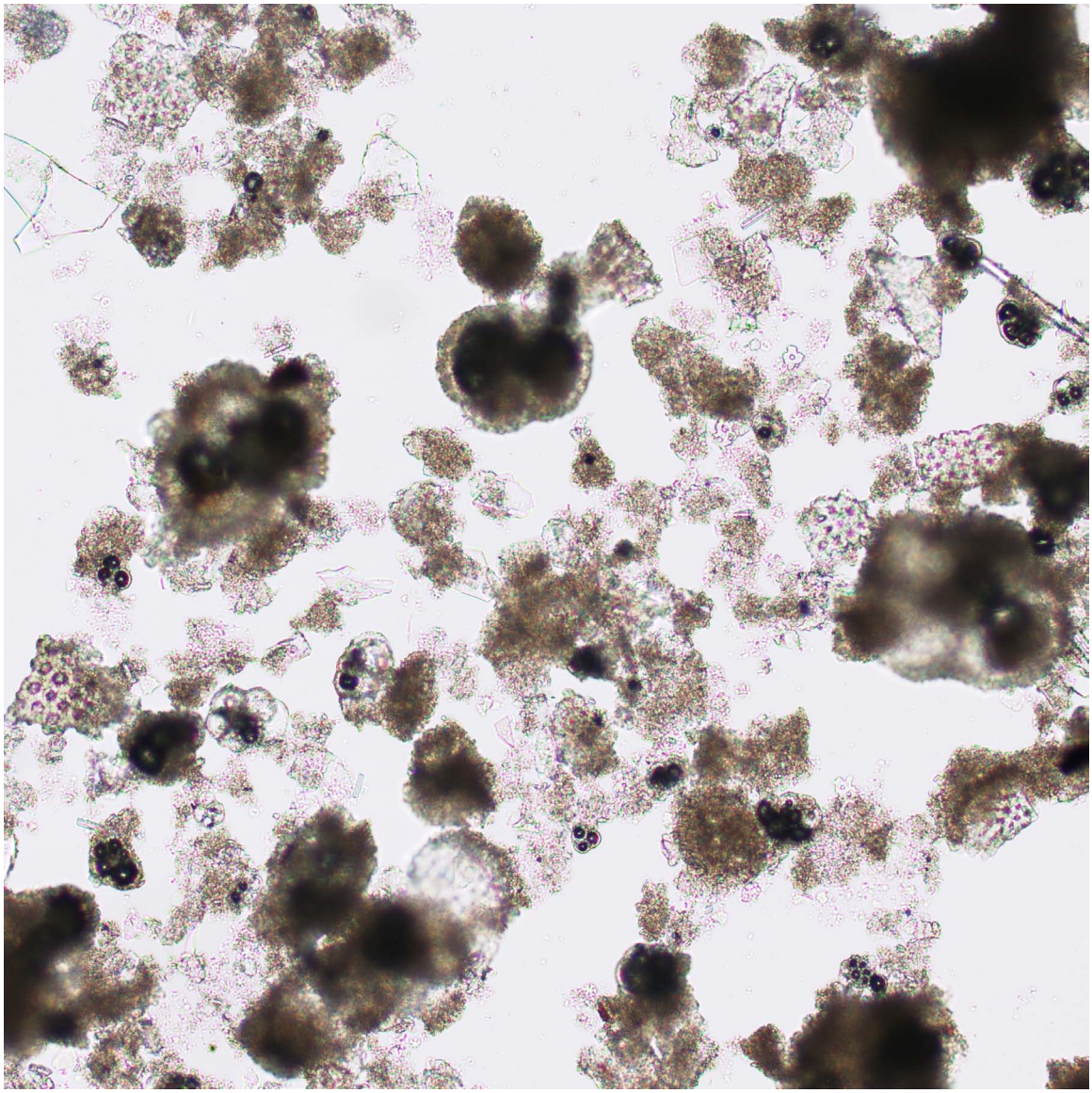

Foram 29.

Larger foraminifera stand high on the slide and so are out of focus in this general view of foraminifer nannofossil ooze consisting of intact foraminifer specimens and fragments along with patches of finer nannofossils.

ODP Sample (early Miocene): Leg 165, Hole 999A, Core 47X, Section 5W, 80 cm

Image ID: B0211/B0212

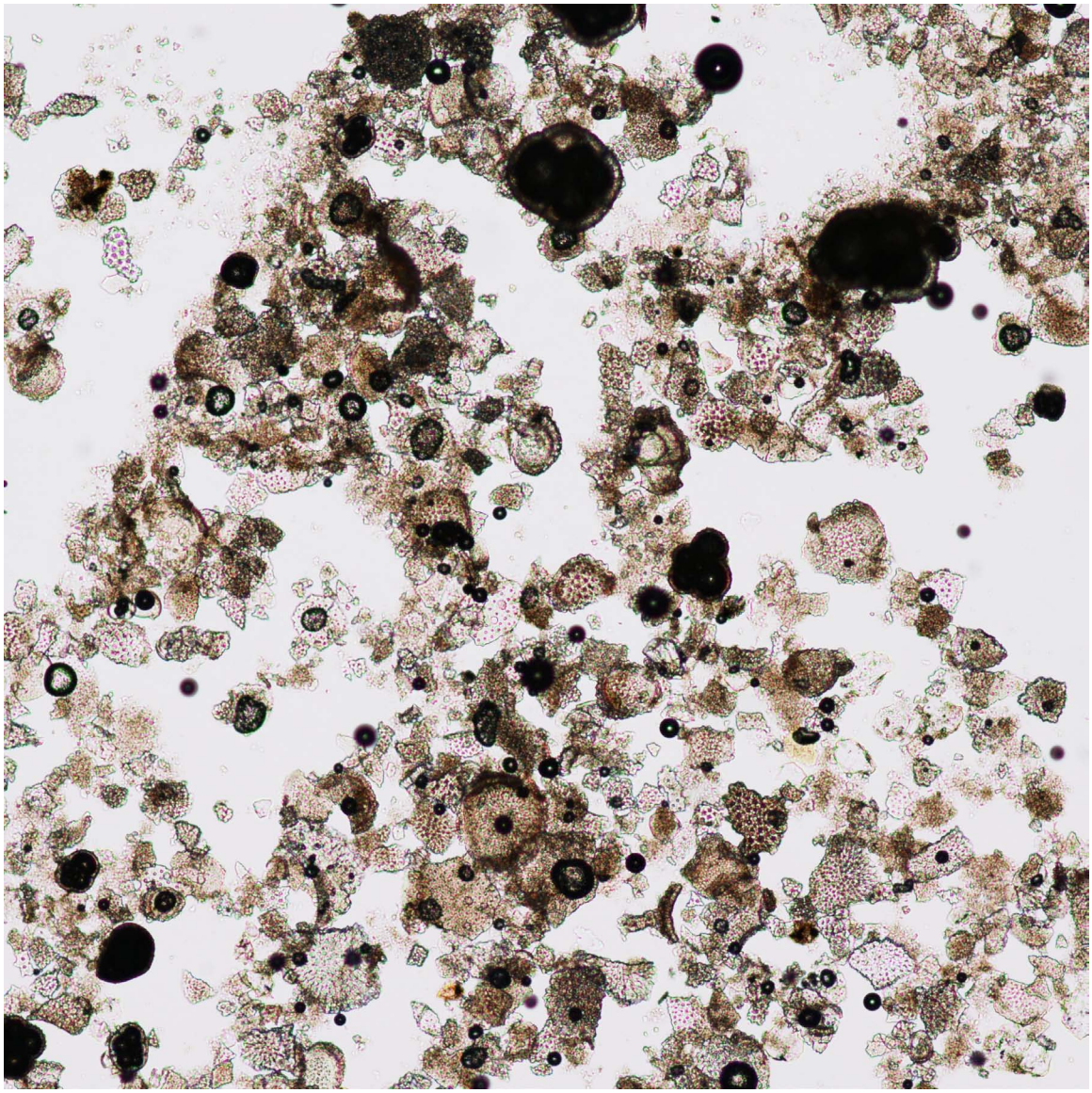

Foram 30.

The black grains are foraminifera with air-filled chambers in this general view of foraminifer ooze with some nannofossils. The percentage of foraminifera is best estimated with polars crossed, so that chambers showing pseudo-uniaxial crosses are obvious.

ODP Sample (early Pleistocene): Leg 103, Hole 637A, Core 7R, Section 2W, 79 cm

Image ID: B0021/B0022

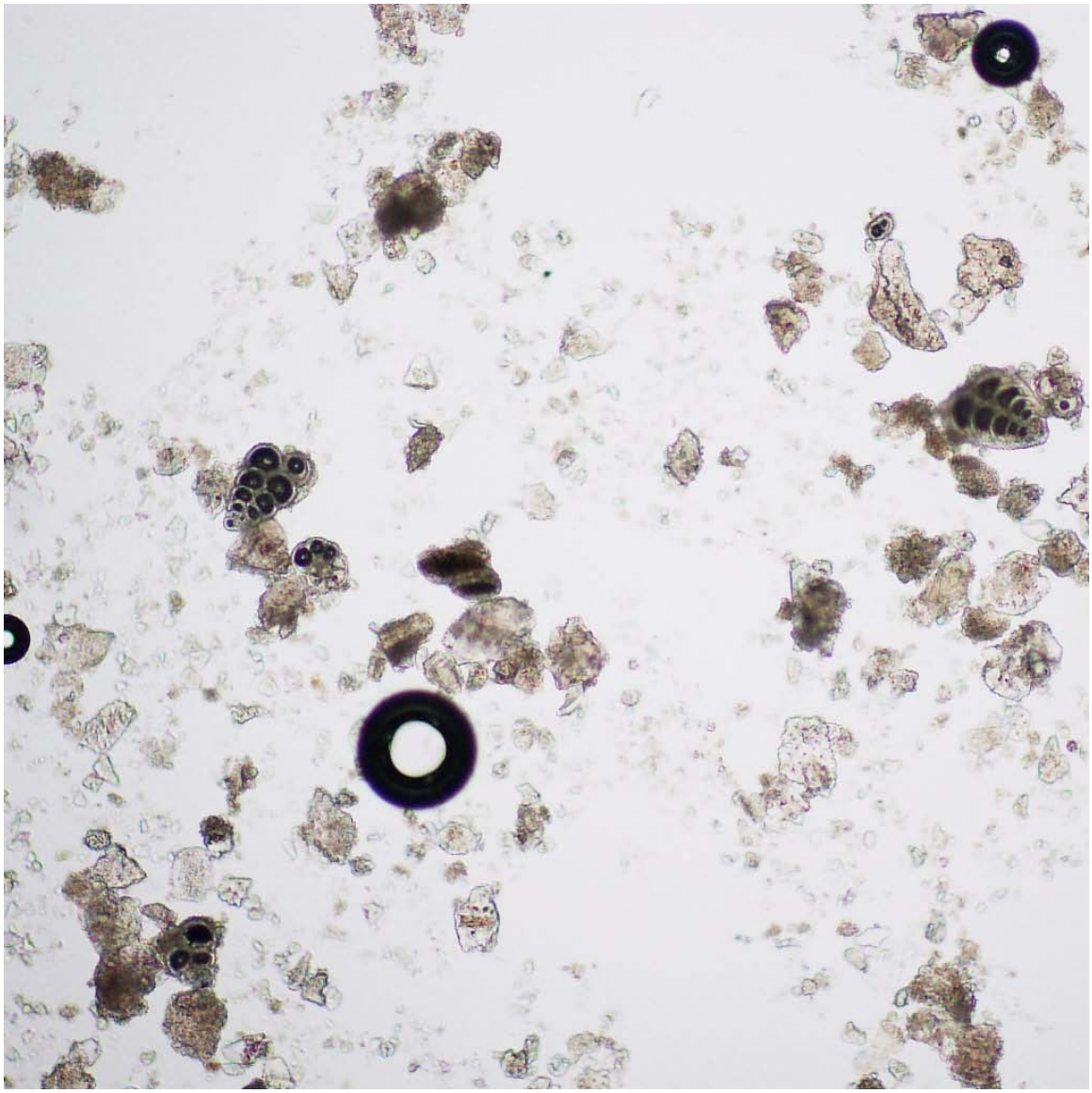

Foram 31.

In this disseminated foraminifer ooze with several intact, biserial foraminifera (circled), the two on the left are planktic and the one on the right is benthic. The benthic foraminifer has less inflated chambers and a thicker wall. The fine matrix includes some silt-sized birefringent micrite (biocalsts?). Large dark circles are bubbles in the epoxy.

DSDP Sample (late Eocene): Leg 21, Hole 209, Core 18, Section 1, 120 cm

Image ID: B0619/B0620

Foram 32.

Biserial benthic foraminifer with elongate (noninflated) chambers amongst other calcareous bioclastic debris.

IODP Sample (late Eocene): Leg 342, Hole 209, Core 18, Section 1, 120 cm

Image ID: B0543/B0544

Foram 33.

Biserial foraminifer with elongate (noninflated) chambers amongst other calcareous bioclastic debris including larger circular, featureless grain that is likely another foraminifer. Note that the sand-sized foraminifera stand above the finer background sediment, which appears out of focus in this view. Small circular features are bubbles in the mounting medium. No image with polars crossed is provided.

ODP Sample (Maastrichtian): Leg 198, Hole 1210B, Core 28H, Section 2W, 30 cm

Image ID: B0586/B0587

Foram 34.

Biserial benthic foraminifer with elongate (noninflated) chambers amongst other calcareous bioclastic debris. Note that the sand-sized foraminifera stand above the surrounding finer and less birefringent, nannofossil-rich sediment on the slide, which appears out of focus in this view.

IODP Sample (late Eocene): Leg 342, Hole 209, Core 18, Section 1, 120 cm

Image ID: B0615/B0616

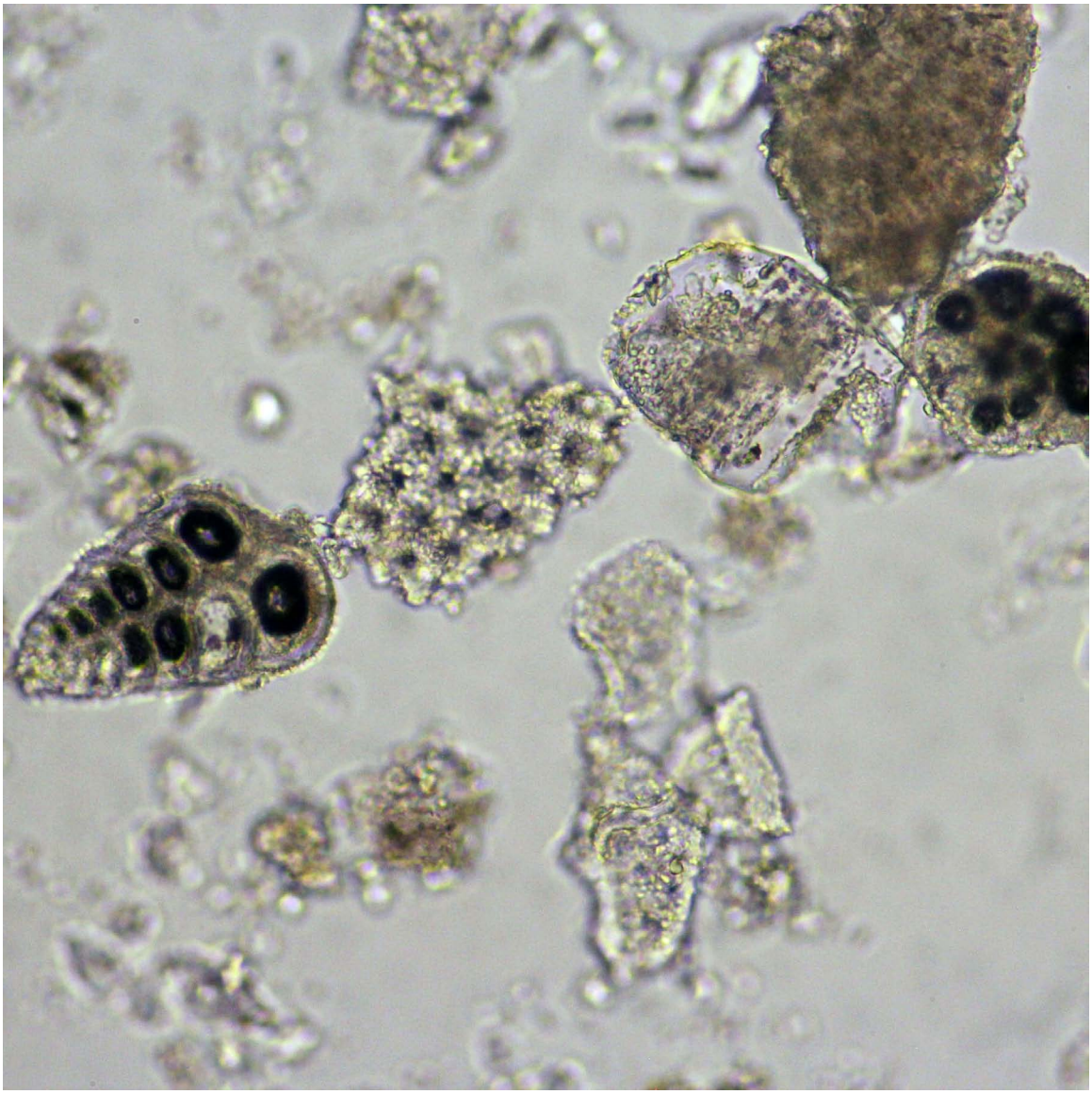

Foram 35.

Calcareous bioclastic sediment with biserial (left) and planispiral (right) planktic foraminifera. Intervening grains are a perforate planktic foraminifer fragment (left) and a semi-rectangular feldspar grain (right).

IODP Sample (late Eocene): Leg 342, Hole 209, Core 18, Section 1, 120 cm

Image ID: B0672/B0673

Foram 36.

The field of view is dominated by a planispiral planktic foraminifer, *Pseudohastigerina*. Note that the sand-sized foraminifera stand above the surrounding finer and less birefringent nannofossil-rich sediment on the slide, which appears out of focus in this view.

ODP Sample (middle Eocene): Leg 122, Hole 673B, Core 6X, Section 4W, 31 cm

Image ID: B0613/B0614

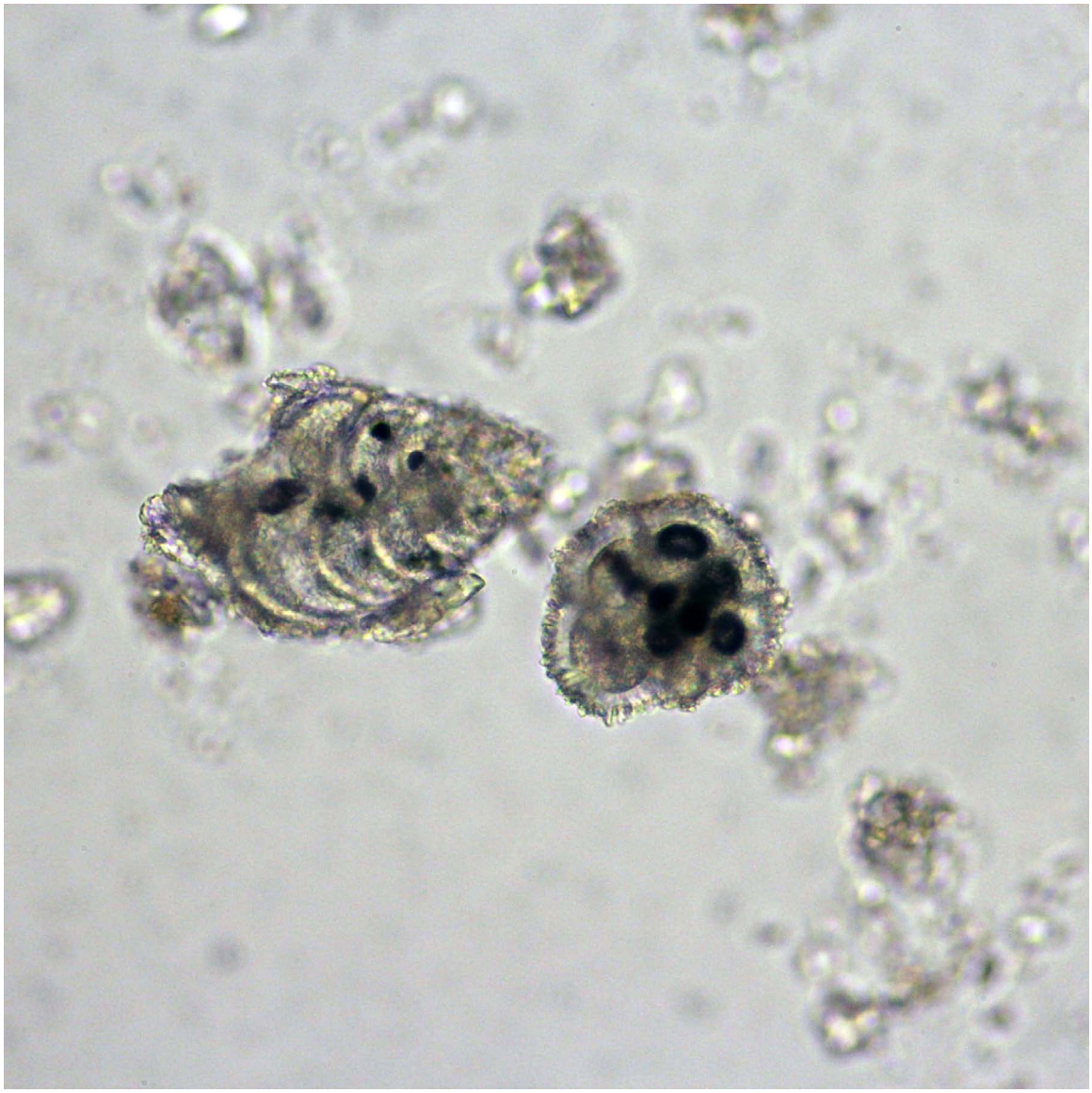

Foram 37.

A biserial benthic foraminifer (left) and a trochospiral planktic foraminifer are shown with darker chambers partly filled by carbonate cement (birefringent) opaque minerals (pyrite) and air bubbles. Note that the sand-sized foraminifera stand above the surrounding finer and less birefringent, nannofossil-rich sediment on the slide, which appears out of focus in this view.

IODP Sample (late Eocene): Leg 342, Hole 209, Core 18, Section 1, 120 cm

Image ID: B0623/B0624

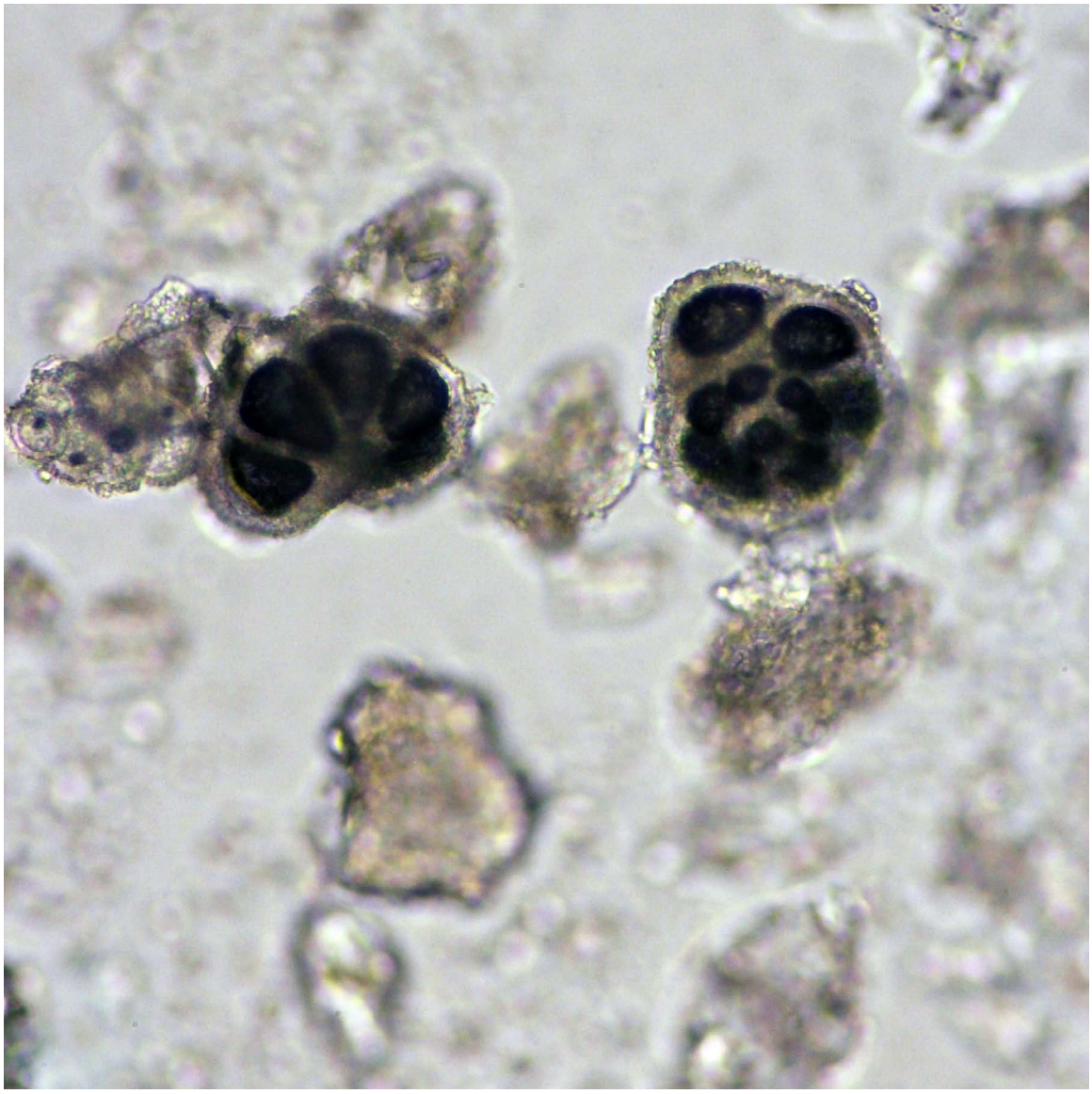

Foram 38.

The focus in this field of view is on two trochospiral benthic foraminifera whose chambers appear dark because of trapped air bubbles. Other, out-of-focus calcareous bioclasts are not identifiable.

IODP Sample (late Eocene): Leg 342, Hole 209, Core 18, Section 1, 120 cm

Image ID: B0545/B0546

Foram 39.

A nannofossil-foraminifer ooze with ribbed calcareous bio-clasts that are likely fragments of the biserial foraminifer.

ODP Sample (Maastrichtian): Leg 198, Hole 1210B, Core 28H, Section 2W, 30 cm

Image ID: B0551/B0552

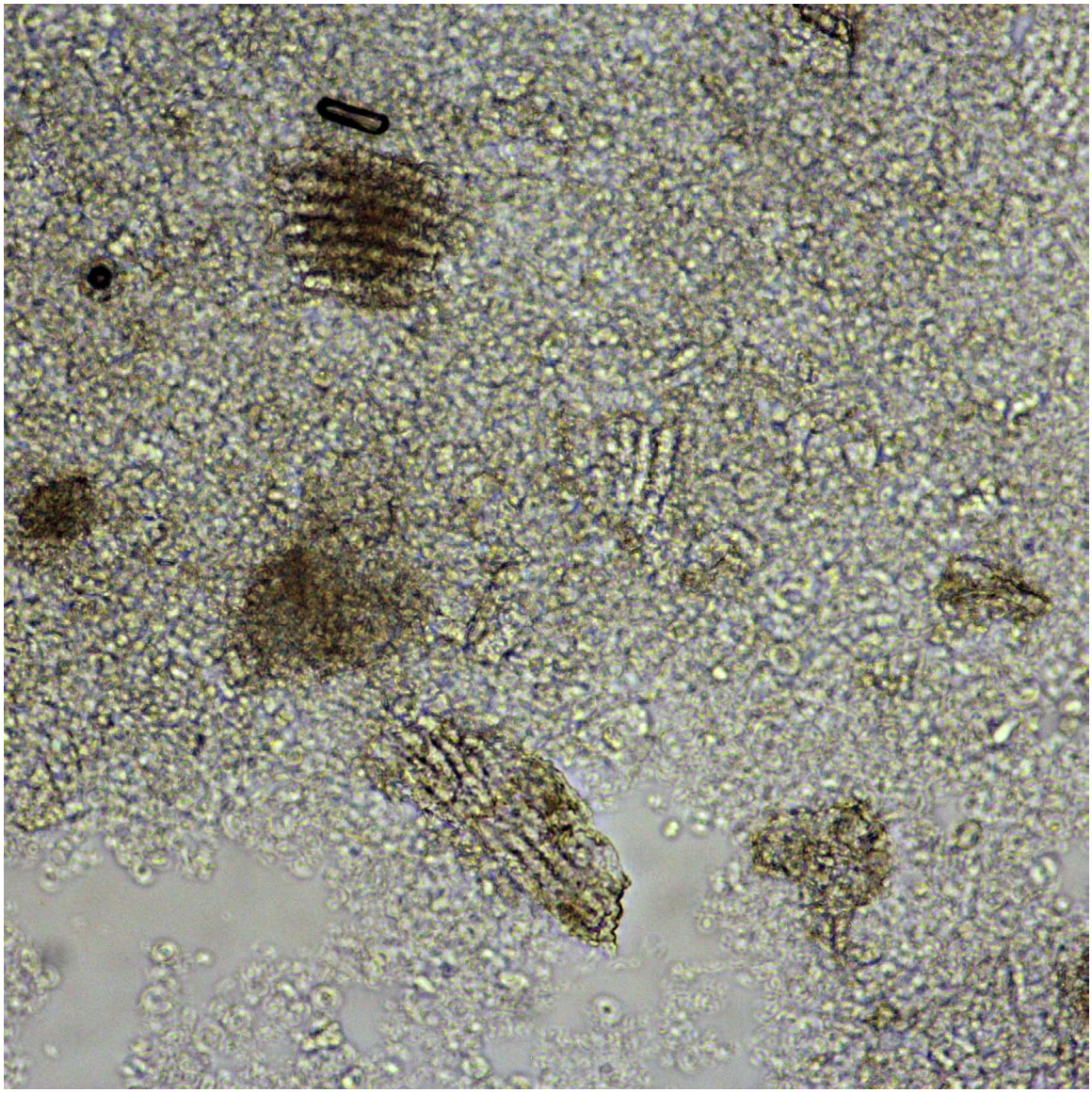

Foram 40.

A larger ribbed fragment of the biserial planktic foraminifer is the focus of this slide, and it is set a mix of nannofossils with other calcareous bioclasts (nannofossil-foraminifer ooze). The smaller nannofossils exhibit lower birefringence and are out of focus.

ODP Sample (Maastrichtian): Leg 198, Hole 1210B, Core 28H, Section 2W, 30 cm

Calcareous Dinoflagellates ("Calcispheres"; Dinocysts)

INTRODUCTION TO CALCAREOUS DINOFLAGELLATES

Overview – Calcareous dinoflagellates are important components of the calcareous phytoplankton in neritic and oceanic settings. The cyst is what is preserved to the rock record, and it typically has an opening (archaeopyle) that was used for excystment. The calcareous walls of the cysts have one or more layers formed by different modes of biomineralization. The Late Jurassic – Cretaceous genus *Pithonella* and Cenozoic genus *Thoracosphaera* (a vegetative/motile stage, not a cyst) are examples. The presence of an operculum-like structure in *Pithonella* reflects the tabulation pattern of dinoflagellates. Calcispheres were near-surface dwellers and are often found in abundance associated with bloom events. The greatest abundance and diversity is in tropical-subtropical waters.

Diagnostic Features – The spherical cysts of calcareous dinoflagellates are typically 10-50 microns in diameter. The Cretaceous calcisphere *Pithonella* has a spherical, elongate, flattened or pyramidal calcareous shell with an apical operculum and apical and antapical pore. They are typically 20-80 μm, up to 180 μm in diameter.

Biology – The calcareous dinoflagellates are a small group of peridinoid dinoflagellates. The calcite crystals in the walls of calcareous cysts are arranged in one of four ways: irregular, radial, oblique, and tangential. Mesozoic *Pithonella* (oblique c-axis crystal orientation) are resting cysts, while *Thoracosphaera* (tangential c-axis crystal orientation) are considered to be the 'shell' of the vegetative (asexual) phase.

Ecology – Autotrophs (or Mixotrophs). Modern calcareous dinoflagellates display species-specific responses to temperature, salinity, upper water column stratification, and nutrient concentration of the photic zone. Some occurrences of calicpheres in the sediment record are associated with bloom events, e.g., *Pithonella* bloom across the Cenomanian-Turonian boundary interval (OAE 2) and *Thoracosphaera* bloom in the basal Danian following the K/Pg boundary mass extinction.

Paleobiogeography – Modern calcareous dinoflagellates are known from all latitudes, and from neritic to oceanic settings. Modern calcareous dinoflagellates experience selective dissolution with increasing water depth, with thinner, more porous forms more prone to dissolution than others. *Pithonella* was common in nearshore and outer shelf to upper slope environments of Tethys and Boreal realms.

Stratigraphic Range – Late Triassic to present.

Key References and Examples:

Bolli, H.M., 1974. Jurassic and Cretaceous Calcisphaerulidae from DSDP Leg 27, eastern Indian Ocean. In, Heirtzler, J.R., Veevers, J.J., et al., Initial Reports of the DSDP, 27:843-907.

Fütterer, D.K., 1978. Distribution of calcareous dinoflagellates in Cenozoic sediments of Site 366, eastern North Atlantic. In, Lancelot, Y., Seibold, E., et al.. Initial Reports of the DSDP, 41:709-737.

Fütterer, D.K., 1984. Pithonelloid calcareous dinoflagellates from the Upper Cretaceous and Cenozoic of the southeastern Atlantic Ocean, DSDP Leg 74. In, Moore, T.C., Jr., Robinowitz, P.D., et al., Initial Reports of the DSDP, 74:533-541.

Gottschling, M., Keupp, H., Plötner, J., Knop, R., Willems, H., and Kirsch, M., 2005. Phylogeny of calcareous dinoflagellates as inferred from ITS and ribosomal sequence data. Molecular Phylogenetics and Evolution, 36: 444-455.

Hart, M.B., 1991. The Late Cenomanian calcisphere global bioevent. Proceedings of the Ussher Society, 7: 413-417.

Hildebrand-Habel, T., and Streng, M., 2003. Calcareous dinoflagellate associations and Maastrichtian-Tertiary climatic change in a high-latitude core (ODP Hole 689B, Maud Rise, Weddell Sea). Palaeogeography, Palaeoclimatology, Palaeoecology, 197: 293-321.

Keupp, H., 1992. Calcareous dinoflagellate cysts from the Lower Cretaceous of Hole 761C, Wombat Plateau, eastern Indian Ocean. In. von Rad, U., Haq, B.U., et al. (Eds.), Proceedings of the Ocean Drilling Program, Initial Report, 122: 497-509.

Kohn, M., and Zonneveld, K.A.F., 2010. Calcification depth and spatial distribution of Thoracosphaera heimii cysts: Implications for palaeoceanographic reconstructions. Deep-Sea Research I, 57: 1543-1560.

Kohring, R., Gottschling, M., and Keupp, H., 2005. Examples for character traits and palaeoecological significance of calcareous dinoflagellates. Paläontologische Zeitschrift, 79(1): 79-91.

Wendler, J., and Willems, H., 2002. Distribution of calcareous dinoflagellate cysts across the Cretaceous-Tertiary boundary (Fish Clay, Stevns Klint, Demark): Implications for our understanding of species-selective extinction. In Koeberl, C., and MacLeod, K.G., eds., GSA Special Paper, 356: 265-275.

Wendler, J.E., Wendler, I., and Huber, B.T., 2013. Revision and evaluation of the systematic affinity of the calcitarch genus Pithonella based on exquisitely preserved Turonian material from Tanzania. Journal of Paleontology, 87(6):1077-1106.

Zonneveld, K.A.F., Meier, K.J.S., Esper, O., Siggelkow, D., Wendler, I., and Willems, H., 2005. The (palaeo-)environmental significance of modern calcareous dinoflagellate cysts: a review. Paläontologische Zeitschrift, 79(1):61-77.

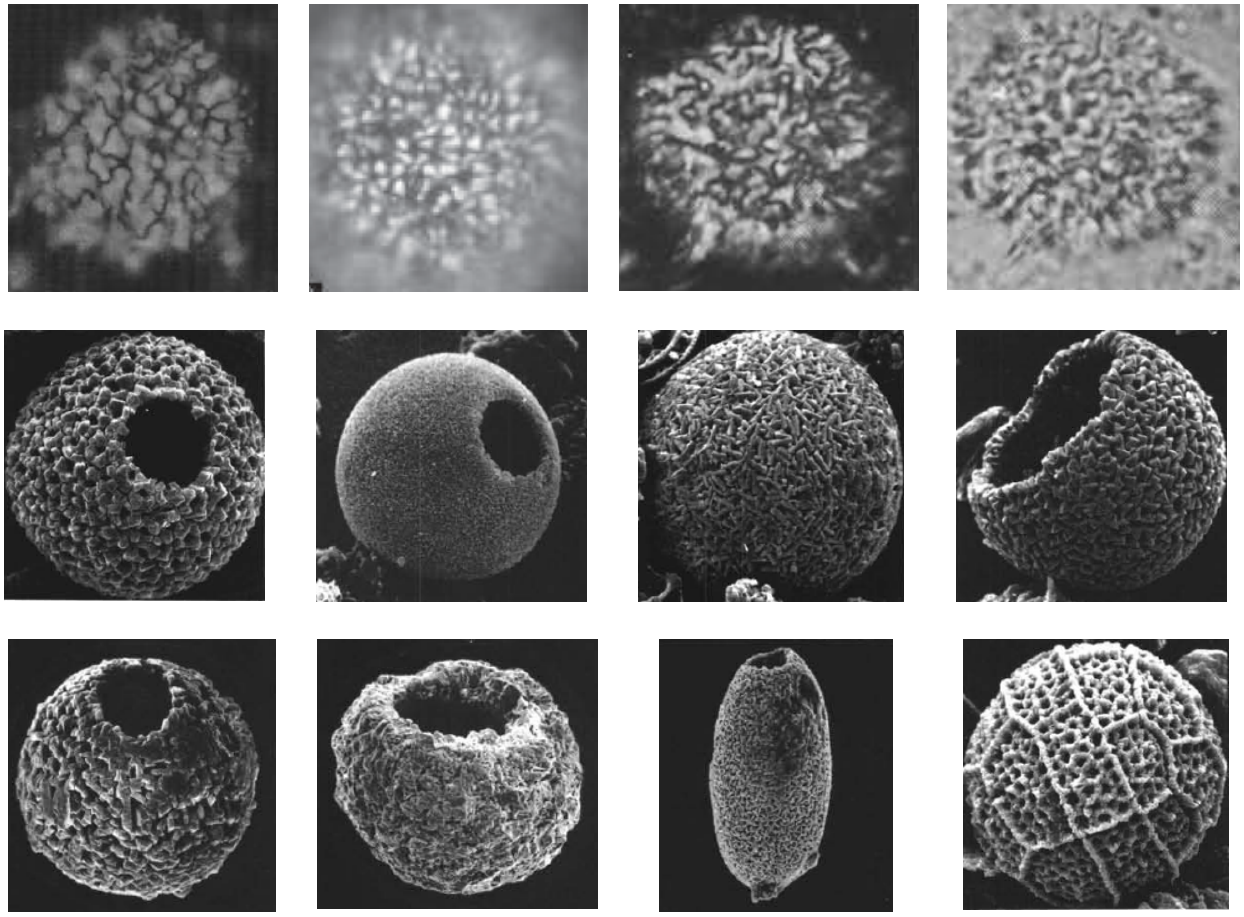

Representative Mesozoic and Cenozoic calcareous dinoflagellates ('calcispheres'). Top row: *Thoracosphaera* sp., 'calcisphere', *Thoracosphaera* cf. *T. saxea*, same specimen (plain light). Second row: *Thoracosphaera heimi, Thoracosphaera granifera, Thoracosphaera tesserula, Thoracosphaera tuberosa*. Bottom row: *Pithonella carterii, Pithonella helentappanae, Pithonella krasheninnikovi, Clciodinellum operosum*. Light microscope photomicrographs (top row) from Wei and Pospichal, 1991; Bown, 2005; Siesser, 1980. SEM images from Bolli, 1974; Fütterer, 1978.

Calcareous Dinoflagellates (“Calcispheres”; Dinocysts)

Calcisphere 1

Calcisphere 2

Calcisphere 3

Calcisphere 4

Calcisphere 5

Calcisphere 6

Image ID: B0617/B0618

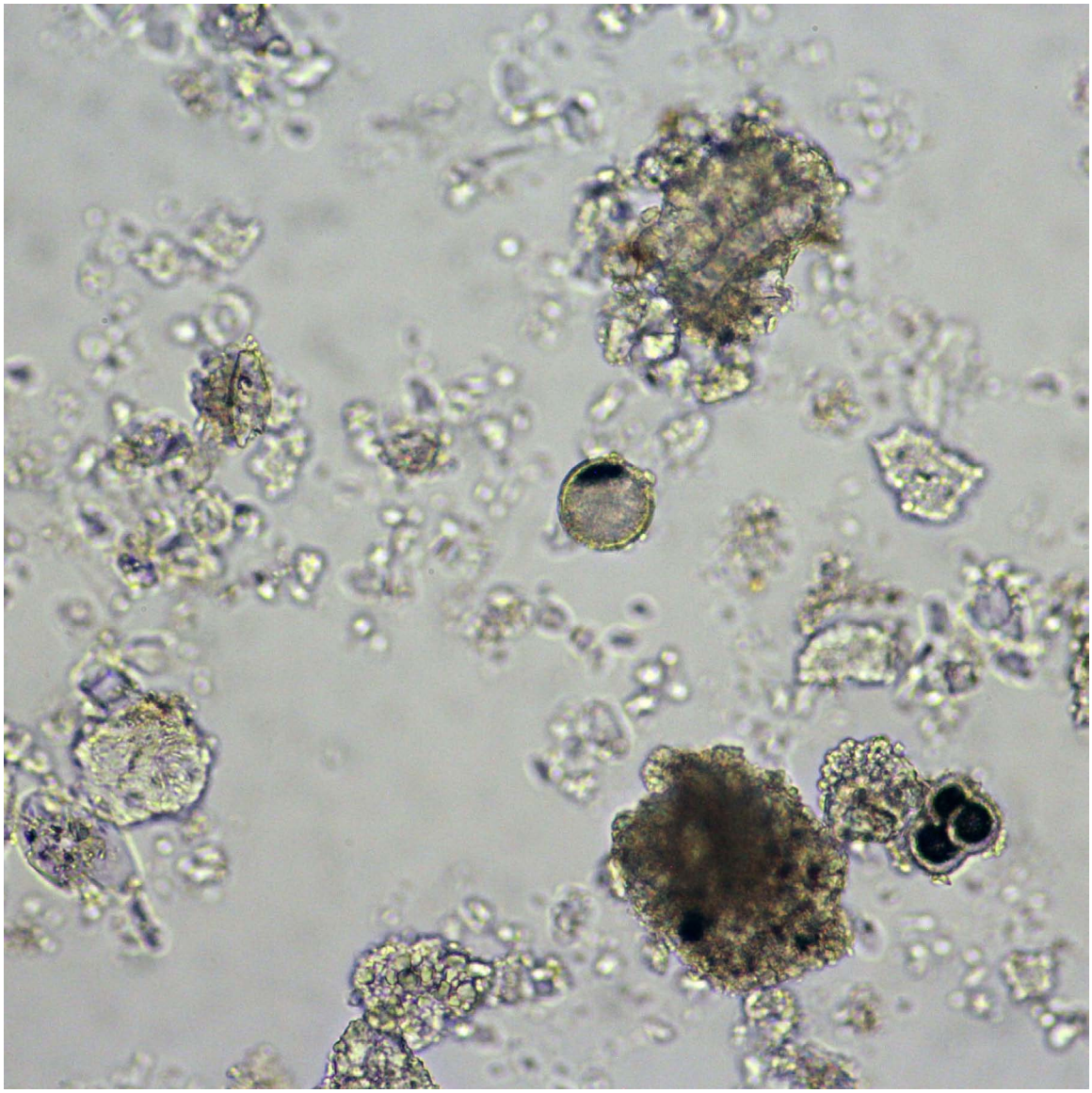

Calcisphere 1.

This field of view is roughly centered on a thin-walled, circular, calcisphere (cyst of a calcareous dinoflagellate) partly filled with opaque (pyrite? Bubble?) and carbonate materials. Other carbonate debris includes foraminifera and micrite that are hard to distinguish because they are mostly out of focus. Note the different birefringence from chambers of planktic foraminifera, which have a distinctive cross extinction pattern not observed in calcispheres.

IODP Sample (late Eocene): Leg 342, Hole 209, Core 18, Section 1, 120 cm

Image ID: B0640/B0641

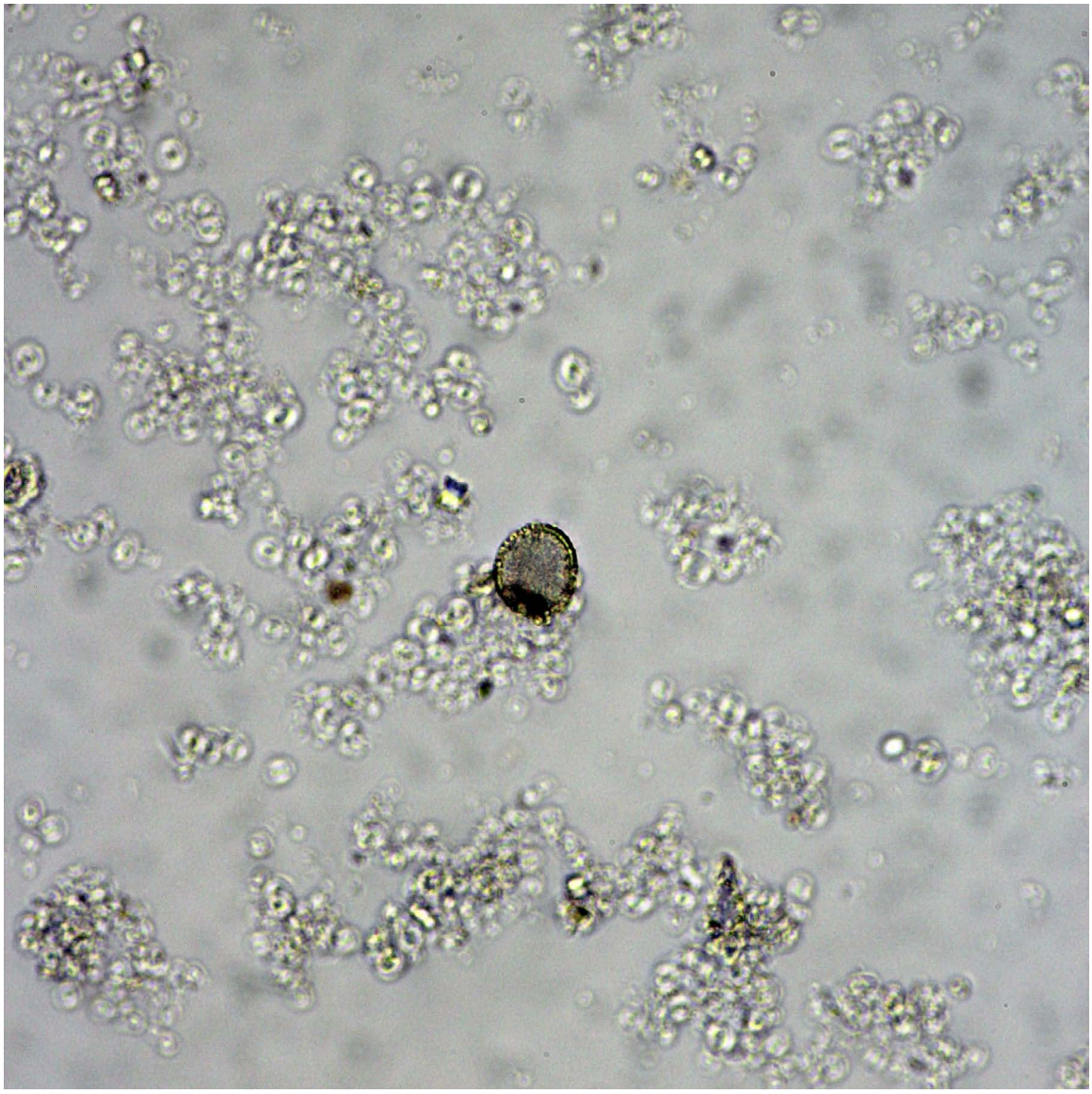

Calcisphere 2.

This field of view is roughly centered on a thin-walled, circular, calcisphere (cyst of a calcareous dinoflagellate) in nannofossil ooze. The calcisphere (in focus) is notably darker than the circular coccoliths that surround it (out of focus).

ODP Sample (Paleocene):Leg 208, Hole 1267A, Core 27X, Section 3W, 53 cm

Image ID: B0714/B0715

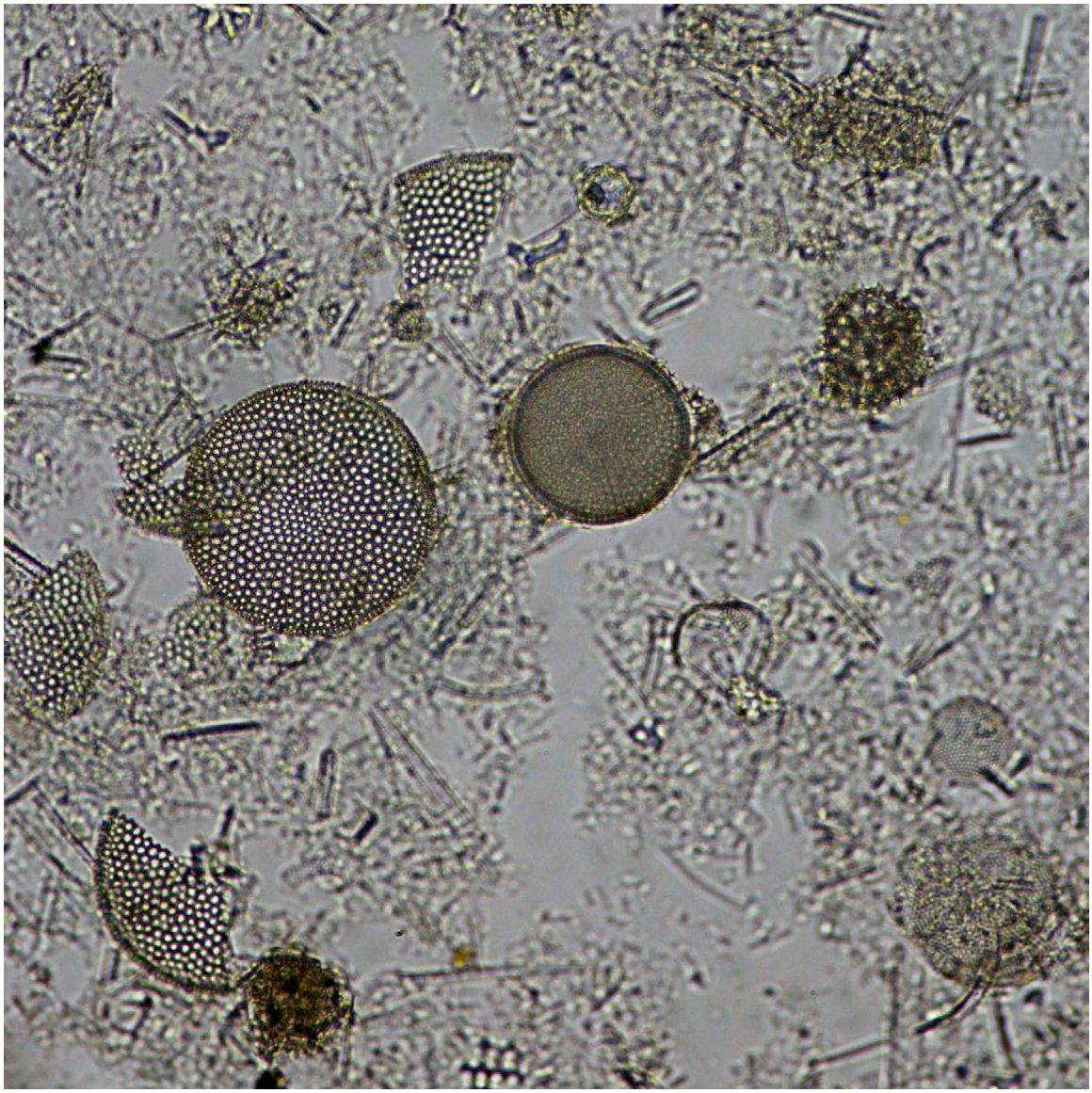

Calcisphere 3.

This mixed siliceous/calcareous ooze contains one carbonate-filled calcareous dinoflagellate that exhibits an aperature (circled). Other calcareous nannofossils and siliceous debris are hard to distinguish because they are mostly out of focus.

DSDP Sample (late Miocene): Leg 38, Hole 847B, Core 21X, Section 3W, 10 cm

Image ID: B0670/B0671

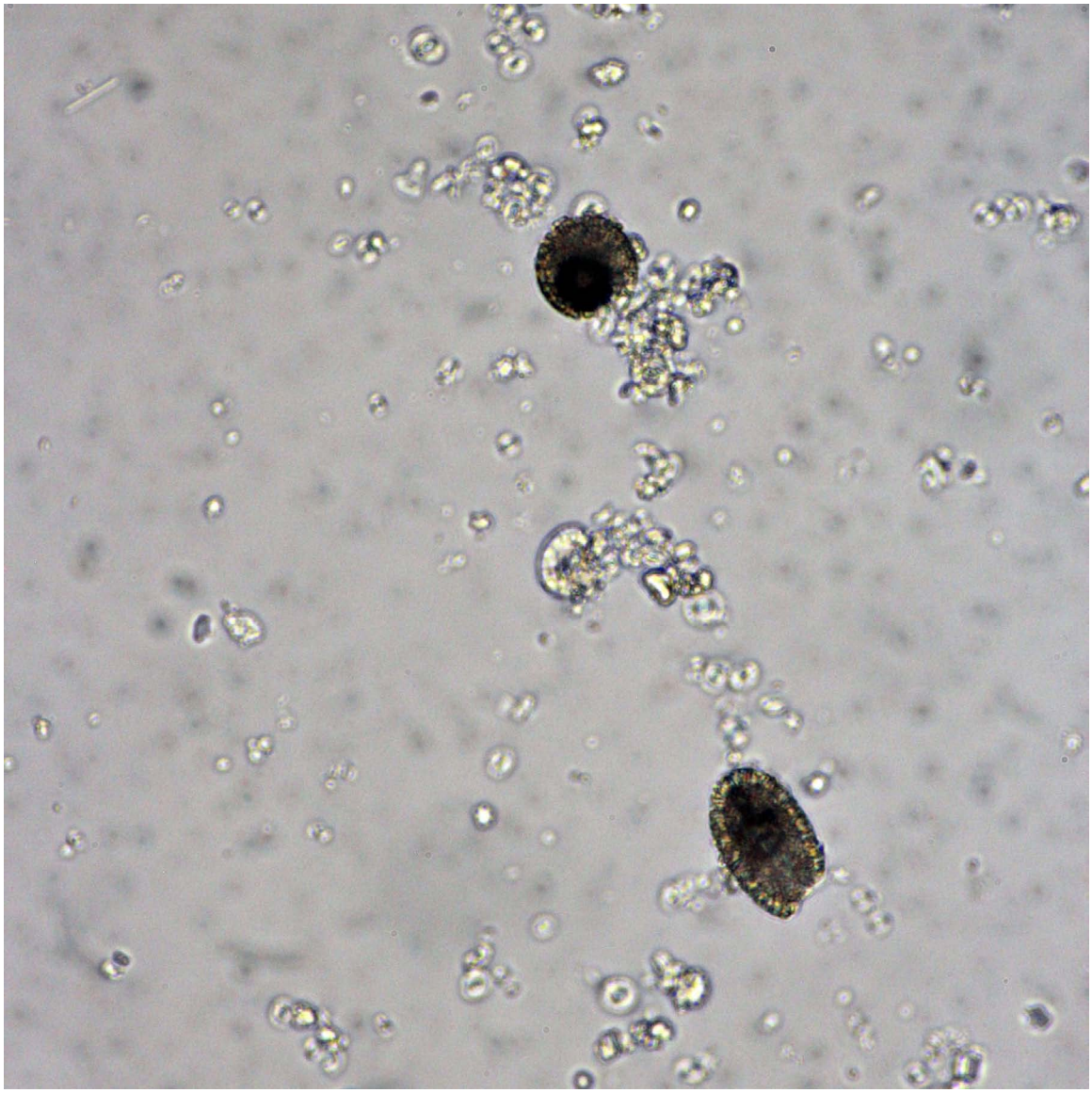

Calcisphere 4.

This nannofossil ooze contains two darker, carbonate-filled, thin-walled calcispheres (cysts of a calcareous dinoflagellate), one round and the other oval, each a different species.

ODP Sample (middle Eocene): Leg 122, Hole 763B, Core 6X, Section 4W, 31 cm

Image ID: B0644/B0645

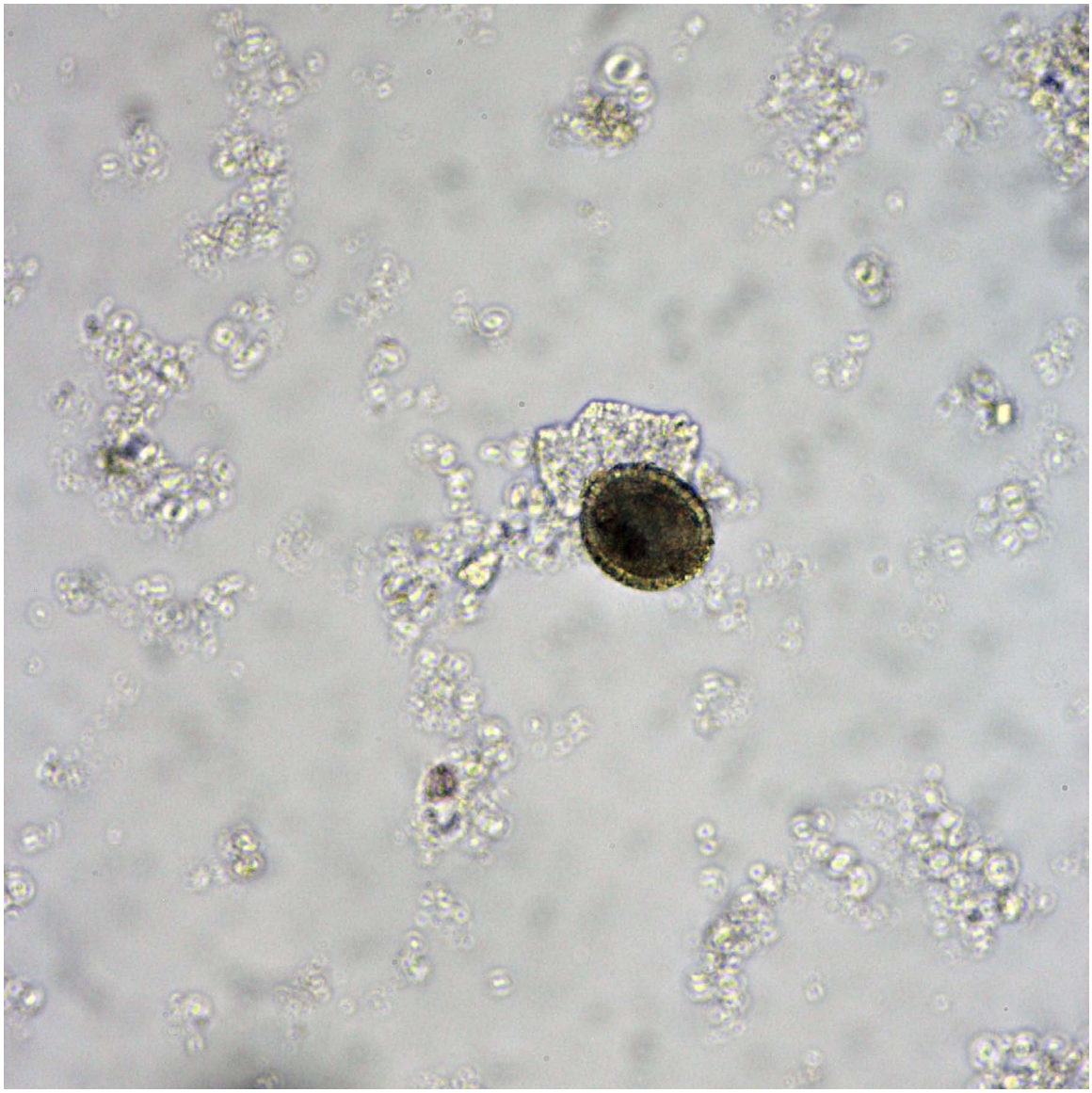

Calcisphere 5.

This field of view is roughly centered on a thin-walled, circular, calcisphere (cyst of a calcareous dinoflagellate), possibly a Thoracosphaera, set in nannofossil ooze. The calcisphere (in focus) is notably darker than the circular coccoliths and other bioclastic debris that surround it (out of focus).

ODP Sample (Paleocene): Leg 208, Hole 1267A, Core 27X, Section 3W, 53 cm

Image ID: B0695/B0696

Calcisphere 6.

This field of view is roughly centered on a circular, calcisphere (cyst of a calcareous dinoflagellate) in nannofossil ooze.The calcisphere (in focus) is notably darker than the circular coccoliths that surround it (out of focus). Also note that this specimen does not have a distinct wall structure, unlike other examples.

ODP Sample (late Eocene): Leg 130, Hole 807C, Core 24R, Section 2W, 35 cm

Calcareous Sponge Spicules

INTRODUCTION TO SPONGES (SILICEOUS AND CALCAREOUS SPICULES)

Overview – Sponges are benthic multicellular animals consisting of a highly porous matrix that allows water to circulate through their bodies. They live attached to the seafloor. Mesohyl is the gelatinous matrix of sponges, consisting of collagen and other polypeptides; spongin is a fibrous collagen protein that provides an internal flexible framework. Many sponges precipitate siliceous (opaline) or calcareous (calcium carbonate) spicules within the mesohyl that provide additional structural support. Sponges with mineralized spicule skeletons can contribute marine sediment in the form of discrete sand-to-silt-size spicules when upon death of the organisms, they decompose and disaggregate.

Diagnostic Features – Amorphous silica (opaline) sponge spicules form around an axis of organic material optically visible as an axial tube in fossil varieties. This axial structure is less defined in the crystalline calcareous spicules, which are surrounded by an organic membrane during growth. In the calcareous spicules, the carbonate is Mg-calcite precipitated as single crystals that exhibit uniform optic orientation when viewed with a petrographic microscope in smear slide and thin section. It is notable that the calcareous spicules break isotropically rather than along mineral cleavage planes as a function of their submicroscopic structure. Calcareous spicules are smooth and range in size from 0.1-10 mm. They are described in terms of the number of axes (-axon) or rays (-actine or -actinal). Siliceous spicules are morphologically more variable. They are described in terms of the number of axes or rays, as well as spicule size, shape and ornamentation. The pointed spicule rays are defined by growth direction. The number of rays can vary from one or two (monoaxon), three (triaxon), to four (tetraxon) or more (polyaxon) and aerose where the rays diverge from a central point. The prefix “acantho-“ is used when the spicule surface is spined. Varieties can be shaped like the letters C or S (sigmas), bow-shaped (toxons), rounded at both ends (strongyles), or knobbed at one or both ends (tylostyle).

Biology – Phylum Porifera

Ecology – Heterotrophs. Sponges occur in freshwater, brackish, and marine environments at all latitudes and water depths, from intertidal to abyssal. Calcareous sponges are more common in warmer, shallower waters.

Stratigraphic Range – Neoproterozoic to present.

Key References and Examples:

Albach, W.J., and McCartney, K., 1992. Siliceous sponge spicules from Site 748. In, Wise, S.W., Jr., Schlich, R., et al., Proceedings of the ODP, Scientific Results, 120: 833-837.

Bergquist, P.R. 1978. Sponges. Hutchinson: London & University of California Press: Berkeley & Los Angeles: 268 p.

Ivanik, M.M., 1983. Paleogene and Neogene sponge spicules from Sites 511, 512, and 513 in the South Atlantic. Initial Reports Deep Sea Drilling Project, 71: 933-950.

McCartney, K., 1987. Siliceous sponge spicules from DSDP Leg 93. In, Van Hinte, J.E., Wise, S.W., Jr., et al., Initial Reports DSDP, 93:815-824.
Palmer, 1988.
Sethmann, I., and Wörheide, G., 2008. Structure and composition of calcareous sponge spicules: A review and comparison to structurally related biominerals. Micron, 39:209-228.

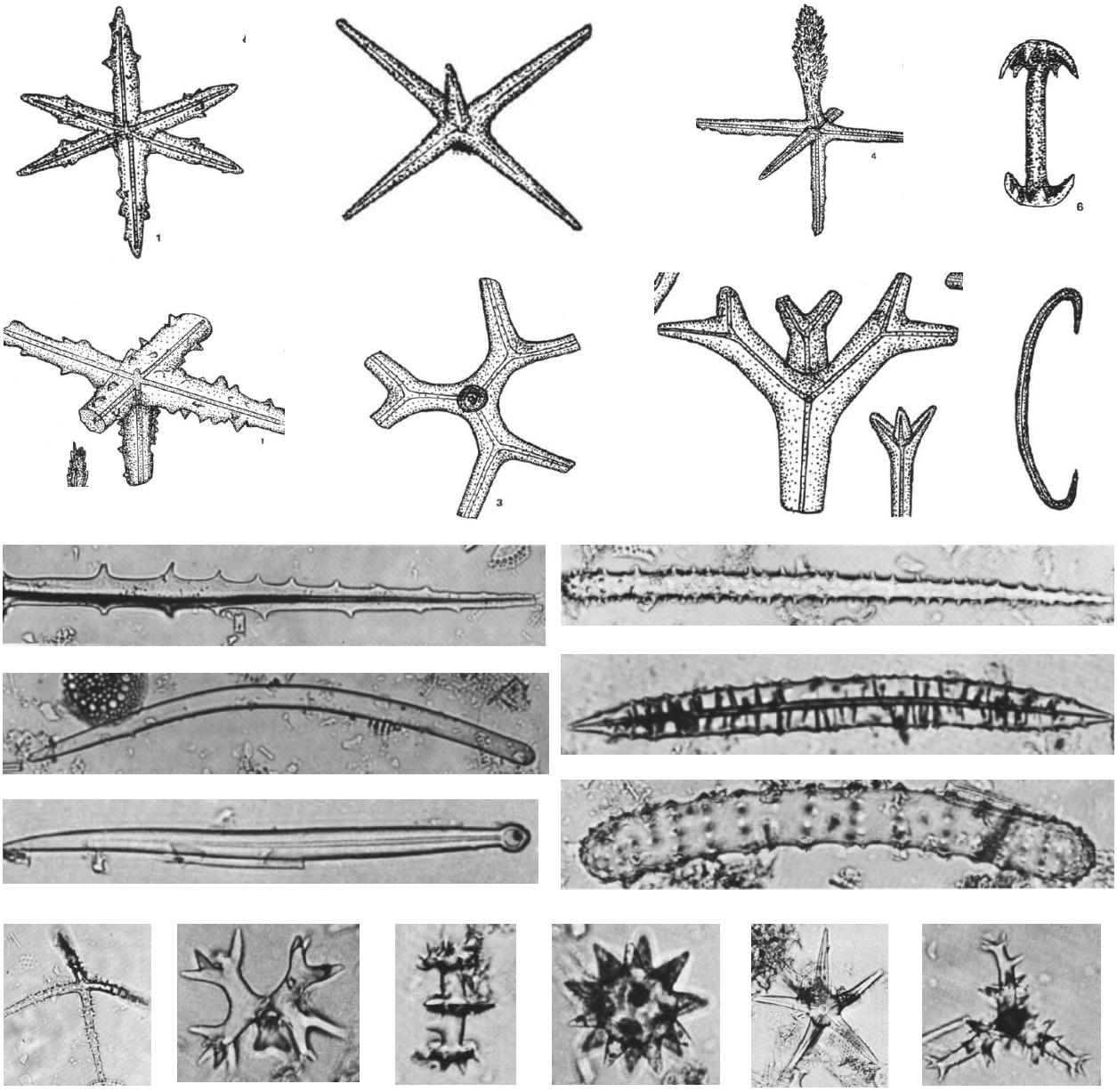

Representative Cenozoic sponge spicules. Top row: Oxyhexactine, thorned; Hexactine; Pinulus; Amphidiscus. Second row: Pentactine; Orthodichotriaenes; Plagiodichotriaenes; Sigma. Third row: ‘serrated spine’, ‘acanthostyle’. Fourth row: ‘syle’, ‘acanthoxea’. Fifth row: ‘tylostyle’, ‘anthrostrongyle’. Bottom row: ‘hexactine’, ‘streptaster’, ‘discorhabd’, ‘spheraster’, ‘oxyaster’, ‘caltrops’. Camera ludida drawings from Ivanik, 1983; Photomicrographs from McCartney, 1987.

Calcareous Sponge Spicules

Calcite spicule 1

Calcite spicule 2

Calcite spicule 3

Calcite spicule 4

Image ID: 0152/0153

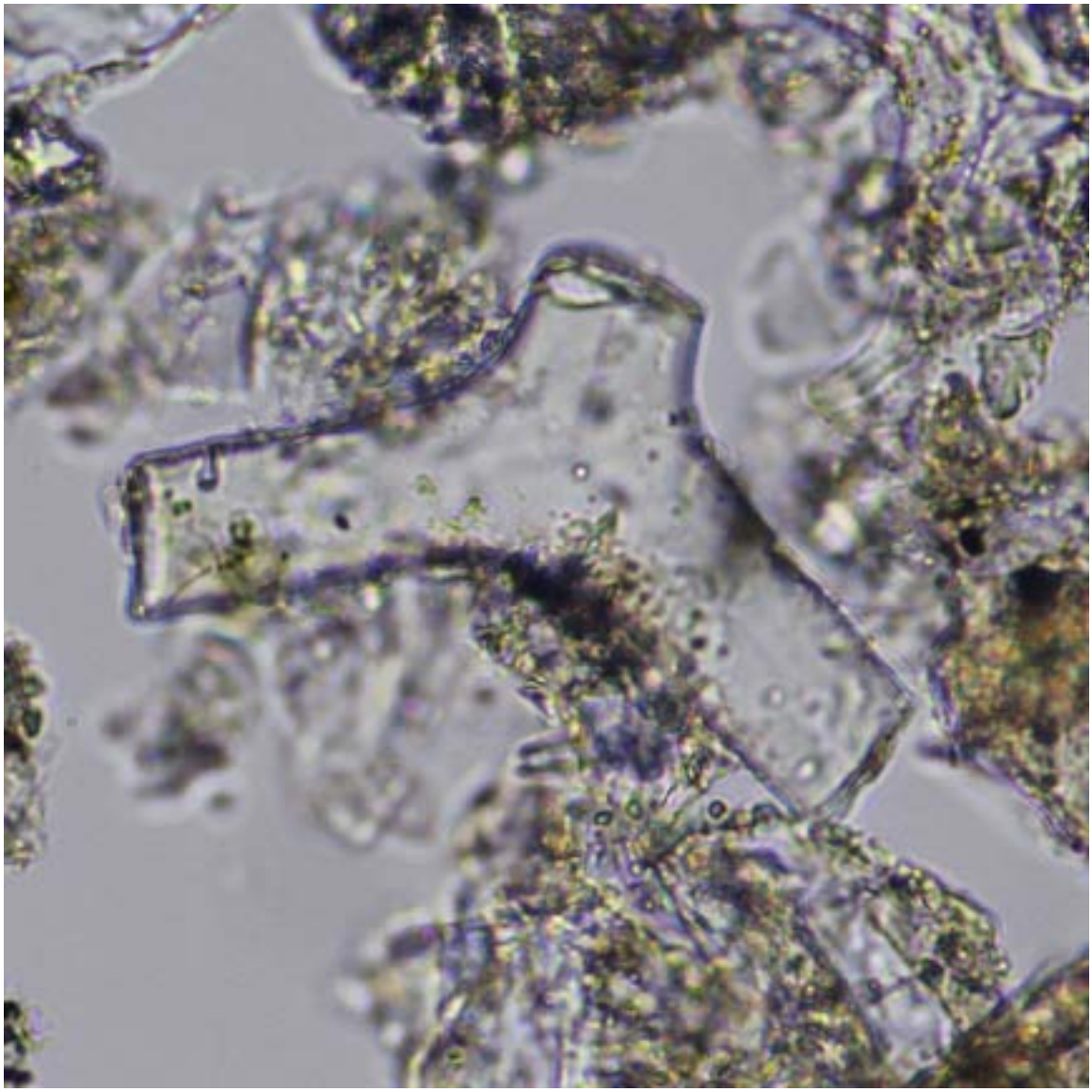

Calcite spicule 1.

Calcareous triaxon sponge spicule where three arms (rays) radiate from a center of origin. Each of the arms (originally pointed?) has broken off along a planar surface, to produce this y-shaped fragment. The single-crystal carbonate mineralogy is evident by the higher and uniform birefringence when polars are crossed. The surrounding material is largely siliceous debris.

IODP Sample (Pleistocene-Holocene): Leg 317, Hole 1352B, Core 11H, Section 2W, 21 cm

Image ID: 0154/0155

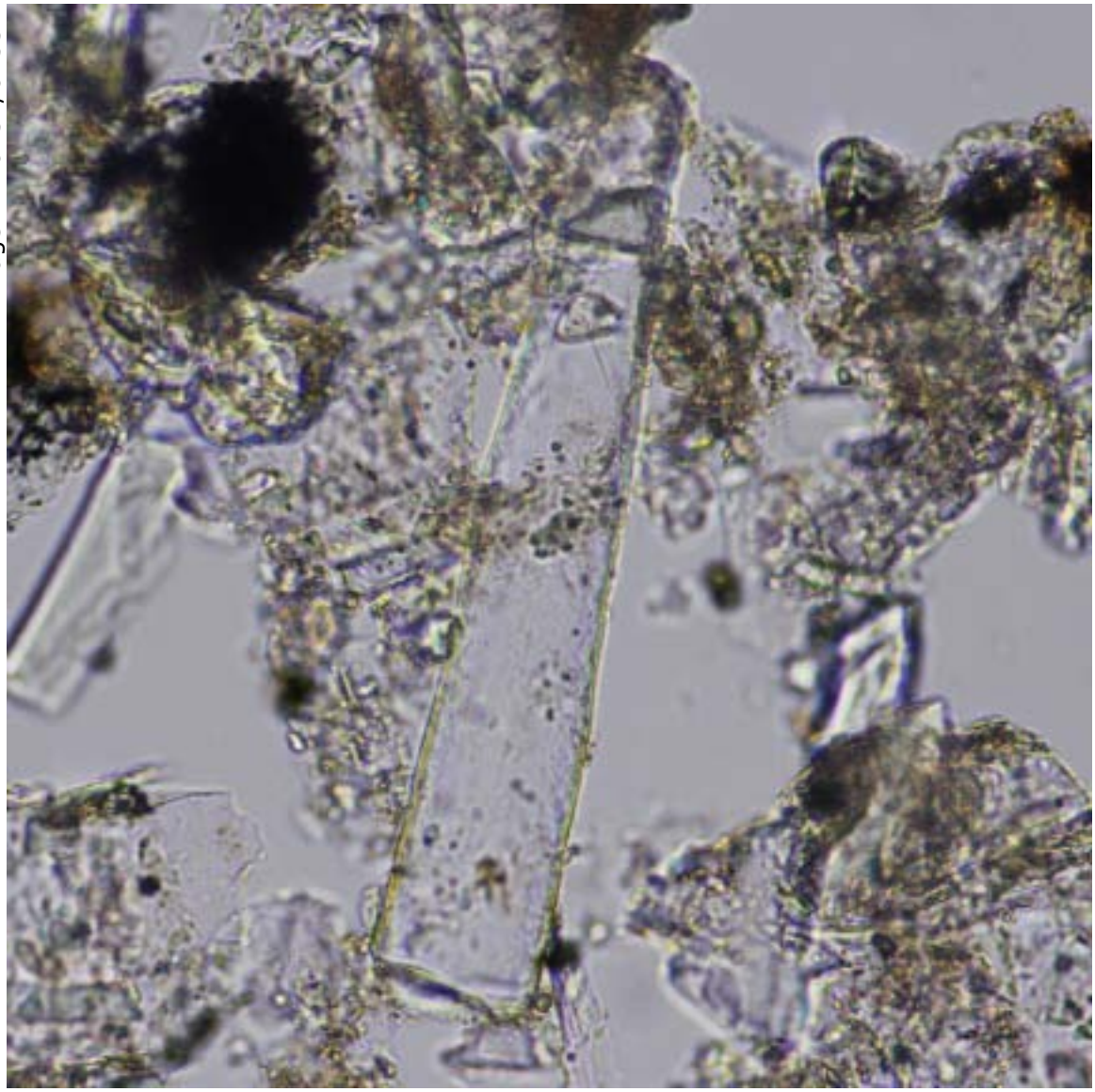

Calcite spicule 2.

A tapered, broken calcite sponge spicule, dominates this field of view. The single-crystal carbonate mineralogy is evident by the higher and uniform birefringence when polars are crossed. The surrounding material is largely siliceous terrigenous debris (clay and silt).

IODP Sample (Pleistocene-Holocene): Leg 317, Hole 1352B, Core 11H, Section 2W, 21 cm

Image ID: 0327/0328

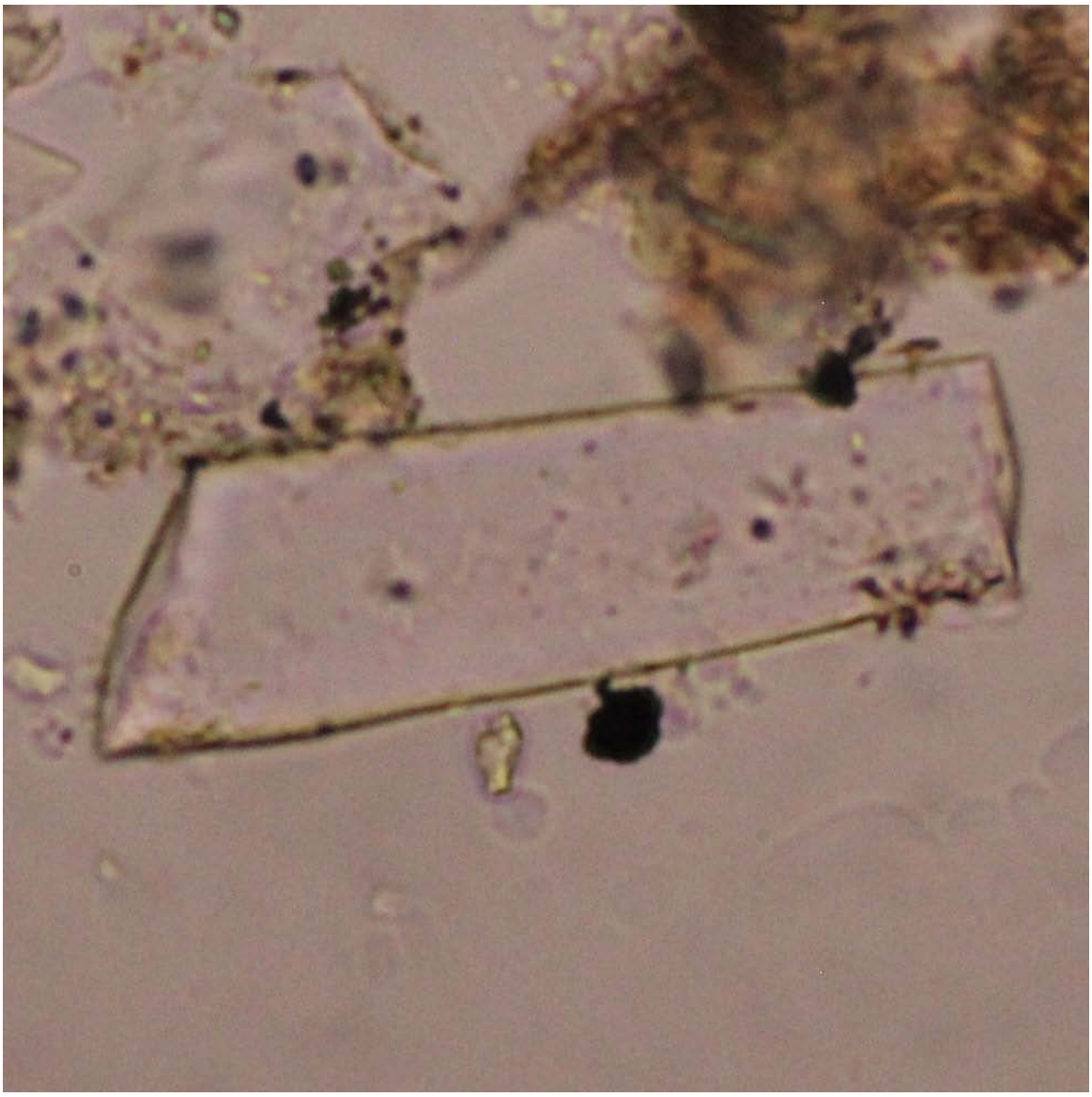

Calcite spicule 3.

Fragment of calcite sponge spicule showing characteristic birefringence and single-crystal optic orientation when polars are crossed. Note that fragment is broken at each end but slightly tapers to the right. Contrast the smooth form of the spicule with the irregular mollusk prism shown in the Mollusk or Bioclast section (check where it ends up?).

ODP Sample (late Pleistocene): Leg 181, Hole 1119C, Core 6H, Section 1W, 43 cm

Image ID: 0320/0321

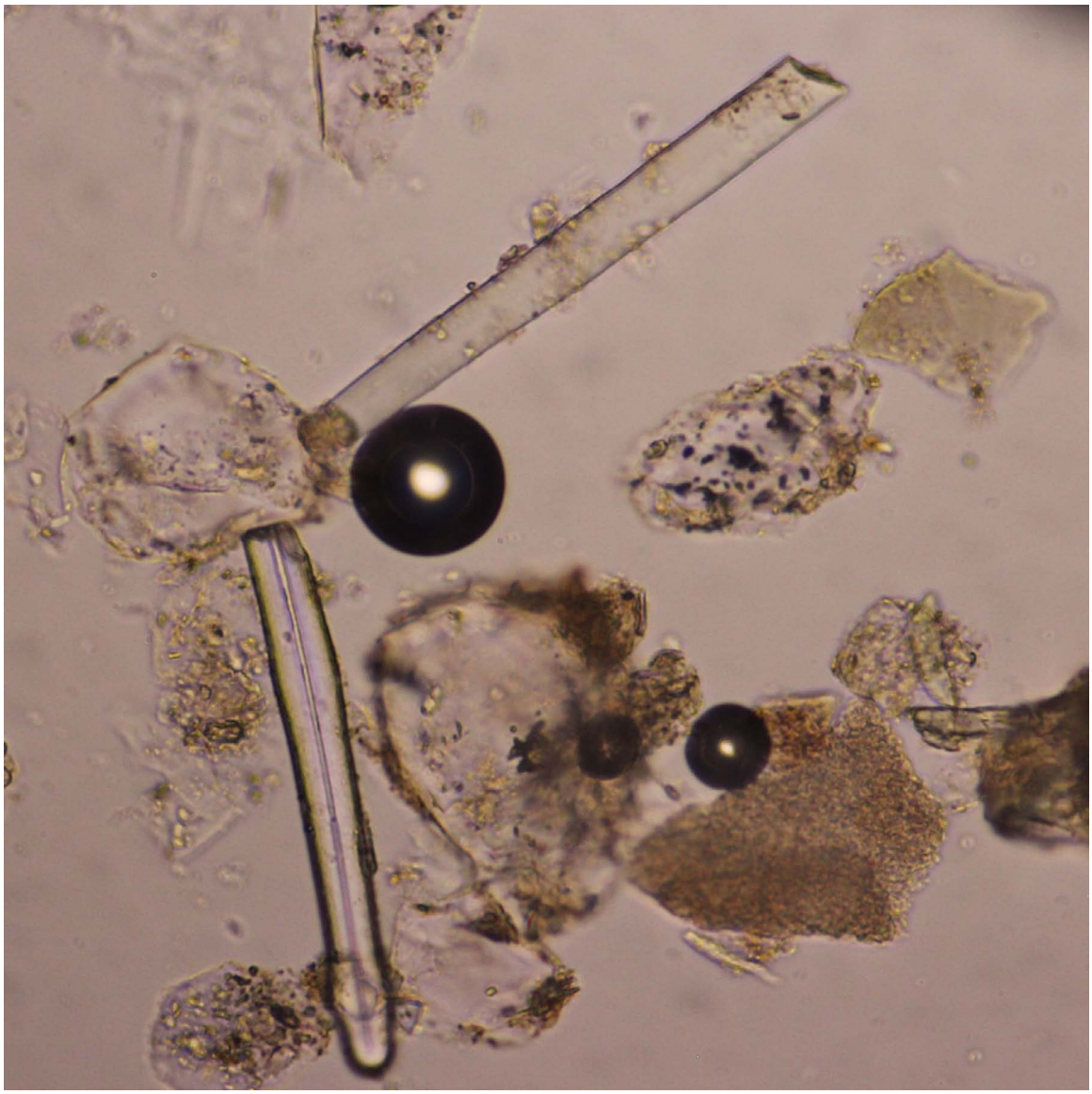

Calcite spicule 4.

Mixed sandy sediment with two linear (monaxon?) sponge spicule fragments, one calcareous (high birefringence) and another siliceous (opaline – isotropic, no birefringence). The siliceous spicule has an axial hollow canal; one end is broken (planar) and the other has a knobbed tip (tylostyle). Both ends of the calcareous spicule are broken but it tapers slightly along its length. As these are fragments, it is impossible to say whether they are monoaxon or not. Other grains in the field of view include quartz and clay-rich lithic fragments.

ODP Sample (late Pleistocene): Leg 181, Hole 1119C, Core 6H, Section 1W, 43 cm

Pteropods

INTRODUCTION TO PTEROPODS

Overview – Planktic gastropods, so-called “sea butterflies”, with shells of aragonite.

Key References:

Bé, A.W.H., and Gilmer, R.W., 1977. A zoogeographic and taxonomic review of euthecosomatous pteropoda. In Ramsey, A.T.S. (Ed.), Oceanic Micropaleontology, 1: 733-808.

Herman, Y., 1978. 5: Pteropods. In Haq, B.U., and Boersma, A. (Eds.), Introduction to Marine Micropaleontology: Elsevier, 151-159

Pteropod 1

Pteropod 2

Image ID: B0329/B0330

Pteropod 1

An elongate pteropod(?) shell dominates the field of view. The very thin shell shows carbonate birefringence when polars are crossed. The dark interior of shell results from air bubbles. The surrounding mud is dominated by nannofossils, most of them very small, with terrigenous clay and silt, orange-brown algal organic matter, and traces of siliceous debris.

ODP Sample (Quaternary): Leg 167, Hole 1014A , Core 1H, Section 2W, 120 cm

Image ID: B0343/B0344

Pteropod 2

The dark interior of the round pteropod(?) shell in the center of the field of view results from air bubbles. The very thin shell shows carbonate birefringence when polars are crossed. The surrounding mud is dominated by terrigenous clay and silt; nannofossils, most very small; and orange-brown organic(?) matter.

ODP Sample (Quaternary): Leg 167, Hole 1015A, Core 25X, Section 2W, 60 cm

Ostracods

INTRODUCTION TO OSTRACODS

Overview – Ovate to kidney-shaped bivalved crustaceans; most are benthic but there are planktic species. Widely distributed in fresh water, estuarine, neritic and deep-sea environments.

Key References:

Pokorny, V., 1978. 4: Ostracodes. In Haq, B.U., and Boersma, A. (Eds.), Introduction to Marine Micropaleontology: Elsevier, 109-149.

Web Resources:
http://www.ucl.ac.uk/GeolSci/micropal/ostracod.html

Ostracod 1

Ostracod 2

Image ID: B0541/B0542

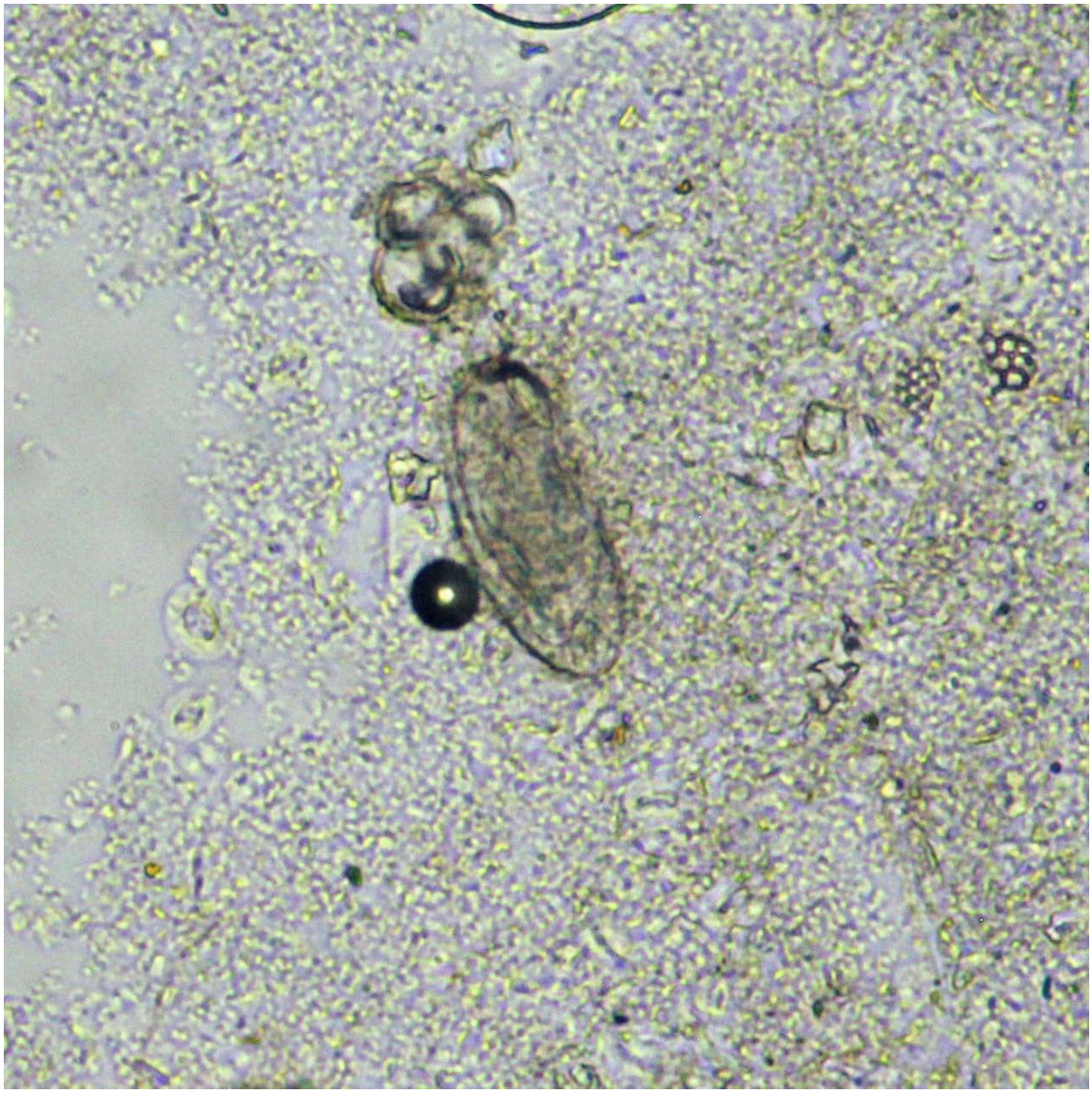

Ostracod 1.

This elongate oval carbonate shell may be an ostracod or a juvenile foraminifer.

ODP Sample (late Pliocene to Pleistocene): Leg 198, Hole 1210B, Core 1H, Section 4W, 50 cm

Image ID: xxx

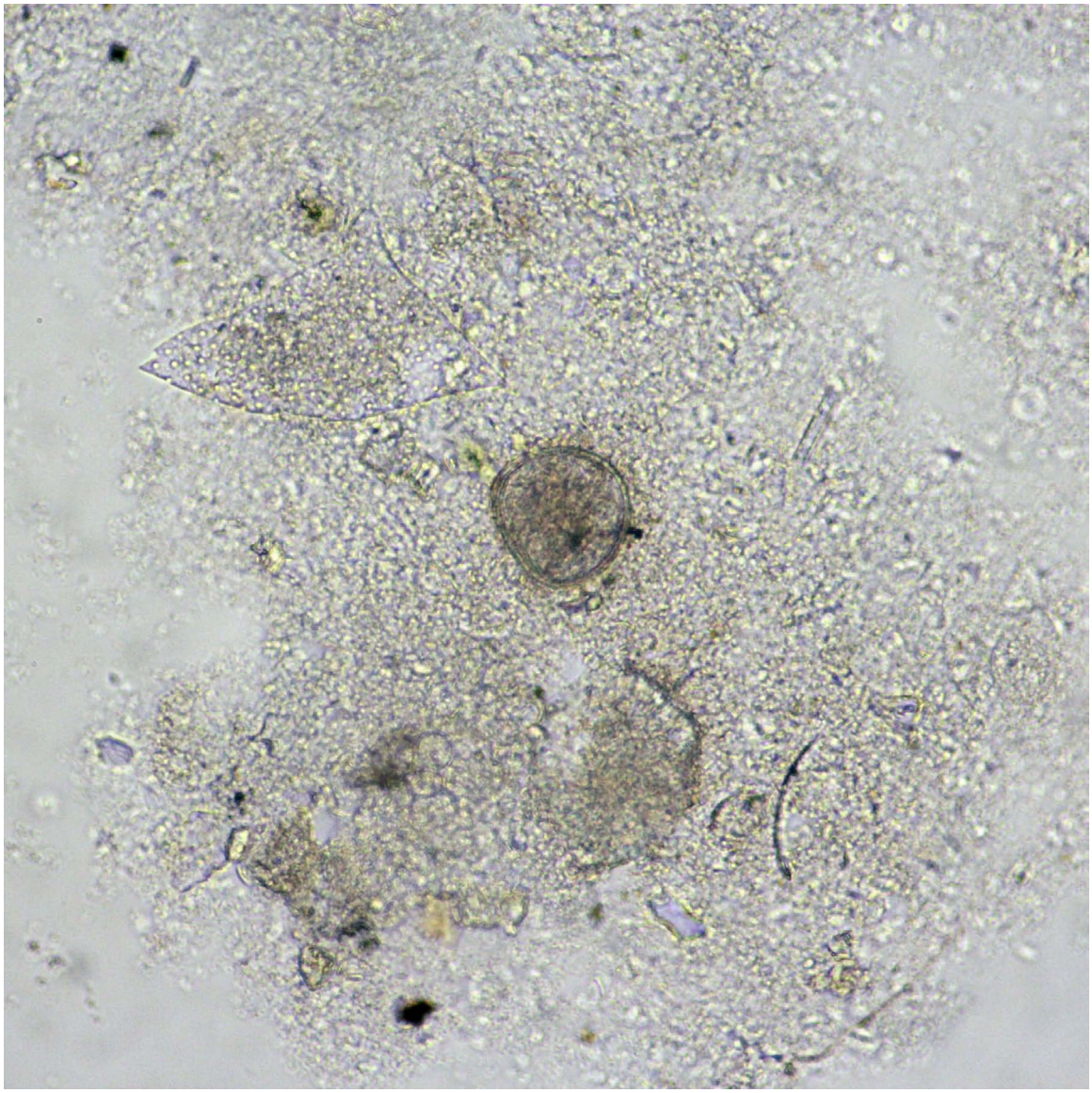

Ostracod 2.

This oval carbonate shell may be an ostracod.

ODP Sample (late Pliocene to Pleistocene): Leg 198, Hole 1210B, Core 1H, Section 44W, 50 cm

Otoliths

INTRODUCTION TO OTOLITHS

Overview – Otoliths are calcareous concretions in the inner ear of ray-finned (teleost) fishes. As summarized by Woydack and Morales-Nin (2001), they are mainly composed of aragonite with minor organic matrix with rhythmic growth zonations at macroscopic to microscopic scales. Their mineralogy makes them prone to diagenetic alteration. Otoliths provide information on fish growth structure and paleoecology. They are common Cenozoic fossils but range back into the Jurassic (e.g., Patterson, 1999).

Key References:

Nolf, D., 1995. Studies on fossil otoliths-the state of the art. in D. Secor, J. M. Dean, and S. Campana, eds. Recent developments in fish otolith research. University of South Carolina Press, Columbia, p. 513-544.

Patterson, W.P., 1999, Oldest isotopically characterized fish otoliths provide insight to Jurassic continental climate of Europe, Geology, v. 27, p. 199-202.

Woydack, A., and Morales-Nin, B., 2001, Growth patterns and biological information in fossil fish otoliths. Paleobiology, v. 27, p. 369-378.

Otolith 1

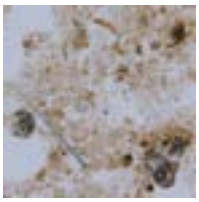

Otolith 2

Image ID: B0331/B0332

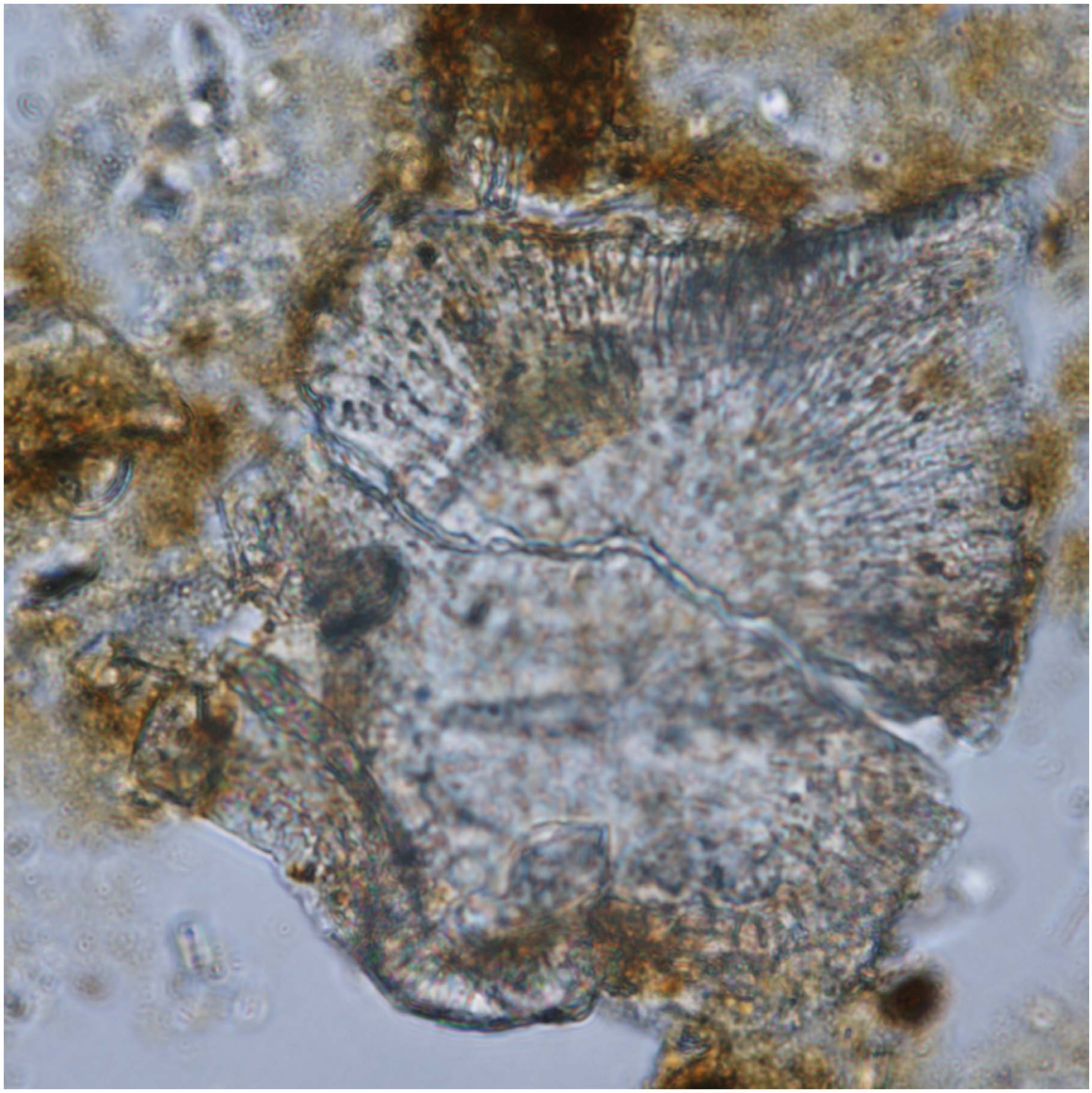

Otolith 1.

Possible fish otolith (calcareous mass referred to as an ear bone or stone). It has an irregular form and shows micro-pores, but not the age rings or banding that would suggest it came from an older fish.

ODP Sample (Quaternary): Leg 167, Hole 1014A, Core 1H, Section 2W, 120 cm

Image ID: B0339/B0340

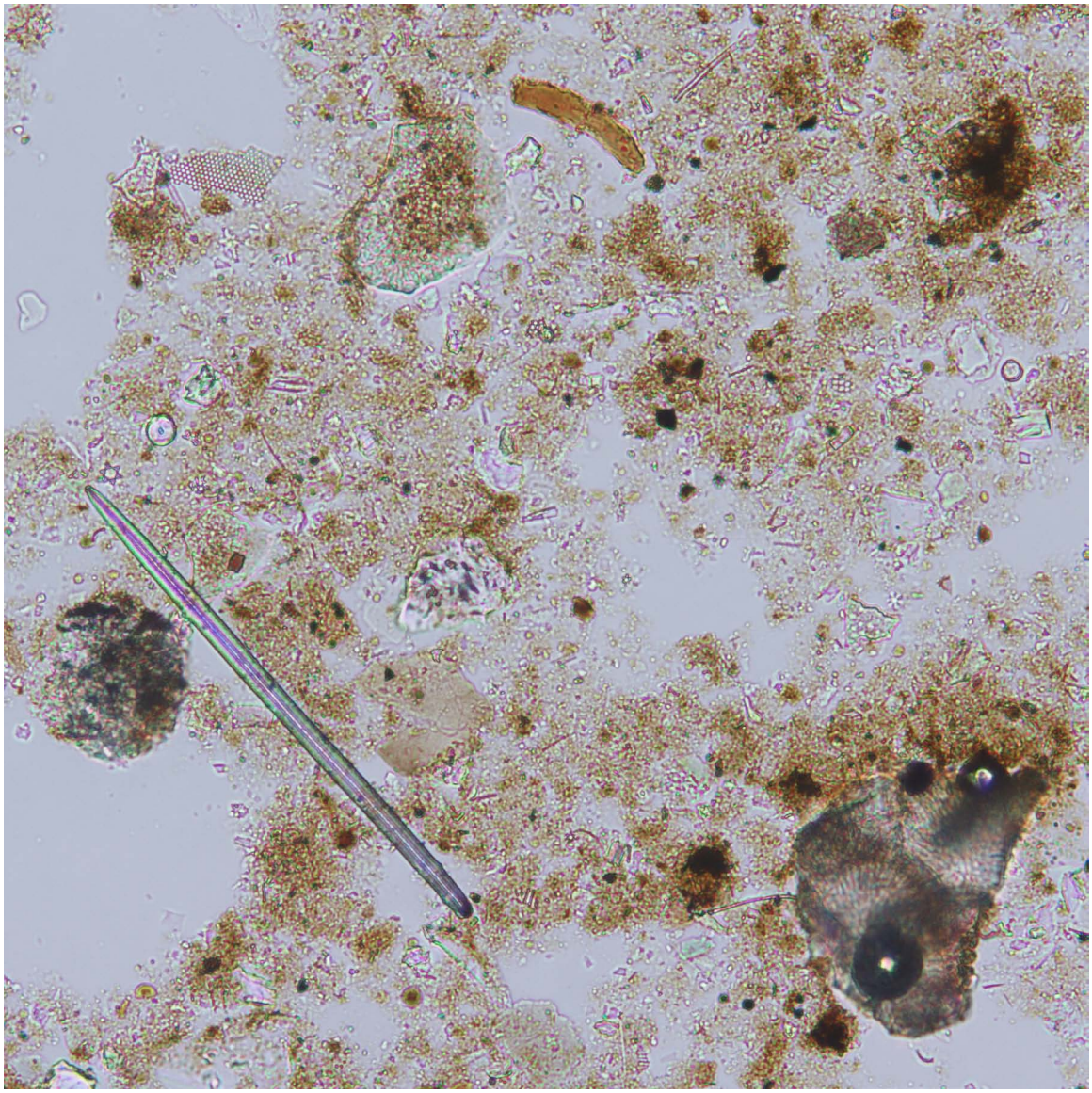

Otolith 2.

Mixed biogenic-terrigenous mud (pelleted?) with an elongate siliceous sponge spicule on left, brown curved phosphatic fragment in top center, and a possible fish otolith in lower right corner.

ODP Sample (Quaternary): Leg 167, Hole 1014A, Core 1H, Section 2W, 120 cm

Tunicate Spicules

INTRODUCTION TO TUNICATE SPICULES

Overview – The fossil record of Urochordata, also known as tunicates or sea squirts, is sparse but some, particularly in the Didemnidae and Pyuridae families, generate microscopic spicules. These microfossils are composed of calcium carbonate (aragonite) and limited to waters shallower than 200 to 500 m.

Diagnostic features – The soft tissue of adult organisms can be embedded with microscopic aragonitic spicules showing concentric to radiating ultrastructures with variable numbers of rays.

Biology – Kingdom Animalia, Subkingdom Eumetazoa, Deuterostomatous adults, Phylum Urochodata.

Ecology – These benthic organisms are hermaphrodites that mostly feed on phytoplankton and are found throughout the world's oceans. Their spicules are mainly limited to shallow water (<200-500m) but can be transported into deeper water by currents.

Stratigraphic Range – Jurassic to Present, but perhaps as old as Precambrian.

Key References:

Jones, B., 1990,Tunicate spicules and their syntaxial overgrowths: examples from the Pleistocene Ironshore Formation, Grand Cayman, British West Indies: Canadian Journal of Earth Sciences, v. 27, p. 525-532.

Scholle, P. A., and Ulmer-Scholle, D.S., 2003. A Color Guide to the Petrography of Carbonate Rocks: Grains, Textures, Porosity, Diagenesis. Memoir, v. 77: Tulsa, Oklahoma, American Association of Petroleum Geologists, 474 p.

Wei, W., 1993, Abundance patterns of tunicate spicules at the Great Barrier Reef – Queensland Plateau transect sites: implications for downslope transport and early Pleistocene initiation of the central Great Barrier Reef: Proceedings of the Ocean Drilling Program, Scientific Results, v. 133, p. 447-453.

Tunicate spicule 1

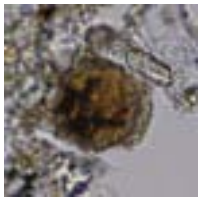

Tunicate spicule 2

Tunicate spicule 3

Tunicate spicule 4

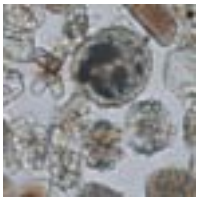

Tunicate spicule 5

Image ID: 0144/0145

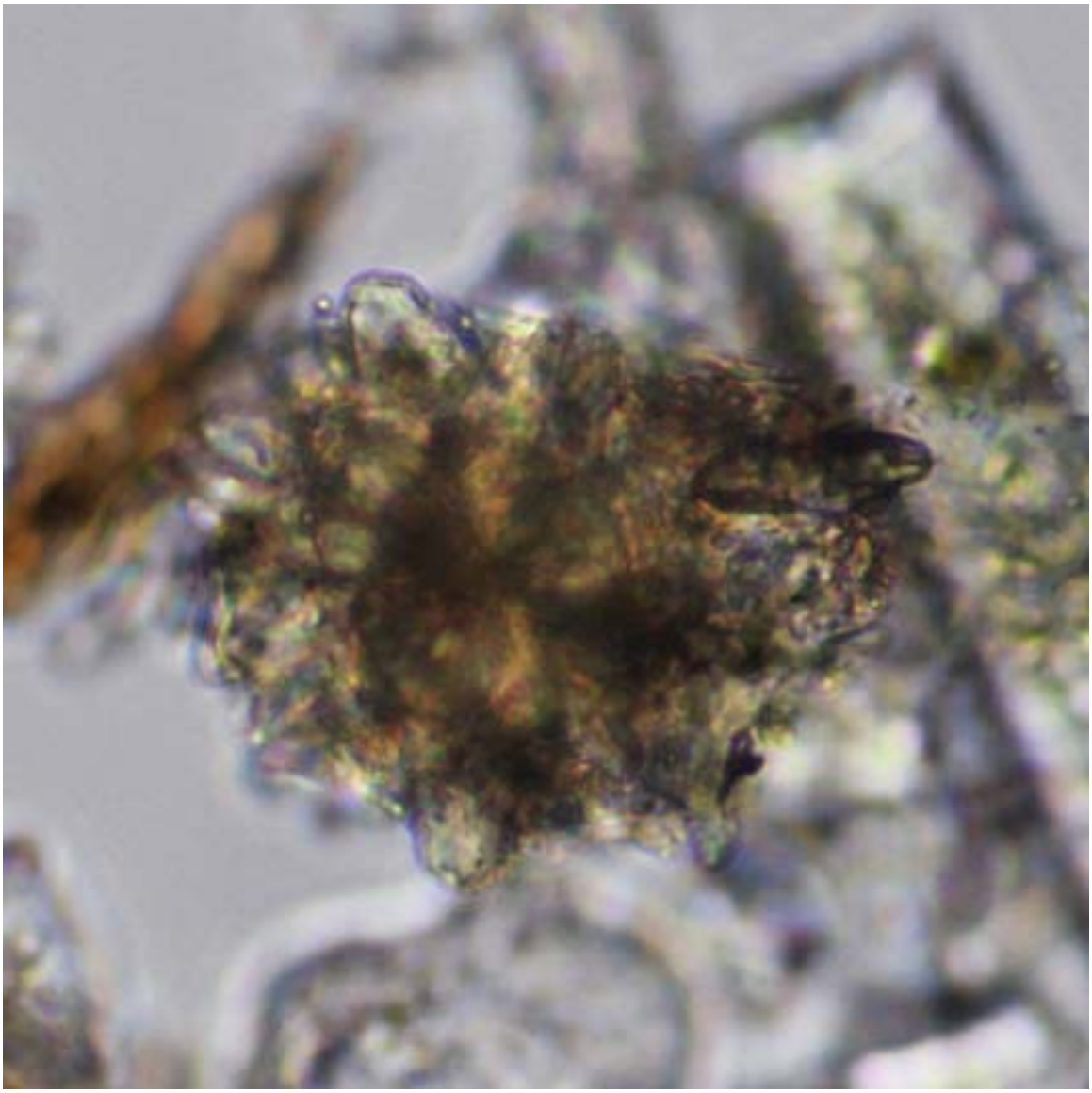

Tunicate spicule 1.

Example of a calcareous tunicate spicule (sclerite) in the form of a spiked sphere. The carbonate mineralogy is evident when polars are crossed.

IODP Sample (Pleistocene-Holocene): Leg 317, Hole 1352B, Core 11H, Section 2W, 21 cm

Image ID: 0158/0159

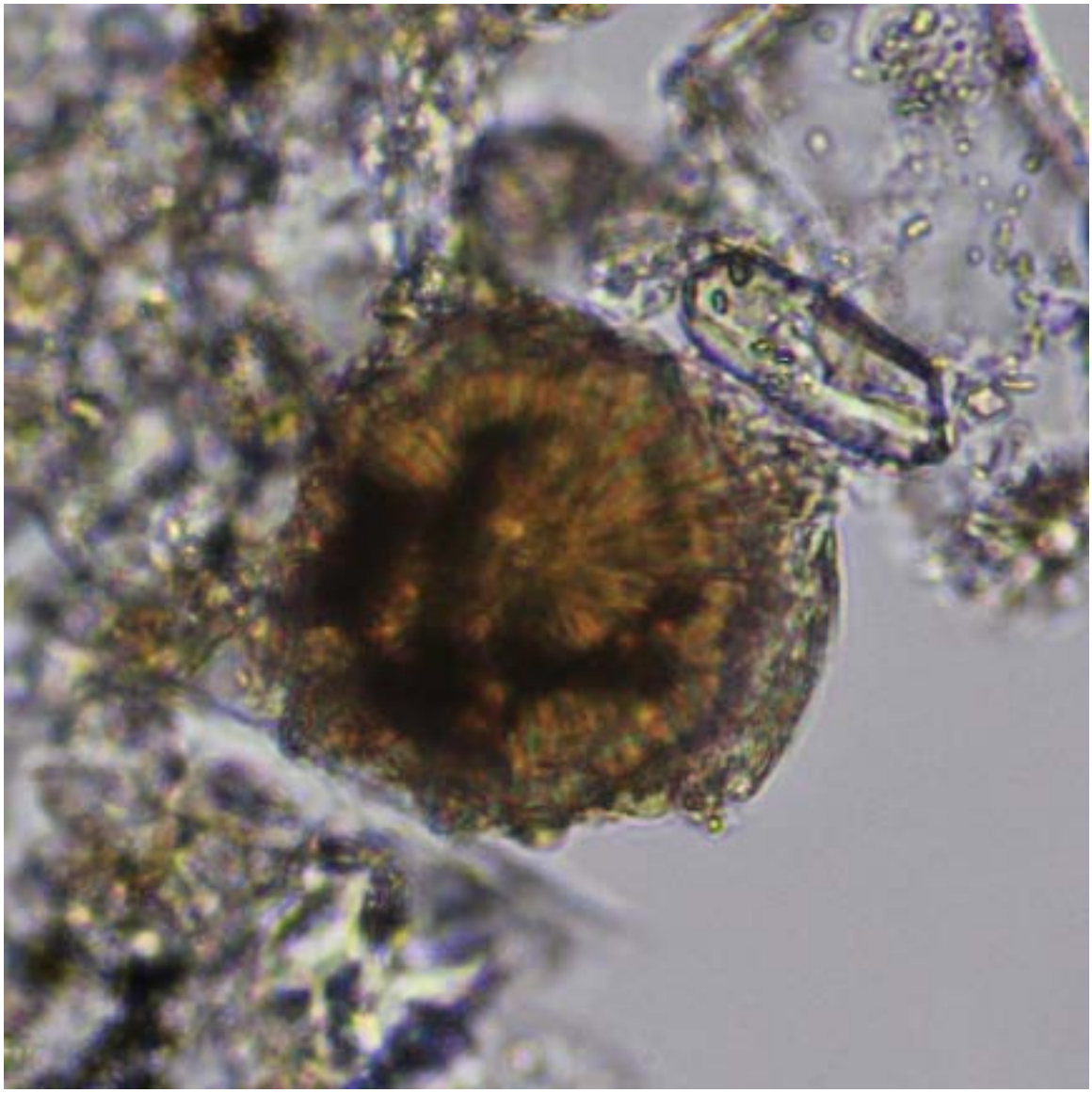

Tunicate spicule 2.

Example of a calcareous tunicate spicule (sclerite) in center of field of view. Its carbonate mineralogy is evident when polars are crossed. The form is that of a sphere with internal fibrous radiating carbonate. Brownish color may be a function of organic matter content.

IODP Sample (Pleistocene-Holocene): Leg 317, Hole 1352B, Core 11H, Section 2W, 21 cm

Image ID: B0357/B0358

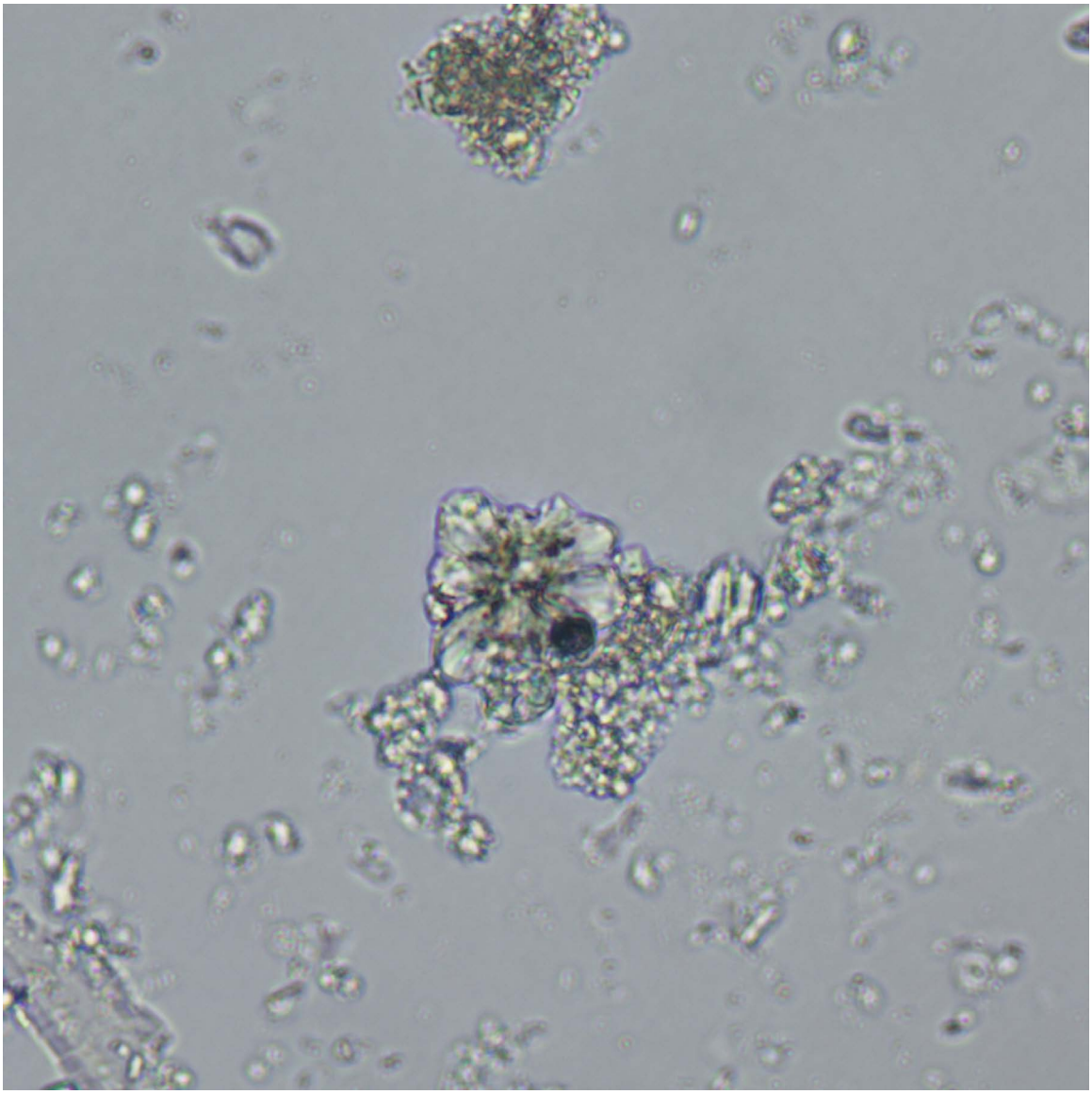

Tunicate spicule 3.

Example of a calcareous tunicate spicule (sclerite) in center of field of view. Its carbonate mineralogy is evident when polars are crossed. The form is that of an irregular fibrous radiating mass of carbonate crystals.

ODP Sample (Pliocene): Leg 101, Hole 628A, Core 2H, Section 1, 47 cm

Image ID: B0359/B0360

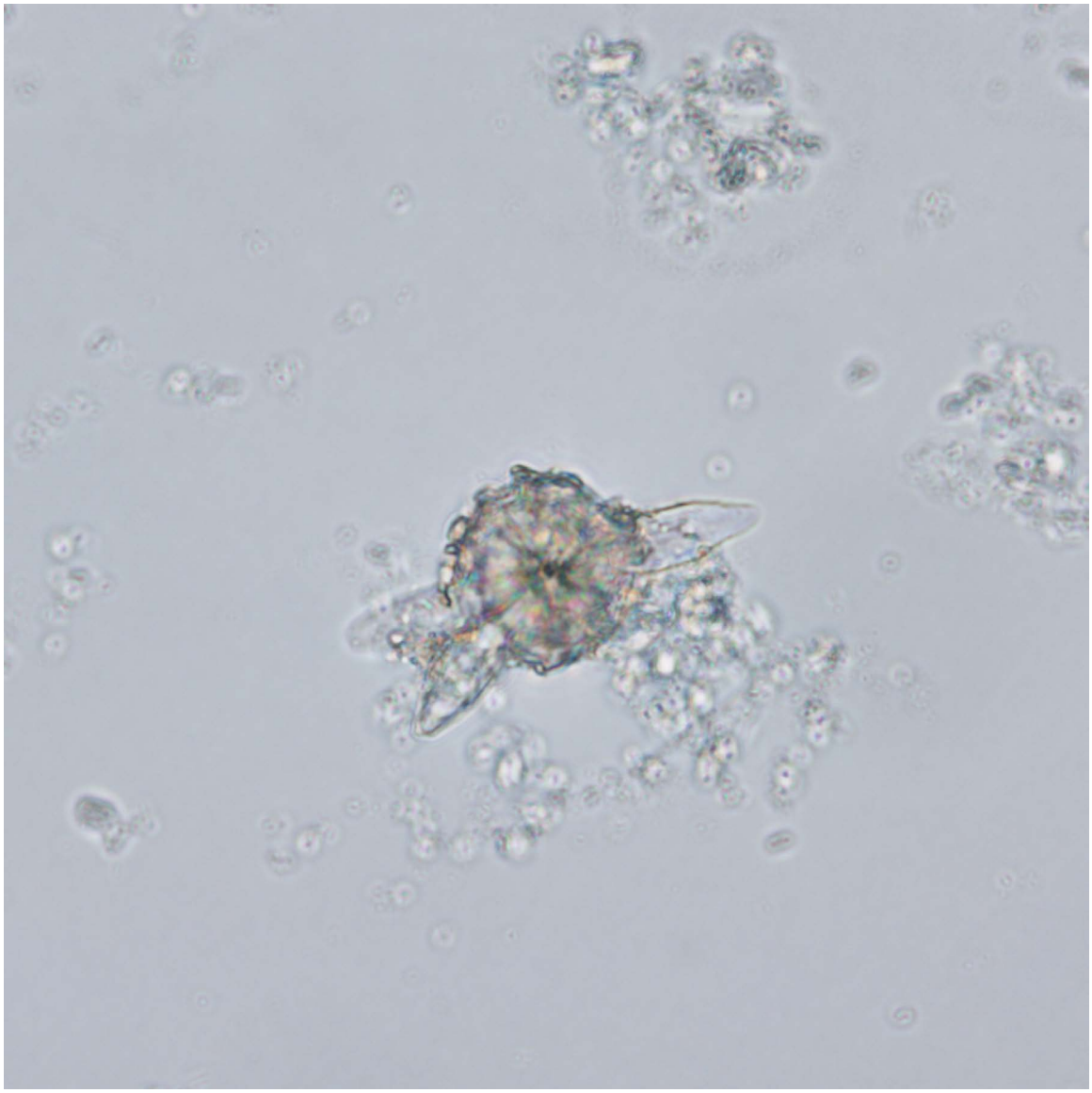

Tunicate spicule 4.

Example of a calcareous tunicate spicule (sclerite) in center of field of view. Its carbonate mineralogy is evident when polars are crossed. The form is that of a sphere with internal fibrous radiating carbonate, with a few larger crystal (spikes) overgrowths?

ODP Sample (Pliocene): Leg 101, Hole 628A, Core 2H, Section 4, 97 cm

Image ID: B0242/B0243

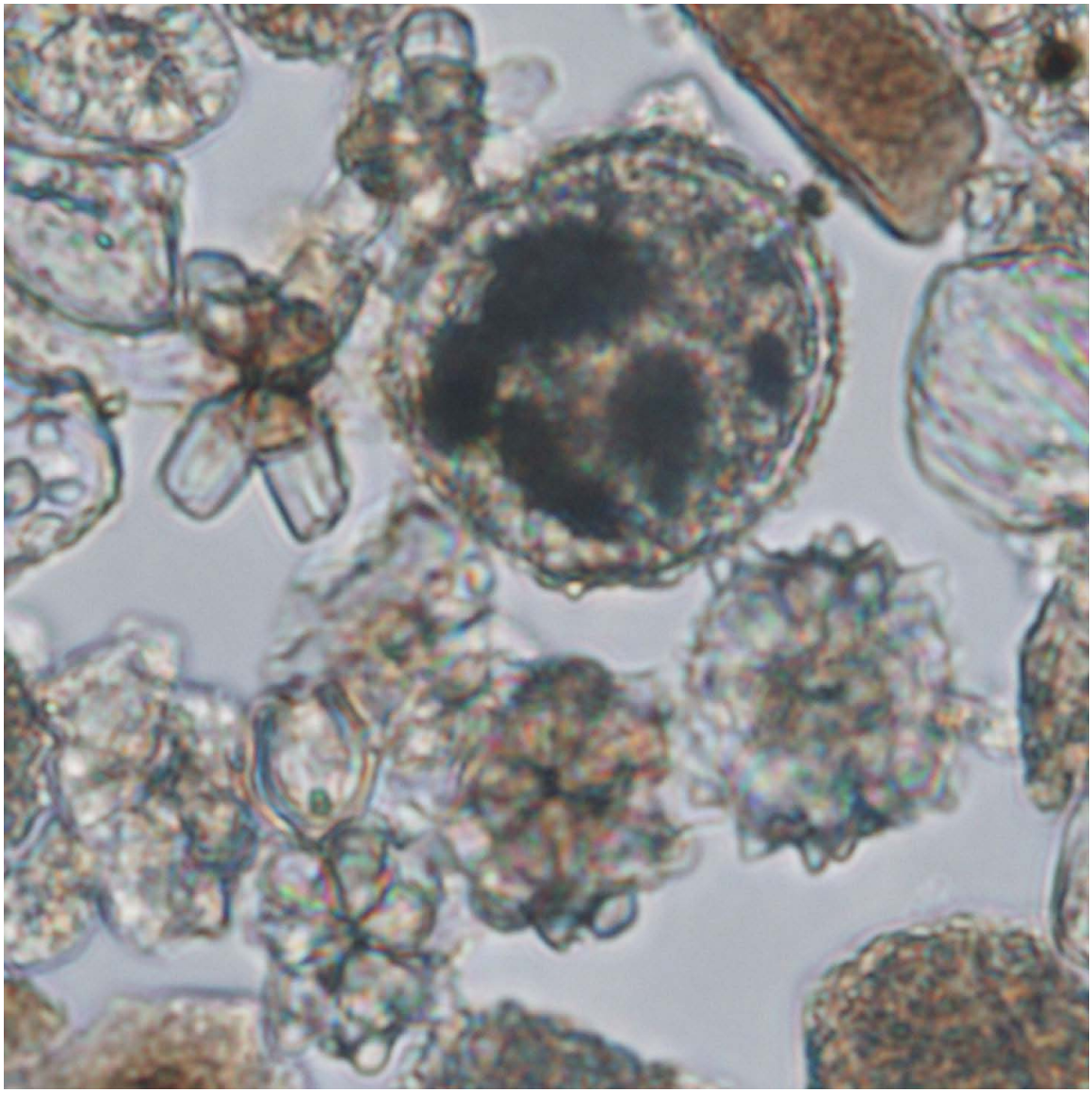

Tunicate spicule 5.

The carbonate and pyrite-cemented foraminifer in the center is surrounded by a variety of tunicate spicules with radial ultrastructure.

ODP Sample (late Pliocene): Leg 172, Hole 1062A, Core 16H, Section 6W, 73 cm

Unspecified Bioclasts

INTRODUCTION TO UNSPECIFIED BIOCLASTS

Carbonate fossil fragments (bioclasts) of indeterminant origin can be present in smear slides. These fragments may be a product of predepositional transport, post-depositional bioturbation, postdepositional diagenesis (e.g., partial dissolution), and/or breakage during smear-slide production.Those produced by predepositional transport can sometimes be differentiated by more rounded shapes. Fragment ultrastructure can sometimes provide clues to its fossil affiliation.


Bioclast 1


Bioclast 2


Bioclast 3


Bioclast 4


Bioclast 5

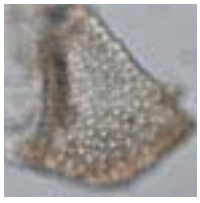
Bioclast 6

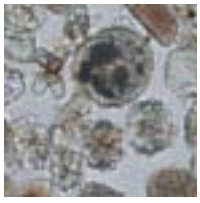
Bioclast 7

Image ID: B0213/B0214

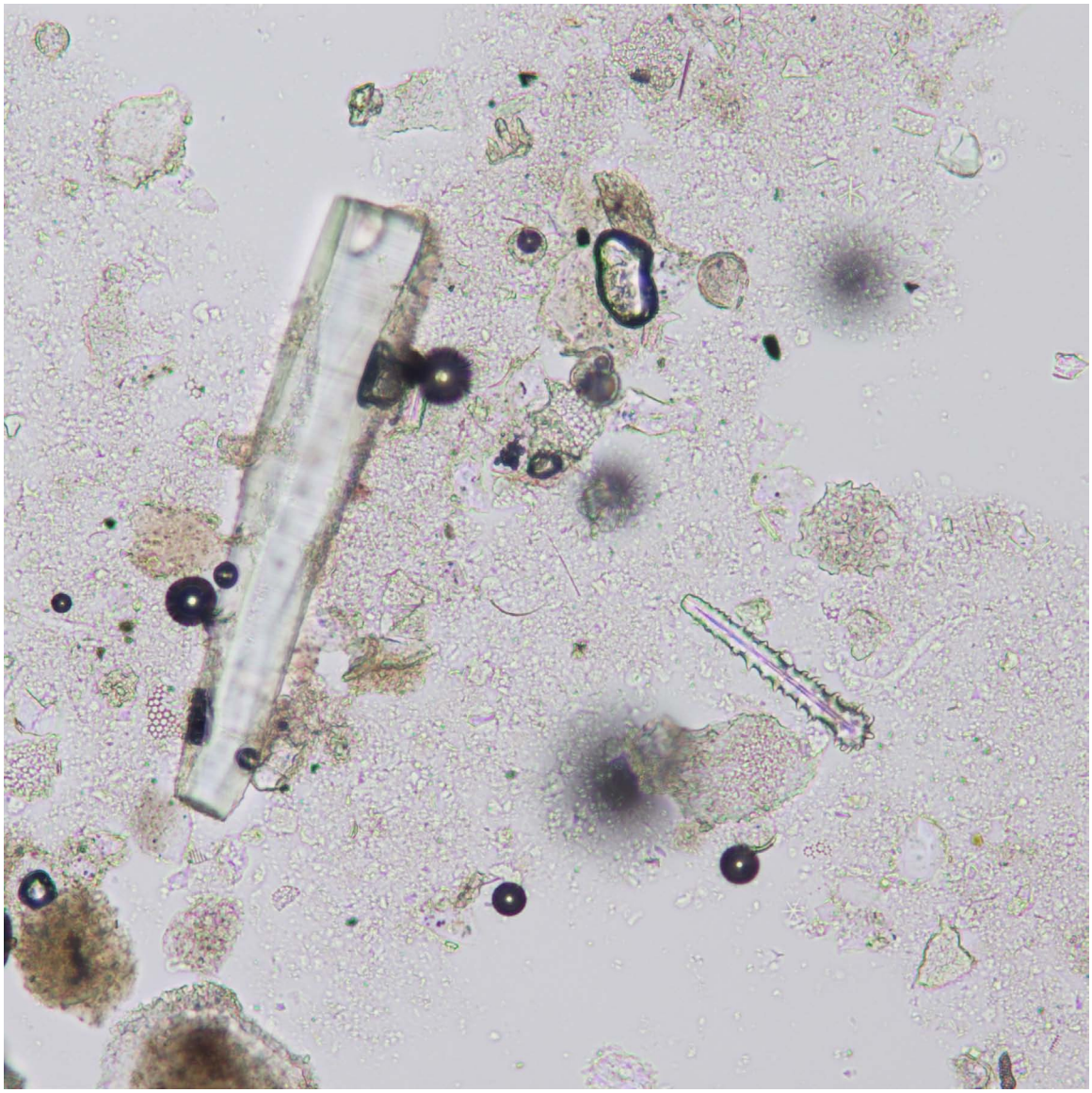

Bioclast 1.

Mixed calcareous ooze with a large carbonate prism that could be a mollusk fragment (prismatic ultrastructure). The other components include a mono-axonic barbed siliceous (nonbirefringent) sponge spicule with a slightly inflated bulbous end (acanthotylostyle), several planktic foraminifera (pseudo-uniaxial cross with nicols crossed), and finer nannofossil matrix.

ODP Sample (Pleistocene): Leg 108, Hole 657A, Core 4H, Section 1W, 34 cm

Image ID: B0353/B0354

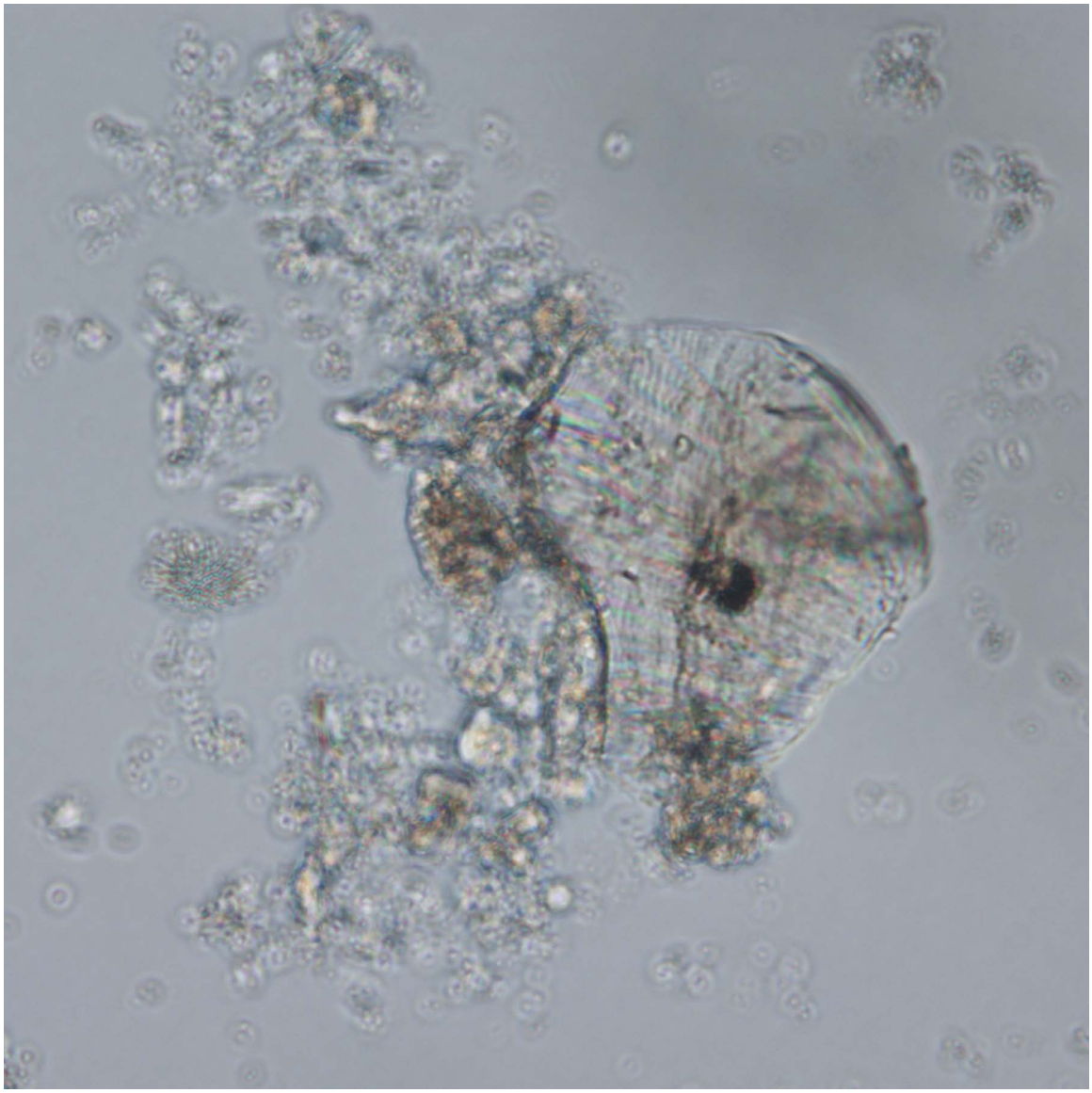

Bioclast 2.

This rounded calcareous bioclast has fibrous ultrastructure under crossed polars and is probably a mollusk fragment. The degree of rounding is consistent with formation and abrasion in a high-energy environment. Such grains can be transported from shallow-water to deeper water in density currents.

ODP Sample (Pleistocene): Leg 101, Hole 628A, Core 1H, Section 1, 51 cm

Image ID: B0215/B0216

Bioclast 3.

This rounded calcareous bioclast has fibrous ultrastructure under crossed polars and is probably a mollusk fragment. The degree of rounding is consistent with formation and abrasion in a high-energy environment. Such grains can be transported from shallow-water to deeper water in density currents.

ODP Sample (Pleistocene): Leg 108, Hole 657A, Core 4H, Section 1W, 34 cm

Image ID: B0507/B0508

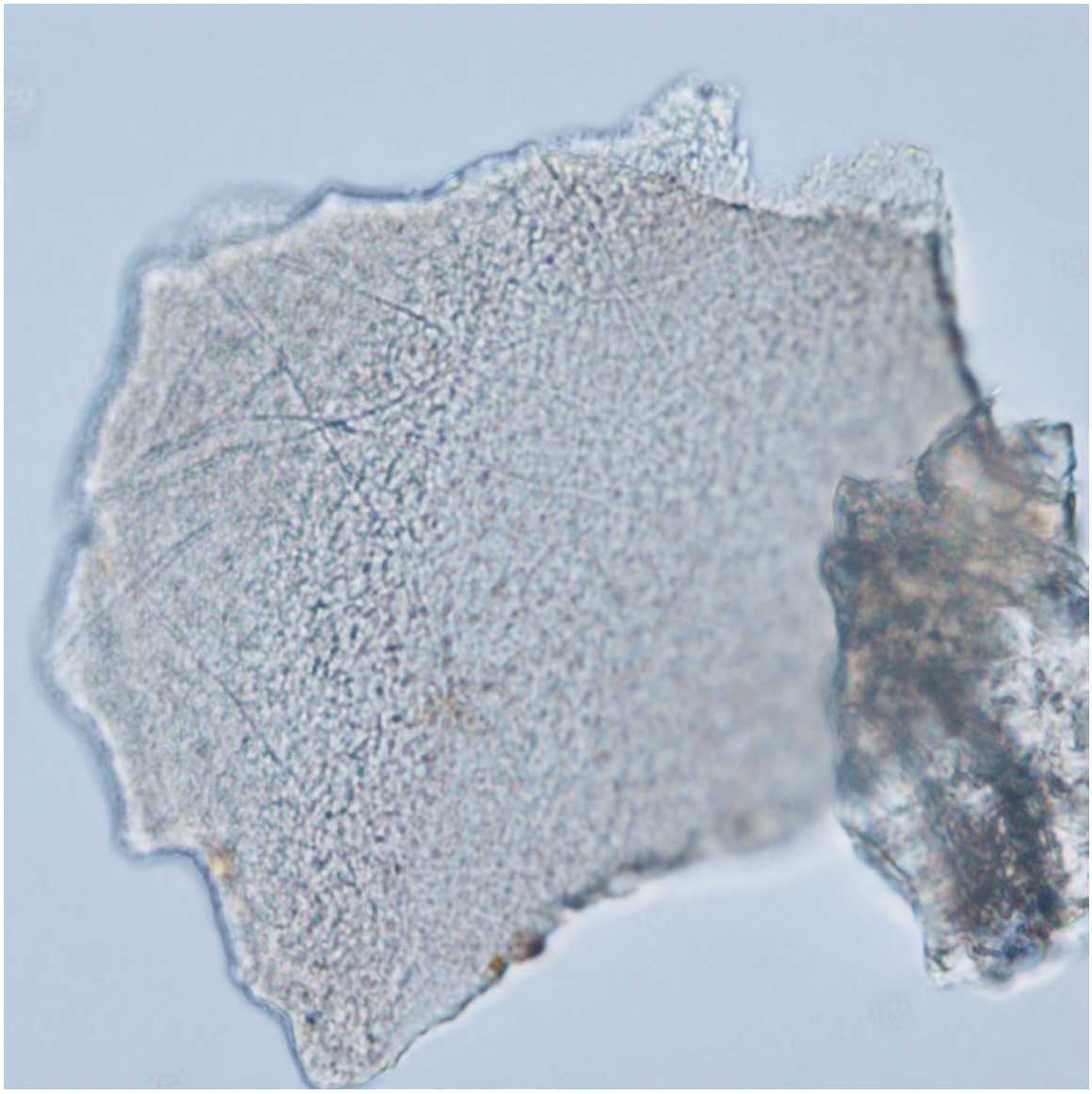

Bioclast 4.

Large angular bioclast of unknown origin with microborings.

ODP Sample (Pleistocene): Leg 121, Hole 752A, Core 1H, Section 1W, 55 cm

Image ID: B0154/B0155

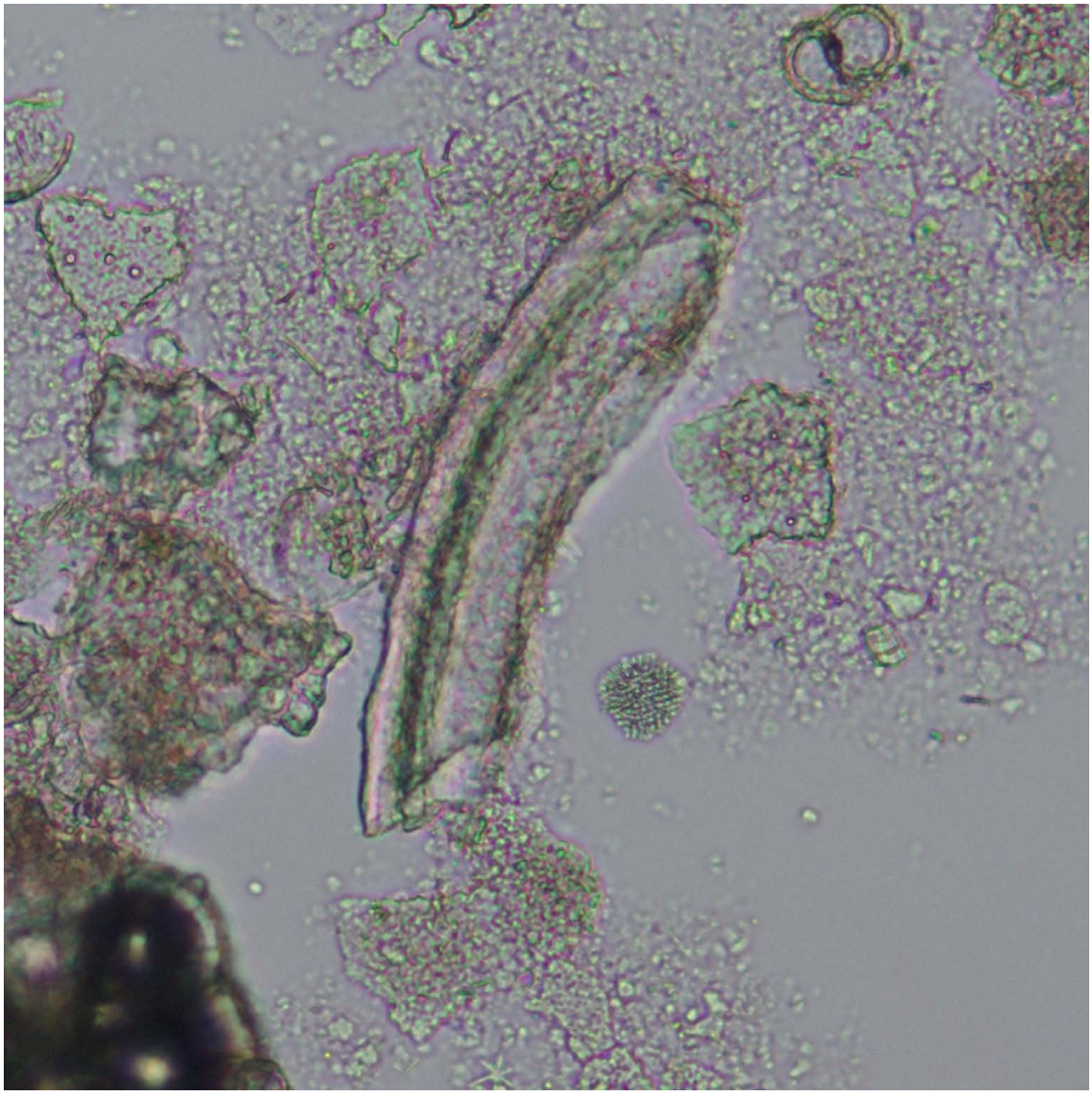

Bioclast 5.

This arcuate bioclast with layered ultrastructure may be a mollusk fragment. It is set in a mixed formainifer-nannofossil ooze.

ODP Sample (Pleistocene): Leg 130, Hole 807A, Core 1H, Section 2W, 93 cm

Image ID: B0164/B0165

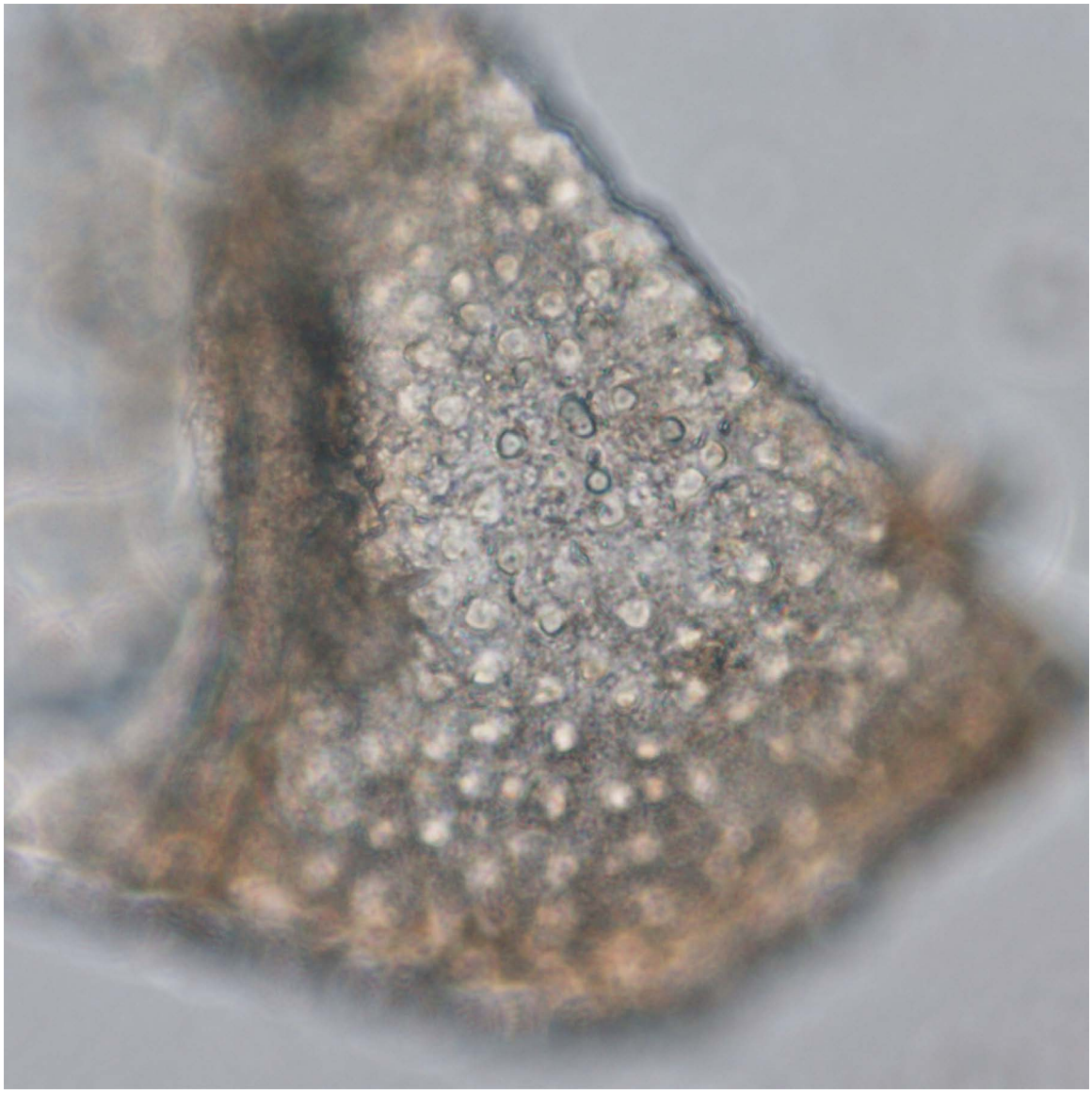

Bioclast 6.

View of knobby surface texture of a bioclast that is either a foraminifer or an ostracod fragment. The darker trace of a pseudo-uniaxial cross can be seen under crossed polars which supports the former interpretation.

ODP Sample (Pleistocene): leg 130, Hole 807A, Core 1H, Section 2W, 93 cm

Image ID: B0242/B0243

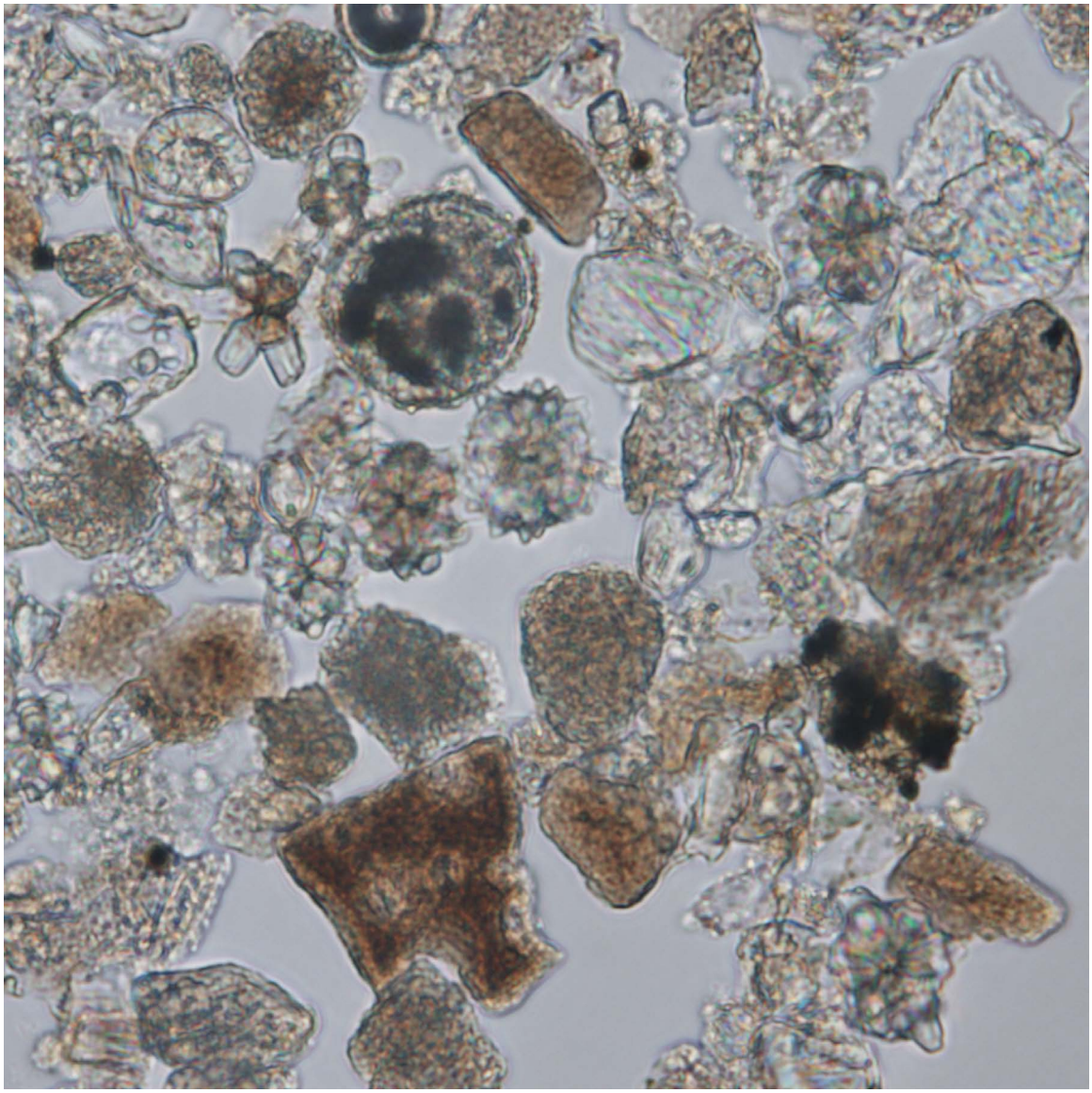

Bioclast 7.

This bioclastic sand includes foraminifera, including fragments of brown miliolids, and tunicate spicules but most fragments are hard to identify. The latter may include mollusc fragments based on their ultrastructure. See Tunicate Spicule 5 images for closer view of some of the debris.

ODP Sample (late Pliocene): Leg 172, Hole 1062A, Core 16H, Section 6W, 73 cm

Other Calcareous Bioclasts (Bolboforma, Echinoderm)

INTRODUCTION TO BOLBOFORMA

Overview – These enigmatic microfossils are suspected to be the cysts of a planktic alga. They are typically single-chambered, subspherical, smooth to strongly ornamented tests with terminal apertures. The tests are 50-150 µm, up to 250 µm in diameter, and composed of monocrystalline calcite. *Bolboforma* have a bipolar distribution in the mid- to high latitudes. They are often associated with hiatuses (episodes of intermediate-water circulation), have punctuated records, typically of monospecific populations, and occur from late early Eocene to late Pliocene, with none recorded in Quaternary to Recent sediments.

Key References:

Crundwell, M.P., Cooke, P.J., Nelson, C.S., and Spiegler, D., 2005. Intraspecific morphological variation in the late Miocene Bolboforma, and implications for their classification, ecology, and biostratigraphic utility. Marine Micropaleontology, 56: 161-176.

Poag, C.W., and Karowe, A.L., 1986. Stratigraphic potential of Bolboforma significantly increased by new finds in the North Atlantic and South Pacific. Palaios, 1: 162-171.

Spiegler, D., 1999. Bolboforma biostratigraphy from the Hatton-Rockall Basin (North Atlantic). In Raymo, M.E., Jansen, E., et al., Eds., Proceedings of the Ocean Drilling Program, Scienctific Results, 162: 35-49.

Spiegler, D., and Spezzaferri, S., 2005. Bolboforma – an overview. Paläontologische Zeitschrift, 79(1): 167-181.

INTRODUCTION TO ECHINODERM SPINES

Overview – Echinoid spines and plates may be components of marine sediments. They are largely present in the sand fraction and not distinguishable as silt-sized fragments. These bioclasts are composed of single crystals of calcite and are identifiable by their shape (e.g., tapered spine, rectangular plates where intact), unit extinction and propensity for developing syntaxial calcite overgrowths as illustrated in Scholle and Ulmer-Scholle (2003). (No images provided)

Key References:

Scholle, P. A., and Ulmer-Scholle, D.S., 2003. A Color Guide to the Petrography of Carbonate Rocks: Grains, Textures, Porosity, Diagenesis. Memoir, v. 77: Tulsa, Oklahoma, American Association of Petroleum Geologists, 474 p.

Diatoms

INTRODUCTION TO DIATOMS

Overview – Single-celled algae with an opaline silica shell (frustule) composed of two identical or dissimilar, interlocking valves. There are both planktic and benthic diatoms.

Diagnostic Features – Diatoms that are circular, oval, cylindrical, or triangular in shape display a radial symmetry; flat, elongate diatoms have bilateral symmetry with or without a central, axial raphe. A girdle band connects the slightly larger epivalve and smaller hypovalve. The valve faces have pores (areolae), and may have short spines or processes. 20-200 µm long/in diameter, up to 2000 µm (2 mm) long.

Biology – Kingdom Protoctista, Subkingdom Heterokonta, Phylum Bacillariophyta. Diatoms are traditionally divided into two orders: centric diatoms (radial symmetry) and pennate (bilateral symmetry). Some species produce a resting spore that may or may not resemble the vegetative cell.

Ecology – Autotrophs. Diatoms occur in marine, sea ice, fresh water, and soil environments.

Paleobiogeography – Widely distributed, but most abundant in nutrient-rich coastal waters and zones of oceanic divergence where upwelling supplies nutrients and dissolved silica to the photic zone. Diatom ooze forms in the arctic/subarctic and in the Southern Ocean.

Stratigraphic Range – Early Jurassic? Mid-Cretaceous (late Aptian/early Albian) to present.

Key References and Examples:

Barron, J.A., 1985. 16: Miocene to Holocene planktic diatoms. In Bolli, H.M., Saunders, J.B., and Perch Nielsen, K. (Eds.), Plankton Stratigraphy: Cambridge (Cambridge Univ. Press), 763-809.

Barron, J.A., 1985. Late Eocene to Holocene diatom biostratigraphy of the equatorial Pacific Ocean, DSDP Leg 85. In, Mayer, L., Theyer, F., et al., Initial Reports of the DSDP, 85:413-456.

Barron, J.A., 1993. 10: Diatoms. In, Lipps, J.H. (Ed.), Fossil Prokaryotes and Protists: Blackwell Scientific Publications, 155-167.

Burckle, L.H., 1978. 10: Marine Diatoms. In Haq, B.U., and Boersma, A. (Eds.), Introduction to Marine Micropaleontology: Elsevier, 245-266.

Ciesielski, P.F., 1983. The Neogene and Quaternary diatom biostratigraphy of subantarctic sediments, DSDP Leg 71. In, Ludwig, W.J., Krasheninnikov, V.A., et al., Initial Reports of the DSDP, 71:635-665.

Fenner, J., 1985. 15: Late Cretaceous to Oligocene planktic diatoms. In Bolli, H.M., Saunders, J.B., and Perch Nielsen, K. (Eds.), Plankton Stratigraphy: Cambridge (Cambridge Univ. Press), 713-762.

Gombos, A.M., Jr., and Ciesielski, P.F., 1983. Late Eocene to early Miocene diatoms

from the southwest Atlantic. In, Ludwig, W.J., Krasheninnikov, V.A., et al., Initial Reports of the DSDP, 71:583-634.

Katz, M.E., Finkel, Z.V., Grzebyk, D., Knoll, A.H., and Falkowski, P.G., 2004. Evolutionary trajectories and biogeochemical impacts of marine eukaryotic phytoplankton. Annual Reviews of Ecology and Evolutionary Systems, 35:523-556.

Katz, M.E., Wright, J.D., Miller, K.G., Cramer, B.S., Fennel, K., and Falkowski, P.G., 2005. Biological overprint of the geological carbon cycle. Marine Geology, 217:323-338.

Web Resources:

http://www.ucl.ac.uk/GeolSci/micropal/diatom.html

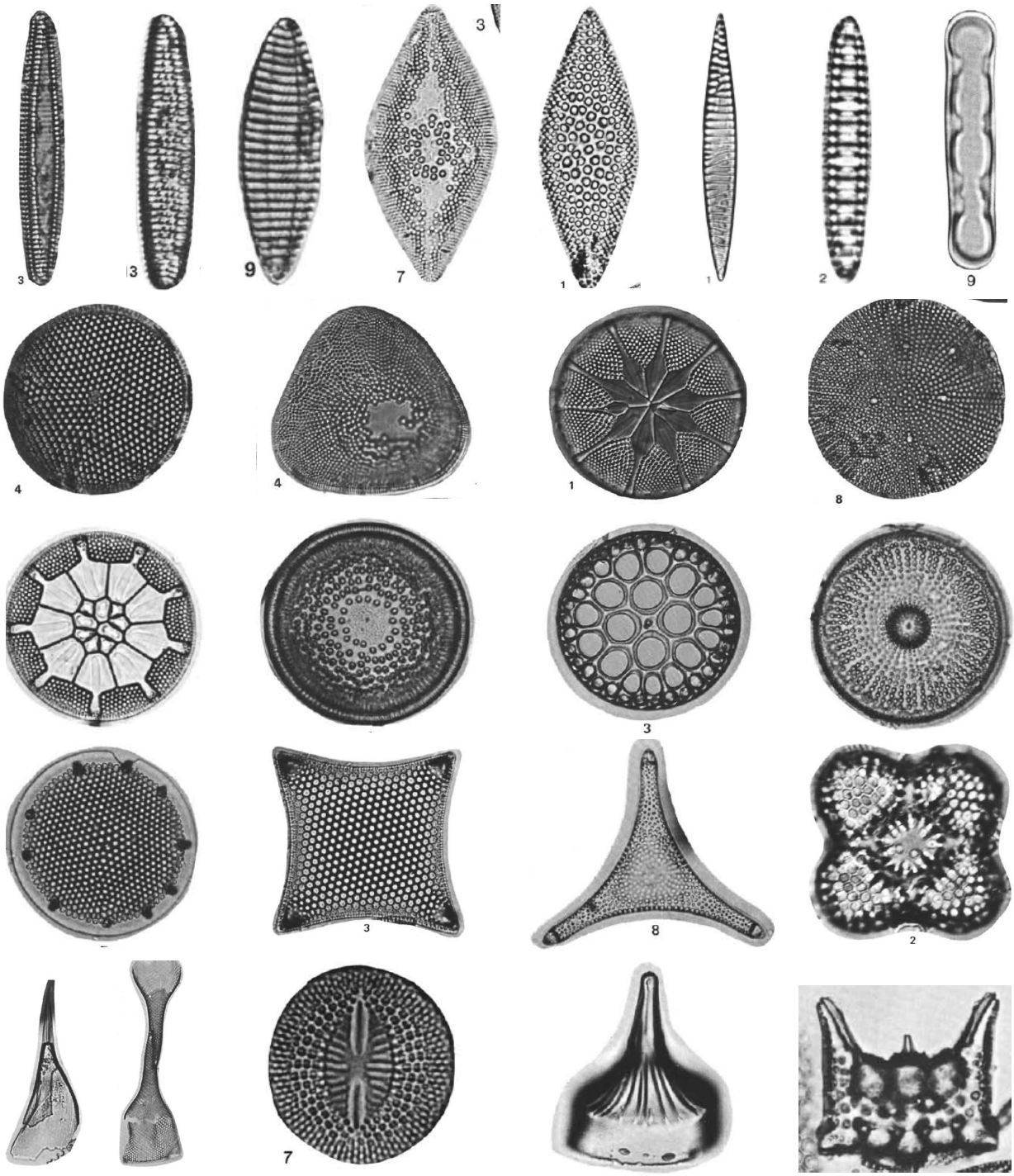

Representative Cenozoic pennate and centric diatoms. Top row (pennate diatoms): *Nitzschia weaver*, *Nitzschia interfrigidaria, Nitzschia miocenica, Cestodiscus peplum, Coscinodiscus rhombicus, Rossielaa praepaleacea, Denticulinopsis hustedtii, Denticulinopsis praedimorpha*. Second row (centric diatoms): *Thalassiosira torokina, Cosmiodiscus insignis forma trianula, Asteromphalus sp., Coscinodiscus vulnificus*. Third row (centric diatoms): *Asterolampra schmidtii, Coscinodiscus superbus, Rocella gelida, Cestodiscus* sp.. Fourth row (centric diatoms): *Stephanopyxis hyalomarginata, Triceratium unguiculatum, Trinacria excavate, Lisitzinia ornata. Bottom row: Rhizosolenia gravida, Pyxilla prolongata, Raphidodiscus marylandicus, Pterotheca major, Hemiaulus* sp. Photomicrographs from Barron, 1985; Ciesielski, 1983; Gombos and Ciesielski, 1983.

Diatoms

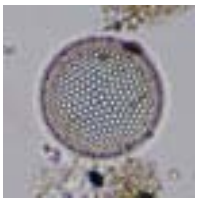
Diatom 1

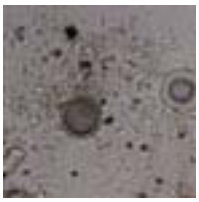
Diatom 2


Diatom 3


Diatom 4

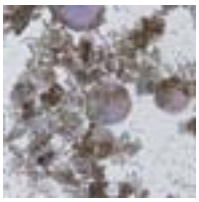
Diatom 5

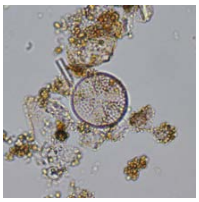
Diatom 6

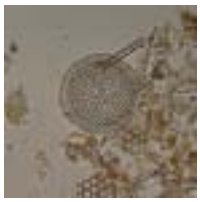
Diatom 7

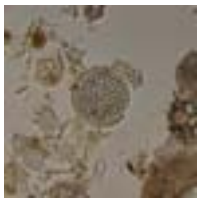
Diatom 8


Diatom 9


Diatom 10


Diatom 11


Diatom 12


Diatom 13


Diatom 14


Diatom 15


Diatom 16


Diatom 17


Diatom 18

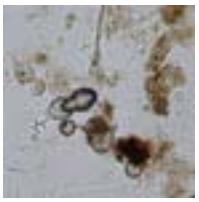
Diatom 19


Diatom 20


Diatom 21


Diatom 22


Diatom 23


Diatom 24


Diatom 25

Diatom 26

Diatom 27

Diatom 28

Image ID: B0026

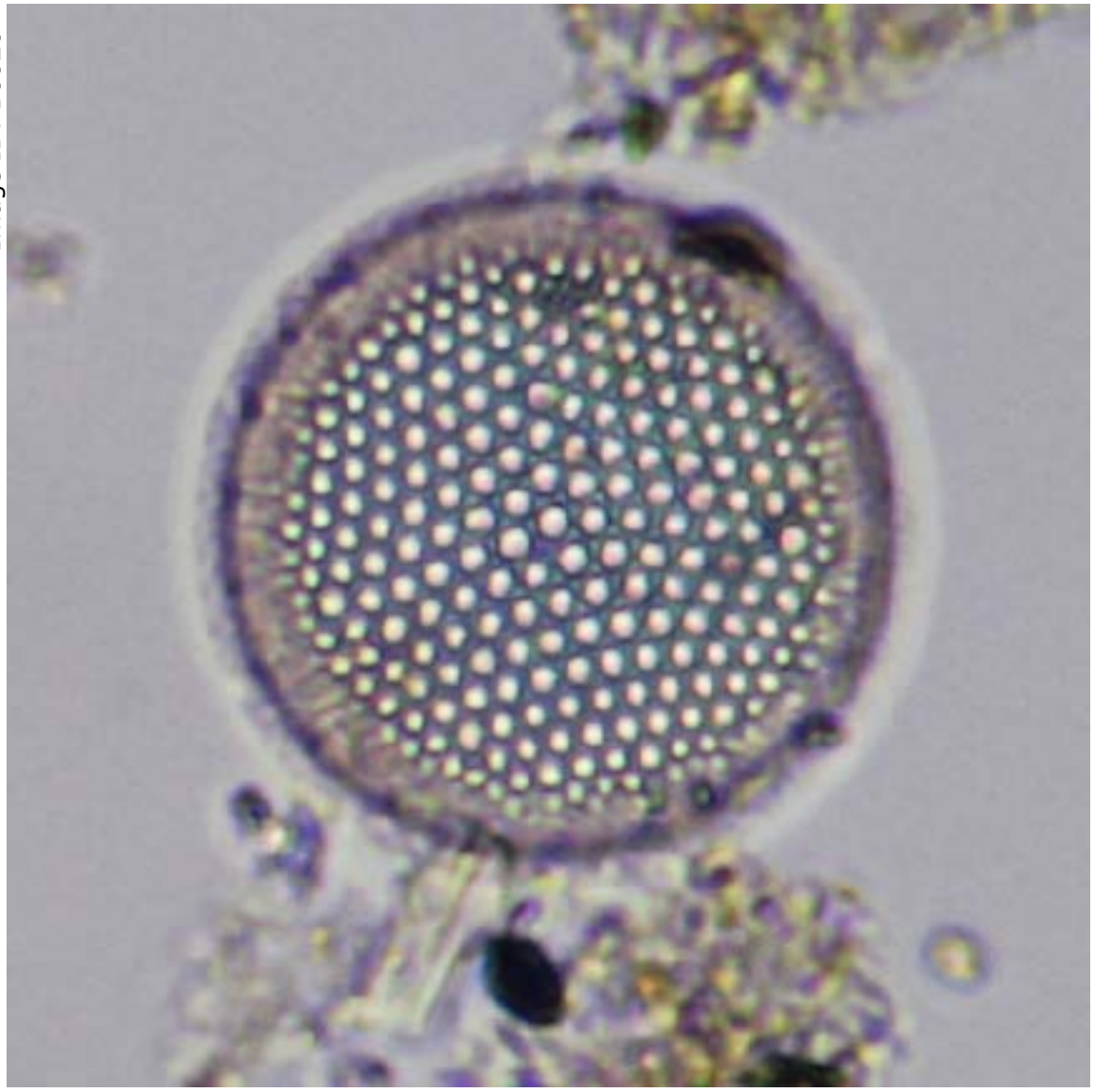

Diatom 1.

Opaline centric diatom valve that is isotropic when polars are crossed. Valve exhibits characteristic honeycomb structure (areolae) also called a sieve plate.

DSDP Sample (late Pleistocene): Leg 64, Hole 474, Core 8, Section 1, 53 cm

Image ID: 0628/0629

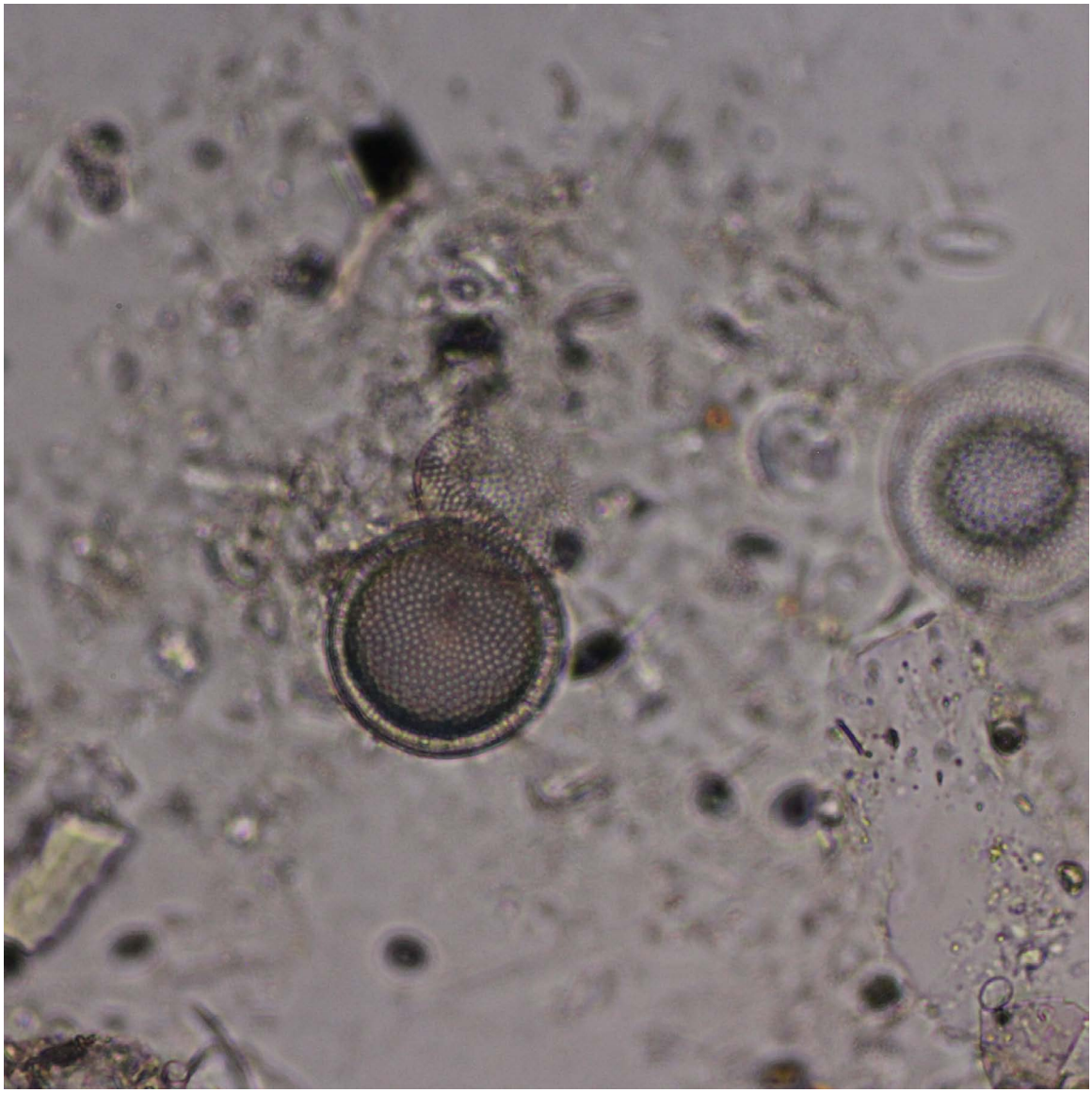

Diatom 2.

Opaline centric diatom valve that is isotropic when polars are crossed. Alternate focus view provides an idea of three dimensionality of the valves.

ODP Sample (Holocene): Leg 178, Hole 1098C, Core 5H, Section 1W, 5 cm

Image ID: 0361

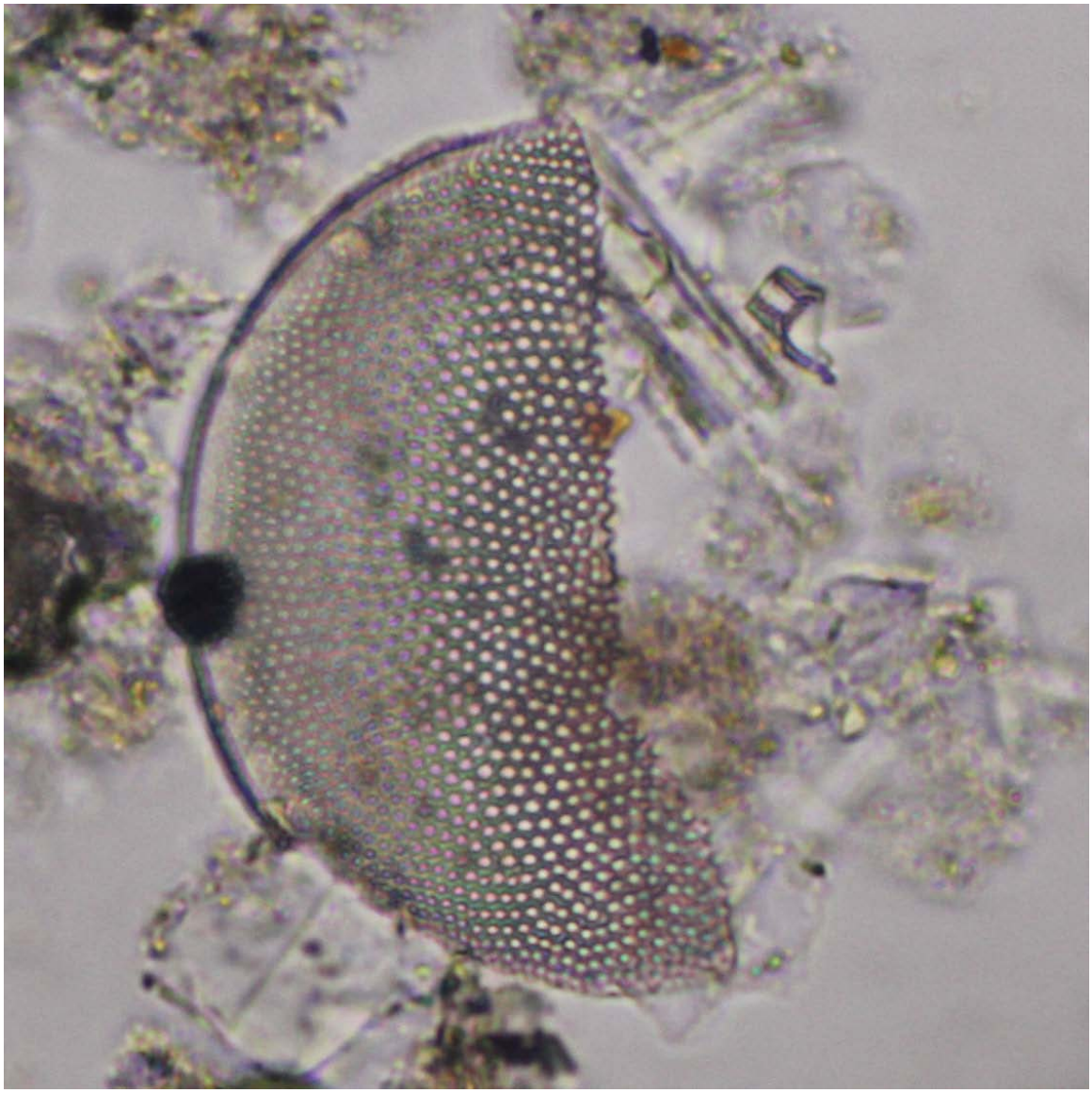

Diatom 3.

Broken opaline centric diatom valve that is isotropic when polars are crossed. It is set in a terrigenous silty mud. No cross-polar view is provided.

DSDP Sample (late Pleistocene): Leg 18, Hole 179, Core 3, Section 3, 30 cm

Image ID: B0422/B0423

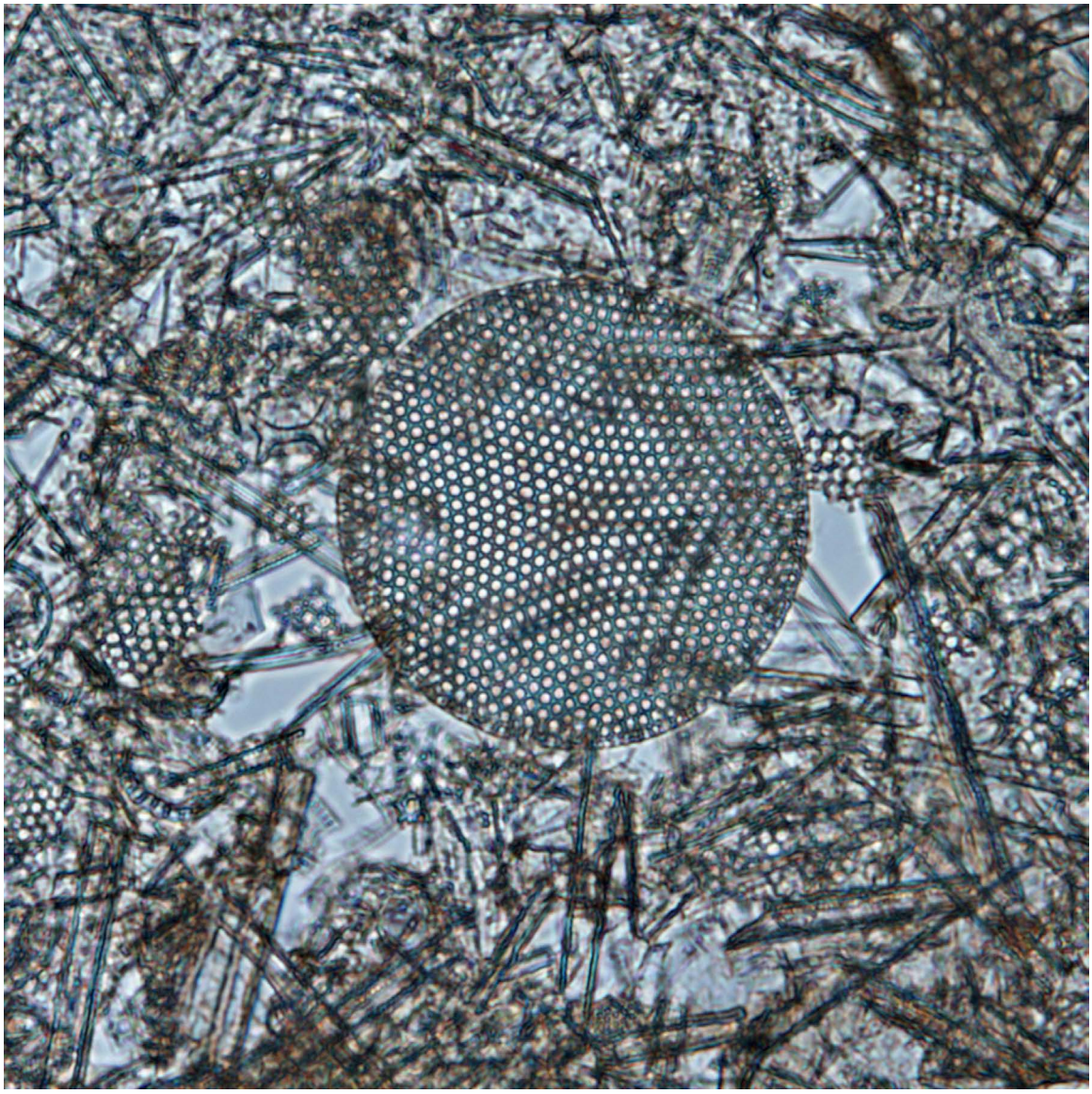

Diatom 4.

Diatom ooze with a complete centric diatom valve set in a mix of pennate and centric fragments. The view completely isotropic when polars are crossed.

ODP Sample (early Pliocene): Leg 113, Hole 690A, Core 1H, Section 6W, 105 cm

Image ID: B0322

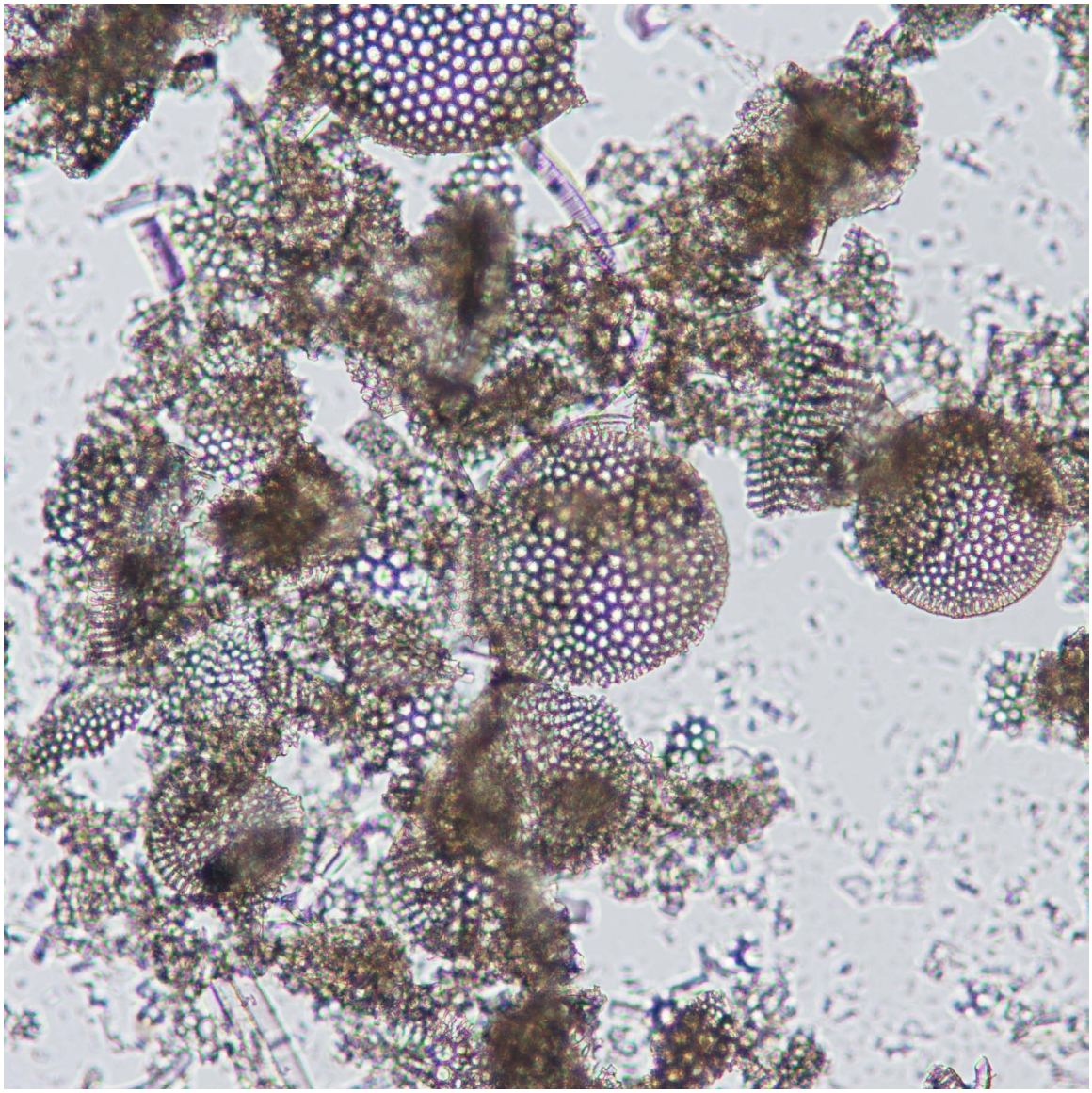

Diatom 5.

This is a clay-rich diatom ooze with several intact centric diatom valves and fragments. The view completely isotropic when polars are crossed, so no cross polar view provided.

ODP Sample (early Pliocene): Leg 145, Hole 881C, Core 23X, Section 1W, 60 cm

Image ID: B0078

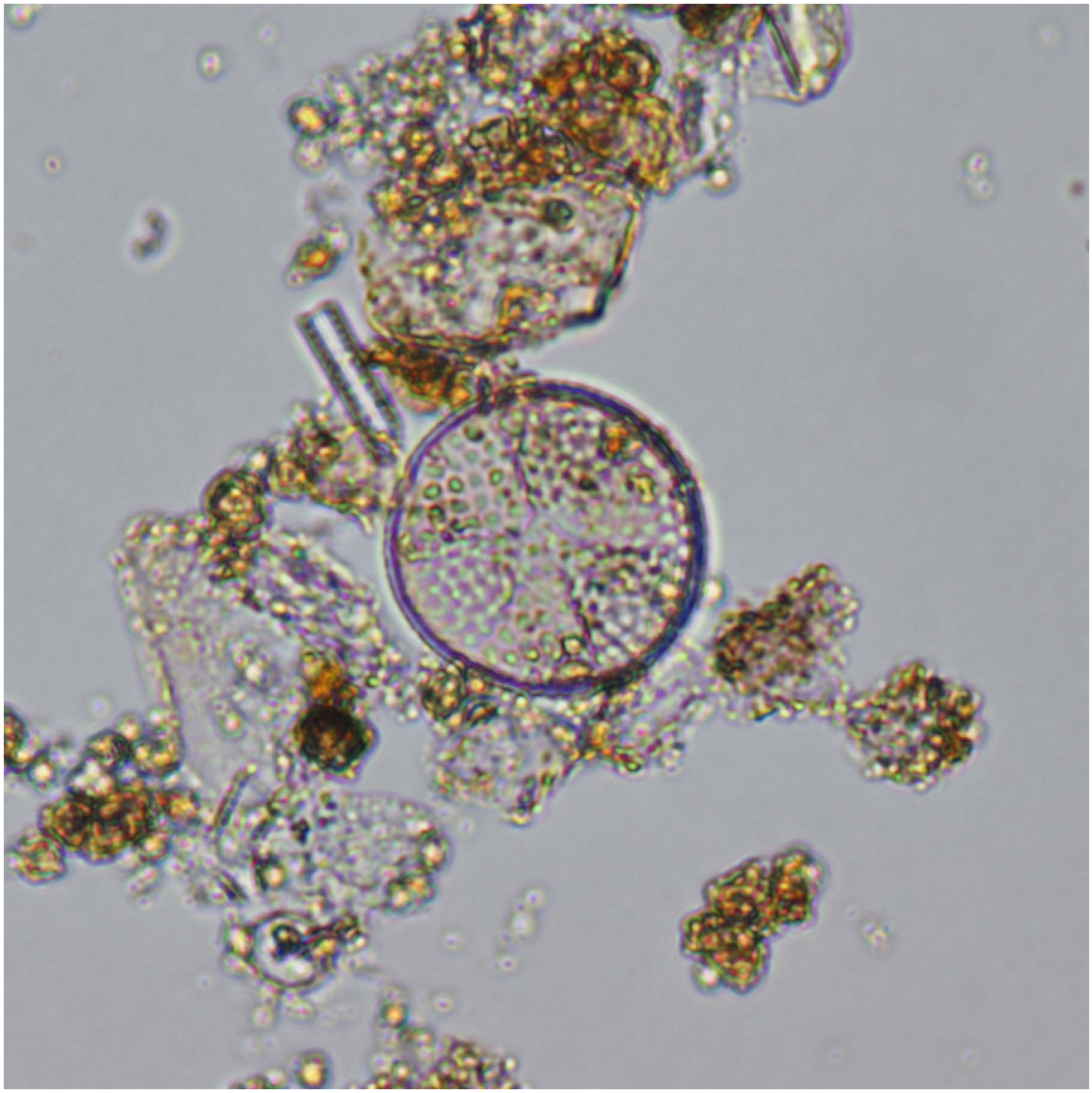

Diatom 6.

An opaline centric diatom valve in the center is isotropic along with surrounding material, so no cross-polar view is provided. Valve exhibits characteristic honeycomb structure (areolae) also called a sieve plate, with a segmented pattern. The valve is textured with alternating raised zones in the shape of pie-like wedges.

DSDP Sample (late Pleistocene): Leg 64, Hole 478, Core 3, Section 3, 133

Image ID: B0057

Diatom 7.

This opaline centric diatom valve and surrounding siliceous sediment made up of diatom fragments are isotropic when polars are crossed so no cross-polar view is provided. The valve exhibits characteristic honeycomb structure (areolae) also called a sieve plate and a distinct rim (girdle in third dimension).

DSDP Sample (Pliocene): Leg 56, Hole 438A, Core 13, Section 3, 64 cm

Image ID: B0060

Diatom 8.

Opaline centric diatom valve that is isotropic when polars are crossed. Valve exhibits characteristic honeycomb structure (areolae) also called a sieve plate and a distinct rim (girdle in third dimension). In the case of this specimen the rim has been partly broken away. No cross-polar view is provided.

DSDP Sample (Pliocene): Leg 56, Hole 438A, Core 13, Section 3, 64 cm

Image ID: B0053

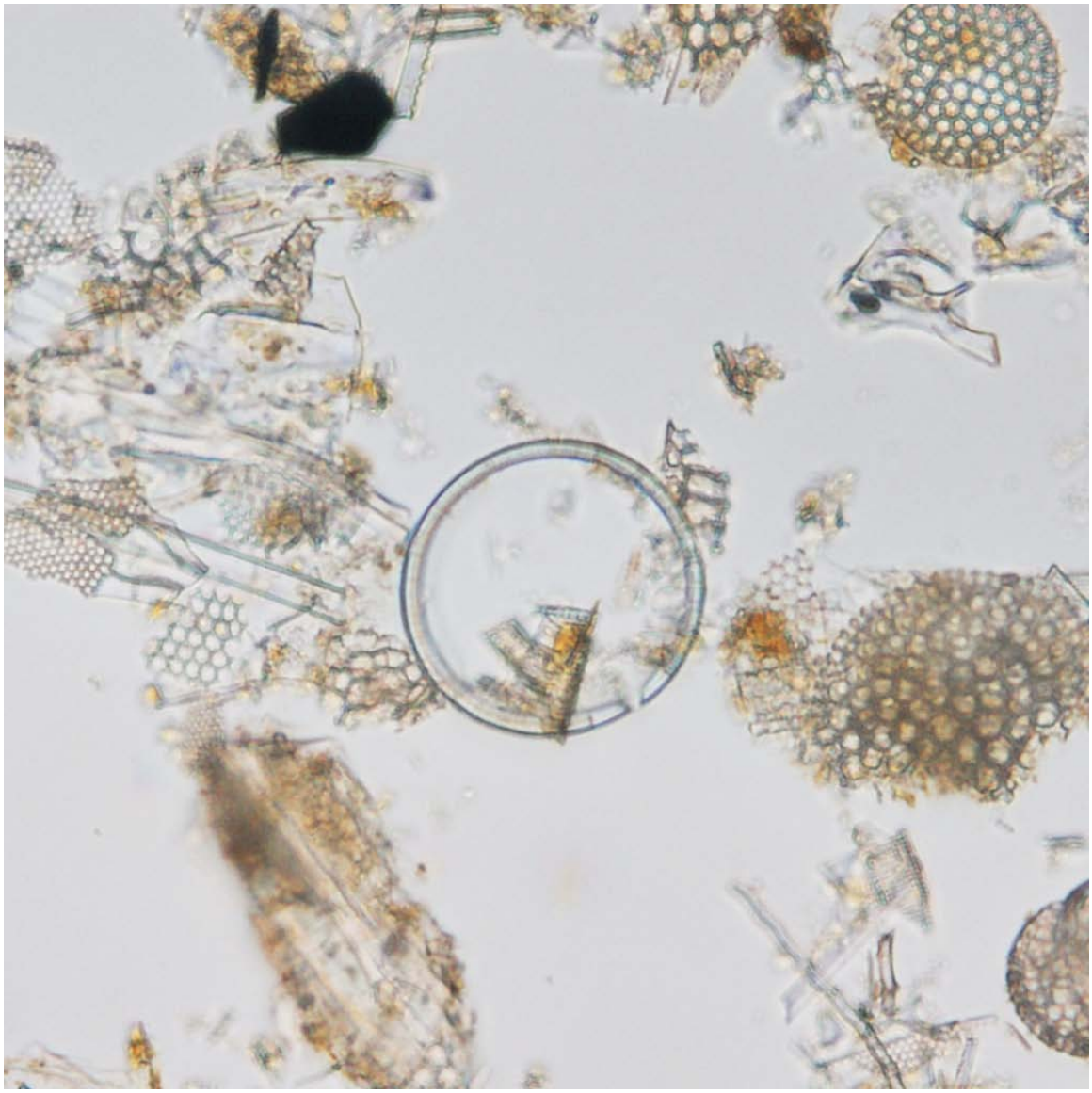

Diatom 9.

This view shows one half of a centric diatom frustrule where the valve rim (girdle) has been separated from the porous sieve plate, leaving a hollow ring. There are also several fragments of vescicular colorless volcanic glass with adhering siliceous bioclastic bits (circled).

DSDP Sample (Pliocene): Leg 56, Hole 438A, Core 13, Section 3, 64 cm

Image ID: B0410/B0411

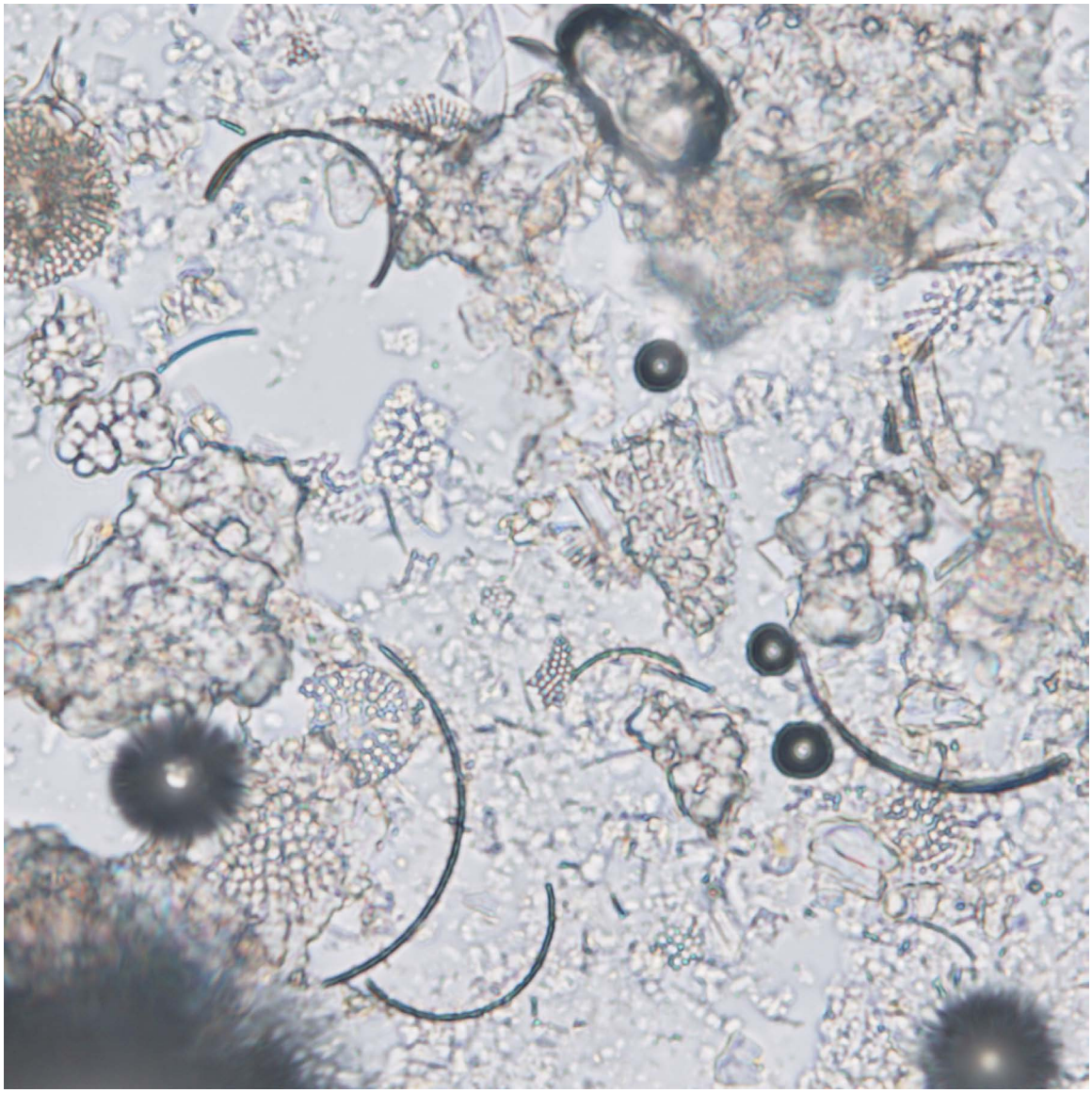

Diatom 10.

In this view, scattered broken rims (girdles) derived from centric diatom valves are set in a mixed calcareous/siliceous ooze as seen by the carbonate birefringence when the polars are crossed.

ODP Sample (early Pliocene): Leg 113, Hole 690A, Core 1H, Section 1, 110 cm

Image ID: B0489/B0490

Diatom 11.

The circular feature in this diatom ooze is most likely a rim (girdle) of a centric diatom. The entire field of view isotropic except for a few coccoliths fragments. Both centric and pennate diatom fragments are present.

ODP Sample (late Miocene-Pleistocene): Leg 119, Hole 738B, Core 2H, Section 1W, 78 cm

Image ID: B0483/B0484

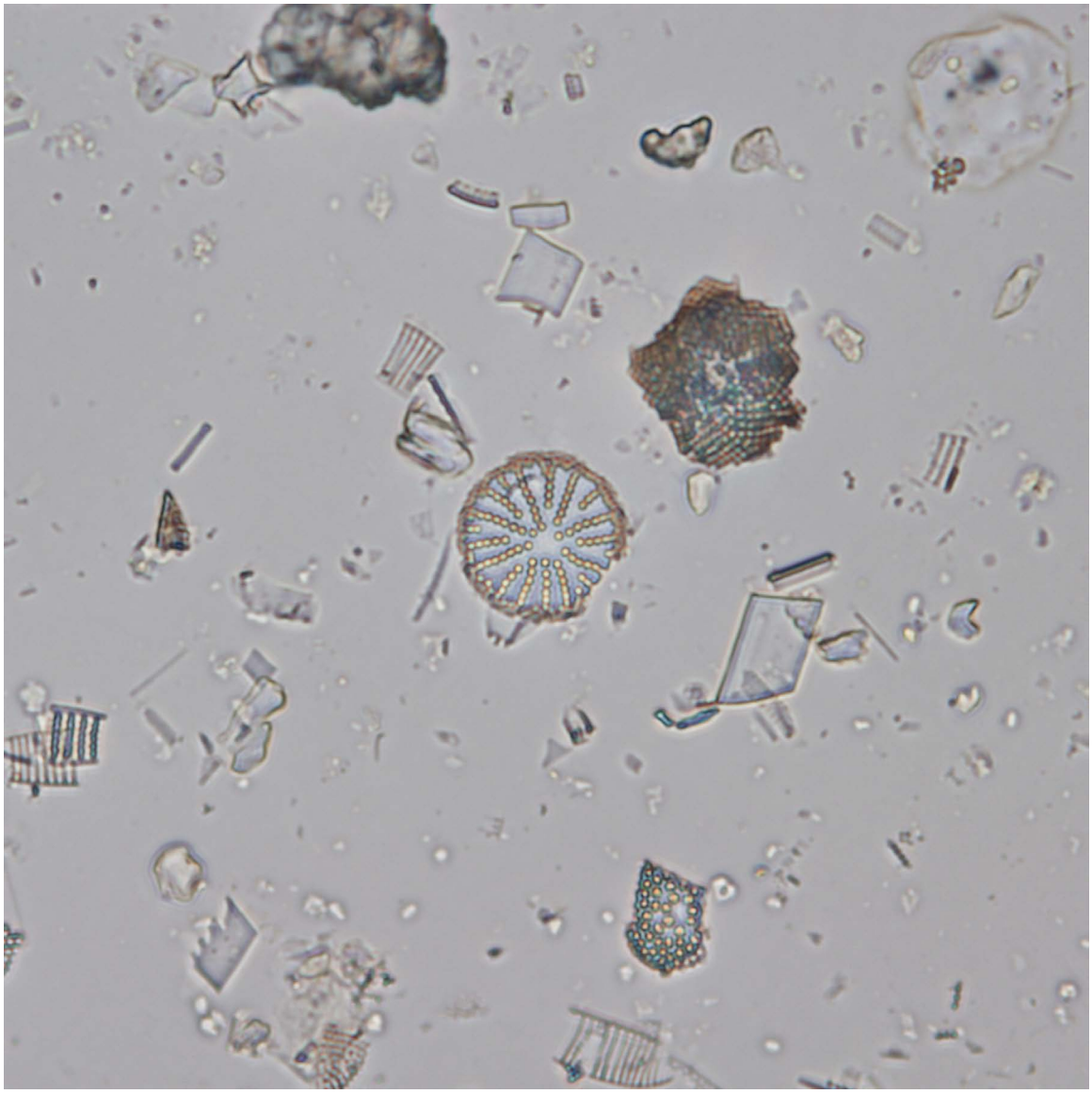

Diatom 12.

The field of view is centered on a centric diatom with raised ribs that is surrounded by siliceous and calcareous debris in a mixed calcareous/siliceous ooze. Note the level to which the debris has been dispersed on the slide.

ODP Sample (late Miocene-Pleistocene): Leg 119, Hole 738B, Core 1H, Section 2W, 69 cm

Image ID: B0058

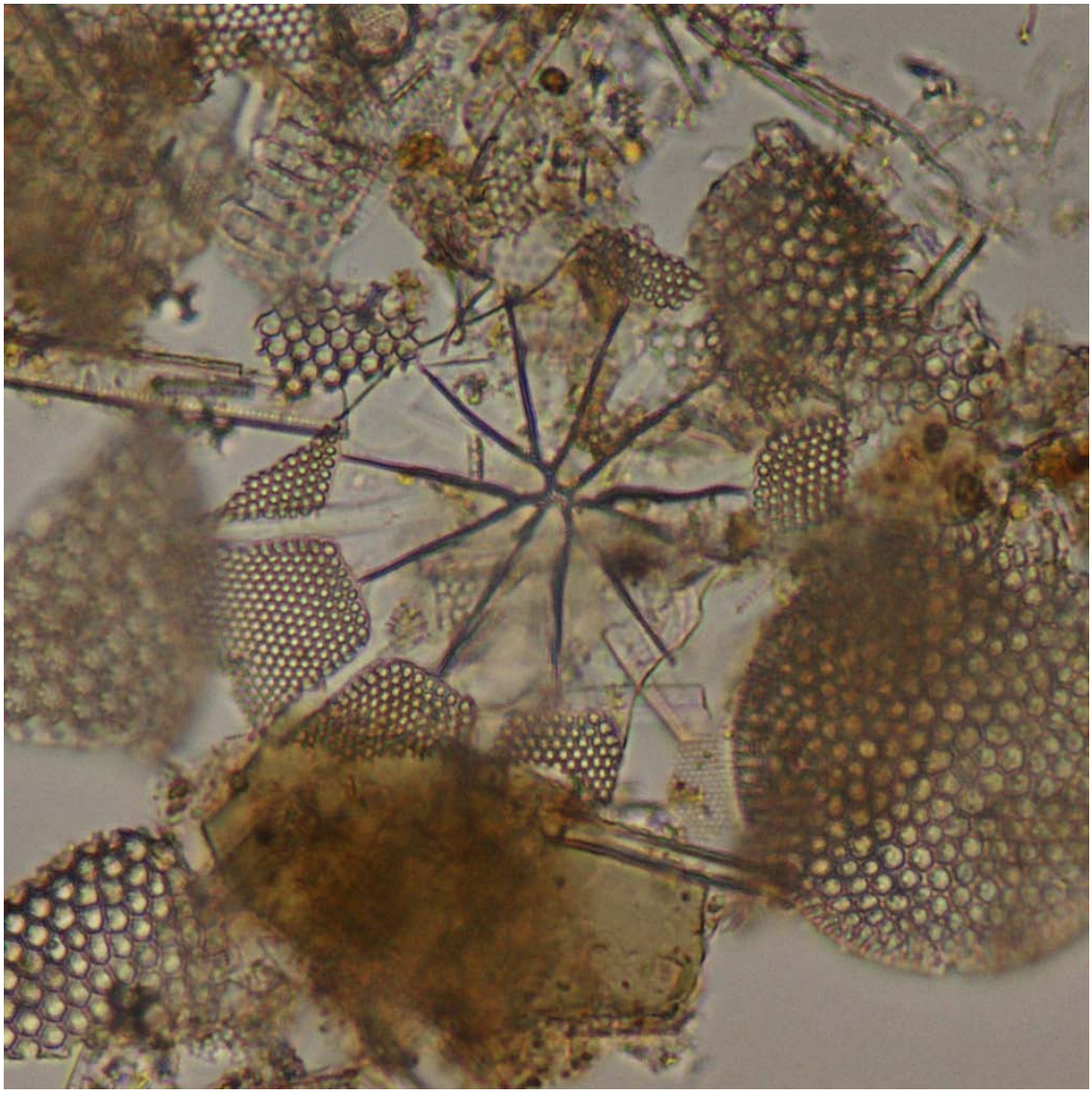

Diatom 13.

In the center of the field of view is a broken centric diatom valve with central hyaline zone and hyaline rays radiating out towards the edge of the valve. It and surrounding diatom debris are all isotropic so no cross-polar view is provided.

DSDP Sample (Pliocene): Leg 56, Hole 438A, Core 13, Section 3, 64 cm

Image ID: B0067

Diatom 14.

In the center of the field of view is an intact centric diatom with a pronounced rim effect that might be a product of stacked valves in an intact, flat lying frustrule. Adjacent to it is a broken centric diatom valve with central hyaline zone and hyaline rays extending out towards the edge of the valve.

DSDP Sample (early Pleistocene): Leg 57, Hole 440B, Core 8, Section 3, 5 cm

Image ID: B0253

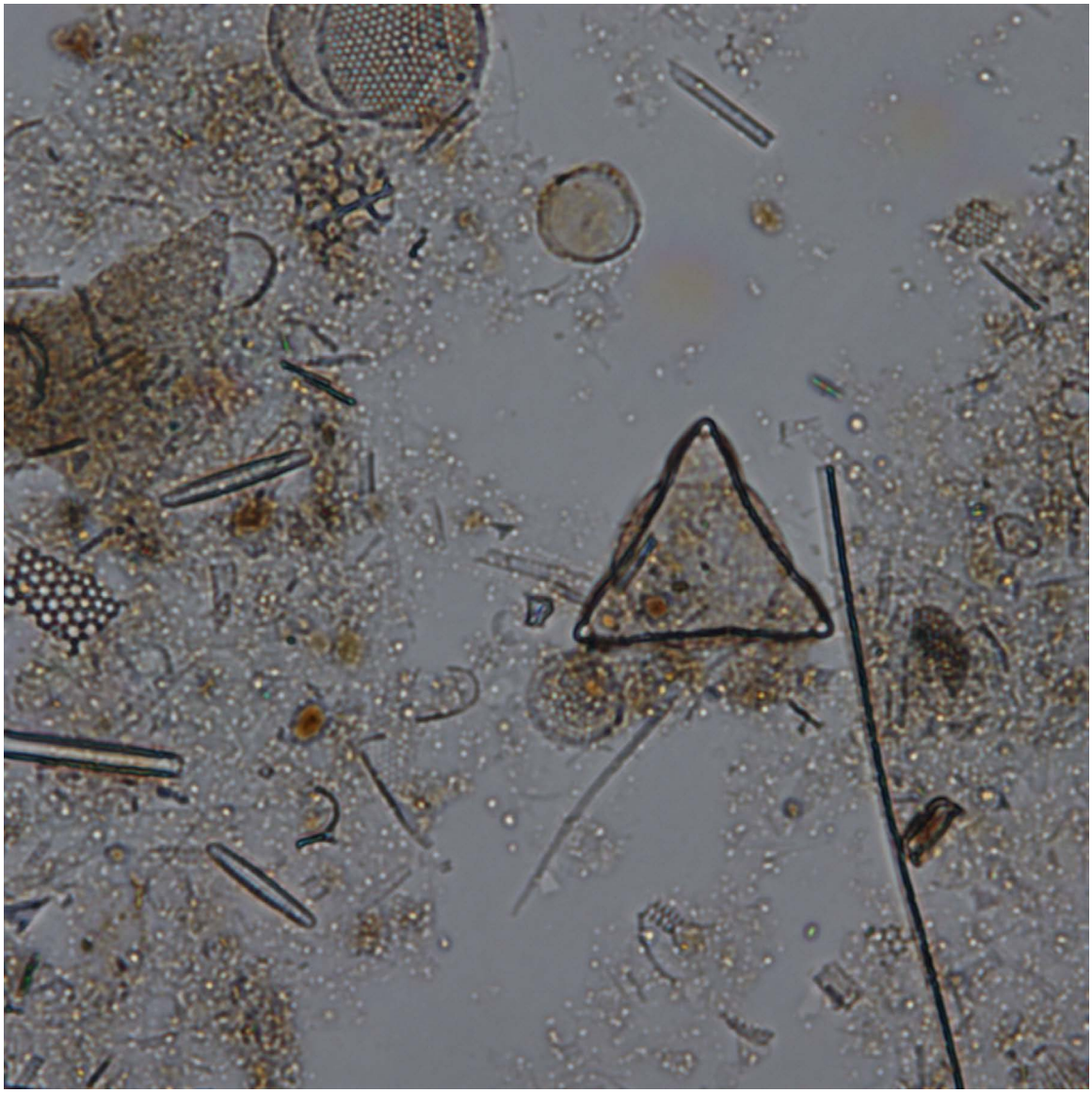

Diatom 15.

A distinct triangular-shaped centric diatom valve lies in the center of this field of view. Note the slightly shifted circular centric diatoms in the upper edge. These are likely frustrule valves slightly disassociated during the smear process. All components are isotropic, so no cross-polar view is provided.

ODP Sample (middle and late Pleistocene): Leg 175, Hole 1075A, Core 8H, Section 2W, 27 cm

Image ID: B0424/B0425

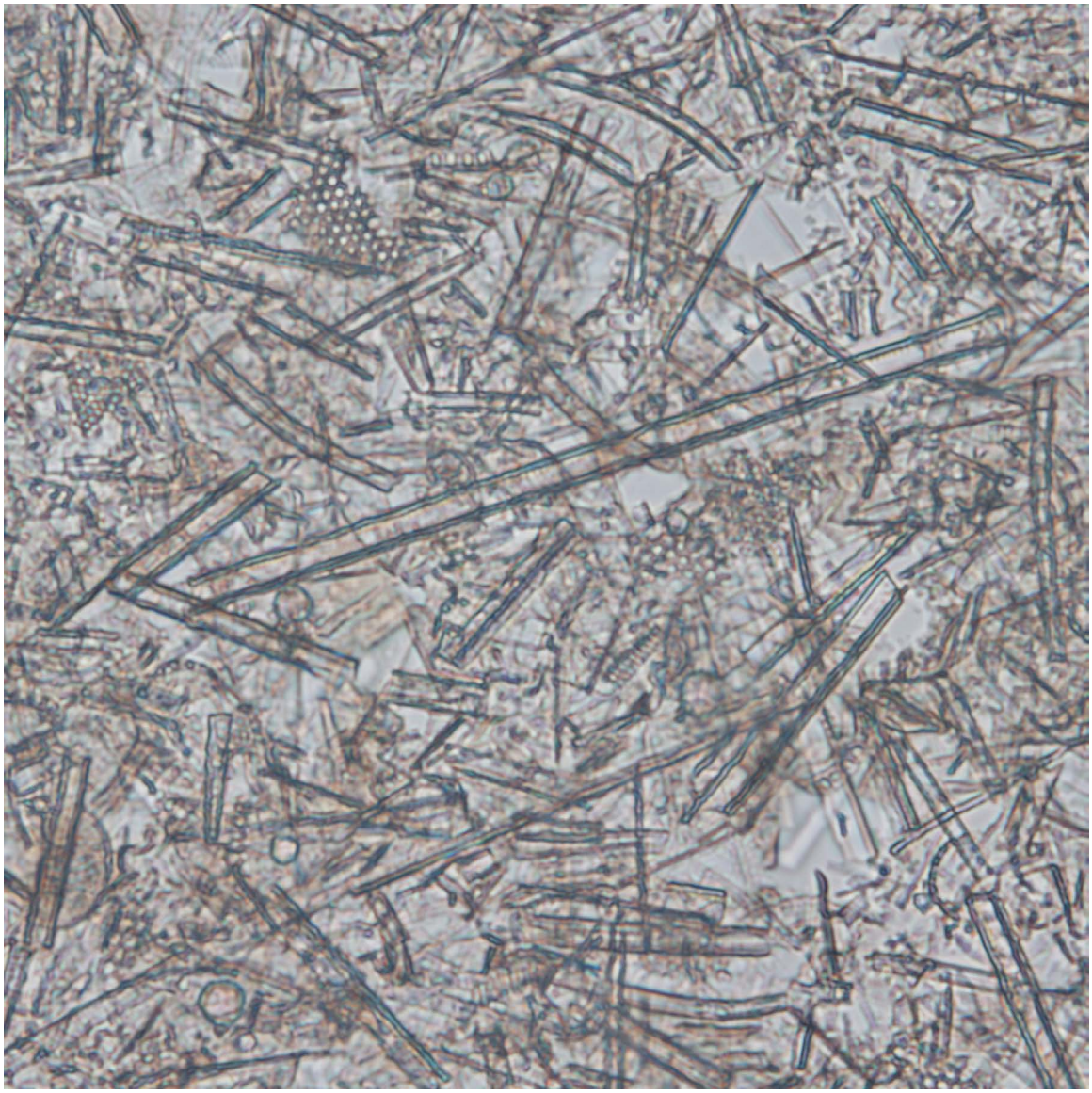

Diatom 16.

Fibrous mat of opaline elongate pennate diatoms with bits of centric diatoms recognizeable by their honeycomb structure. The entire sediment is isotropic as shown by the black cross-polar view.

ODP Sample (early Pliocene): Leg 113, Hole 690A, Core 1H, Section 6W, 105 cm

Image ID: B0134/B0135

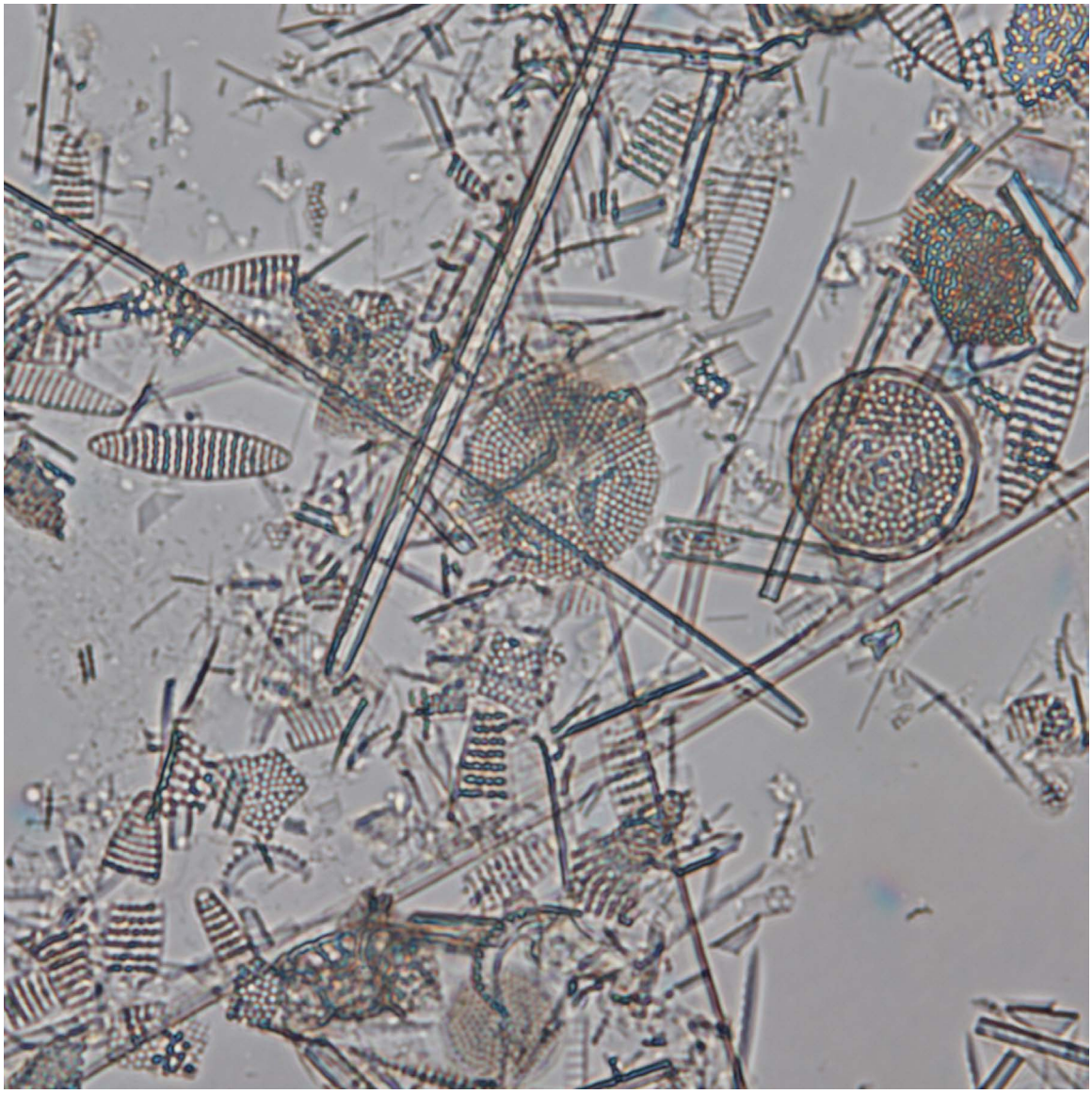

Diatom 17.

This is a diatom ooze consisting of a mix of centric and pennate diatoms, mostly fragmented. The circular, honeycomb textured valves are centric diatoms, whereas the elongate and striped football shaped valves are pennate diatoms. Only sparse calcareous biogenic debris can be seen with polars crossed.

ODP Sample (Pleistocene): Leg 177, Hole 1093A, Core 1H, Section 2W, 17 cm

Image ID: B0434/B0435

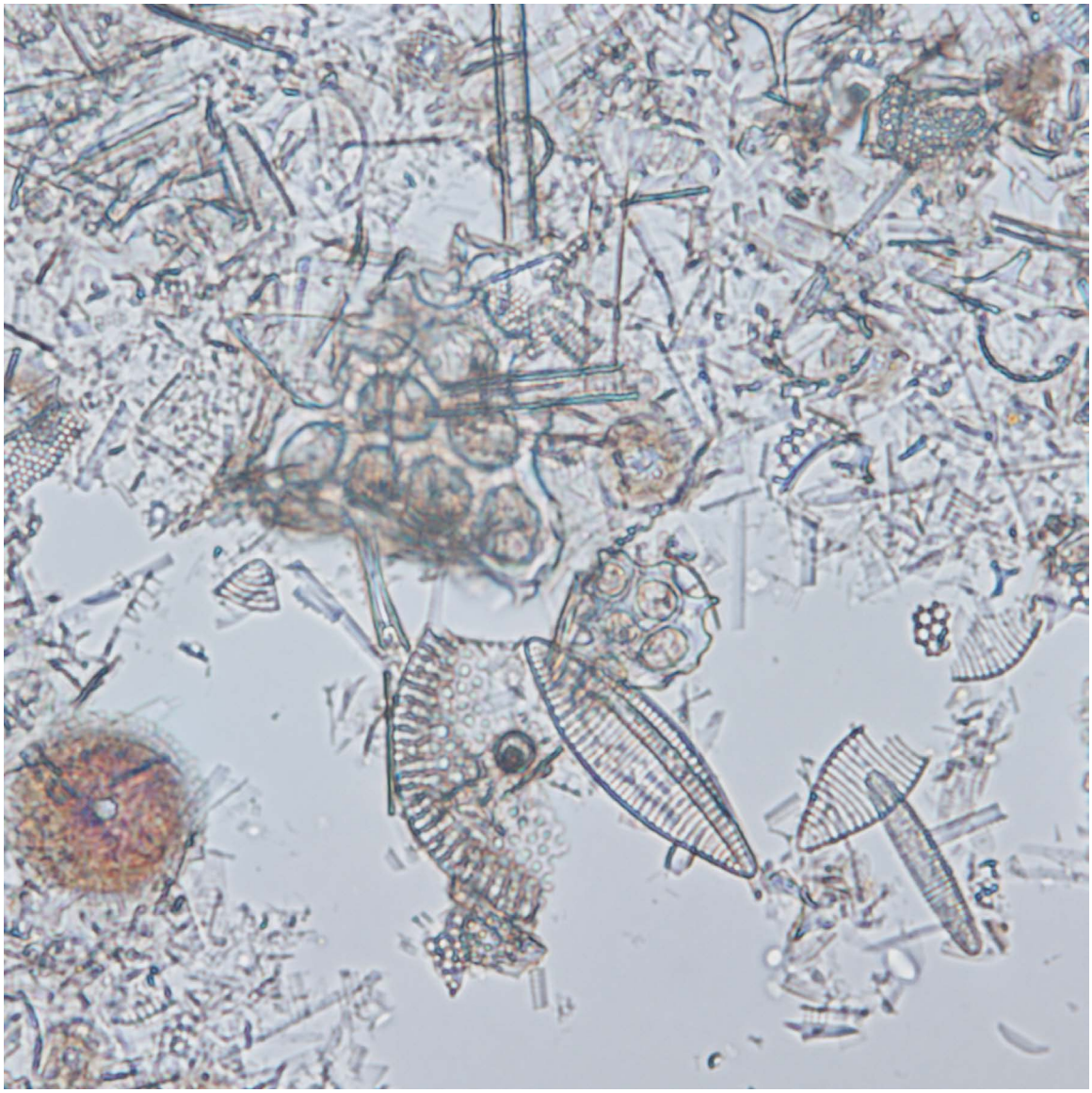

Diatom 18.

Siliceous ooze with football-shaped pennate diatoms in the lower right corner of the slide. Large skeletal fragment in the center is a radiolarian. Almost the entire field of view is isotropic with only a few birefringnet fragments of mineral silt or carbonate biogenic debris. The orange-color of the centric diatom in lower left corner is likely a function of diffraction of light through an intact frustule (both valves).

ODP Sample (early Pliocene): Leg 113, Hole 690B, Core 2H, Section 2W, 120 cm

Image ID: B0247

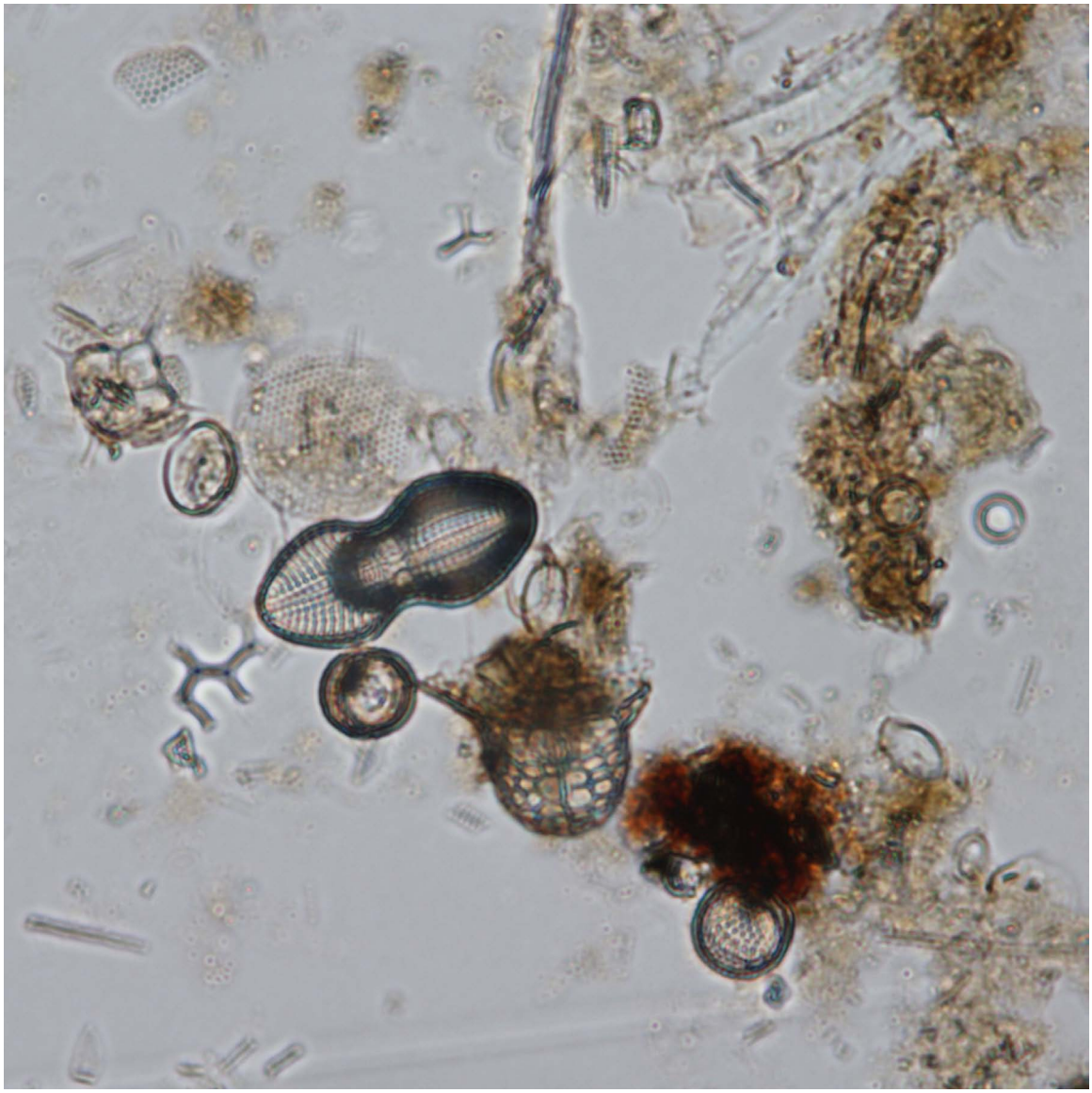

Diatom 19.

This image of organic-rich siliceous ooze is focused on the peanut-shaped pennate diatom in the center of the field of view. Bilateral symmetry of pore structure is partly masked by a large bubble in the test. Other siliceous debris include a radiolarian, intact frustules of small centric diatoms and a silicoflagellate.

ODP Sample (late and middle Pleistocene): Leg 175, Hole 1075B, Core 2H, Section 2W, 15 cm

Image ID: B0454/B0455

Diatom 20.

These pennate diatoms resemble paper clips and are minor components of the surrounding nannofossil ooze. Note their variable internal structure. Coccoliths are readily distinguished when polars are crossed.

ODP Sample (middle Miocene): Leg 113, Hole 690B, Core 5H, Section 2W, 57 cm

Image ID: B0450/B0451

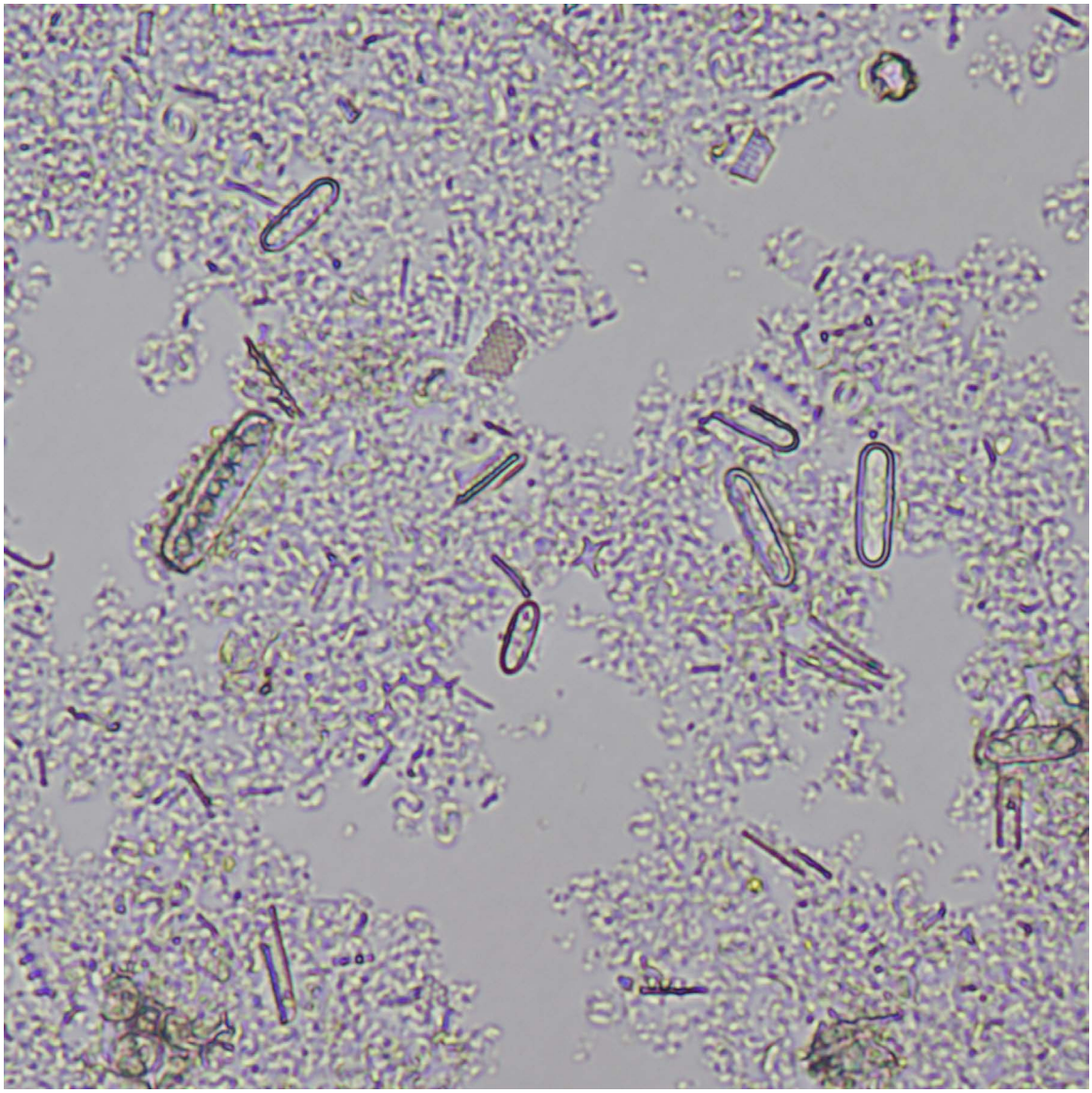

Diatom 21.

These pennate diatoms resemble paper clips and are minor components of the surrounding nannofossil ooze. Note their variable internal structure. Coccoliths are readily distinguished with polars crossed. Linear opaline fragments may be parts of these pennate diatoms or radiolarian spicules.

ODP Sample (middle Miocene): Leg 113, Hole 690B, Core 5H, Section 2W, 57 cm

Image ID: B0056

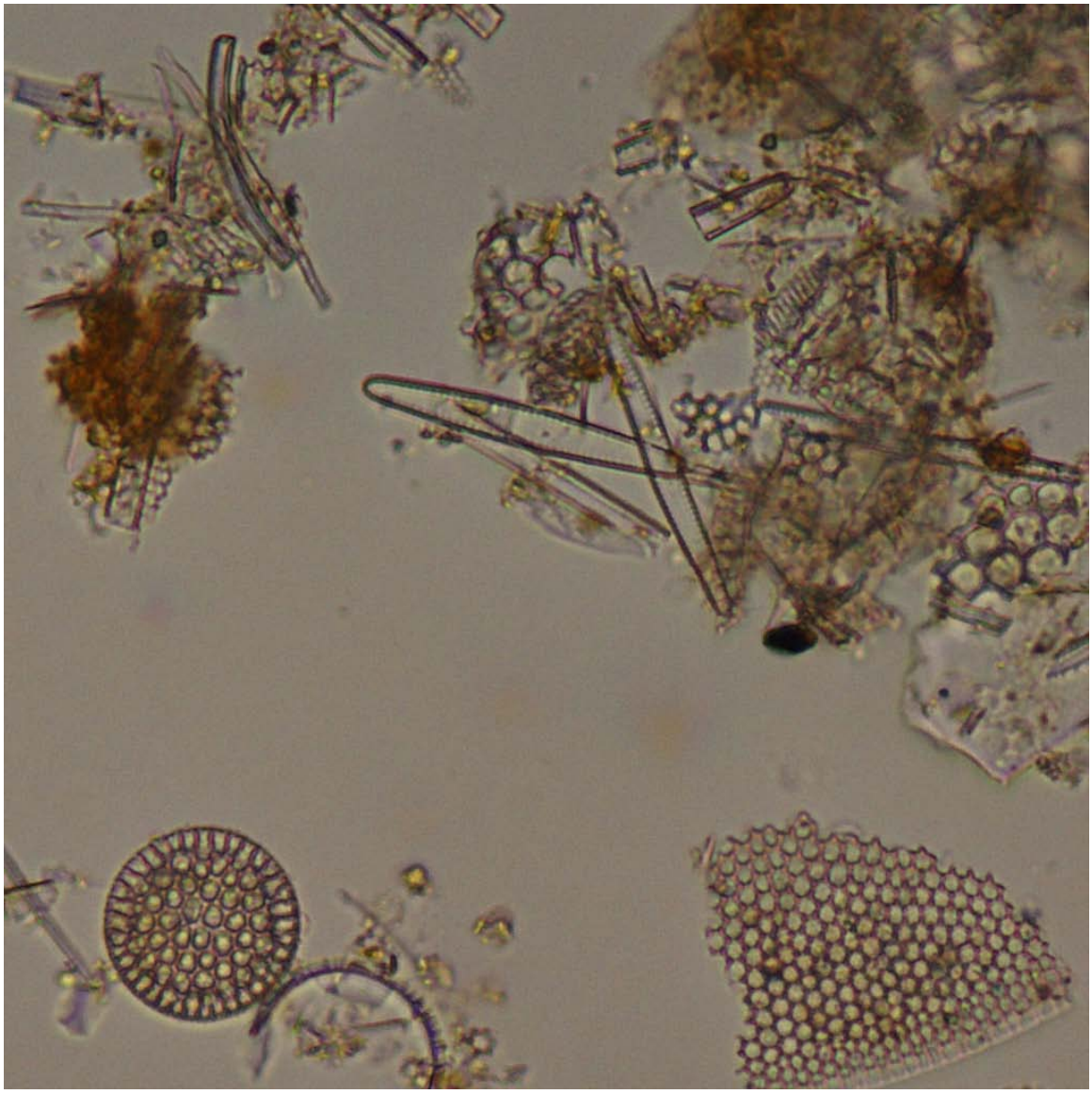

Diatom 22.

Several elongate pennate diatoms are clusted in the center of this field of view. Other siliceous debris is mostly porous centric fragments. No cross-polar view is provided.

DSDP Sample (early-late Pliocene): Leg 56, Hole 438A, Core 13, Section 3, 64 cm

Image ID: 0625

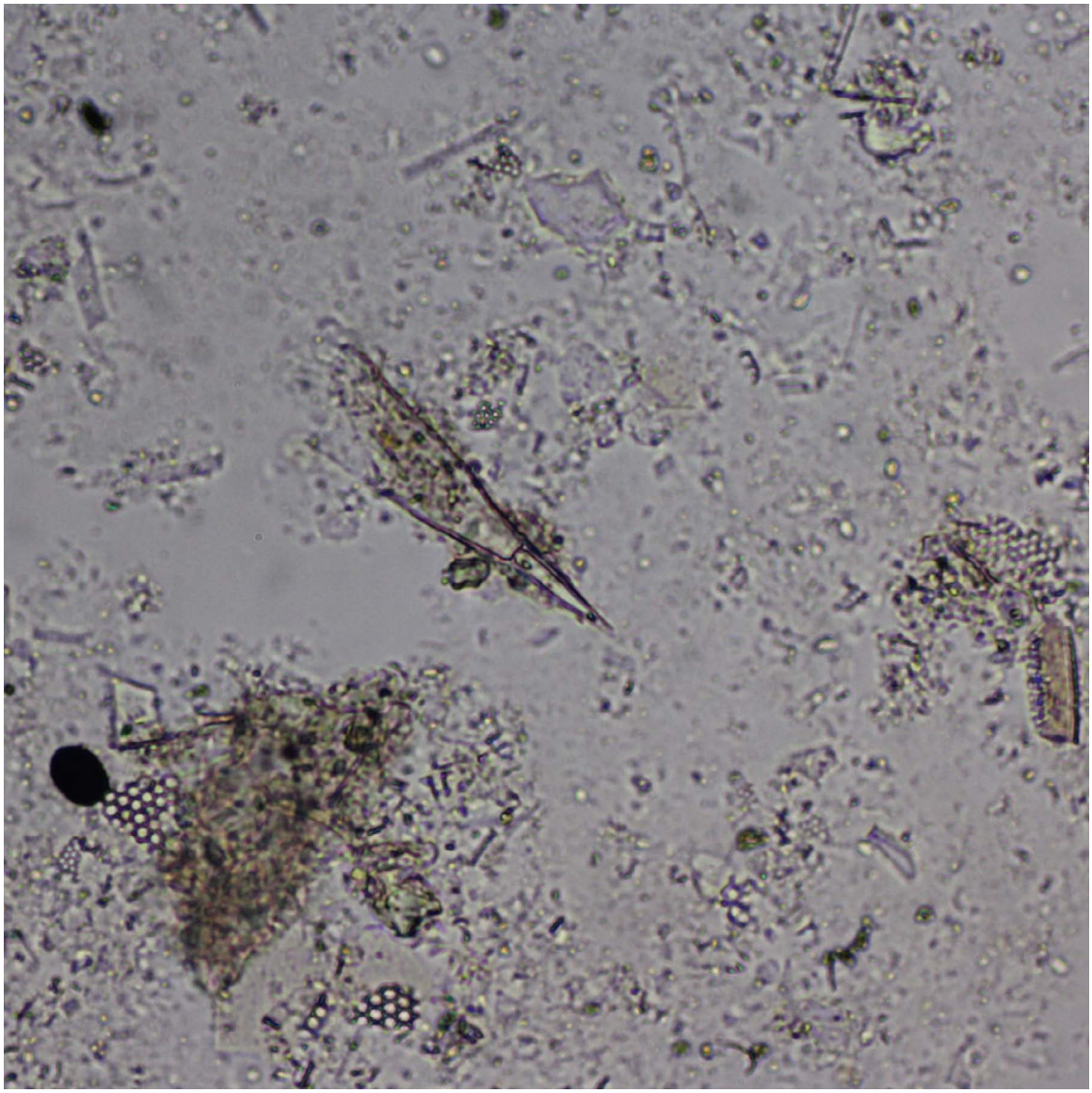

Diatom 23.

Pointed, cone-shaped pennate diatom lies in the center of this field of view. This is a *Rhizosolenia* diatom, that can be a major mat-former in the equatorial Pacific. No cross-polar view is provided.

ODP Sample (early Pliocene): Leg 178, Hole 1097A, Core 34R, Section 1W, 16 cm

Image ID: 0622

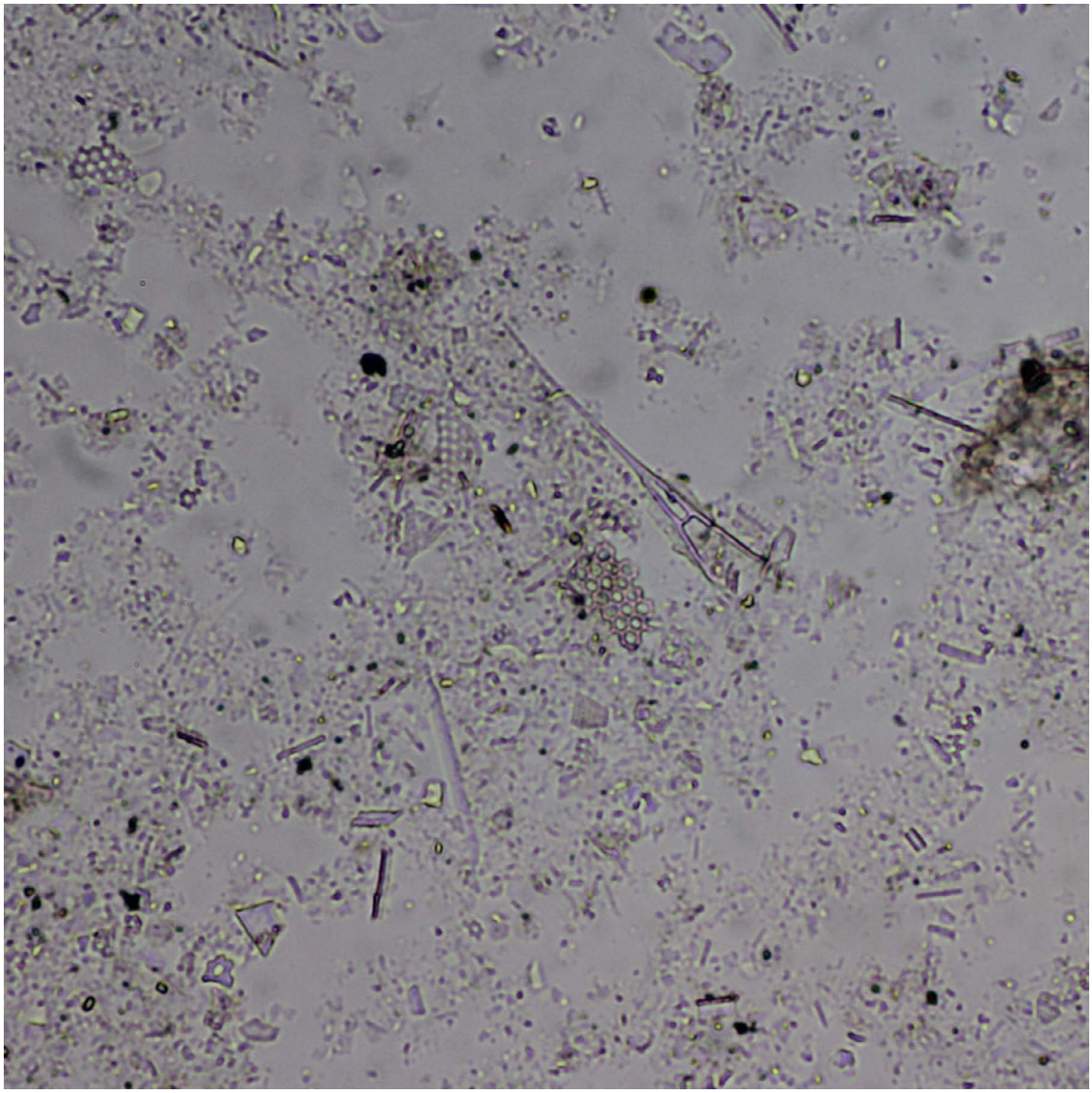

Diatom 24.

A pointed, cone-shaped pennate diatom (*Rhizosolenia*) lies in the center of this field of view. No cross-polar view is provided.

ODP Sample (early Pliocene): Leg 178, Hole 1097A, Core 34R, Section 1W, 16 cm

Image ID: B0491

Diatom 25.

Several pointed, cone-shaped pennate diatoms (*Rhyzolenia*) lie in the center of this field of view. They and the other siliceous debris are isotropic so no cross-polar view is provided.

ODP Sample (late Miocene-Pleistocene): Leg 119, Hole 738B, Core 2H, Section 1W, 78 cm

Image ID: B0493

Diatom 26.

Pointed, cone-shaped pennate diatom lies in the center of this field of view. Other pennate and centric debris is present. Note the fine radiating texture of the centric diatom valve which has been separated from its girdle. No cross polar view is provided as all material is isotropic.

ODP Sample (late Miocene-Pleistocene): Leg 119, Hole 738B, Core 2H, Section 1W, 78 cm

Image ID: B0706/B0707

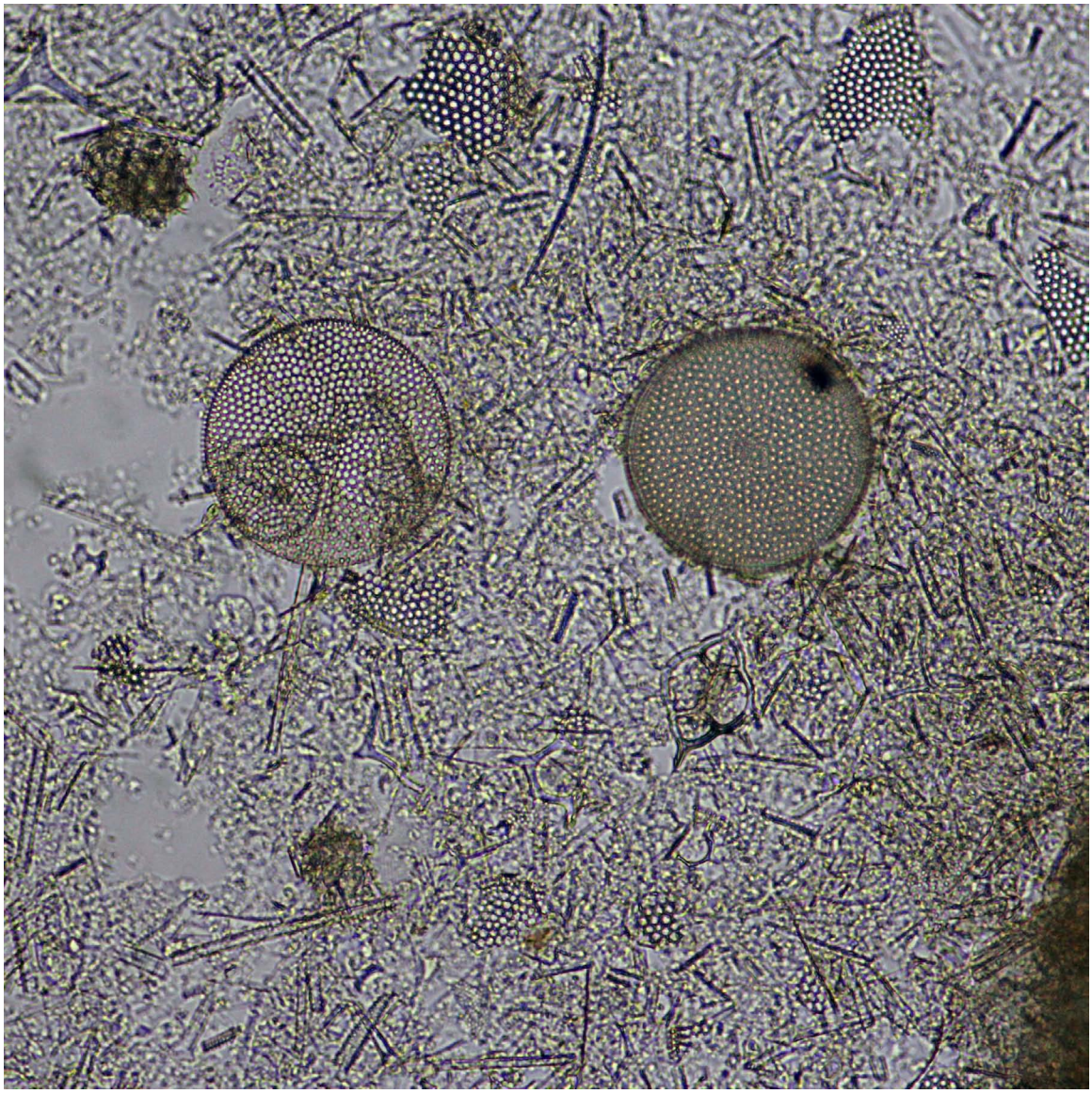

Diatom 27.

Ooze containing a variety of elongate tube-like pennate fragments, with one large intact pennate diatom in the center of the field of view. Fragments of centric diatoms are also present. When polars are crossed, it is apparent that this is a mixed siliceous/calcareous ooze with a significant (30-40%) proportion of birefringent nannofossils (grey pinwheels), whereas the opaline diatoms are nonbirefringent. Review of the plane light view shows the presence of faint star and circular shapes characteristic of nannofossils.

DSDP Sample (late Miocene): Leg 38, Hole 845A, Core 15H, Section 2W, 10 cm

Image ID: B0718/B0719

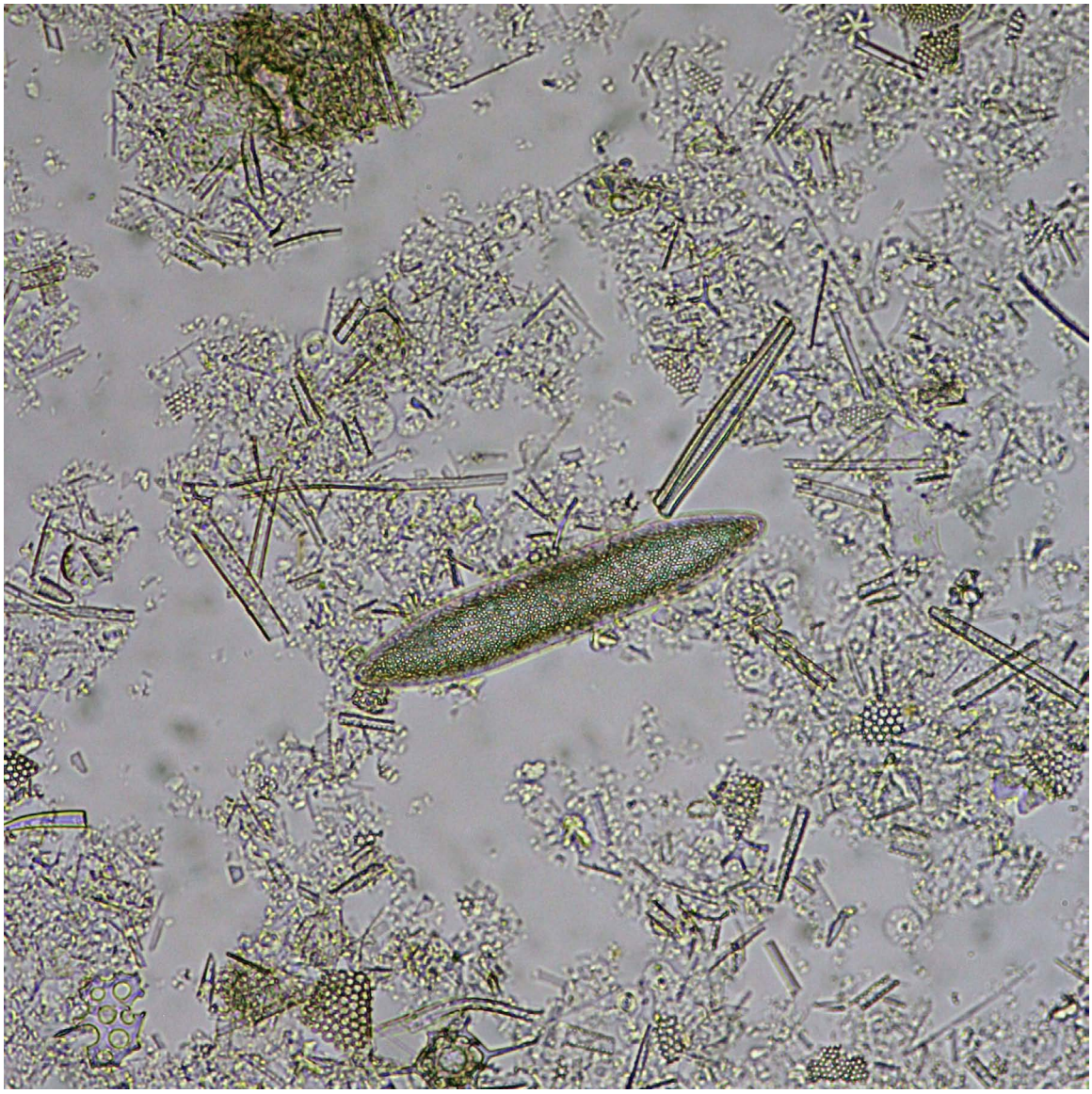

Diatom 28.

In plane light, several centric diatoms can be seen in this sample, along with other fragments of both pennate and centric diatoms and silicoflagellates. When polars are crossed, it is apparent that this sediment is a mixed siliceous/calcareous ooze with a significant (30-40%) proportion of nannofossils (grey pinwheels) and some micrite of uncertain origin (bioclast?) with higher birefringence.

DSDP Sample (late Miocene): Leg 38, Hole 845A, Core 15H, Section 2W, 10 cm

Radiolarians

INTRODUCTION TO RADIOLARIANS

Overview – Radiolarians are a highly diverse group of planktonic protists with skeletal elements composed of opaline silica. They have a long geologic history and occur throughout the world ocean, from the near-surface to abyssal water depths. They are most abundant in areas of upwelling. There are two major Cenozoic groups with distinctive skeletons, the conical-shaped nassellarians and spherical to discoidal-shaped spumellarians.

Diagnostic Features –A radiolarian shell differs from a planktic foraminiferal test in having a siliceous framework, rather than a perforate calcareous wall. The Nassellarians are generally conical in shape and may have multiple uniserial 'chambers' with or without basal spines or terminal, apical spine and cephalus; they can resemble spaceships. The Spumellarians range in shape from spherical to ellipsoidal to discoidal. They typically display radial symmetry and may have concentric shells connected by solid bars. The radiolarian shell lattice has rather large pores and may have primary and secondary spines. In some, a delicate siliceous framework resembles a mesh and appears 'spongy'. ~30-2000 µm (2 mm).

Biology – Kingdom Protoctista, Subkingdom Akonta, Phylum Actinopoda. The Phaeodarians are probably not related to the other radiolarians; the Acantharia form their shells from strontium sulfate. Both groups are very rarely preserved. The Polycystina have two major groups: the Nassellarians and Spumellarians. Like the planktic foraminifera, many species of radiolarians contain algal symbionts.

Ecology – Heterotrophs. Open marine; near-surface to many hundreds of meters water depth.

Paleobiogeography – Radiolarian abundance is strongly related to the availability of dissolved silica, typically in areas of upwelling; radiolarian-rich sediments are found beneath areas of highly productive surface waters, especially in the area of the equatorial divergence. Radiolarians are also found in red clay sediments below the calcite compensation depth.

Stratigraphic Range – Cambrian to present

Key References and Examples:

Anderson, O.R., 1983. Radiolaria. Springer-Verlag, New York, USA, 365 pp.

Casey, R.E., 1993. 13: Radiolaria. In Lipps, J.H. (Ed.), Fossil Prokaryotes and Protists: Blackwell Scientific Publications, 249-284.

Kling, S.A., 1978. 9: Radiolaria. In Haq, B.U., and Boersma, A. (Eds.), Introduction to Marine Micropaleontology: Elsevier, 203-244.

Morley, J.J., 1985. Radiolarians from the northwest Pacific, DSDP Leg 86. In, Heath, G.R., Burckle, L.H., et al., Initial Reports of the DSDP, 86:399-422.

Sanfilippo, A., and Riedel, W.R., 1985. 13: Cretaceous radiolarian. In Bolli, H.M., Saunders, J.B., and Perch Nielsen, K. (Eds.), Plankton Stratigraphy: Cambridge (Cambridge Univ. Press), 573-630.

Sanfilippo, A., Westberg-Smith, M.J., and Riedel, W.R., 1985. 14: Cenozoic radiolarian. In Bolli, H.M., Saunders, J.B., and Perch Nielsen, K. (Eds.), Plankton Stratigraphy: Cambridge (Cambridge Univ. Press), 631-712.
Weaver, F.M., 1983. Cenozoic radiolarians from the southwest Atlantic, Falkland Plateau region, DSDP Leg 71. In, Ludwig, W.J., Krasheninnikov, V.A., et al., Initial Reports of the DSDP, 71:667-686.

Web Resources:

http://www.ucl.ac.uk/GeolSci/micropal/radiolaria.html
http://www.ucmp.berkeley.edu/protista/radiolaria/rads.html
Line drawings of Ernst Haeckel, 1862: http://caliban.mpiz-koeln.mpg.de/haeckel/radiolarien/
http://www.radiolaria.org

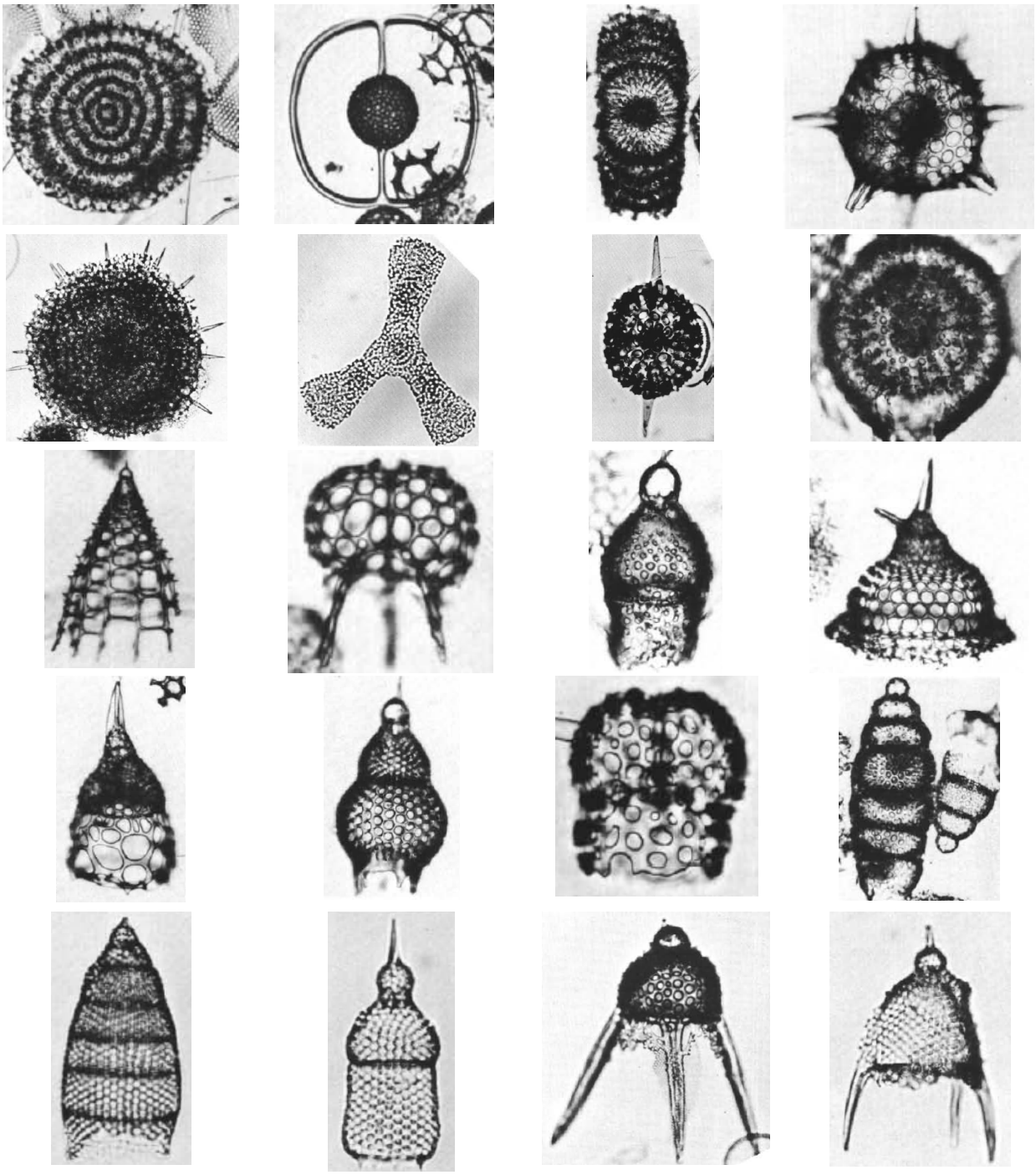

Representative Cenozoic spumellarian and nassellarian radiolarians. Top row (spumellarian radiolarians): *Stylodictya validispina, Saturnalis circularis, Diartus hughesi, Actinomma tanyacantha*. Second row (spumellarian radiolarians): S*pongotrochus(?) venustum, Euchitonia sp., Druppatractus acquilonius, Sphaeropyle robusta*. Third row (nassellarian radiolarians): *Peripyramis circumtexta, Triceraspyris antarctica, Theocorys redondoensis, Clathrocyclas bicornis*. Fourth row (nassellarian radiolarians): *Lamprocyrtis heteroporos, Lamprocyclas aegles, Dendrospyris haysi, Stichocorys peregrina*. Bottom row (nassellarian radiolarians): *Eucyrtidium acuminatum, Theocorythium trachelium dianae, Lychnocanoma grande, Pterocanium prismatium*. Photomicrographs from Weaver, 1983; Morley, 1985.

Radiolarians


Radiolarian 1


Radiolarian 2

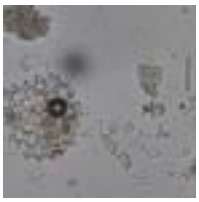
Radiolarian 3


Radiolarian 4


Radiolarian 5


Radiolarian 6


Radiolarian 7


Radiolarian 8

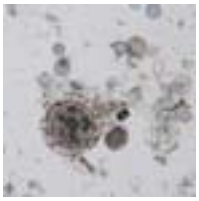
Radiolarian 9


Radiolarian 10


Radiolarian 11


Radiolarian 12


Radiolarian 13


Radiolarian 14

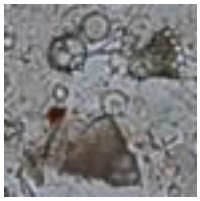
Radiolarian 15


Radiolarian 16


Radiolarian 17


Radiolarian 18

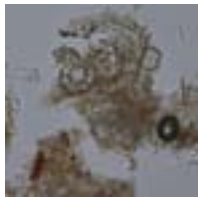
Radiolarian 19


Radiolarian 20


Radiolarian 21

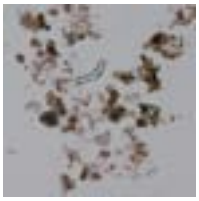
Radiolarian 22


Radiolarian 23

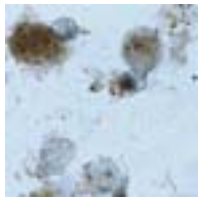
Radiolarian 24


Radiolarian 25

Radiolarians

Radiolarian 26

Radiolarian 27

Radiolarian 28

Radiolarian 29

Image ID: 0148/0149

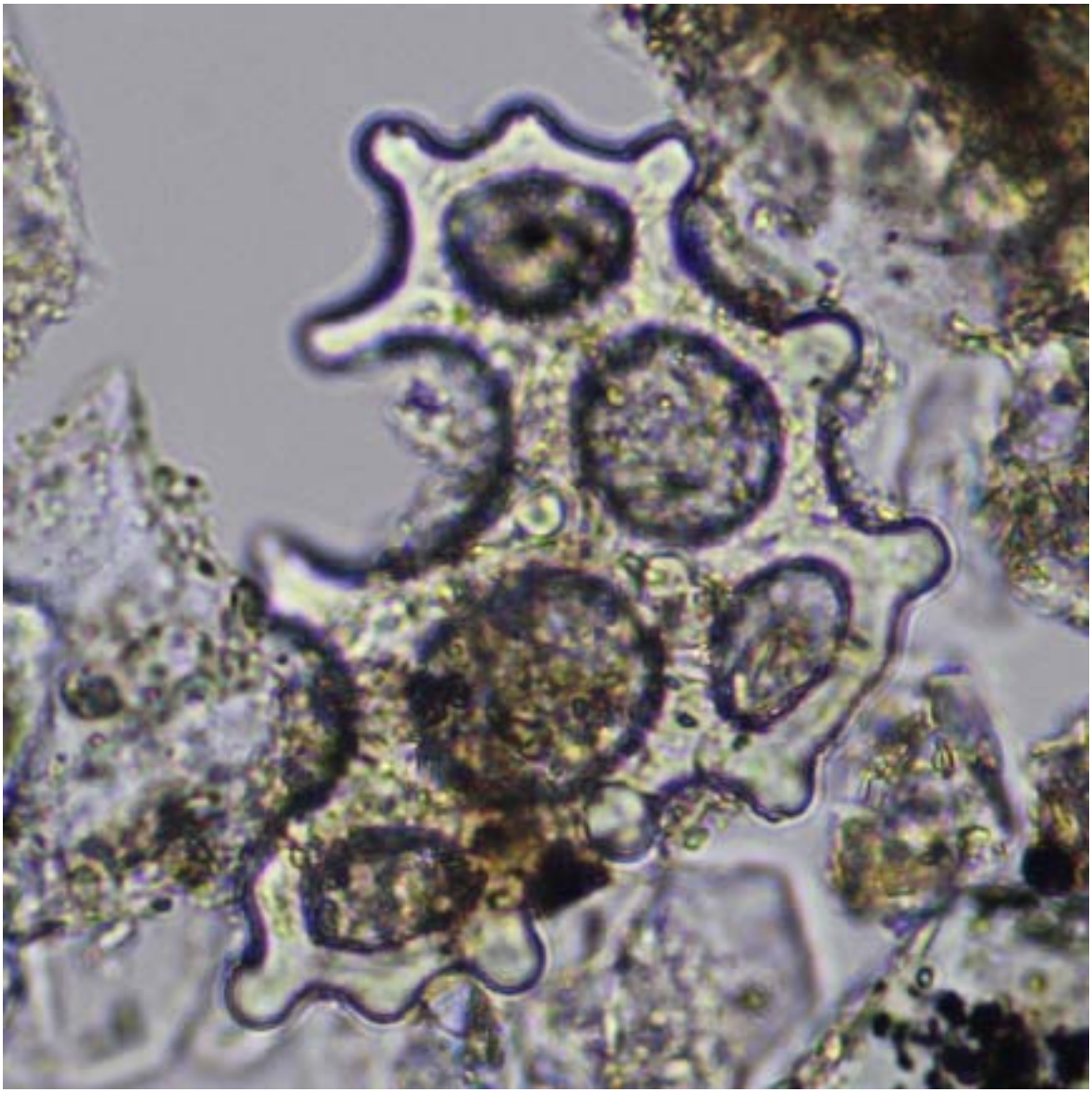

Radiolarian 1.

Porous sand-size skeletal fragment of a radiolarian in a dominantly terrigenous sediment. The opaline fragment is isotropic with no birefringence when polars are crossed. Rounded edges of the broken latticed wall suggest that this fragment may be a reworked bioclast that was abraded during transport. Although pores are generally hexagonal in shape, they may be rounded by precipitation of silica. Surrounding grains include quartz and feldspar based on their optical properties, e.g., low birefringence and relief.

IODP Sample (Pleistocene-Holocene): Leg 317, Hole 1352B, Core 11H, Section 2W, 21 cm

Image ID: B0039/B0040

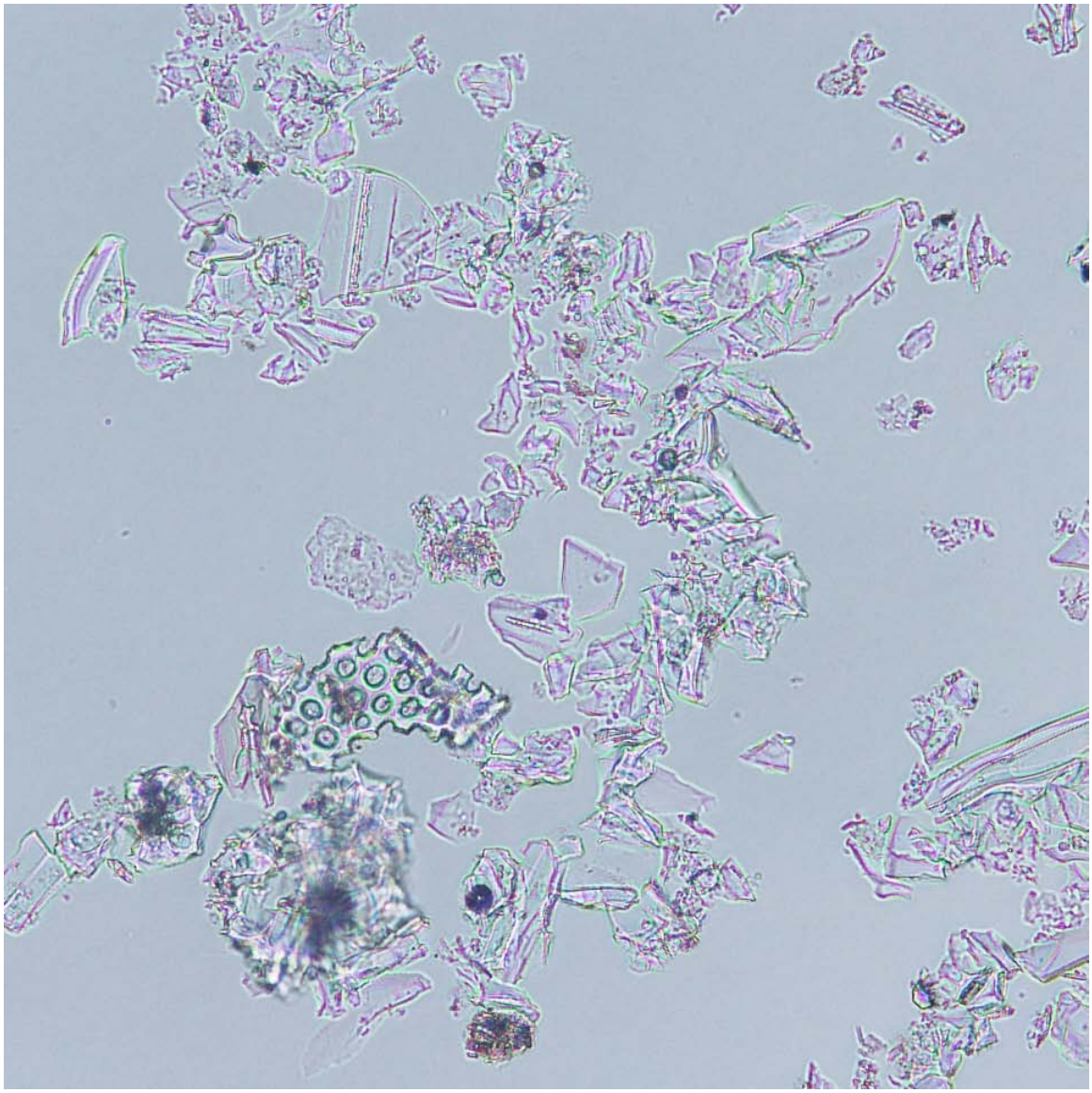

Radiolarian 2.

In this vitric ash composed of colorless glass shards, one siliceous biogenic fragment stands out. It is a latticed skeletal wall fragment from a radiolarian (circled). Under crossed polars, the opaline radiolarian fragment and the vitric components are isotropic, with only minor birefringent components (e.g., mineral inclusions in glass and carbonate including nannofossils).

DSDP Sample (middle Eocene): Leg 119, Hole 286, Core 28, Section 2, 146 cm

Image ID: B0481/B0482

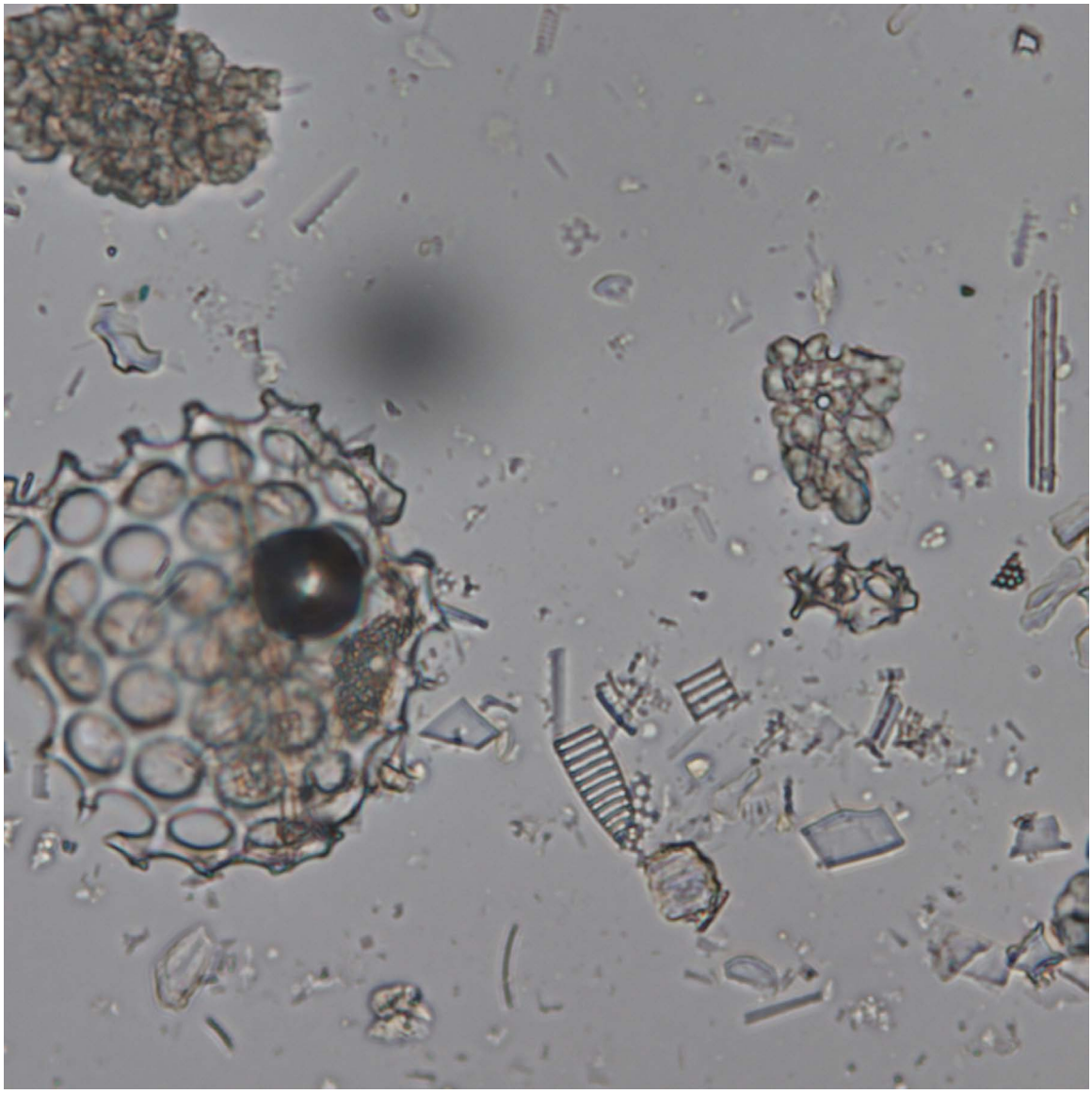

Radiolarian 3.

The rounded shape of this porous radiolarian specimen (on left) is apparent from the variable focus, with the apex being slightly out of focus as compared to the edges of the fragment in the plane-light view. When the alternate view layer is selected, the top is in focus and the outer rim goes out of focus. Other biogenic debris in the field of view includes larger fragments of foraminifera (higher relief) and more delicate diatom fragments. Only the former would show birefringence with polars crossed (not shown).

ODP Sample (Quaternary): Leg 119, Hole 738B, Core 1H, Section 2W, 69 cm

Image ID: 0402/0403

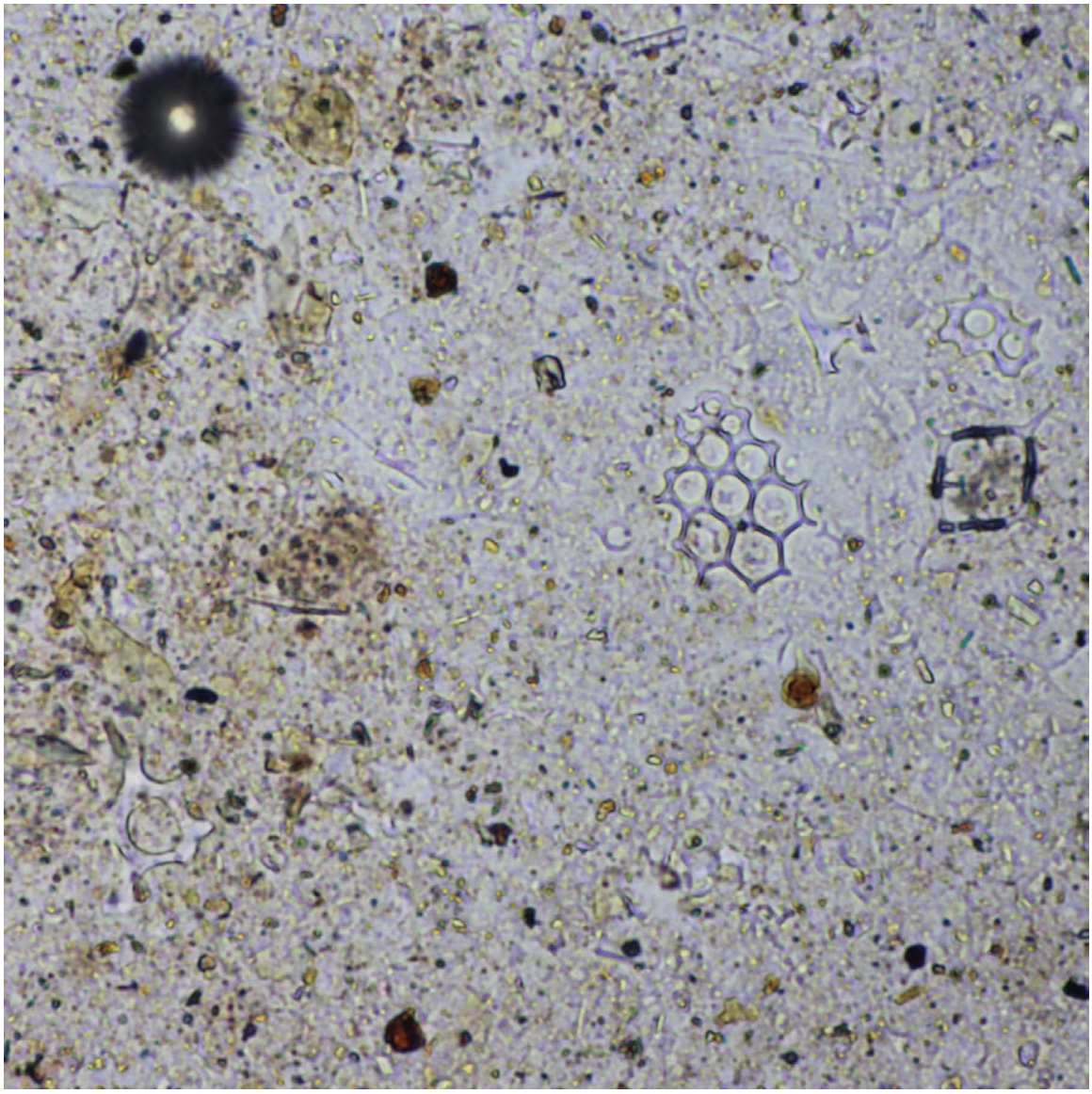

Radiolarian 4.

Densely packed smear slide of hemipelagic mud showing numerous latticed-wall radiolarian fragments some with hexagonal lattice pores and others where the hexagons have been modified (rounded) by precipitation of silica. One diamond-shaped silicoflagellate is present (darker outline), middle right. With polars crossed, opaline biogenic debris shows no birefringence, in contrast to abundant white to grey silt-size fragments of quartz and feldspar. The reddish Fe-oxides are visible in both plane light and with polars crossed. Note small round, dark bubble in upper left corner.

DSDP Sample (late Pleistocene): Leg 86, Hole 576B, Core 1H, Section 1, 2 cm

Image ID: B0414/B0415

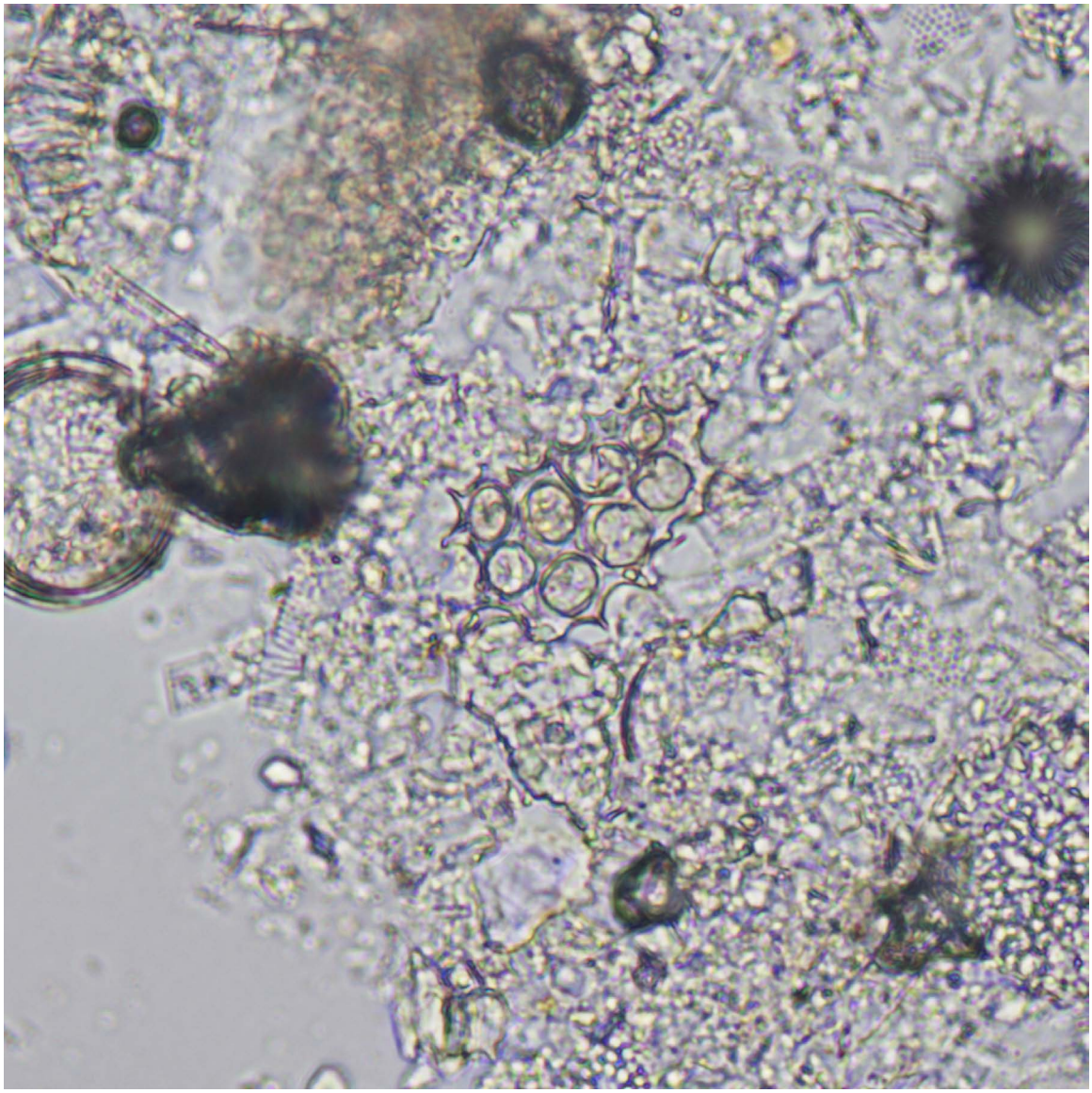

Radiolarian 5.

This opaline radiolarian fragment is readily identifiable by the regular, porous nature of the opaline skeletal fragment and its isotropic nature with polars crossed. Birefringent carbonate (micrite) can be seen in the cross-polar view.

ODP Sample (late Pliocene): Leg 113, Hole 690A, Core 1H, Section 1, 110 cm

Image ID: B0314

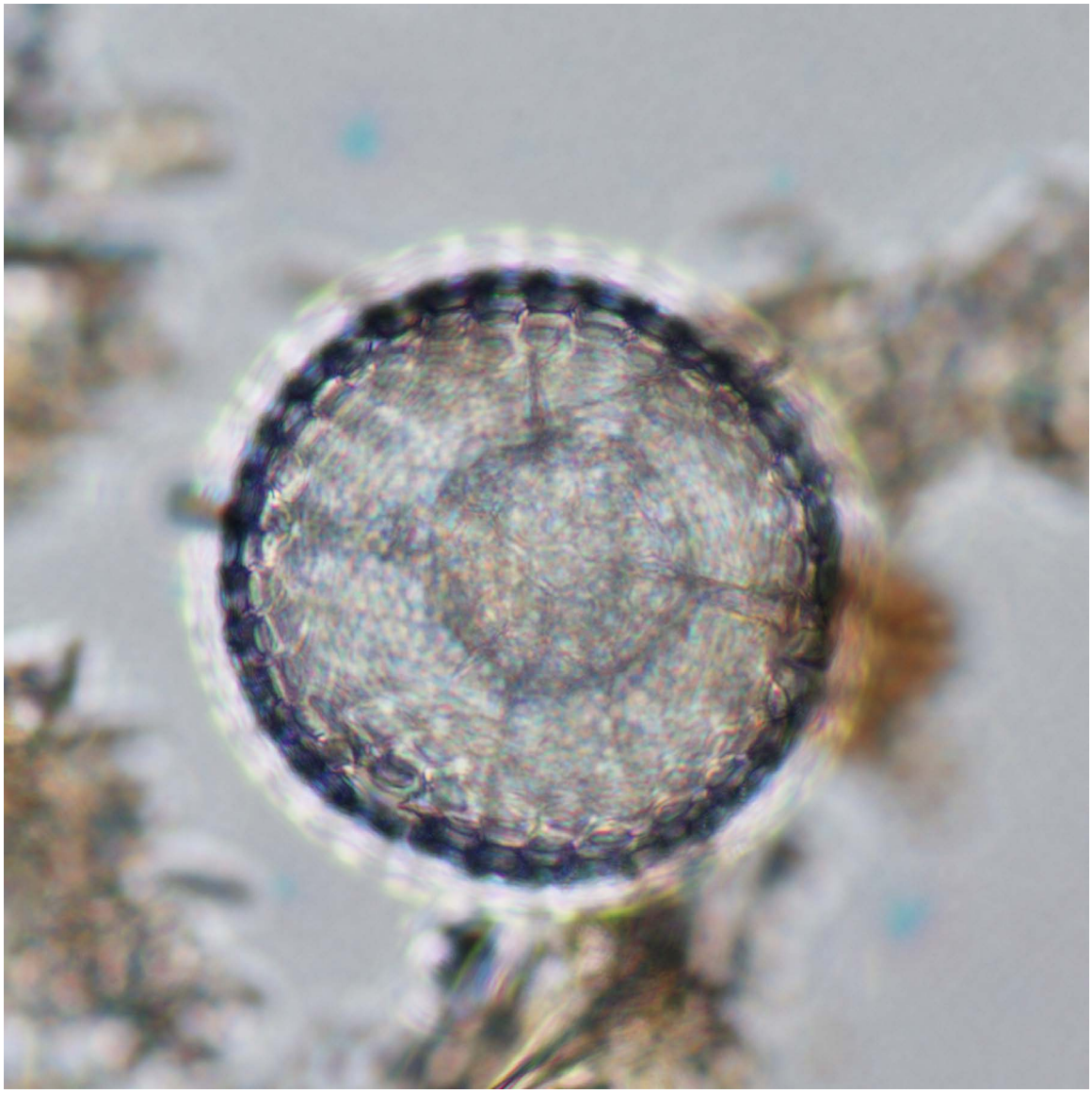

Radiolarian 6.

This Spumellarian radiolarian exhibits an external cortical shell with an internal medullary shell suspended by bars. To show this internal structure both shells are slightly out of focus. The specimen is composed of isotropic opal but no crossed polar view is provided.

ODP Sample (late Miocene): Leg 138, Hole 845A, Core 15H, Section 2W, 10 cm

Image ID: B0315

Radiolarian 7.

Excellent example of a Spumellarian radiolarian composed of isotropic opal, so no view with polars crossed is provided.

ODP Sample (late Miocene): Leg 138, Hole 845A, Core 15H, Section 2W, 10 cm

Image ID: B0296

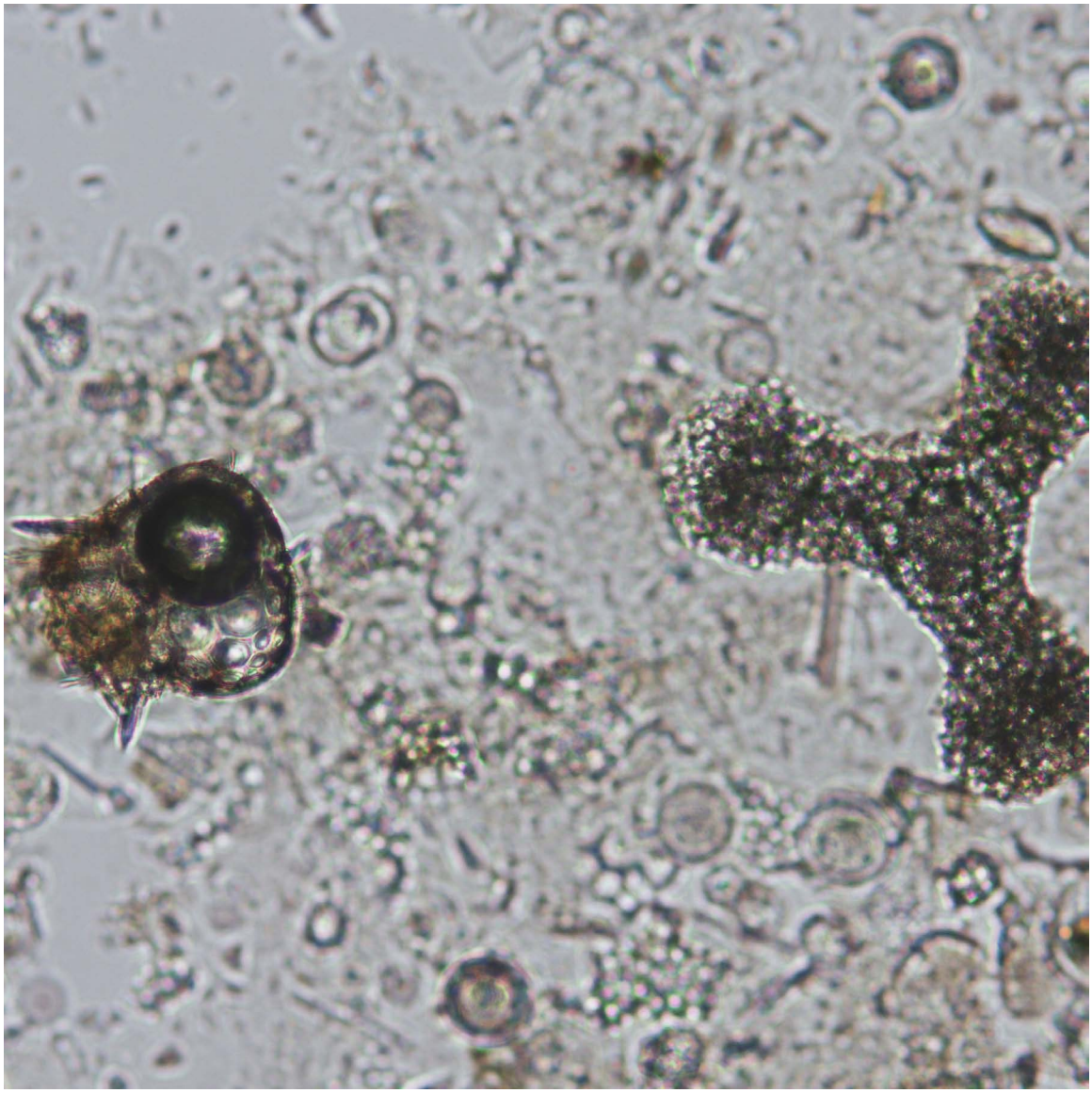

Radiolarian 8.

Excellent examples of larger radiolarians, a Nasellarian on the left and a Spumellarian on the right, set in a finer-grained diatomaceous ooze. All the biogenic debris is isotropic opal so no view with polars crossed is provided.

ODP Sample (Pleistocene): Leg 138, Hole 845A, Core 2H, Section 6W, 120 cm

Image ID: B0285

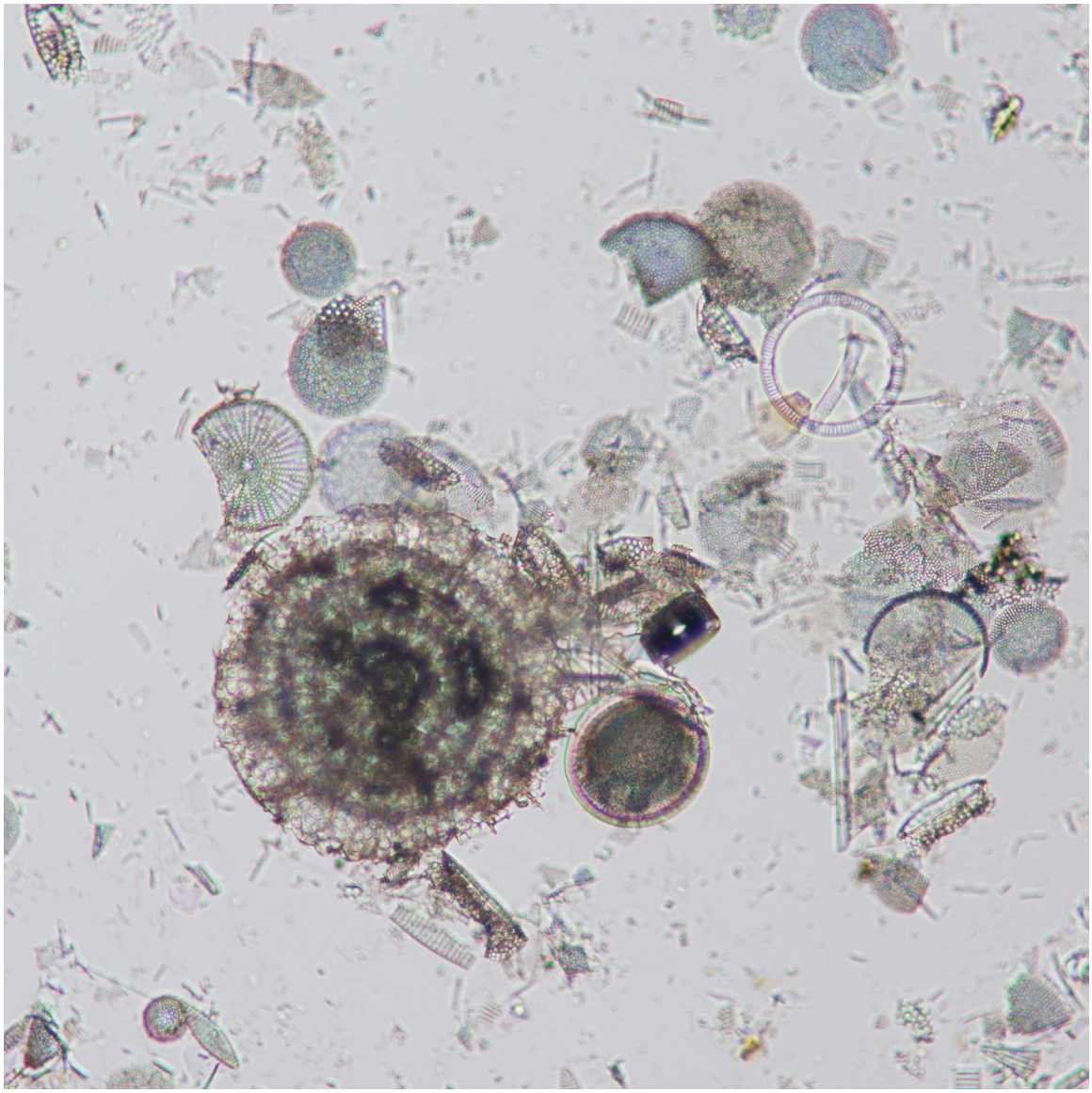

Radiolarian 9.

Large, disk-shaped Spumellarian radiolarian surrounded by variably preserved centric diatoms including one intact frustrule (darker circular feature to right of radiolarian), individual circular valves, valve rims (girdles), and smaller fragments. Note scale differences among these siliceous bioclasts, with the radiolarian being much larger.

ODP Sample (Quaternary): Leg 119, Hole 745B, Core 5H, Section 1W, 65 cm

Image ID: B0250

Radiolarian 10.

A large skeletal element (sagittal ring) of a Nassellarian radiolarian dominates this field of view. The background sediment is organic rich (tan/brown) and largely composed of various diatom fragments. All siliceous bioclasts are opaline with no birefringence, so no cross-polar view is provided.

ODP Sample (late and middle Pleistocene): Leg 175, Hole 1075A, Core 5H, Section 6W, 6 cm

Image ID: B0298

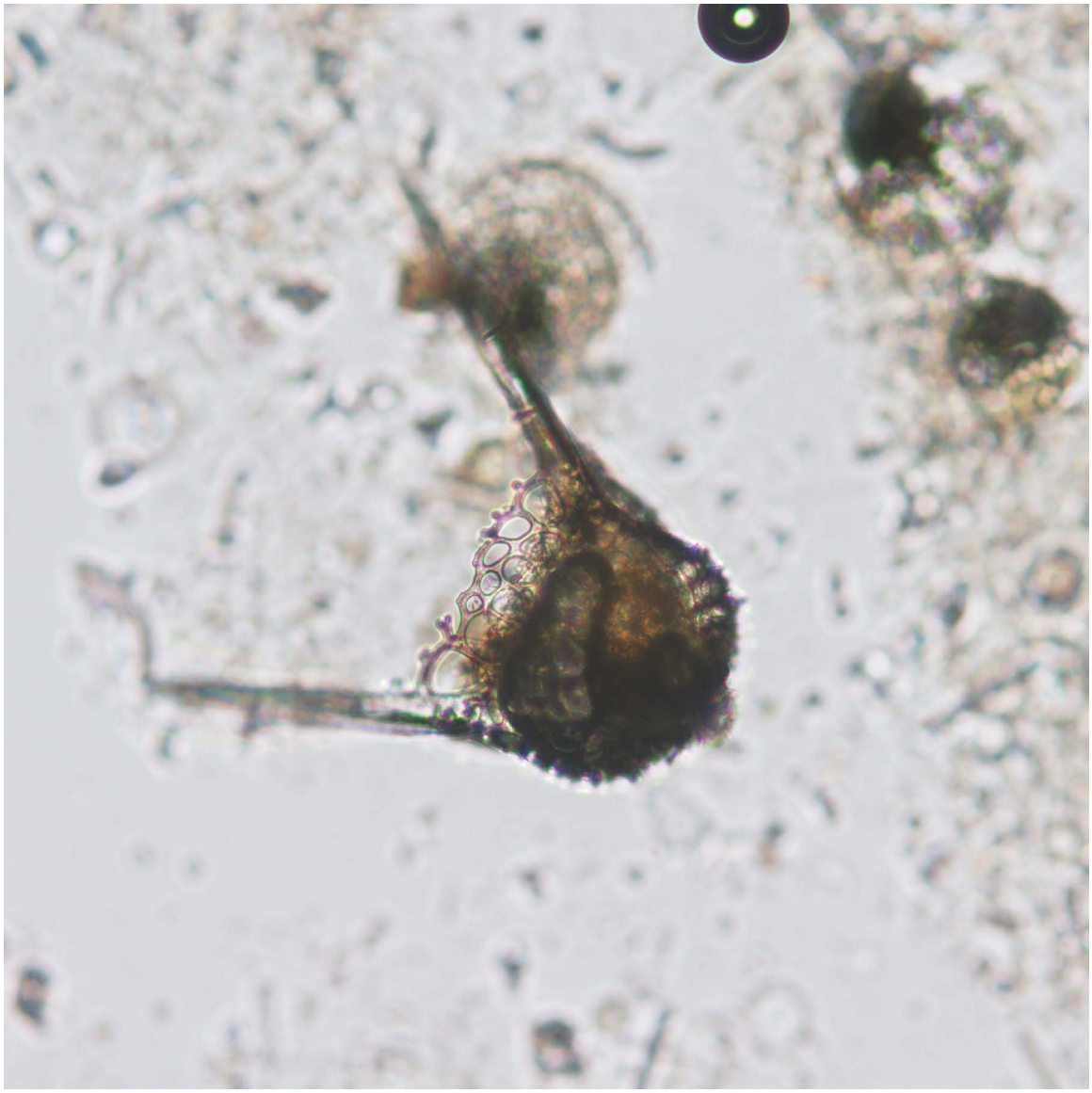

Radiolarian 11.

Large helmet-shaped Nassellarian radiolarian. Two prominent spicules are visible in this view. This specimen is opaline with no birefringence, so no cross-polar view is provided.

ODP Sample (Pleistocene): Leg 138, Hole 845A, Core 2H, Section 6W, 120 cm

Image ID: B0295

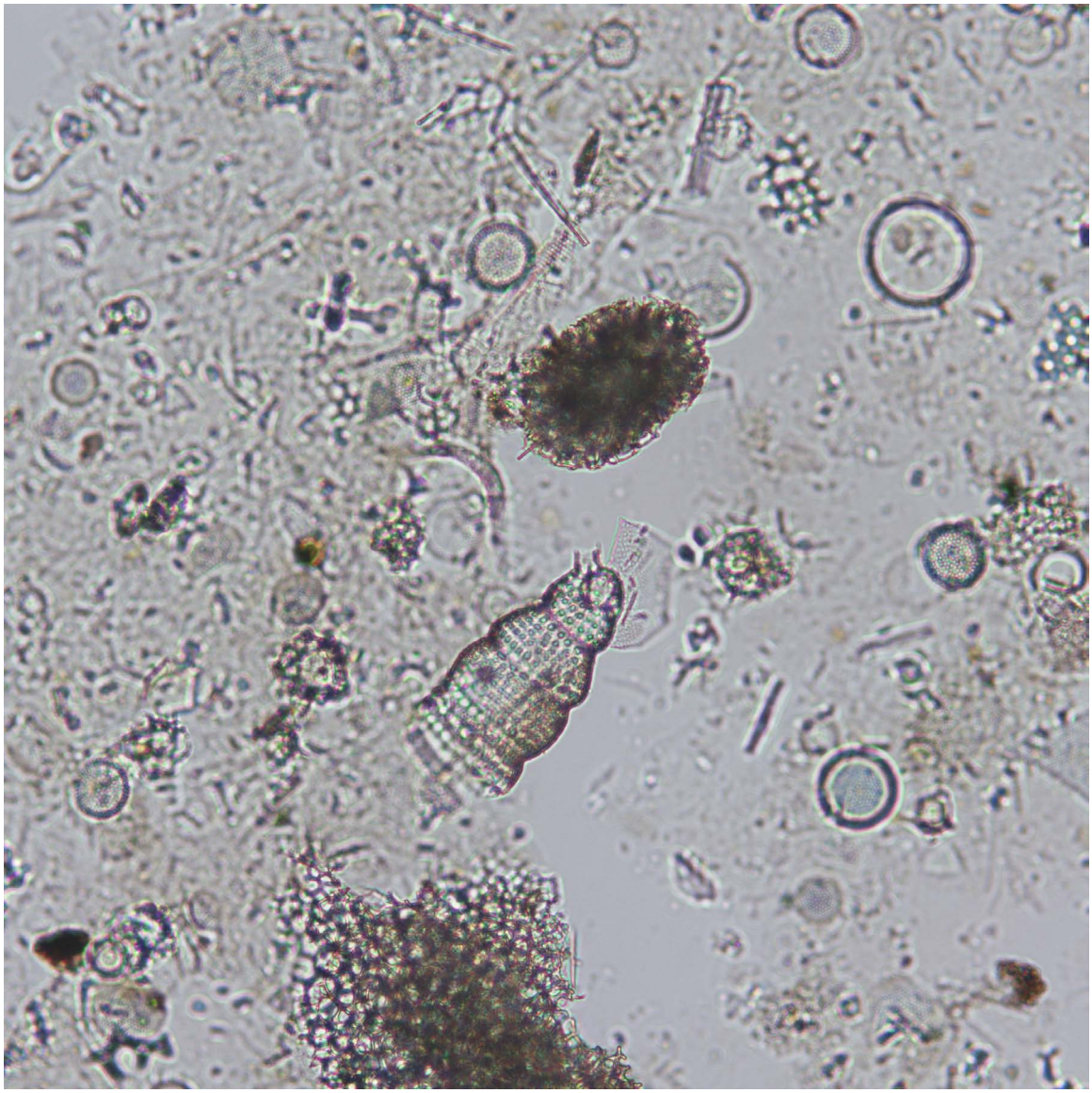

Radiolarian 12.

Jointed, bell-shaped Nassellarian radiolarian in center of field of view. Other darker grains above and below may also be matrix-filled radiolarian (Spumellarians). Much of the debris in the surrounding sediment is diatom fragments. The bio-clasts in this specimen are all opaline with no birefringence, so no cross-polar view is provided.

ODP Sample (Pleistocene): Leg 138, Hole 845A, Core 2H, Section 6W, 120 cm

Image ID: B0299/B0230

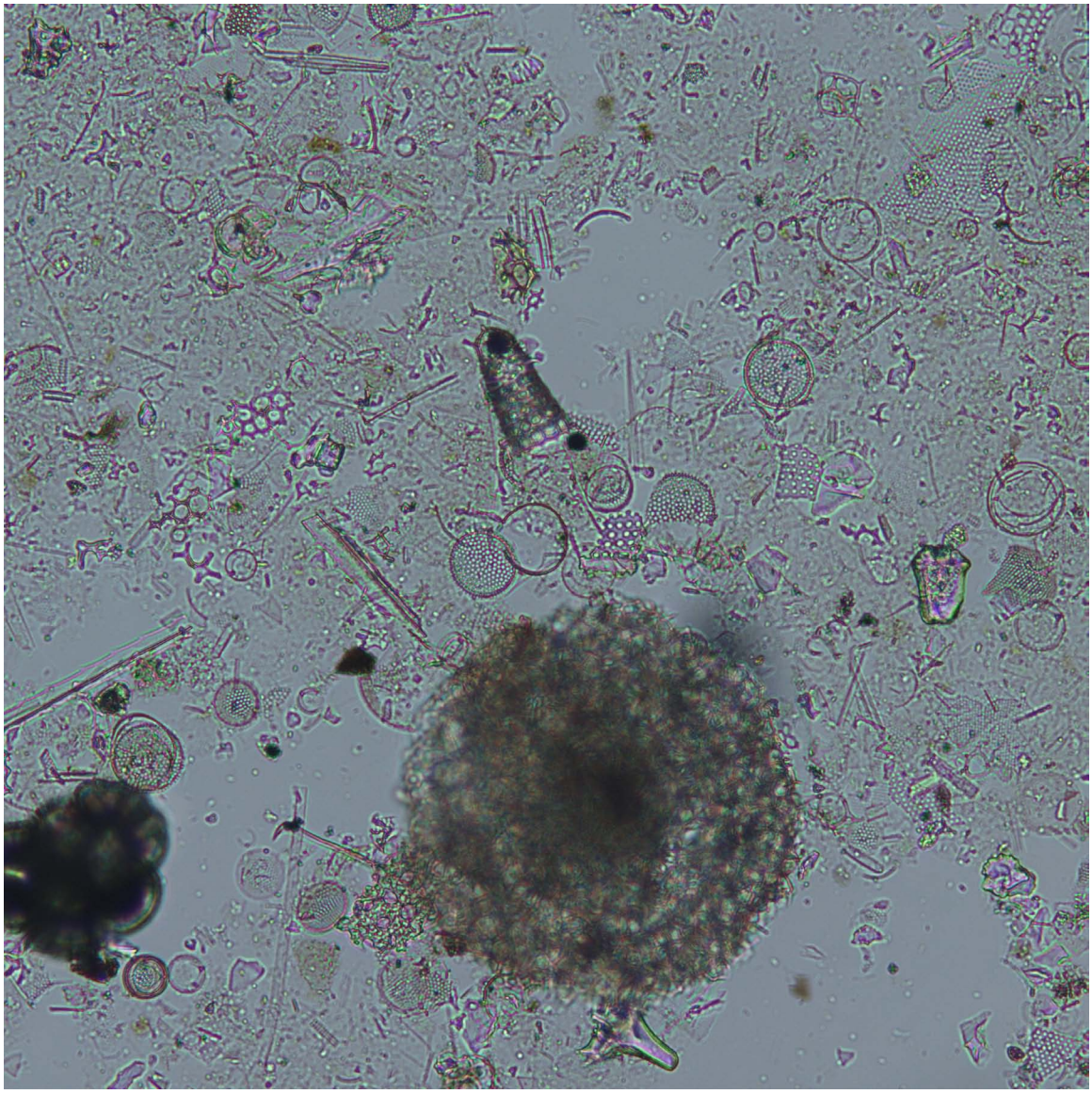

Radiolarian 13.

Large, disk-shaped Spumellarian (bottom center) and small, thimble-shaped Nassellarian (center) radiolarians, with a dark chambered foraminifer in lower left corner. The surrounding sediment is dominated by variably preserved centric diatoms including one intact frustrule, individual circular valves, valve rims (girdles) and smaller fragments. Note the difference in scale for these circular siliceous bioclasts, with the radiolarian being much larger. With polars partly crossed, the clay component is much more evident, along with a small foram forming a bright point in the upper left quadrant.
ODP Sample (Pleistocene): Leg 138, Hole 845A, Core 2H, Section 6W, 120 cm

Image ID: B0301/B0302

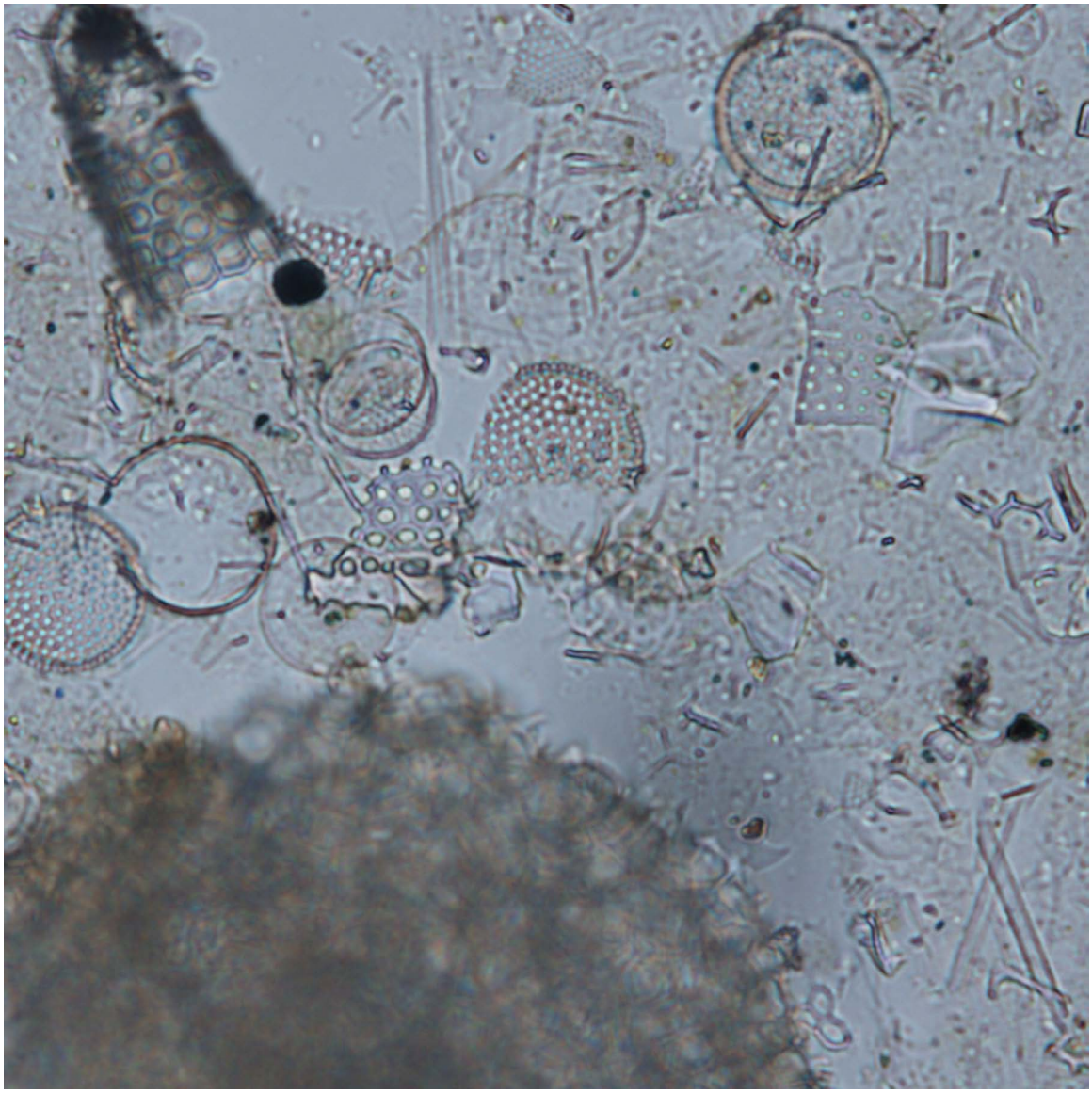

Radiolarian 14.

Closer view of large, disk-shaped Spumellarian (bottom center) and small, thimble-shaped Nassellarian (upper left) radiolarian seen in previous image, providing finer detail. Note the displaced valves of a frustrule below the circular opaque (pyrite framboid?).

ODP Sample (Pleistocene): Leg 138, Hole 845A, Core 2H, Section 6W, 120 cm

Image ID: B0297

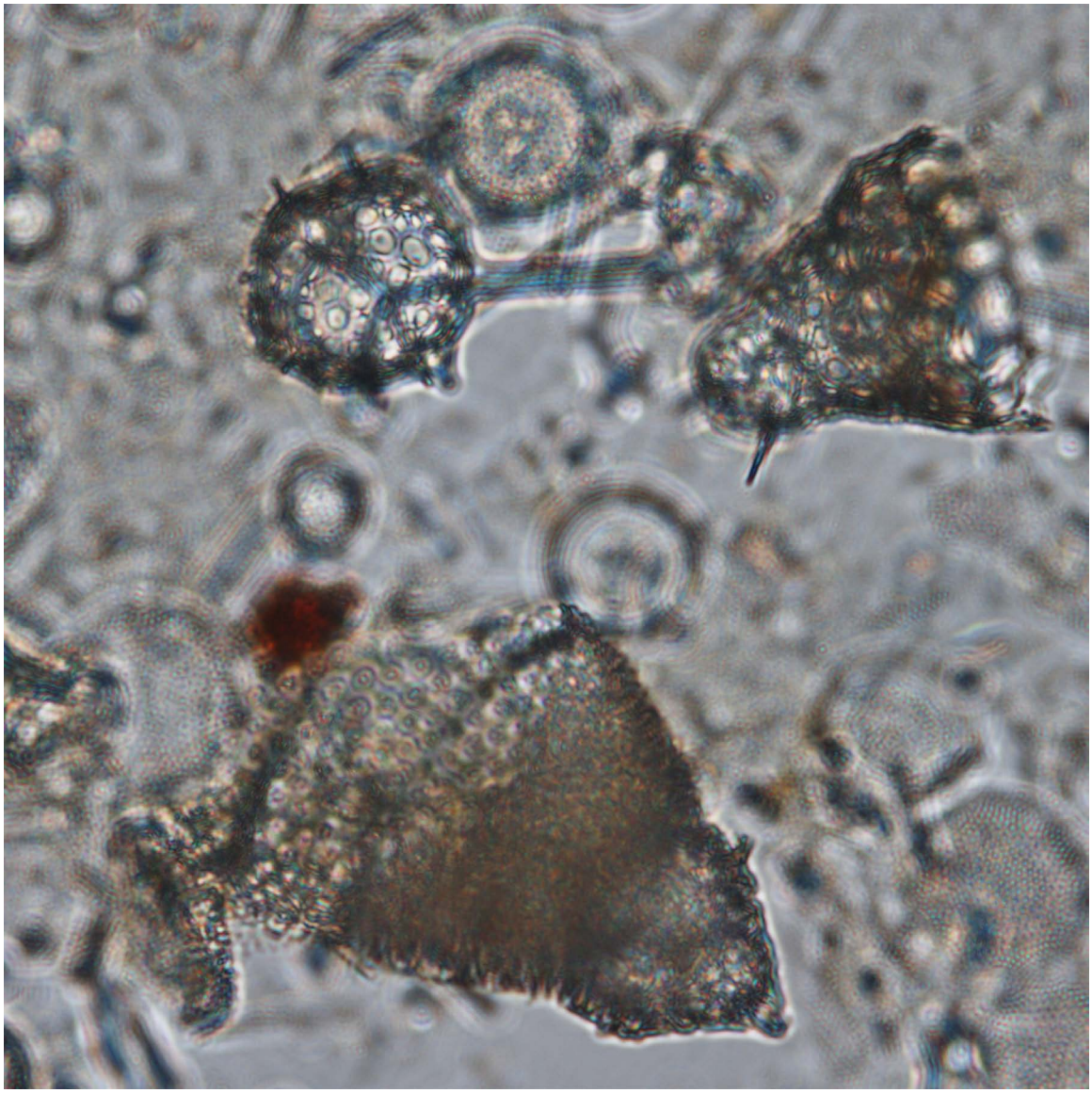

Radiolarian 15.

More circular Spumellarian (top left) and two darker, cone- or bell-shaped Nassellarian radiaolarians are set in an out-of-focus background sediment of centric diatoms. All are opaline and isotropic, so no view with polars crossed.

ODP Sample (Pleistocene): Leg 138, Hole 845A, Core 2H, Section 6W, 120 cm

Image ID: B0736

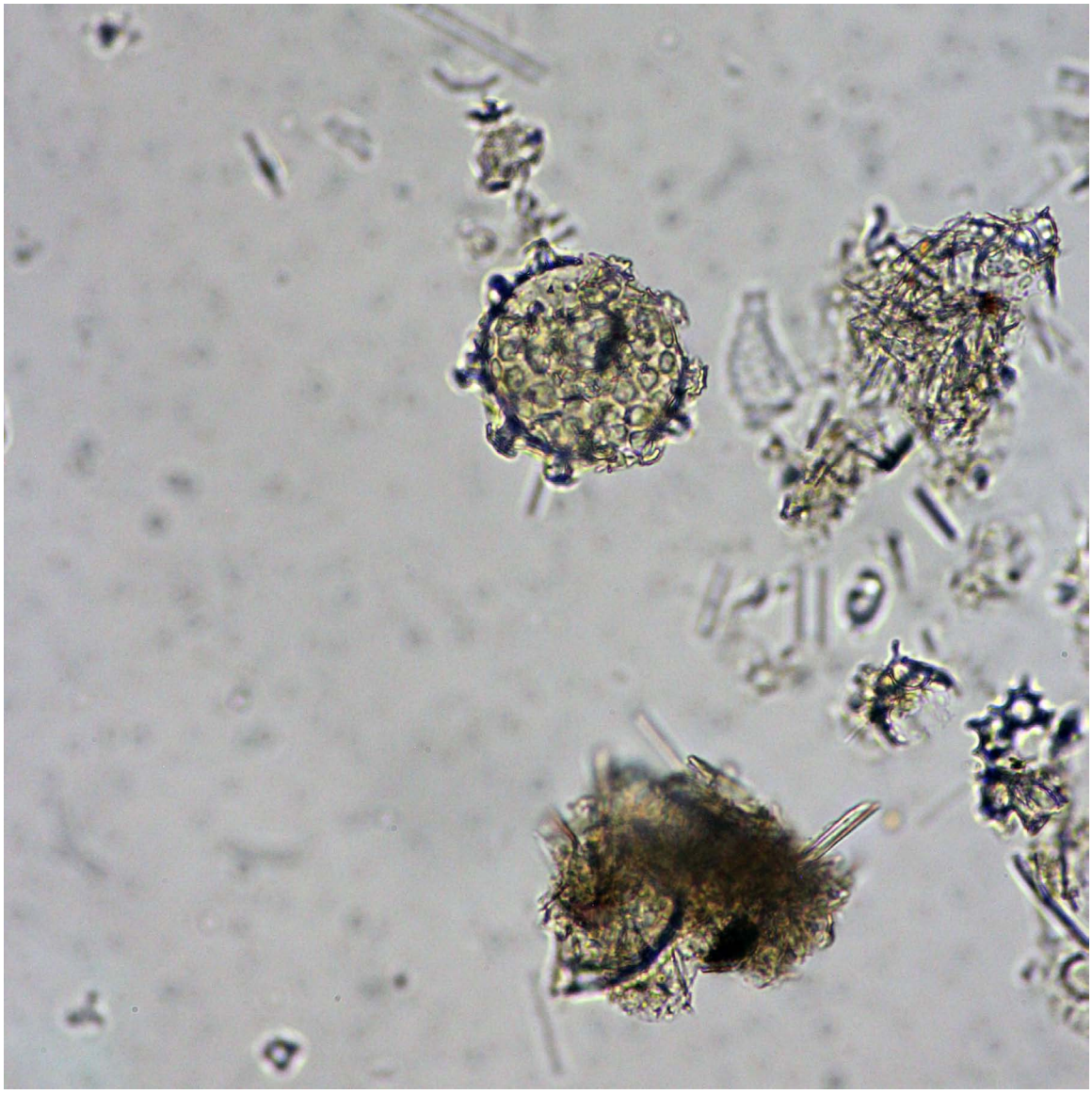

Radiolarian 16.

This spherical radiolarian exhibits processes extending off its round surface. The test and surrounding finer biogenic fragments are composed of isotropic opal, so no view with polars cross is provided.

DSDP Sample (late Miocene): Leg 38, Hole 845A, Core 15H, Section 2W, 10 cm

Image ID: 0410

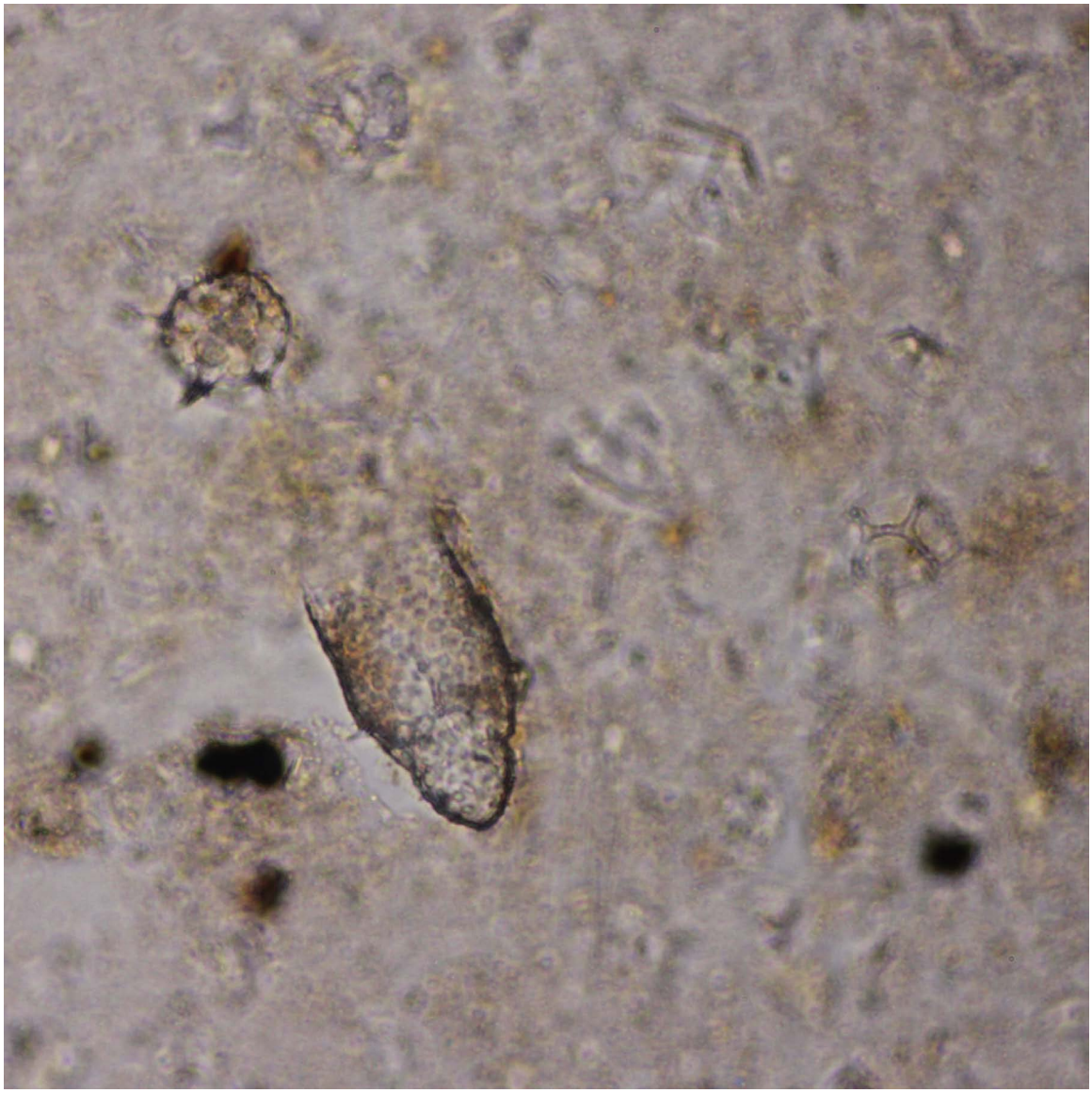

Radiolarian 17.

This view is focused on a nonsymmetrical cone-shaped Nassellarian radiolarian and a nearby spherical and spined radiolarian (Astrosphaerins). All are isotropic opal as evidenced by their lack of birefringence in the cross-polar view.

DSDP Sample (late Pleistocene): Leg 86, Hole 576B, Core 1H, Section 1, 6 cm

Image ID: B0123/B0124/B0125

Radiolarian 18.

This is a close-up view of a Nassellarian radiolarian. Click on the alternate view layer for a different level of focus which provides some information on the three-dimensionality of these opaline bioclasts.

ODP Sample (late Pliocene): Leg 141, Hole 859D, Core 1R, Section 1W, 120 cm

Image ID: B0312

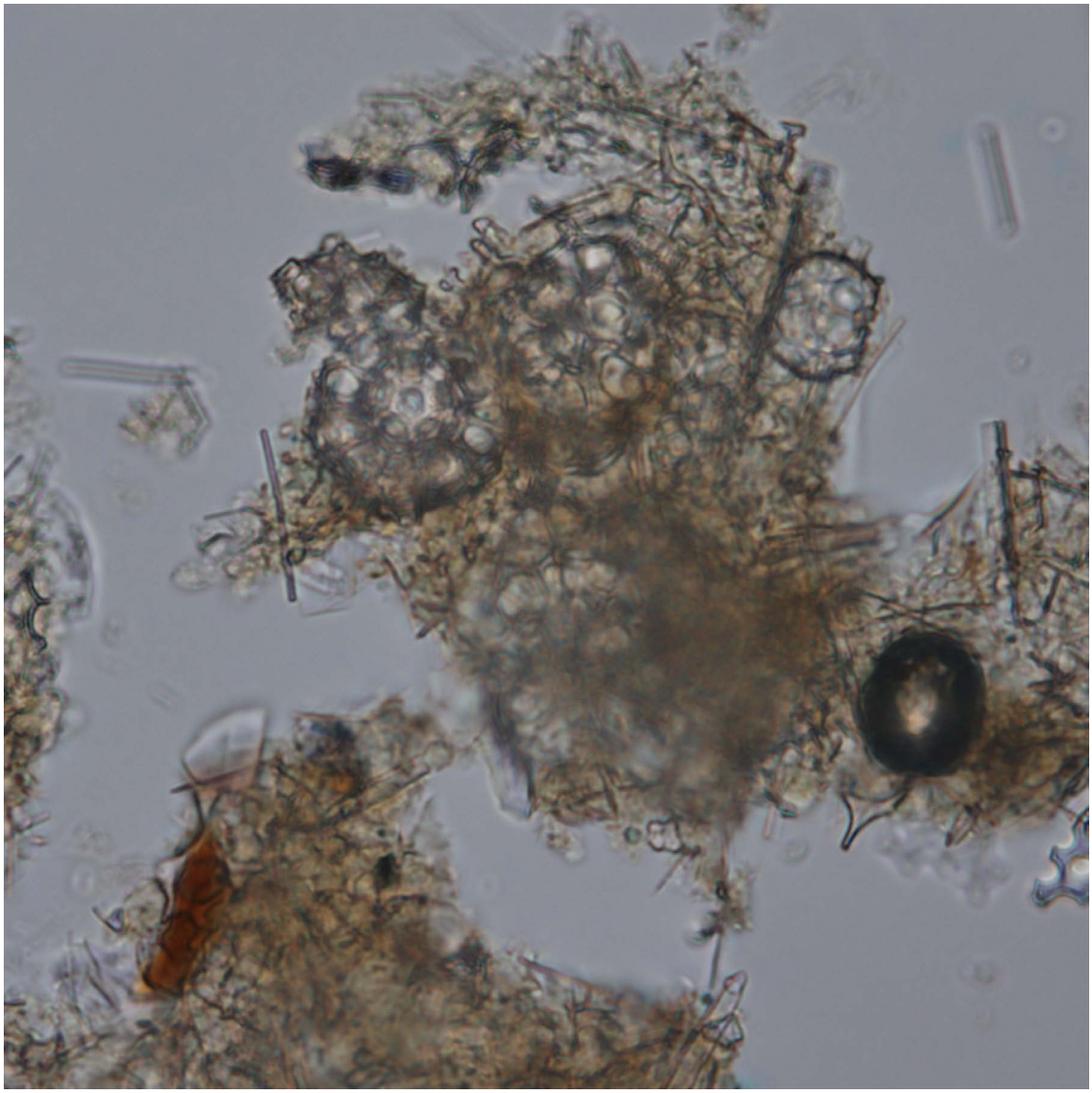

Radiolarian 19.

This sample of radiolarian ooze is a mixture of potentially both Spumellarian and Nassellarian radiolarian fragments in clumps. At least one of the circular radiolarians (far right) may be a view looking at the top of a Nassellarian specimen. Note the fine linear elements that are likely radiolarian spicules. Compare these delicate structures to those of the more bulky siliceous sponge spicules elsewhere in this volume, which are characterized by the presence of axial pores. Brownish matrix within clumps likely consists of some organic matter with clay. All the pictured components are non-birefringent, so no cross-polar view is provided.

ODP Sample (late Miocene): Leg 138, Hole 845A, Core 15H, Section

Image ID: B0311

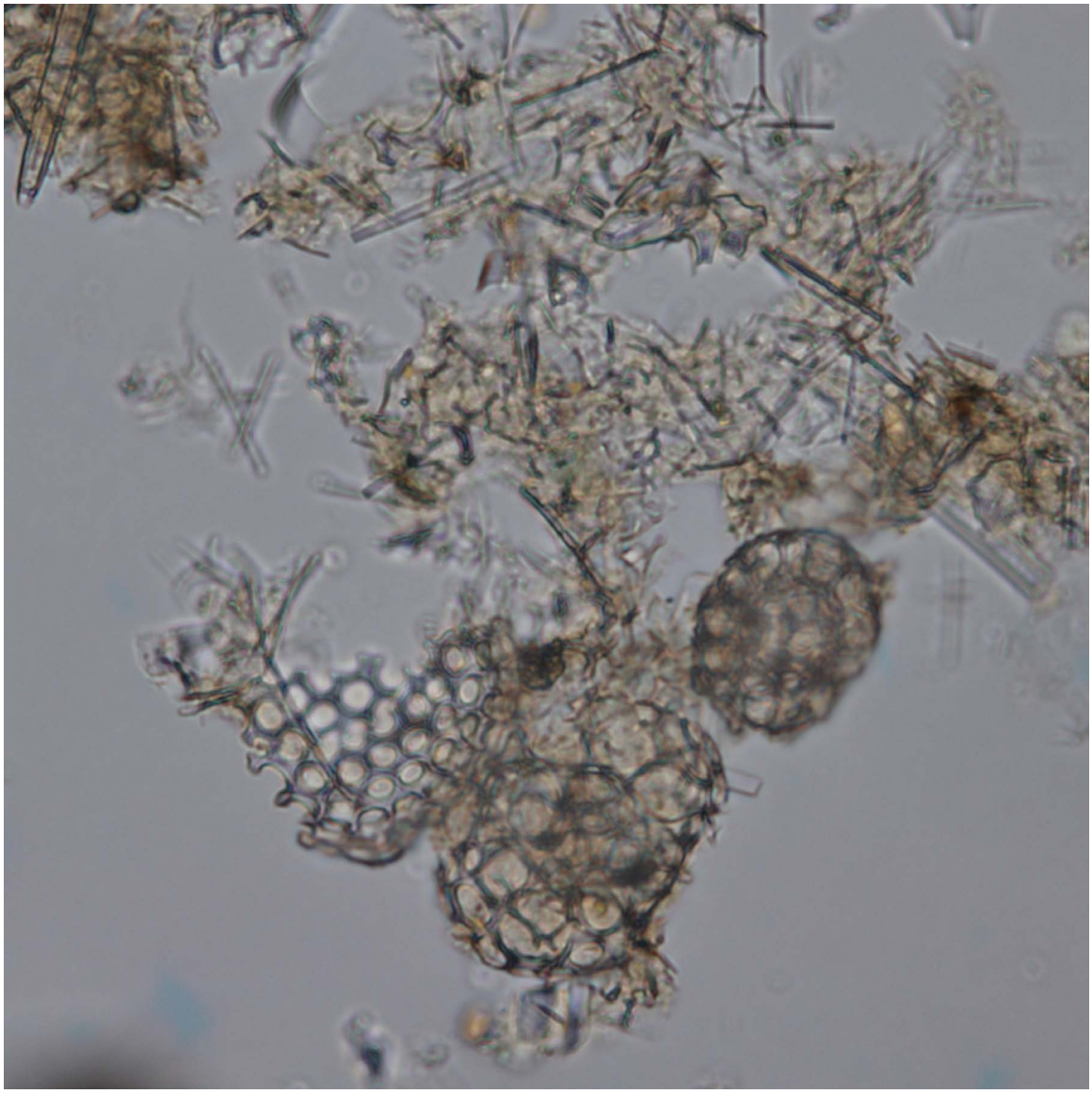

Radiolarian 20.

This sample of radiolarian ooze is a mixture of potentially both Spumellarian and Nassellarian radiolarian fragments. Organic-rich (brown) clumps are crisscrossed by fine linear elements that are likely radiolarian spicules. Compare these delicate structures to those of the more bulky siliceous sponge spicules, which are characterized by the presence of axial pores. All the pictured components are non-birefringent, so no cross-polar view is provided.

ODP Sample (late Miocene): Leg 138, Hole 845A, Core 15H, Section 2W, 10 cm

Image ID: B0252

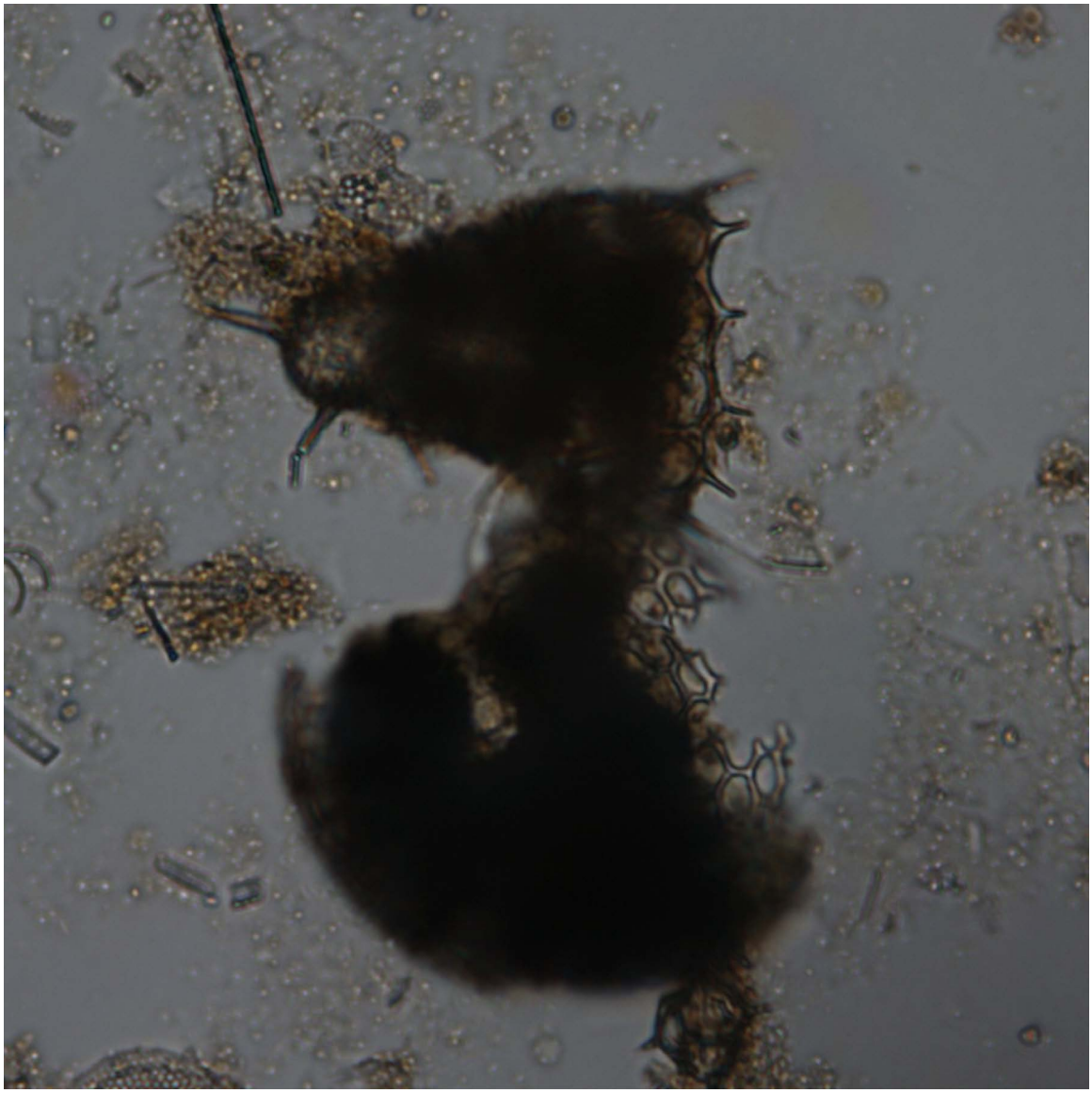

Radiolarian 21.

These radiolarians are opaque-filled, with one showing a spined bell-shaped profile characteristic of a Nassellarian. All the pictured components are non-birefringent, so no cross-polar view is provided.

ODP Sample (late and middle Pleistocene): Leg 175, Hole 1075A, Core 8H, Section 2W, 27 cm

Image ID: B0310

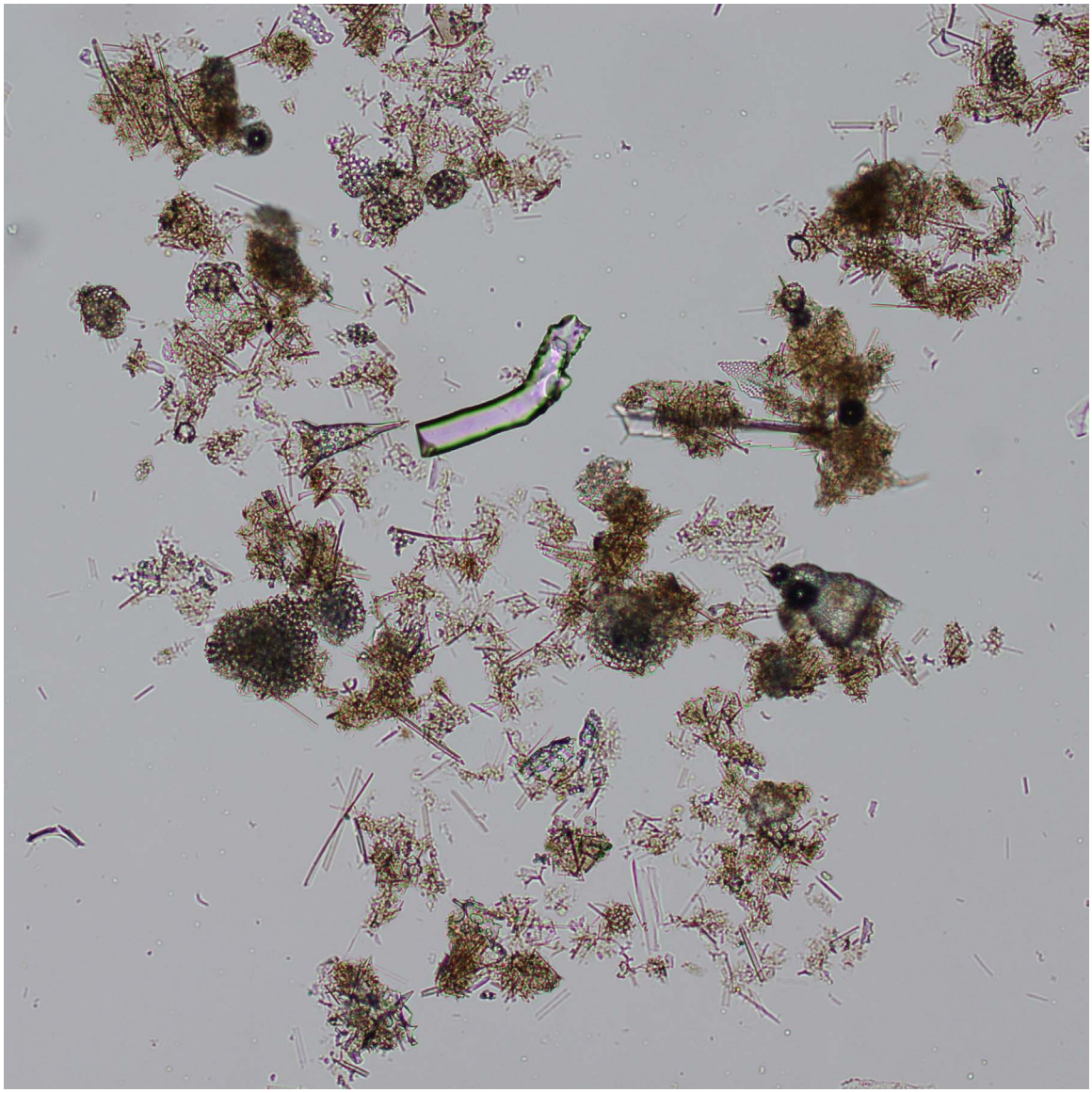

Radiolarian 22.

General view of radiolarian ooze composed of whole to fragmented Spumellarian (round and darker) and Nassellarian (cone-shaped and lighter) radiolarians with numerous fine and one coarse, serated, radiolarians spines. The higher relief bioclast with a bent elbow shape is likely a sponge spicule, but no axial pore is apparent, leaving its origin indeterminant. All the pictured components are non-birefringent, so no cross-polar view is provided.

ODP Sample (late Miocene): Leg 138, Hole 845A, Core 15H, Section 2W, 10 cm

Image ID: B0316/B0317

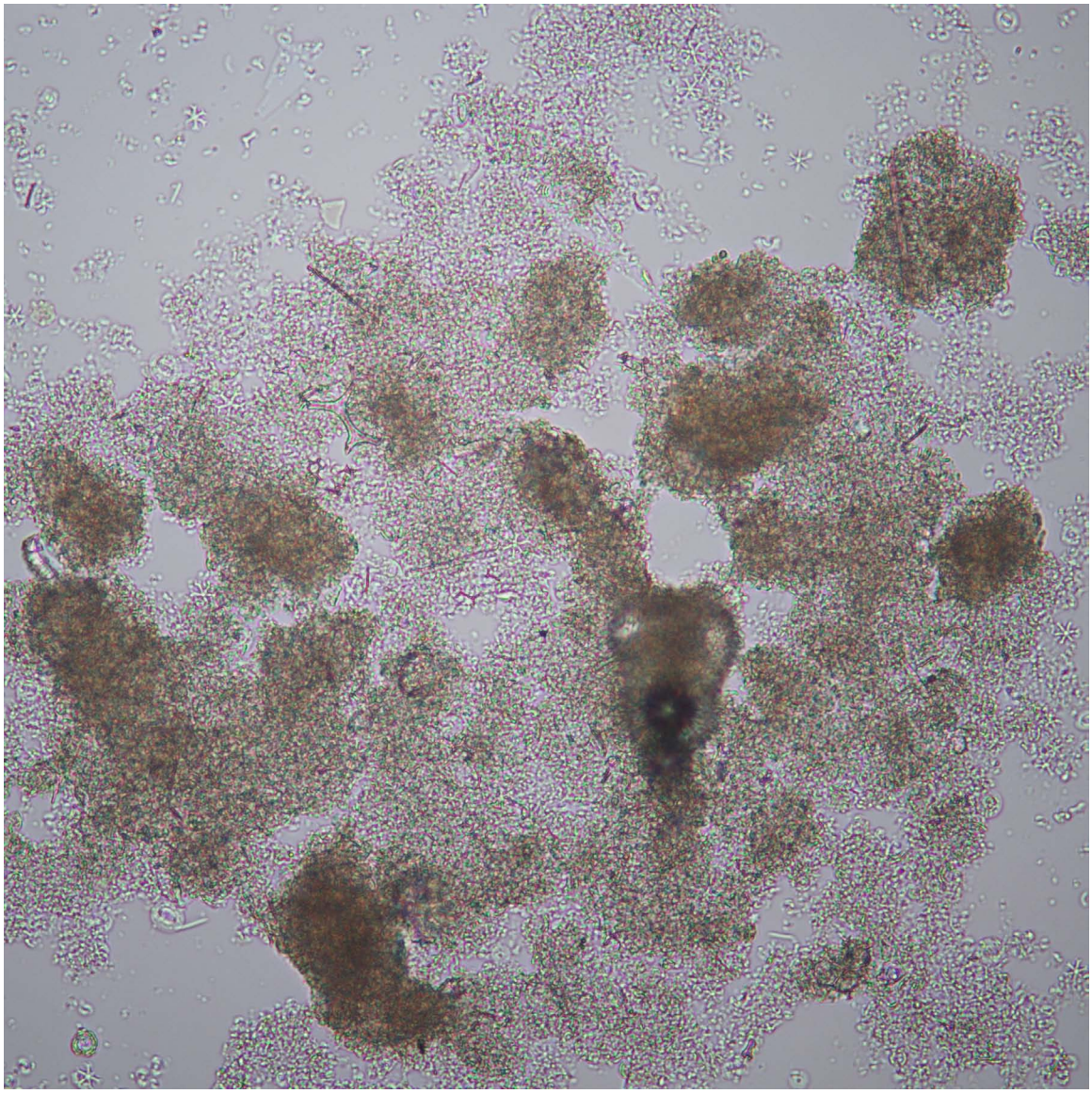

Radiolarian 23.

General view of slightly pelleted (rounded clumps) nannofossil ooze with some radiolarian components, whole to fragmented. The former as one larger Nassellarian radiolarian in the center of the field of view with darker trapped air bubbles (circled) and the latter as sparse lattice-work fragments. This shows the importance of looking at high to low magnification and variable focus to identify siliceous elements in calcareous oozes, where these components are masked by the birefringence of calcareous components.

ODP Sample (middle Miocene): Leg 138, Hole 845A, Core 17H, Section 2W, 20 cm

Image ID: B0274/B0275

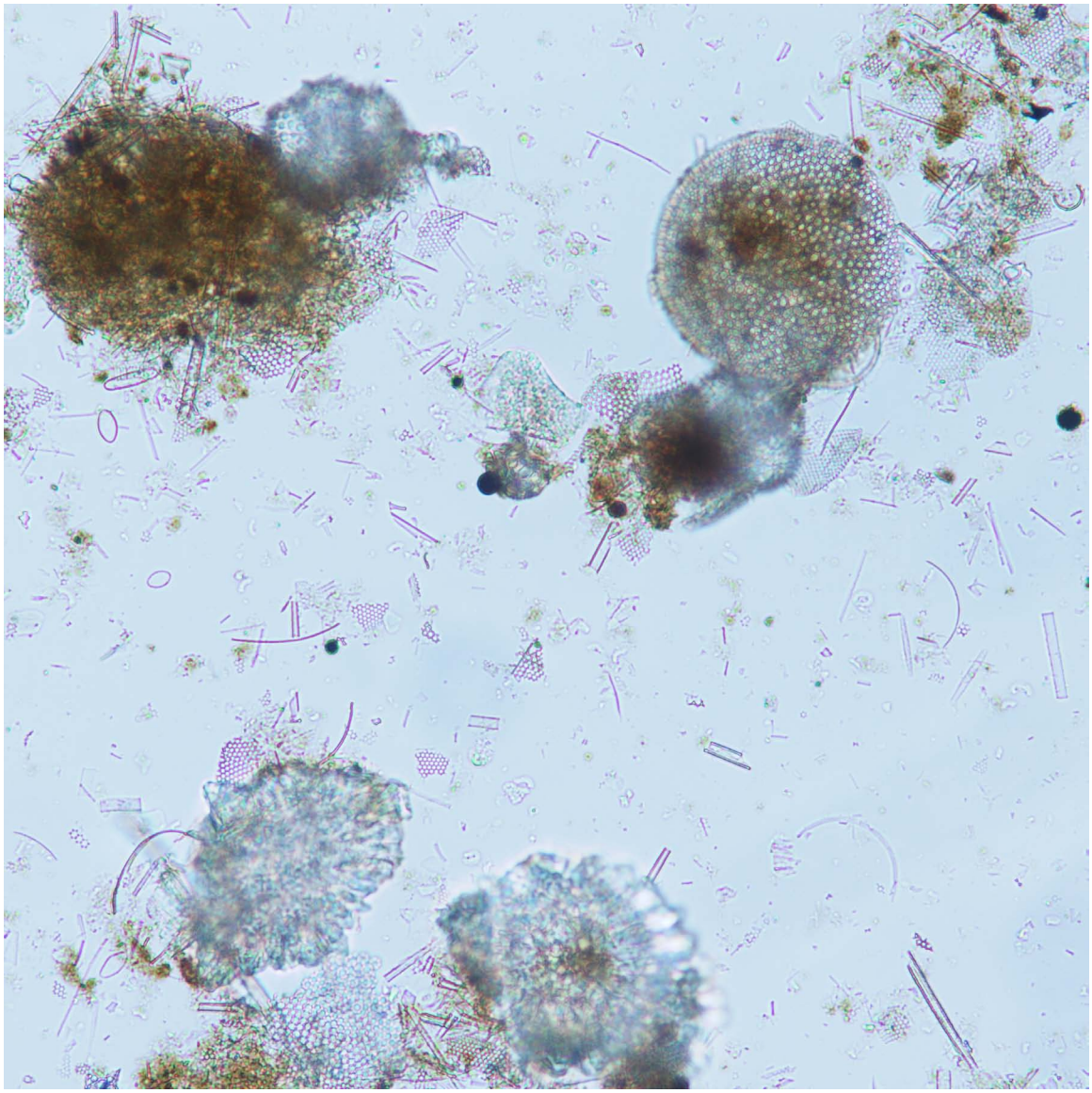

Radiolarian 24.

Mixed biogenic sediment dominated by siliceous components such as centric and pennate diatoms, but containing a few radiolarians and foraminifera. The foraminifera are readily identifiable by their shape and relief in plane light and their characteristically high birefringence with pseudo-uniaxial crosses under crossed polars, in contrast to the larger (round) diatom and greyish, out-of-focus radiolarians which are isotropic under crossed polars. The brownish matrix is likely organic-rich clay. Note the dispersed circular opaques, likely framboidal pyrite. ODP Sample (Quaternary): Leg 128, Hole 799A, Core 3H, Section 1W, 125 cm

Image ID: B0735

Radiolarian 25.

Another example of a Spumellarian radiolarian composed of isotropic opal, so no view with polars cross is provided.

DSDP Sample (late Miocene): Leg 38, Hole 845A, Core 1H, Section 2W, 10 cm

Image ID: B0732

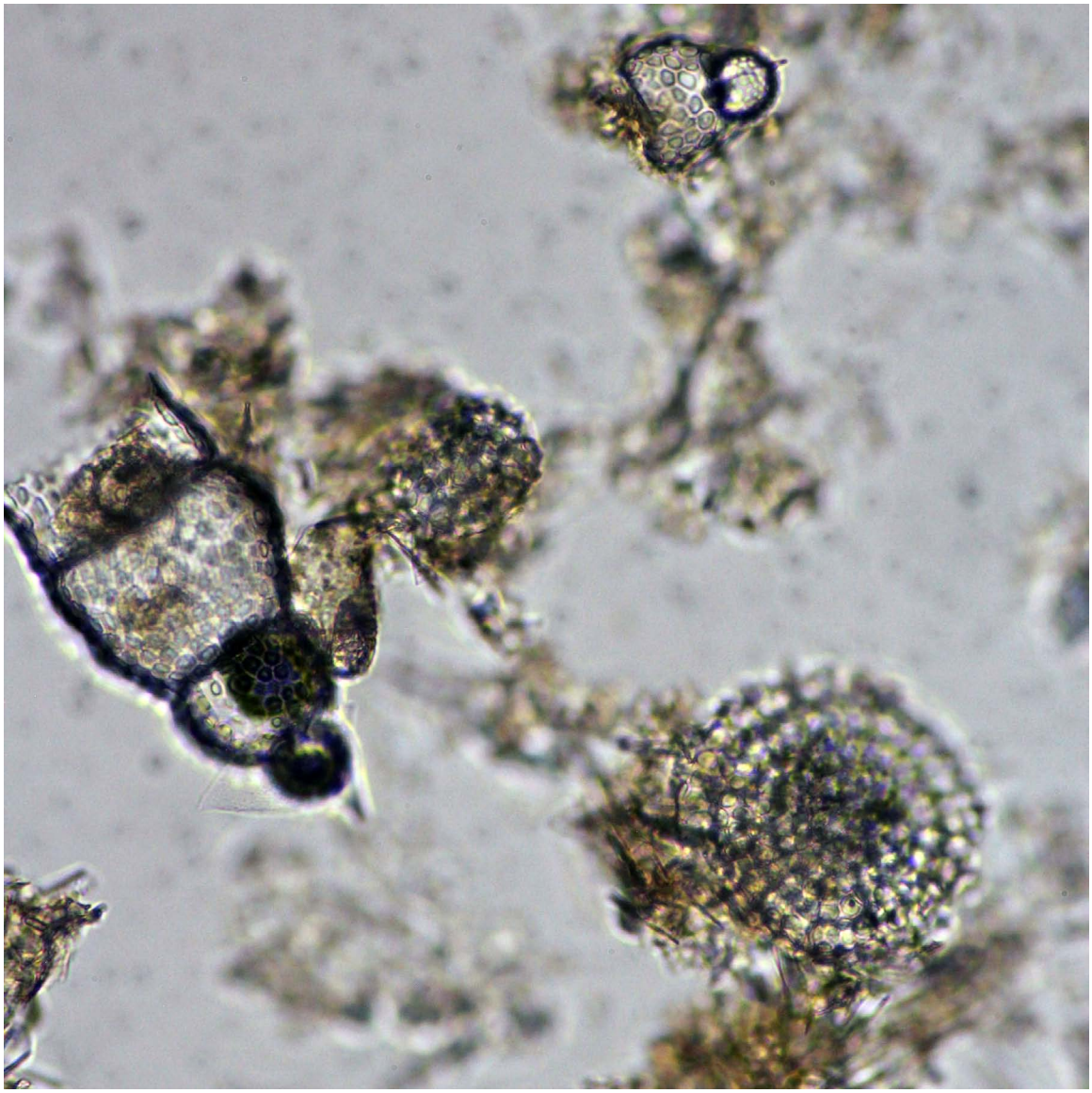

Radiolarian 26.

This image of siliceous ooze includes two bell-shaped Nassellarian radiolarians and a disk-shaped Spumellarian in the lower right corner. The radiolarian and fine surrounding sediment are all isotropic/nonbirefringent, so no view with polars cross is provided.

DSDP Sample (late Miocene): Leg 38, Hole 845A, Core 15H, Section 2W, 10 cm

Image ID: B0739

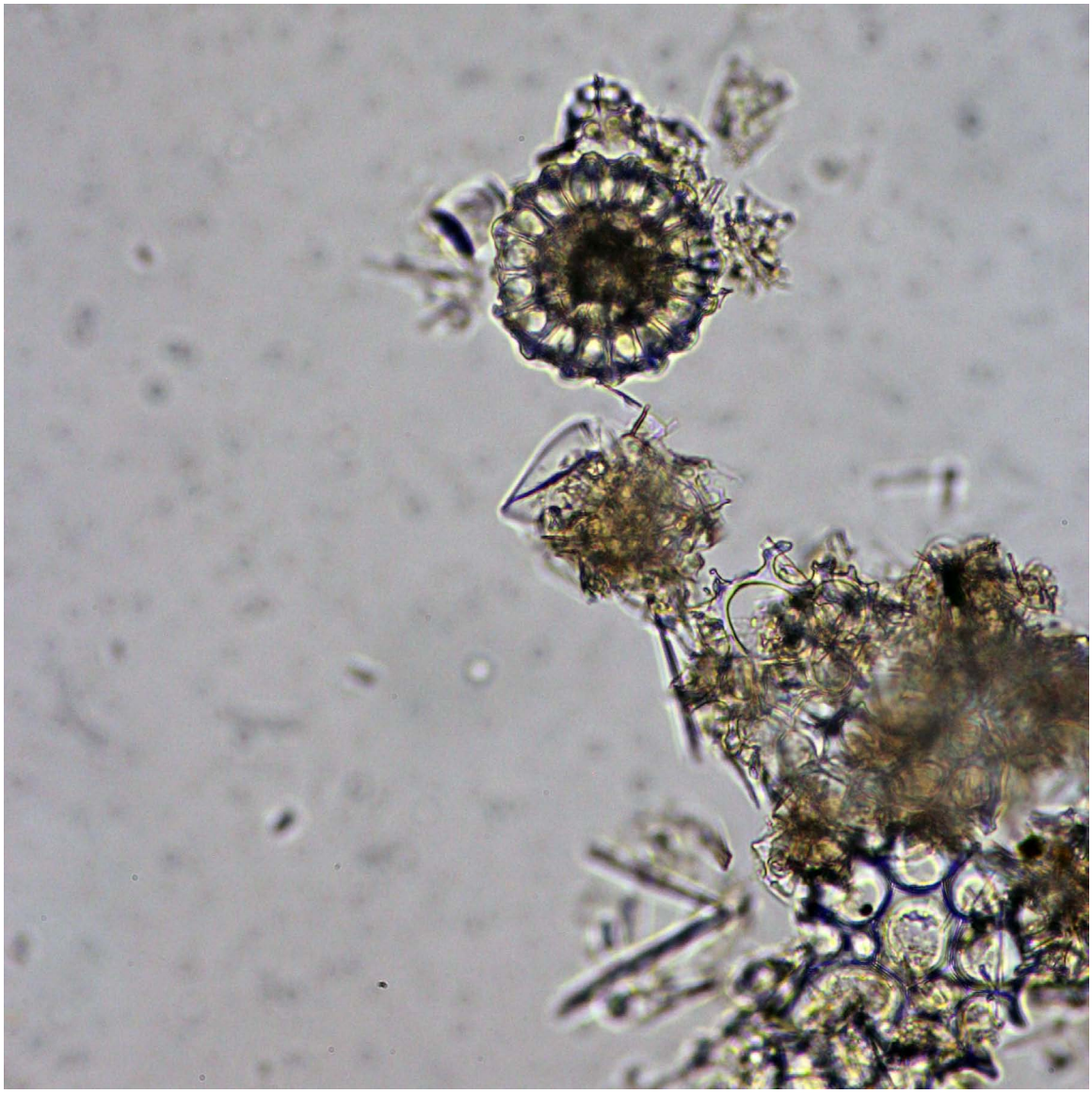

Radiolarian 27.

This is a round Spumellarian radiolarian in a siliceous sediment that contains other fragments of other radiolarians as indicated by their cellular texture. The radiolarians and associated sediment are composed of isotropic opal, so no view with polars cross is provided.

DSDP Sample (late Miocene): Leg 38, Hole 845A, Core 15H, Section 2W, 10 cm

Image ID: B0741/B0742

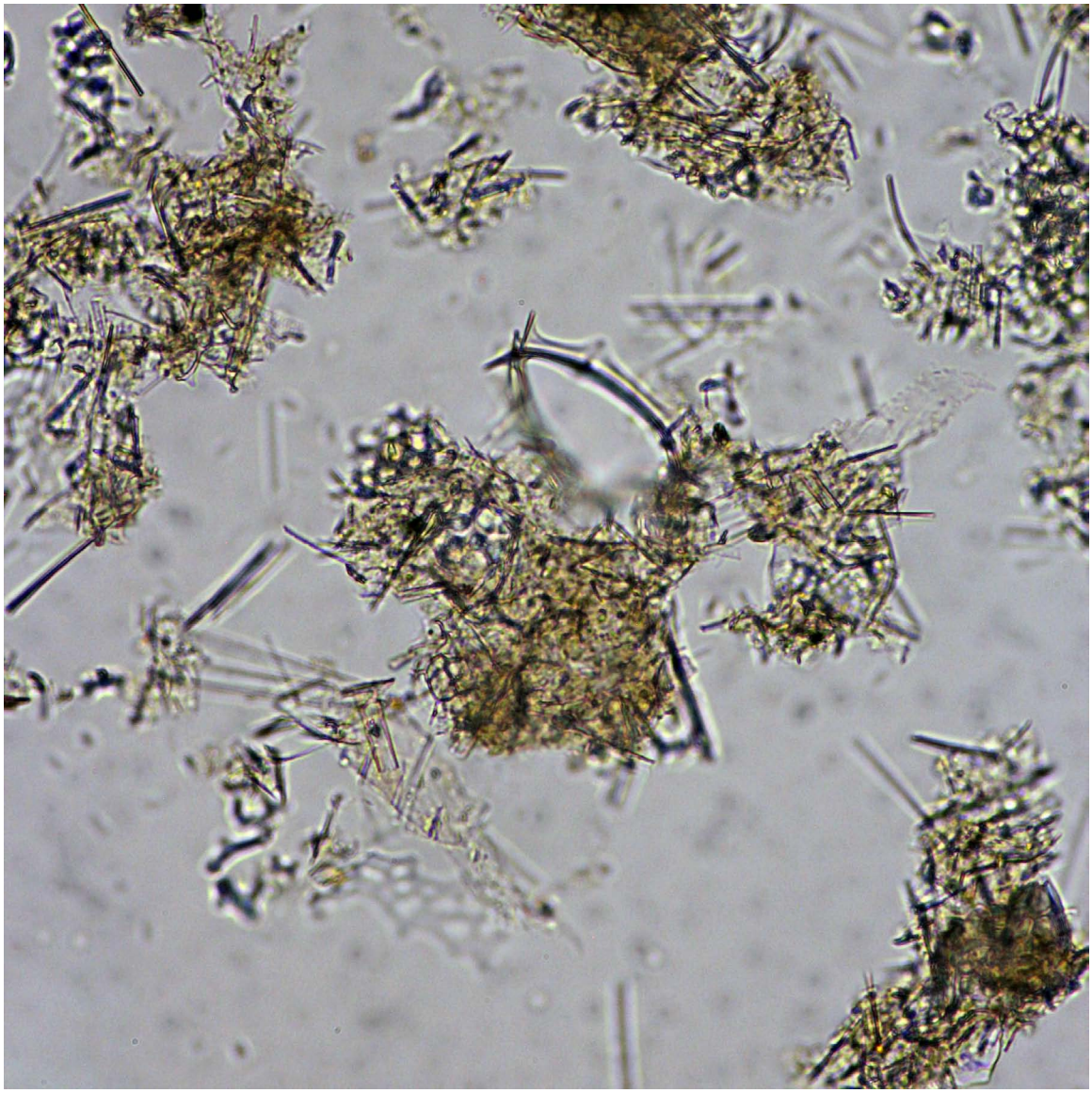

Radiolarian 28.

Siliceous ooze with common fragments of radiolarian spines (thin filaments) and one slightly curved radiolarian skeletal fragment. All are isotropic, so no view with polars crossed is provided, but the alternate view at a different focus illustrates the ring morphology of the fragment.

DSDP Sample (late Miocene): Leg 38, Hole 845A, Core 15H, Section 2W, 10 cm

Image ID: xxx

Radiolarian 29.

Siliceous ooze with common elongate fragments of pennate diatoms and one small spiked radiolarian(?) that stands out because of its higher relief (see alternate focus level). All are isotropic, so no view with polars crossed is provided.

DSDP Sample (late Miocene): Leg 38, Hole 845A, Core 15H, Section 2W, 10 cm

Other Siliceous Bioclast

Silicoflagellates

INTRODUCTION TO SILICOFLAGELLATES

Overview – Silicoflagellates are planktonic marine algae with a single flagellum and a relatively simple skeletal framework of opaline silica. They are most abundant in areas of upwelling and oceanic divergence. Silicoflagellates are useful for biostratigraphy, particularly at higher latitudes. Their assemblages display distinct zonal patterns.

Diagnostic Features – The simple internal skeleton of the silicoflagellates is composed of connected hollow rods, similar to siliceous sponge spicules, typically with spines. The skeleton of Cenozoic silicoflagellates has two primary parts: a basal ring can be polygonal, elliptical or circular in shape, and an apical structure or apical apparatus (hemispherical shape). The apical structure is connected to the basal ring by struts. Mid-Cretaceous forms lack a basal ring, which first appears in the Late Cretaceous (Santonian-Campanian boundary). 10-100 µm, up to 500 µm.

Biology – Kingdom Protoctista, Subkingdom Heterokonta, Phylum Chrysomonada (Chrysophyta), Class Dictyochophyceae

Ecology – Autotrophs. Open marine.

Paleobiogeography – The distributions of Distephanus, a genus with an basal ring and apical structure having an apical ring ('window'), and Dictyocha, a genus characterized by a basal ring and apical structure having a apical bar rather than a apical ring, have been useful for distinguishing cooler and warmer surface water masses, respectively.

Stratigraphic Range – Mid-Cretaceous (latest Aptian-early Albian) to present.

Key References and Examples:

Bukry, D., 1985. Tropical Pacific silicoflagellate zonation and paleotemperature trends of the late Cenozoic. In, Mayer, L., Theyer, F., et al., Initial Reports of the DSDP, 85:477-497.

Bukry, D., 1986a. Miocene silicoflagellates from Chatham Rise, DSDP Site 594. In, Kennett, J.P., von der Borch, C.C., et al., Initial Reports of the DSDP, 90:925-937.

Bukry, D., 1986b. Eocene siliceous and calcareous phytoplankton, DSDP Leg 95. In, Poag, C.W., Watts, A.B., et al., Initial Reports of the DSDP, 95:395-415.

Dumitrica, P., 2014. Double skeletons of silicoflagellates: Their reciprocal position and taxonomical and paleobiological values. Revue de Micropaléontolgie, 57: 57-74.

Haq, B.U., 1978. 11: Silicoflagellates and Ebridians. In Haq, B.U., and Boersma, A. (Eds.), Introduction to Marine Micropaleontology: Elsevier, 267-275.

McCartney, K., 1993. 9: Chrysophystes and Silicoflagellates. In Lipps, J.H. (Ed.), Fossil Prokaryotes and Protists: Blackwell Scientific Publications, 141-154.

McCartney, K., Witkowski, J., and Harwood, D.M., 2010. Early evolution of the silicoflagellates during the Cretaceous. Marine Micropaleontology, 77:83-100.

McCartney, K., Witkowski, J., and Harwood, D.M., 2014. New insights into skeletal morphology of the oldest known silicoflagellates: Variramus, Cornua and Gleserocha gen. nov. Revue de Micropaléontolgie, 57: 75-91.
Perch-Nielsen, K., 1985. 17: Silicoflagellates. In Bolli, H.M., Saunders, J.B., and Perch Nielsen, K. (Eds.), Plankton Stratigraphy: Cambridge (Cambridge Univ. Press), 811-846.

Web Resources:
http://www.ucmp.berkeley.edu/chromista/silicoflagellata.html
http://eol.org/pages/3505/details

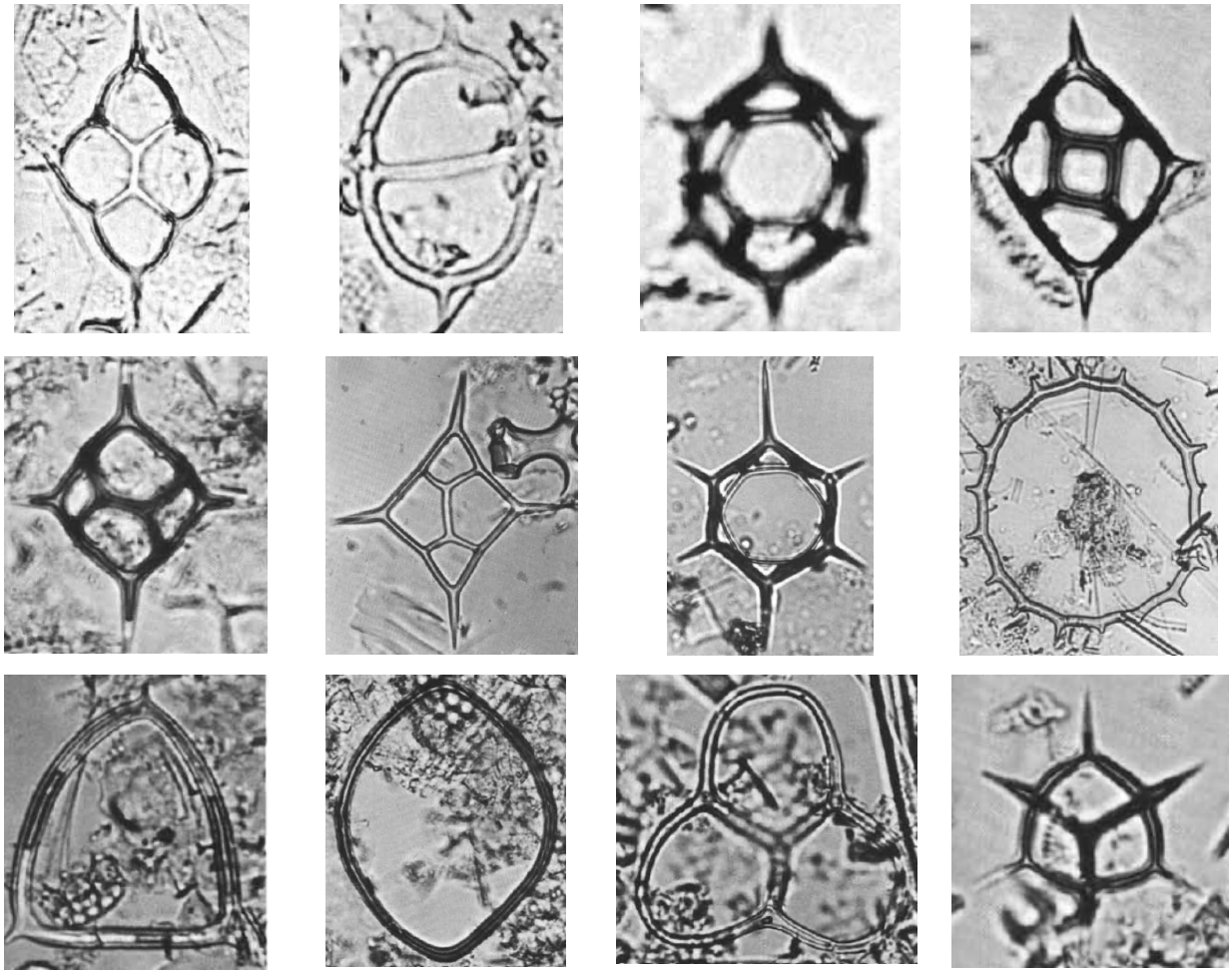

Representative Cenozoic silicoflagellates. Top row: *Dictyocha perfecta, Dictyocha pons, Distephanus speculum patulus, Distephanus crux scutulatus*. Second row: *Dictyocha cf. D. byronalis, Dictyocha fibula augusta, Distephanus speculum minutus, Mesocena dumitricae.* Bottom row: *Bachmannocena apiculata monolineata, Bachmannocena connudata, Corbisema inermis ballantina, Dictyocha hexacantha*. Photomicrographs from Bukry, 1985, 1986a, b.

Silicoflagellates

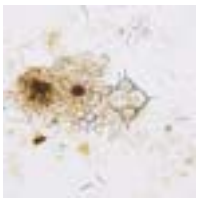
Silico 1


Silico 2


Silico 3


Silico 4


Silico 5


Silico 6

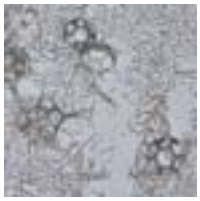
Silico 7


Silico 8


Silico 9


Silico 10

Image ID: B0103/B0104

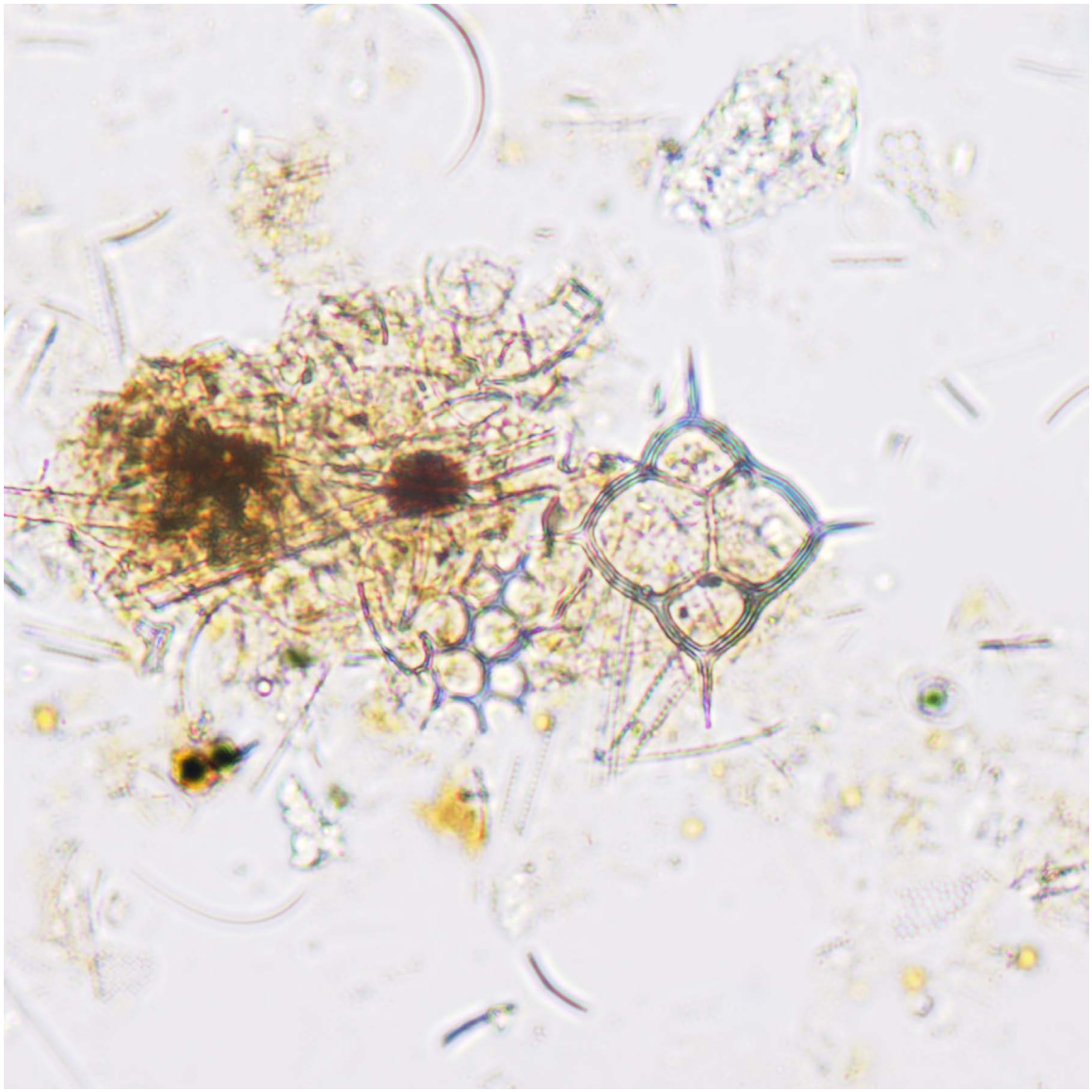

Silicoflagellate 1.

This view shows a single specimen of a dictyocid silicoflagellate with a central apical bar in a siliceous ooze. Other noteworthy components include radiolarian, pennate diatom fragment, and reddish brown organic matter. some calcarous biogenic debris is evident when the polars are crossed.

ODP Sample (Quaternary): Leg 112, Hole 688A, Core 2H, Section 5W, 74 cm

Image ID: B0109/B0110

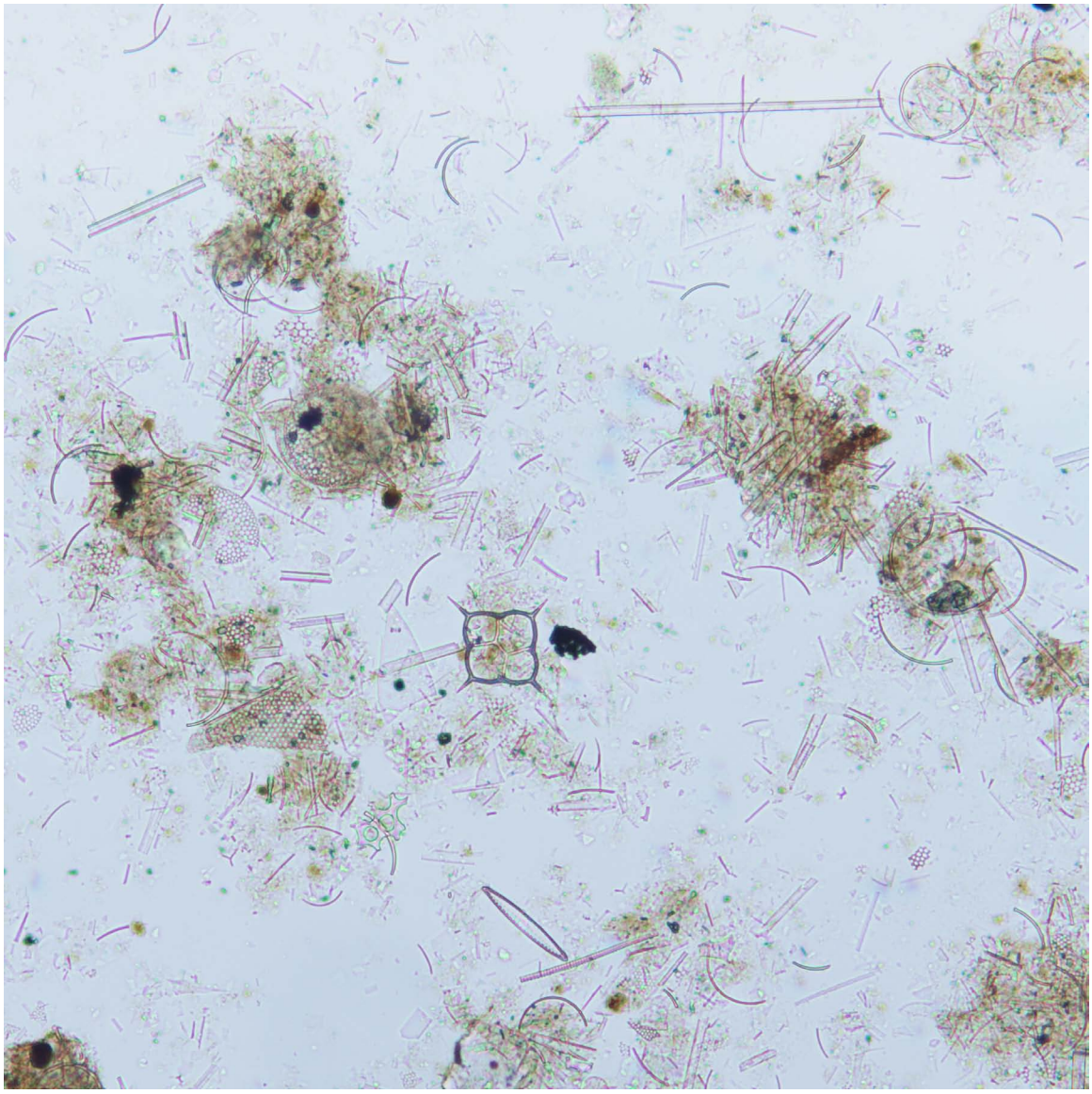

Silicoflagellate 2.

In the center of this field of view of diatom ooze is a dictyocid silicoflagellate where its central structure including an apical bar is slightly out of focus (zoom to 200% to see central bars). The cross-polar view shows the presence of some carbonate of unknown affinity.

ODP Sample (Quaternary): Leg 112, Hole 688A, Core 2H, Section 5W, 74 cm

Image ID: 0382

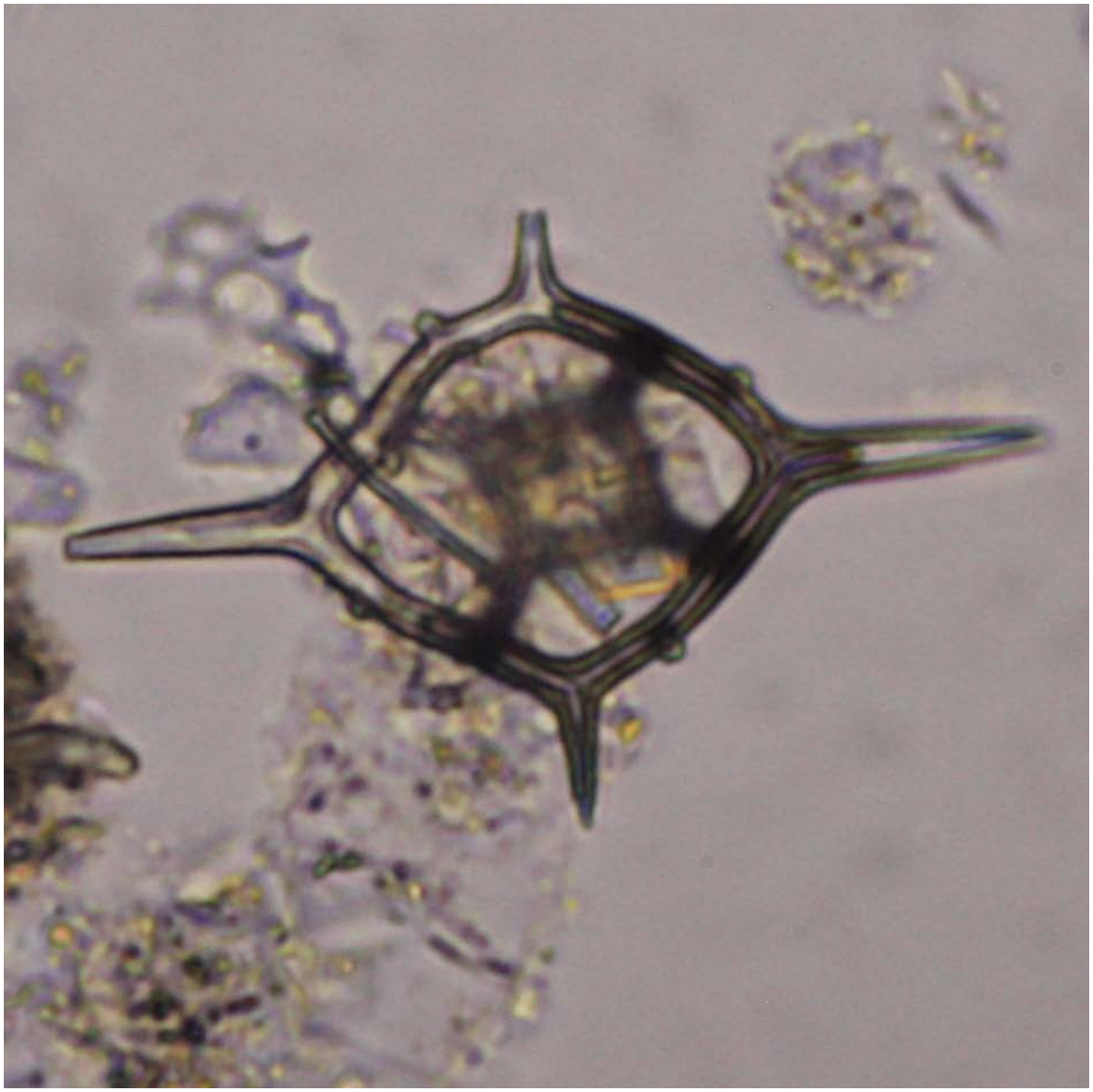

Silicoflagellate 3.

This is a specimen of a distephanid silicoflagellate with a distinctive apical window slightly out of focus.

DSDP Sample (Pliocene): Leg 18, Hole 179, Core 10, Section 3, 78 cm

Image ID: B0055

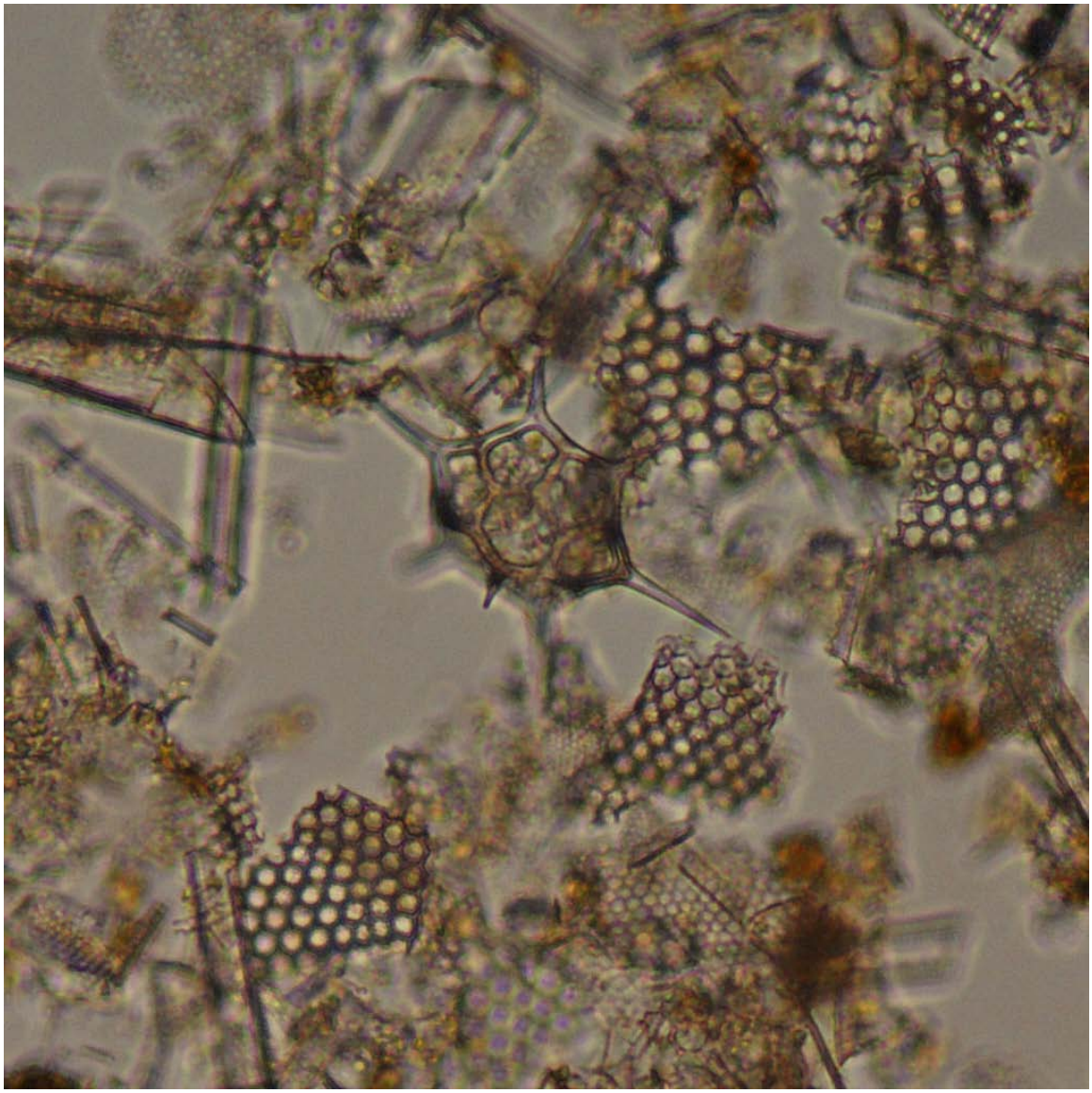

Silicoflagellate 4.

In the center of this image is an oblique view of a distephanid silicoflagellate set in an ooze largely composed of diatom fragments. All are isotropic, so no cross-polar view is provided.

DSDP Sample (early to late Pliocene): Leg 57, Hole 438A, Core 13, Section 3, 64 cm

Image ID: B0442/B0443

Silicoflagellate 5.

This is a specimen of a distephanid silicoflagellate with central apical window structure that is slightly out of focus. All components are isotropic so no cross-polar view is provided.

ODP Sample (early Pliocene): Leg 113, Hole 690B, Core 3H, Section 3W, 50 cm

Image ID: B0432/B0433

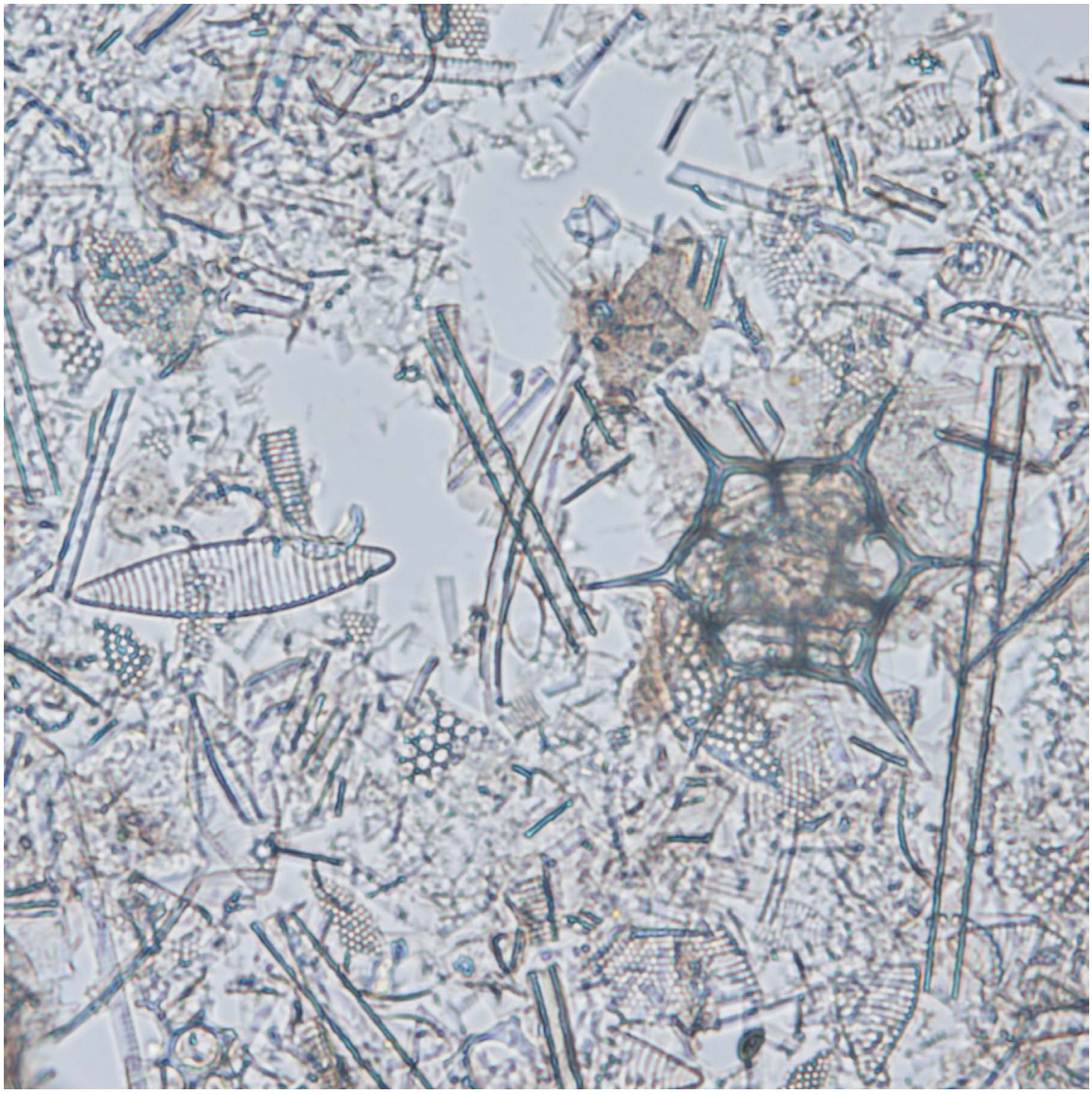

Silicoflagellate 6.

This is diatom ooze with a large distephanid silicoflagellate with central apical window structure that is slightly out of focus on the right. A variety of pennate diatoms, mostly fragmented, are also present. There is some birefringent mineral matter of unknown origin, possibly terrigenous minerals or carbonate debris.

ODP Sample (early Pliocene): Leg 113, Hole 690B, Core 2H, Section 2W, 120 cm

Image ID: B0444/B0445

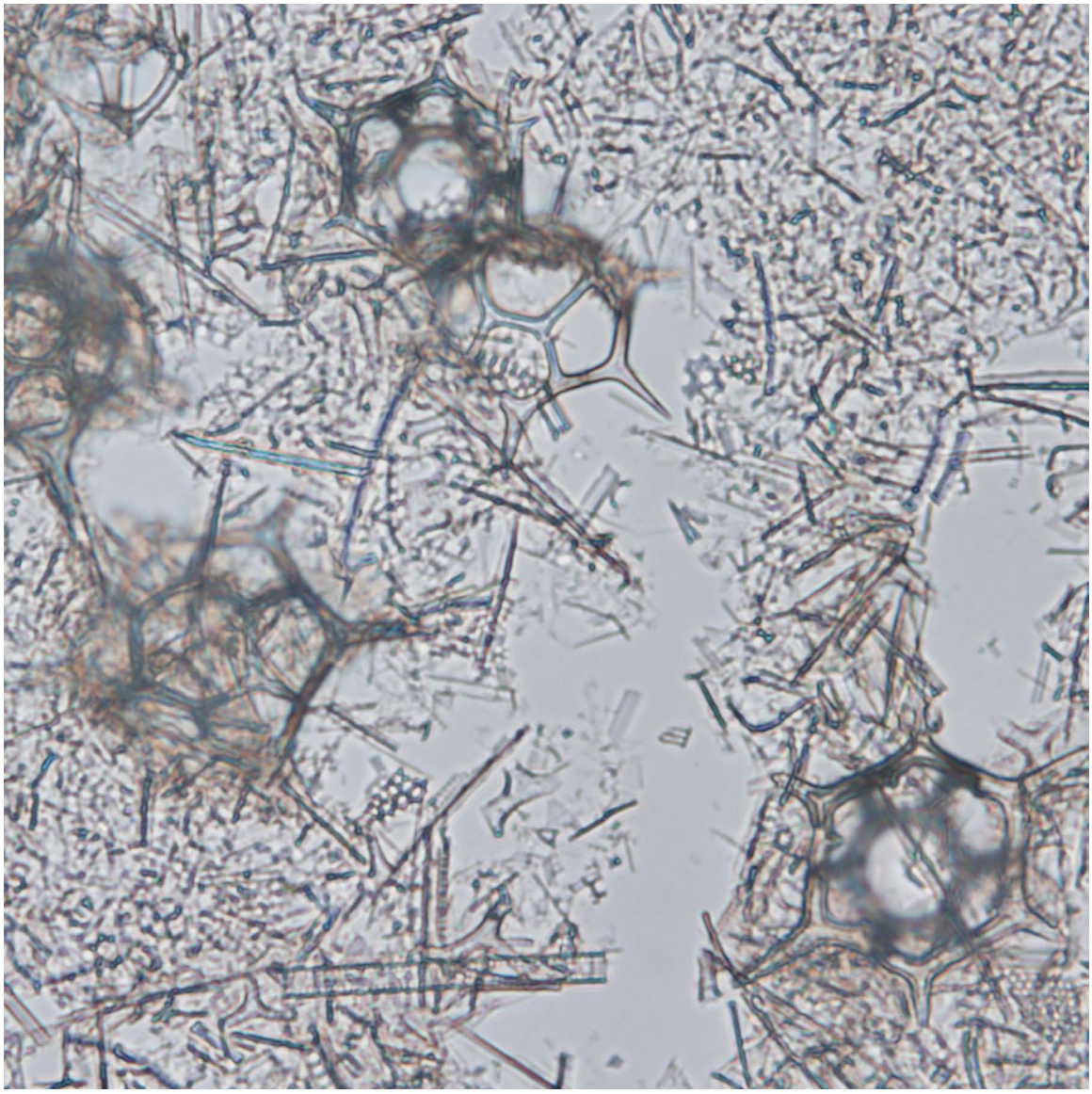

Silicoflagellate 7.

This sample shows several larger specimens of distephanid silicofglagellates with central apical window structures set in a largely isotropic, fine siliceous ooze.

ODP Sample (early Pliocene): Leg 113, Hole 690B, Core 3H, Section 3W, 50 cm

Image ID: B0438/B0439

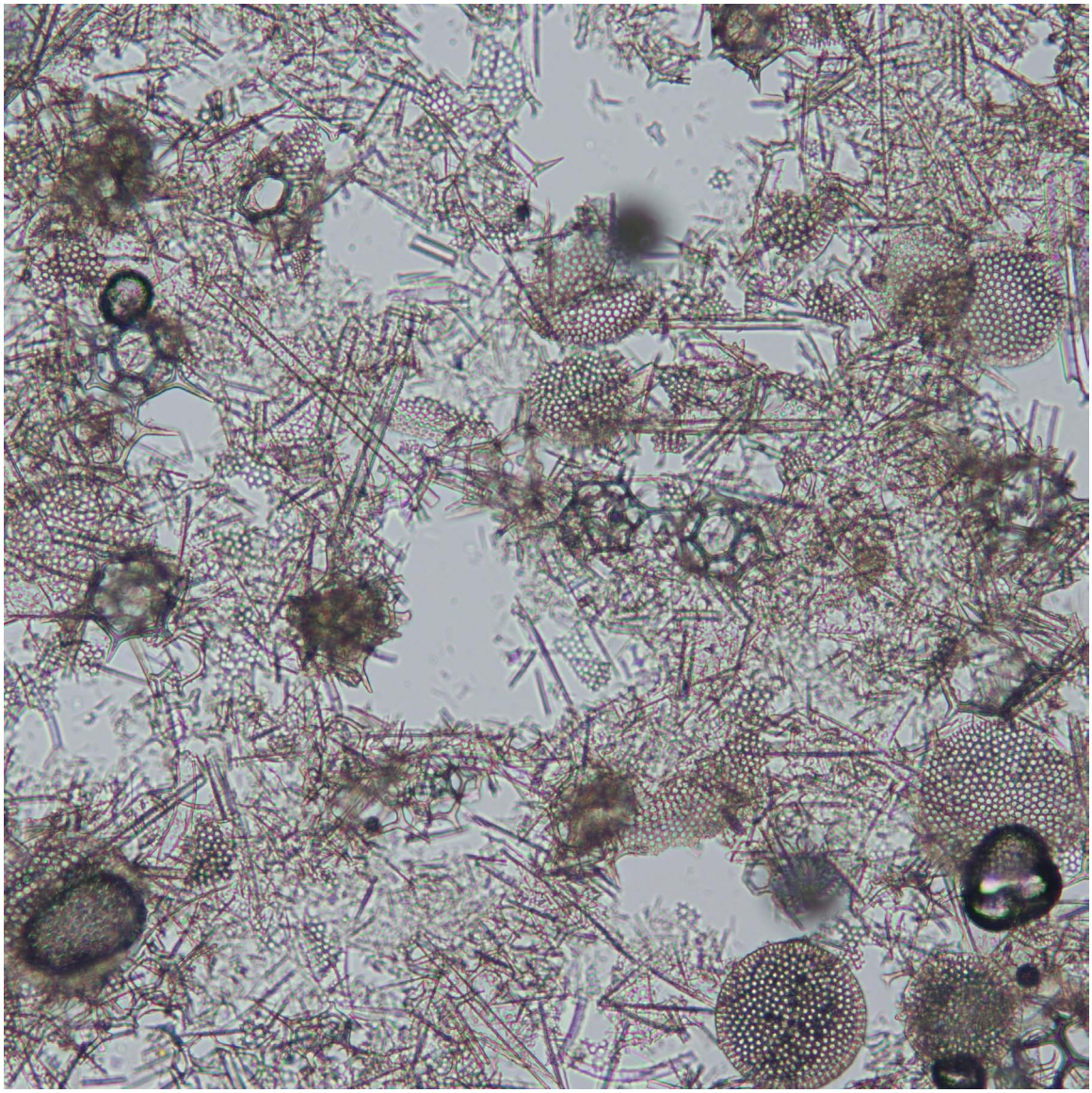

Silicoflagellate 8.

This diatom ooze (pennate and centric varieties) contains over 10 specimens of distephanid silicoflagellates. Its purity is attested to by the total absence of birefringence when polars are crossed.

ODP Sample (early Pliocene): Leg 113, Hole 690B, Core 3H, Section 3W, 50 cm

Image ID: 0415/0416

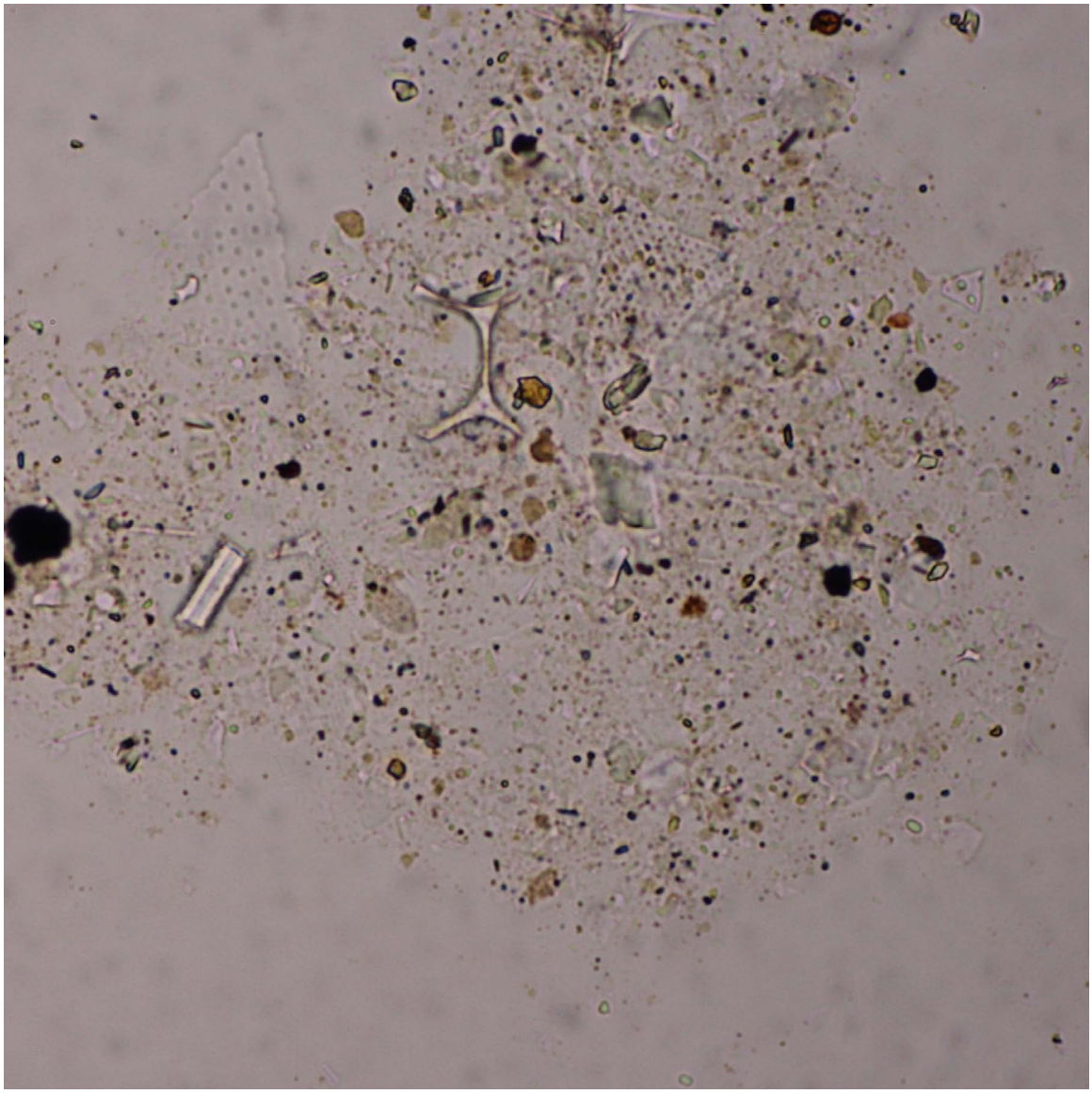

Silicoflagellate 9.

The geometry of the colorless opaline, I-shaped fragment in this mud suggests that it is a piece of sillicoflagellate or radiolarian. Note the triangular pieces of centric diatoms.

DSDP Sample (late Pleistocene): Leg 86, Hole 576B, Core 1H, Section 1W, 112 cm

Image ID: B0710/B0711

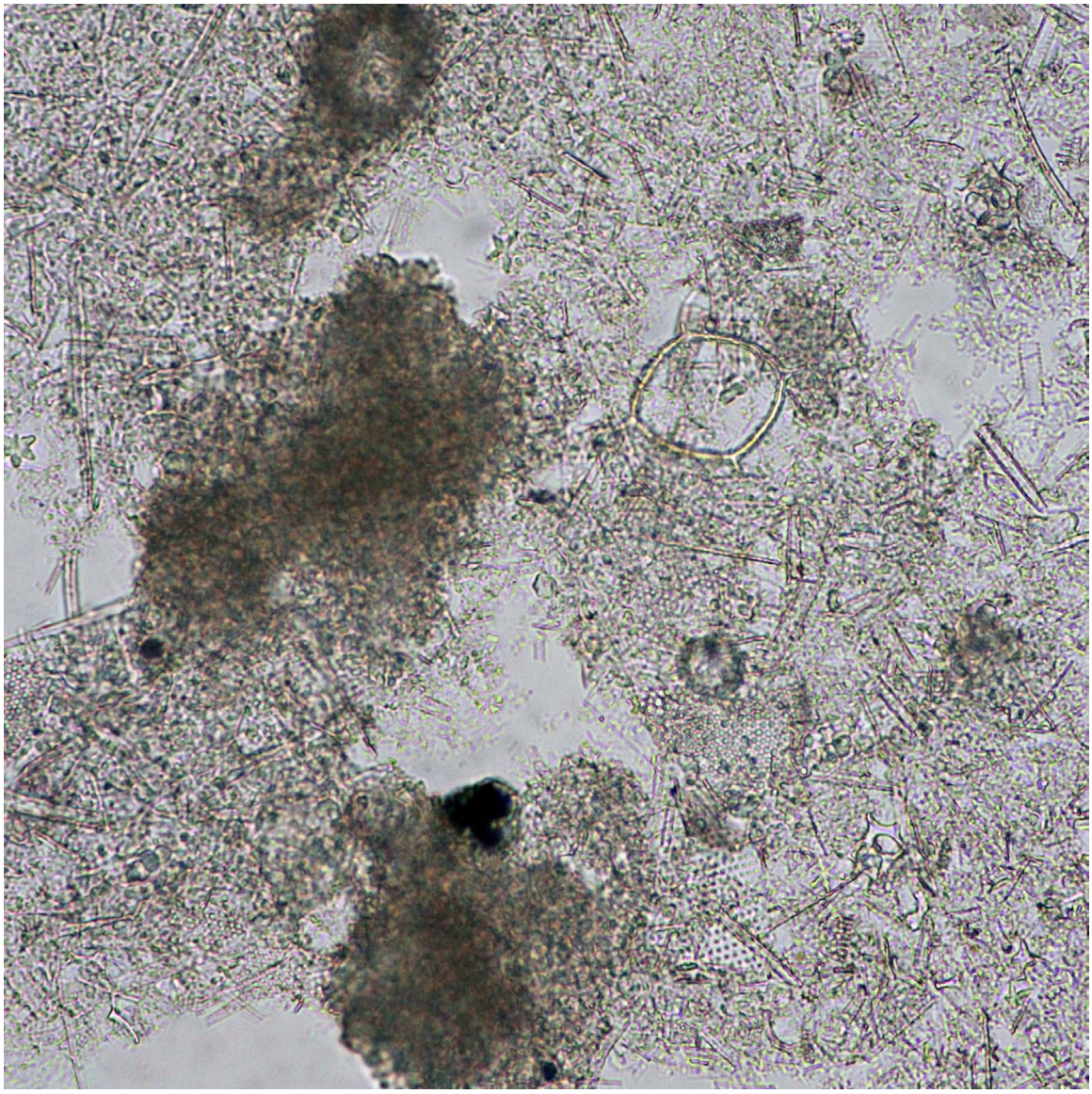

Silicoflagellate 10.

A simple, open, diamond- to oval-shaped silicoflagellate (circled) stands out in this mixed siliceous/calcareous ooze comprising nonbirefringent fragments of pennate and centric diatoms, and birefringent nannofossils with micrite and a few small foraminifera most easily discerned when polars are crossed.

DSDP Sample (late Miocene): Leg 38, Hole 845A, Core 15H, Section 2W, 10 cm

Ebridians

INTRODUCTION TO EBRIDIANS

Overview – Flagellated protists, similar in general form to the silicoflagellates, distinguished by their simple internal siliceous skeleton composed of solid, angular elements.

Diagnostic Features – Simple skeleton of solid elements with angular edges (triradial, cross, or T-shaped in cross-section): consisting of bars, rings, and spines. These elements may have jagged (reticulated) edges in some species. Initial elements are tetraxial or triradial to which other structural elements are added. Lacks distinctive basal ring of silicoflagellates. 15-65 µm in diameter, generally <25 µm.

Biology – Ebridians share many cellular characteristics with the heterotrophic dinoflagellates, including the two flagella of differing lengths (Ernissee and McCartney, 1993; UCL webpage on dinos), but other research suggests that they are closely related to euglenoid flagellates (Hargraves, 2002).

Ecology – Heterotrophs and mixotrophs, possibly autotrophs. Best known from coastal and neritic waters, as well as bays and estuaries.

Stratigraphic Range – Cenozoic, with peak diversity in the Eocene – Miocene.

Key References:

Ernissee, J.J., and McCartney, K., 1993. 8: Ebridians. In Lipps, J.H. (Ed.), Fossil Prokaryotes and Protists: Blackwell Scientific Publications, 131-140.

Haq, B.U., 1978. 11: Silicoflagellates and Ebridians. In Haq, B.U., and Boersma, A. (Eds.), Introduction to Marine Micropaleontology: Elsevier, 267-275.

Hargraves, P.E., 2002. The ebridian flagellates Ebria and Hermesinum. Plankton Biology and Ecology, 49(1): 9-16.

Ling, H.Y., 1984. Paleogene silicoflagellates and ebridians from the Goban Spur, Northeastern Atlantic. In, de Graciansky, P.C., Poag, C.W., et al., Initial Reports, DSDP 80:663-668.

Locker, S., and Martini, E., 1986. Ebridians and actiniscidians from the southwest Pacific. In, Kennett, J.P., von der Borch, C.C., et al., Initial Reports, DSDP 90:939-951.

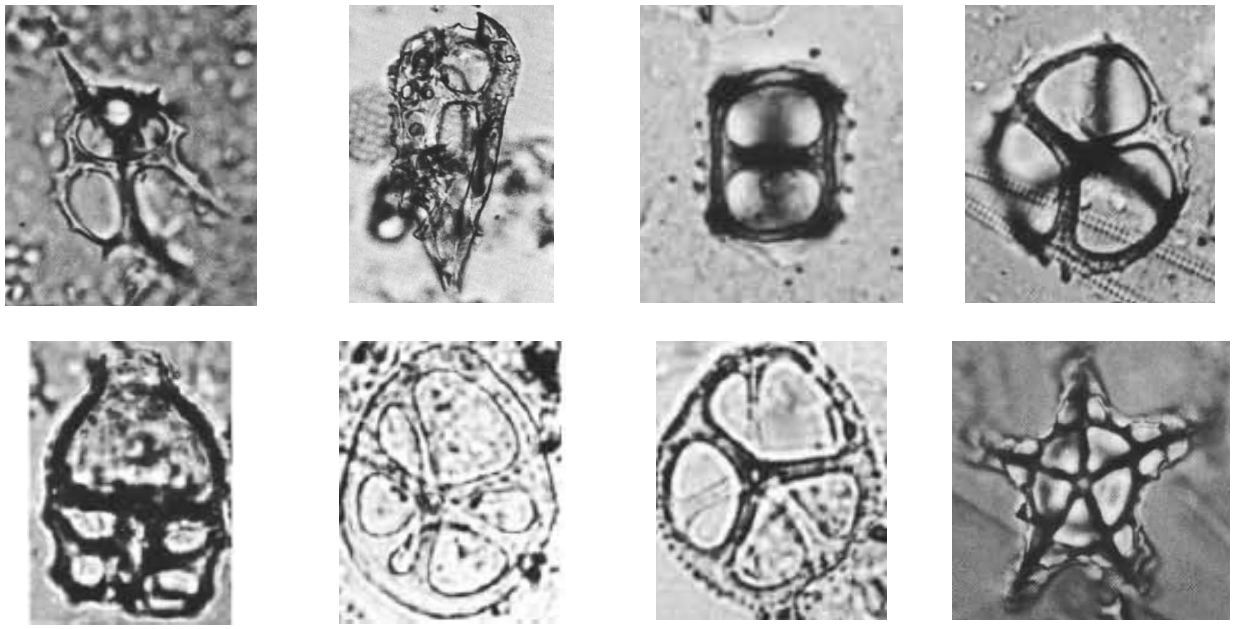

Representative Cenozoic ebridians and actiniscidian. Top row: *Hermesinum obliquum, Micromarsupium anceps, Ammodochium serotinum, Ebriopsis cornuta*. Bottom row: *Ammodochium rectangulare, Ebriopsis antiqua antiqua, Ebriopsis crenulata, Actiniscus pentasterias.* Photomicrographs from Ling, 1984; Locker and Martini, 1986.

Siliceous Sponge Spicules

INTRODUCTION TO SPONGES (SILICEOUS AND CALCAREOUS SPICULES)

Overview – Sponges are benthic multicellular animals consisting of a highly porous matrix that allows water to circulate through their bodies. They live attached to the seafloor. Mesohyl is the gelatinous matrix of sponges, consisting of collagen and other polypeptides; spongin is a fibrous collagen protein that provides an internal flexible framework. Many sponges precipitate siliceous (opaline) or calcareous (calcium carbonate) spicules within the mesohyl that provide additional structural support. Sponges with mineralized spicule skeletons can contribute marine sediment in the form of discrete sand-to-silt-size spicules when upon death of the organisms, they decompose and disaggregate.

Diagnostic Features – Amorphous silica (opaline) sponge spicules form around an axis of organic material optically visible as an axial tube in fossil varieties. This axial structure is less defined in the crystalline calcareous spicules, which are surrounded by an organic membrane during growth. In the calcareous spicules, the carbonate is Mg-calcite precipitated as single crystals that exhibit uniform optic orientation when viewed with a petrographic microscope in smear slide and thin section. It is notable that the calcareous spicules break isotropically rather than along mineral cleavage planes as a function of their submicroscopic structure. Calcareous spicules are smooth and range in size from 0.1-10 mm. They are described in terms of the number of axes (-axon) or rays (-actine or -actinal). Siliceous spicules are morphologically more variable. They are described in terms of the number of axes or rays, as well as spicule size, shape and ornamentation. The pointed spicule rays are defined by growth direction. The number of rays can vary from one or two (monoaxon), three (triaxon), to four (tetraxon) or more (polyaxon) and aerose where the rays diverge from a central point. The prefix “acantho-“ is used when the spicule surface is spined. Varieties can be shaped like the letters C or S (sigmas), bow-shaped (toxons), rounded at both ends (strongyles), or knobbed at one or both ends (tylostyle).

Biology – Phylum Porifera

Ecology – Heterotrophs. Sponges occur in freshwater, brackish, and marine environments at all latitudes and water depths, from intertidal to abyssal. Calcareous sponges are more common in warmer, shallower waters.

Stratigraphic Range – Neoproterozoic to present.

Key References and Examples:

Albach, W.J., and McCartney, K., 1992. Siliceous sponge spicules from Site 748. In, Wise, S.W., Jr., Schlich, R., et al., Proceedings of the ODP, Scientific Results, 120: 833-837.

Bergquist, P.R. 1978. Sponges. Hutchinson: London & University of California Press: Berkeley & Los Angeles: 268 p.

Ivanik, M.M., 1983. Paleogene and Neogene sponge spicules from Sites 511, 512, and 513 in the South Atlantic. Initial Reports Deep Sea Drilling Project, 71: 933-950.

McCartney, K., 1987. Siliceous sponge spicules from DSDP Leg 93. In, Van Hinte, J.E., Wise, S.W., Jr., et al., Initial Reports DSDP, 93: 815-824.
Sethmann, I., and Wörheide, G., 2008. Structure and composition of calcareous sponge spicules: A review and comparison to structurally related biominerals. Micron, 39: 209-228.

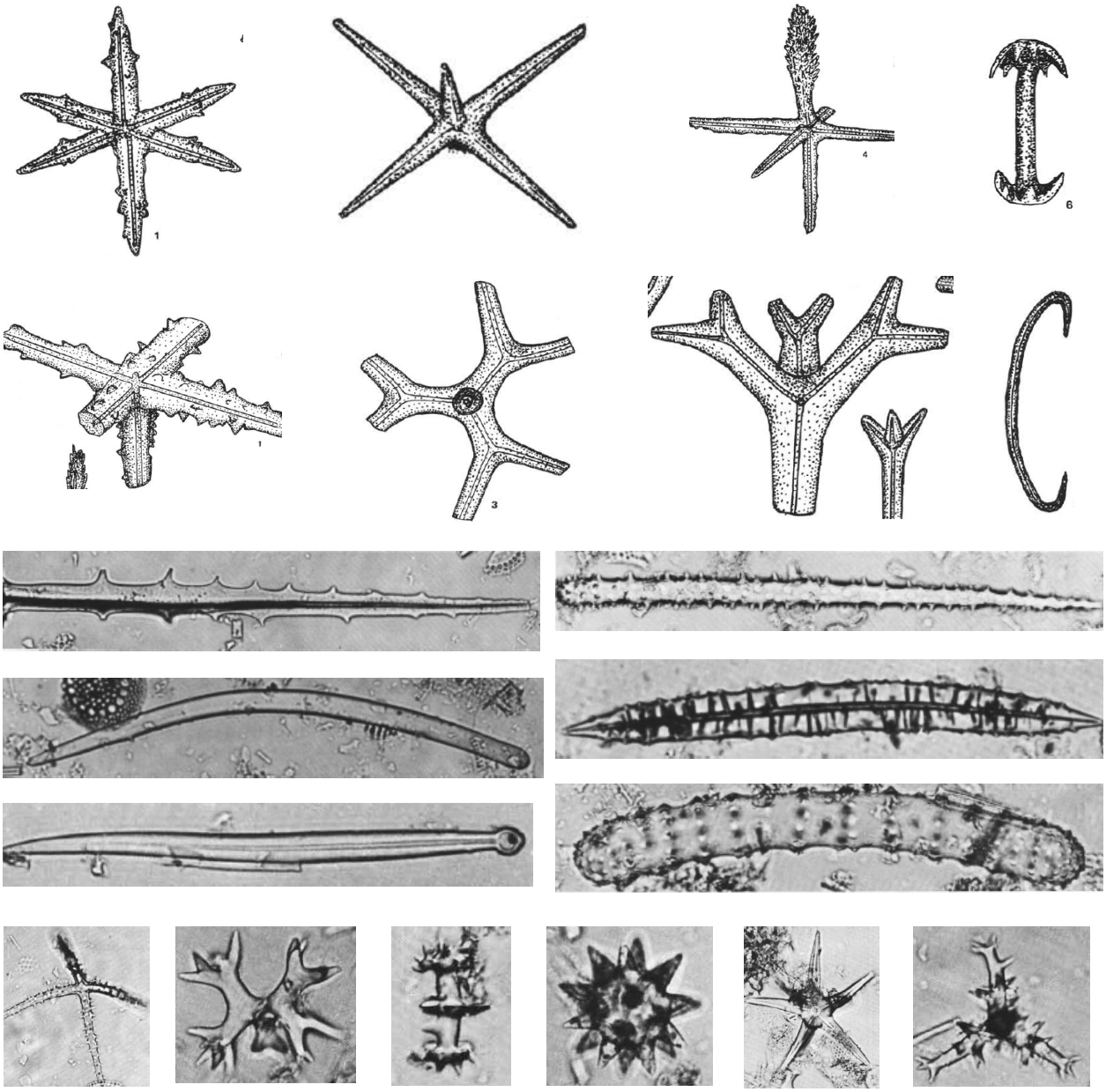

Representative Cenozoic sponge spicules. Top row: Oxyhexactine, thorned; Hexactine; Pinulus; Amphidiscus. Second row: Pentactine; Orthodichotriaenes; Plagiodichotriaenes; Sigma. Third row: ‘serrated spine’, ‘acanthostyle’. Fourth row: ‘syle’, ‘acanthoxea’. Fifth row: ‘tylostyle’, ‘anthrostrongyle’. Bottom row: ‘hexactine’, ‘streptaster’, ‘discorhabd’, ‘spheraster’, ‘oxyaster’, ‘caltrops’. Camera ludida drawings from Ivanik, 1983; Photomicrographs from McCartney, 1987.

Siliceous Sponge Spicules


Sponge spicule 1


Sponge spicule 2


Sponge spicule 3


Sponge spicule 4


Sponge spicule 5


Sponge spicule 6


Sponge spicule 7

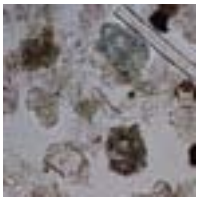
Sponge spicule 8


Sponge spicule 9


Sponge spicule 10


Sponge spicule 11

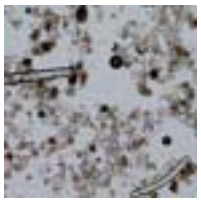
Sponge spicule 12


Sponge spicule 13


Sponge spicule 14


Sponge spicule 15

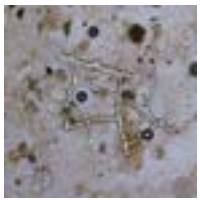
Sponge spicule 16


Sponge spicule 17

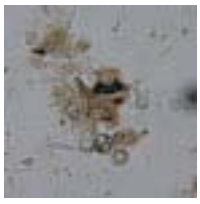
Sponge spicule 18


Sponge spicule 19


Sponge spicule 20


Sponge spicule 21


Sponge spicule 22

Image ID: 0194

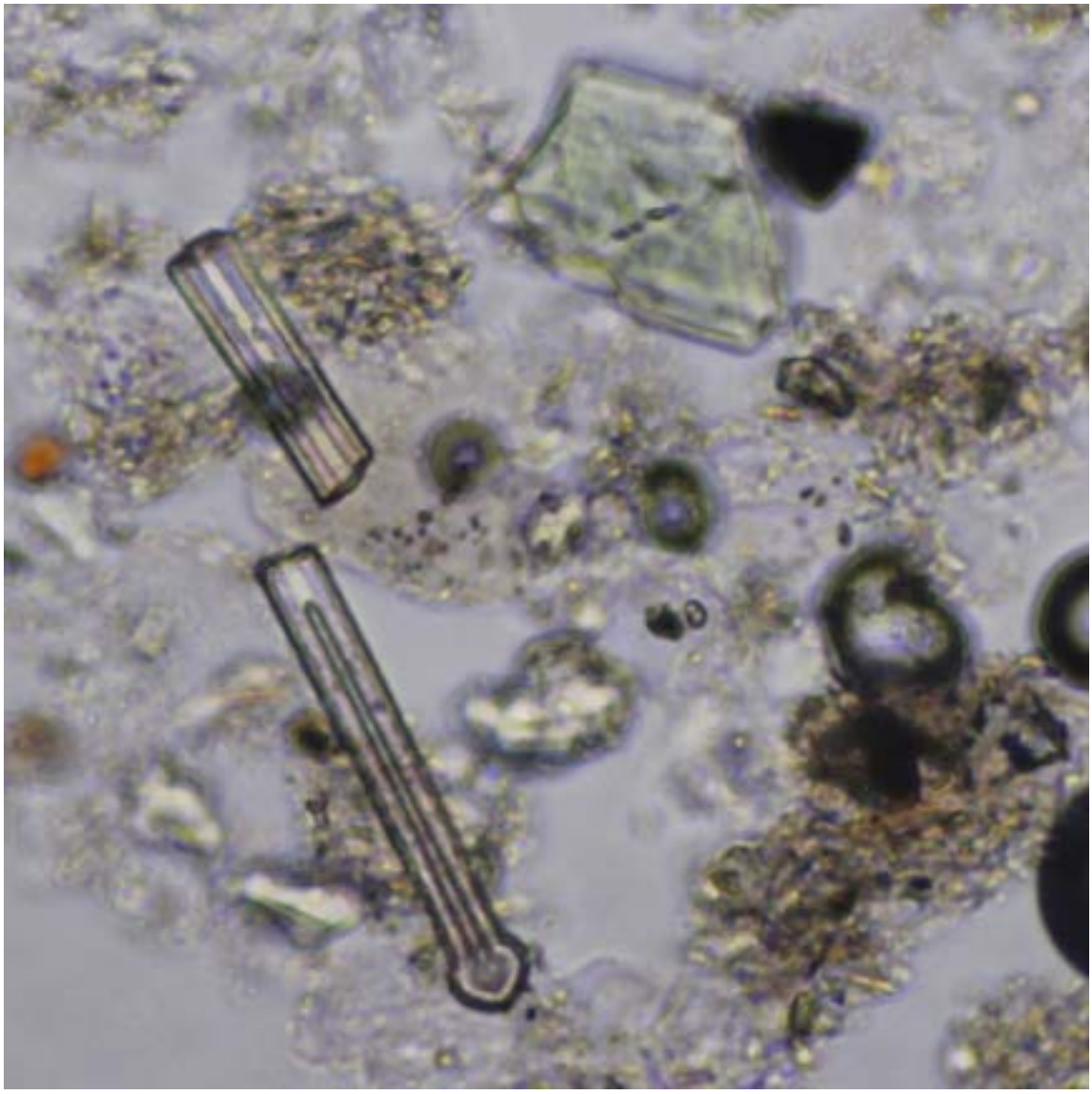

Sponge spicule 1.

Broken fragments of a siliceous (opaline) sponge spicule with a distinct axial tube and knobbed end (Tylostyle). The spicule was fractured during smear creation, with two pieces still proximal to one another in this field of view. The surrounding grains are terrigenous silt, mainly dense minerals and lithic fragments. Note that there is no crossed polar view for this image.

ODP Sample (early Pleistocene): Leg 141, Hole 861C, Core 15X, Section 2, 40 cm

Image ID: 0326

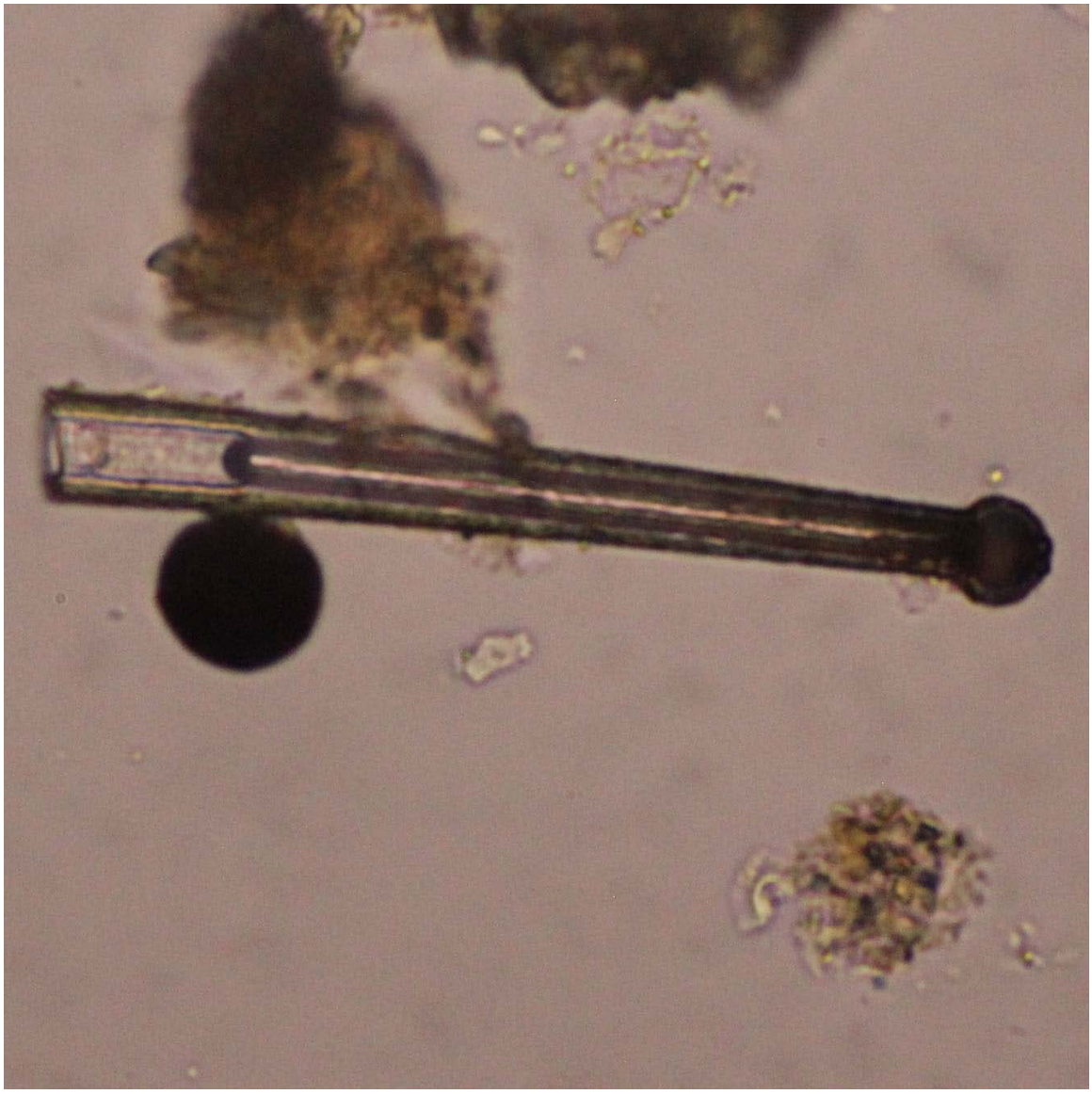

Sponge spicule 2.

Broken fragments of a siliceous (opaline) sponge spicule with a distinct axial tube and knobbed end (Tylostyle) in contact with a perfectly circular authigenic opaque grain (pyrite framboid?). The other grains in this field of view are likely clumps of clay matrix. Note that there is no crossed polar view for this image, as each of the components (biogenic, authigenic and detrital) is not birefringent.

ODP Sample (late Pleistocene): Leg 181, Hole 1119C, Core 6H, Section 1W, 43 cm

Image ID: B0029/B0030

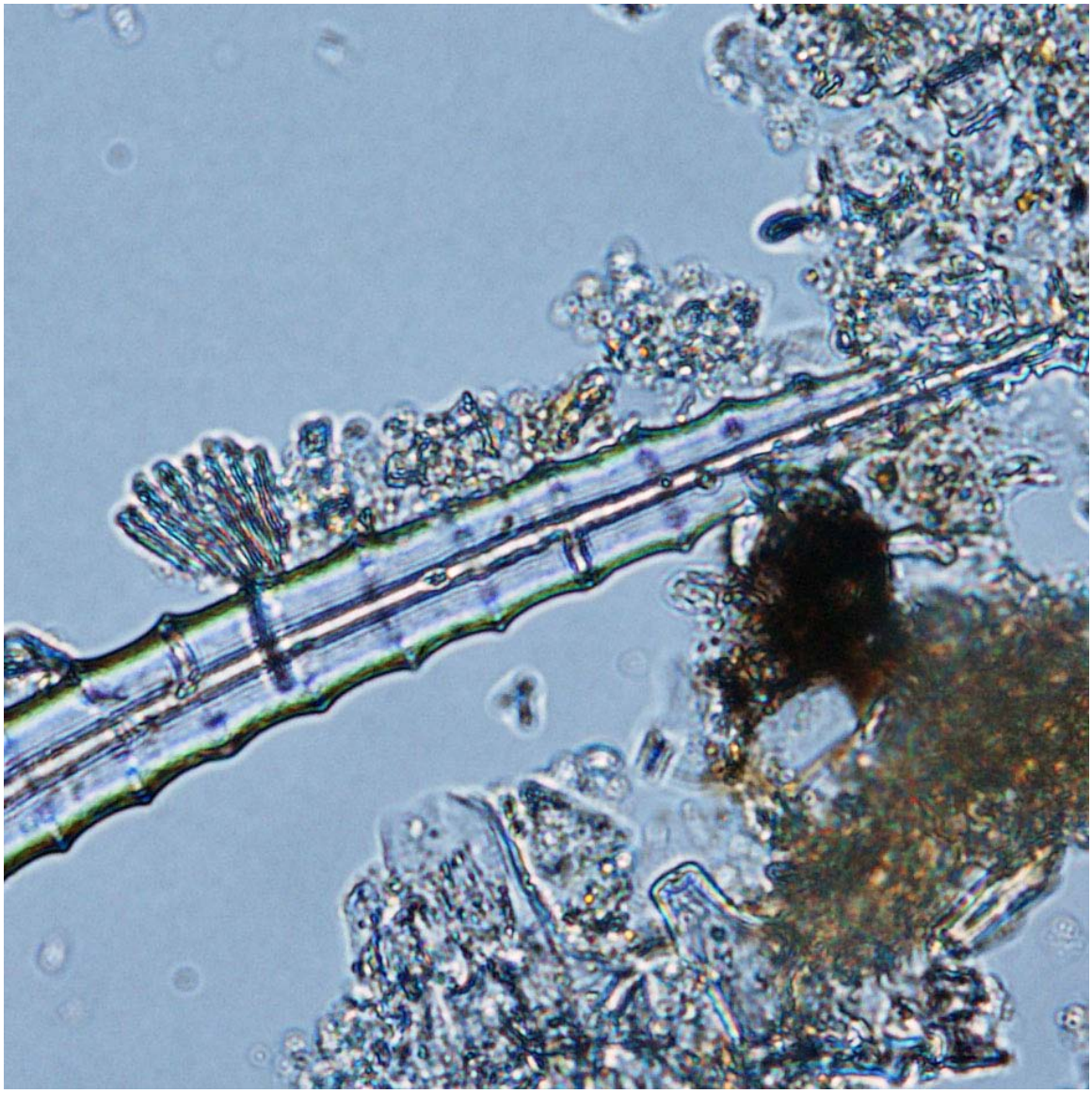

Sponge spicule 3.

A slightly tapered siliceous sponge spicule with a distinct axial tube but less pronounced spines (Acanthoxea ?) that appear as small bumps on the surface of the spicule. With polars crossed, the opaline nature (isotropic) of the spicule is evident. Other non-birefringent silt-size fragments are volcanic glass and/or authigenic zeolites, with minor birefringent clay to silt-size mineral (crystal?) components.

DSDP Sample (late Eocene): Leg 30, Hole 286, Core 10, Section 4, 79 cm

Image ID: B0035/B0036

Sponge spicule 4.

A close-up view of a spined siliceous sponge spicule fragment with more pronounced spines and a distinct axial tube. It can only be described as "Acantho-" without further information on the geometry and morphology of the spine. With nicols crossed, the opaline spine is isotropic and partly defined by the slightly birefringent clay/carbonate(?) matrix adhering to it.

DSDP Sample (late Eocene): Leg 30, Hole 286, Core 10, Section 4, 79 cm

Image ID: B0051/B0052

Sponge spicule 5.

A prominent sponge broken siliceous sponge spicule has an axial tube and a rounded end with no knob (Strongyle). The surrounding siliceous ooze consists mainly of centric (mesh-like texture) and pennate (thin parallel elements) diatom fragments and one very small round radiolarian. The locally birefringent, brown-colored matrix consists of organic matter, clay minerals, and silt-to-clay-size minerals.

DSDP Sample (early-late Pliocene): Leg 56, Hole 438A, Core 13, Section 3, 64 cm

Image ID: B0037/B0038

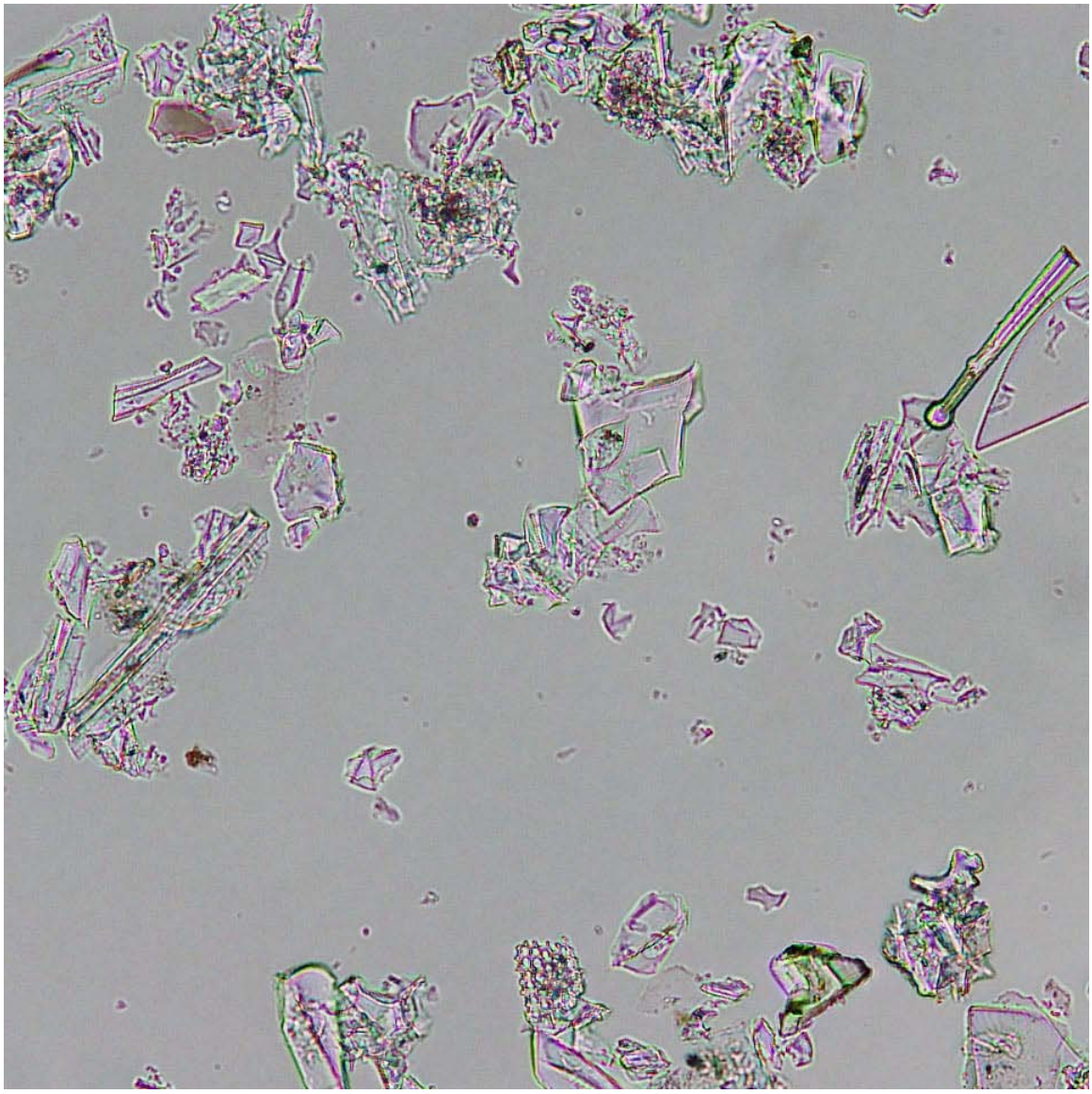

Sponge spicule 6.

This sample of volcanic ash is composed of colorless volcanic glass with one broken siliceous sponge spicule (Tylostyle or Strongyle) in the upper right for comparison (circled). Both glass fragments and opaline spicule are non-birefringent (isotropic) under crossed polars, but the shape (bulbous end) and axial tube of the spicule distinguishes it. The birefringent components are crystal fragments or microlites in glass (plagioclase and plagioclase), and a few small nannofossils with characteristic pin-wheel first-order birefringence.

DSDP Sample (middle Miocene): Leg 30, Hole 286 , Core 28, Section 2, 148 cm

Image ID: B0065

Sponge spicule 7.

Siliceous ooze with fragments of sponge spicules, one with a smooth surface and another spined (Acantho-), but both distinguished by their axial tubes, and other smaller fragments of centric diatoms distinguished by their mesh-like textures. Intermixed, angular silt grains may be colorless volcanic glass. Brown matrix is likely a combination of organic matter and clay minerals. All components are essentially isotropic, so no crossed-polar view is shown.

DSDP Sample (early Pleistocene): Leg 56, Hole 440B, Core 8, Section 3, 5 cm

Image ID: 0684/0683

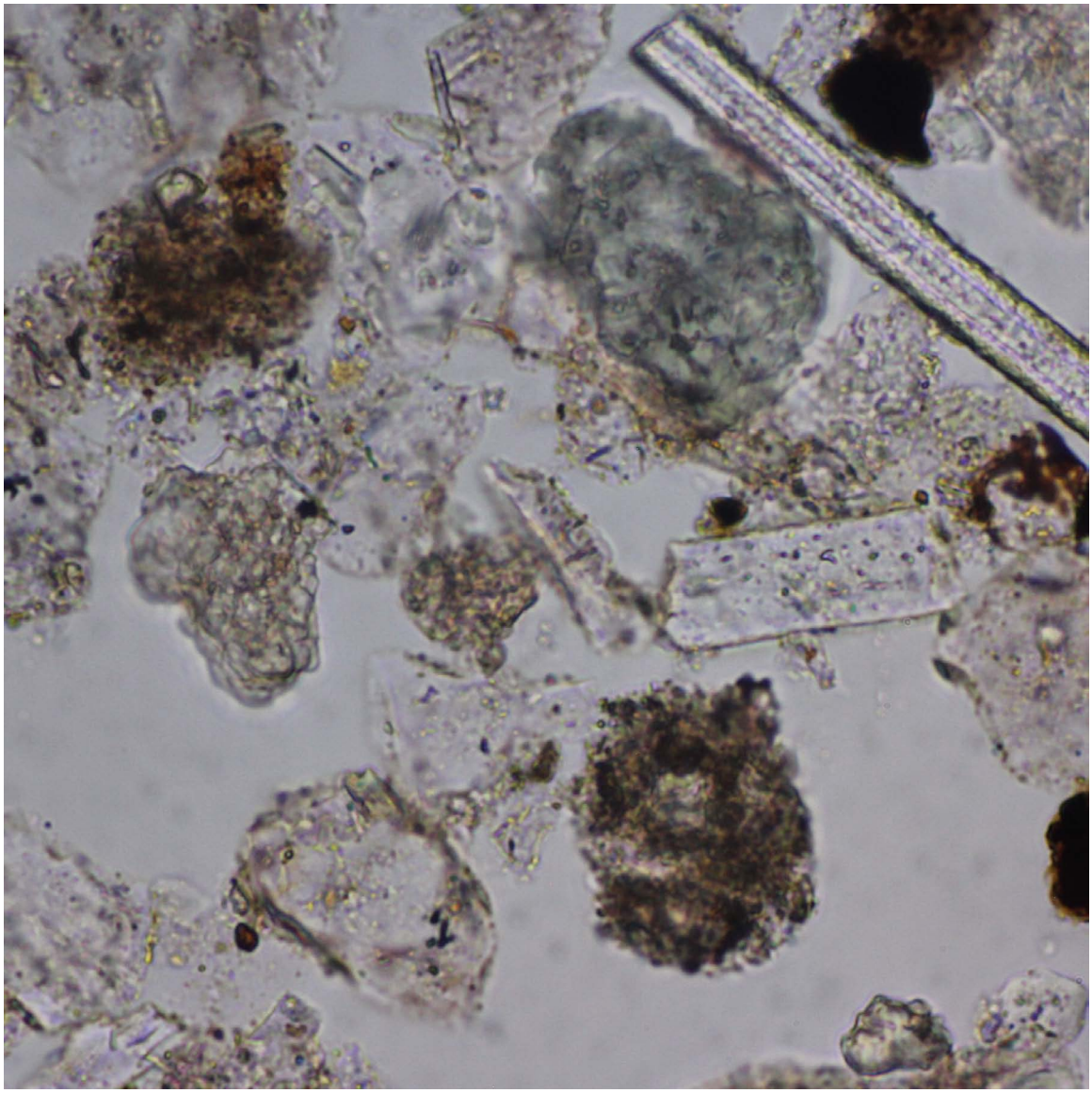

Sponge spicule 8.

A diverse detrital grain assemblage includes quartz, feldspar, carbonate, and brown sedimentary lithic fragments with one prominent siliceous sponge spicule. This opaline spicule has a higher relief than the surrounding grains, but no birefringence and a poorly defined axial tube.

DSDP Sample (Pleistocene): Leg 96, Hole 614A, Core 5H, Section 2W, 26 cm

Image ID: 0623

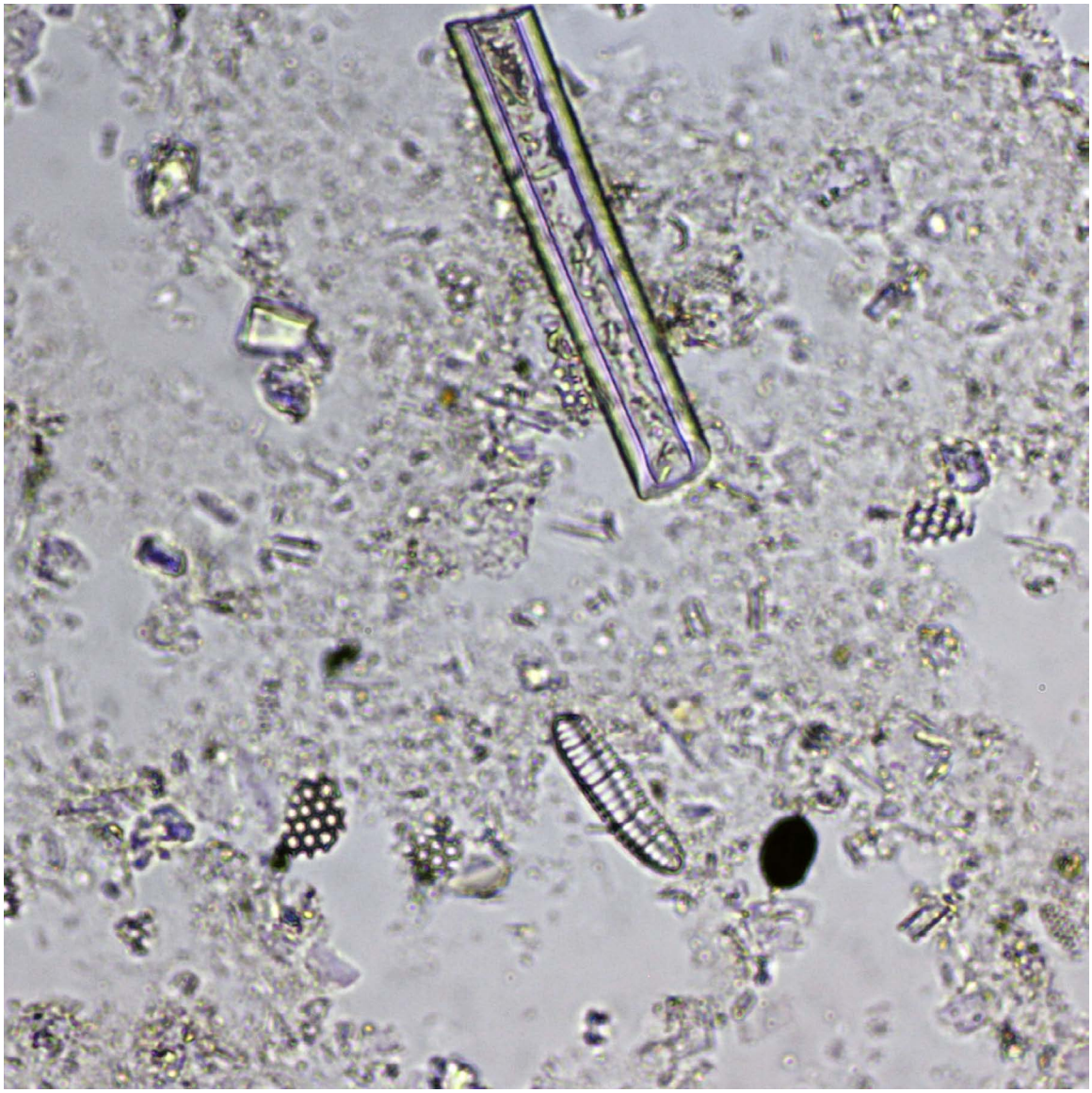

Sponge spicule 9.

Broken siliceous sponge spicule fragment with a wide axial tube that appears to be stuffed with clay-size matrix. The surrounding silt- and clay-size matrix includes fine fragments of centric diatoms distinguishable by their mesh-like texture. The overall low birefringence of this sample precludes a cross-nicols view. Some distinct high relief detrital(?) mineral grains are present.

IODP Sample (early Pliocene): Leg 178, Hole 1097A, Core 34R, Section 1W, 16 cm

Image ID: B0367/B0368

Sponge spicule 10.

Broken fragment of smooth-surfaced, tapered siliceous sponge spicule where wide axial tube is mostly filled by micritic carbonate. The contrast between the isotropic opaline spicule and highly birefringent carbonate is striking under crossed polars. Micritic carbonate outside of the axial pore space adjacent to the spicule and elsewhere in the field of view is slightly more coarsely crystalline than that in the spicule.

IODP Sample (late Pleistocene): Leg 317, Hole 628A, Core 15H, Section 2, 52 cm

Image ID: B0430/B0431

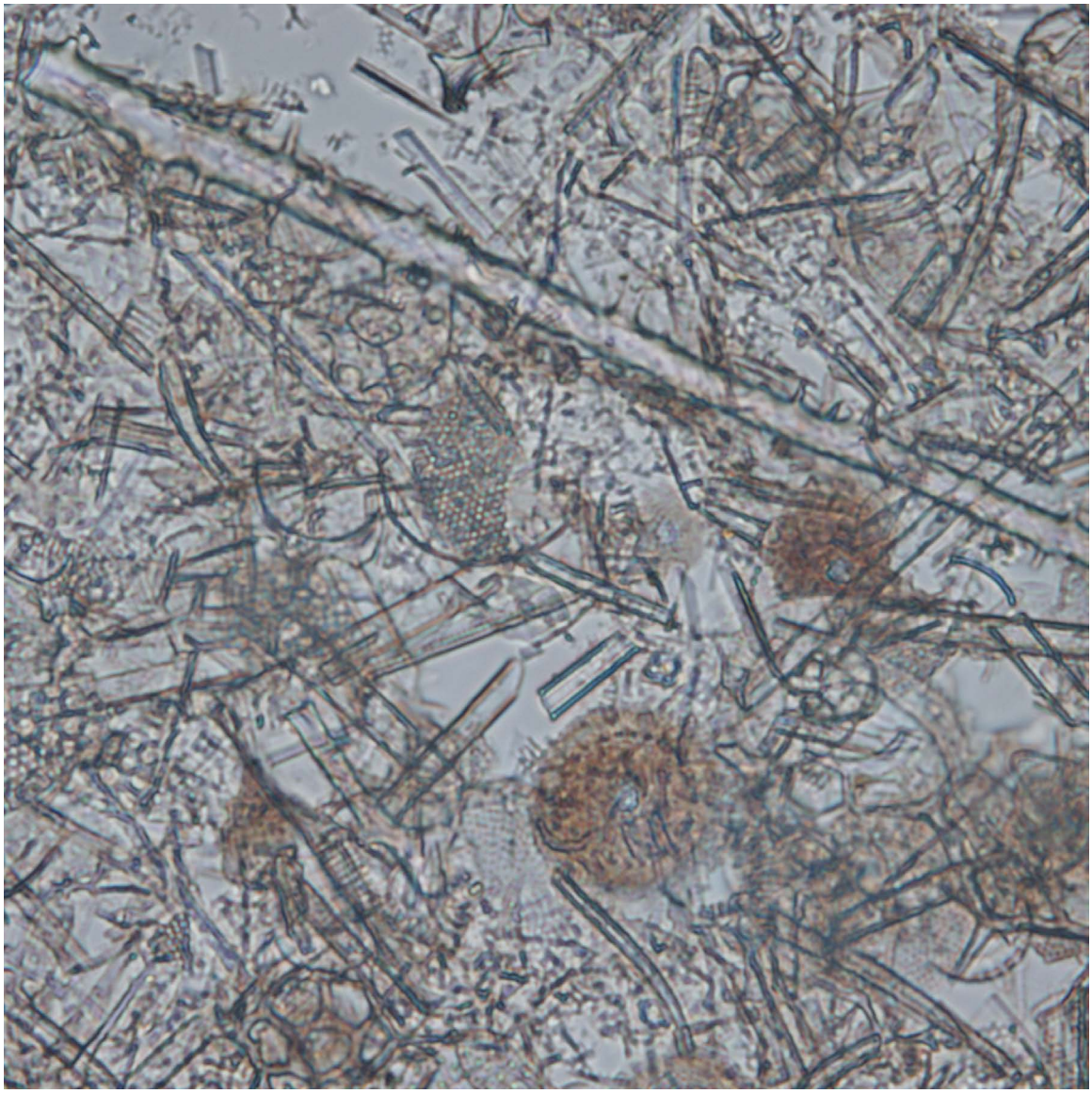

Sponge spicule 11.

The siliceous ooze in this field of view is dominated by frustule fragments of needle-shaped pennate diatoms. These contrast with a longer spiny (acantho-) siliceous sponge spicule that extends across the field of view from upper left to right; the spicule has an axial pore that is just barely discernable in the upper left end of the spicule. Circular, more complete diatom valves appear brownish, an optical illusion because of their very fine meshwork texture, a regular, repeating pattern which is also visible in fragments throughout the field of view. The pattern is more visible in these fragments because they are likely derived from large specimens.

ODP Sample (early Pliocene): Leg 113, Hole 690B, Core 2H, Section 2W, 120 cm

Image ID: B0027/B0028

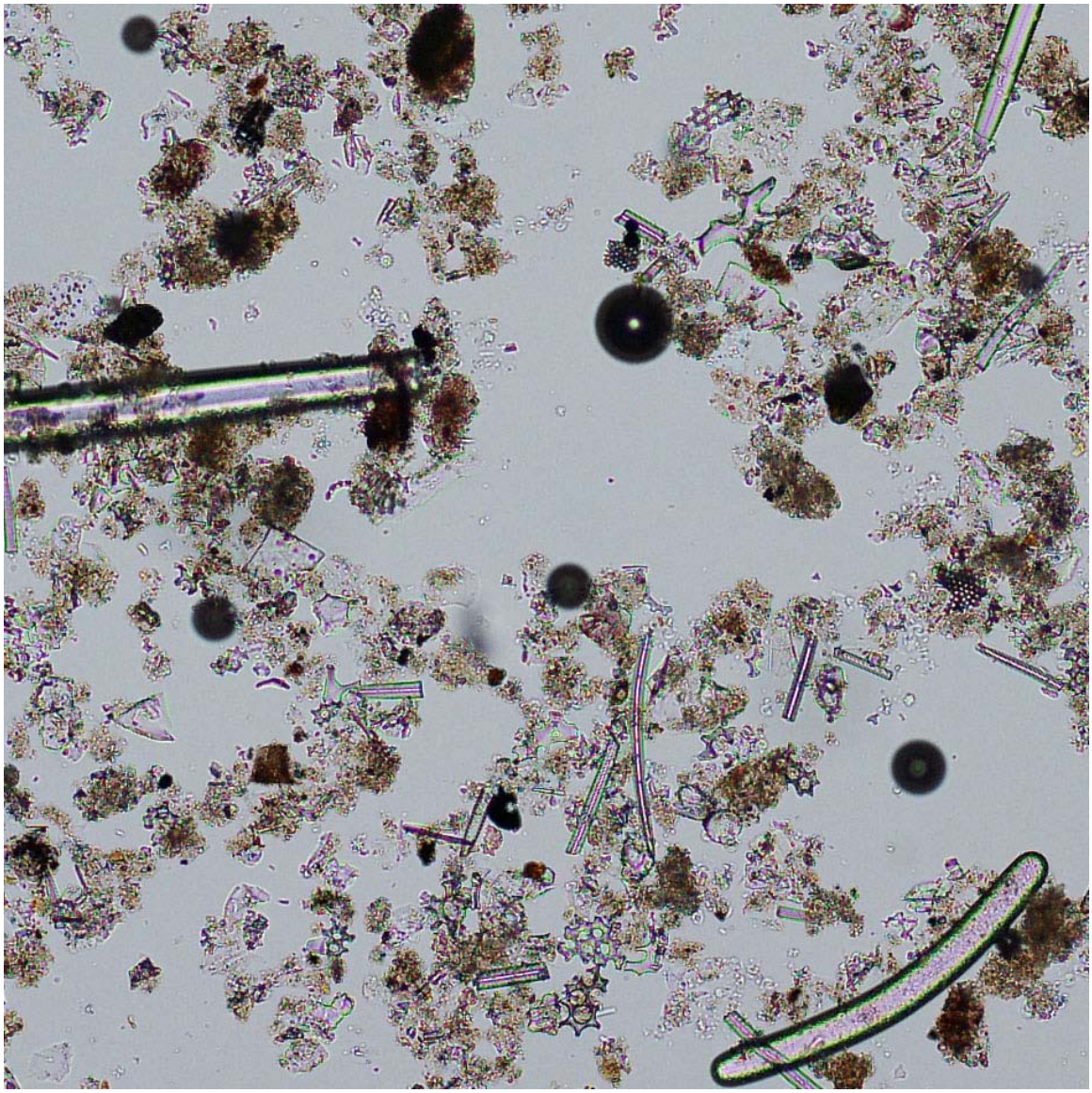

Sponge Spicule 12.

This is a mixed sediment of terrigenous silt and clay, biosiliceous debris, and carbonate. The axial pore is not in focus in the doubly rounded spicule (Strongyle) in the lower right corner.

DSDP Sample (late Eocene): Leg 30, Hole 286, Core 10, Section 4, 79 cm

Image ID: B0469/B0470

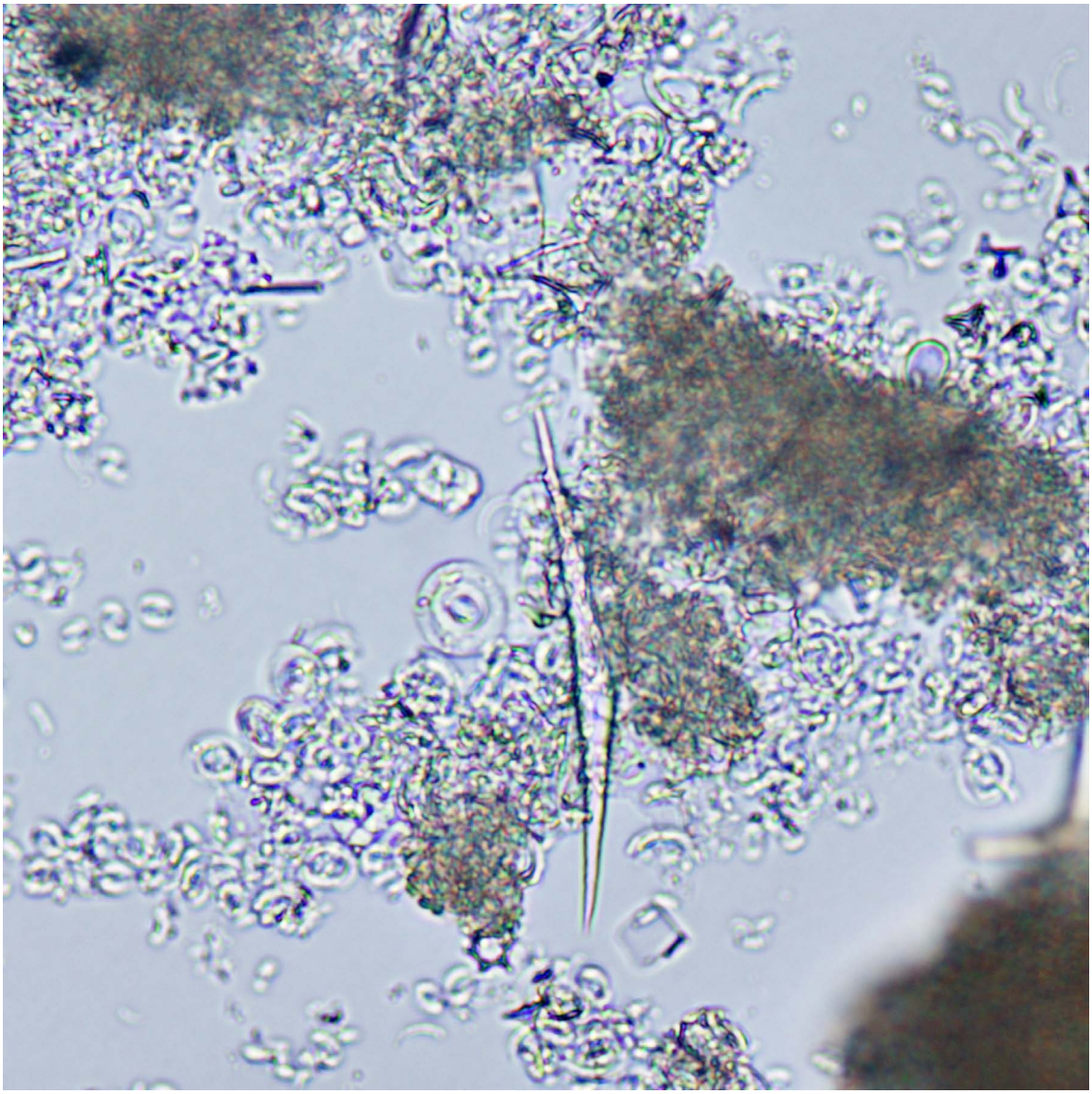

Sponge spicule 13.

This ooze consist of variably size nannofossils (coccoliths) with minor siliceous biogenic debris including a distinct siliceous spicule in the center of the field of view. This doubly tapered opaline spicule lacks an axial pore, and so may be part of another organism, perhaps a radiolarian. The nannofossils exhibit their characteristic birefringence with polars crossed, but some larger (~10 micron) coccoliths range up to first-order red. The ooze takes on the appearance of chalk in tan clumps where the nannofossils are more closely packed.
ODP Sample (early Oligocene): Leg 113, Hole 690B, Core 10H, Section 6W, 120 cm

Image ID: B0369/B0370

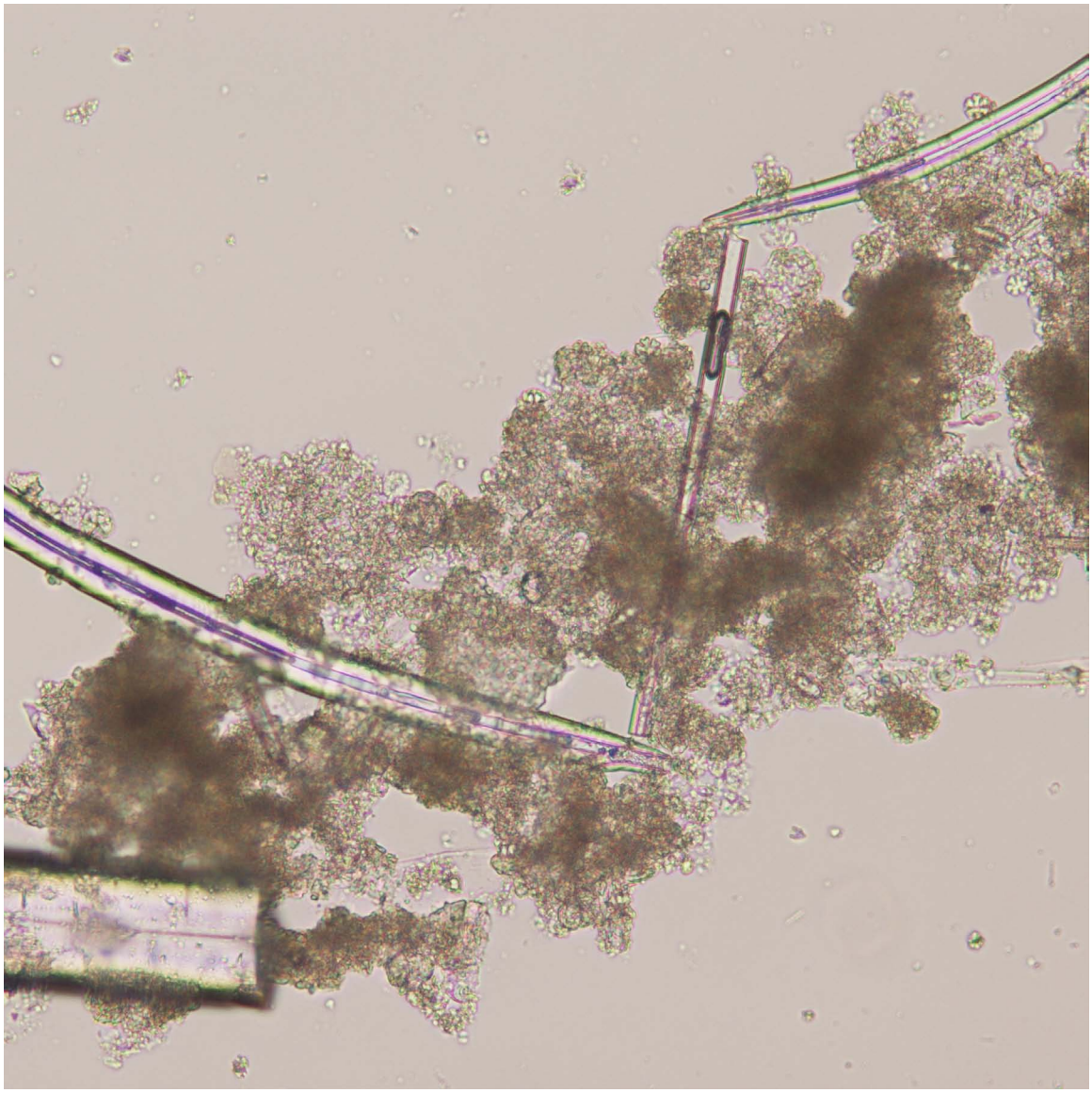

Sponge spicule 14.

Four broken fragments of siliceous mono-axon spicules ranging in thickness from 50 to <10 microns. The thinner spicules appear to taper and show pronounced axial pores, but note the thickest example in lower left corner has a very thin axial pore. These spicule fragments are set in a brownish semi-consolidated ooze/chalk. Note that the birefringence of the surrounding carbonate can be seen through the translucent, non-birefringent opaline spicules.

ODP Sample (late Oligocene): Leg 101, Hole 628A, Core 17H, Section 3, 52 cm

Image ID: B0460/B0461

Sponge spicule 15.

This smear slide shows a clump of siliceous ooze, largely composed of very fine fragments of diatomaceous debris in which a large doubly-tapered siliceous sponge spicule (Oxea) is set. The large bulbous brown grain is likely organic (algal spore?) and that there is some disseminated algal organic matter (brown dots) throughout the otherwise siliceous sediment, the opaline nature of which is demonstrated in the largely black field of view in the crossed-polar view. ODP Sample (Miocene): Leg 113, Hole 690B, Core 5H, Section 4W, 67 cm

Image ID: B0138/B0139

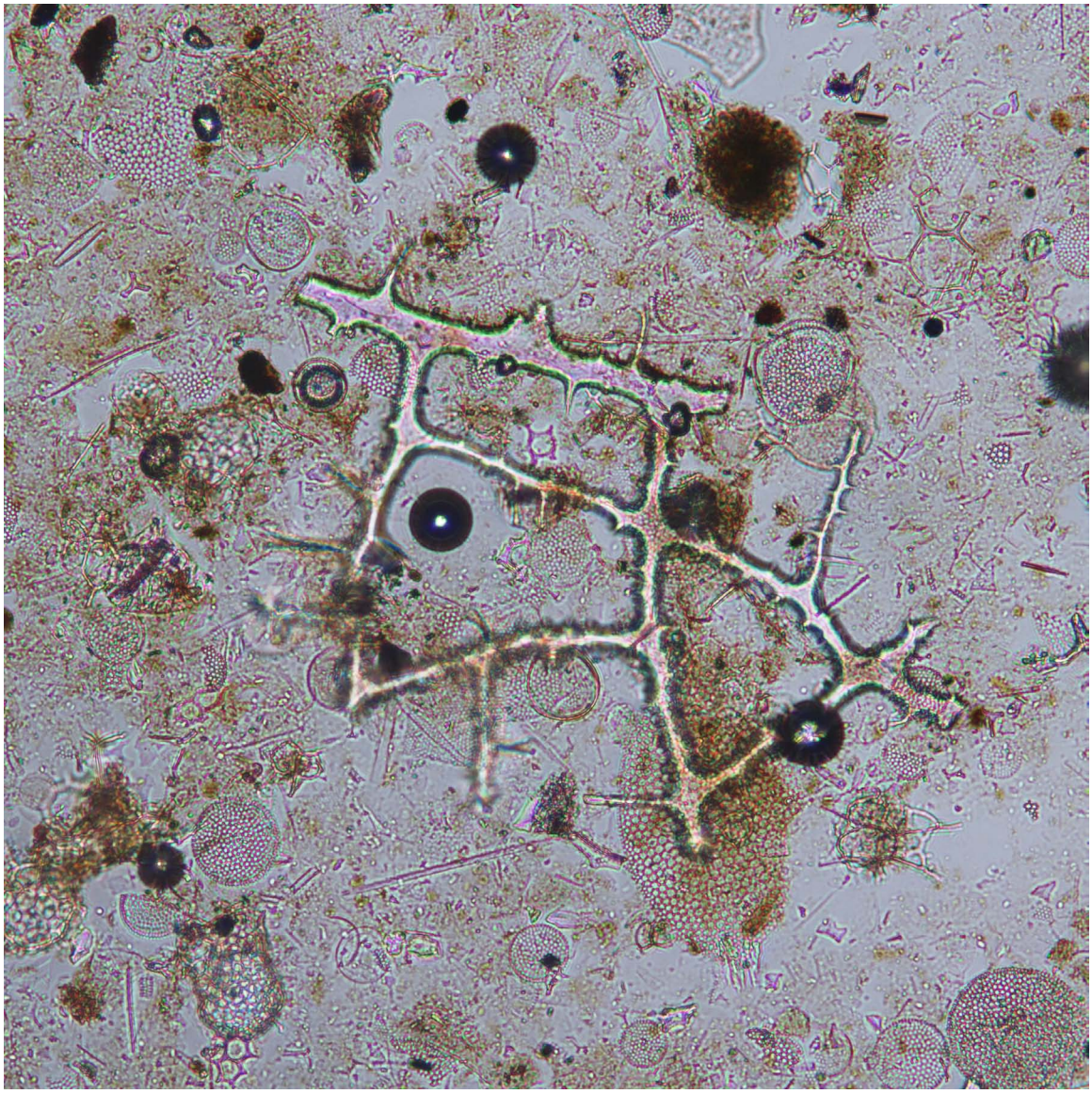

Sponge spicule 16.

This mesh-like network of oplaline silica (fused spicules?) may be a fragment of a "superficial dermal sponging fiber skeleton" as pictured in Bergquist (1978). It is set in radiolarian ooze with brown (organic?) clumps.

ODP Sample (Pleistocene): Leg 138, Hole 845A, Core 1H, Section 1W, 66 cm

Image ID: B0251

Sponge spicule 17.

Unusual, star-shaped siliceous microfossil, potentially a sponge spicule (pentactine microsclere) or ebridian, but most likely an actiniscidian. The background sediment is organic rich (tan/brown) and largely composed of various diatoms and diatom fragments. All siliceous bioclasts are opaline with no birefringence, so no cross-polar view is provided.

ODP Sample (late and middle Pleistocene): Leg 175, Hole 1075A, Core 5H, Section 6W, 6 cm

Image ID: B0246

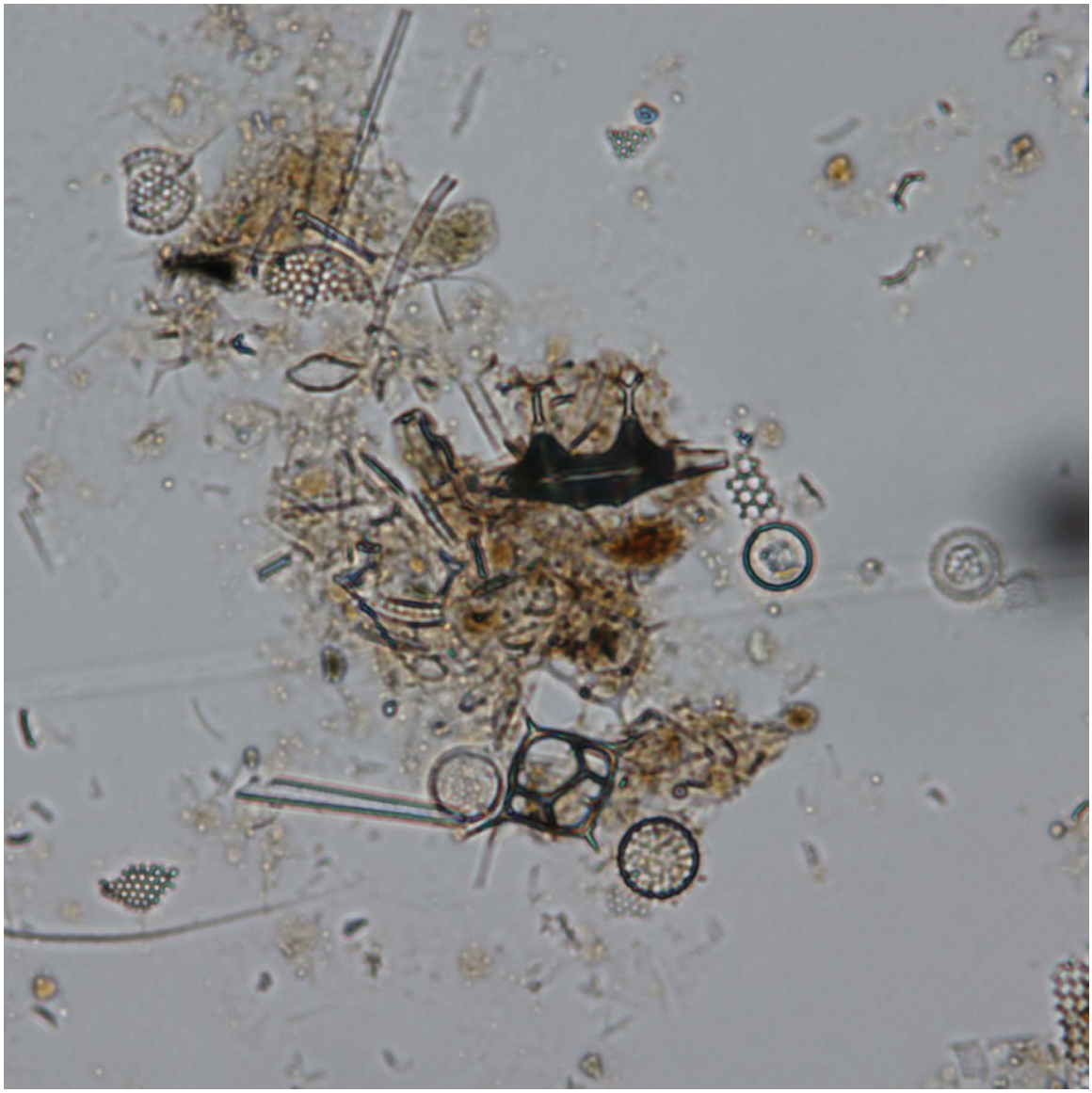

Sponge Spicule 18.

This unusual-shaped opaline bioclast may be a sponge spicule. It is set in a siliceous ooze with some clay and organic matter. No cross-polar view is provided as the components do not exhibit birefringence.

ODP Sample (late and middle Pleistocene): Leg 175 Hole 1075B, Core 2H, Section 2W, 15 cm

Image ID: B0565

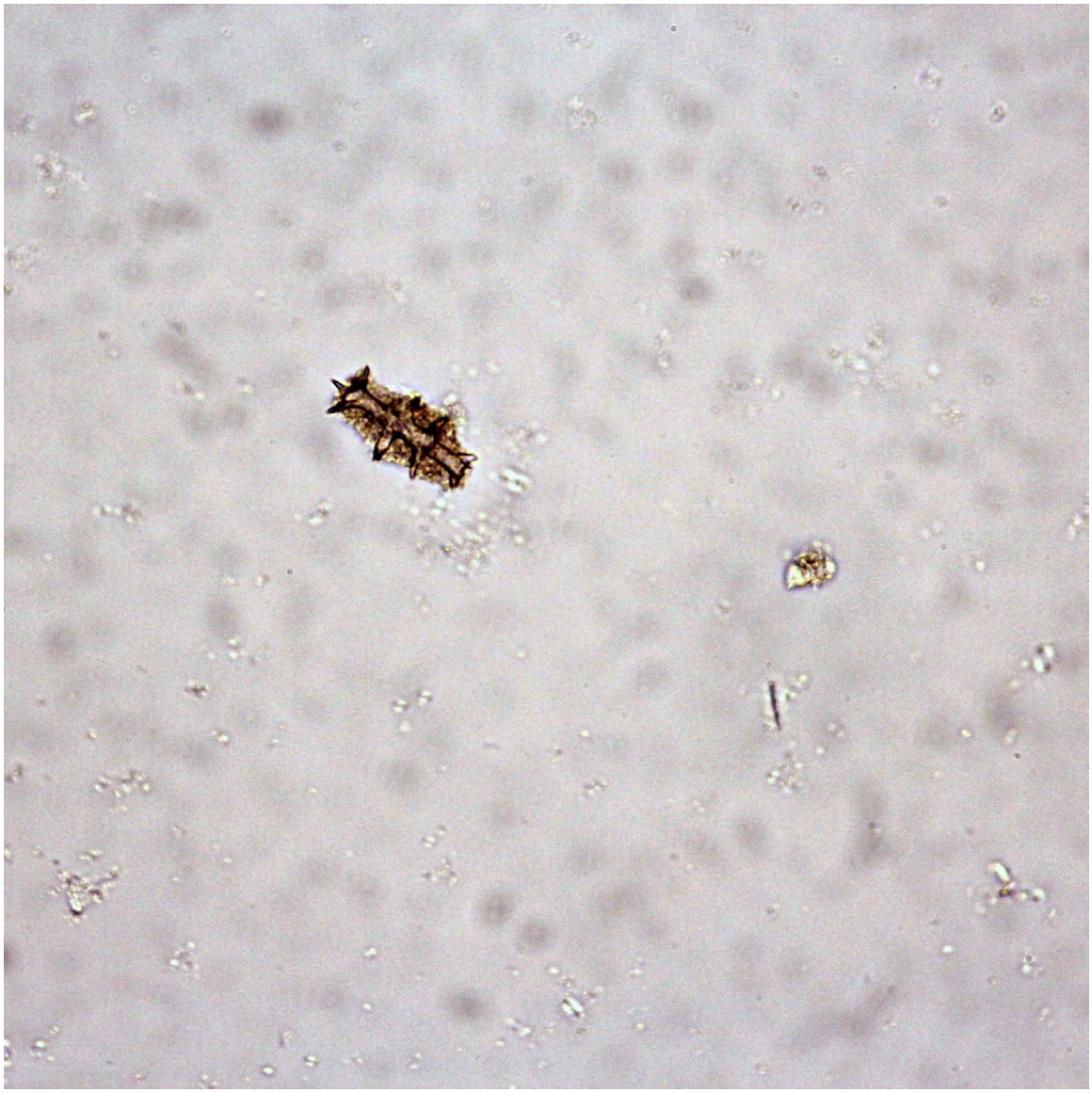

Sponge spicule 19.

A small sponge spicule or microsclere with distinct barbs and adhering brownish sediment dominates this field of view. Focus is on the fine spicule structure, which likely rests higher on the slide, above the surrounding fine sediment, which appears out of focus (blurred). Note that there is no crossed polar view for this image.

ODP Sample (late Pliocene): Leg 162, Hole 982A, Core 5H, Section 3W, 110 cm

Image ID: B0563/B0564

Sponge spicule 20.

A well-dispersed smear slide of calcareous ooze with a variety of bioclasts including a distinct tetraxon (?) sponge spicule with high relief in the center of the field of view above a long man-made (?) brownish fiber. Both of these components are isotropic under crossed polars. The majority of the sediment is gray with nicols crossed, consisting of circular nannofossils with characteristic pinwheel birefringence. A large trochospirally-coiled planktic foraminifer appears dark in plane light because of air bubbles in its chambers, but exhibits characteristic carbonate birefringence with nicols crossed.
ODP Sample (late Pliocene): Leg 162, Hole 982A, Core 5H, Section 3W, 110 cm

Image ID: B0572/B0573

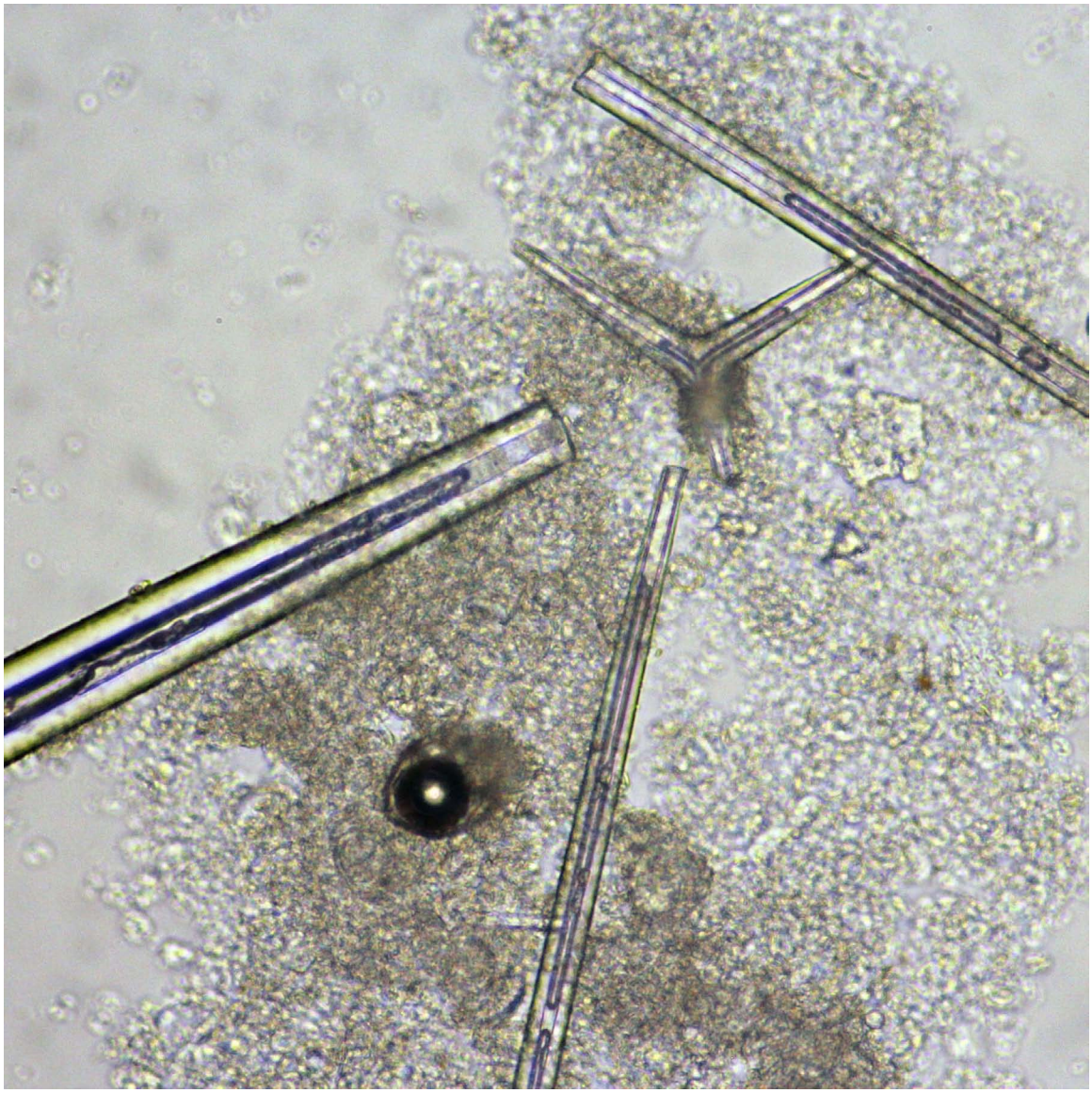

Sponge spicule 21.

Four sponge spicules, one triaxon, flanked by three monoaxon (?) fragments (note all have broken tips) with distinct axial tubes emphasized where they are partly filled with bubbles of air or water. These appear as ghosts with polars crossed, as they are amorphous silica set in a birefringent calcareous, largely nannofossil, ooze. The focus is on the larger spicules, leaving the surrounding, finer-grained sediment out of focus. Ooze color in plane light is a function of nannofossil density, darker tan where more closely packed.

ODP Sample (middle Miocene): Leg 162, Hole 982A, Core 43X, Section 1W, 20 cm

Image ID: B0574/B0575

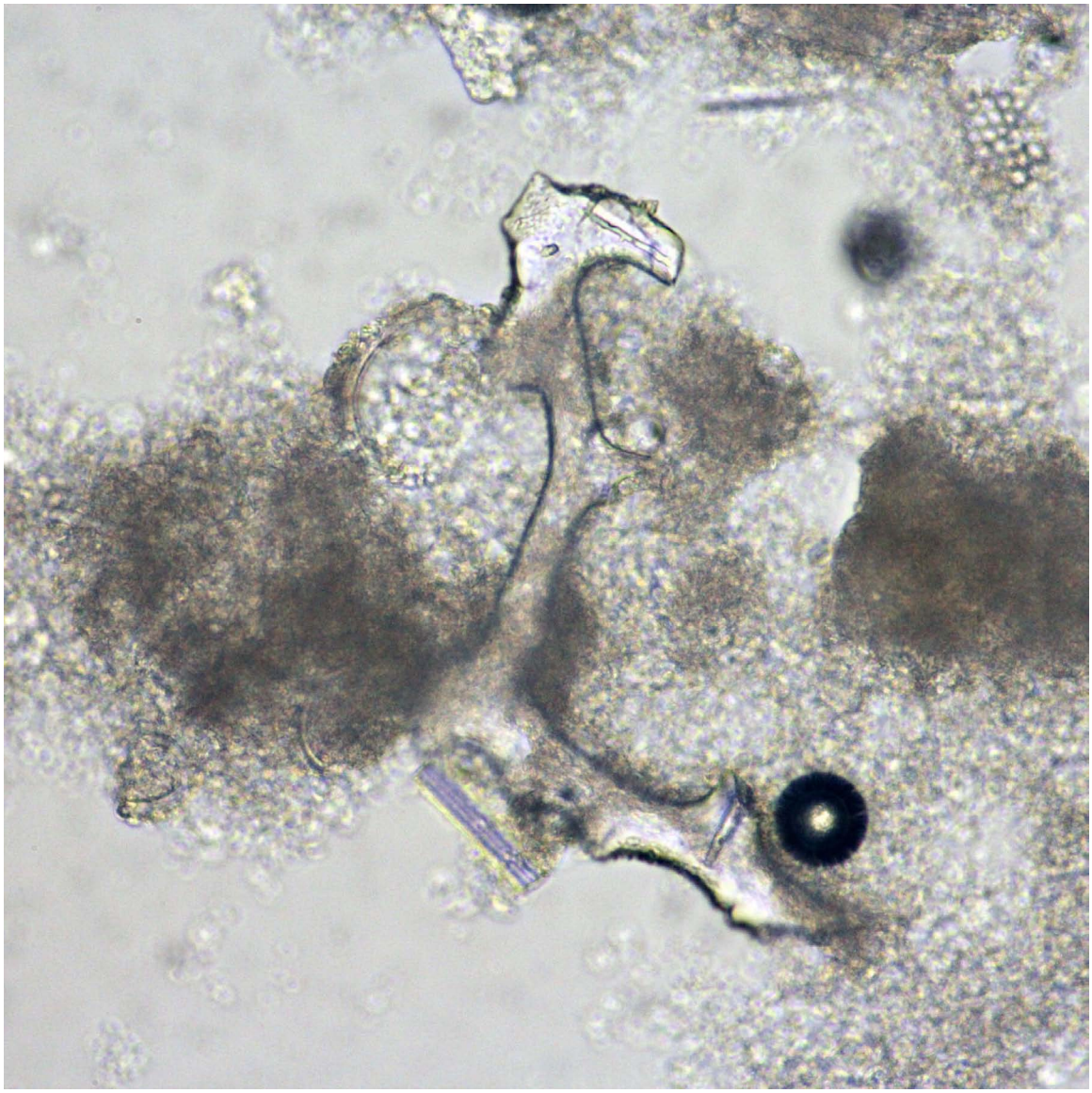

Sponge spicule 22.

This is an irregular fragment of a sponge megasclere, whose amorphous silica composition is evident when polars are crossed and the birefringence of underlying carbonate debris is transmitted through. It is set in a birefringent calcareous, largely nannofossil, ooze that is largely out of focus and contains some other siliceous biogenic debris and curved planktic foraminifer fragments. Ooze color in plane light is a function of nannofossil density, darker tan where more closely packed. Dark circle is a bubble in the epoxy.

ODP Sample (middle Miocene): Leg 162, Hole 982A, Core 43X, Section 1W, 20 cm

Phosphatic Bioclasts and Particles

INTRODUCTION TO PHOSPHATIC BIOCLASTS AND PARTICLES

Amorphous (collophane) to crystalline (calcium fluorapatite) phosphatic debris in marine sediments can include hard parts of fish (scales, bones and teeth) and shelly organisms such as lingulid brachiopods, gastropods (Lowenstam, 1972; Schenau and De Lange, 2000), as well as authigenic phases as encrustation of grains, pellets/coprolites, nodules, and hard grounds (Garrison and Kastner, 1990). Here we show some fragments of likely biogenic and of potentially nonbiogenic origin. Note the color variations from pale yellow to amber, the variability in crystallinity (amorphous, nonbirefringent to crystalline and slightly birefringent), and the potential to mistake with organic matter.

Fish (bone, teeth, scales)

INTRODUCTION TO FISH (BONE, TEETH, SCALES)

Overview – Fragments of phosphatic hard parts of fish or their tiny teeth.

Key References and Examples:

Doyle, P.S, and Riedel, W.R., 1980. Ichthyoliths from Site 436, northwest Pacific, Leg 56, DSDP. In, Initial Reports DSDP, 56:887-893.

Doyle, P.S, and Riedel, W.R., 1985a. Ichthyolith biostratigraphy of western North Pacific pelagic clays, DSDP Leg 86. In, Heath, G.R., Burckle, L.H., et al., Initial Reports DSDP, 86:349-366.

Doyle, P.S, and Riedel, W.R., 1985b. 19: Cenozoic and Late Cretaceous Ichthyoliths. In Bolli, H.M., Saunders, J.B., and Perch Nielsen, K. (Eds.), Plankton Stratigraphy:

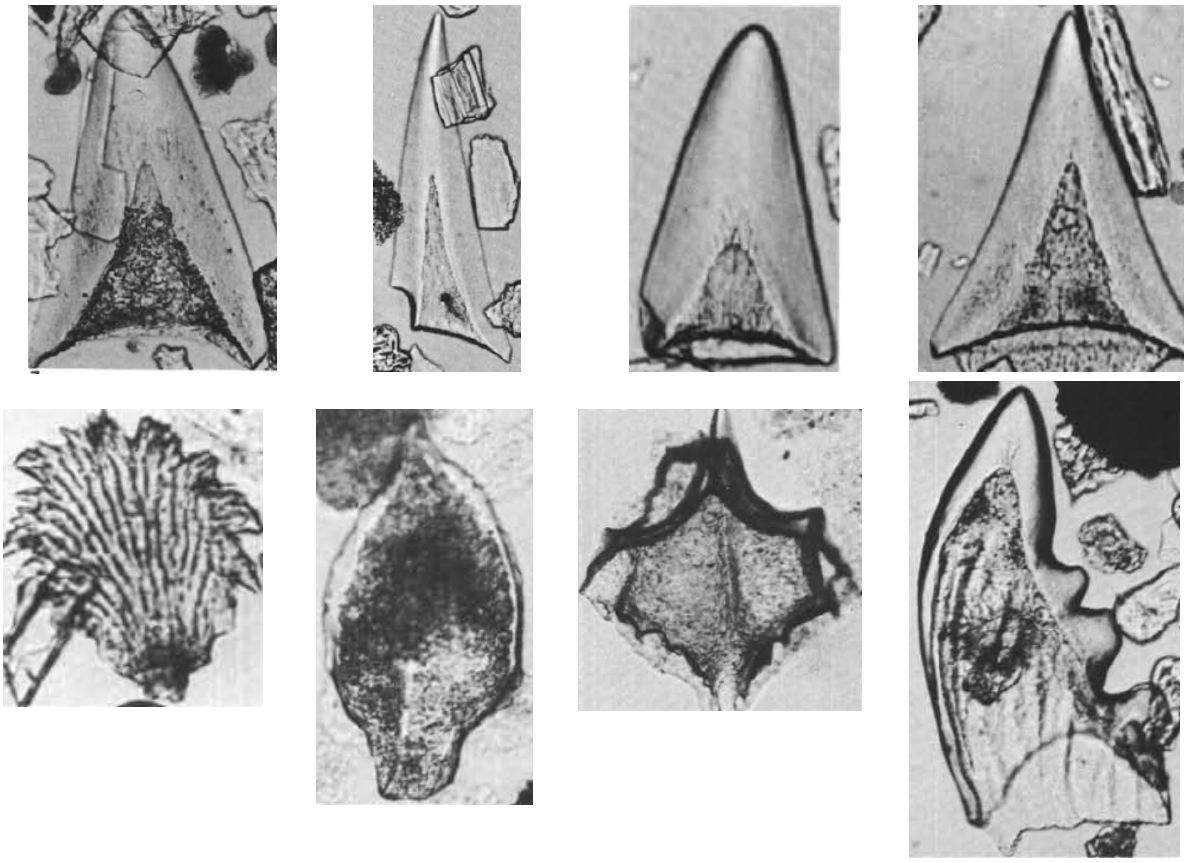

Representative Late Cretaceous and Cenozoic fish teeth and bone.
Photomicrographs from Doyle and Riedel, 1980, 1985.

Phosphatic Bioclasts and Particles

Phosphatic particle 1

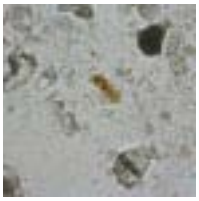

Phosphatic particle 2

Phosphatic particle 3

Phosphatic particle 4

Phosphatic particle 5

Phosphatic particle 6

Image ID: B0656/B0657

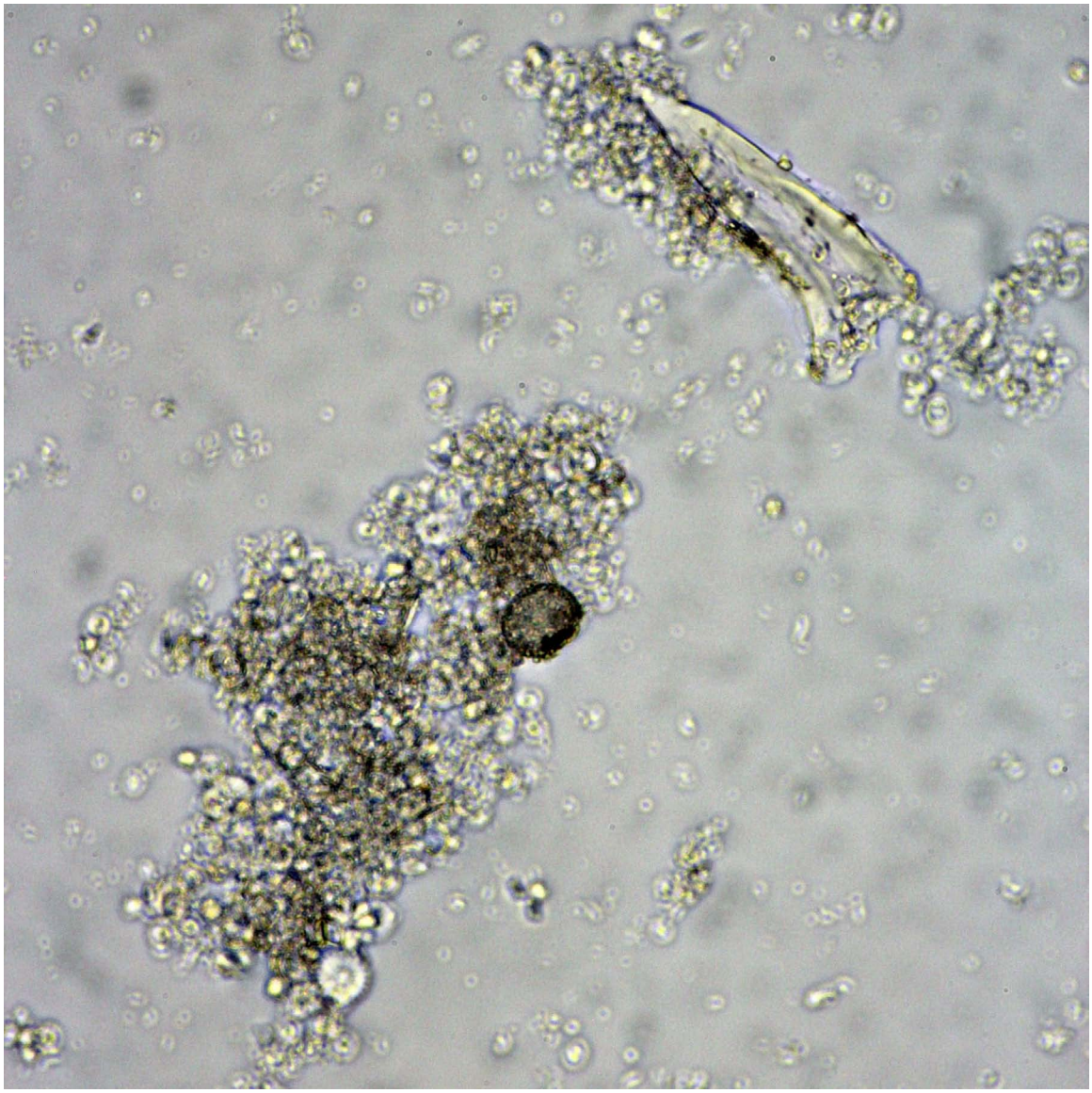

Phosphatic particle 1.

Distinctly pointed and zoned (dentine in center?) fish tooth in upper right is partly coated by calcareous nannofossil ooze. The very low birefringence of tooth is characteristic of bone debris composed of calcium fluorapatite. In the center of the field of view is a dark circular calcisphere in a brownish clump of nannofossil ooze (poorly disaggregated chalk?).

ODP Sample (Paleocene?): Leg 208, Hole 1267A, Core 23H, Section 1W, 60 cm

Image ID: B0594/B0595

Phosphatic particle 2.

The field of view is centered on a fragment of amber-colored collophane (?) that is zoned (growth bands?), translucent and nonbirefringent. The origin of this fragment is indeterminant. It could also be organic matter of some sort. The surrounding sediment is a mix of micrite, nannofossils, bioclasts, and terrigenous detritus.

IODP Sample (late Eocene): Leg 342, Hole 209, Core 18, Section 1, 120 cm

Image ID: B0318/B0319

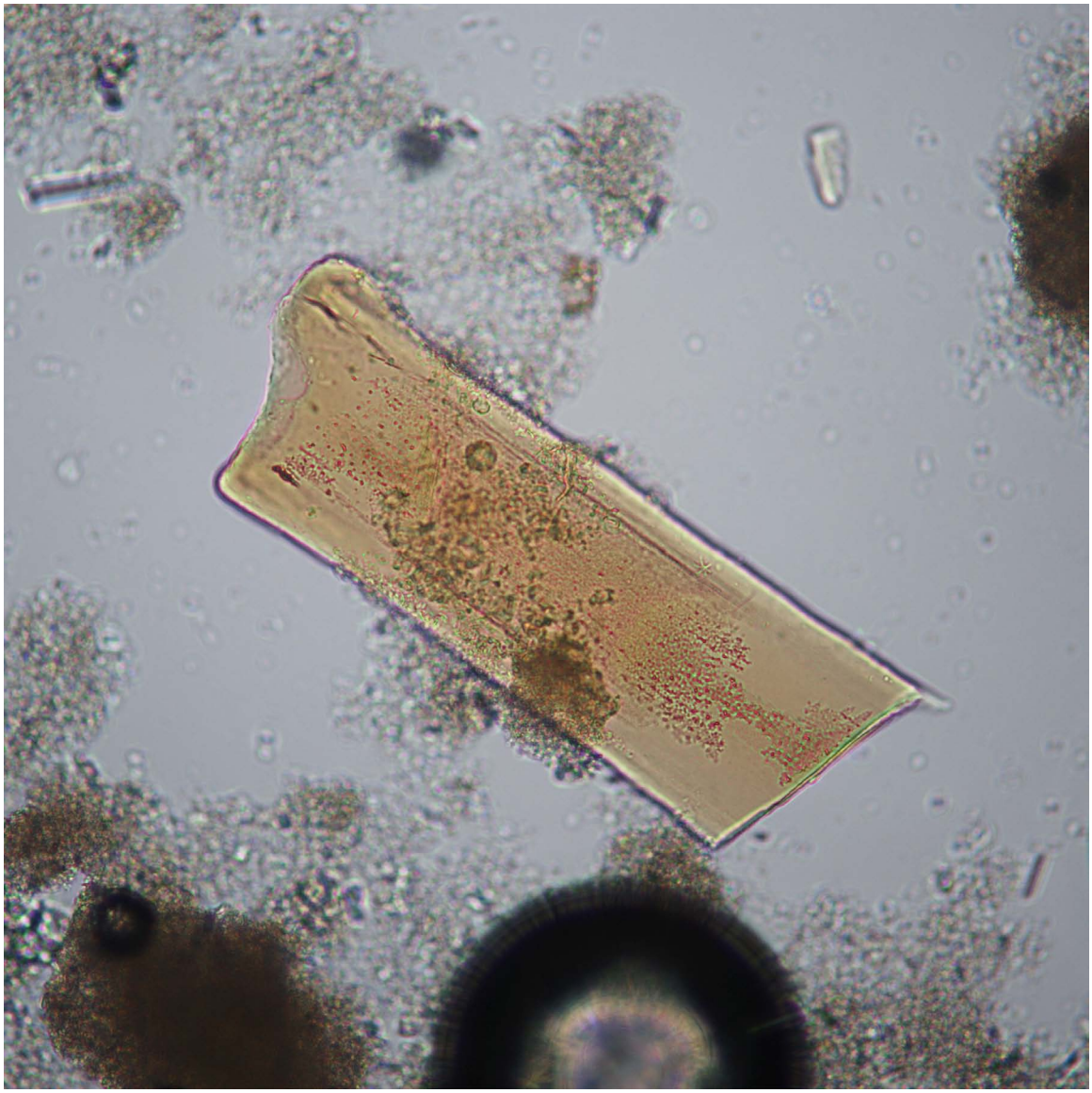

Phosphatic particle 3.

This amber-colored, semi-rectangular fragment exhibits the characteristic color and birefringence of fish bone debris.

ODP Sample (middle Miocene): Leg 138, Hole 845A, Core 17H, Section 2W, 20 cm

Image ID: B0231/B0232

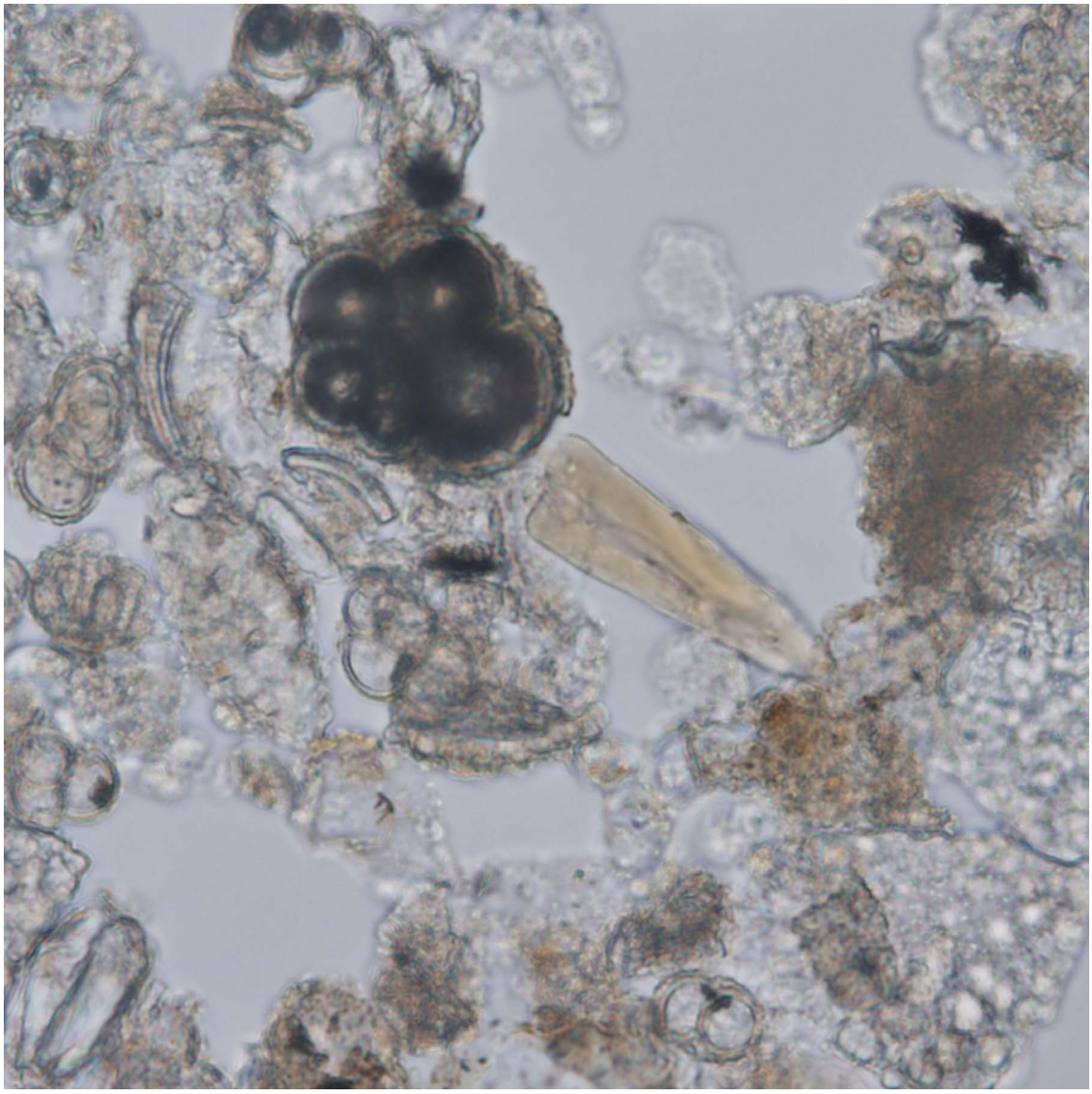

Phosphatic particle 4.

The light amber tapered and zoned fragment in the center of the field of view may be a piece of fish debris (bone or tooth?). Note that it is amorphous (nonbirefringent) and set in a bioclastic sediment including foraminifera, both whole and fragmental.

ODP Sample (late Pliocene-Pleistocene): Leg 157, Hole 950A, Core 9H, Section 6W, 93 cm

Image ID: B0313

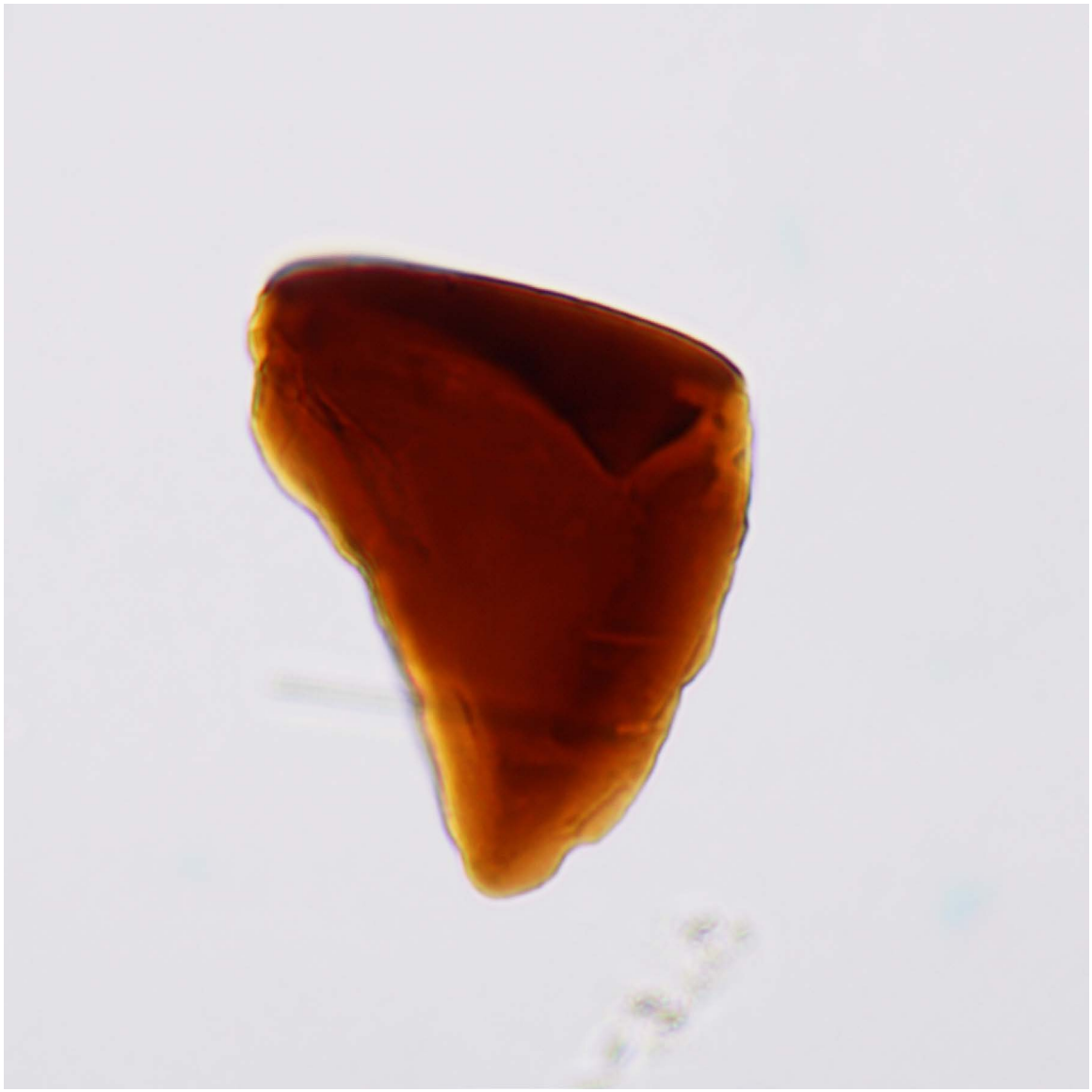

Phosphatic particle 5.

This dark amber fragment has the shape and zonation of a fish tooth or scale. The grain is not birefringent, so no image with polars crossed is provided.

ODP Sample (late Miocene): Leg 138, Hole 845A, Core 15H, Section 2W, 10 cm

Image ID: B0625/B0626

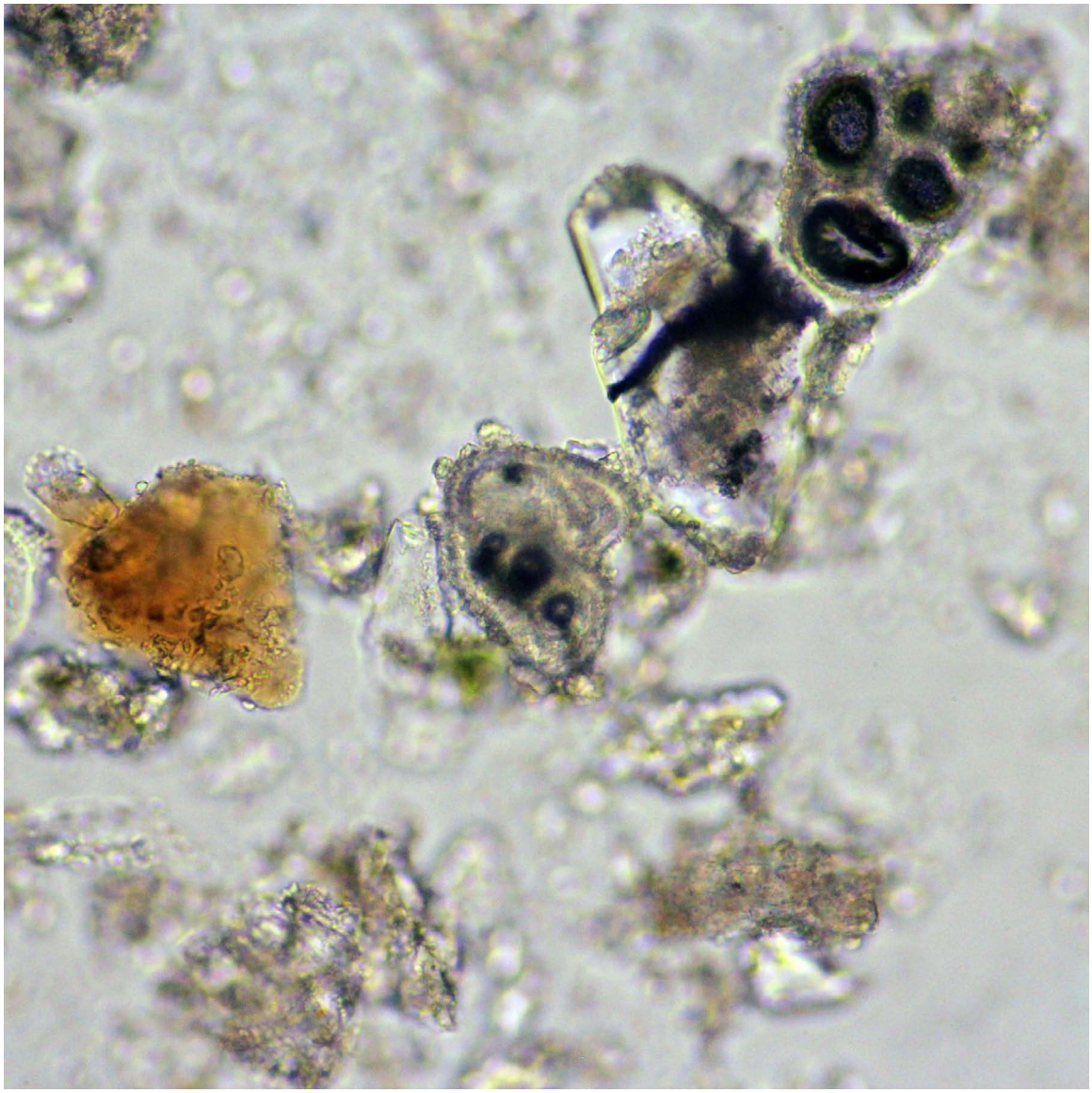

Phosphatic particle 6.

The amber fragment on the left may be phosphatic or organic debris. Other grains include a small piece of glauconite, several whole foraminifera and feldspar. The nonsymmetrical foraminifer in the center of the field of view is an edge view of a juvenile *Turborotalia cerroazulensis*.

IODP Sample (late Eocene): Leg 342, Hole 209, Core 18, Section 1, 120 cm

Organic Matter

INTRODUCTION TO ORGANIC MATTER

Identification of organic matter (OM) in smear slides is challenging. The more standard method for organic petrography is accomplished on polished specimens (whole rock or organic concentrates) observed in reflected light microscopy. The following list provides guidance on identification of OM in smear slides. If significant OM is suspected based on smear slide observations it is wise to check this determination by comparison to shipboard sediment analysis of total organic carbon (TOC).

- Color: organic matter in smear slides displays diverse colors, ranging across pale yellow, darker yellow, amber, red, red-brown, brown, and black (opaque).
- Birefringence: Generally, isotropic, but may display first order birefringence and some undulosity in larger particles.
- Index of refraction: Phosphate grains display a similar range of colors and birefringence and these can be discriminated from OM based on the higher index of refraction in phosphate minerals
- Shape or morphology: phosphatic particles (see section on fish debris) have a distinct range of forms that relate to their origin as fish bones, teeth, and scales; likewise organic particles arising as algal cells or spores, wood, dinoflagellates, etc. have distinct forms.

Key organic matter types as seen in smear slides:

1. Amorphous dispersed OM. Distributed as extremely fine material this OM type has no discernible particles and is recognized mainly based on a distinctly brownish color in the clay-size fraction and, possibly, association with an abundance of larger OM particles. It is essential to check the presence of such OM against bulk analyses of TOC. This type of OM is in many cases accompanied by a large quantity of planktic siliceous debris.

2. Fine particulate red-brown OM. Perhaps the most common OM type observed in smear slides, this material is typically of coarse clay to fine silt-size (2 – 20 μ). Although this OM takes the form of discrete particles there is essentially no internal structure discernible beyond a sort of granularity at the micron scale. This type of OM is typically accompanied by a large quantity of planktic siliceous debris.

3. Structured particles of marine OM. A wide range of structured OM types relate to algal cells and spores. These are distinct from the OM types 1 and 2 above in having discernible walls and other morphological features.

4. Structured particles of terrestrial OM. Generally grouped as “woody fragments”, this material may be quite abundant in the silty and even sandy portions of turbidites. It’s important to recall that even log-size pieces of wood can be transported far into the ocean basins.

5. Several specific microfossils have purely organic compositions and have very distinct structures that can be used to identify the taxonomic affinity of the fossil: Dino-flagellates, tintinids, and foraminifer linings are some of these distinct forms.

Organic matter examples are arranged roughly in order, proceeding from type 1 to type 5, from structureless to highly structured.

Pollen and Spores

INTRODUCTION TO POLLEN AND SPORES

Overview – Dark-colored, compressed ovate to triangular to spherical shaped particles composed of sporopollenin, a tough, chemically resistant material composed of biopolymers. Terrestrial pollen and spores can be transported great distances into the marine realm by wind and turbidity currents. Long geologic record.

Key References and Examples:

Bratzeva, G.M., 1983. Spores and pollen from Cenozoic sediments of the Falkland Plateau, Site 511, DSDP Leg 71. In, Ludwig, W.J, Krasheninnikov, V.A., et al., Initial Reports, DSDP, 71:907-932.

Heusser, L., 1978. 14: Spores and Pollen in the Marine Realm. In Haq, B.U., and Boersma, A. (Eds.), Introduction to Marine Micropaleontology: Elsevier, 327-339.

Web Resources:

http://www.ucl.ac.uk/GeolSci/micropal/spore.html

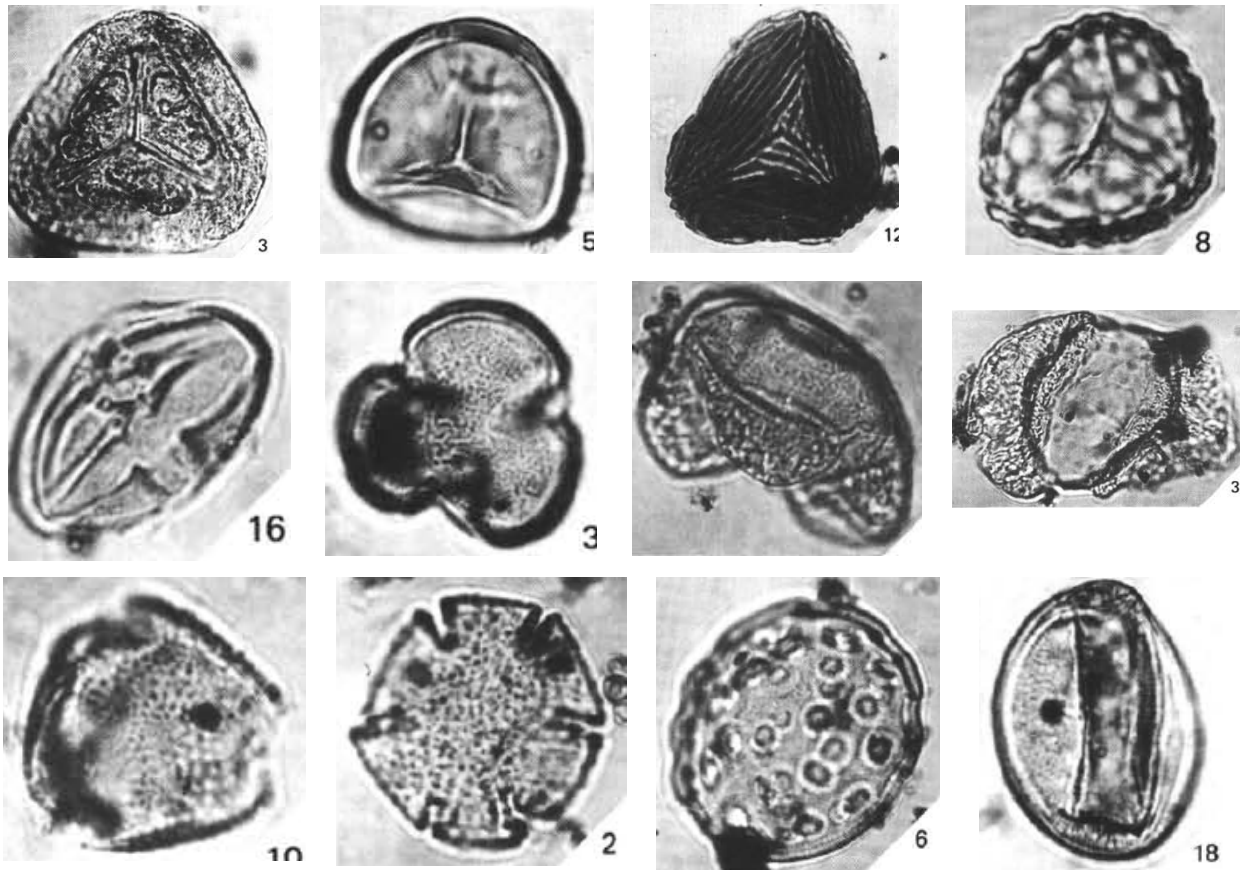

Representative Cenozoic pollen. Top row: *Cyatheacidites sp., Cingutriletes australis, Cicatricosisporites australiensis, Lycopodiumsporites* sp.. Second row: *Rhoipites striatoreticulatus, Tricolpites cf. T. brevicolpus, Microcachrydites antarcticus, Podocarpidites marwickii*. Bottom row: *Proteacidites cf. P. retiformis, Nothofagidites asperus, Parsonsidites cf. P. conspicuous, Polygonum* sp. Photomicrographs from Bratzeva, 1983.

Dinoflagellates (Organic-Walled Dinocysts)

INTRODUCTION TO DINOFLAGELLATES

Overview – Unicellular, bi-flagellated protists that produce a resistant biopolymer dinosporin cyst (sporopollenin-like), or a calcareous cyst in the case of the calcareous dinoflagellates ('calcispheres'; e.g., Pithonella, Thoracospaera, Operculodinella, and Cervisiella); it is the cysts which are typically preserved to the rock record. Resting cysts are produced during times of unfavorable environmental conditions or for reproduction. Only a fraction of the living species produce a cyst that is capable of preservation to the sediment record.

Diagnostic Features – Dark-colored to transluscent organic wall that resembles the motile phase (theca) or consists of a structure with spine-like projections (processes); these are referred to proximate and chordate cysts, respectively. 15-100 µm in diameter; up to 2 mm. Excystment opening may be visible (archeopyle).

Biology – Kingdom Protoctista, Subkingdom Alveolata, Phylum Dinomastigota. Dinoflagellates include both autotrophic and heterotrophic (or mixotrophic) forms. The life cycle of some/many dinoflagellates includes the formation of an organic or calcareous cyst. These cysts are functionally for resting (dormant stage) following the sexual part of their life cycle, or for vegetative (asexual) reproduction; cysts have great potential to become preserved as fossils.

Ecology – Most are marine; neritic to oceanic. Many modern species are cosmopolitan and broadly tolerant of temperature and salinity variations. Together with the diatoms and coccolithophorids, the dinoflagellates are among the most important eukaryotic primary producers.

Paleobiogeography – Widely distributed. Especially abundant in neritic environments, and mixing zones associated with oceanic fronts.

Stratigraphic Range – Silurian? Late Triassic – present

Key References and Examples:

Below, R., 1984. Aptian to Cenomanian dinoflagellate cysts from the Mazagan Plateau, northwest Africa (Sites 545 and 547, DSDP Leg 79). In, Hinz, K., Winterer, E.L., et al., Initial Reports DSDP, 79:621-649.

Brown, S., and Downie, C., 1984. Dinoflagellate cyst biostratigraphy of late Paleocene and early Eocene sediments from Holes 552, 553A, and 555, Leg 81, DSDP (Rockall Plateau). In, Roberts, D.G., Schnitker, D., et al., Initial Reports DSDP, 81:565-579.

Bujak, J.P., and Williams, G.L., 1979. Dinoflagellate diversity through time. Marine Micropaleontology, 4:1-12.

Edwards, L.E., 1984. Miocene dinocysts from DSDP Leg 81, Rockall Plateau, eastern North Atlantic. In, Roberts, D.G., Schnitker, D., et al., Initial Reports DSDP, 81:581-594.

Edwards, L.E., 1993. 7: Dinoflagellates. In Lipps, J.H. (Ed.), Fossil Prokaryotes and

Protists: Blackwell Scientific Publications, 105-129.
Katz, M.E., Finkel, Z.V., Grzebyk, D., Knoll, A.H., and Falkowski, P.G., 2004. Evolutionary trajectories and biogeochemical impacts of marine eukaryotic phytoplankton. Annual Reviews of Ecology and Evolutionary Systems, 35:523-556.
Pross, J., and Brinkhuis, H., 2005. Organic-walled dinoflagellate cysts as paleoenvironmental indicators in the Paleogene; a synopsis of concepts. Paläontologische Zeitschrift, 79(1):53-59.
Williams, G.L., 1978. 13: Dinoflagellates, Acritarchs and Tasmanitids. In Haq, B.U., and Boersma, A. (Eds.), Introduction to Marine Micropaleontology: Elsevier, 293-326.
Williams, G.L., and Bujak, J.P, 1985. Mesozoic and Cenozoic dinoflagellates. In Bolli, H.M., Saunders, J.B., and Perch Nielsen, K. (Eds.), Plankton Stratigraphy: Cambridge (Cambridge Univ. Press), 847-964.

Web Resources:
http://www.ucl.ac.uk/GeolSci/micropal/dinoflagellate.html

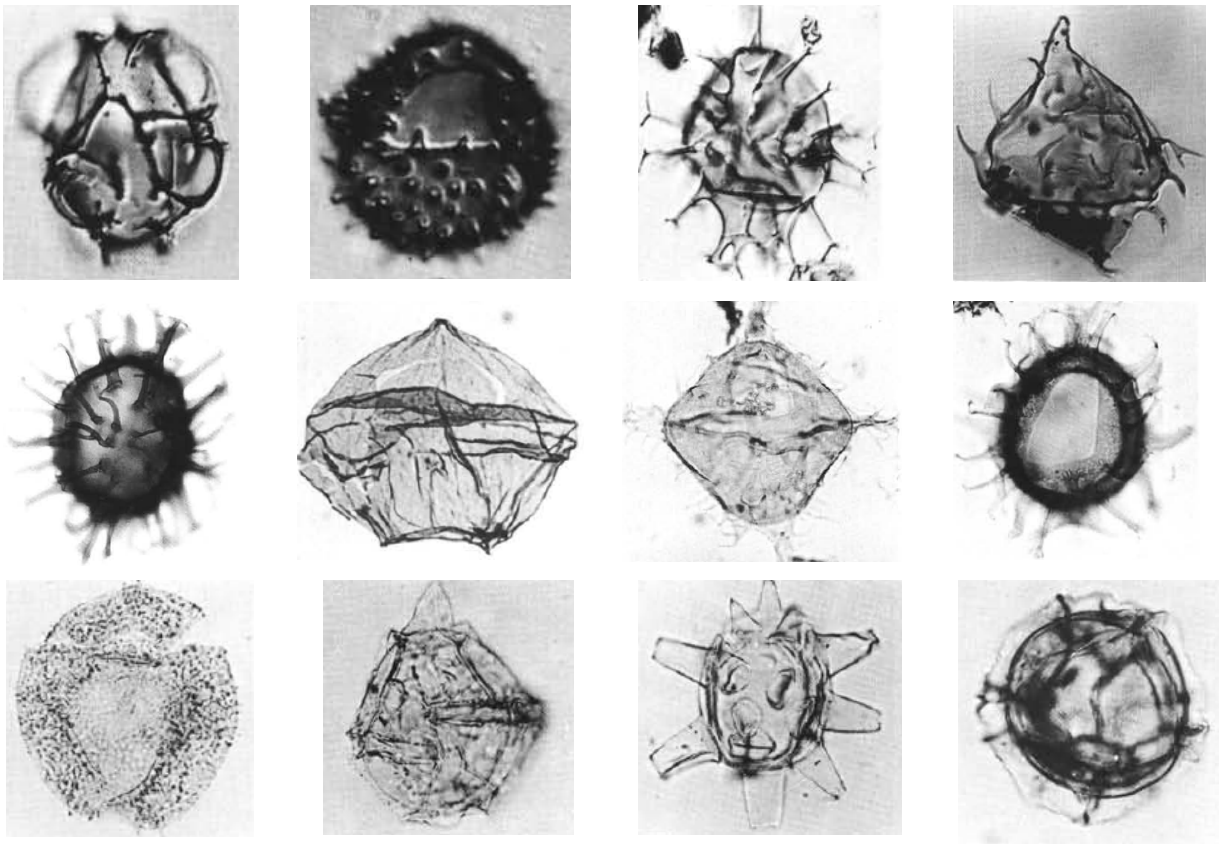

Representative Cretaceous and Cenozoic dinoflagellates. Top row: *Cannosphaeropsis?, Operculodinium sp., Spiniferites mirabilis; Fibrocysta? fusiforma*. Second row: *Lejeunecysia spatiosa, Wetzeliella similis, Fibrocysta* sp.. Bottom row: *Cyclonephelium paucimarginatum, Gonyaulacysta helicoidea, Litosphaeridium siphoniphorum, Pterodinium cingulatum*. Photomicrographs from Edwards, 1984; Brown and Downie, 1984; Below, 1984.

Tintinnids

INTRODUCTION TO TINTINNIDS

Overview – Choreotrich ciliates with simple vase-shaped lorica; geologically preserved species are composed of tiny mineral grains in a protein matrix (i.e., agglutinated wall). These microzooplankton graze on phytoplankton. Distributions include: cosmopolitan, estuarine, neritic, tropical-subtropical, boreal, and austral. Paleozoic-Mesozoic Calpionellids have similar shells of calcite; it is unclear whether they are tintinnids or ciliates of any type. Thecamoebians have a somewhat similar agglutinated vase-shaped test, but are restricted to freshwater environments.

Key References and Examples:

Dolan, J.R., and Gallegos, C.L., 2001. Estuarine diversity of tintinnids (planktonic ciliates). Journal of Plankton Research, 23(9): 1009-1027.

Eicher, D.L., 1965. Cretaceous tintinnids from the western interior of the United States. Micropaleontology, 11: 449-456.

Lipps, J.H., Stoeck, T., and Dunthorn, M., 2013. Fossil tintinnids. In Dolan, J., Montagnes, D., Agatha, S., Coats, W., and Stoecker, D. (Eds.). Biology and Ecology of Tintinnid Ciliates: Models for Marine Plankton. West Sussex: Wiley-Blackwell, 186-197.

Pierce, R.W., and Turner, J.T., 1993. Global biogeography of marine tintinids. Marine Ecology Progress Series, 94: 11-26.

Tappan, H., 1993. 14: Tintinnids. In Lipps, J.H. (Ed.), Fossil Prokaryotes and Protists: Blackwell Scientific Publications, 285-303.

Organic Matter


Organic matter 1


Organic matter 2

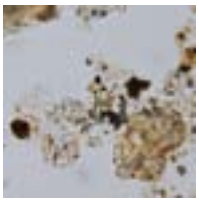
Organic matter 3

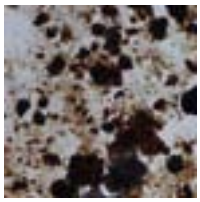
Organic matter 4

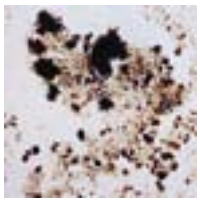
Organic matter 5


Organic matter 6


Organic matter 7

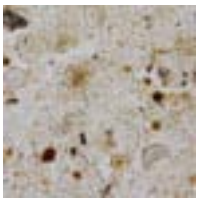
Organic matter 8

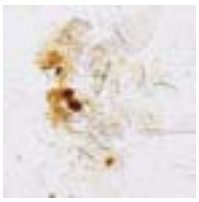
Organic matter 9

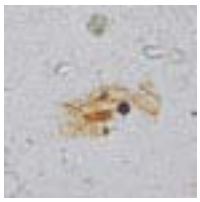
Organic matter 10


Organic matter 11


Organic matter 12


Organic matter 13

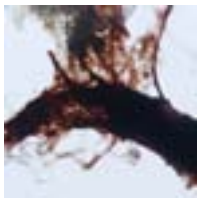
Organic matter 14

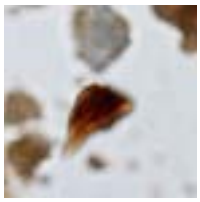
Organic matter 15

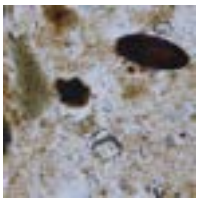
Organic matter 16


Organic matter 17


Organic matter 18


Organic matter 19


Organic matter 20


Organic matter 21

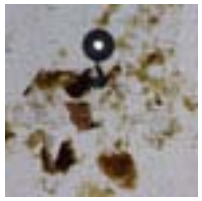
Organic matter 22

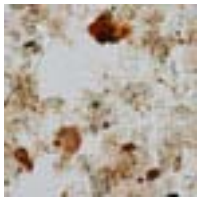
Organic matter 23


Organic matter 24

Image ID: B0111/B0112

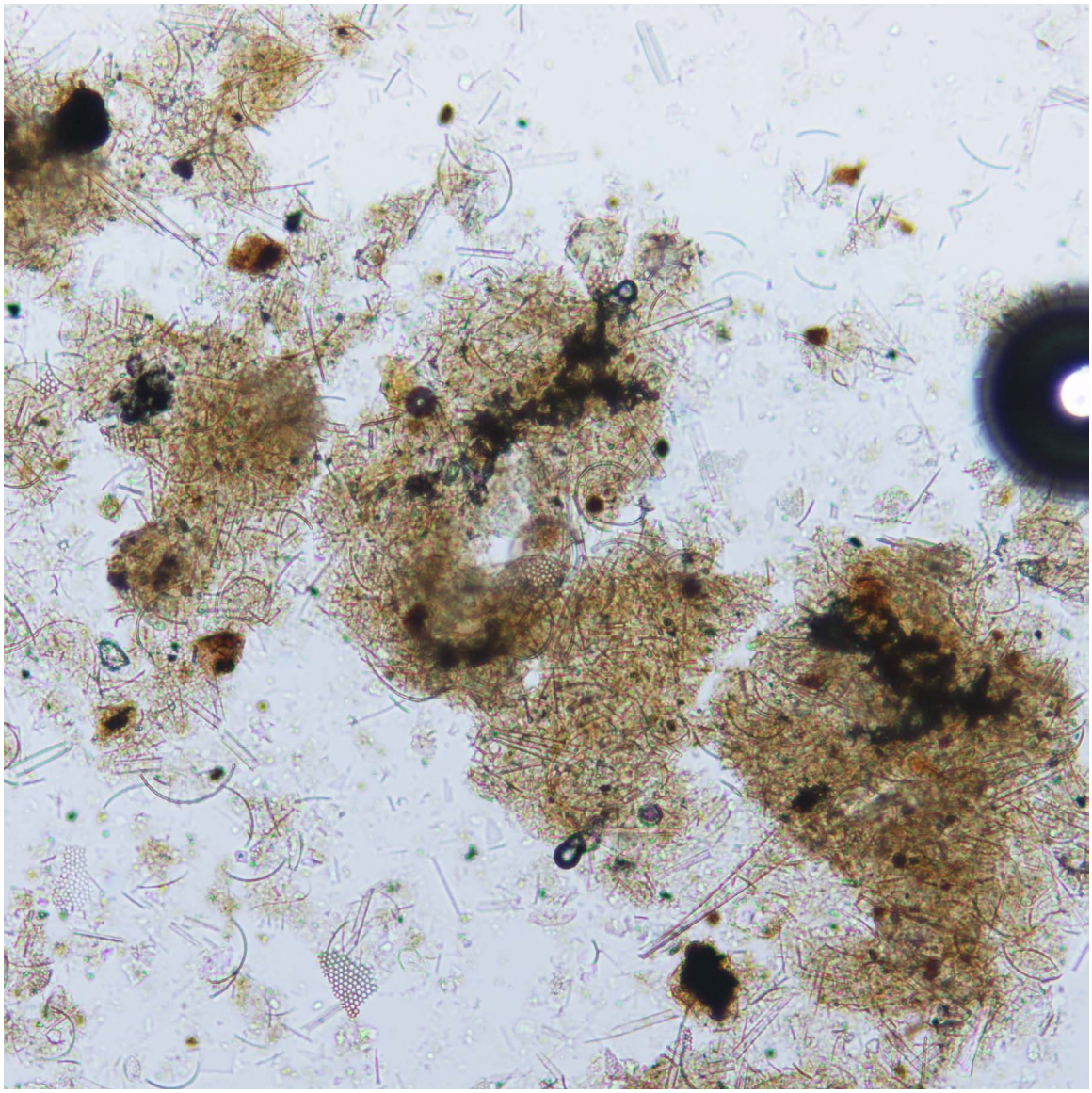

Organic matter 1.

The organic content of this sample is suggested mainly by the brownish color of the clay-size fraction and a few red-brown particles of lower silt-size. A sample such as this should spark a quick inspection of shipboard bulk analyses of total organic carbon (TOC).

ODP Sample (Quaternary): Leg 112, Hole 688A, Core 2H, Section 5W, 74 cm

Image ID: B0150/B0151

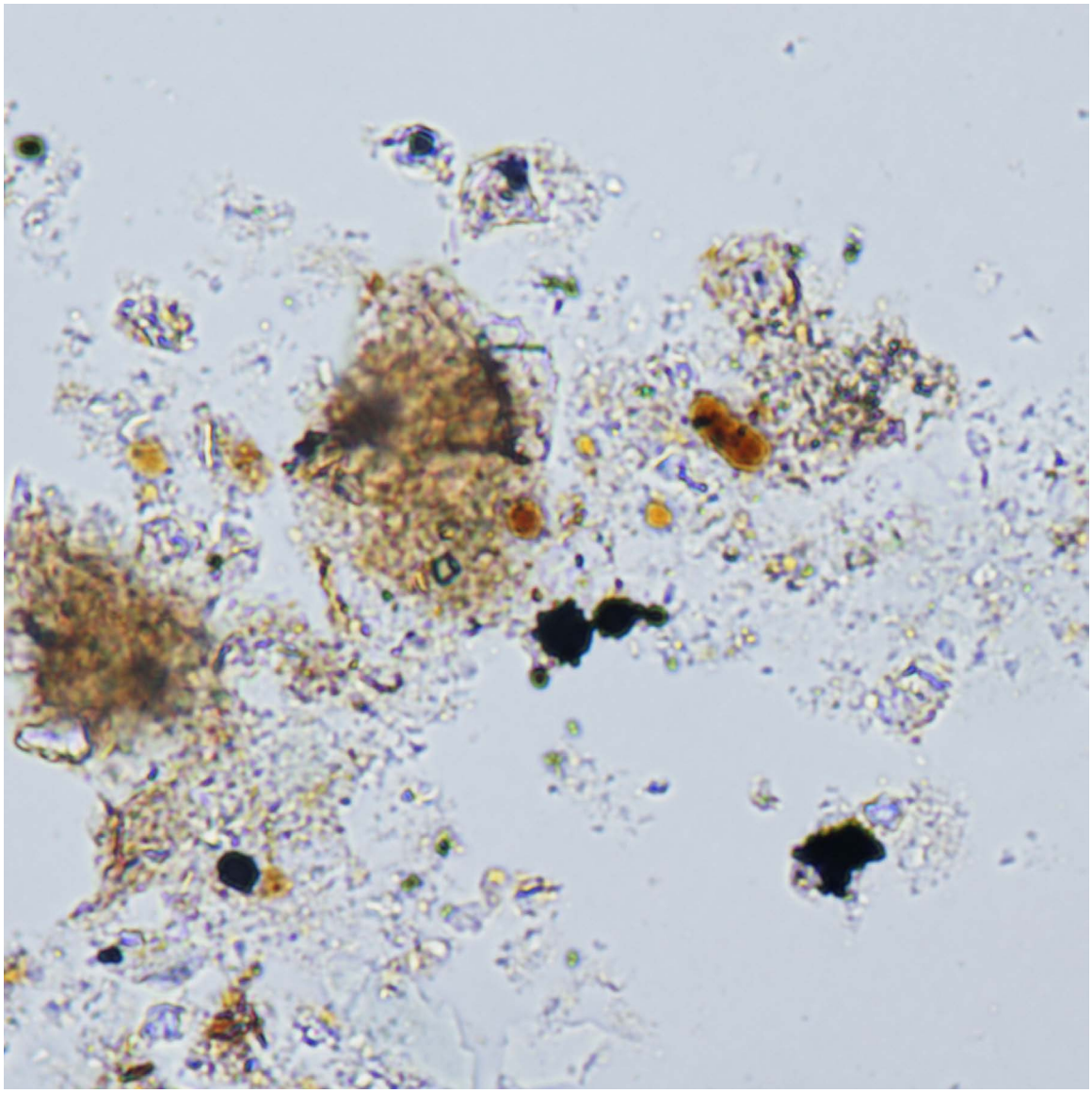

Organic matter 2.

Particulate and dispersed organic matter is commonly associated with pyrite framboids as shown in this mud sample.

ODP Sample (middle Eocene): Leg 112, Hole 688E, Core 35R, Section 1W, 80 cm

Image ID: B0072/B0073

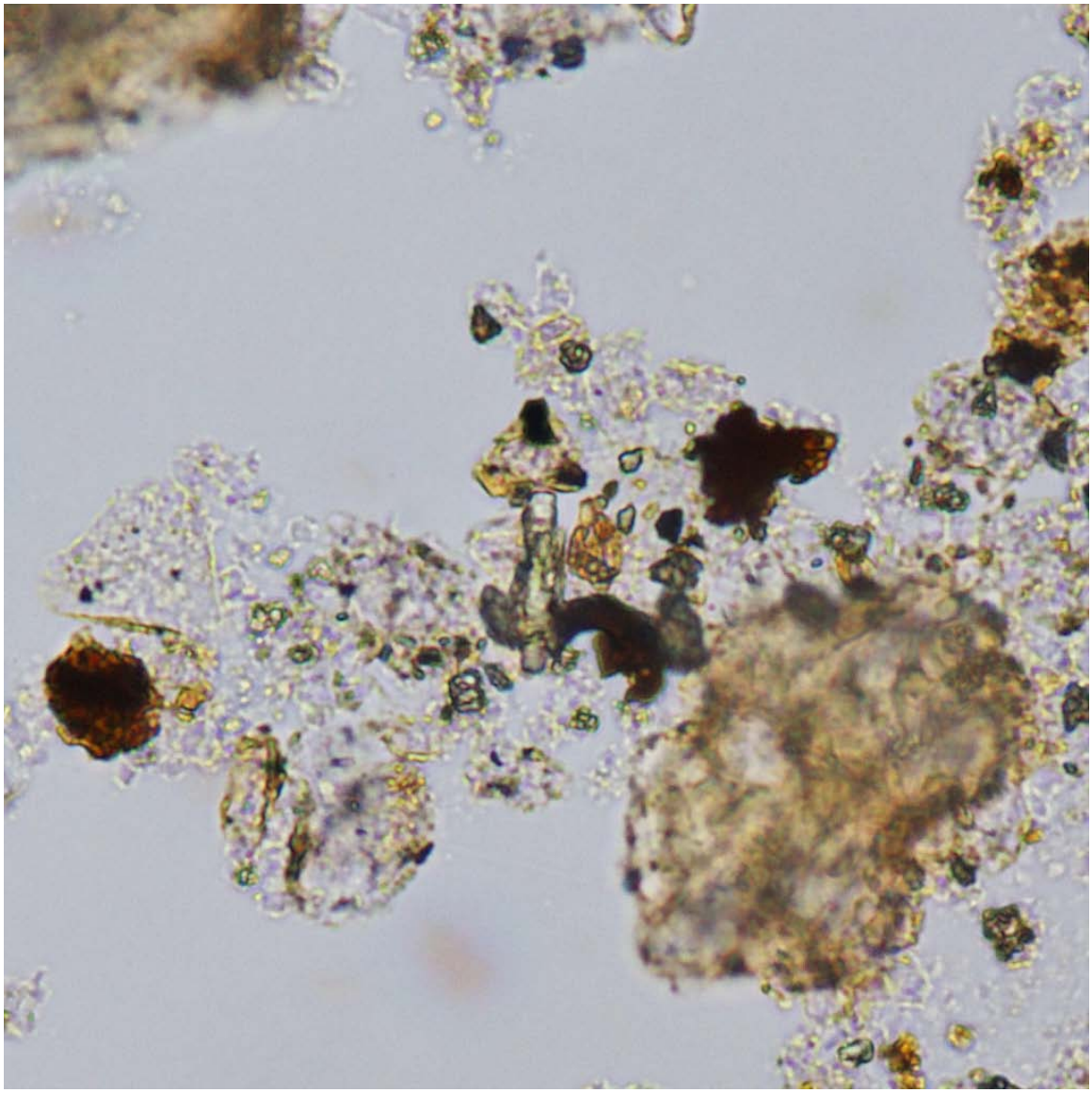

Organic matter 3.

The most common particulate organic matter form seen in smear slides is red-brown in color, equant but irregular in shape, and largely structureless. Marine algal remains are a likely source.

DSDP Sample (?): Leg 64, Hole 477A, Core 7, Section 1, 160 cm

Image ID: 0572/0573

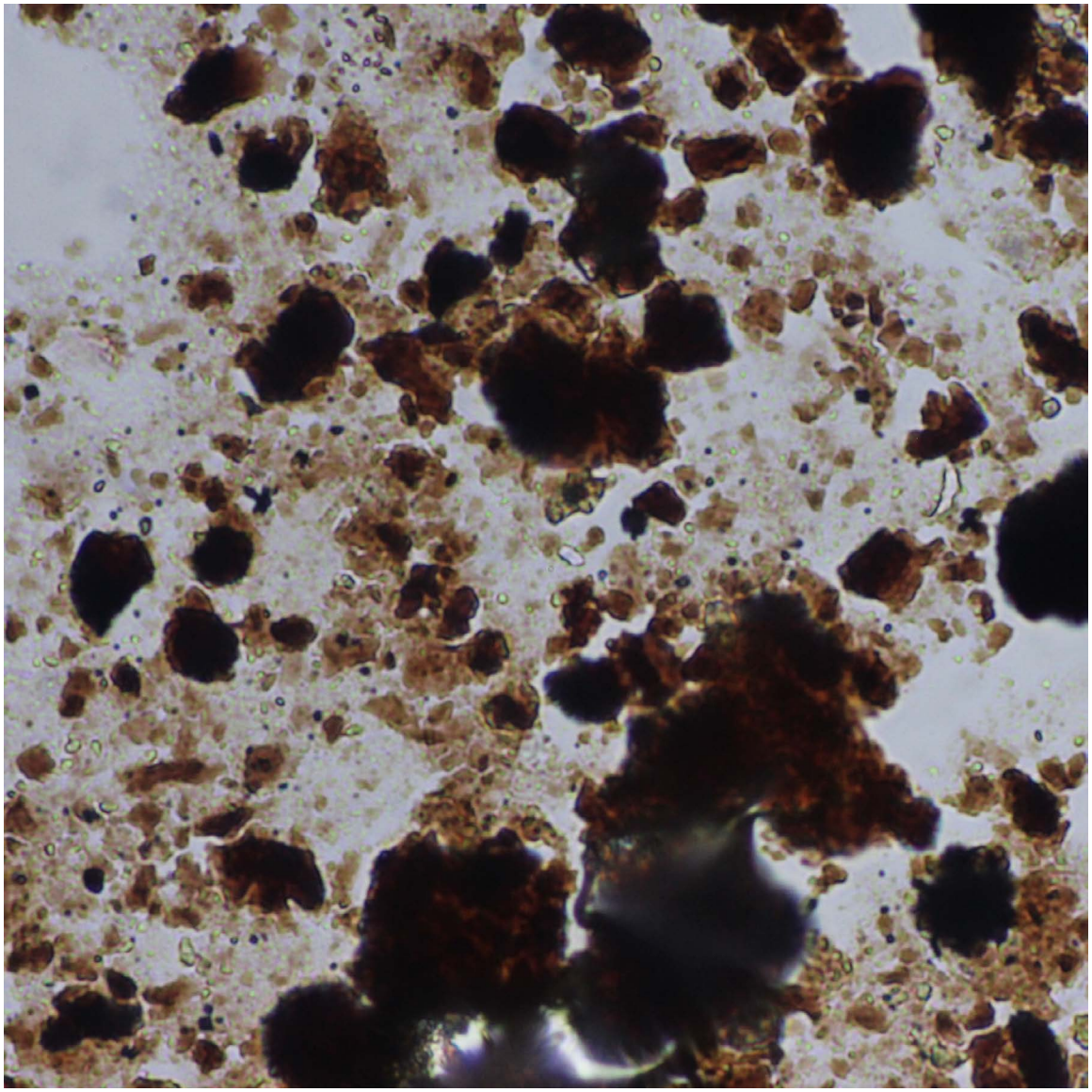

Organic matter 4.

Organic matter in this specimen is strikingly abundance (20% by shipboard analysis). Interpreted as a peat, this material does not however display any particles with the distinctive structures associated with woody organic matter. Organic matter particles here range from clay size to upper silt size and are generally equant but still irregular and structureless.

ODP Sample (Campanian): Leg 144, Hole 877A, Core 20R, Section 1W, 81 cm

Image ID: 0568/0569

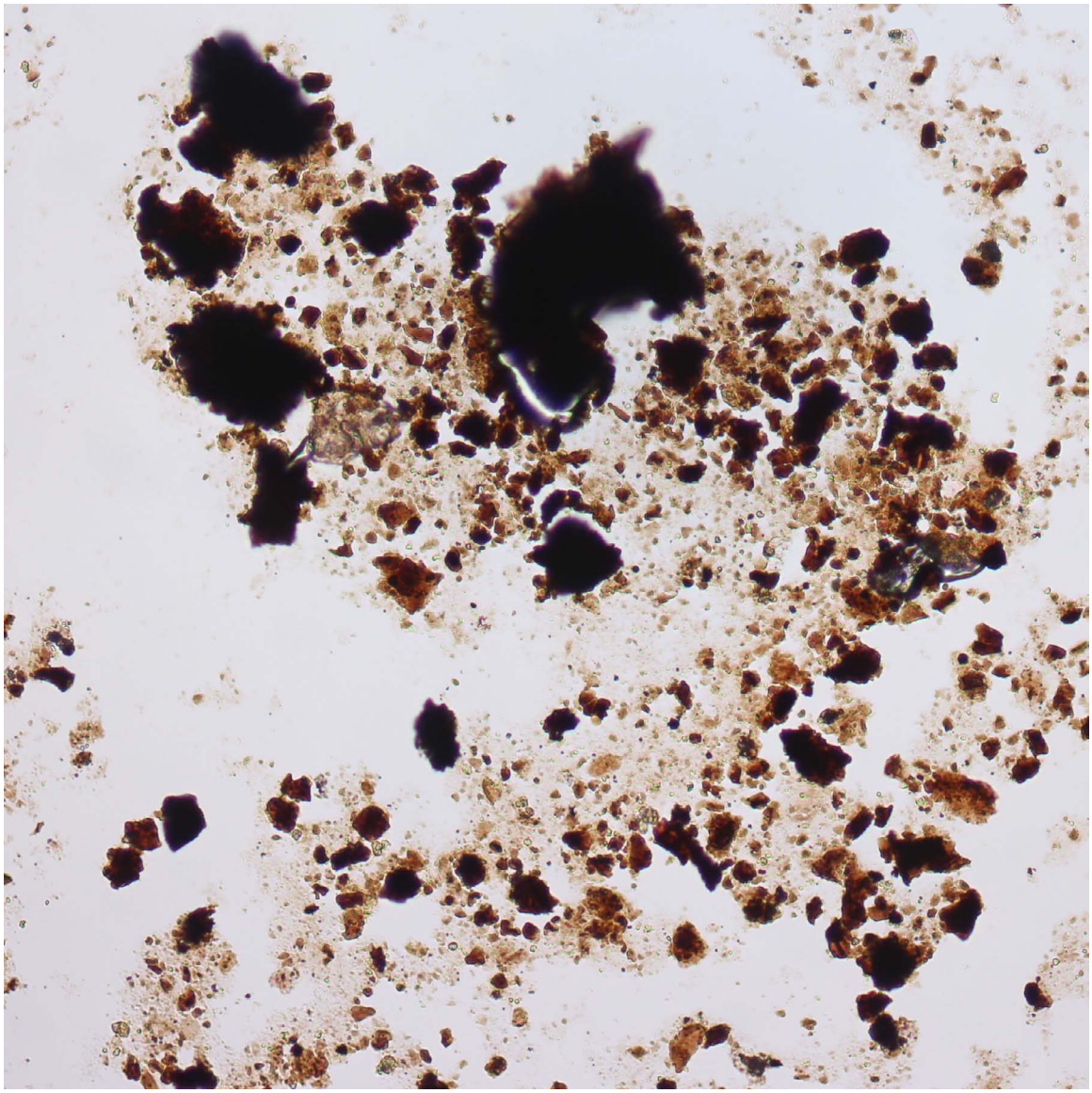

Organic matter 5.

A lower magnification view of the organic matter seen in Organic Matter 4 image. Again, organic matter particles here range from clay size to upper silt size and are generally equant but still irregular and structureless. Examine the cross-polar view to appreciate the mineral components.

ODP Sample (Campanian): Leg 144, Hole 877A, Core 20R, Section 1W, 81 cm

Image ID: B0276/B0277

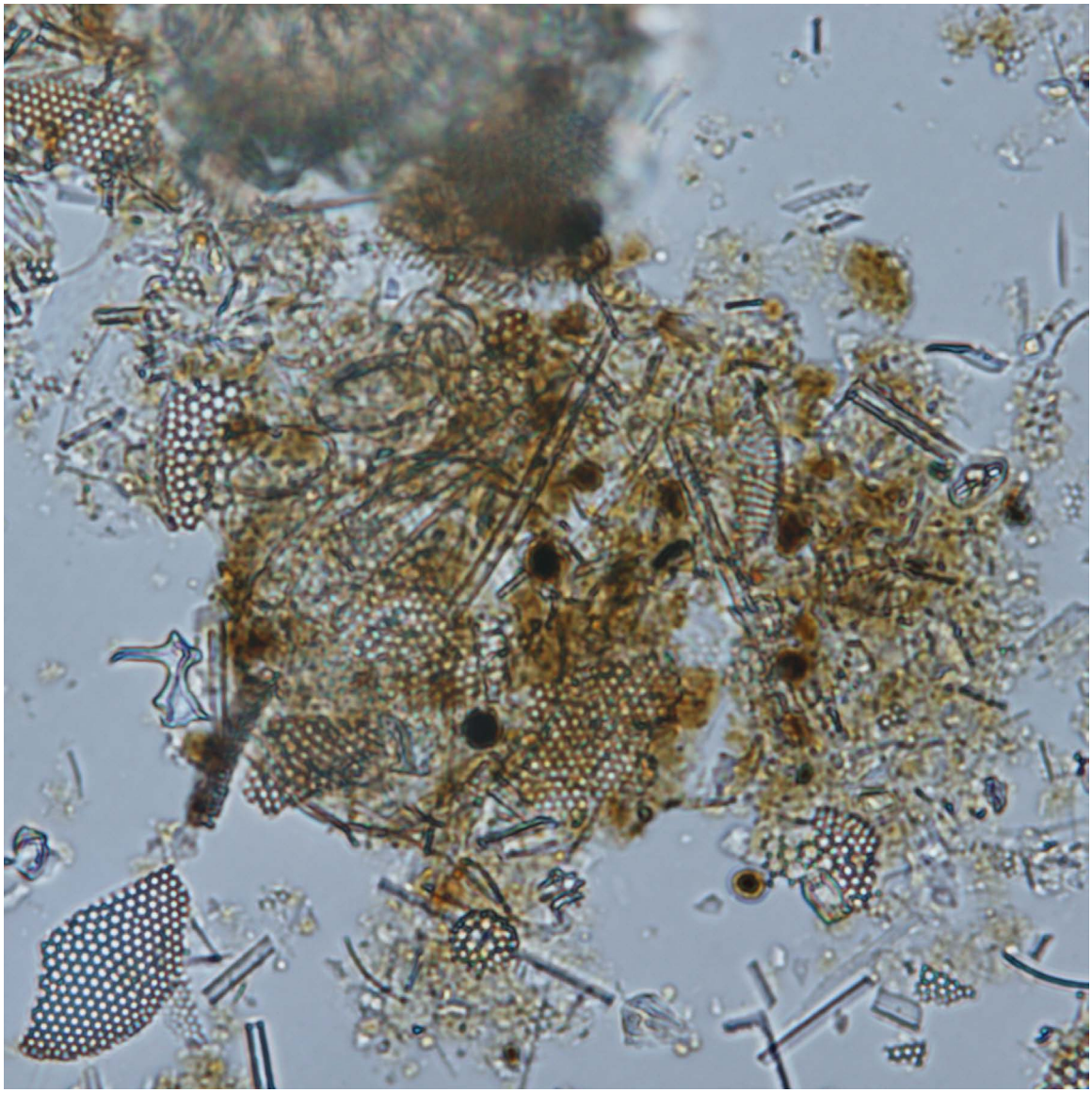

Organic matter 6.

The dominant organic matter here is amorphous material dispersed through the clay-size fraction, giving the material a brownish color. The shape and uniform size of the discrete particles here suggests algal cells. Close inspection reveals distinct walls in many of these.

ODP Sample (Quaternary): Leg 128, Hole 799A, Core 3H, Section 1W, 125 cm

Image ID: B0462

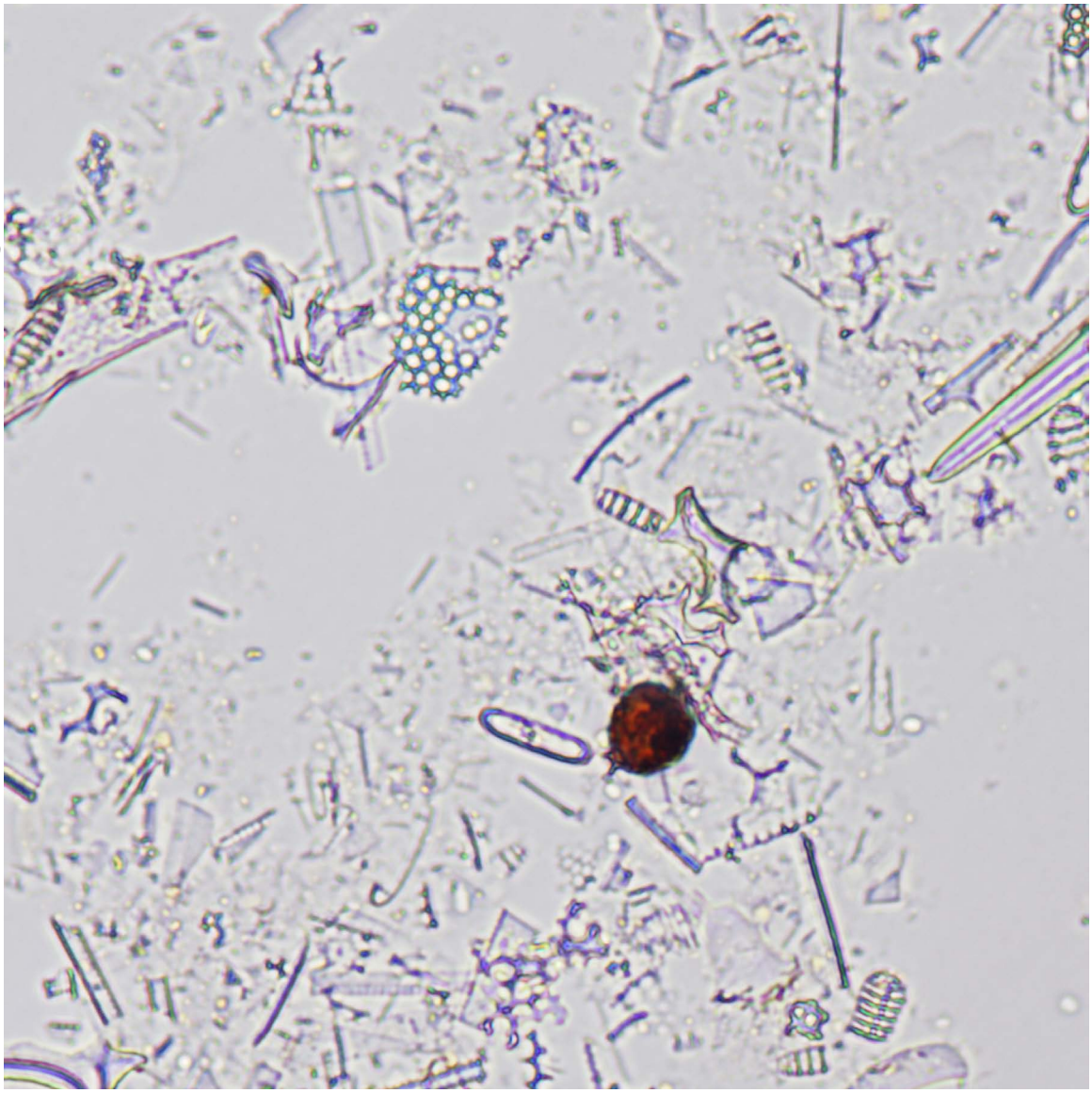

Organic matter 7.

This small spherical organic particle is in a siliceous ooze dominated by diatoms. Note the subtle presence of a wall and a few spiky protuberances. This is a possible algal cell or spore.

ODP Sample (middle Miocene): Leg 113, Hole 690B, Core 5H, Section 4W, 67 cm

Image ID: B0197/B0198

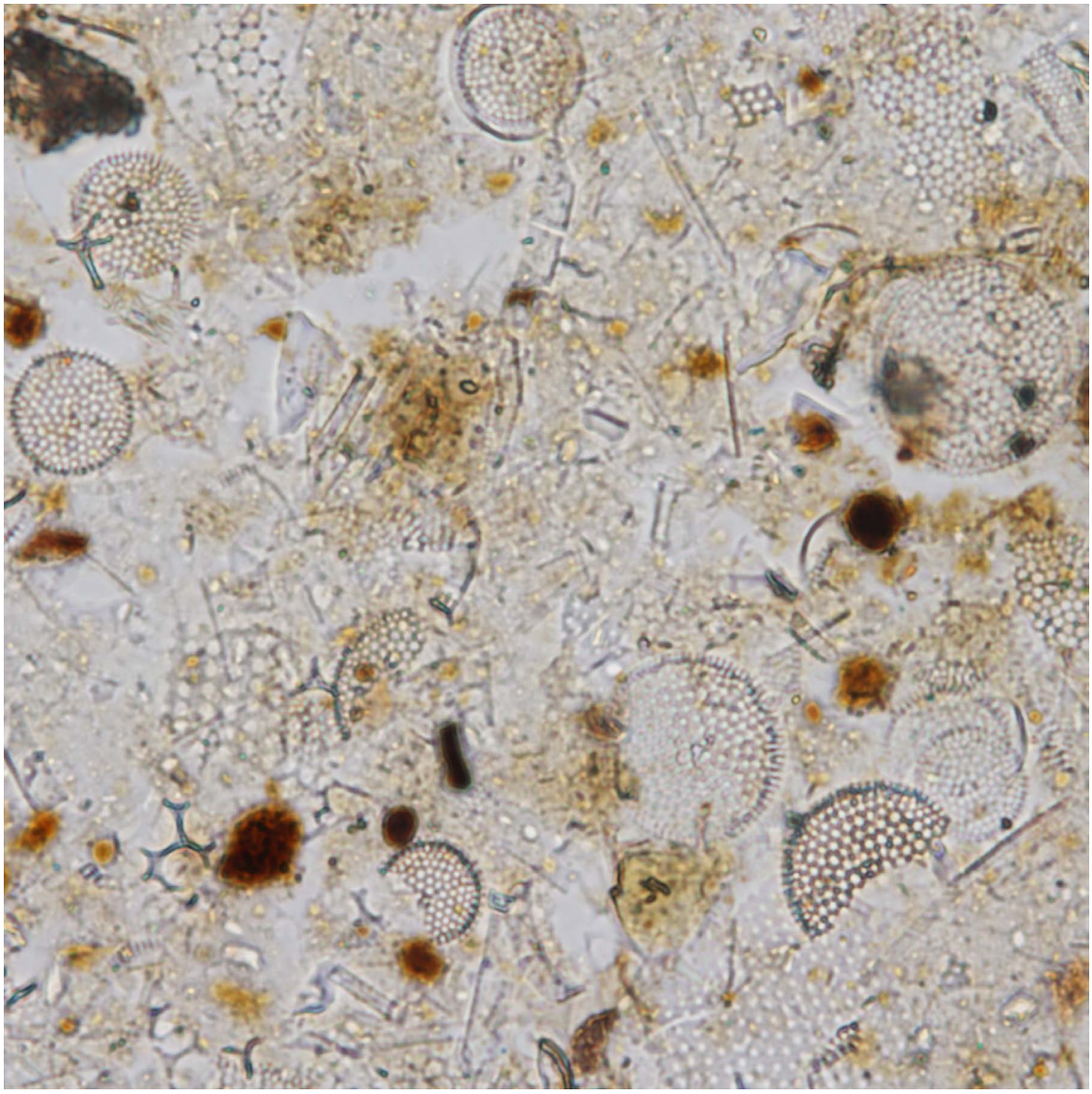

Organic matter 8.

This sample contains a mix of clay-size dispersed organic matter, that makes splotches of yellow color, and discrete particulate organic matter. Many of the particles have equant but irregular shapes and are essentially structureless. Two of the larger particles however are nearly spherical and have clear walls. These can be more confidently attributed to marine algae.

ODP Sample (Pleistocene): Leg 138, Hole 845A, Core 1H, Section 1W, 66 cm

Image ID: B0107/B0108

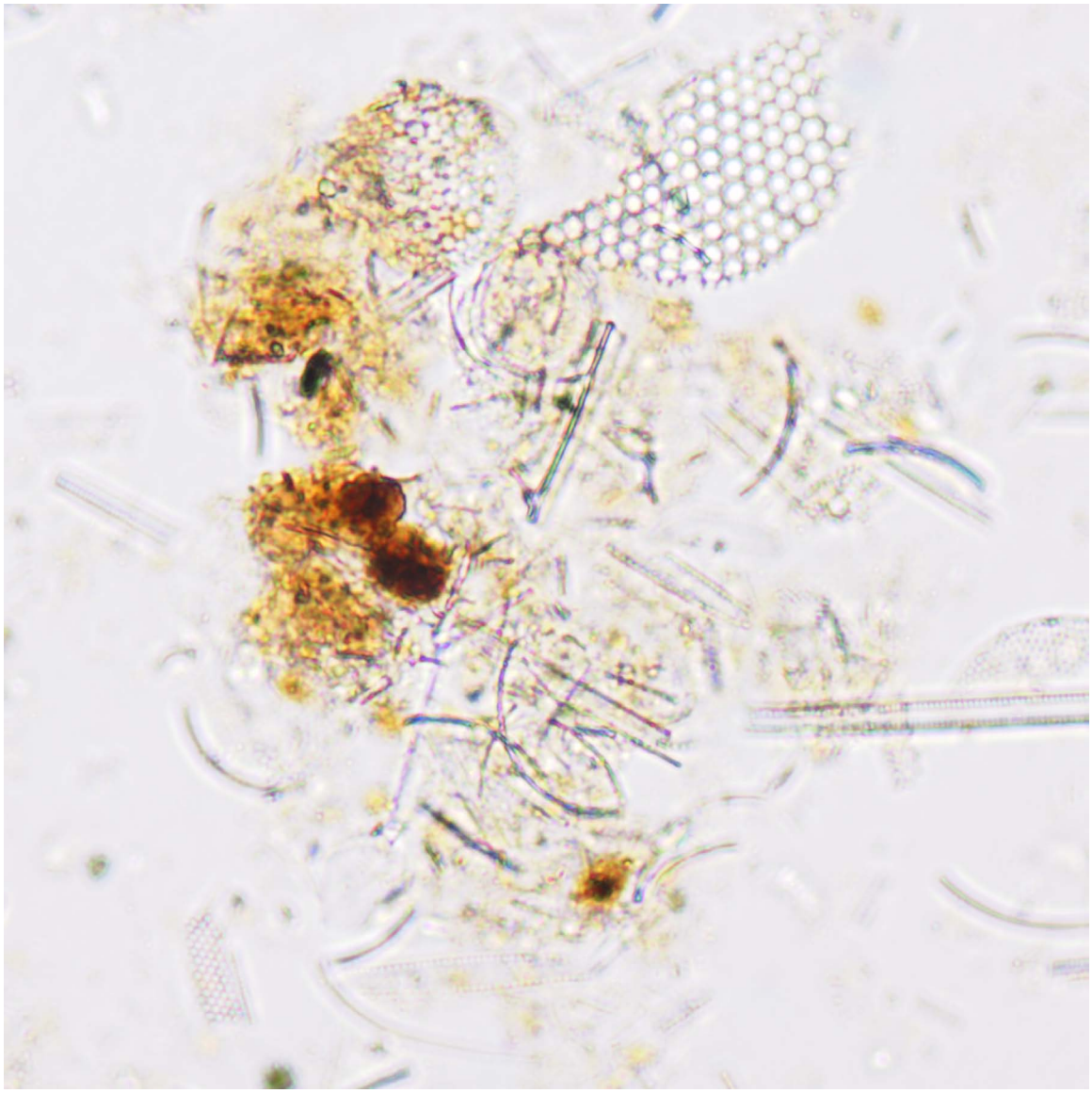

Organic matter 9.

In addition to dispersed structureless organic matter this image includes particles of more discrete form. The size and shape of this material suggests possible algal cells

ODP Sample (Quaternary): Leg 112, Hole 688A, Core 2H, Section 5W, 74 cm

Image ID: B023/B0234

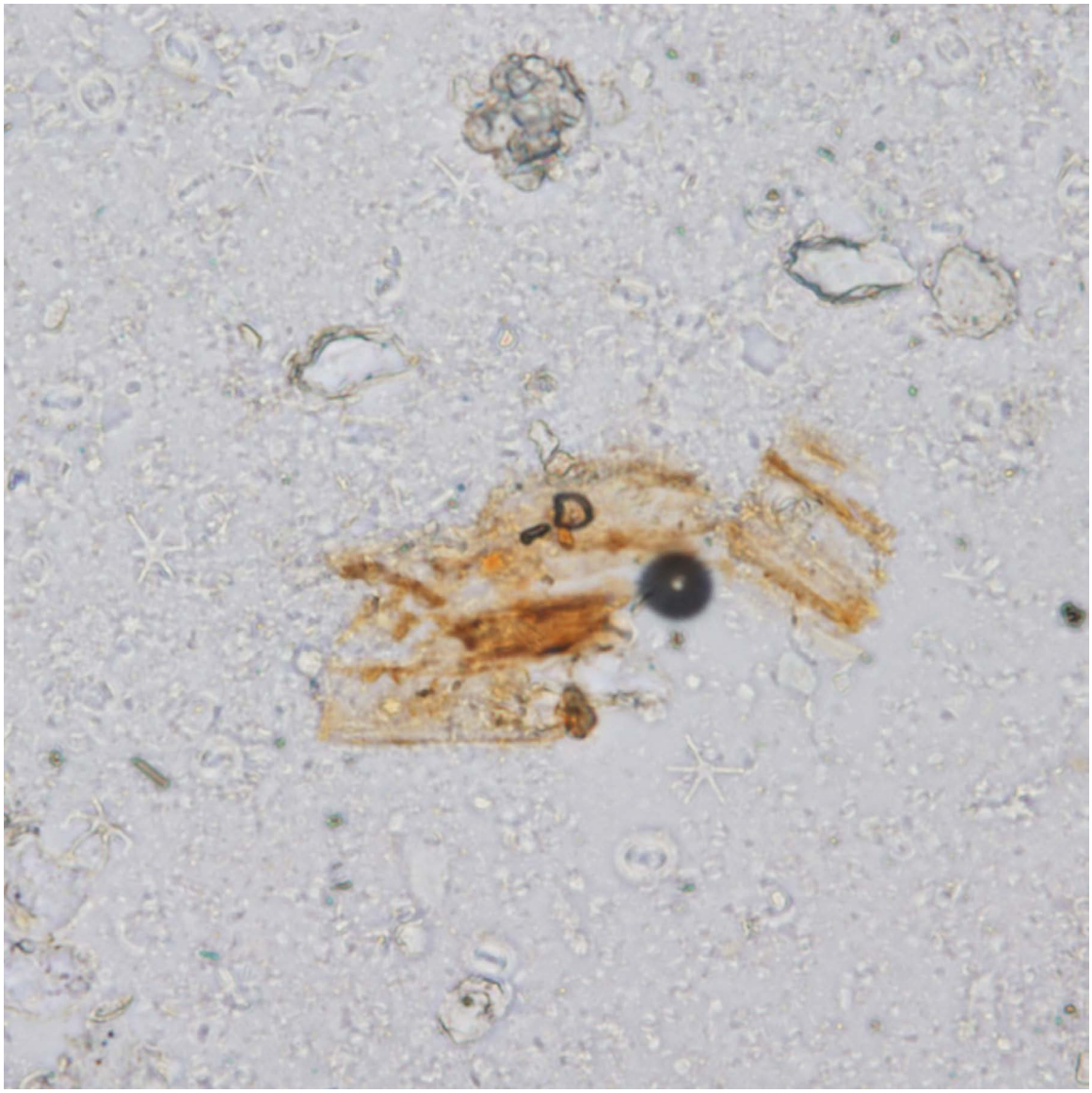

Organic matter 10.

This fragmented reddish-orange wood is broken parallel to the elongated pores. Dark feature is a bubble in the optical adhesive.

ODP Sample (late Pliocene-Pleistocene): Leg 157, Hole 950A, Core 9H, Section 6W, 101 cm

Image ID: 0337

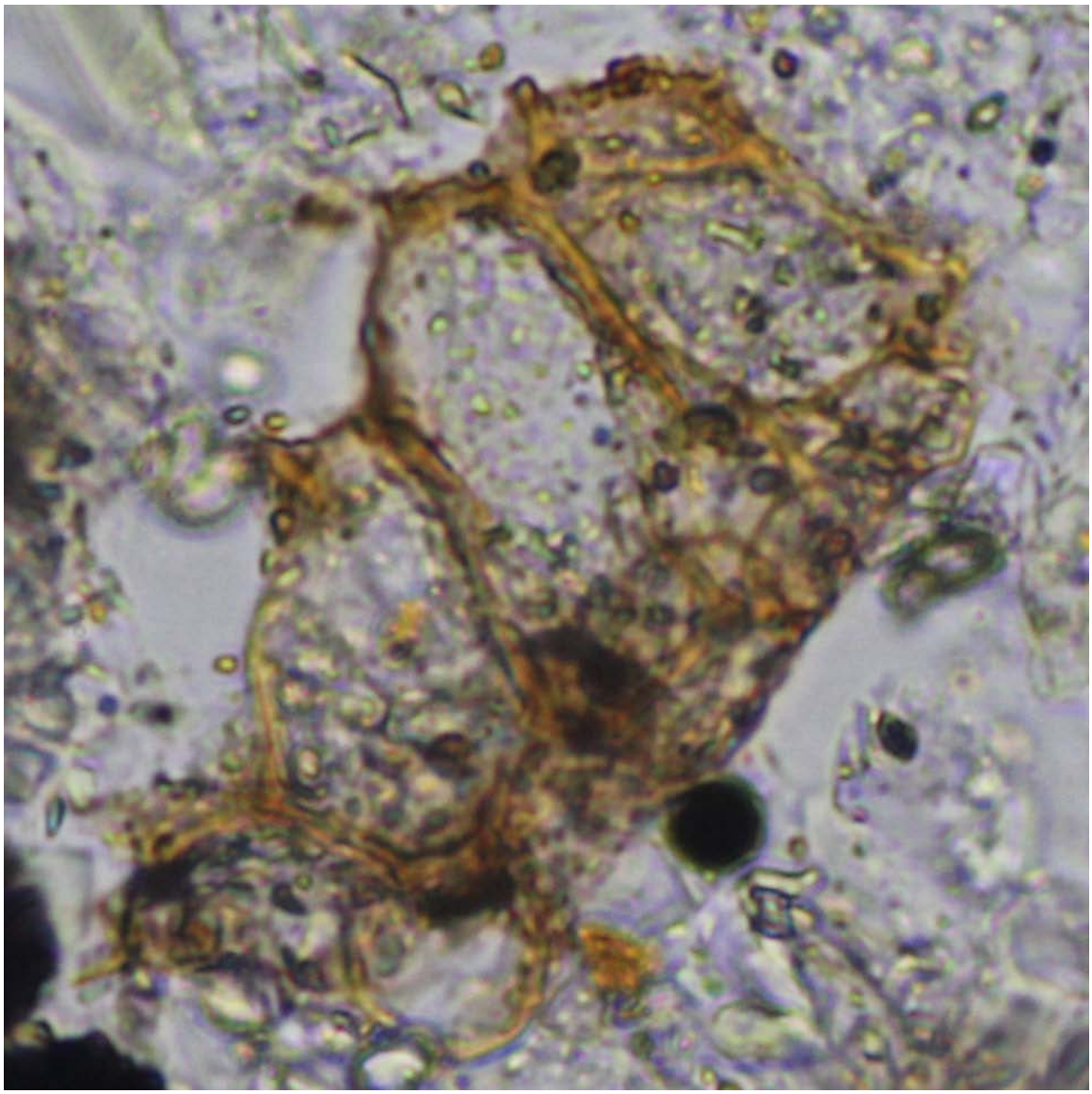

Organic matter 11.

The typical structure of wood consists of walls that surround pores spaces. Here, several pores are intact with complete walls.

IODP Sample (Pleistocene-Holocene): Leg 317, Hole 1352B, Core 2H, Section 2W, 117 cm

Image ID: B0203/B0204

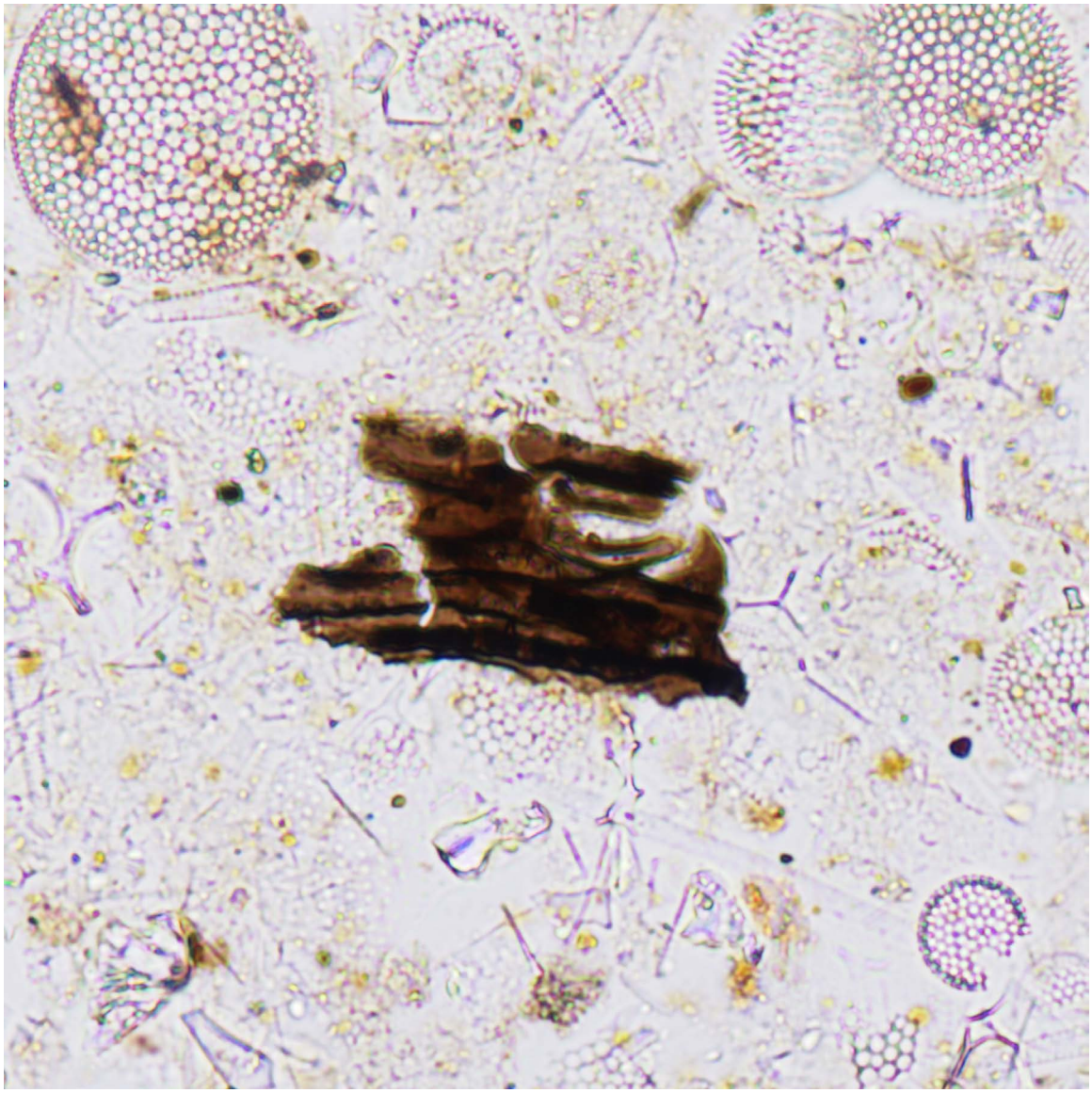

Organic matter 12.

The typical structure of wood consists of walls that surround pores spaces. Here, the fragment is broken parallel to the pores, revealing a sort of fibrous structure that arises from the elongated strands of cellulosic material that line the pores. It is set in and organic-rich diatom ooze.

ODP Sample (Pleistocene): Leg 138, Hole 845A, Core 1H, Section 1W, 66 cm

Image ID: 0041/0042

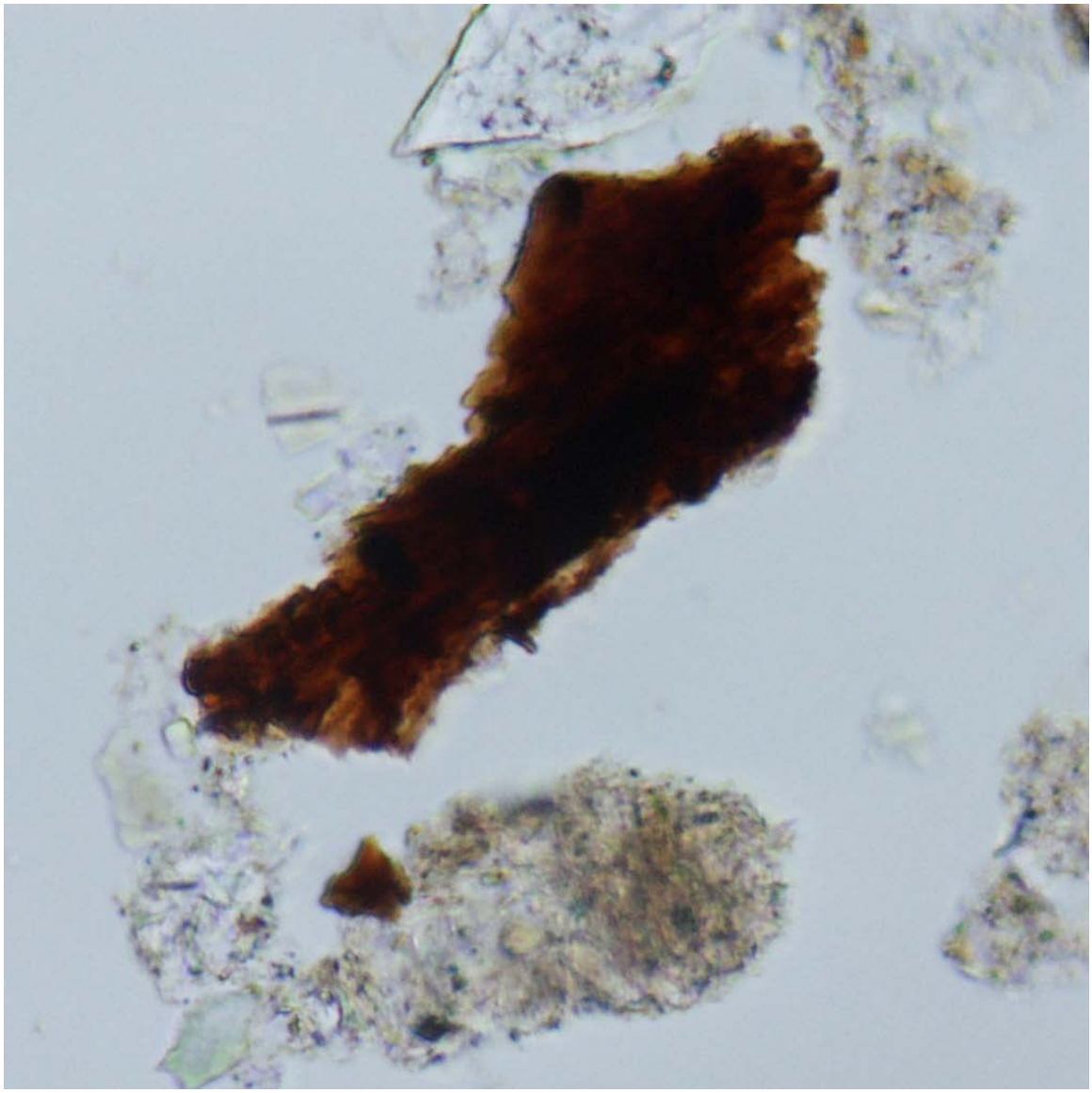

Organic matter 13.

This elongate woody particle is broken parallel to the pores. The fibrous nature of the material can be seen on the ends and along the edges.

DSDP Sample (late Miocene): Leg 31, Hole 297, Core 20, Section 2, 141 cm

Image ID: B0121/B0122

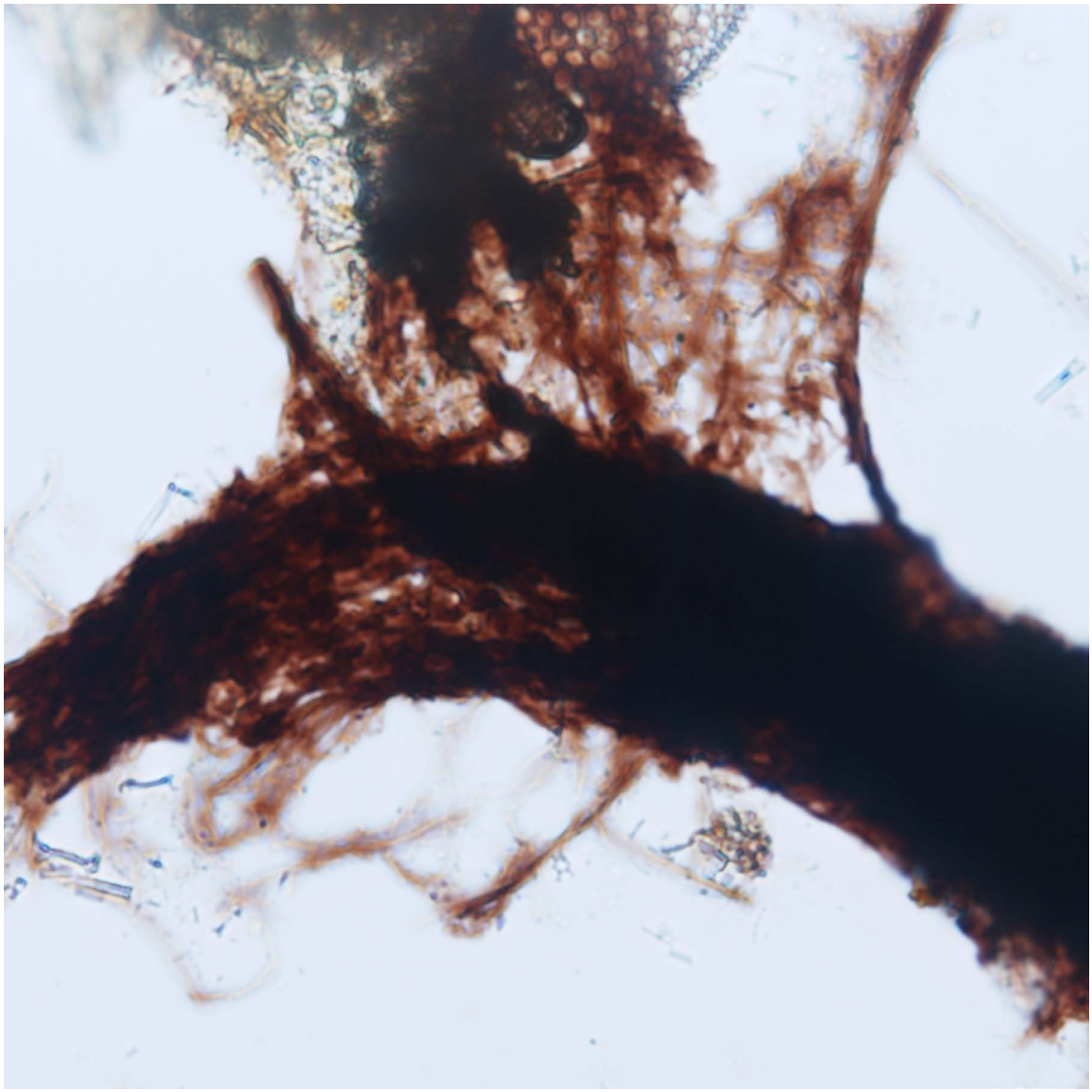

Organic matter 14.

This woody particle is bent and has spalled several fibers. These fibers arise from the stringy cellulosic material that lines the pores in the wood, forming the pore walls.

ODP Sample (late Miocene): Leg 141, Hole 859D, Core 1R, Section 1W, 120 cm

Image ID: B0117/B0118

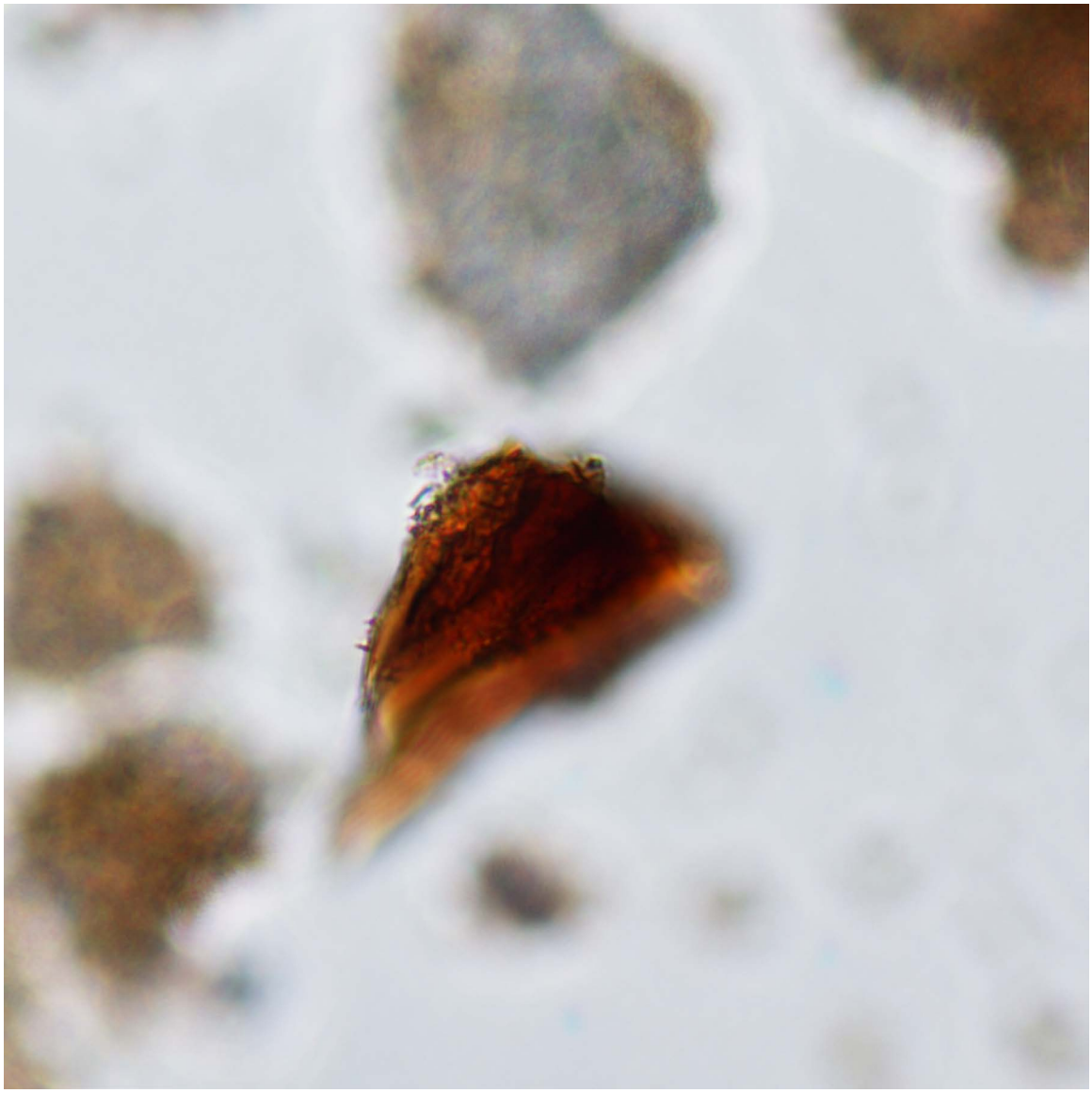

Organic matter 15.

This OM particle is relatively thick and is thus not fully in focus. The focused surface has ridges. The nature of this particle, wood or spore fragment, is uncertain. When confronted with such particles it's time to scan the slide for similar grains that might reveal the identity more fully.

ODP Sample (early Miocene): Leg 112, Hole 688E, Core 26R, Section 1W, 65 cm

Image ID: B0333/B0334

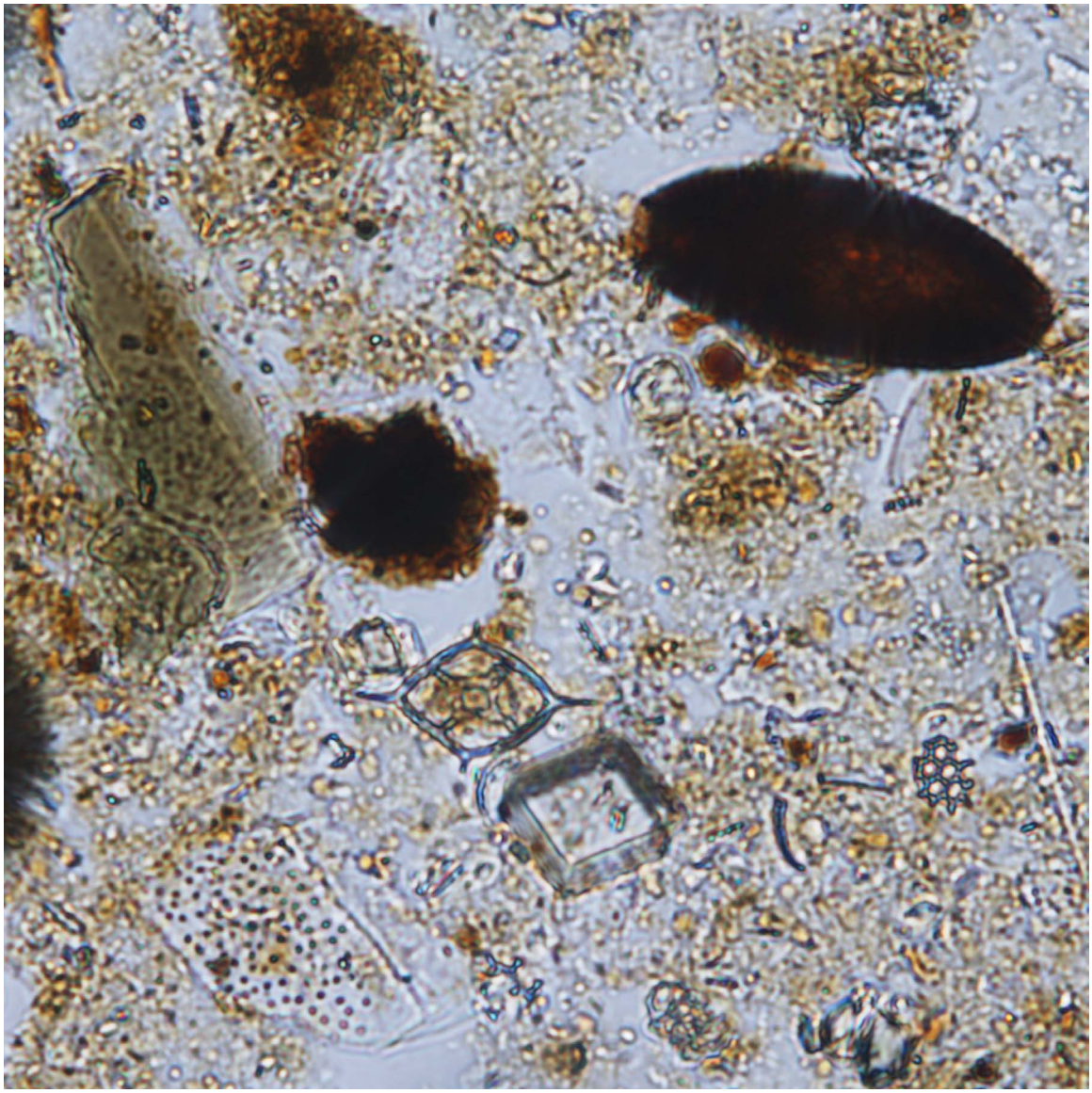

Organic matter 16.

Diverse OM types in this sample include amorphous dispersed clay-size material; irregular particles of clay- and lower-silt size, possible walled cells, and one large oblate particle that may be an some type of spore. Other things to observe here are a silicoflagellate, a foraminifer fragment with clear pores, an elongate dense mineral (probable amphibole), and a euhedral carbonate crystal (possible dolomite).

ODP Sample (Quaternary): Leg 167, Hole 1014A, Core 1H, Section 2W,

Image ID: 0150/0151

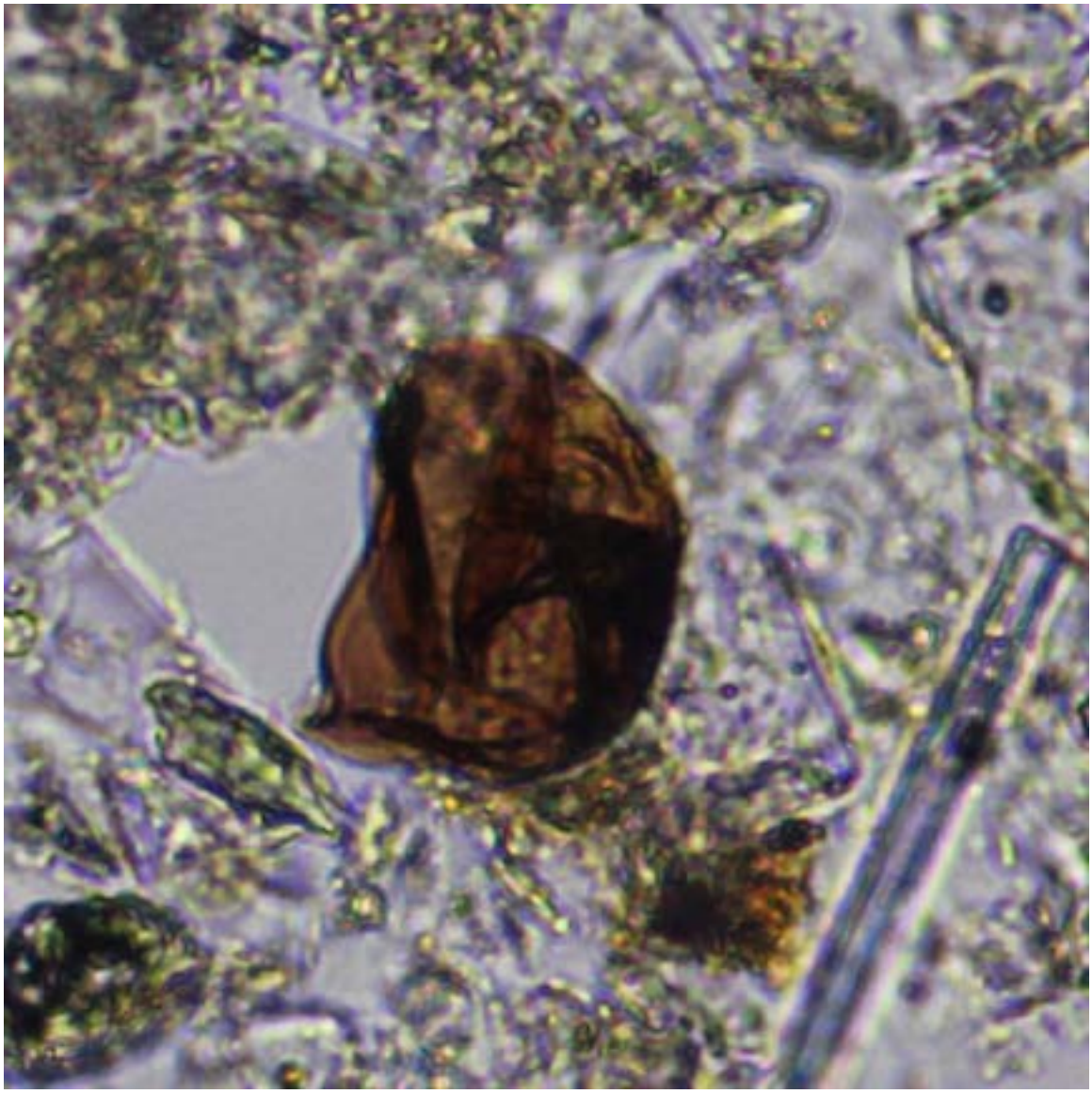

Organic matter 17.

The wrinkled surface of this large organic particle is typical of many spores and pollens.

IODP Sample (Pleistocene-Holocene): Leg 317, Hole 1352B, Core 11H, Section 2W, 21 cm

Image ID: B0201/B0202

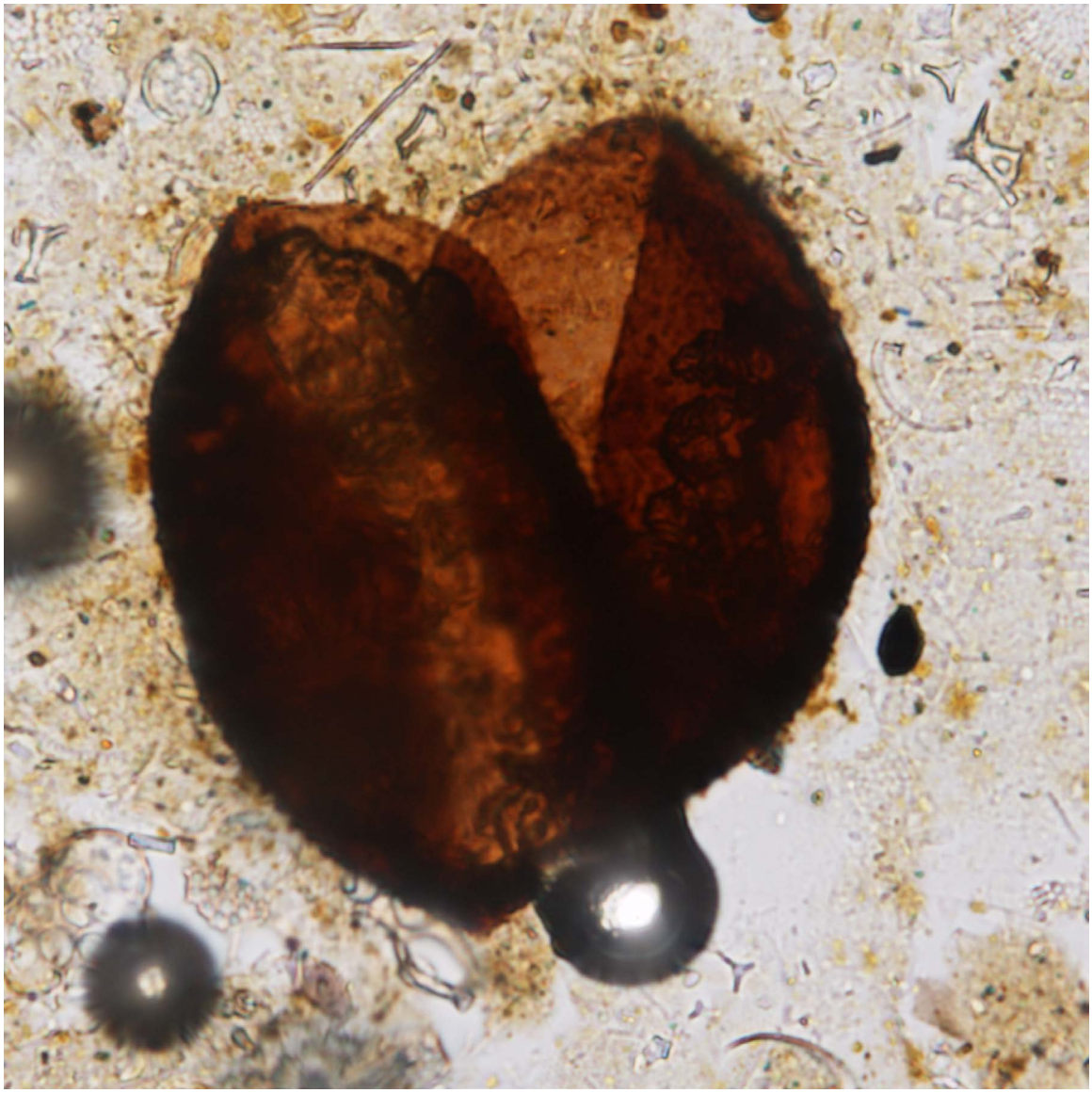

Organic matter 18.

This large particle, probably some sort of spore, has two distinct parts and a slightly bumpy surface.

ODP Sample (Pleistocene): Leg 138, Hole 845A, Core 1H, Section 1W, 66 cm

Image ID: B0303/B0304

Organic matter 19.

An intact grain of pollen or a spore.

ODP Sample (late Miocene): Leg 138, Hole 845A, Core 15H, Section 2W, 10 cm

Image ID: B0337/B0338

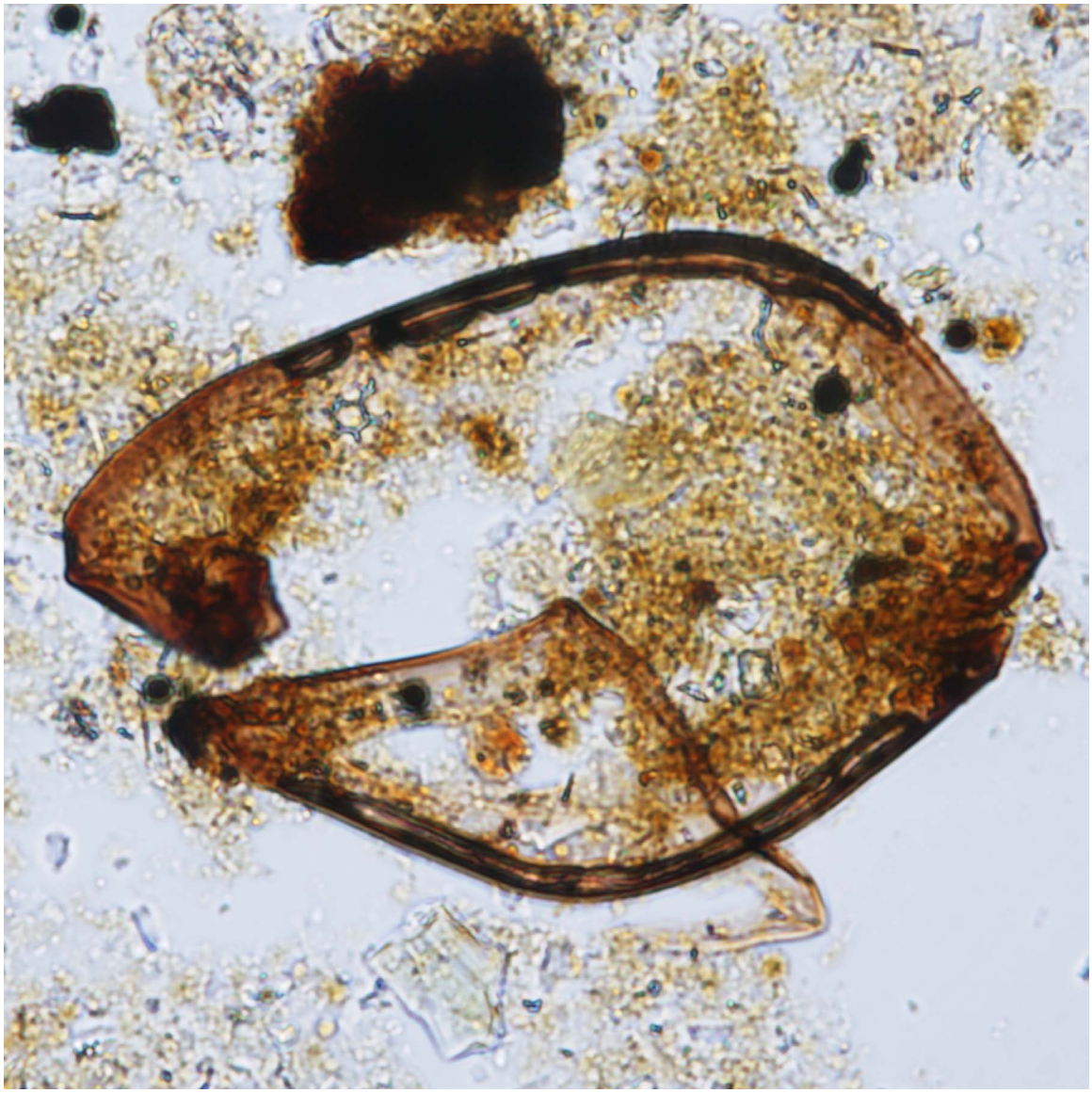

Organic matter 20.

This is a larger semi-intact spore or pollen.

ODP Sample (Quaternary): Leg 167, Hole 1014A, Core 1H, Section 2W, 120 cm

Image ID: 0509/0510

Organic matter 21.

This organic particle shows delicate fibrous protrusions and is possibly a spore.

ODP Sample (Pleistocene-Holocene): Leg 139, Hole 858B, Core 1H, Section 2W, 106 cm

Image ID: 0654/0655

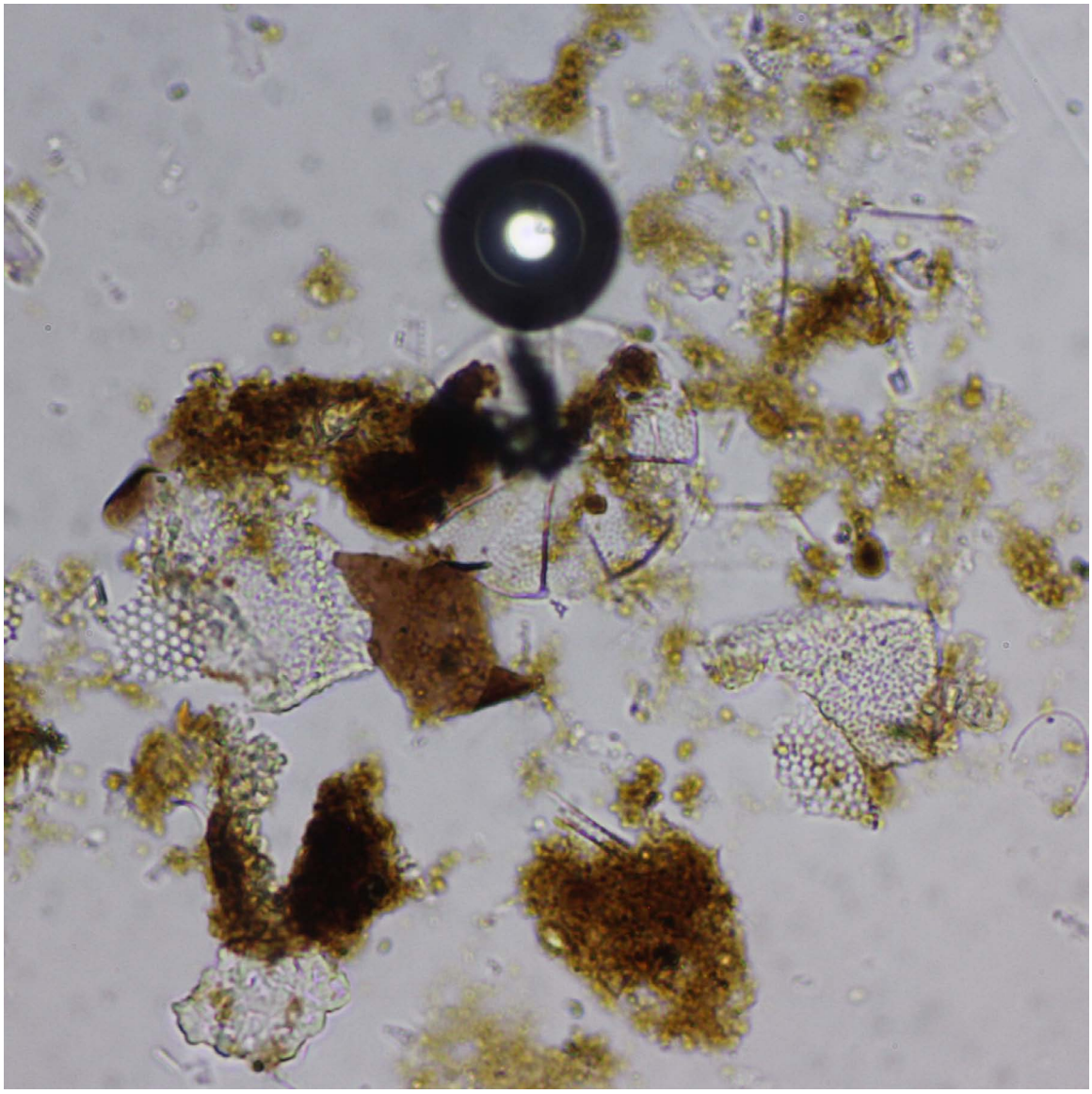

Organic matter 22.

In the center of the field of view below the distinct bubble in the epoxy is an opaline centric diatom valve partly obscured by opaque minerals or organic debris. The valve is textured with alternating raised zones in the shape of pie-like wedges. The groundmass is dark and likely organic rich.

ODP Sample (Pleistocene-Holocene): Leg 201, Hole 1228A, Core 1H, Section 2W, 20 cm

Image ID: B0015/B0016

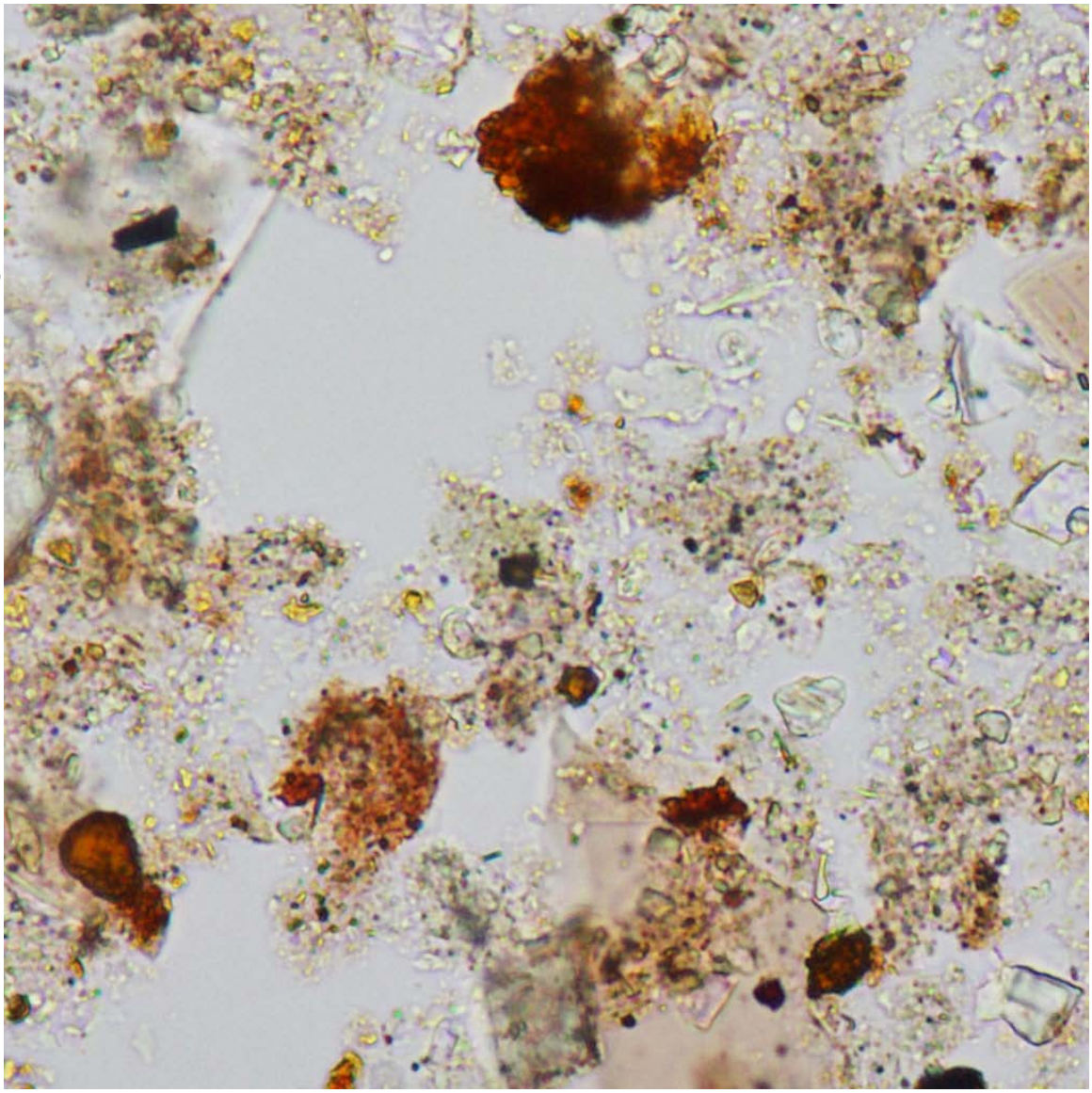

Organic matter 23.

Calcareous mixed terrigenous sediment with detrital brownish (organic?) clay and silt (mica). The higher relief grains are carbonate (micrite) of uncertain affinity, best seen with polars crossed. Sparse coccoliths are not discernible in plane light, but can be seen with polars crossed as white/grey/black circular pinwheels. One larger coccolith exhibits first-order yellow birefringence. Note mica grains show no birefringence because they lie flat with their c-axes perpendicular to the field of view.

DSDP Sample (late Miocene/Messinian):Leg 13, Hole 132, Core 22, Section 1, 12 cm

Image ID: B0105/B0106

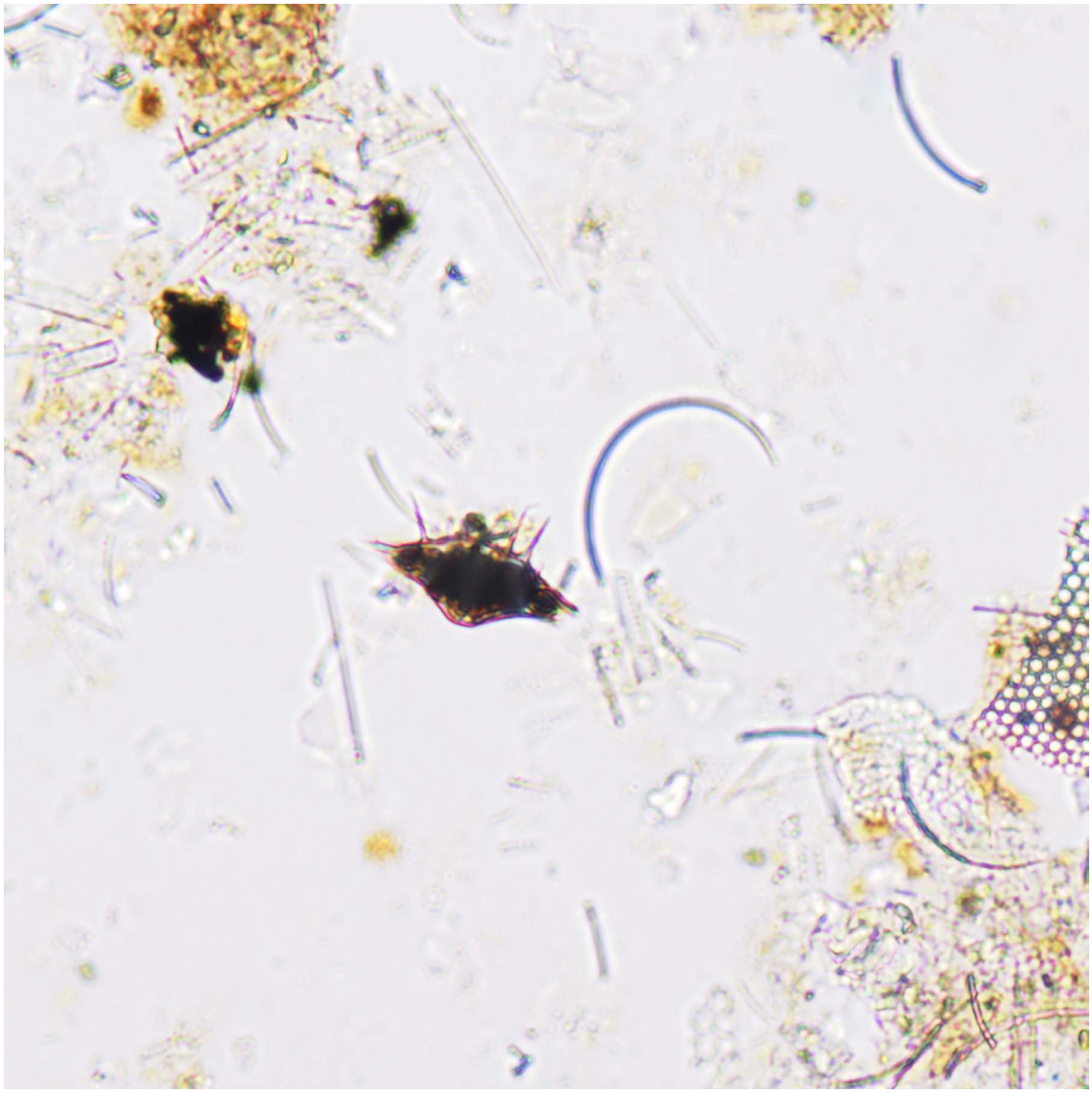

Organic matter 24.

It is difficult to determine whether this is an opaque-filled spikey pollen grain or siliceous microfossil set in a diatom-rich sediment.

ODP Sample (Quaternary): Leg 112, Hole 688A, Core 2H, Section 5W, 74 cm

Sediment Aggregates (Pellets)

INTRODUCTION TO SEDIMENT AGGREGATES (PELLETS)

Sediment aggregates are important components in fine-grained sediment. So strong is the tendency of clay-size particles to clump together, it may, in fact, be rare for clay-size particles to travel as independent particles. Aggregates arise from a variety of chemical and mechanical processes: electrostatic charges on small particles cause them to clump together; sticky biofilms secreted by planktic and benthic microbes trap sediment particles; feeders both small and large in the water column create a rain of particles onto the seafloor; sediment feeders on or in the sediment excrete lumps of sediment; reworking of sediment lithified by early cementation on the seafloor. Sediment aggregates formed by passage of sediment through the digestive tract of invertebrate organisms are called pellets. Pellets can be subdivided into ones that fall from the water column and ones formed within the sediment. Excretions of vertebrates, mostly generated in the water column, are typically designated coprolites and are unlikely to be observed in smear slides, though it is possible these may be noted in visual core observations. Coprolites are typically aggregates of phosphatic particles or nannofossils. Sediment aggregates formed by reworking of cemented seafloor are called intraclasts and in deep sea sediments these are most commonly cemented by pyrite, glauconite, or phosphate minerals. Intraclasts cemented by carbonate minerals are common in shallow water settings, but rare in deep sea sediments.

In smear slides it is a challenge to discriminate natural sediment aggregates from lumps of mud that simply failed to fully disaggregate during smear slide production. This problem becomes especially acute as the sediment becomes more compacted and lithified in the deeper sections of a hole. The following list provides guidance on the recognition of possible sediment aggregates in smear slides:

1) Distinct shapes with well-defined edges
2) Uniform size, color, and texture.
3) Color and texture that contrasts with that of the surrounding mud.
4) Internal structure (rare).

Pellets

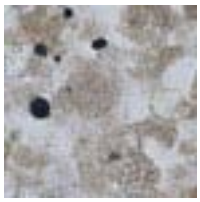
Pellets 1

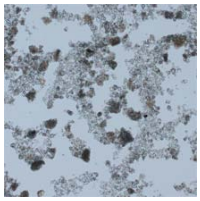
Pellets 2

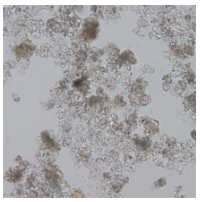
Pellets 3

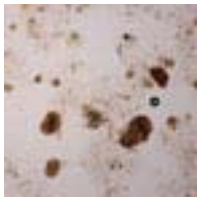
Pellets 4


Pellets 5

Image ID: B221/B222

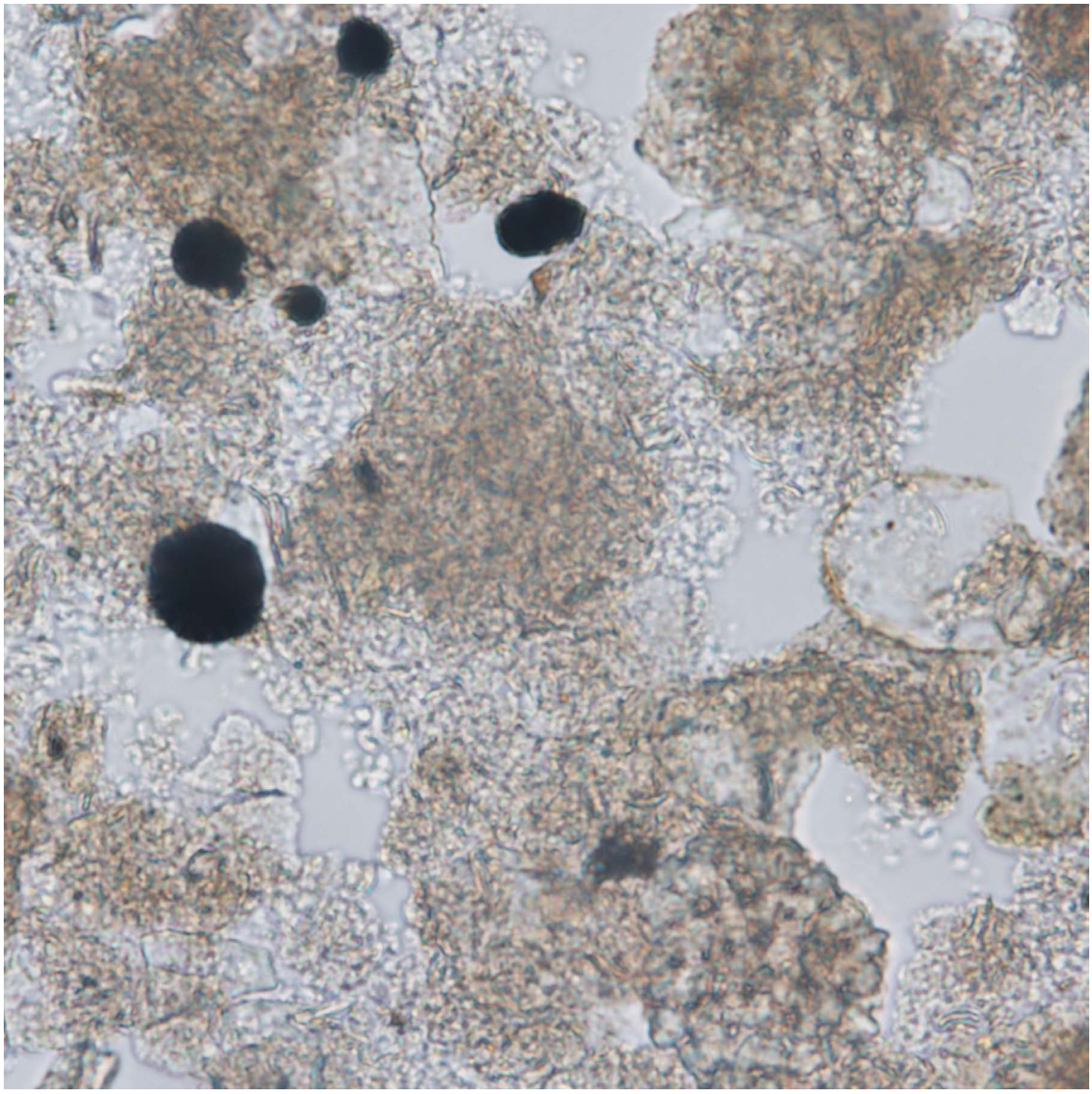

Pellets 1.

Structureless, round clump of material in the center of the field of view, tan in plain light, is shown to consist of tightly packed, slightly birefringent nannofossils with polars crossed. This clump is likely a fecal pellet. Elsewhere in the slide is a semi-circular perforate foraminifer fragment (lower right corner) and opaque pyrite framboids.

ODP Sample (Pleistocene): Leg 108, Hole 659B, Core 4H, Section 1W, 106 cm

Image ID: B0093/B0094

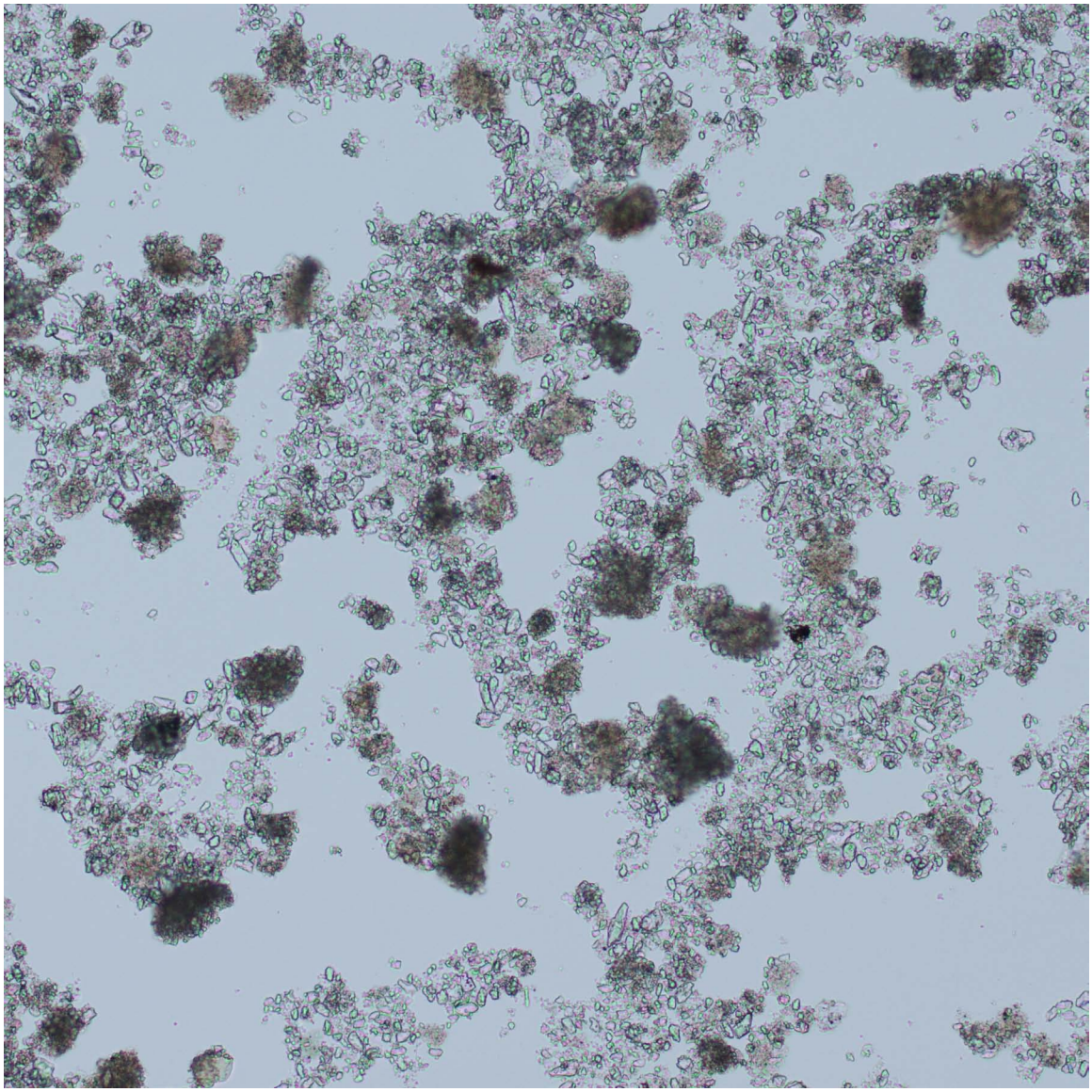

Pellets 2.

These darker clumps of fine carbonate (nannofossils?) dispersed amongst carbonate micrite of uncertain origin, but likely biogenic origin, may be pellets.

ODP Sample (early-middle Cenomanian): Leg 101, Hole 627A, Core 42, Section 4, 145 cm

Image ID: B0095/B0096

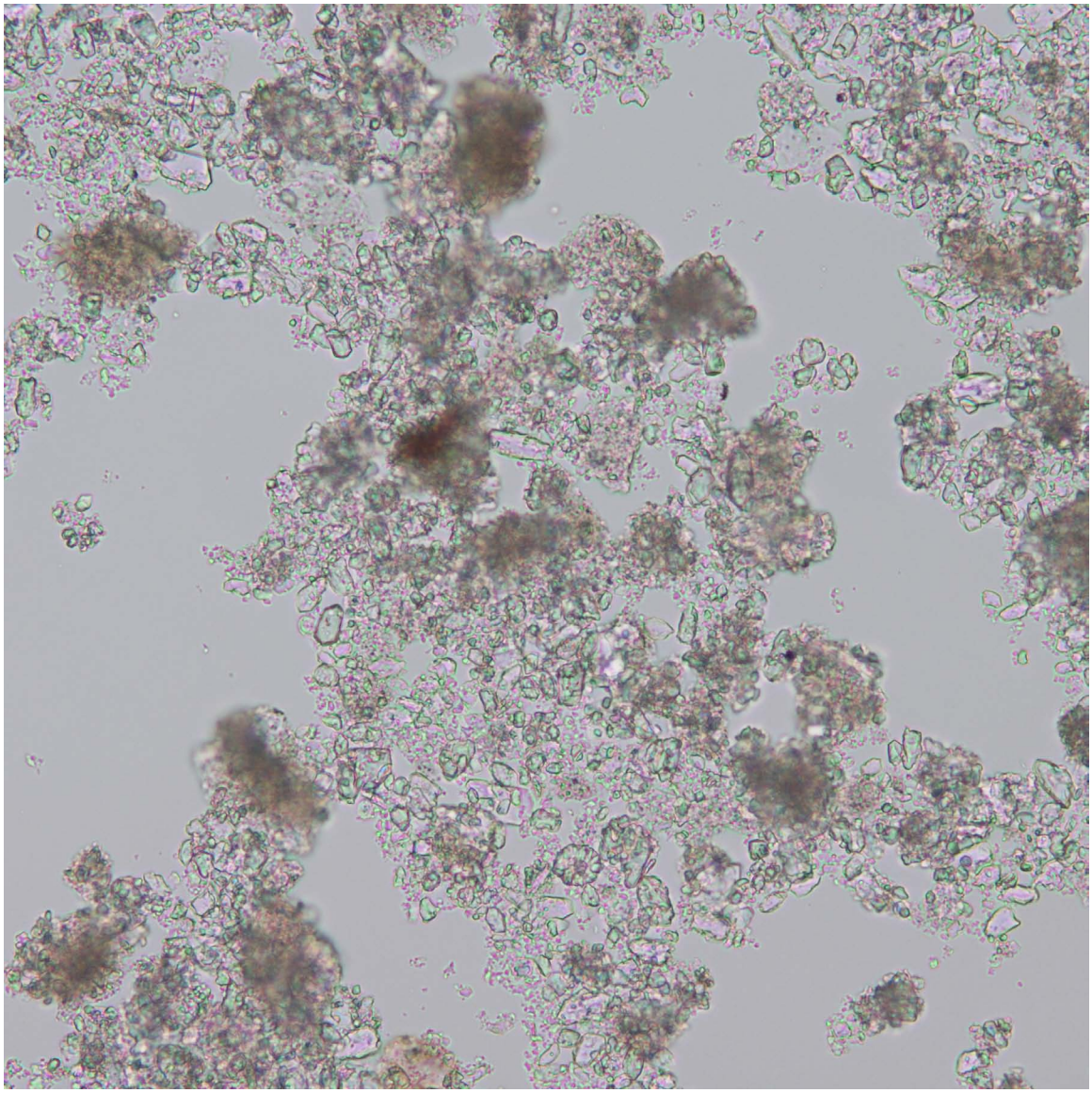

Pellets 3.

This view shows darker clumps of fine carbonate (nannofossils?) dispersed amongst carbonate micrite of uncertain, but likely biogenic origin. Some distinct calcareous nannofossils are present.

ODP Sample (early-middle Cenomanian): Leg 101, Hole 627A, Core 42, Section 4, 145 cm

Image ID: 00454/0455

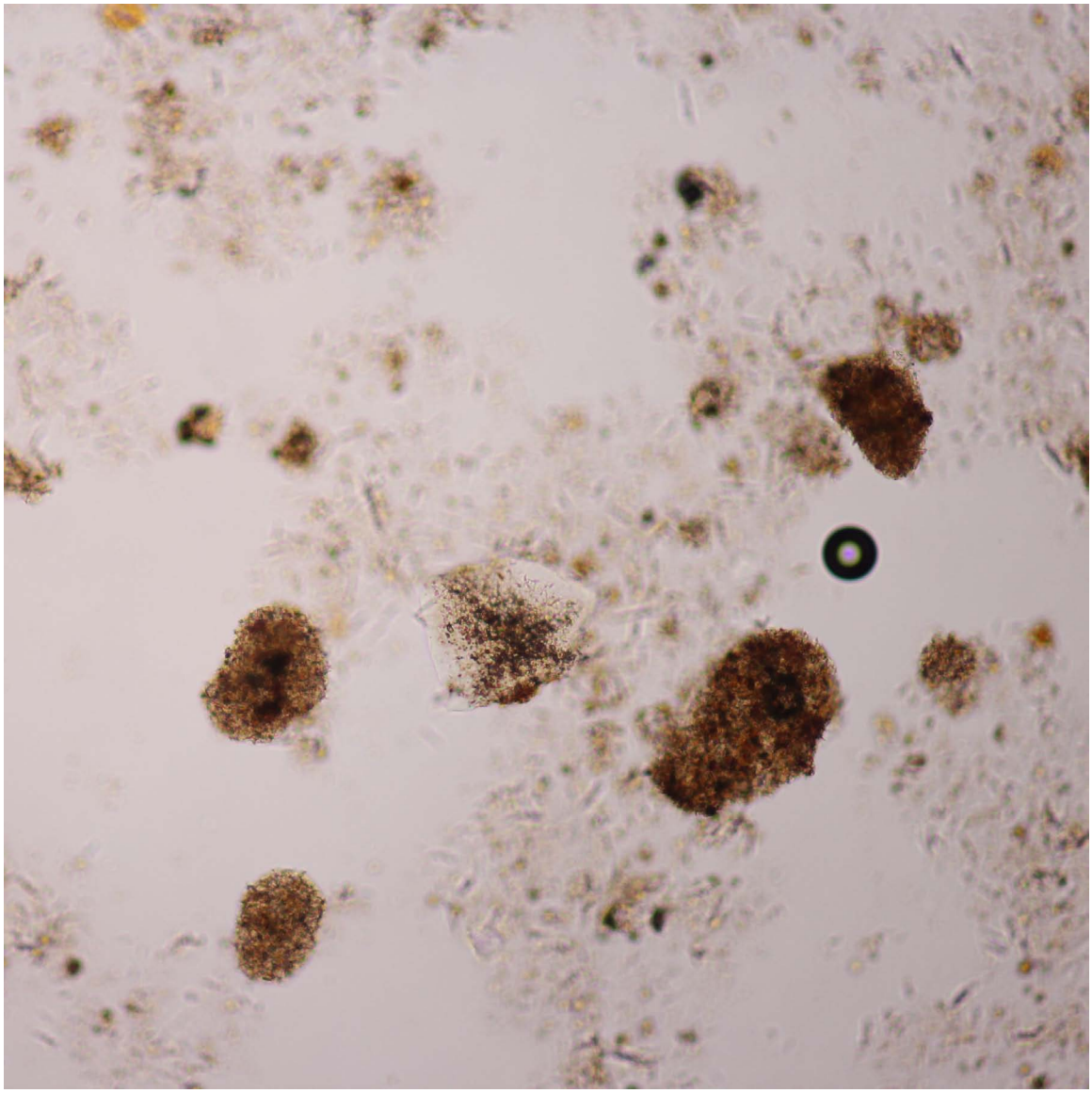

Pellets 4.

General view with undisaggregated clumps or pellets likley composed of a mixture of clay and carbonate based on their birefringence.

DSDP Sample (middle Miocene): Leg 91, Hole 596, Core 1, Section 4, 52 cm

Image ID: B0219/B0220

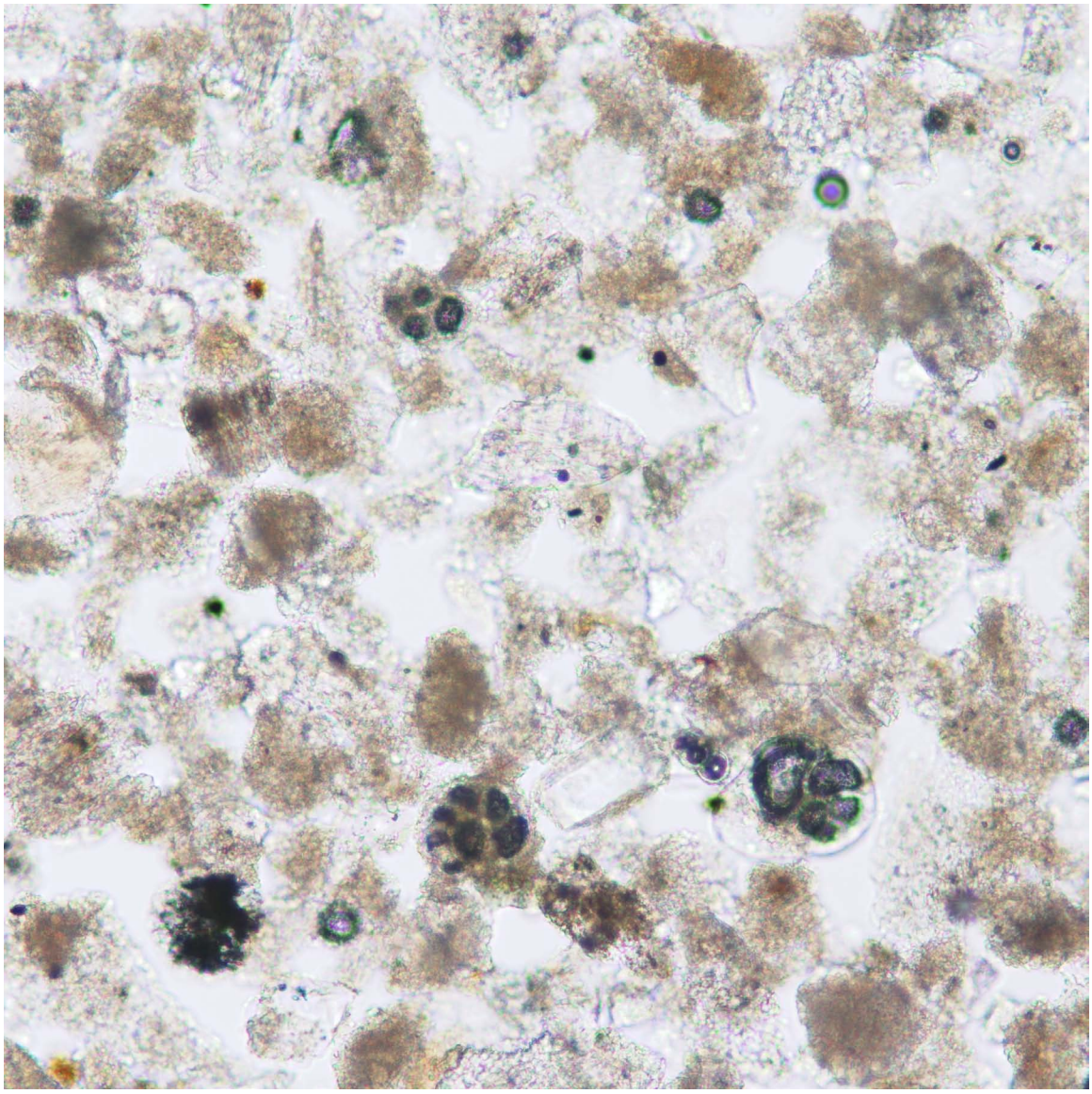

Pellets 5.

This field of view shows bioclastic silt including whole forams and possible micritic pellets.

ODP Sample (late Pliocene): Leg 108, Hole 657A, Core 9H, Section 3W, 31 cm

Authigenic Minerals & Diagenetic Features

INTRODUCTION TO AUTHIGENIC MINERALS & DIAGENETIC FEATURES

Diagenesis encompasses all the chemical and mechanical processes that affect sediment in the part of the rock cycle between deposition and metamorphism and between either of these and weathering. Both chemical and mechanical processes can be biologically mediated, especially in the earliest stages of diagenesis near the sediment-water interface.

Smear slides require sediment that is only weakly consolidated and, thus, extensive cementation is not commonly observed in samples prepared as smears. Incipient cements that grow within intergranular spaces in unconsolidated mud are the most commonly observed diagenetic features in smear slides. Pyrite framboids and dolomite rhombs are common products of bacterial sulfate reduction. Localization of pyrite within fossils is a very common result of reducing conditions that are not uniformly distributed in the sediment. Microcrystalline calcite cement commonly nucleates on both the external and internal surfaces of nannofossils and foraminifer tests. Other common early cements that form under conditions of slow sedimentation are glauconite and phosphate and these may form distinct crusts that can be observed in visual core observations. Reworking of these cemented crusts can yield small intraclasts of glauconite or phosphate that occur in the silt fraction.

Grain alteration is another diagenetic process, typically observed in the deeper, older sections of a particular hole. In grain alteration, unstable grains begin to express their reaction potential as they dissolve in pore fluids, followed in some cases by re-precipitation of authigenic materials within and between the dissolved grains. Grain alteration initially leads to a subtle coarsening of clay-size carbonate and the erasure of the distinctive morphologies in certain nannofossil populations. For example certain nannofossils (e.g., some placoliths) tend to dissolve with diagenesis, whereas others (e.g., discoasters) tend to overgrow. Discoasters show a long term evolutionary morphological trend from Paleogene multi-rayed plate-like ones to thinner Neogene ones with fewer rays. Thus through time, discoasters becoming progressively less robust, with fewer rays, even if there is diagenetic overprinting. For example, shipboard scientists on ODP Leg 130 erred in attributing the change in Site 806 samples from thin-rayed late Pliocene discoasters to progressively more robust middle to lower Miocene discoasters, to overgrowth processes only (Personal Communication, J. Firth).

Similarly, bio-siliceous debris loses the delicate morphologies of diatoms and radiolarian as they are replaced by authigenic silica or carbonate. Sponge spicules are more resistant to this process but they too ultimately succumb to replacement. Extensive replacement is typically accompanied by cementation and so only rare and incipient instances of replacement are typically
observed in smear slides.

Kroenke, K.W., Berger, W.H., Janecek, T.R., et al., 1991. Proceedings Ocean Drilling Program. Initial Reports, College Station, TX, 130.

Authigenic Minerals & Diagenetic Features

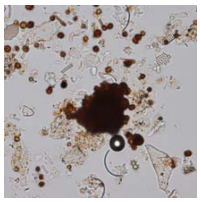
Siderite 1

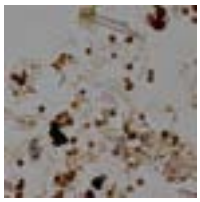
Siderite 2


Siderite 3


Carbonate 1

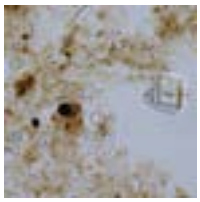
Carbonate 2


Carbonate 3

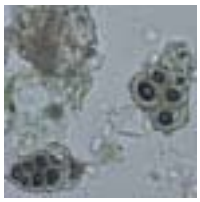
Carbonate 4


Carbonate 5


Carbonate 6


Carbonate 7


Carbonate 8


Glauconite 1


Glauconite 2


Glauconite 3

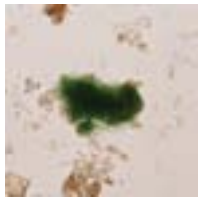
Glauconite 4


Glauconite 5


Silica 1


Silica 2

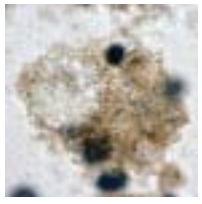
Silica 3


Silica 4

Zeolite 1

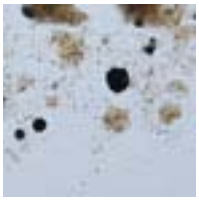

Pyrite 1

Pyrite 2

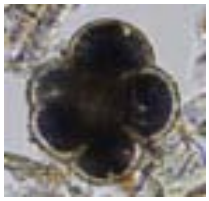

Pyrite 3

Pyrite 4

Pyrite 5

Dissolution 1

Dissolution 2

Image ID: 0091/0092

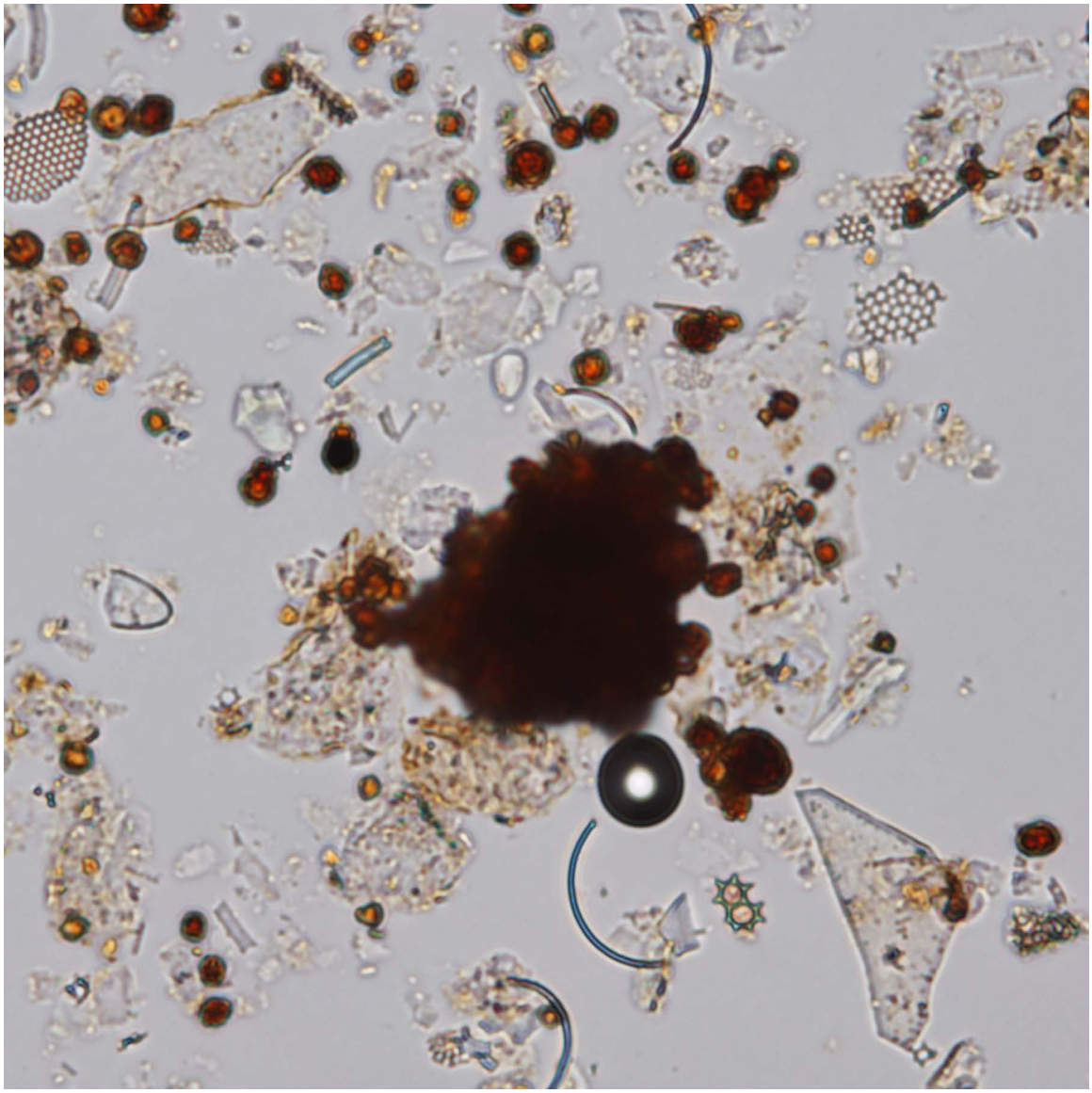

Siderite 1.

Without direct compositional data (by XRD or EDS) it is not possible to say with certainty that these small red-orange crystals are siderite (FeCO3). Supporting observations are the color, high relief, size, and shape. Siderite is not intrinsically red or brown however the Fe2+ of the siderite is readily oxidized and submicroscopic crystals of Fe-oxide-hydroxide can color the crystals. Associated grains here include many diatom fragments.

DSDP Sample (late Pleistocene): Leg 64, Hole 479, Core 26, Section 6, 120 cm

Image ID: B0092

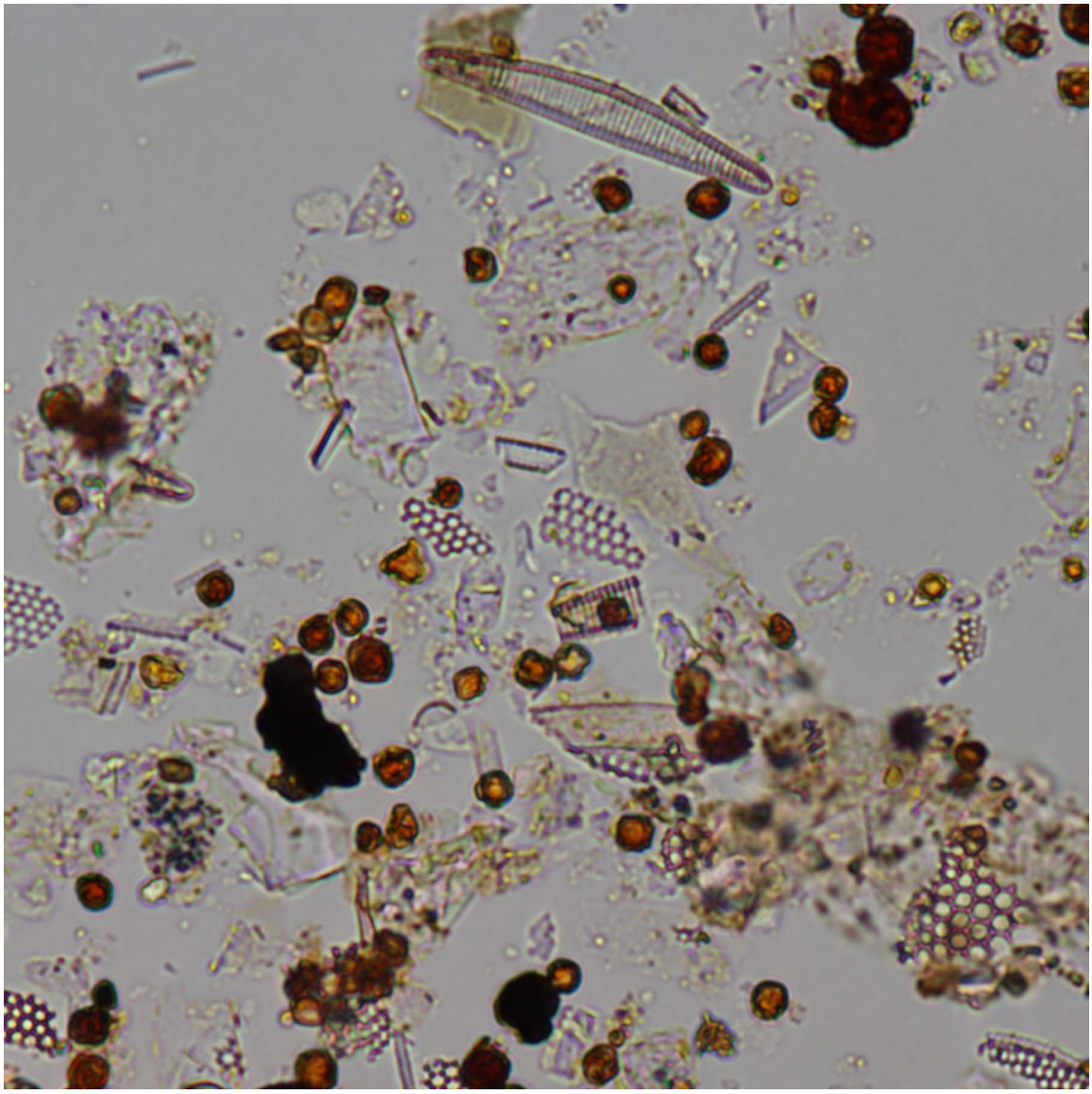

Siderite 2.

Similar to Siderite 1. Note the rhomb-shapes of a few crystals. Other crystals appear to be tiny rosettes. Again these are set in a diatom-rich sediment.

DSDP Sample (late Pleistocene): Leg 64, Hole 479, Core 26, Section 6, 120 cm

Image ID: B0557/B0558

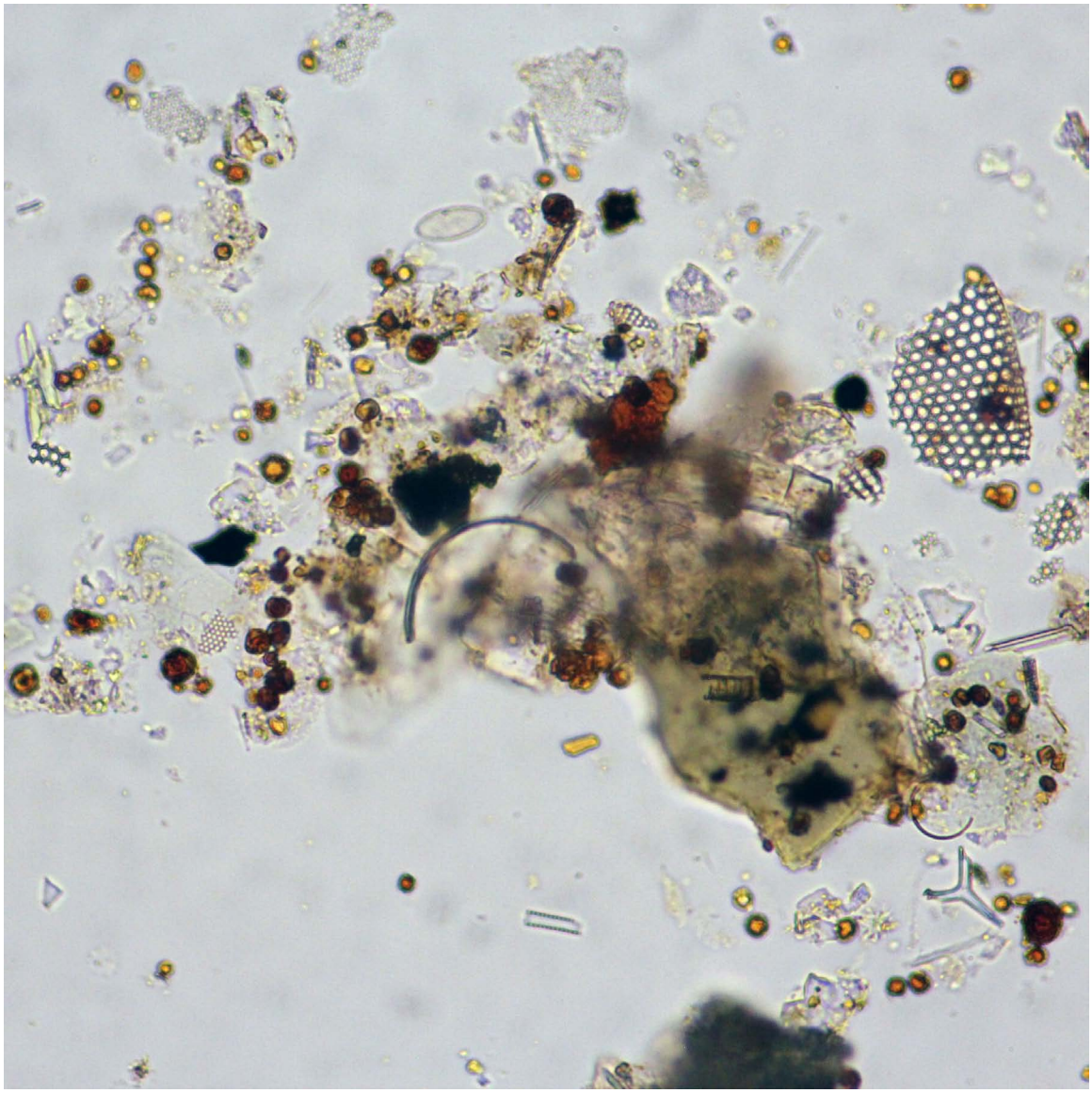

Siderite 3.

This is a mixed sediment that contains terrigenous debris (greenish biotite flake, quartz and feldspar), centric diatom debris and orange/brown birefringent authigenic carbonate that maybe siderite.

DSDP Sample (late Quaternary): Leg 64, Hole 479, Core 26, Section 6, 120 cm

Image ID: 0658/0659

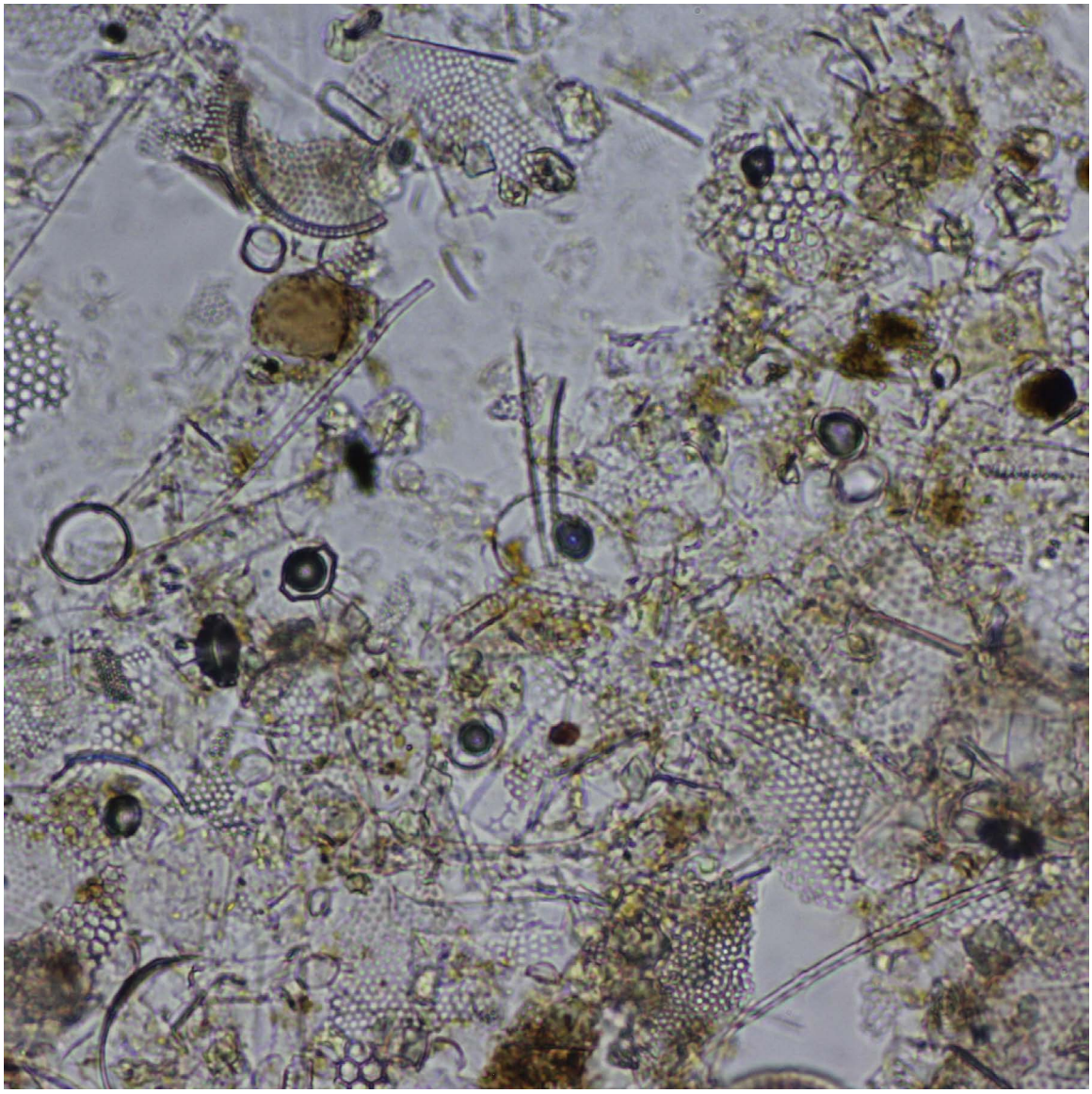

Carbonate 1.

Calcite (CaCO3) and dolomite (CaMg(CO3)2) cannot be discriminated on the basis of their optical properties. Both can take rhombic form, although this is more common for dolomite. Dolomite is also a common early diagenetic component in marine muds, especially in the case that these muds are exposed to conditions of low oxygenation. The carbonate component of this specimen is best appreciated in the cross-polar view where the rhomb shapes of many crystals becomes evident, suggesting, but not proving, that a portion of the carbonate here is dolomite. Associated grains here are mostly diatom debris.
ODP Sample (Pleistocene): Leg 201, Hole 1229A, Core 2H, Section 6W, 26 cm

Image ID: B0335/B0336

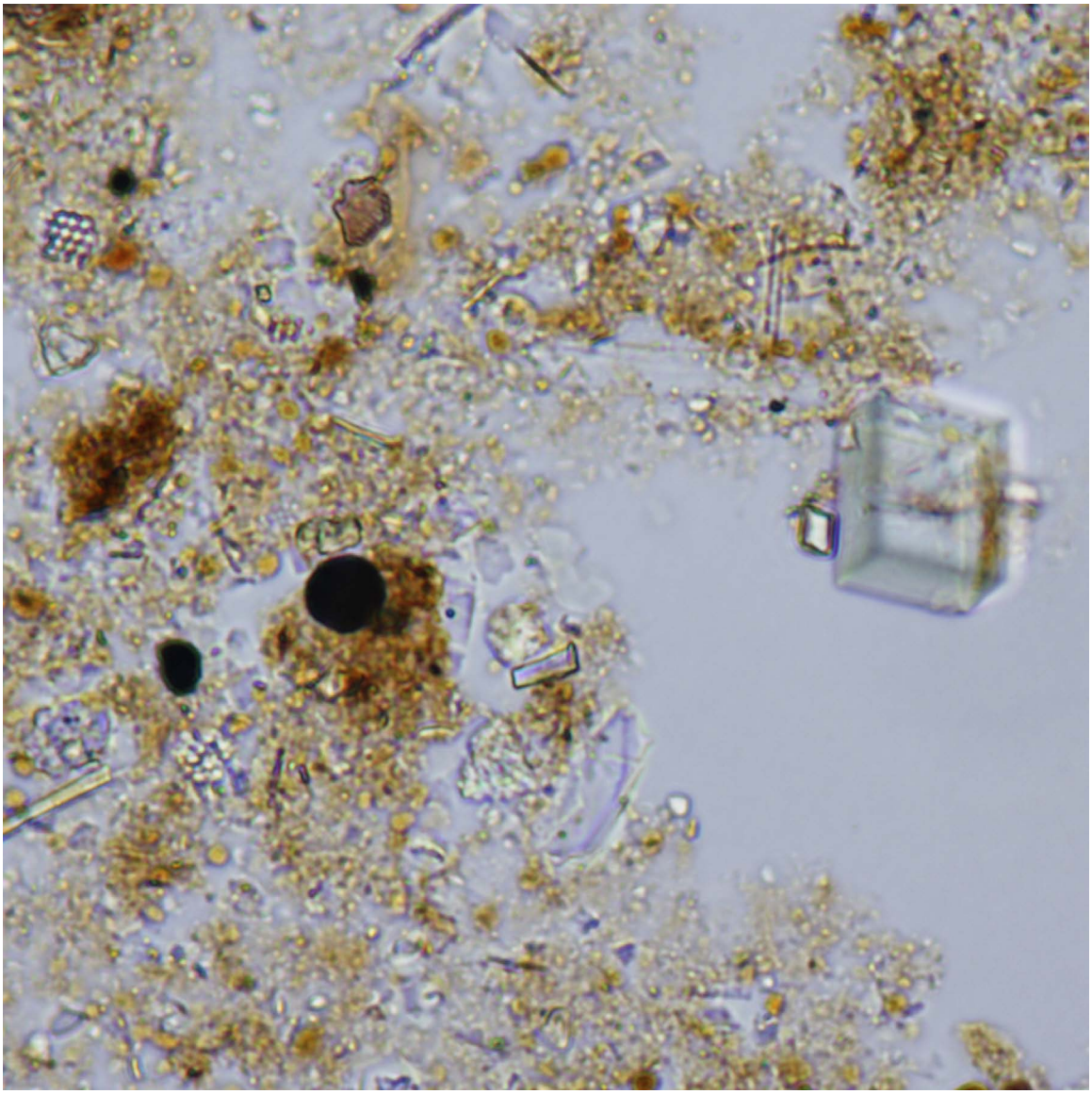

Carbonate 2.

Brownish color in plane light suggests an organic-rich composition for this mud. Some organic matter is present as discrete brownish particles (e.g., circled region). Go to the cross-polar view to gain an appreciation of the carbonate content. The large rhomb on the image right-size is probably dolomite. Black sphere is a pyrite framboid.

ODP Sample (Quaternary): Leg 167, Hole 1014A, Core 1H, Section 2W, 120 cm

Image ID: B0017/B0018

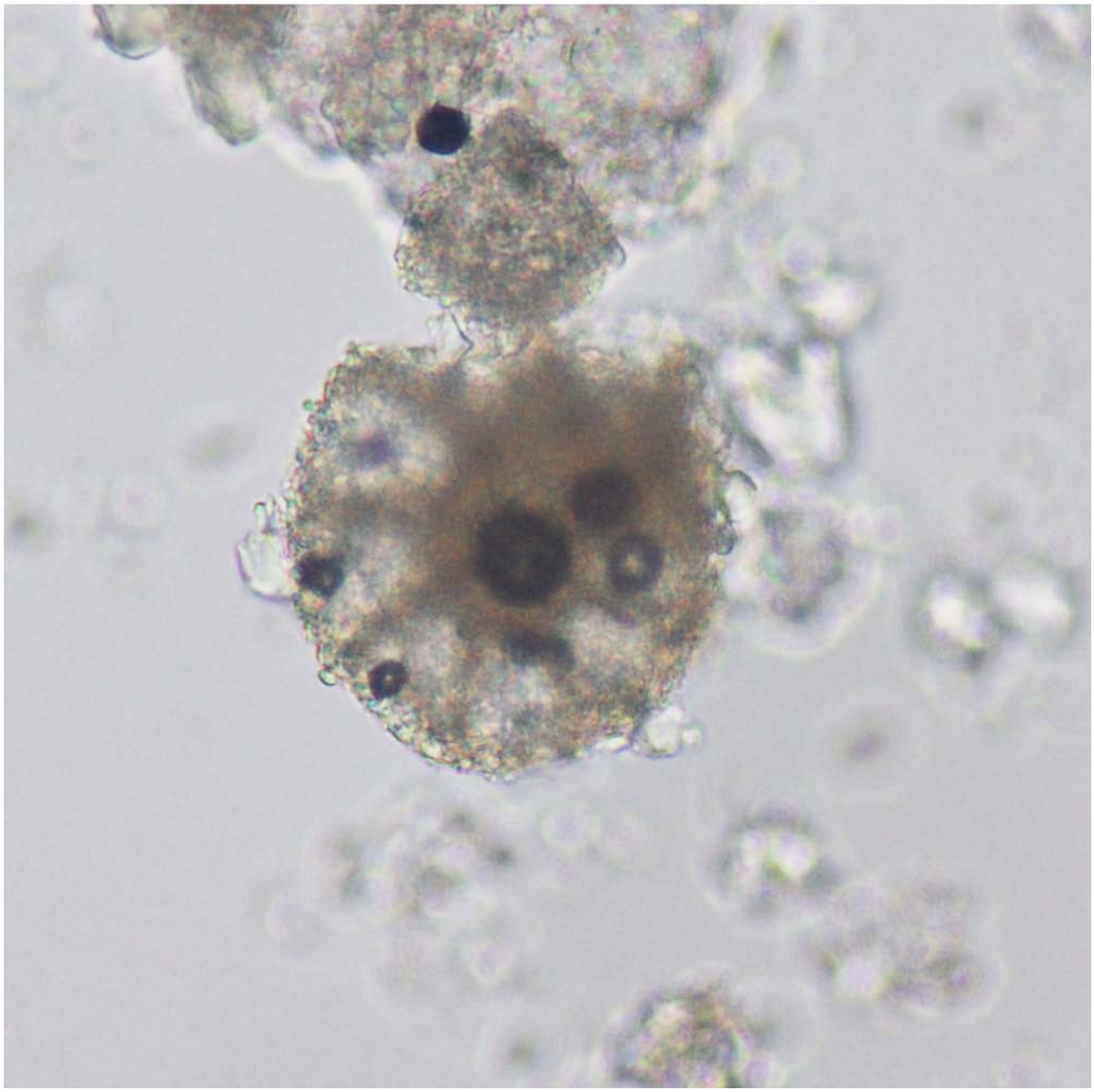

Carbonate 3.

This possible benthic foraminifer has its chambers filled with microcrystalline calcite cement.

DSDP Sample (late Eocene): Leg 21, Hole 209, Core 18, Section 1, 120 cm

Image ID: B0025/B0026

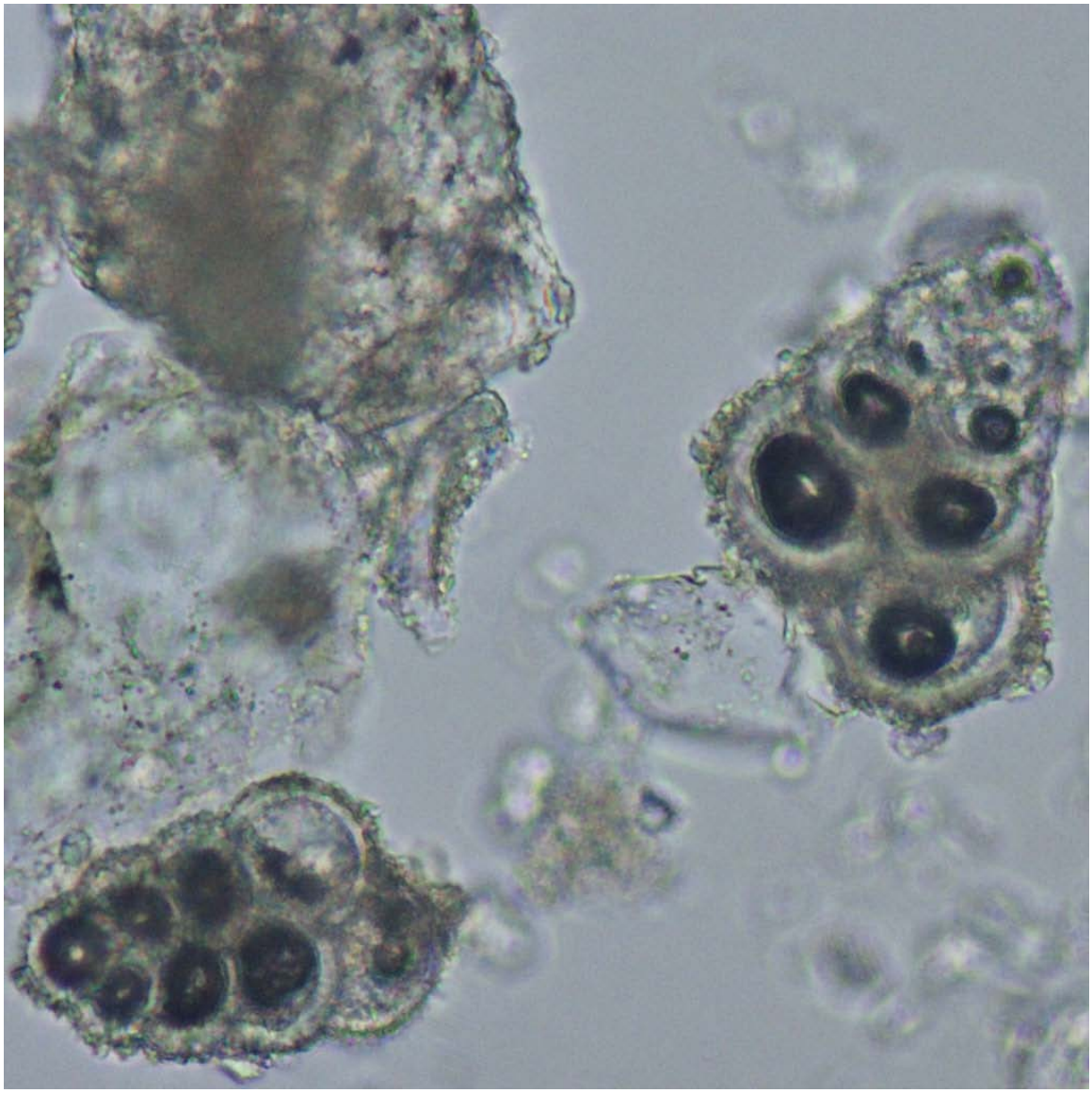

Carbonate 4.

These biserial planktic foraminifera are encrusted and filled with microcrystalline calcite cement.

DSDP Sample (late Eocene): Leg 21, Hole 209, Core 18, Section 1, 120 cm

Image ID: B0514/B0515

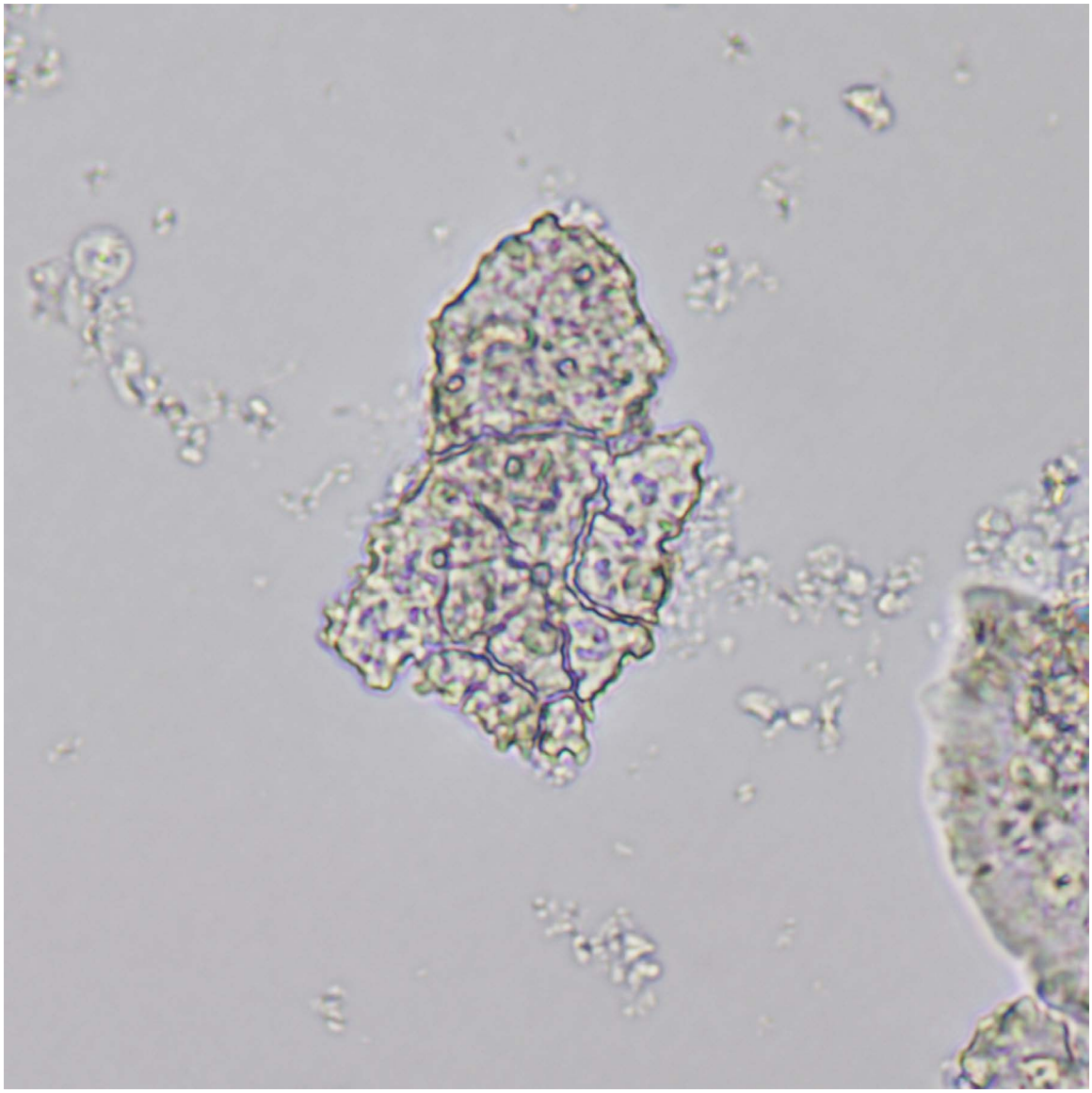

Carbonate 5.

This porous foraminifer fragment exhibits irregular micro-channels (microborings?) and is relatively nonbirefringent owing to its orientation on the slide.

ODP Sample (early Pliocene): Leg 121, Hole 752A, Core 2H, Section 5W, 20 cm

Image ID: B0750/B0751

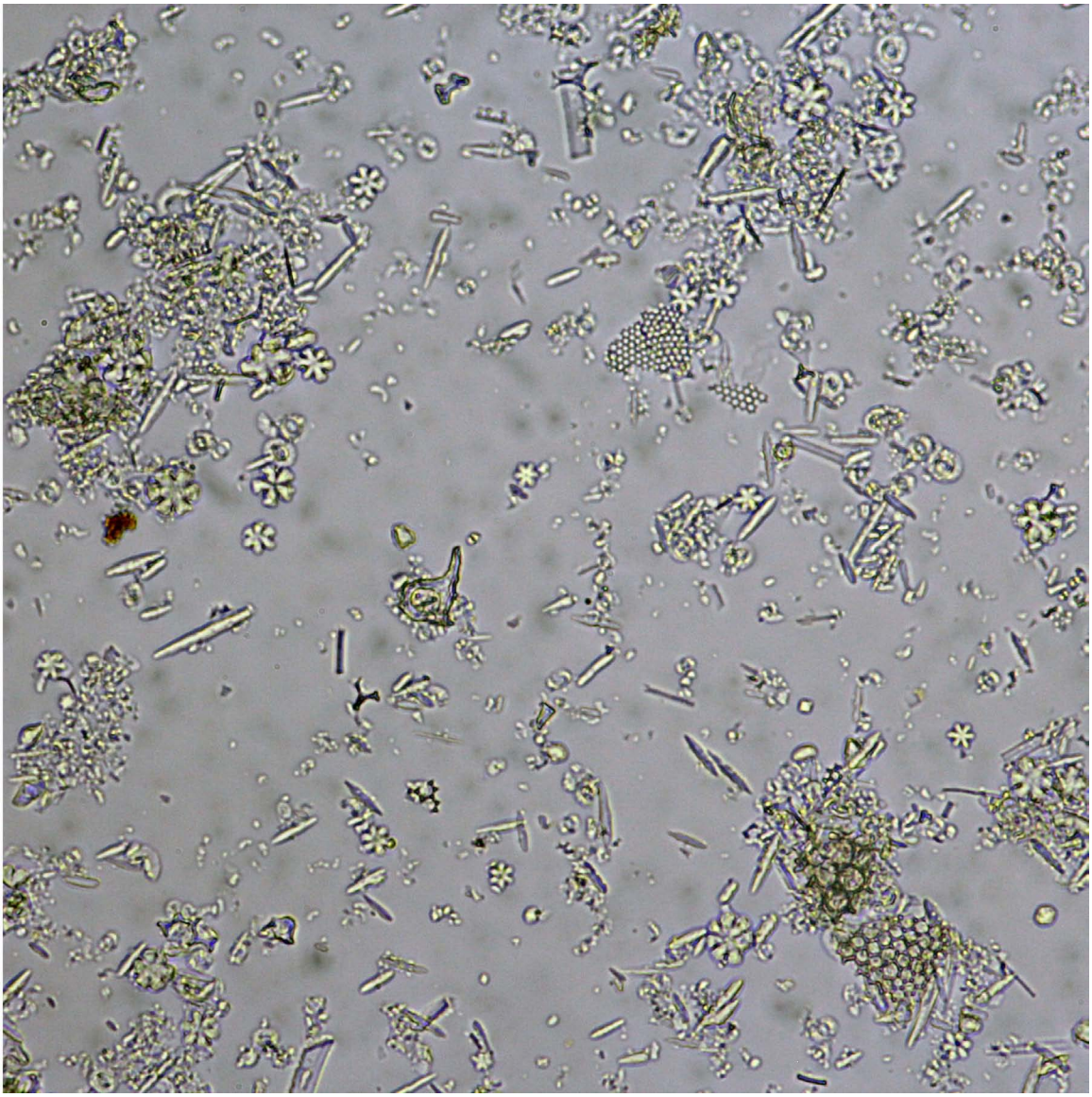

Carbonate 6.

Carbonate ooze with coccoliths, discoasters, and authigenic carbonate needles of uncertain mineralogy. Additional components include diatom fragments with characteristic cellular texture.

ODP Sample (late Oligocene/early Miocene): Leg 199, Hole 1219A, Core 6H, Section 2W, 6 cm

Image ID: B0588/B0589

Carbonate 7.

Calcareous bioclastic sediment where one fragment (thin echinoderm?) in center of the field of view exhibits carbonate overgrowth cementation. The carbonate cement is colorless and transluscent.

IODP Sample (late Eocene): Leg 342, Hole 209, Core 18, Section 1, 120 cm

Image ID: B0700/B0701

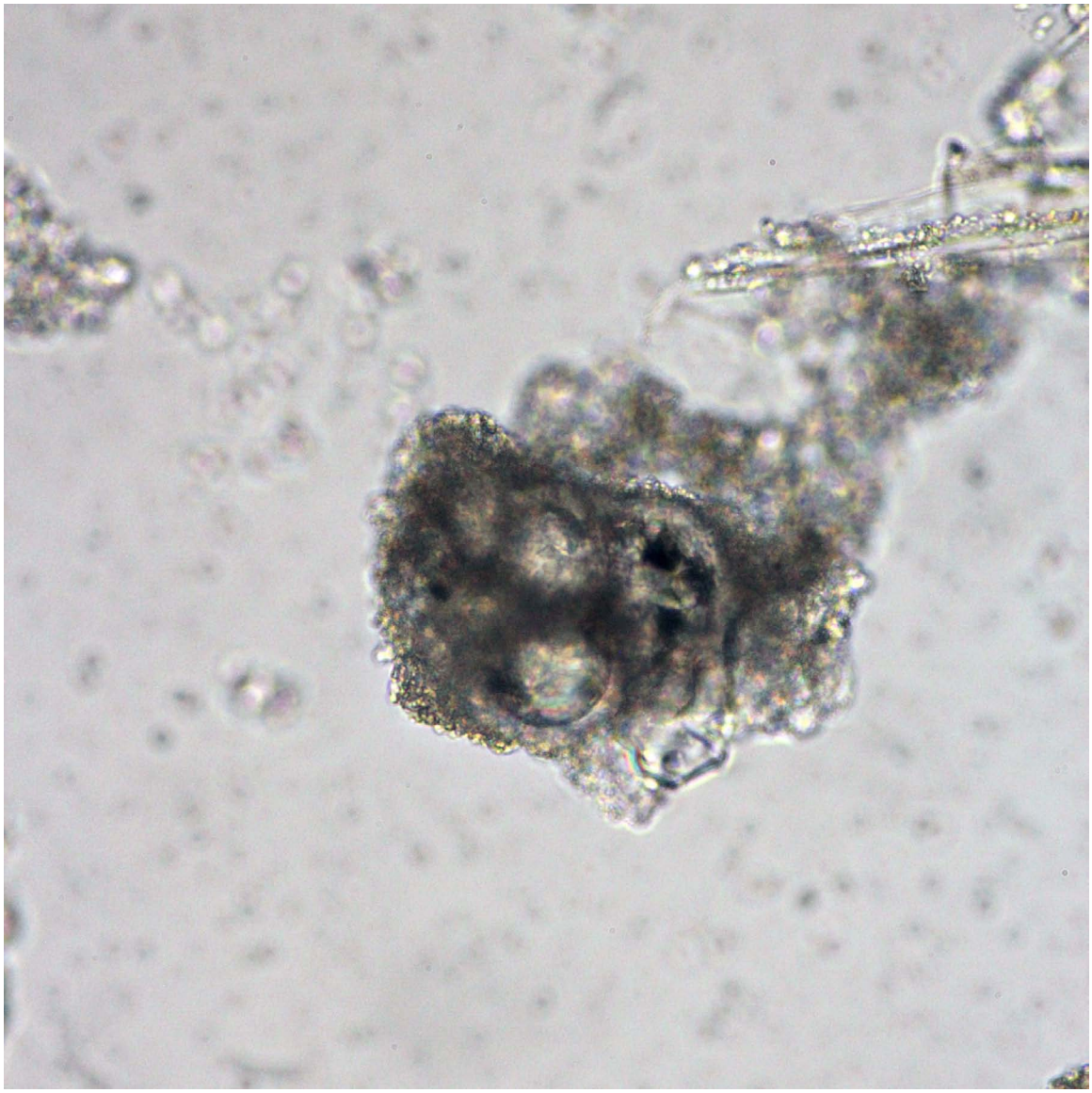

Carbonate 8.

The "ugly grain" in the center of this field of view is a recrystallized biserial foraminifer filled and partly encased by carbonate cement, indicating that the sediment is semilithified.

ODP Sample (Maastrichtian): Leg 130, Hole 807C, Core 57R, Section 2W, 70 cm

Image ID: B0306/B0307

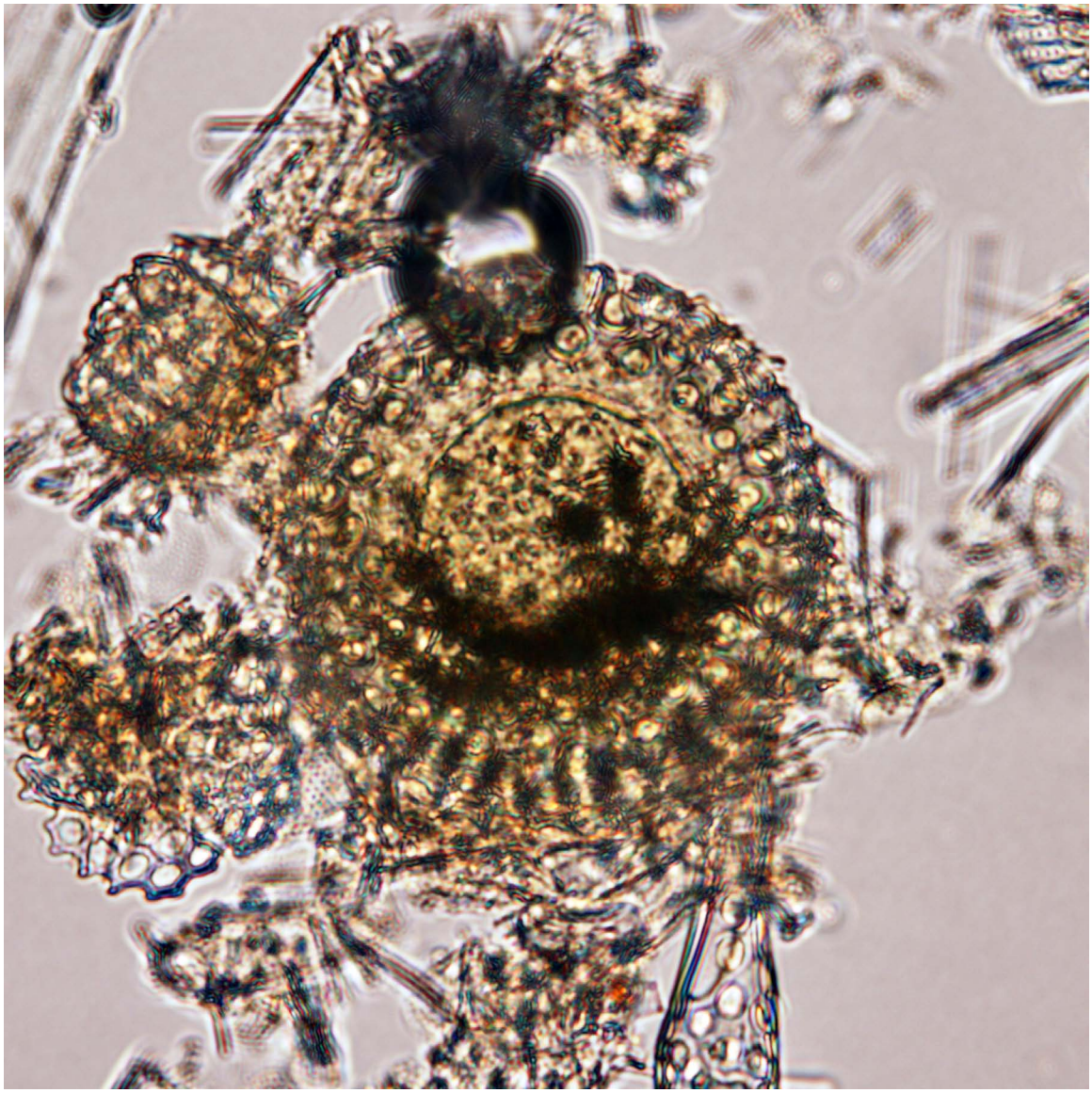

Glauconite 1.

Brownish green color of this radiolarian results from a filling of glauconite (possibly oxidized). Glauconite is a common feature of early marine diagenesis under conditions of slow sediment accumulation. Glauconite forms cements and surface crusts that are reworked as detrital particles.

ODP Sample (late Miocene): Leg 138, Hole 845A, Core 15H, Section 2W, 10 cm

Image ID: B0510/B0511

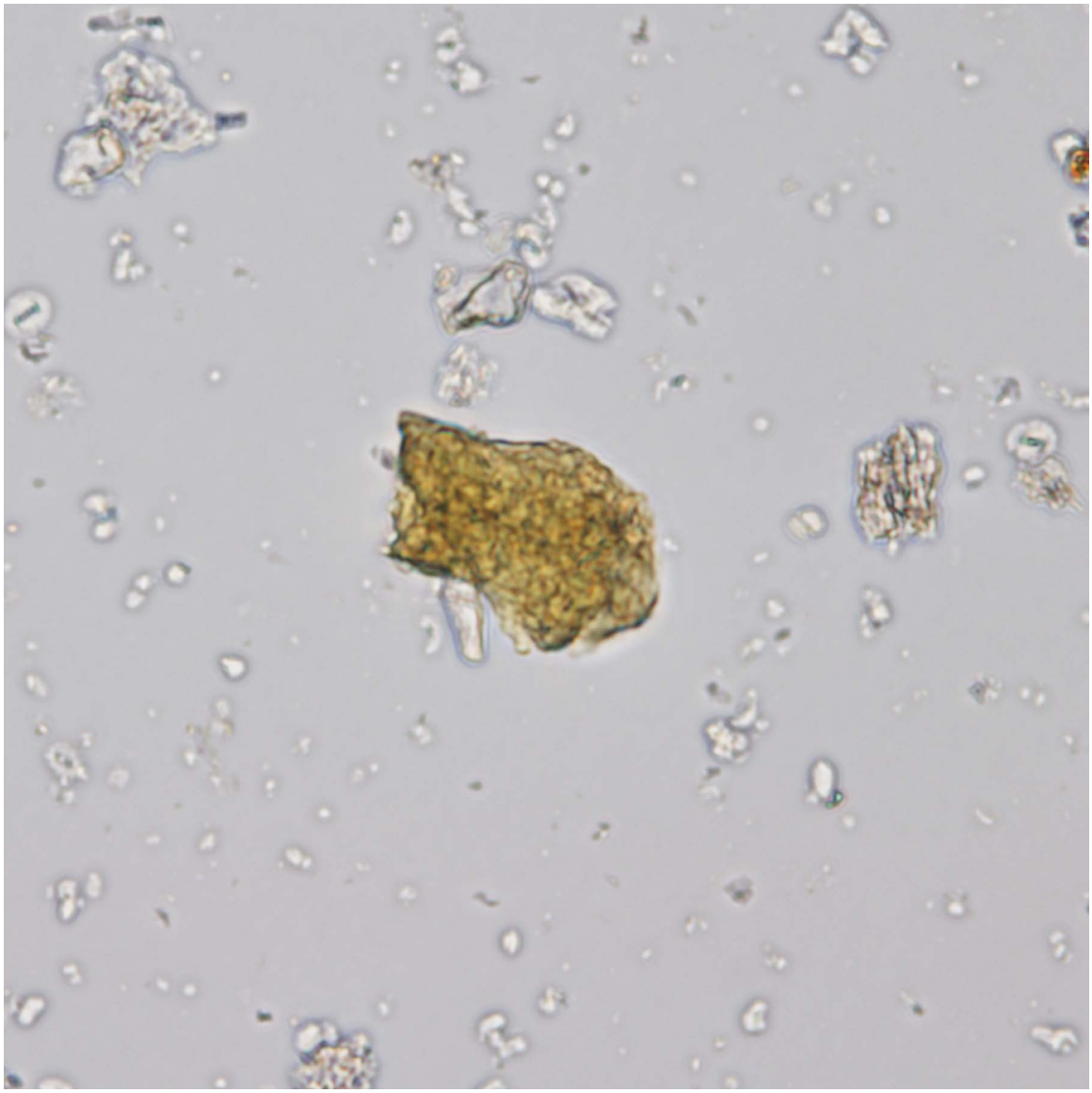

Glauconite 2.

The brownish color of this grain is not typical of glauconite except in cases where the glauconite is oxidized. The texture and birefringence as revealed by the cross-polar image is typical of glauconite however.

ODP Sample (Pleistocene): Leg 121, Hole 752A, Core 1H, Section 6W, 90 cm

Image ID: B0115/B0116

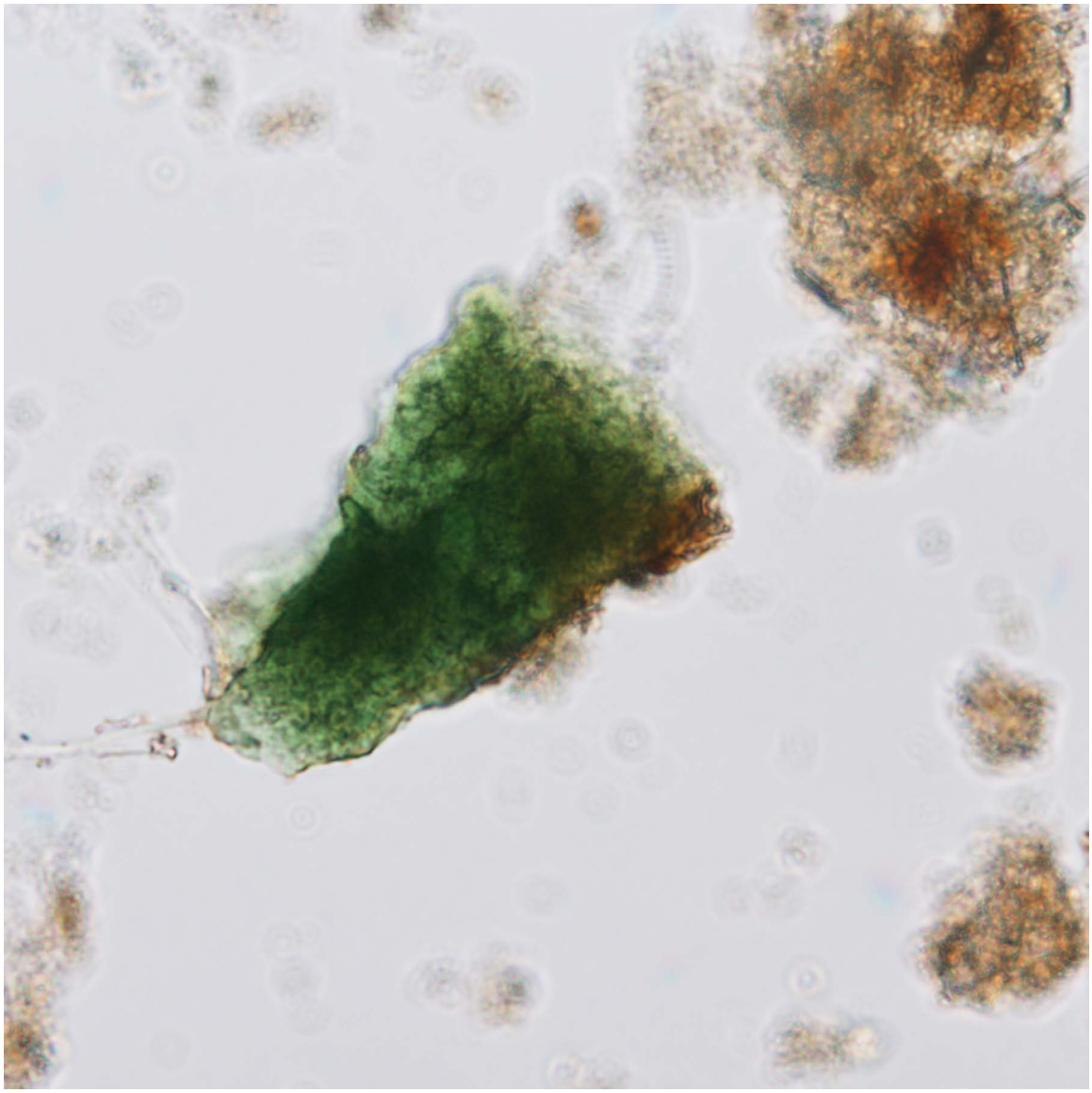

Glauconite 3.

This grain is the typical color and texture of glauconite ($(K,Na)(Fe_3+,Al,Mg)_2(Si,Al)_4O_{10}(OH)_2$), lacking only the usual rounded (pellet) shape.

ODP Sample (early Miocene): Leg 112, Hole 688E, Core 26R, Section 1W, 65 cm

Image ID: B0119/B0120

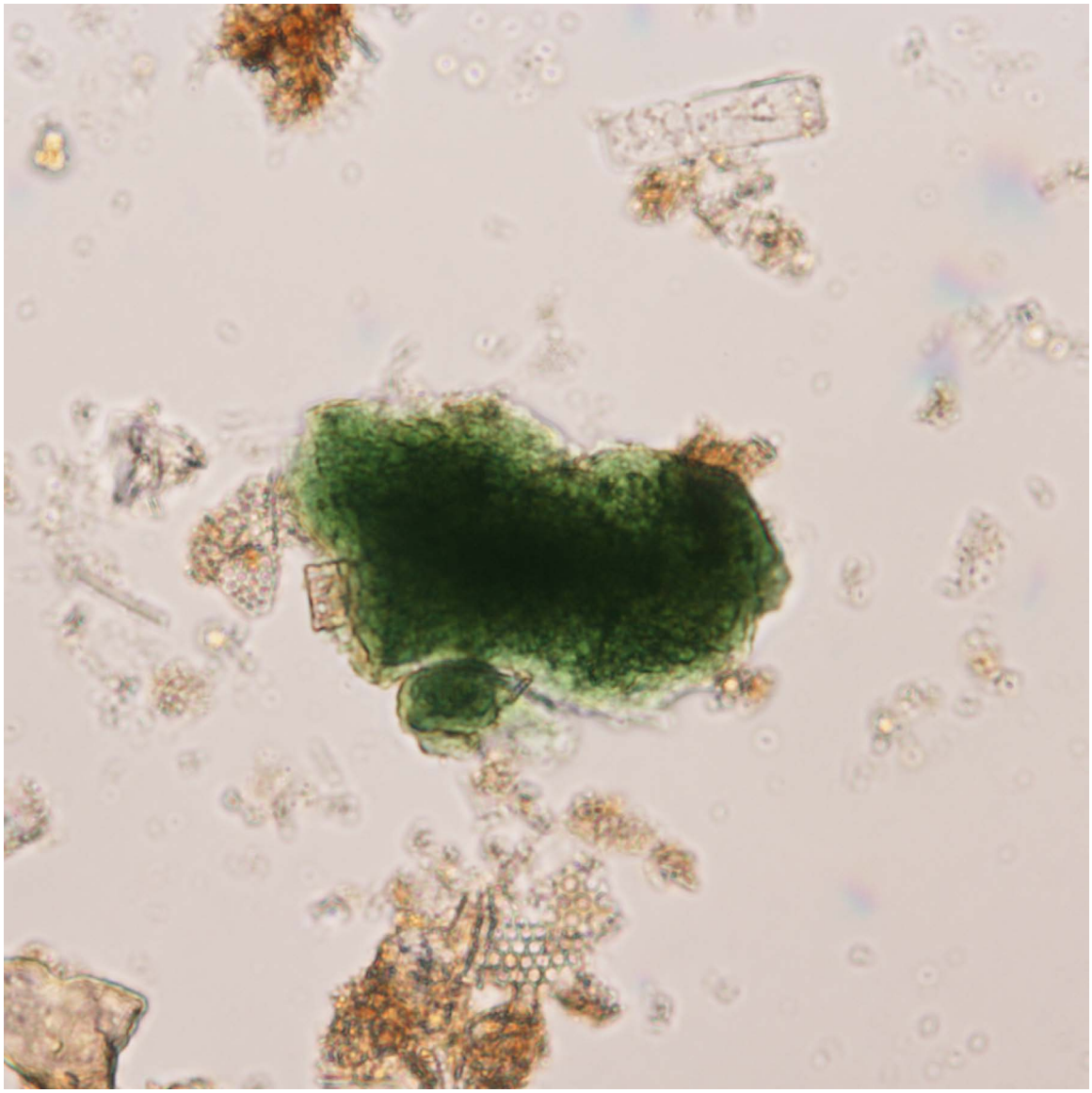

Glauconite 4.

Like glauconite 3 this grain shows typical color and texture but not the typical rounded (pellet) shape.

ODP Sample (early Miocene): Leg 112, Hole 688E, Core 26R, Section 1W, 65 cm

Image ID: B0286/B0287

Glauconite 5.

This is a typical glauconite grain with associated bio-siliceous debris (mostly diatoms).

ODP Sample (Quaternary): Leg 119, Hole 745B, Core 5H, Section 1W, 65 cm

Image ID: B0529/B0530

Silica 1.

The grain in this field of view is a silicified radiolarian with zoned chalcedony. The yellow to red birefringence of the silica indicates the grain is slightly thicker than 30 microns.

ODP Sample (Albian-Cenomanian): Leg 130, Hole 807C, Core 71R, Section 6W, 95 cm

Image ID: B0527/B0528

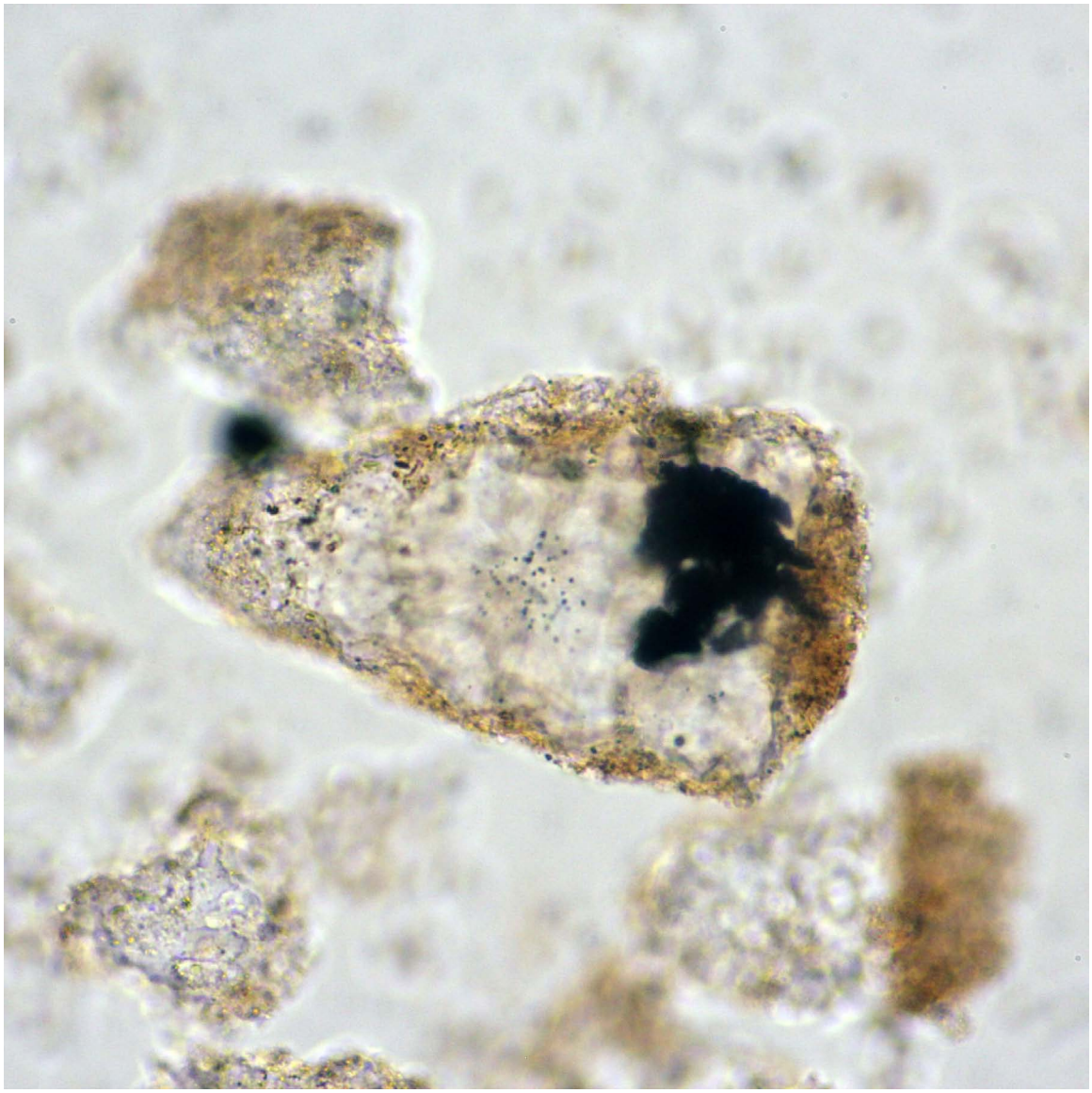

Silica 2.

The grain in this field of view is a silicified cone-shaped Nassellarian radiolarian partly filled by opaques (pyrite?) with adhering birefingent host clay-rich sediment.

ODP Sample (Albian-Cenomanian): Leg 130, Hole 807C, Core 71R, Section 6W, 95 cm

Image ID: B0522/B0523

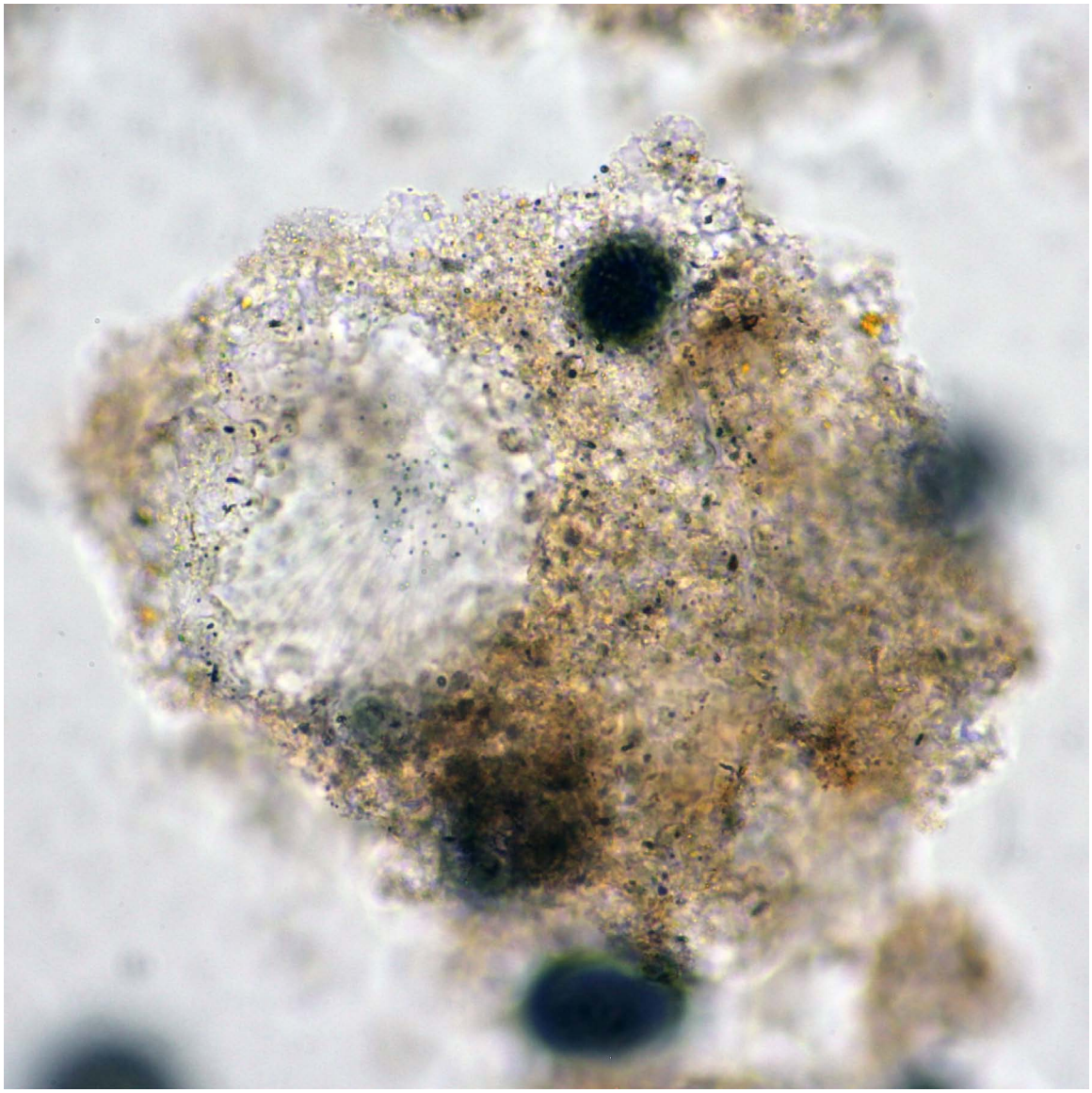

Silica 3.

This a silicified radiolarian set in a fragment of partly silicified clay-rich host sediment. Note the slight fibrous texture to the pore-filling silica.

ODP Sample (Albian-Cenomanian): Leg 130, Hole 807C, Core 71R, Section 6W, 95 cm

Image ID: B0520/B0521

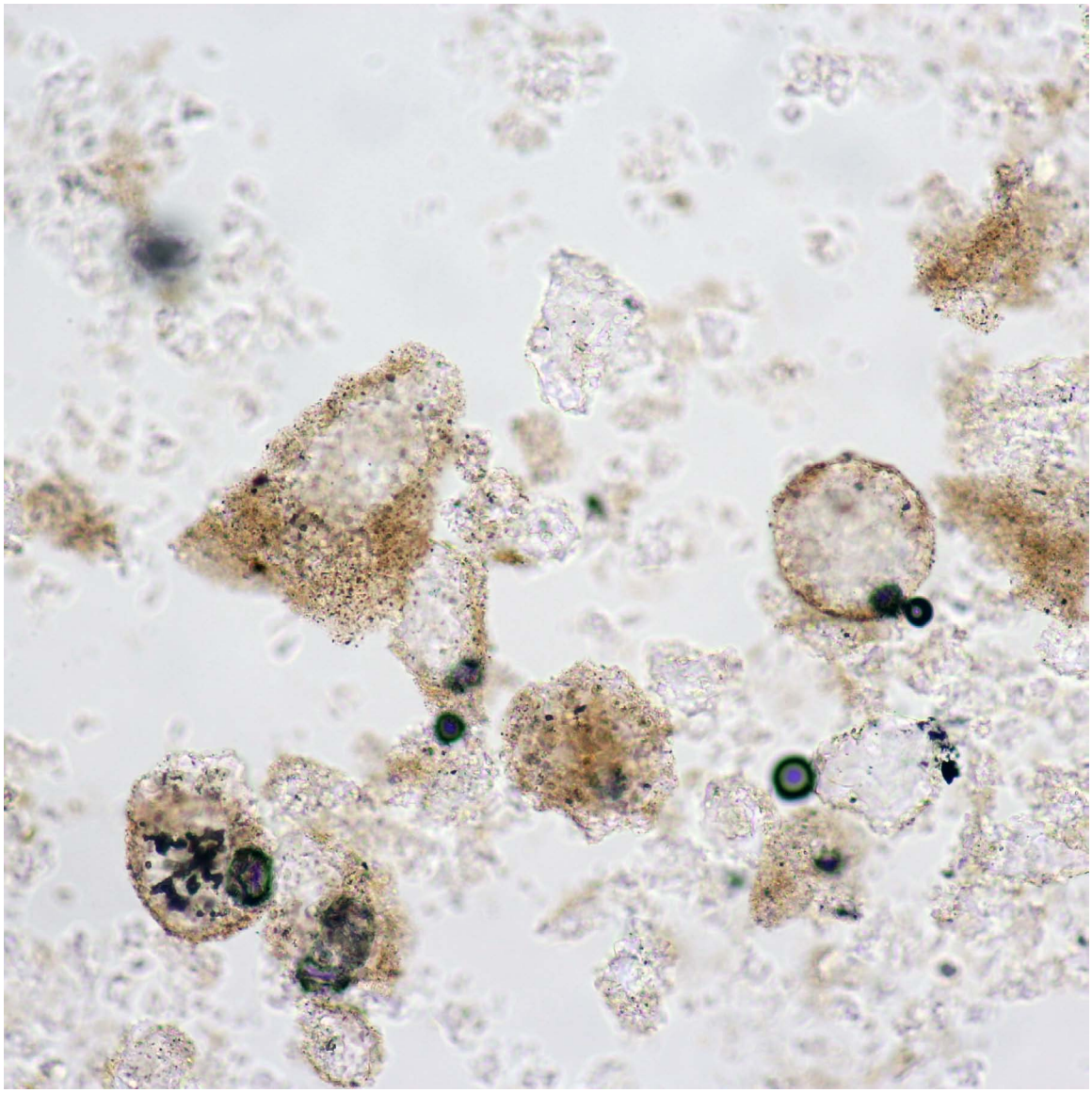

Silica 4.

View of semilithified radiolarian clay with circular to cone-shaped, silica-filled and replaced radiolarian. Some dark blebs are opaque minerals (pyrite?), others are bubbles in the epoxy.

ODP Sample (Albian-Cenomanian): Leg 130, Hole 807C, Core 71R, Section 6W, 95 cm

Image ID: B0223/B0224

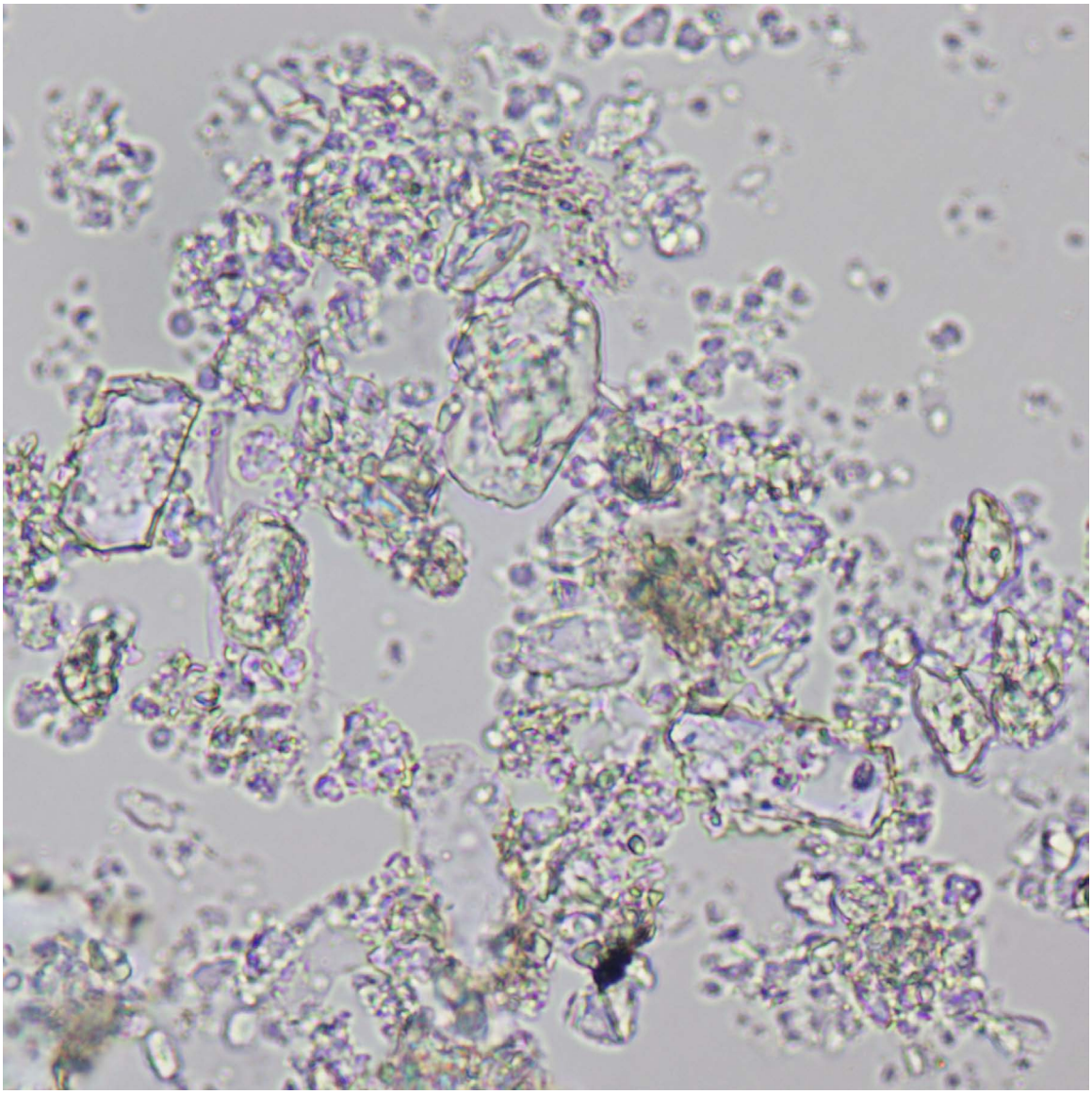

Zeolite 1.

Mix of anhedral calcite of silt- and clay-size and near-isotropic crystals of low-relief and euhedral to subhedral form that are probably zeolites. One crystal with typical clinoptilolite form is circled.

ODP Sample (middle Eocene): Leg 110, Hole 672A, Core 95X, Section CC, 110 cm

Image ID: B0142/B0143

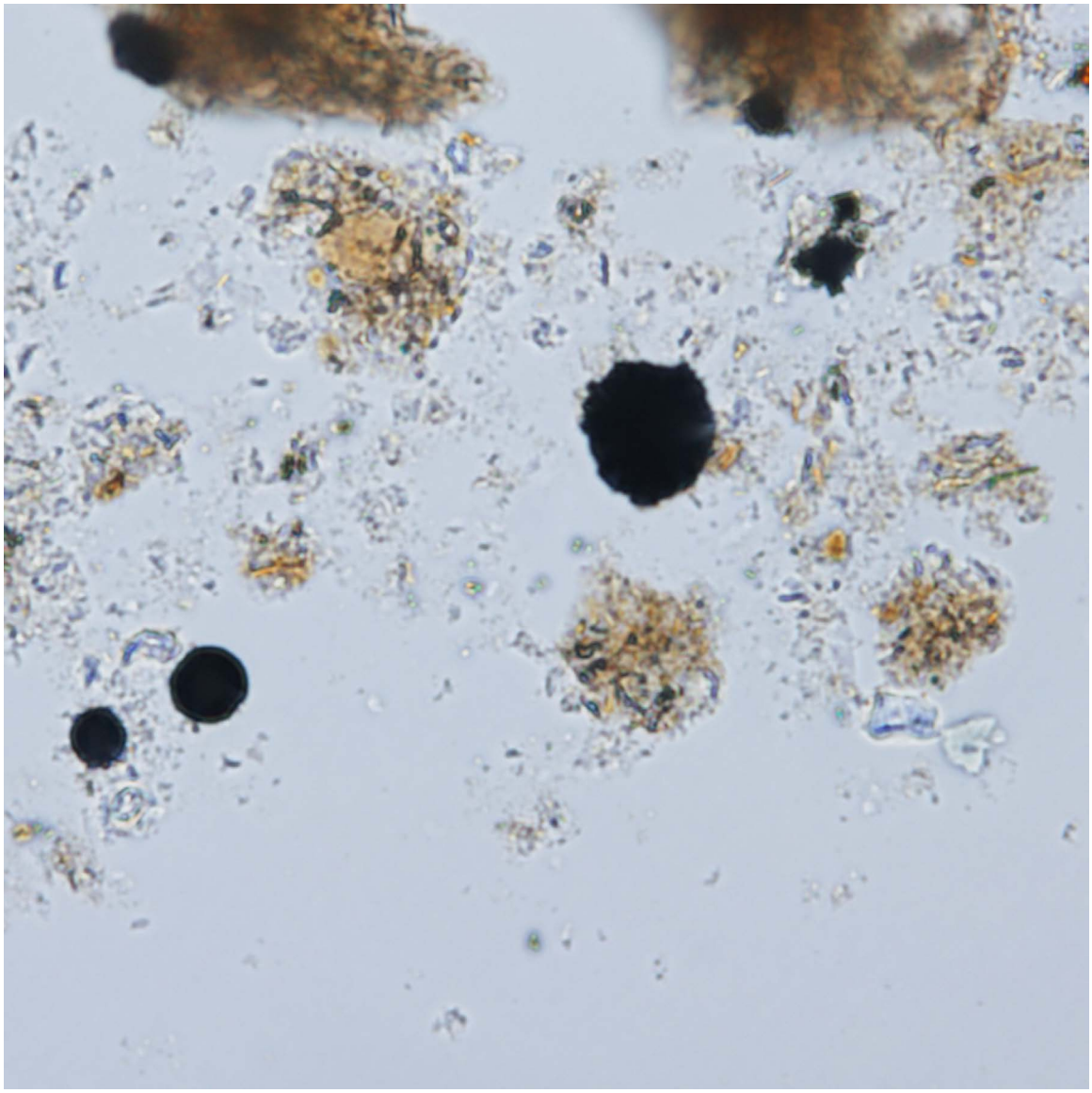

Pyrite 1.

Isolated pyrite (FeS_2) framboids are opaque in transmitted light. A reflected light source must be used to see the typical gold metallic color.

ODP Sample (middle Eocene): Leg 112, Hole 688E, Core 35R, Section 1W, 80 cm

Image ID: B0152/B0153

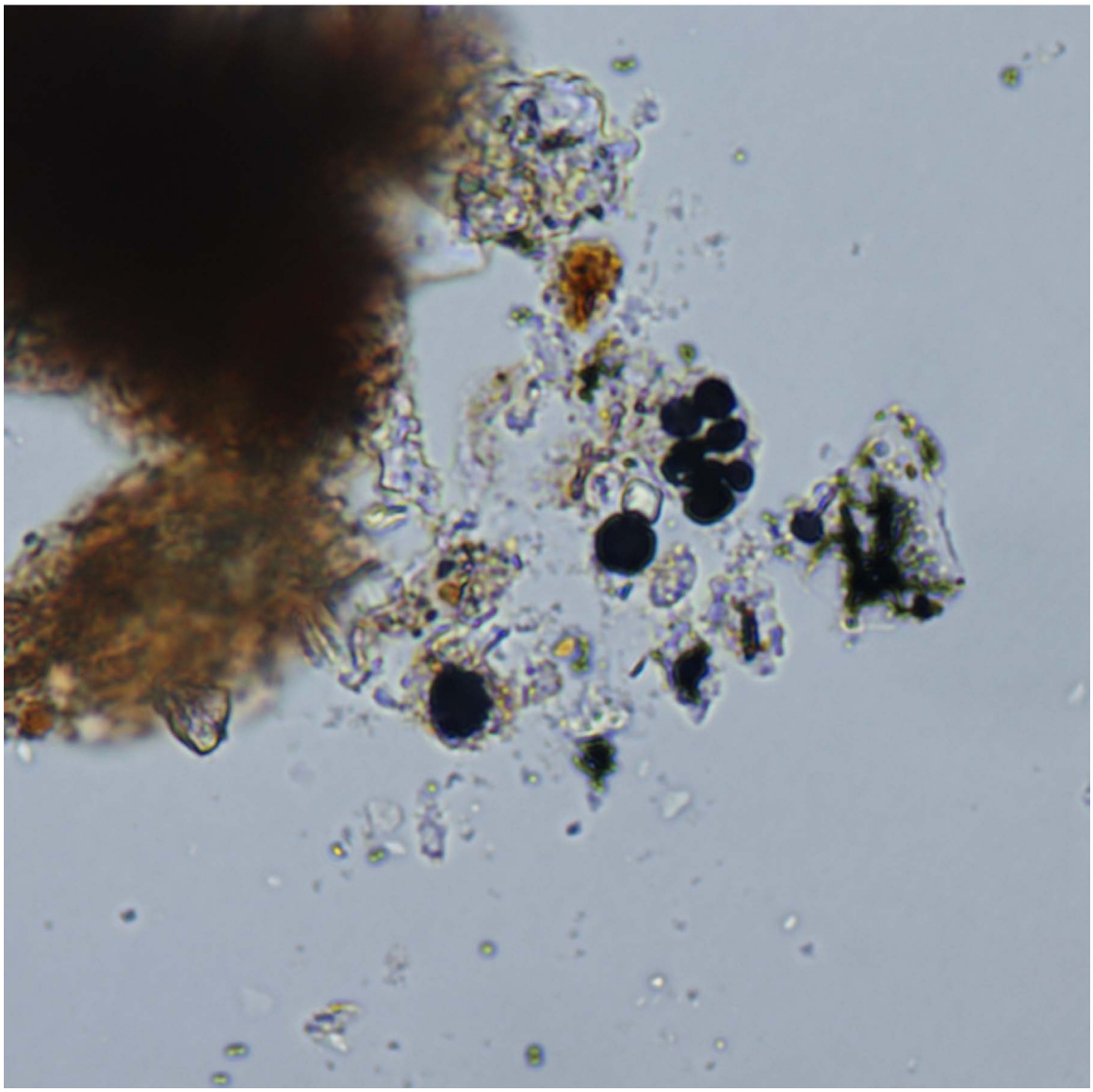

Pyrite 2.

Opaque, isolated pyrite framboids and a framboid cluster are present in this field of view. Both habits are common for pyrite in marine sediments.

ODP Sample (middle Eocene): Leg 112, Hole 688E, Core 35R, Section 1W, 80 cm

Image ID: 0071

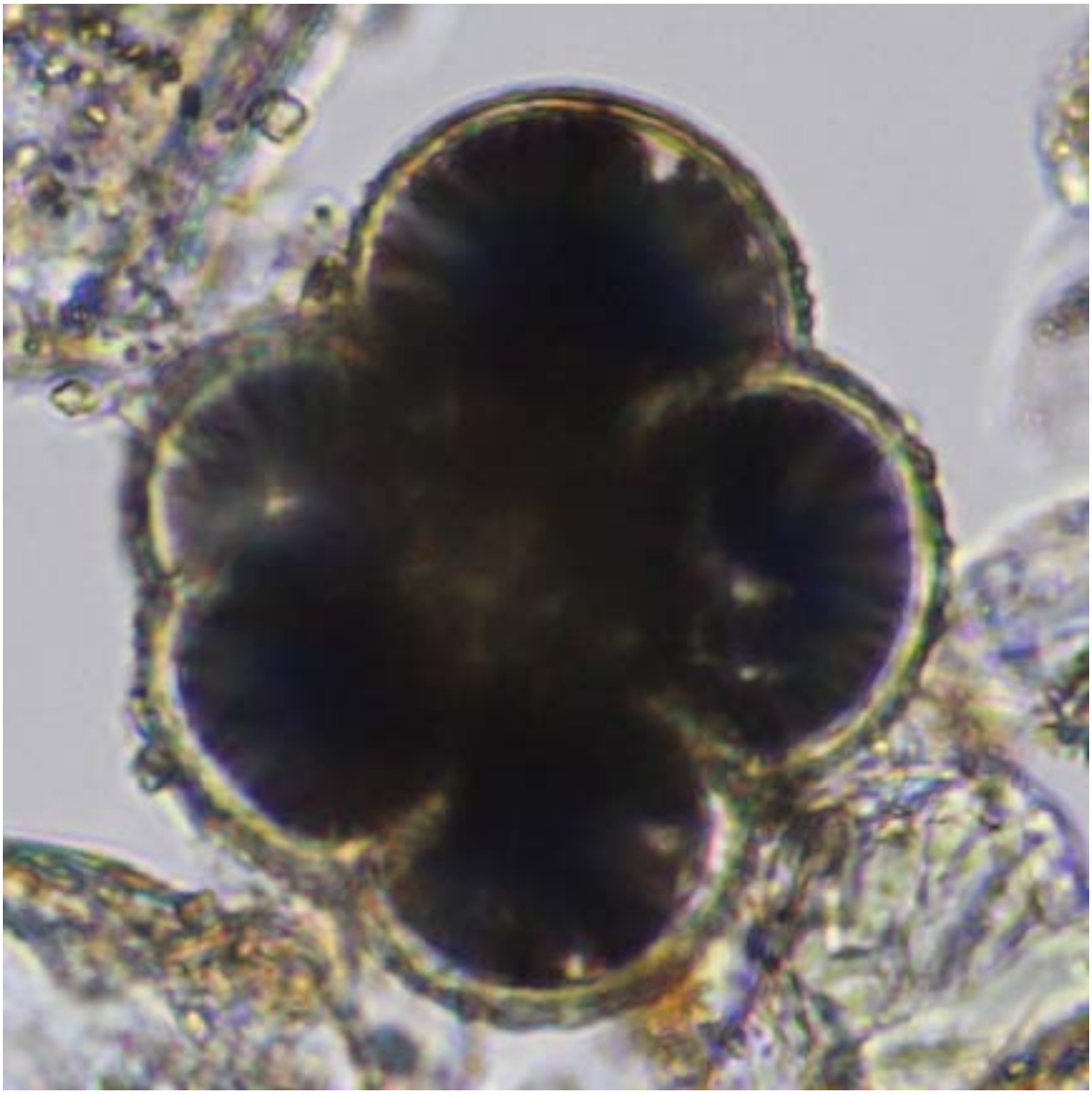

Pyrite 3.

A pyrite-filled foraminifer. Foraminifer chambers provide locally reducing environments favorable for localized nucleation of pyrite in sediment that may have been more generally under oxidizing conditions.

ODP Sample (middle to late Pleistocene): Leg 181, Hole 1119C, Core 10A, Section 2W, 125 cm

Image ID: B0355/B0356

Pyrite 4.

The dark, nearly opaque fillings with these foraminifer chambers may contain pyrite or they may be a mixture of pyrite, organic matter, and detrital clay.

ODP Sample (Pliocene): Leg 101, Hole 628A, Core 2H, Section 1, 47 cm

Image ID: B0205/B0206

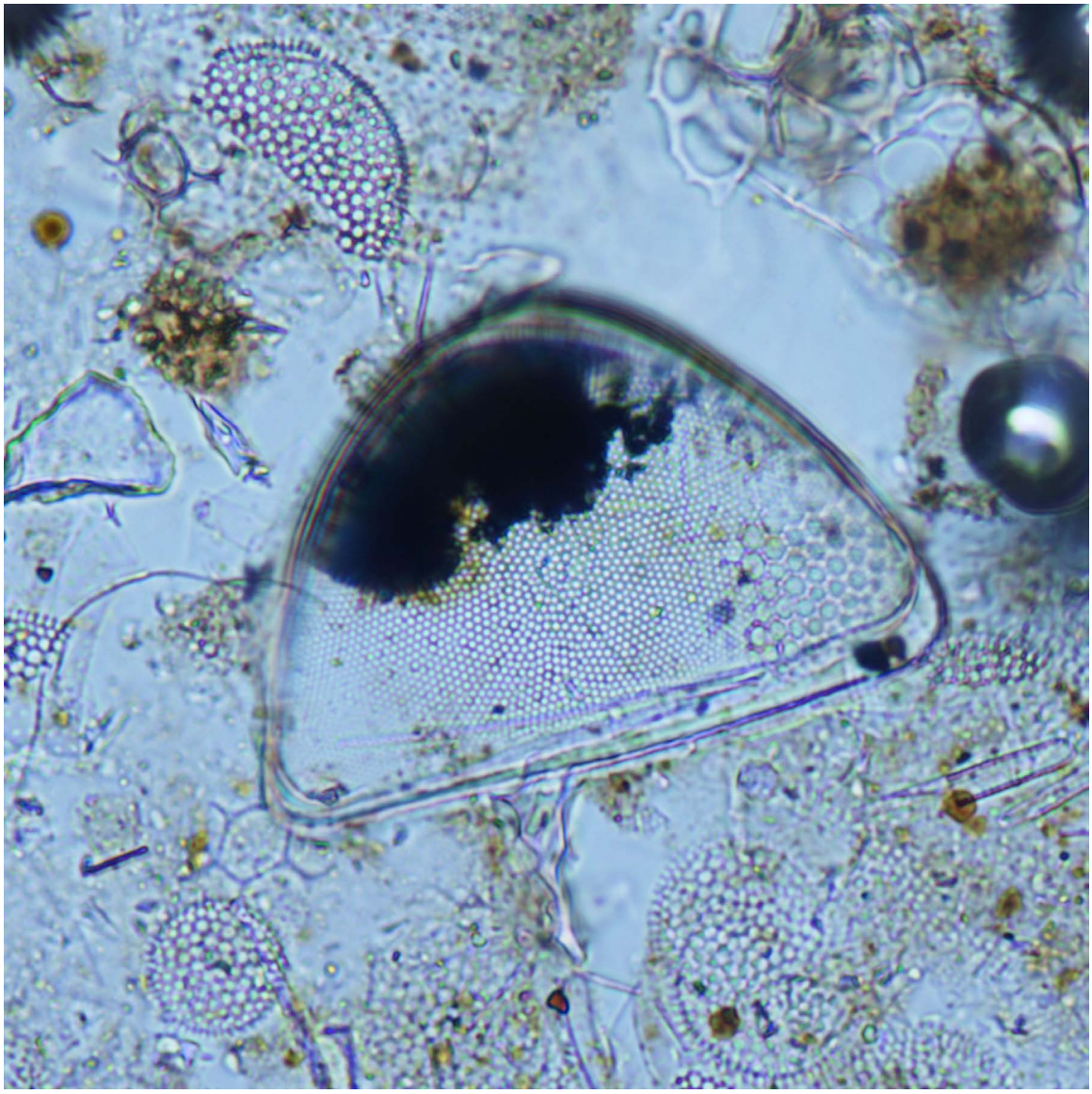

Pyrite 5.

This diatom frustrule is partly filled with microcrystalline pyrite.

ODP Sample (Pleistocene): Leg 138, Hole 845A, Core 1H, Section 1W, 66 cm

Image ID: B0458/B0459

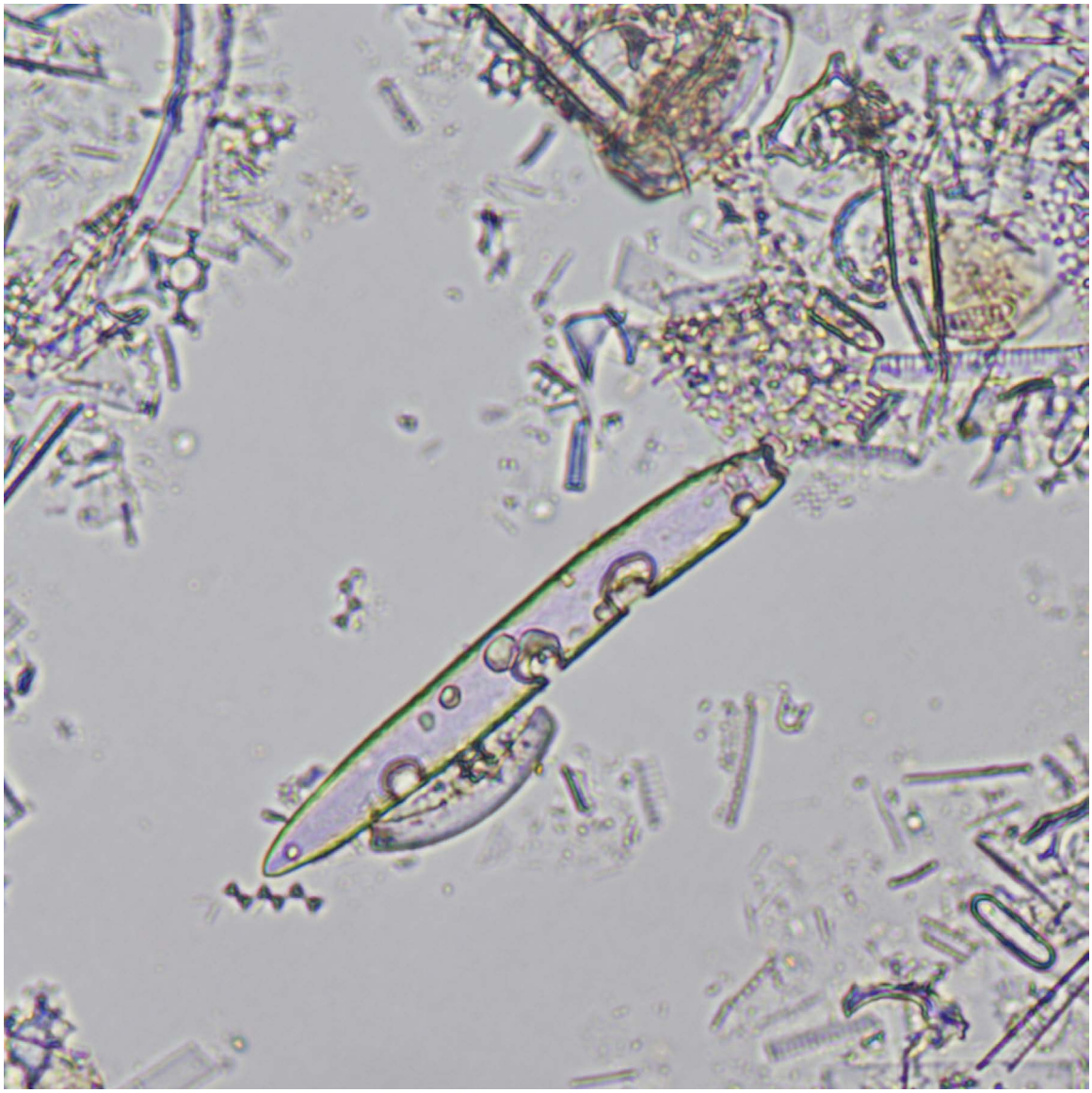

Dissolution 1.

Sponge spicule with borings. Diagenesis includes both chemical and mechanical processes and in both cases the agent of those processes can be biologic. Here a sponge spicule has been eaten away, most likely by a boring organism. Alternative explanation would be that this is a purely inorganic dissolution, but in such a case we would expect to see other spicules similarly affected. Associated grains are diatoms.

ODP Sample (middle Miocene): Leg 113, Hole 690B, Core 5H, Section 4W, 67 cm

Image ID: B0693/B0694

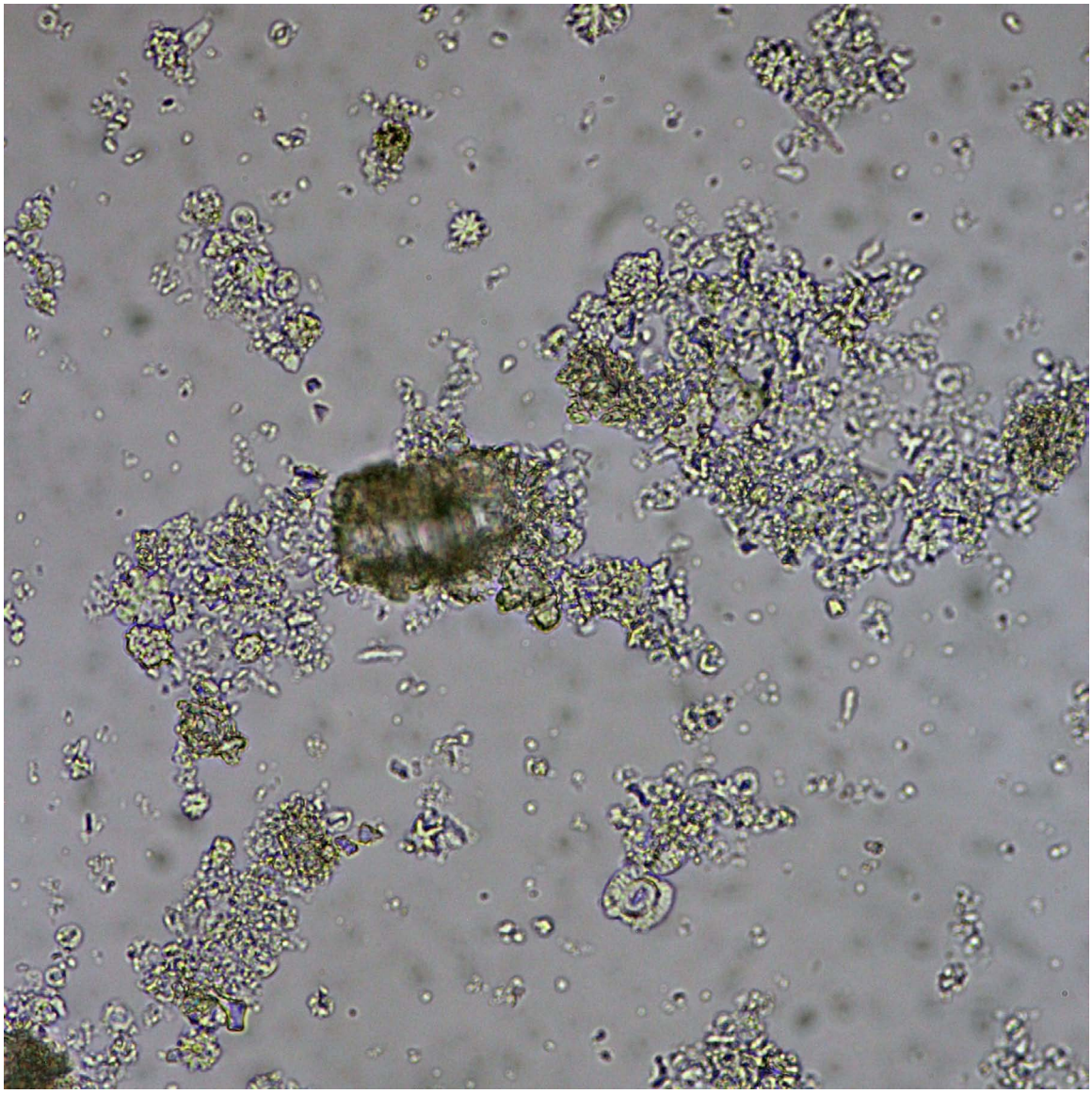

Dissolution 2.

In this nannofossil ooze there is evidence for dissolution of one of the larger coccoliths in the lower center where it appears as blunted rather than fully oval (circled).

ODP Sample (late Eocene): Leg 130, Hole 24R, Core 2W, Section 35, 35 cm

Micrite

INTRODUCTION TO MICRITE

Micrite is one of several terms applied in thin section and smear slide descriptions to crystalline clay-size carbonate (<4 μm) matrix of potentially biogenic and authigenic origin. Micarb and carbonate mud are essentially synonyms for micrite. Modern carbonate mud in deeper marine environments is typically dominated by calcite and Mg-calcite though significant components of aragonite and dolomite are common. Mineralogy of clay-size carbonate needs to be confirmed by XRD bulk analysis as the optical properties of these possible carbonate minerals are not definitive (no matter the crystal size). Most micrite is believed to form by the mechanical breakdown of skeletal carbonate, including that formed in the water column and on the sea bed. By the time the particles have been reduced to clay-size, however, identification of the original grain type is challenging using light microscopy alone. Calcareous nannoplankton and benthic algae are two sources of voluminous carbonate mud. Calcareous nannonplankton (LINK to SECTION) dominate in carbonate-rich sediments of the deep sea, whereas the remains of calcareous algae are a feature of slope environments that receive sediments generated in the surrounding shallow-water carbonate factories. Clay-size nannoplankton often retain ultrastructure sufficient to be identifiable in smear slides. When lithified into chalk, nannoplankton components become less distinct especially when viewed in thin section, where the term micrite is often applied to the bulk sediment, and micritic carbonate is in part authigenic (including both cement and grain replacement). Samples partially transitioned from nannofossil ooze to chalk appear in smear slides as mixtures of nannofossils, with increasing birefringence and overgrowth, accompanied by finely crystalline authigenic carbonate.

Description of carbonate mud is one of the great challenges of smear slide petrography and presents an opportunity to stretch your powers of observation. Very fine silt and clay-size particles are smaller than the standard 30 micron thickness that is used for assessment of birefringence and thus they display lower-order colors under cross polarization than we typically associate with these minerals. It is advised that you make your first shipboard estimates of carbonate content on samples that are then tested by XRD, allowing you to calibrate your eye. In general, the particle size of micrite is coarser than typical clay-size clay minerals, typically in the range of 0.5 to 4 micrometers whereas clay mineral particles are much smaller, typically 1 micrometer or less. Fine-grained carbonate sediment has considerable reaction potential in early diagenesis, especially the Mg-calcite and aragonite components. Such grains may dissolve and then reprecipitate as authigenic calcite. The incipient stages of this process may occur prior to significant lithification (as described above), and thus, it is good to carefully inspect the micrite for evidence of crystal euhedra.

Find a portion of the slide where there particles are well dispersed and using the highest magnification objective focus your attention on the particles from about 4 microns to the smallest ones you can see, in both plane- and cross-polarized light. In

plane light, most carbonate crystals will manifest a distinct change in index with rotation of the stage, helping you to discriminate tiny carbonate from tiny quartz and feldspar. First, note carbonate particles that can be attributed to identifiable allochems such as nannofossils (link to section). Next, turn your attention to particles that cannot be readily assigned to known taxa. Observe the range of particle shapes (equant, bladed, or needle-like) and the degree of euhedrality (anhedral, subhedral, euhedral). Note whether the grains are mono- or polycrystalline. In samples where micrite has begun to lithify by precipitation of grain-binding cement the sediment may no longer disperse well during smear slide production and the micrite may appear as microcrystalline aggregates. Nonetheless, these small fragments of lithified sediment can be observed in smear slides and observations can be made on the size, shape, and euhedrality of the component crystals.

Changes in the character of the micrite across the stratigraphy may relate to changes in the mix of sediment sources as well as to diagenesis. Thus, careful observations of this finest fraction can yield useful data that can be combined with observation of the silt-size fraction to give a more comprehensive sediment description.


Micrite 1

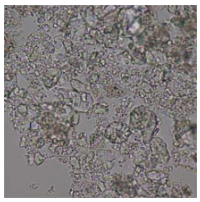
Micrite 2

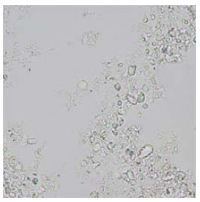
Micrite 3


Micrite 4


Micrite 5


Micrite 6

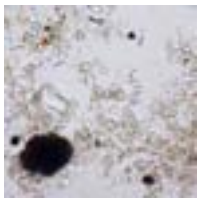
Micrite 7


Micrite 8


Micrite 9

Image ID: B0363/B0364

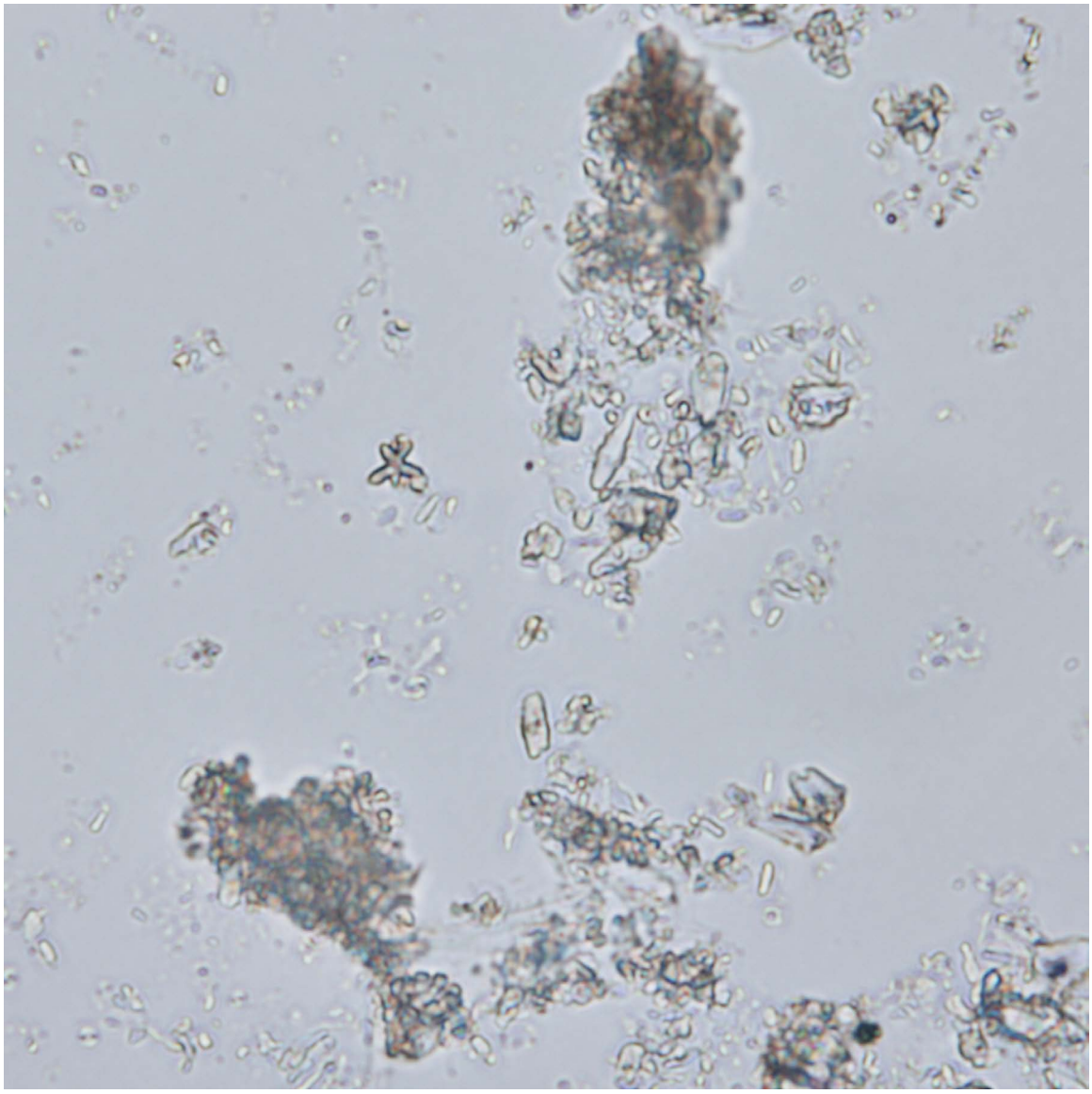

Micrite 1.

Birefringent silt-sized carbonate (micrite) of uncertain (biogenic?) origin intermixed with calcareous nannofossils including coccoliths and discoasterids. Sediment from Little Bahama Bank.

ODP Sample (late Miocene): Leg 101, Hole 628A, Core 4H, Section 3, 95 cm

Image ID: B0097/B0098

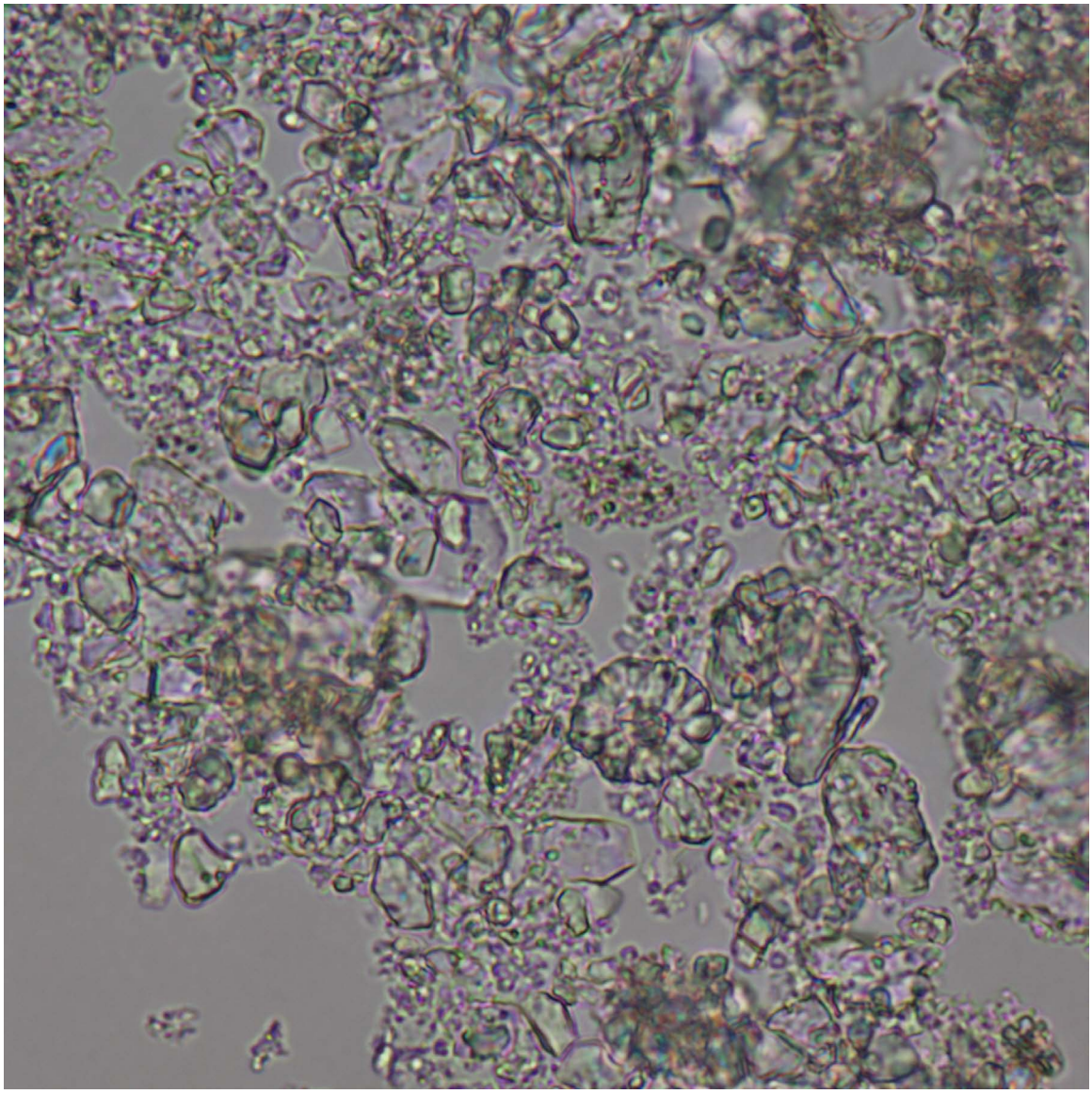

Micrite 2.

Birefringent anhedral silt-sized carbonate (micrite) of uncertain origin. Note the circular slightly birefringent recrystallized nannofossil in lower center (circled) that suggests at least some of the carbonate is of biogenic origin. Sediment from Blake Plateau.

ODP Sample (early-middle Cenomanian): Leg 101, Hole 627A, Core 42, Section 4, 145 cm

Image ID: B0099/B0100

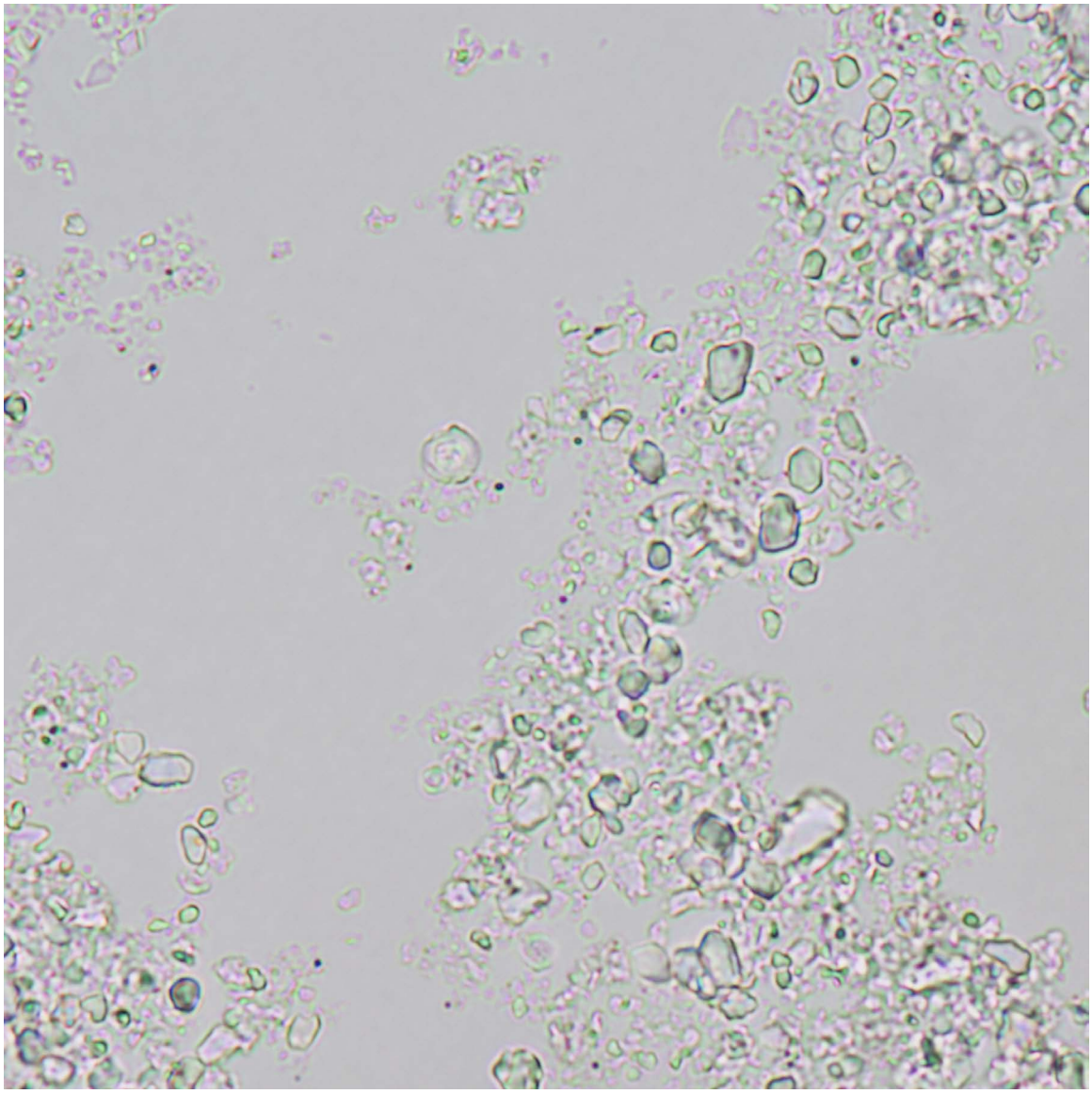

Micrite 3.

Calcareous ooze consisting of a mix of lower relief circular nannofossils with low birefringence (swirls) and slightly higher relief anhedral silt-sized carbonate (micrite) of uncertain origin, potentially bioclastic debris such as fragments of Braarudosphaerid nannofossils. Sediment sample from Blake Plateau.

ODP Sample (early-middle Cenomanian): Leg 101, Hole 627A, Core 42, Section 2, 145 cm

Image ID: B0019/B0020

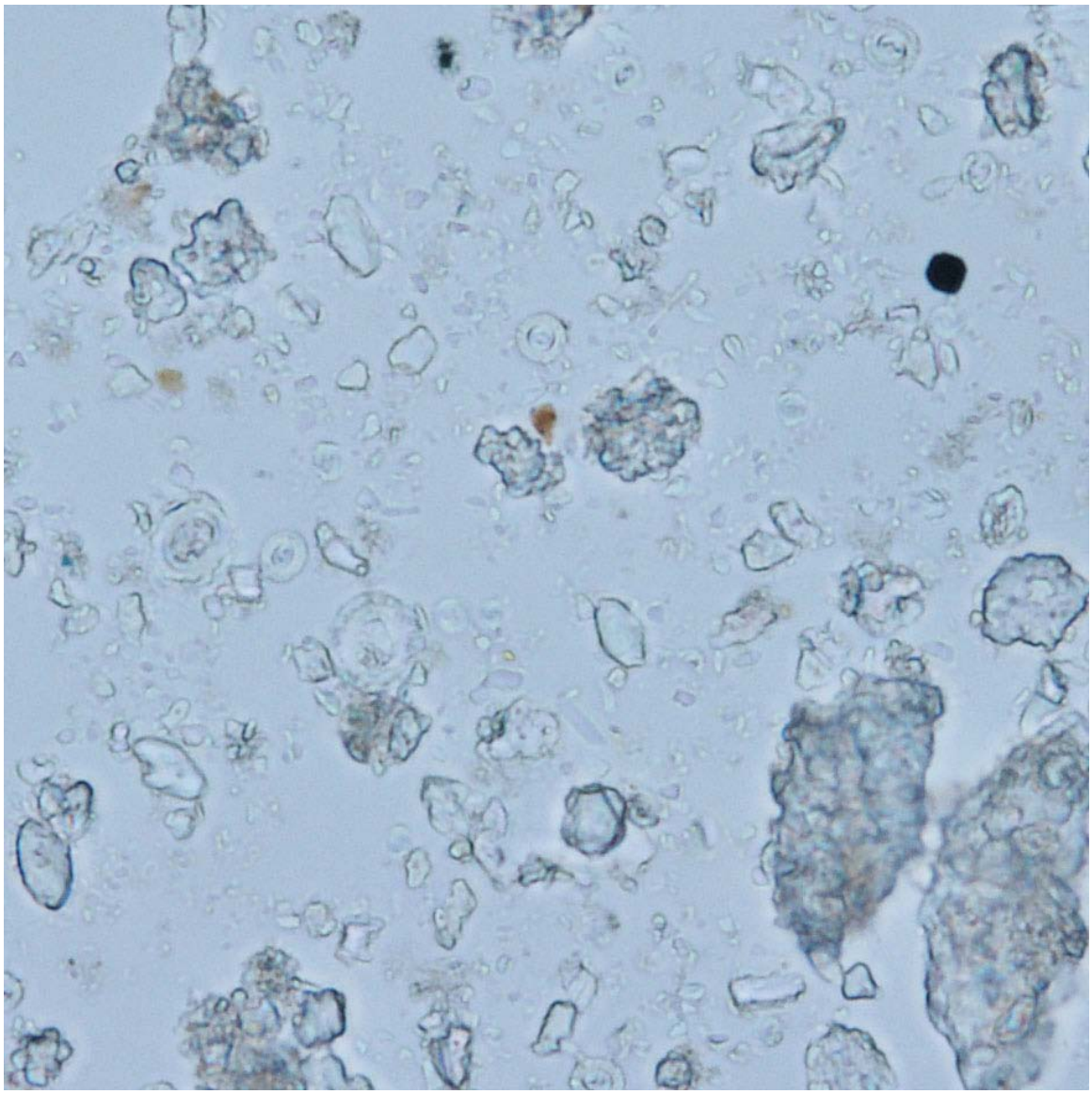

Micrite 4.

Calcareous ooze consisting of a mix of lower relief circular nannofossils with low birefringence (swirls) and slightly higher relief anhedral silt-sized carbonate (micrite) of uncertain origin. The larger higher relief sand-sized bits are likely fragments of foraminifera or lithified bits of chalk. The latter is more likely as this is Eocene sediment from the Queensland Plateau.

DSDP Sample (late Eocene): Leg 21, Hole 209, Core 18, Section 1, 120 cm

Image ID: 0472/0473

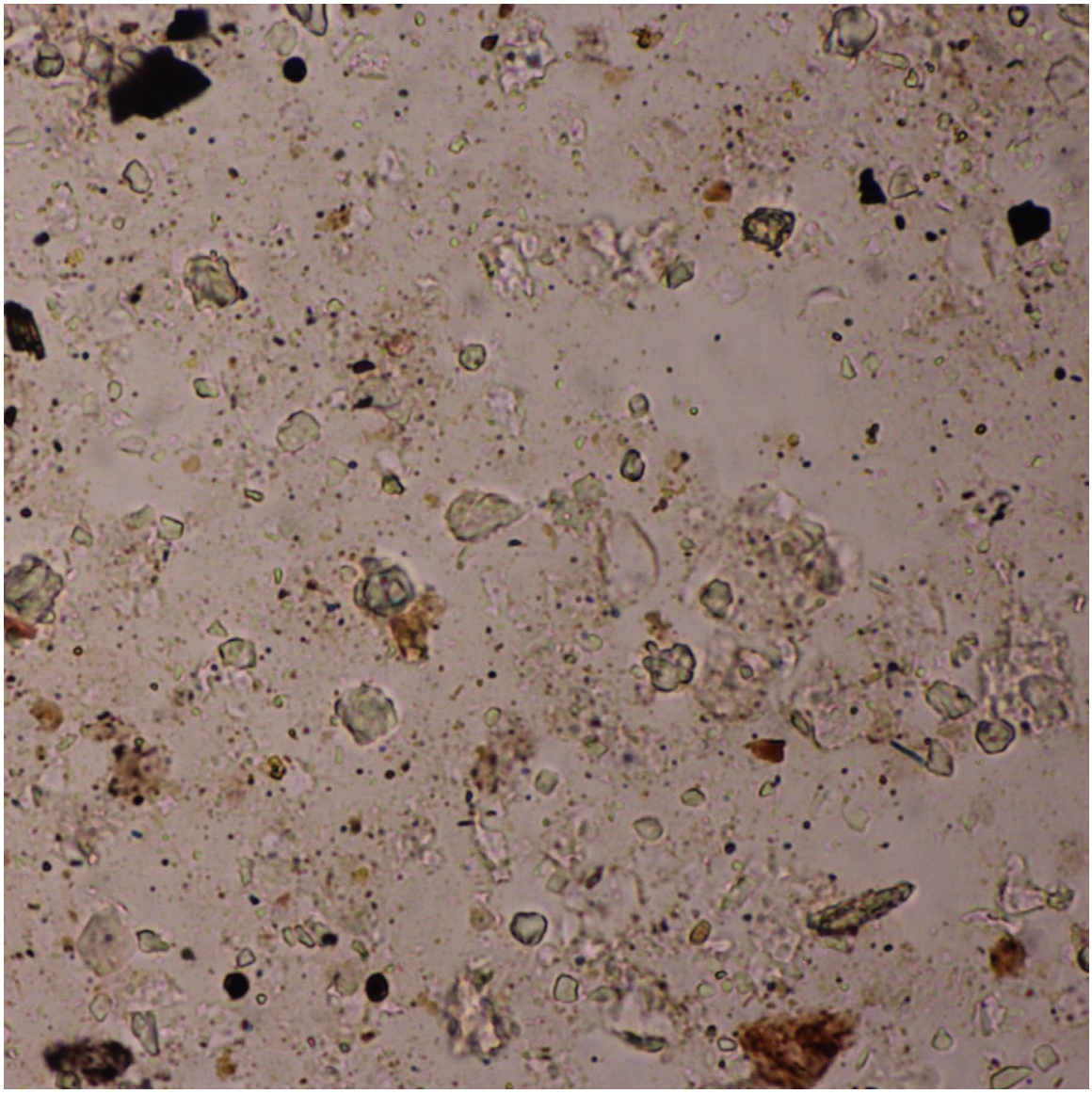

Micrite 5.

Mixed calcareous-terrigenous mud from Mississippi Fan, with common silt-sized carbonate of uncertain origin (micrite). Carbonate could be detrital and a product of glacial erosion of Paleozoic carbonate rocks. Note that Holocene nannofossils may be very small and so mudline carbonate content may be greater than expected. There are larger nannofossils as well as fine silt-sized material with grey birefringence that could be nannofossils.

DSDP Sample (Pleistocene): Leg 96, Hole 614, Core 2H, Section 1W, 22 cm

Image ID: B0351/B0352

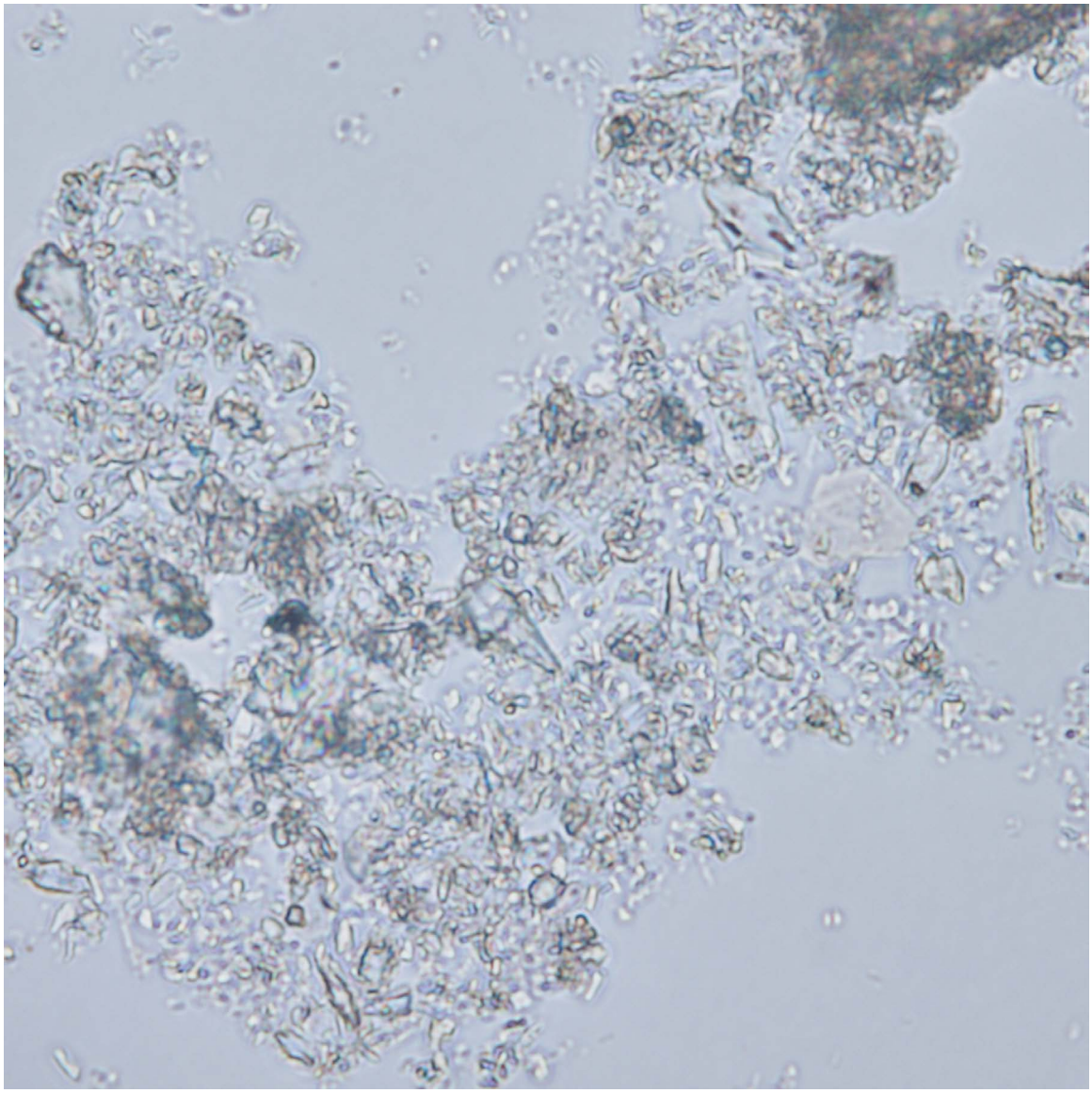

Micrite 6.

Micrite mud/ooze from Little Bahama Bank consisting of bi-refringent, silt-sized carbonate of likely biogenic origin and less birefringent calcareous nannofossils. The latter can be best identified as vague oval to circular structures in plain light.

ODP Sample (Pleistocene): Leg 101, Hole 628A, Core 1H, Section 1, 51 cm

Image ID: B0347/B0348

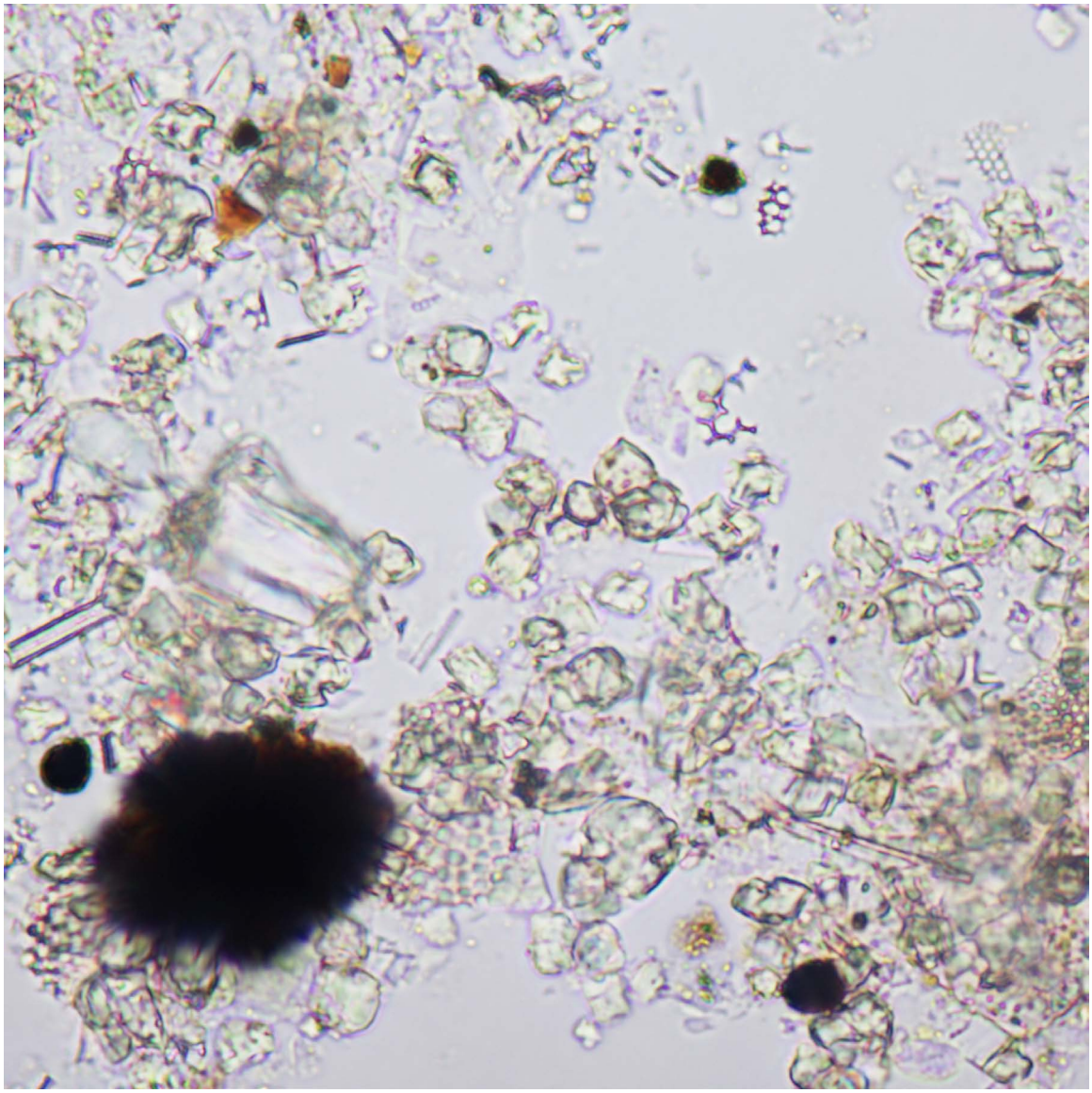

Micrite 7.

Sediment composed mainly of silt-sized authigenic carbonate (micrite) with irregular to semi-euhedral forms. There are traces of siliceous and carbonate biogenic debris, and opaque (pyrite?) grains.

ODP Sample (Pliocene): Leg 167, Hole 1022A, Core 25X, Section 2W, 60 cm

Image ID: B0239/B0240

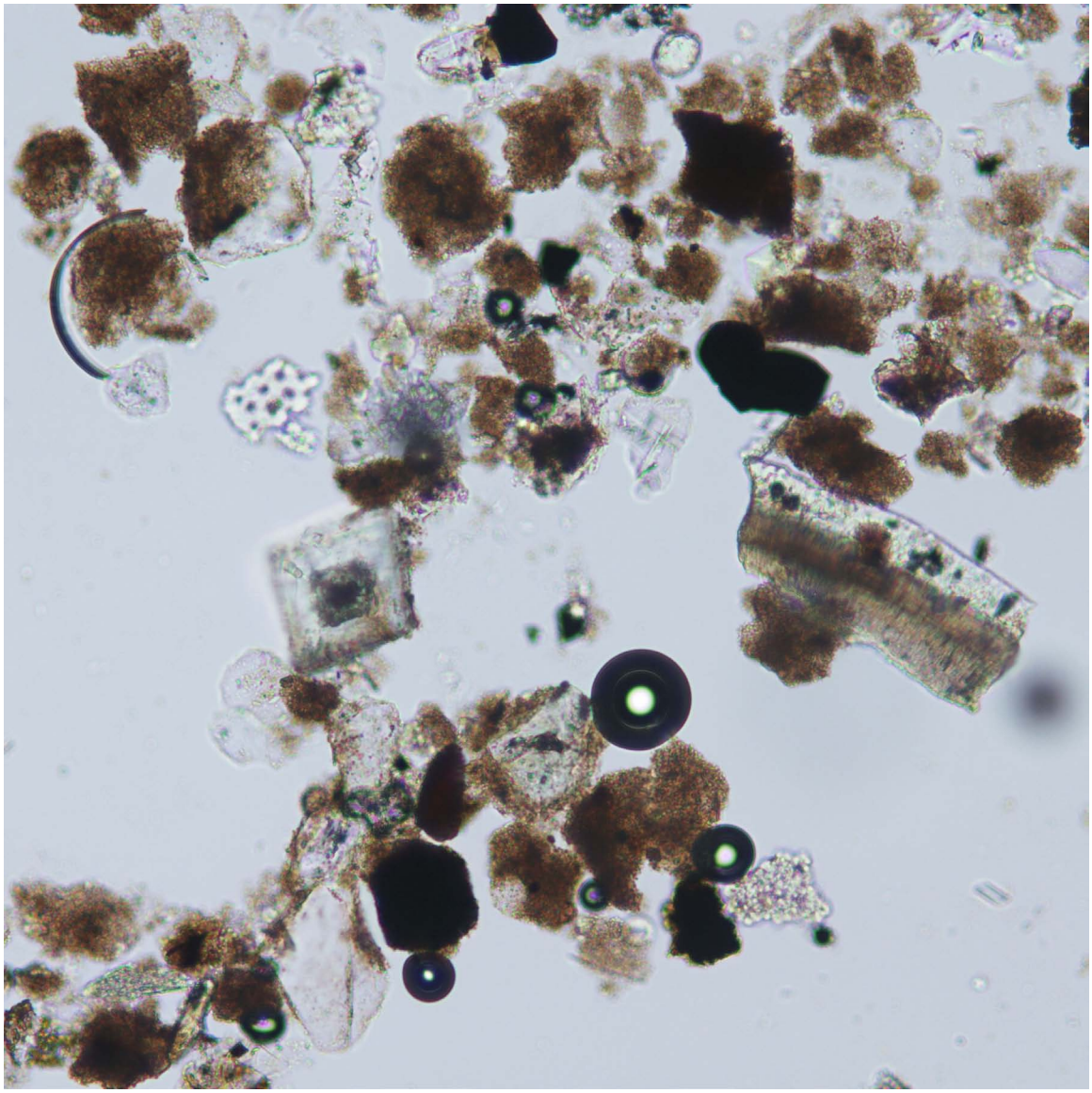

Micrite 8

Authigenic zoned carbonate rhomb in sandy/silty mudstone. Rectangular mollusk fragment shows subparallel growth lines between darker and lighter ultrastrutures.

ODP Sample (Cretaceous): Leg 121, Hole 752A, Core 41X, Section 7W, 6 cm

Image ID: B0393/B0394

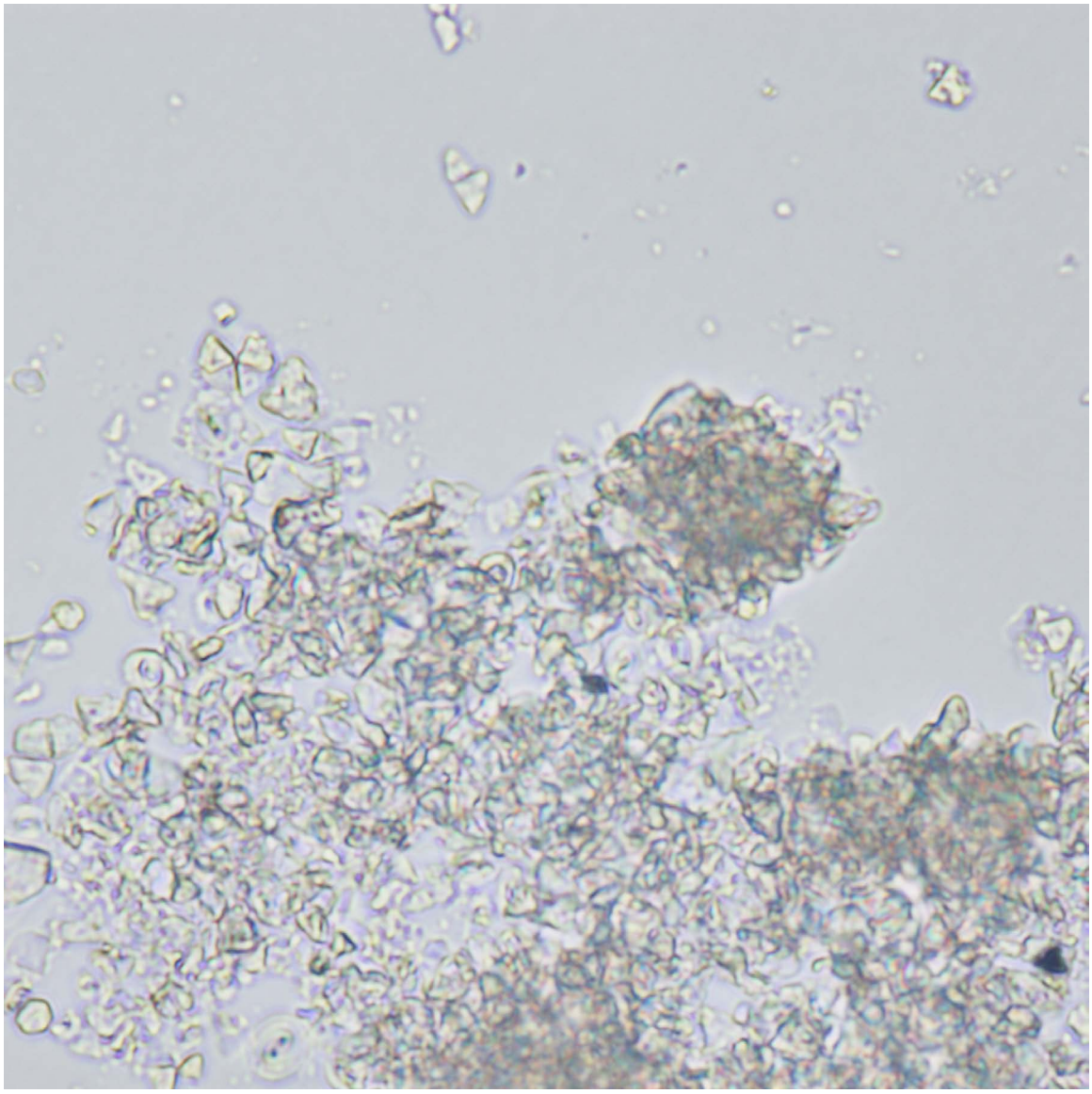

Micrite 9.

If braarurdosphaerids are mostly disarticulated, concetrations of fragments may be mistaken for authigenic carbonate crystals (see micrite images). With polars crossed, however, partly articulated pentaliths and fragments provide hints of biogenic origin.

ODP Sample (early Oligocene to late Eocene): Leg 101, Hole 628A, Core 29X, Section 1, 52 cm

Smear Slide Artifacts

INTRODUCTION TO ARTIFACTS

All smear slides contain features related to minor defects created during smear slide production. Bubbles in the optical adhesive, fibers from the laboratory environment, toothpick fragments, and small bits of plastic and metal from the coring equipment are just some of the possible artifacts that will be observed in smear slides. It is important for the petrographer to be familiar the appearance of artifacts so that they are not mistaken for natural features and also so that no microscope time is wasted in puzzling out the presence and meaning of artifacts. Review the methods section for guidance on minimizing artifacts in smear slides. Additional examples of artifacts can be seen in Part I of the Smear Slide Atlas.

Marsaglia, K., Milliken, K., and Doran, L., 2013. IODP digital reference for smear slide analysis of marine mud. Part 1: Methodology and atlas of siliciclastic and volcanogenic components. IODP Technical Note 1. doi:10.2204/iodp.tn.1.2013

Bubbles 1

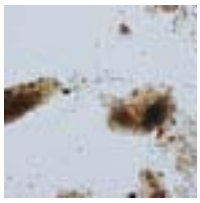

Fibers 1

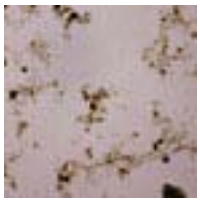

Fibers 2

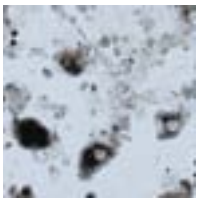

Fibers 3

Fibers 4

Fibers 5

Toothpick 1

Toothpick 2

Plastic 1

Plastic 2

Image ID: 0626/0627

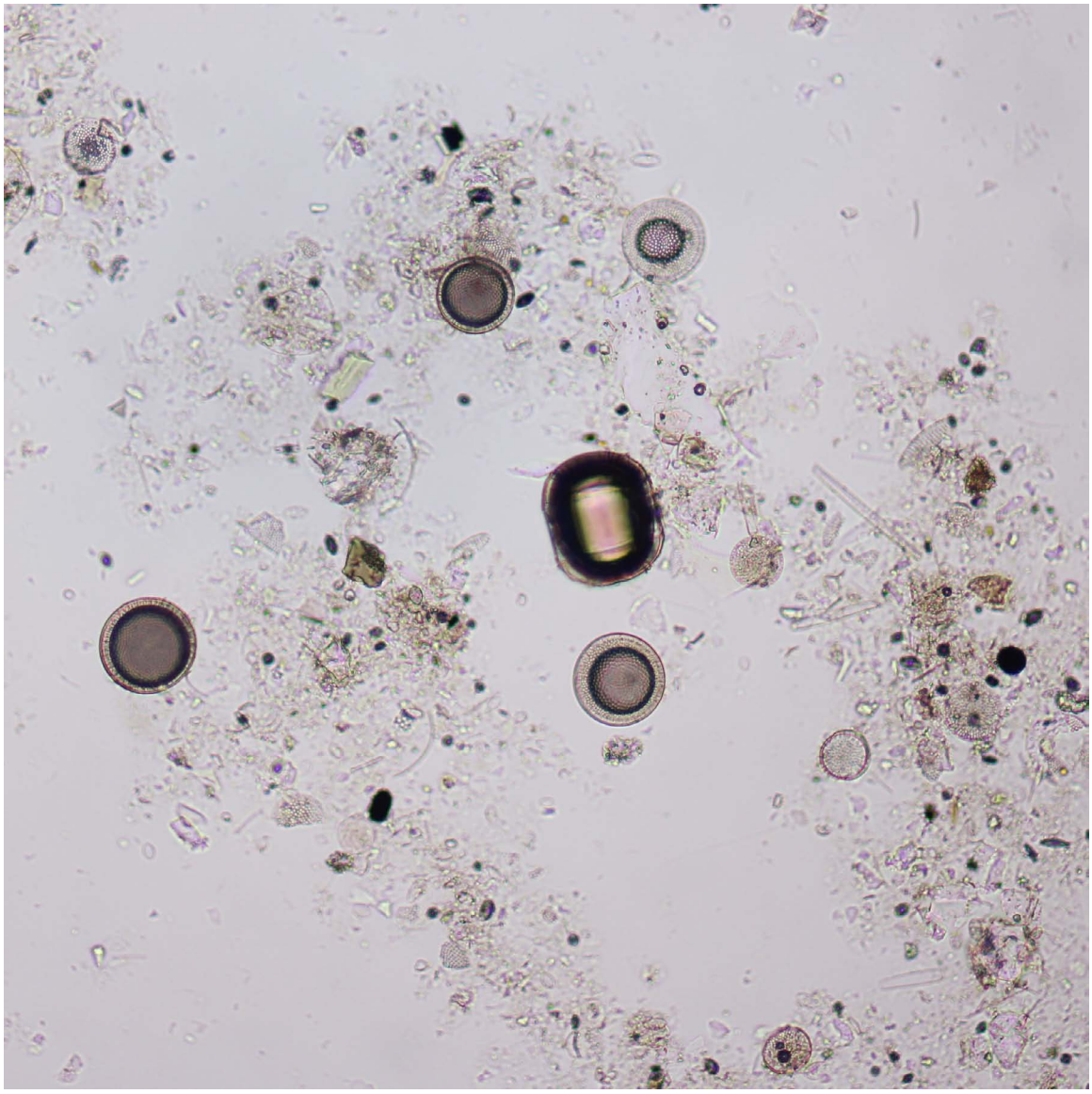

Bubbles 1.

It is nearly impossible to make a smear slide without trapping a few bubbles in the optical adhesive. See methods section for advice on how to minimize bubbles.

Bubbles are easily trapped on large or irregular grains and within large intragranular pores. In this image, several large bubbles are localized above diatom frustrules. Dark rims on bubbles relate to the large contrast in optical index between the gas-filled bubbles and the optical adhesive.

ODP Sample: Leg 178, Hole 1098C, Core 5H, Section 1W, 5 cm

Image ID: B0146/B0147

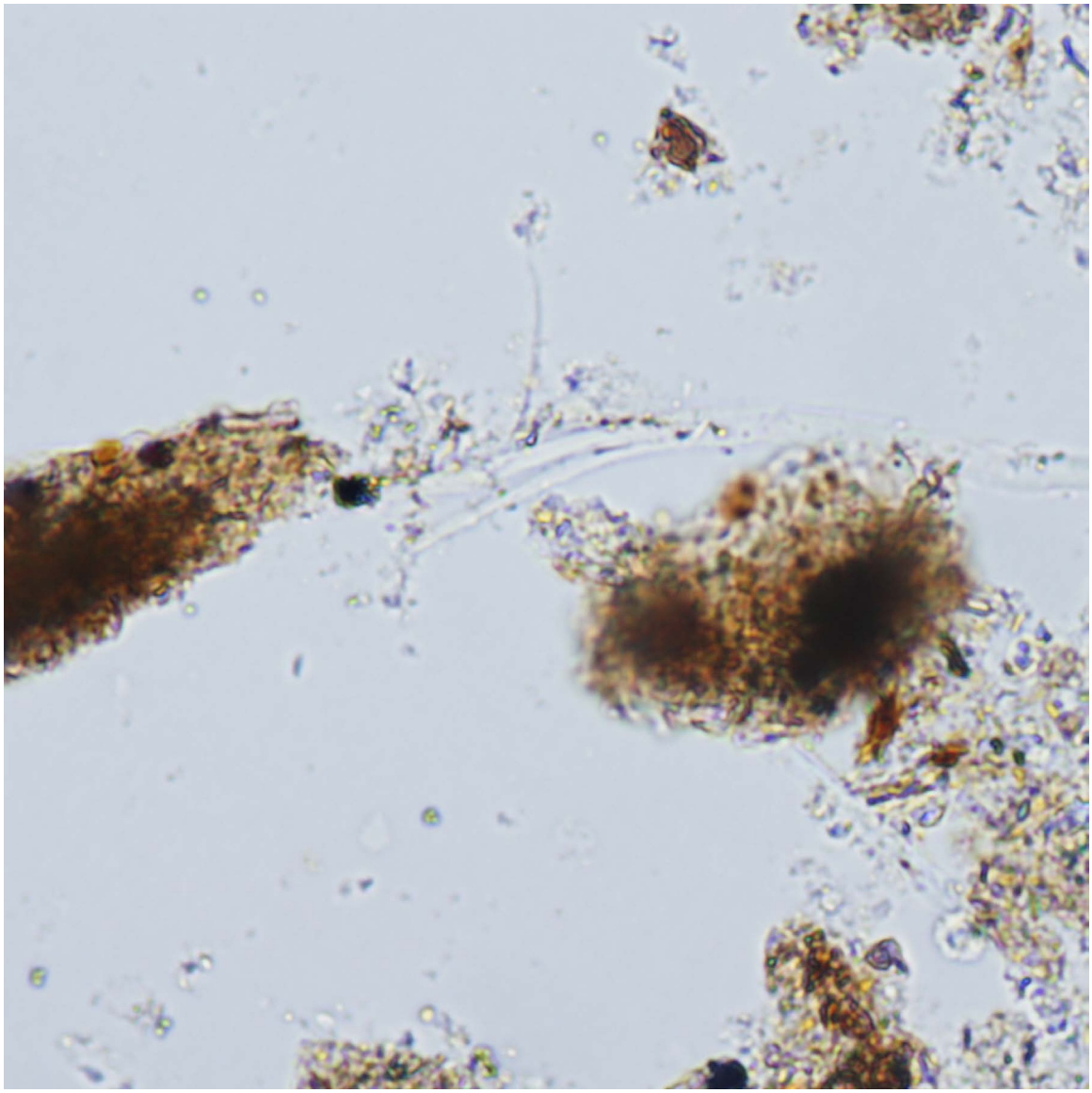

Fibers 1.

Smear slides would need to be made in a clean room to keep them free of fiber contamination, so obviously, most smear slides will have some amount of fiber. Wool, cotton, and polyester are shed from clothing. Shredded plastic can be derived from the core liner. Tooth picks used to disperse the sediment during smear slide production shed wood fibers. Most fibers have some degree of birefringence and because fibers tend to be bent or twisted there is also undulosity.
In this image, a fiber of unknown origin has low birefringence and prominent undulosity.
ODP Sample: Leg 112, Hole 688E, Core 35R, Section 1W, 80 cm

Image ID: 0648/0649

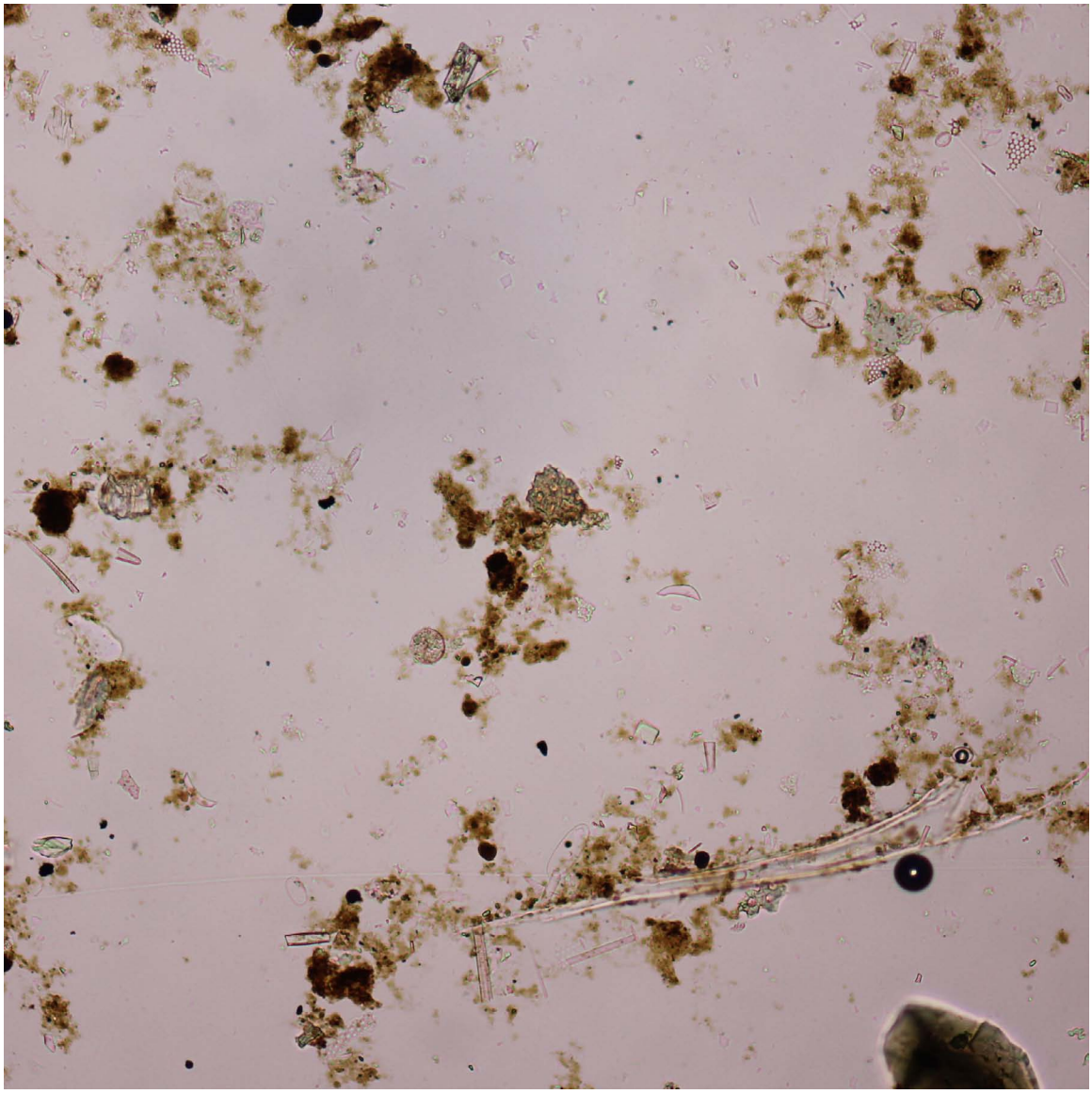

Fibers 2.

A long fiber with upper first order birefringence stretches across the lower part of the slide. Note the adhering sediment.

IODP Sample: Hole 1228A, Core 1H, Section 2W, 20 cm

Image ID: B0397/B0398/B0399

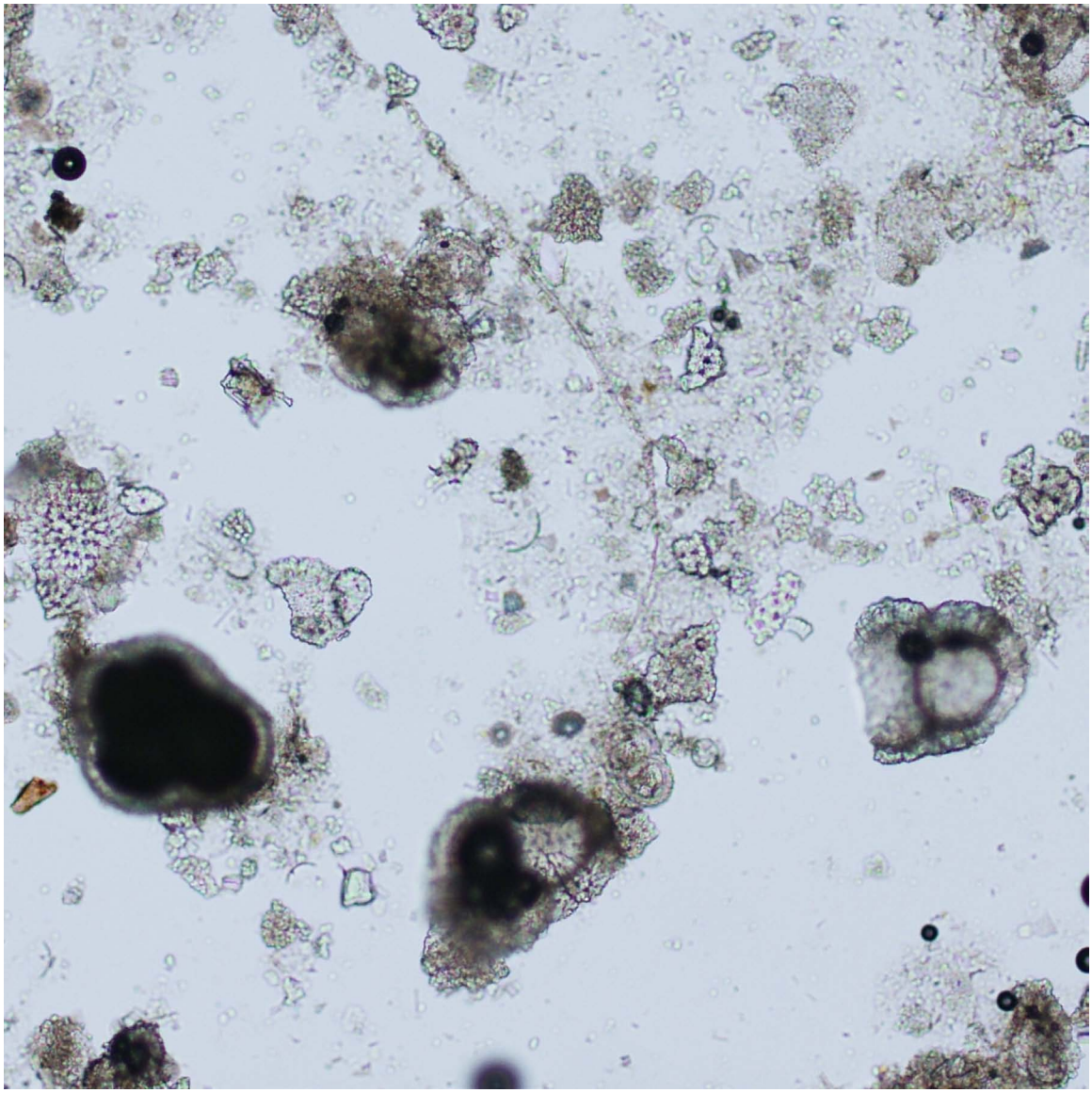

Fibers 3.

A thin fiber with first order birefringence winds through the center of the field of view of foraminifer nannofossil ooze.

ODP Sample: Hole 690A, Core 1H, Section 1, 110 cm

Image ID: B0290/B0291

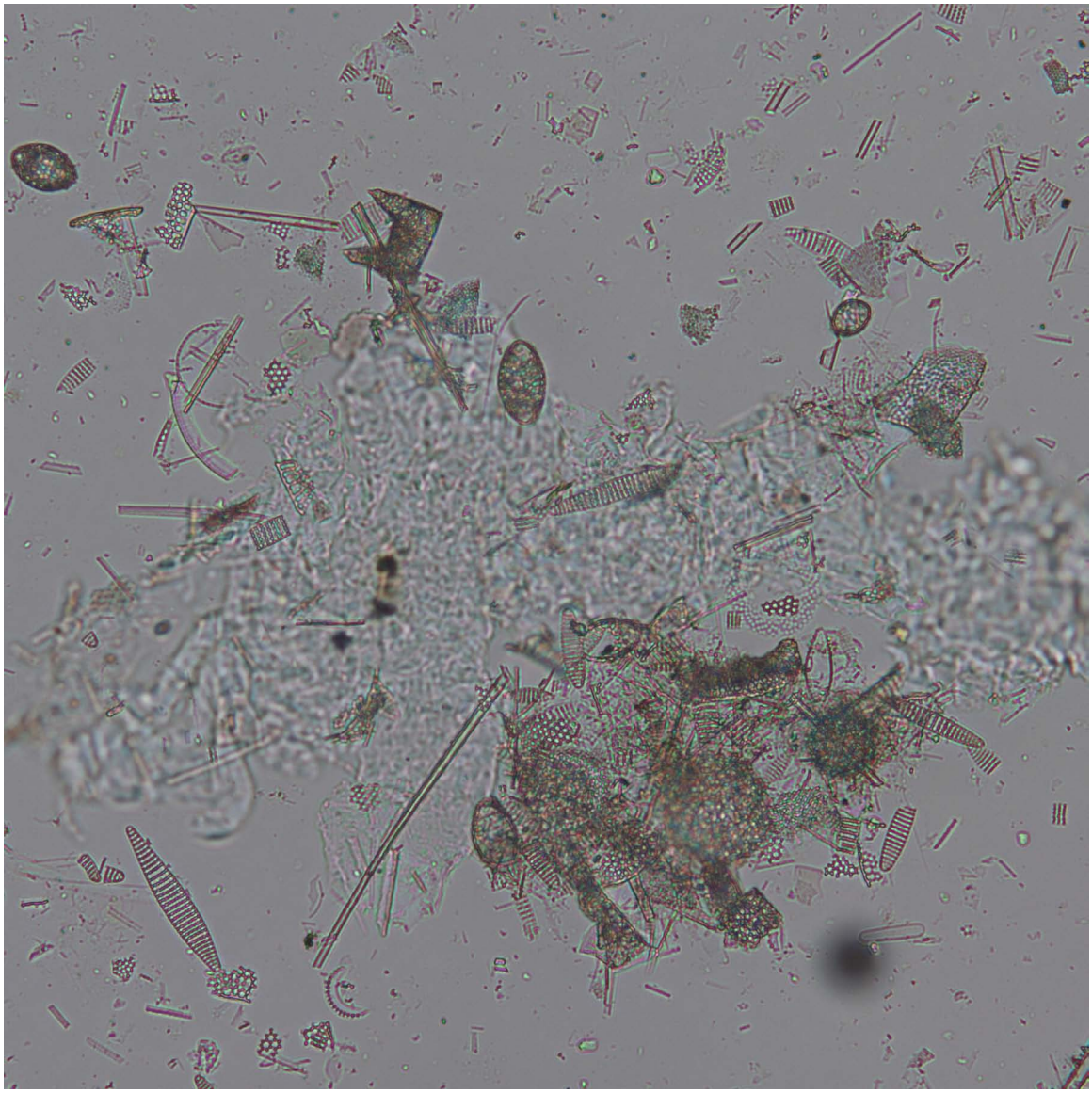

Fibers 4.

Fragment of a laboratory paper wipe displays a fine fibrous structure. Surrounding sediment is dominated by diatoms.

ODP Sample: Hole 745B, Core 5H, Section 1W, 65 cm

Image ID: B0308/B0309

Fibers 5.

The high birefringence of these fibers suggests that it is composed of a synthetic material.

ODP Sample: Hole 845A, Core 15H, Section 2W, 10 cm

Image ID: B0248/B0249

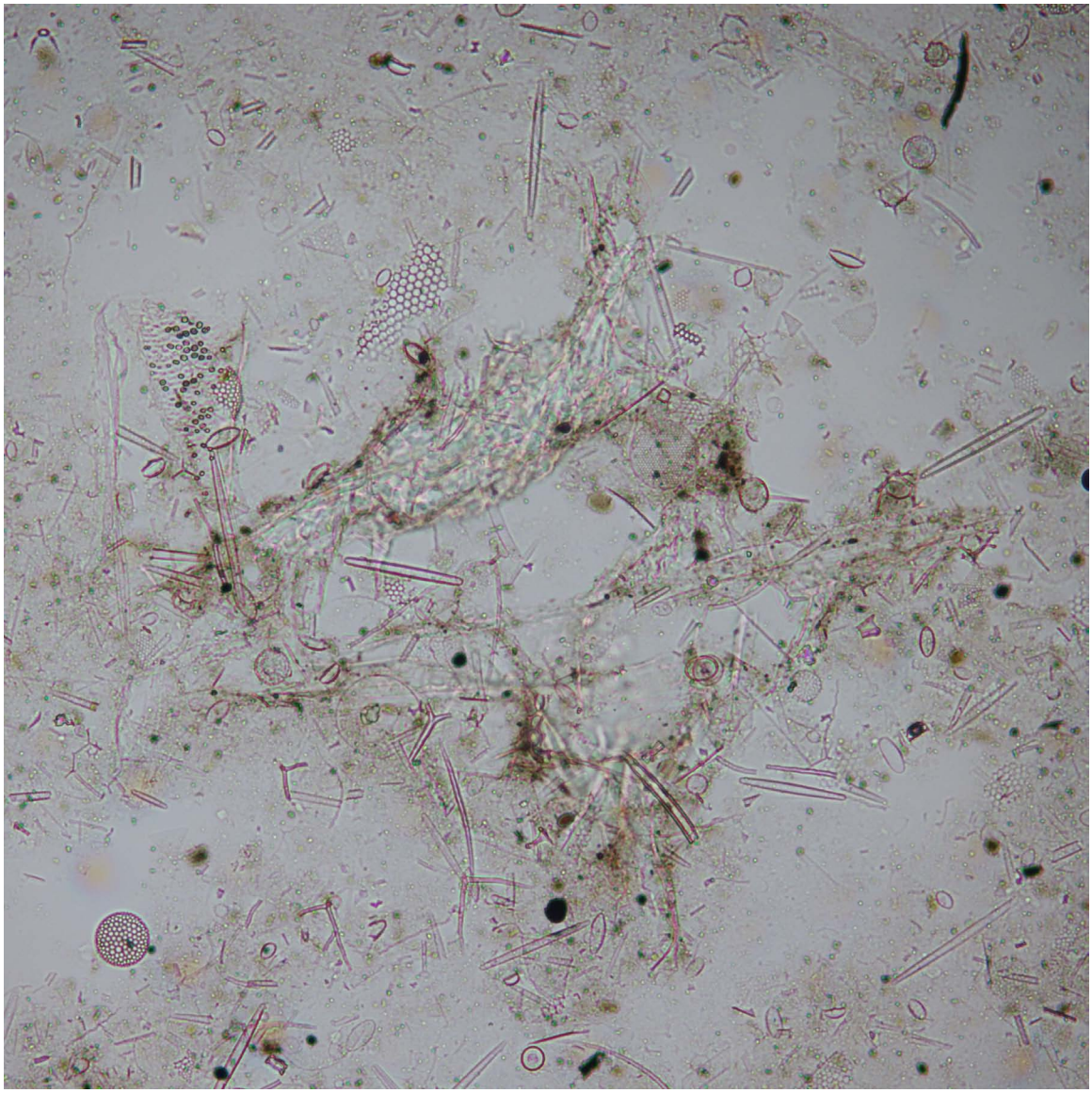

Toothpick 1.

A mass of wood fibers from a toothpick is spectaculalry evident under crossed polars. A portion of toothpick on left side shows nice cellular structure.

ODP Sample: Hole 1075B, Core 3H, Section 6W, 32 cm

Image ID: B0604/B605/B0606

Toothpick 2.

Curved toothpick fragment showing the fine cellular woody texture and first order birefringence. The high birefringence of the surrounding sediment suggests that this sediment might be semi-lithified. The harder the sediment, the more likely the toothpick will fragment during smear-slide production. In such samples the smearing might be best accomplished with a steel spatula.

IODP Sample: Leg 342, Hole 209, Core 18, Section 1, 120 cm

Image ID: B0305

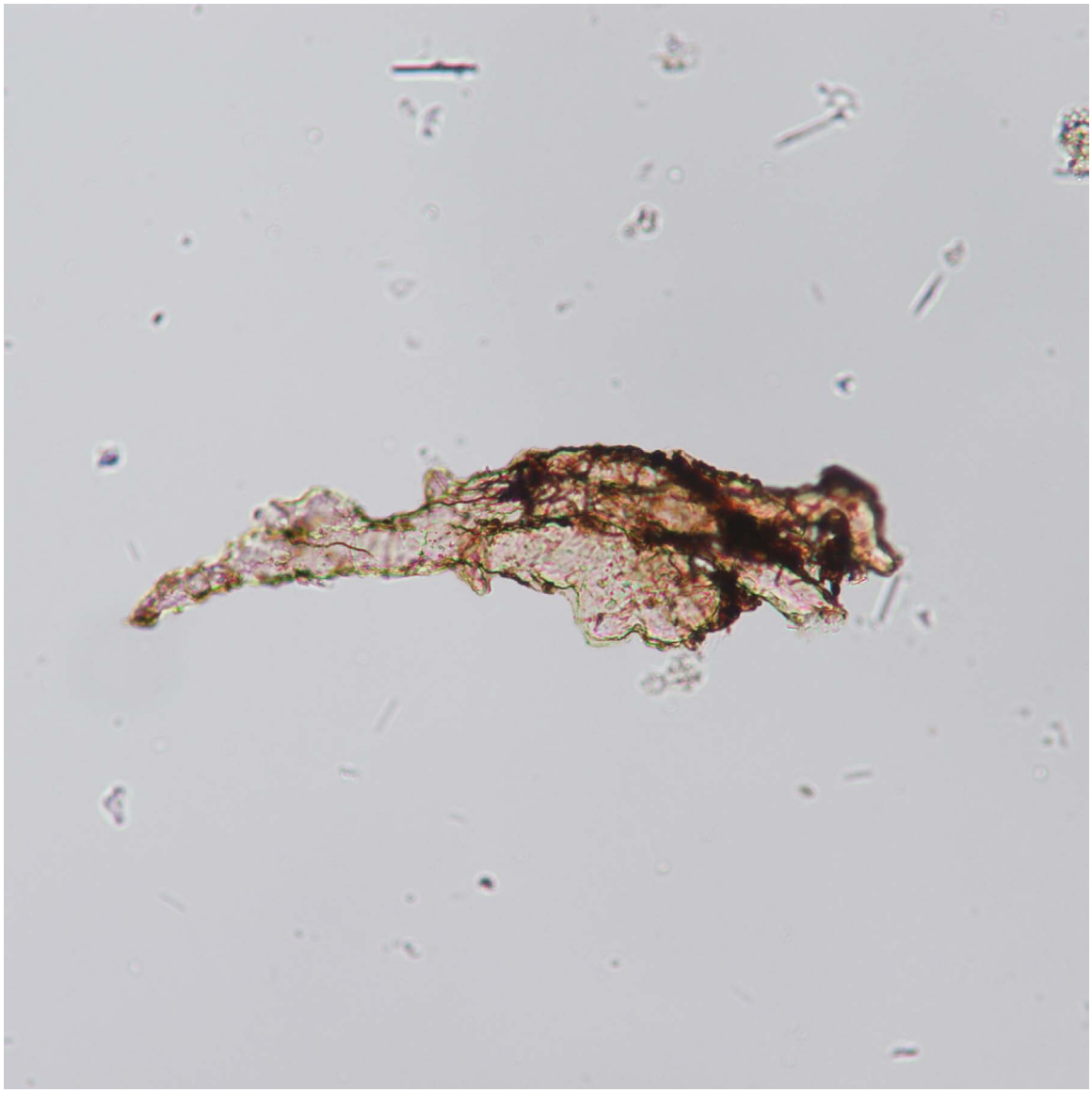

Plastic 1.

This irregular, unknown contaminant fiber is possible plastic.

ODP Sample: Hole 845A, Core 15H, Section 2W, 10 cm

Image ID: B0148/B0149

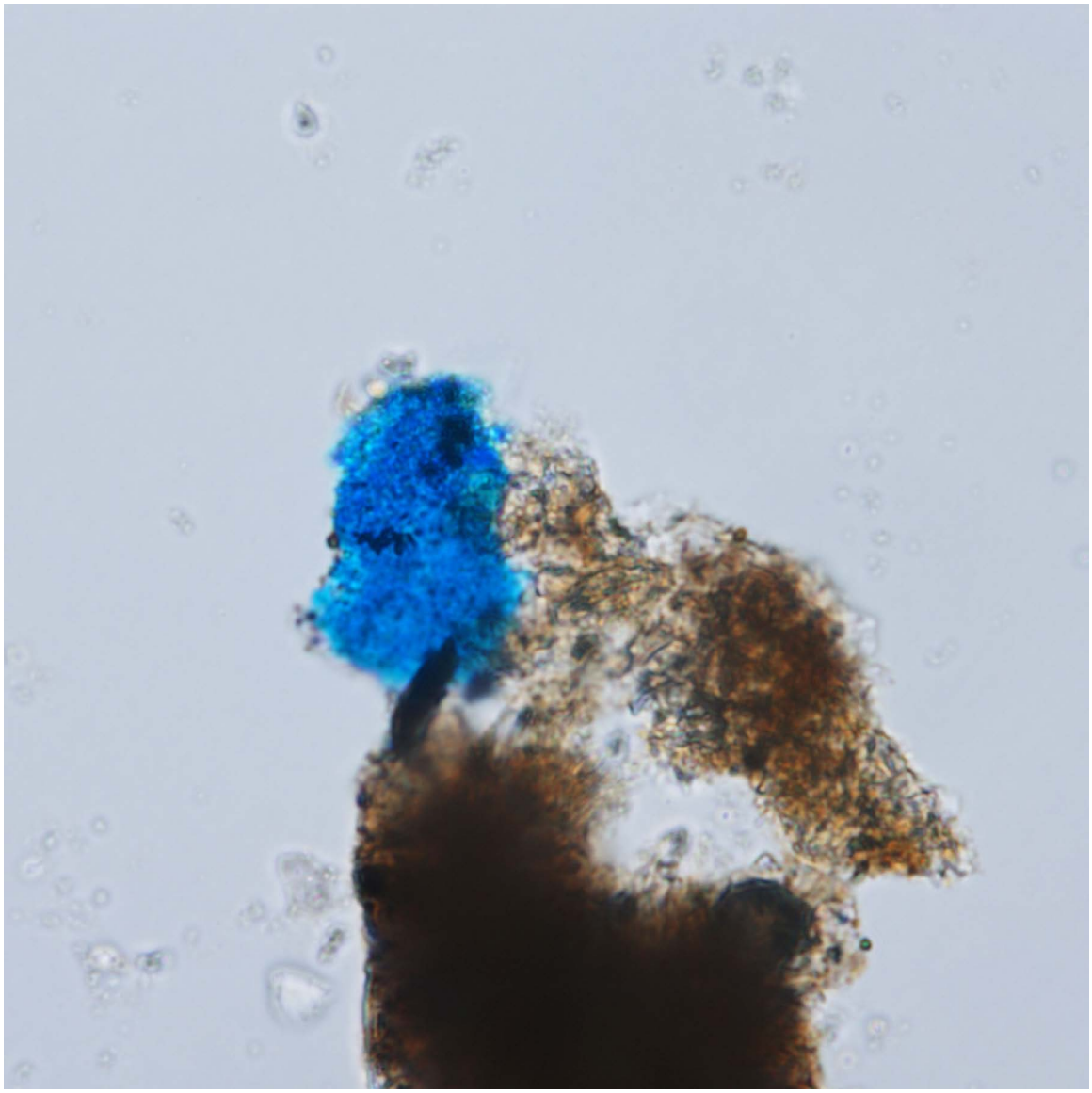

Plastic 2.

Blue plastic bits are most likely derived from the core liner or end caps used to seal off the core sections after they are cut.

ODP Sample: Hole 688E, Core 35R, Section 1W, 80 cm

Tutorial - Introduction

The image atlas provides guidelines for identification of individual biogenic components in smear slides, whereas the following tutorial section provides detailed examples to aid in estimating percentages of components for the purpose of naming the sediment, as well as to hone skills in general component identification. Each of these samples is included in the shipboard/repository smear-slide reference set. Note that this tutorial complements the tutorial section of Part I of this Atlas (Marsaglia et al., 2013), which provided a series of images for several end-member examples of terrigenous and volcanogenic sediment types.

Each tutorial example is first introduced with a written overview followed by two images/views at different magnifications and/or showing different areas of the slide. These have been annotated for identification of components and to illustrate the process of estimating percentages as described in Mazzullo and Graham (1988; http://www-odp.tamu.edu/publications/tnotes/digital/tnote_08.pdf).

The first step in the smear-slide description of biogenic sediments is determining the types and proportions of biogenic components. The second step is determining the presence and texture of nonbiogenic sediment present, namely the proportions of terrigenous/volcanic clay-sized (≤4 µm), silt-sized (4- to 63-µm), and sand-sized (63- to 2,000-µm) material. The grain size is determined using a graduated scale eyepiece reticle that has been calibrated with an optical micrometer so that the 4-µm and63-µm cutoffs for various magnifications, e.g., 10×, 20×, 40×, and 60×, are known. These grain-size estimates are most important for naming terrigenous (e.g., silty clay, sandy silty clay, etc.) and in mixed sediments these terms may be used as modifiers (Mazzullo and Graham (1988). Percentages in the smear slide can be estimated using comparator charts (e.g., Mazzullo and Graham, 1988). The proportions of these biogenic and nonbiogenic components determine the name of the sediment as outlined earlier in this Atlas (link to section). The third step involves the identification and estimation of percentages of authigenic phases that may be used as modifiers.

Note that many of the examples in this tutorial contain both silt- and sand-sized biogenic components. The coarser grains prop up the coverslip to a height that prevents focusing at high magnification on finer surrounding material. This is particularly problematic when the sediment is a mixture of very fine (e.g., nannofossils) and coarse (e.g., foraminifera) components. Segregating the coarser sand fraction in the sediment slurry to one end of the glass slide with the toothpick allows for focusing on fines in the “thin” end, yet maintains a sense of the proportion of coarser material on the “thick” end of the finished smear slide. The alternative method of making the slurry on the coverslip discussed earlier in this volume minimizes this problem. In truth, the proportion of sand-sized foraminifera and radiolarians may be best estimated in the core with a hand

lens. Relative percentages have to be adjusted and should be coordinated with the core describers to avoid misnomers in sediments where there is a wide range of grain sizes.

Lastly, the composition of biogenic sediments should take into consideration other shipboard analyses, such as XRD and carbonate. Where possible, these analyses should be coordinated on the same lithological horizon. In biogenic dominated sediments, color can be a good indicator of sediment composition once baselines have been established with pared analyses. However, there are some caveats to comparing geochemical/mineralogical data sets: 1) biogenic components are often microporous, so petrographically estimated percentages may not directly correspond to bulk mineralogical proportions; 2) opaline microfossil components are amorphous and proportions are not easily determined from XRD analyses; and 3) in mixed sediments it may be difficult to extract information, e.g., clay proportion if terrigenous silt or siliceous debris is present, in a calcareous sediment. It is important to realize that bioturbation may result in sediment heterogeneity on a mm scale (e.g., burrow fills), so core describers must be careful to select truly representative examples of sediment types for combined smear, XRD and carbonate analyses.

Mixed Calcareous/Siliceous Ooze Example (1)

This sample is from a site in the Weddell Sea on the southwestern flank of the Maud Rise located in ~3km water depth. The sediment was described by shipboard scientists as diatom-bearing foraminifer ooze. Its simple two-component composition makes it an excellent teaching tool for estimating percentages.

Percentages are calibrated by first estimating the percentage of the field of view filled with a component (either using comparison charts or grid counts) and then correcting it to reflect the percentage of the field of view filled with sediment. For example, a component estimated at 20% of the field of view, a view that in turn was only half filled (50%) by sediment, would constitute 40% of the sediment sample.

It may be prudent to try to pick several representative field of views, calculate percentages in each and then use the average. With this in mind, two views are shown below for comparison.

Example 1A

Example 1B

Image ID: B0454/B0455

Mixed Ooze Tutorial 1A (also Diatom 20).

In this field of view, approximately 75% is covered by biogenic debris, mostly (92%) nannofossils exhibiting low birefringence (pinwheels) and lesser (8%; arrowed) pennate diatoms, whole and linear fragments composed of amorphous opal without birefringence. The latter look like ornate paper clips and larger fragments are arrowed in image info layer. Compare these percentages to those for Mixed Ooze Tutorial 1B.

ODP Sample (middle Miocene): Leg 113, Hole 690B, Core 5H, Section 2W, 57 cm

Image ID: B0450/B0451

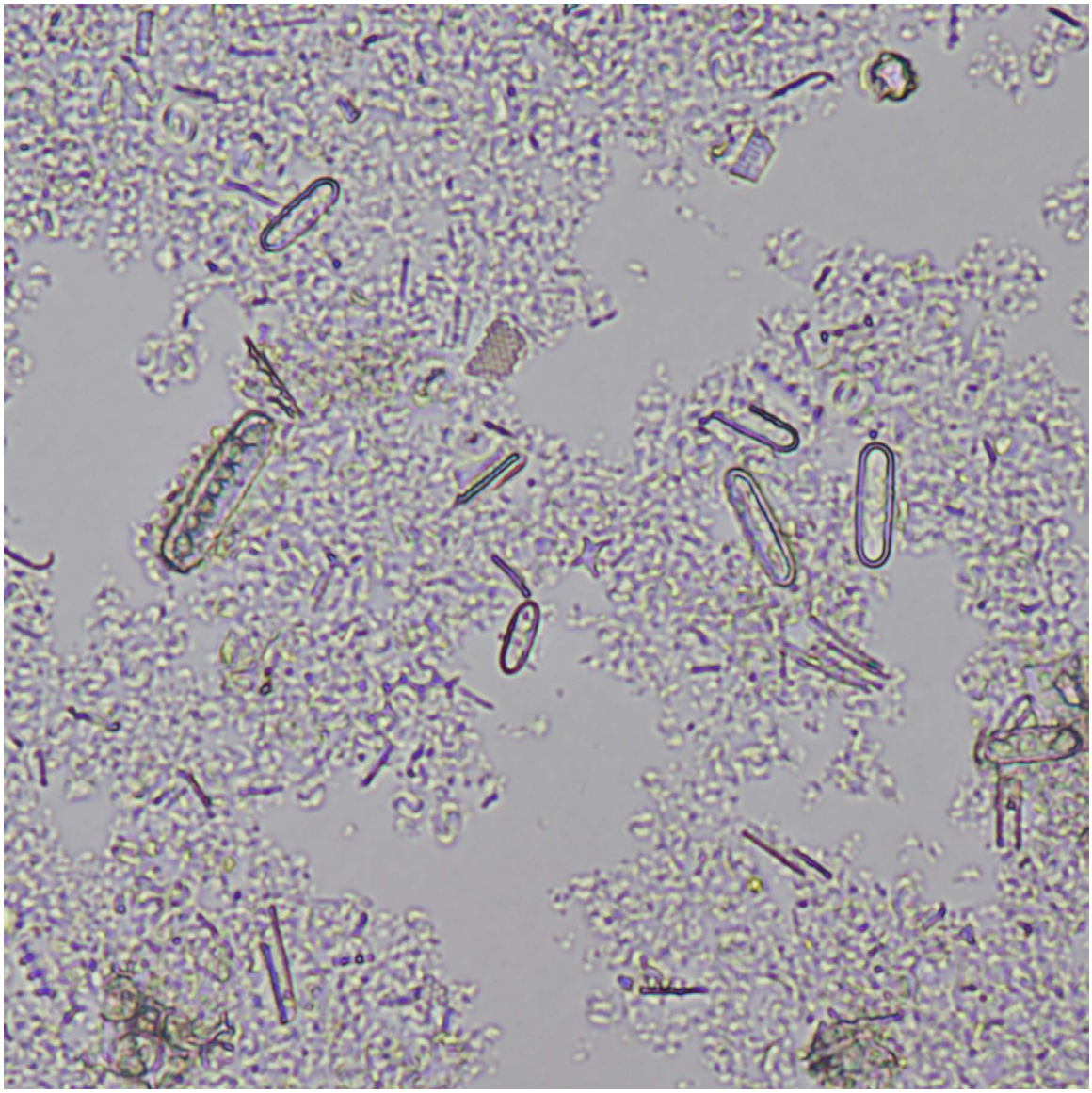

Mixed Ooze Tutorial 1B (also Diatom 21).

In this his alternate filed of view of the same sample in Mixed Ooze tutorial 1A, there is slightly more material with ~80% of the field of view covered by biogenic debris. The percentages of biogenic components are effectively identical to those determined in tutorial 1A with 91% nannofossils and 9% Pennate diatoms.

ODP Sample (middle Miocene): Leg 113, Hole 690B, Core 5H, Section 2W, 57 cm

Calcareous Ooze Example (2)

This sample is from the uppermost few meters of sediment that accumulated at a near-equatorial site on the Ontong Java Plateau that was drilled in 2805 m water depth. Shipboard scientists found roughly subequal amounts of foraminfers and nannofossils in this first core, similar to the proportions described below in a series of images taken at increasing magnification. They described the core as Nannofossil Ooze with Foraminifera to Foraminifer Nannofossil Ooze.

Example 2A

Example 2B

Image ID: B0161/B0162/B0163

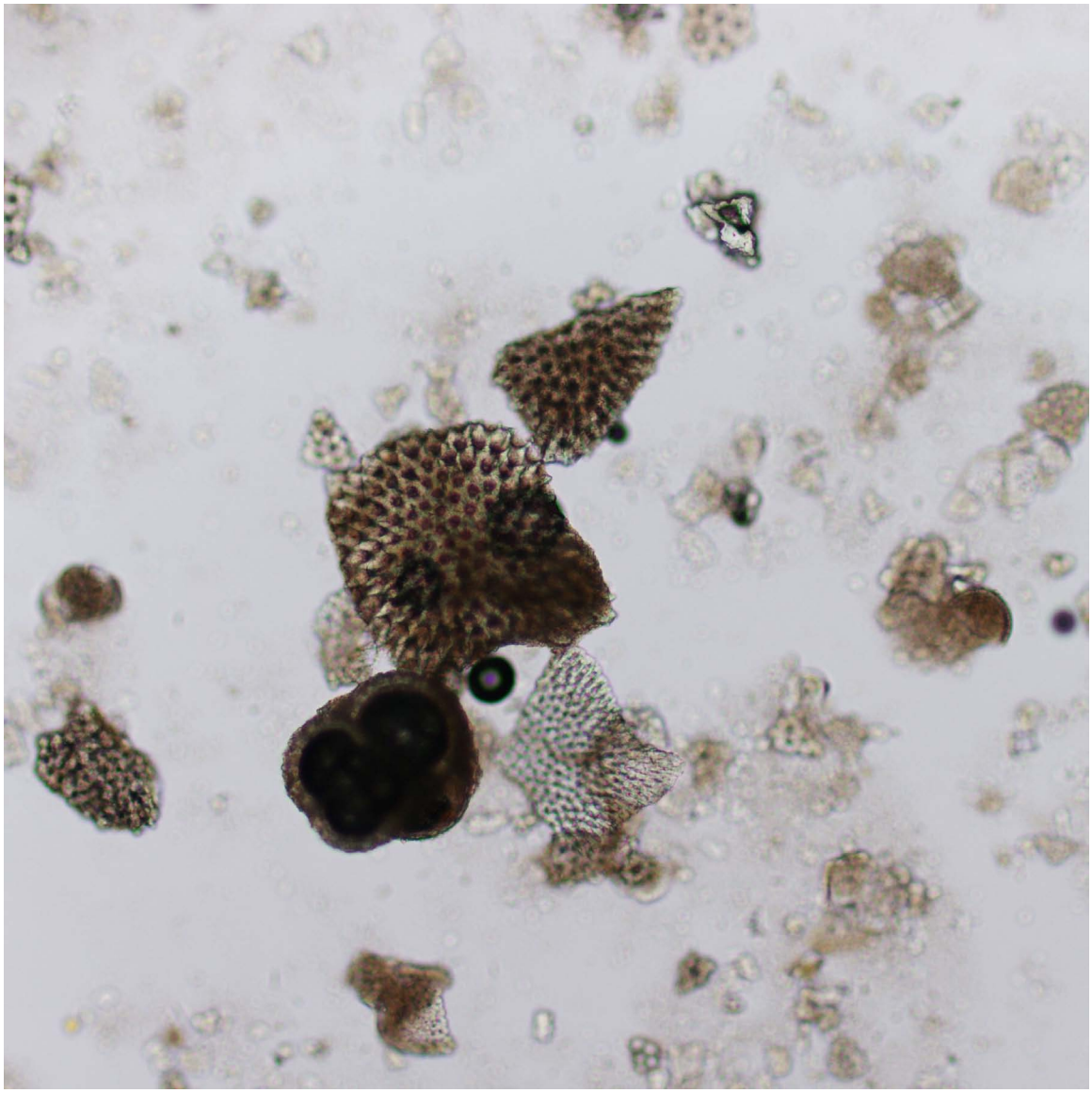

Calcareous Ooze Tutorial 2A (also Foram 23).

This low magnification view focuses on larger, darker, microporous foraminifer fragments (marked with f's in image information) and a large intact planktic foraminifer (marked with p). With polars crossed, many more foraminifer fragments are identifiable via their pseudo-uniaxial cross birefringence (e.g., +), along with significant, variably birefringent, finer-grained material. Using birefringence as a guide, roughly half of the field of view is filled with material, and this material is roughly equally divided between the coarser foraminifera and fragments, and finer material. The nature of the latter is best discerned at higher magnification (see Tutorial 2B).

ODP Sample (Pleistocene): Leg 130, Hole 807A, Core 1H, Section 2W, 93 cm

Image ID: B0159/B0160

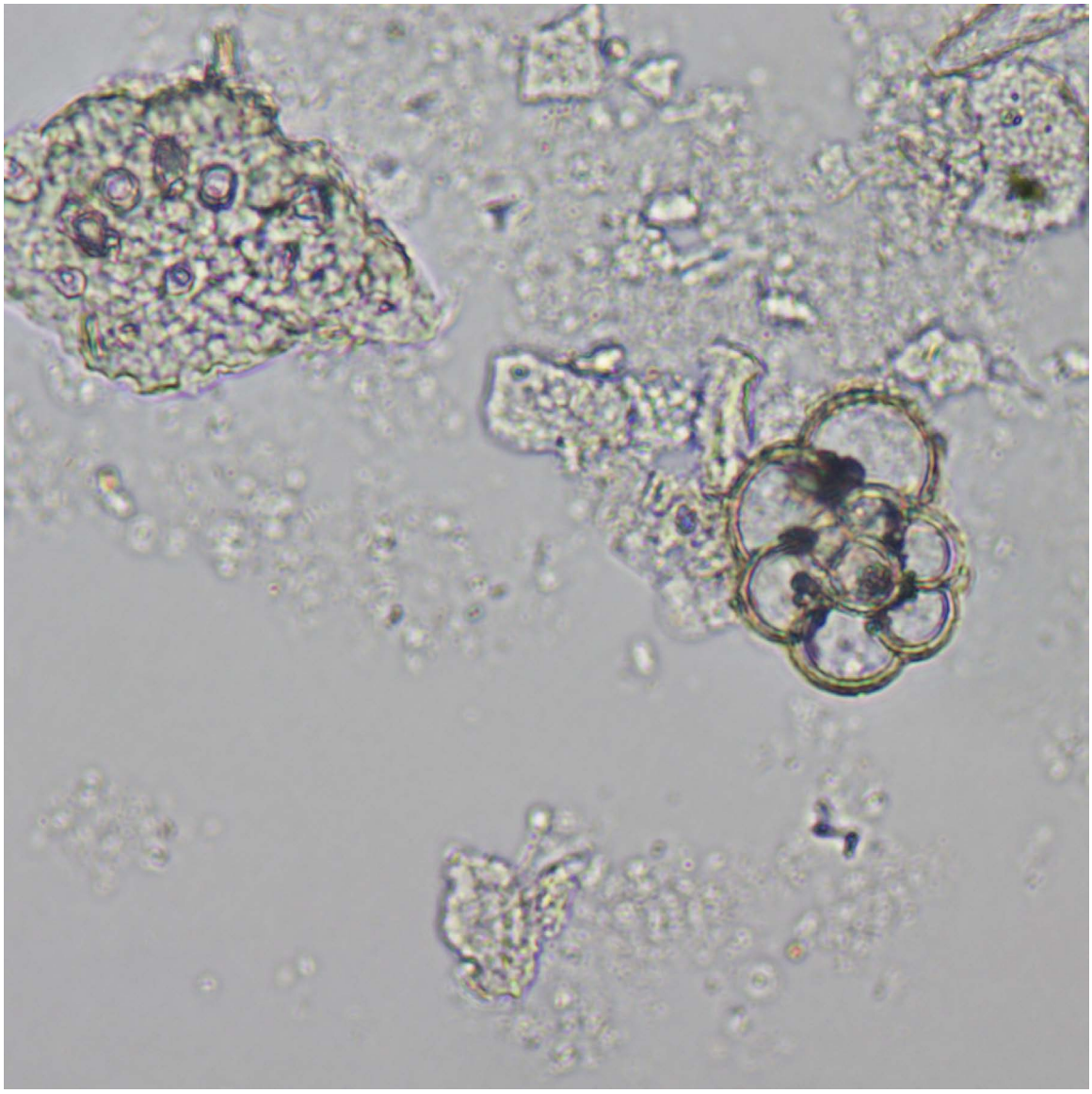

Calcareous Ooze Tutorial 2B (also Foram 2).

Even at higher magnification, the nannofossils are just barley discernible as fuzzy, out-of-focus circular features with very low birefringence (circled in red). Other higher relief bits are foraminfer test fragments (f). These exhibit low birefringence because of the orientation of the fragments, which are lying flat on the slide (also see description in Atlas on p. 73 for more detail). The field of view is approximately 60% filled with biogenic debris consisting of an approximately equal proportion of nannofossils and foraminifera (total of fragments and whole whorled specimen (p)).

ODP Sample (Pleistocene): Leg 130, Hole 807A, Core 1H, Section 2W, 93 cm

Mixed Siliceous/Calcareous Ooze Example (3)

Site 1172 is located on the eastern side of the East Tasman Plateau. This sample comes from an Oligocene interval described by shipboard sedimentologists as mainly clay- to foram-bearing nannofossil chalk with ashy siltstone. Smear slides below this interval were noted to contain diatoms, foraminifera, radiolarians, and sponge spicules.

Example 3

Image ID: B0281/B0282

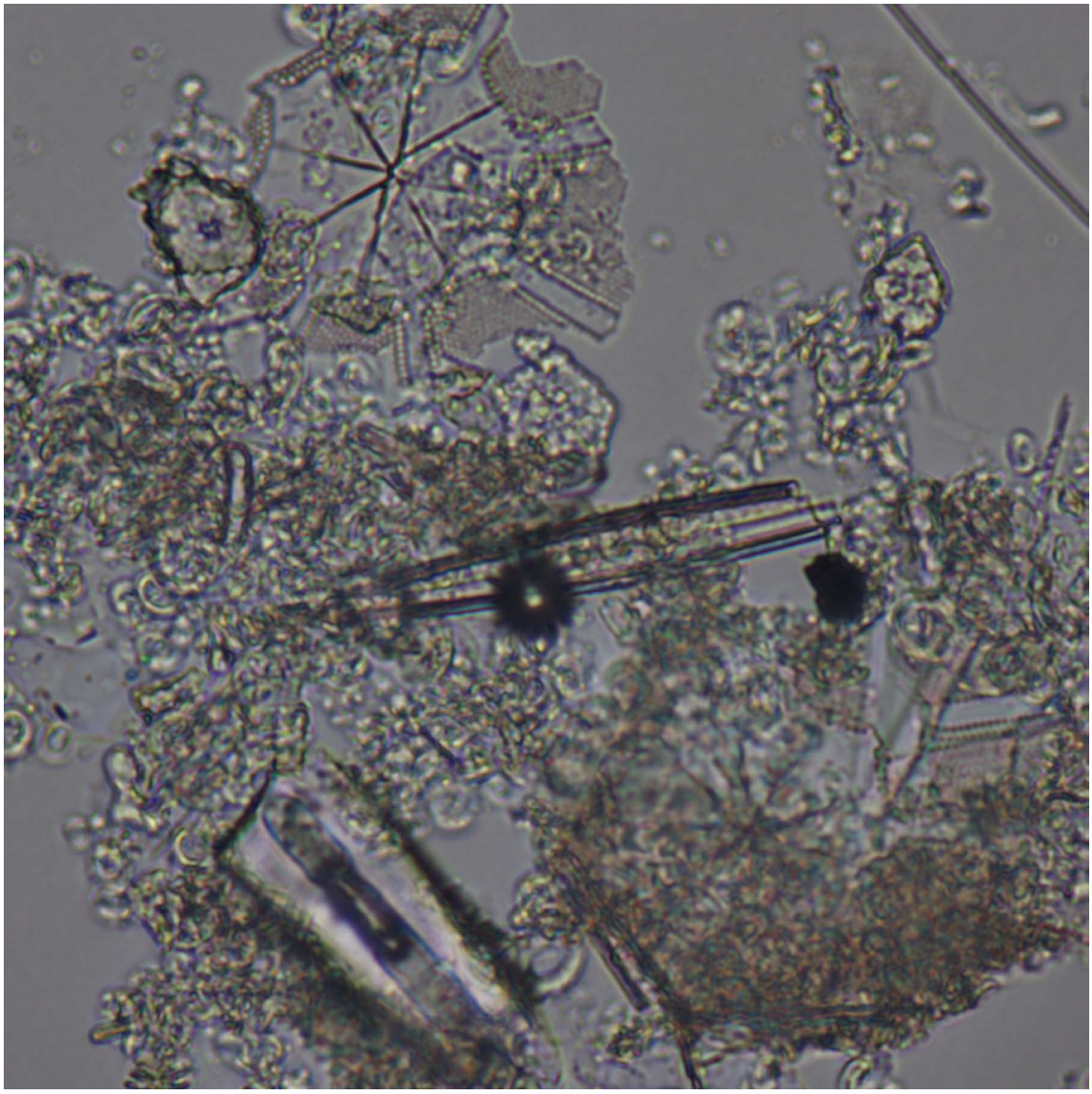

Mixed Ooze Tutorial 3.

Approximately 20% of field of view is void space. Visual estimates of component totals that accommodate this void space are as follows: nannofossils (N; 60%), diatoms (D; 20%), coarse micrite (M; 9%), sponge spicules (S; 5%), volcanic debris (V; 3%), detrital quartz (Q; 2%) and opaque minerals (1%). The coarse micrite may be foraminifer fragments. An out-of-focus region in the lower right quadrant (F) exhibits some birefringence suggesting the presence of nannofossils/micrite but a vague radial pattern similar to that exhibited by the diatom above in left upper left quadrant, suggests that a diatom may be lying on or above carbonate components decreasing the apparent focus. This area was counted partly as "carbonate" and partly as "diatom" to accommodate this. Total carbonate measurements (shipboard analyses) ranged from 64-78% in this core, in line with the 69% total calcareous components visually estimated in this field of view.

IODP/ODP/DSDP Sample: Hole 1172A, Core 38X, Section 5W, 78 cm

Siliceous Ooze Example (4)

This high-latitude sample from the Maud Rise in the Weddell Sea is a fairly pure siliceous ooze dominated by diatoms with significant silicoflagellates. The site is situated on the southwestern flank of the Maud Rise in ~3km water depth. Two views are provided one at low and another at high magnification to provide information on component percentages.

Example 4A

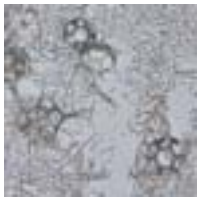

Example 4B

Image ID: B0438/B0439

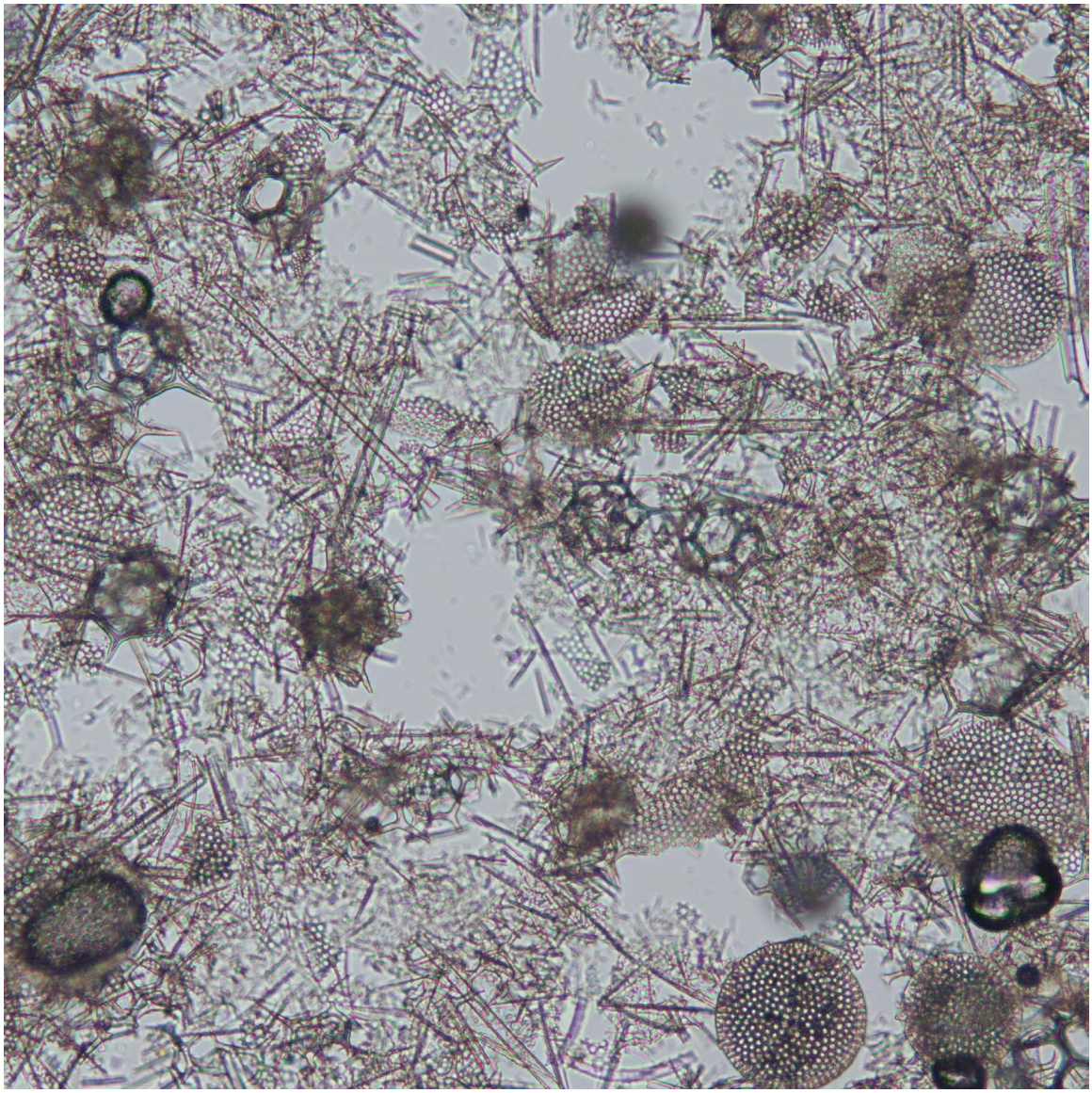

Siliceous Ooze Tutorial 4A (also Silicoflagellate 8).

This smear shows a rather densely packed diatom ooze covering ~90% of the field of view. There are several distinct components including intact Distephanid silicoflagellates (10% of the sediment; marked as D in image annotation layer) and circular centric diatom valves (15% of the sediment; C), the remainder (75%) being a felted mass of pennate diatoms (linear elements; P), and diatom and silicoflagellate fragments. The next image shows the nature and make-up of that fragmental matrix. There are no birefringent components (e.g., calcareous bioclasts) in this sample, as indicated in the crossed-polar view.
ODP Sample (early Pliocene): Leg 113, Hole 690B, Core 3H, Section 3W, 50 cm

Image ID: B0444/B0445

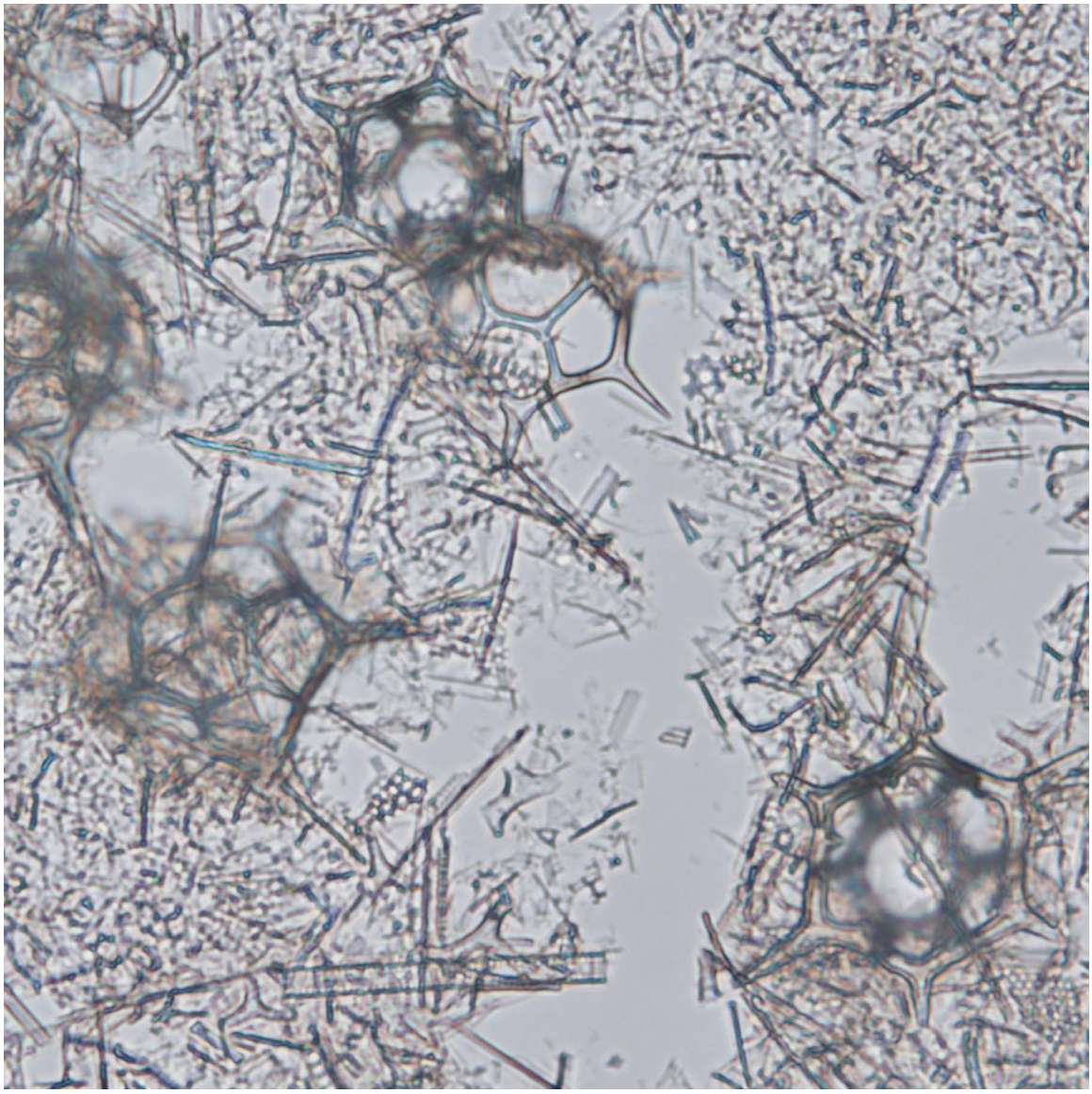

Siliceous Ooze Tutorial 4B (also Sillicoflagellate 7).

This field of view is ~90% covered by siliceous microfossils with a cluster of distephanid silicoflagellate specimens (marked as D in the image annotation layer). These larger specimens constitute 25% of the biogenic debris. Within the finer matrix there are distinct fragments exhibiting the cellular texture of centric diatoms (circled in red), parallel linear structures of penate diatoms (P) and branched fragments of silicoflagellates (circled in yellow). When polars are crossed, a trace of unidentified clay-sized birefringent components (e.g., calcareous bioclasts) can be seen in this sample. A non-birefringent terrigenous clay component cannot be ruled out, but the isolated nature of the site location indicates this is unlikely.

ODP Sample (early Pliocene): Leg 113, Hole 690B, Core 3H, Section 3W, 50 cm

Organic-rich Siliceous Ooze with Carbonate Example (5)

This sediment comes from the continental shelf of Peru at a site drilled in a water depth of ~150 m, a location drilled because of known presence of organic-rich, sulfate-depleted, methane-rich sediments.

Example 5

Image ID: 0658/0659

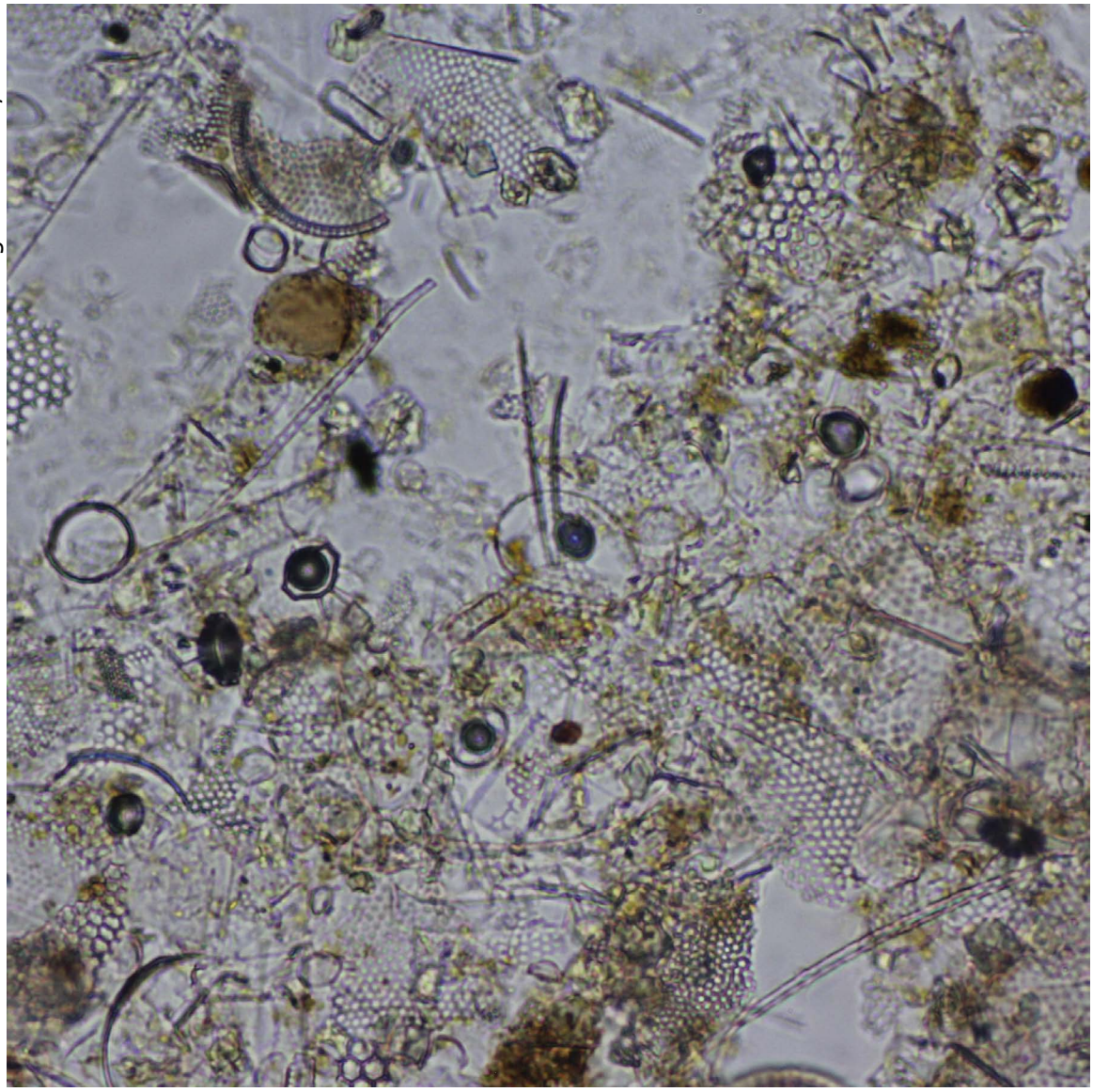

Organic-rich Ooze Example 5 (also Carbonate 1).

There are several important components in this diatomaceous sample, including organic matter (labeled O in image information layer) and birefringent authigenic carbonate (a few marked with C), likely dolomite based on shipboard XRD analyses of other intervals. The proportion of the former is best estimated in plane light whereas the latter is best estimated with polars crossed. The rather closely packed sediment fills ~85% of the field of view. With polars crossed, the birefringent carbonate content (~10% of the sediment) becomes apparent. In plane light, pale brown to tan organic matter (a few marked with O) is slightly more abundant (~15%). The remainder of the sediment (~75%) is nonbirefringnet, opaline biogenic debris that appears to be mainly fragments of centric diatoms based on their meshlike textures (m). Organic and carbonate content in sediment such as this should be verified by shipboard geochemical analyses.

ODP Sample (Pleistocene): Leg 201, Hole 1229A, Core 2H, Section 6W, 26 cm

Siliceous Ooze Example (6)

This sample contains several types of siliceous biogenic debris, from large sand-sized radiolarian and foraminifera, to finer diatoms and clay-sized material, to vitric volcanic fragments. Initially the photograph was taken to illustrate the presence of clay-sized matrix, which upon closer examination at high magnification is likely to be composed of very small nannofossils. These very small, clay size, nannofossils are characteristic of Pleistocene-age sediments. They are often in the first cores recovered on a cruise and often not identified until shipboard carbonate analyses reveal their presence. The two views show the importance of estimating the percentage of sand-sized material at lower magnification and finer material at higher magnification.

Example 6A

Example 6B

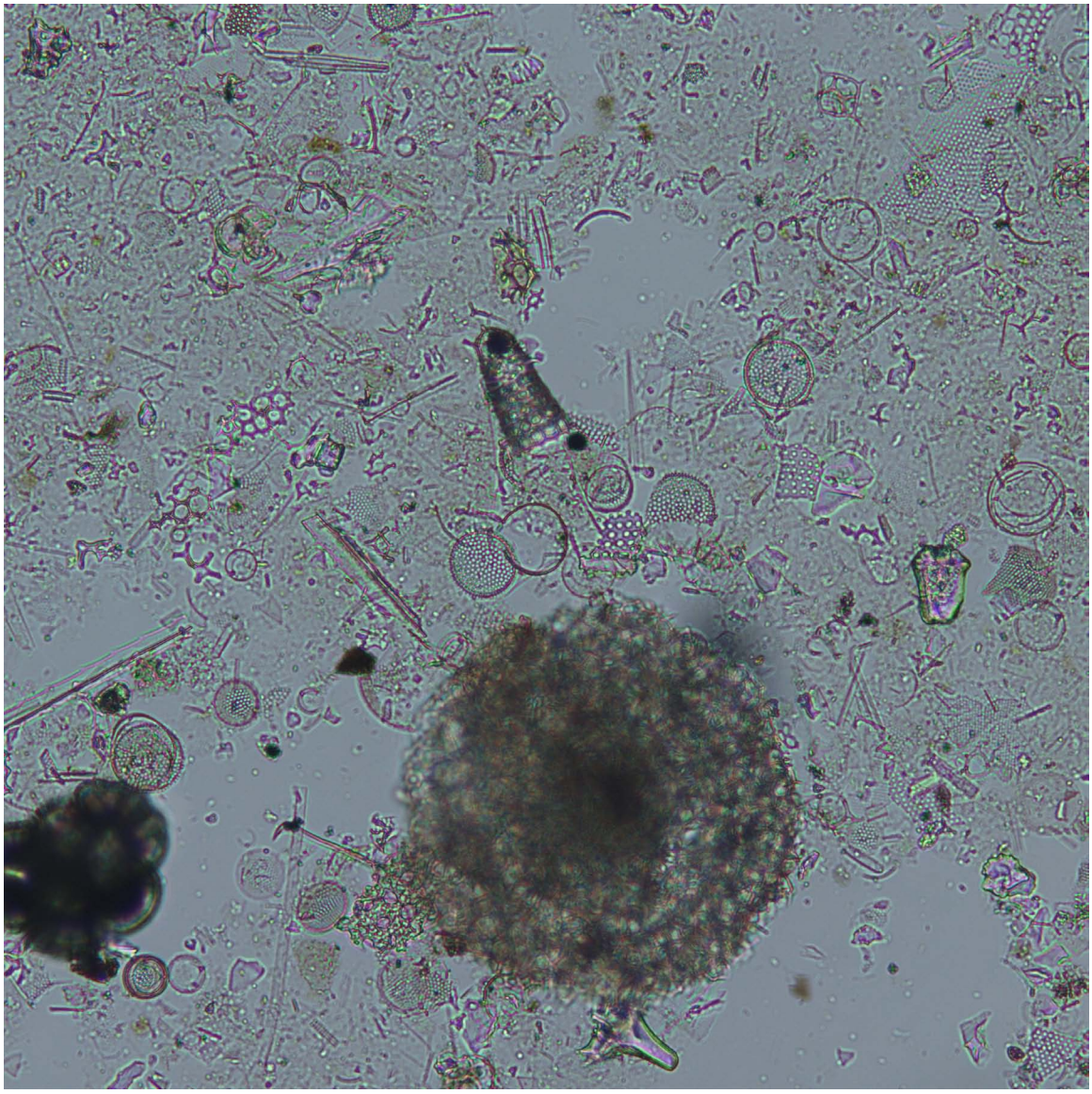

Siliceous Ooze Tutorial 6A (Radiolarian 13).

Roughly 90% of this low magnification field of view is filled by sediment, showing several larger sand-sized components. A large Spumellarian (S) radiolarian dominates the field of view, and it, with a smaller thimble-shaped Nassellarian (N) radiolarian, form ~10% of the sediment. The other large grain, a foraminifer (F), forms ~2% of the sediment. There are several fragments of colorless volcanic glass (V), which stand out with slightly higher relief from the surrounding biosiliceous debris, including many centric diatoms. The square (see image annotation layer) shows the location of a larger magnification view (Siliceous Ooze Tutorial 6B) where the distinction between diatoms and fine matrix is better defined.

ODP Sample (Pleistocene): Leg 138, Hole 845A, Core 2H, Section 6W, 120 cm

Image ID: B0301/B0302

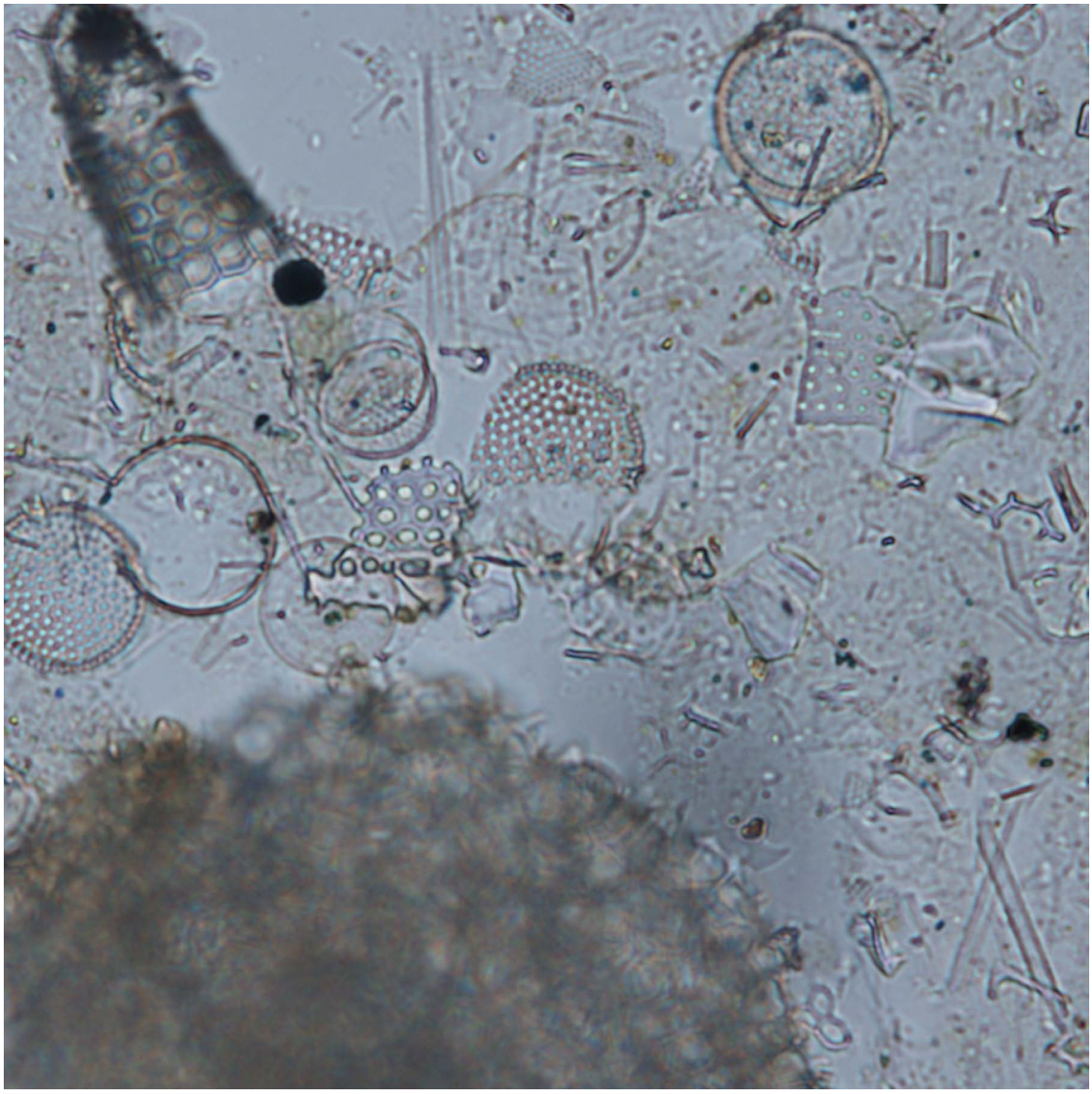

Siliceous Ooze Tutorial 6B (also Radiolarian 14).

In this higher magnification view, again 90% filled by sediment, the radiolaria are disproportionately emphasized (30%). However, the nature and compositional makeup of the finer matrix is clarified; it includes fragments of radiolarians (circled yellow), minor colorless volcanic glass (V), a trace of framboidal pyrite (Py), and common centric to pennate diatoms (30%; D). The clay-sized fraction (~40%) does show subtle circular structures and low birefringence, which suggests that it is at least in part (20%?) composed of fine nannofossils (examples circled in red). Indeed, carbonate measurements in core just below this sample show up to 25% carbonate.

ODP Sample (Pleistocene): Leg 138, Hole 845A, Core 2H, Section 6W, 120 cm

Smear Slide Reference Set for Phase I: Siliciclastic and Volcaniclastic Components Jan-14-2013

Slide Number	Sample Locations and Descriptions			Hole-core-section-top of interval (cm)	Tutorial Examples
ARTIFICIAL MIXTURES & END MEMBERS					
1	~100% clay	End members and mixtures of samples from Holes		576B-7H-6-36	
2	75:25 clay:silt	576B (NW Pacific Ocean clay) &		&	
3	50:50 clay:silt	646A (North Atlantic Ocean silt) &		646A-4H-4-130	
4	25:50 clay:silt	861A (Chilean forearc SE Pacific sand)		&	
5	~100% silt			861A-1H-5-61	
6	33:33:33 clay:silt:sand				
7	100% sand				
CLAY/SHALE					
8	Deep Sea Clay(stone) NW Pacific Ocean	Brown clay		576B-1H-1-112	
9	Deep Sea Clay(stone) NW Pacific Ocean	Brown clay		576B-3H-6-68	Clay T1
10	Deep Sea Clay(stone) NW Pacific Ocean	Brown clay		576B-6H-3-59	
11	Deep Sea Clay(stone) North Pacific Ocean	Red clay		1179C-24H-4-11	
12	Deep Sea Clay(stone) Central Pacific Ocean	Zeolitic clay		842B-3H-4-66	Clay T3
13	Deep Sea Clay(stone) South Pacific Ocean	Palygorskite(?) clay		596-1H-4-52	
14	Eastern Mediterranean Sea	Organic-rich clay (sapropel)		964A-4H-56	
15	Atlantic Ocean	Black shale		1258C-27R-3-24	
SILTY/MUDDY SUITES					
16	Mississippi Fan Gulf of Mexico (silty)	Regional samples (submarine fans)		614A-11H-1-73	Silt T1
17	Mississippi Fan Gulf of Mexico (clayey)	"		615-5H-6-85	
18	Mississippi Fan Gulf of Mexico (sandy)	"		615-43H-1-85	
19	Amazon Fan central Atlantic Ocean (clayey)	"		931A-3H-3-64	
20	Amazon Fan central Atlantic Ocean (muddy)	"		936A-5H-1-110	
21	Amazon Fan central Atlantic Ocean (silty)	"		931B-14X-4-63	
22	Amazon Fan Central Atlantic Ocean (sandy)	"		946A-8H-2-119	
23	Canterbury Margin NZ (silty) Pacific Ocean	Regional samples (slope)		1352B-2H-2-117	
24	Canterbury Margin NZ (clayey) Pacific Ocean	"		1352B-5H4-97	
25	Canterbury Margin NZ (contourite) Pacific Ocean	"		1119C-10H-2-125	
26	Galicia margin NE Atlantic Ocean	"		637A-7R-3-33	
27	North America / Alaska NW Pacific Ocean	Regional samples (ocean basin)		178-34-5-12	
28	North America / Alaska NW Pacific Ocean	"		178-47-2-0	
29	North America / Alaska NW Pacific Ocean	"		179-21-1-134	
30	North Atlantic Ocean	"		647A-8R-2-64	
31	Atlantic Ocean off North Africa	"		952A-24X-3-22	
32	Atlantic Ocean off North Africa	"		657A-5H-3-127	
33	Southern Ocean near Antarctica	"		1096B-4H-1-106	Mud T2
34	East Pacific Ocean off Peru	"		1228A-15H-1-50	
35	Pacific Ocean off Baja California	"		474A-13-4-101	
VOLCANICLASTICS					
36	Izu-Bonin Arc in western Pacific Ocean	Intraoceanic magmatic arc		791A-34-CC-12	Volcanic T1
37	Izu-Bonin Arc in western Pacific Ocean	"		791B-62R-1-3	Volcanic T2
38	Chilean forearc SE Pacific Ocean	Continental magmatic arc		1232A-12H-1-125	
39	Chilean forearc SE Pacific Ocean	"		1232A-9H-2-69	
40	Chilean forearc SE Pacific Ocean	"		861A-1H-5-61	Mud T1
OTHER					
41	Pacific Ocean guyot	Paleosol		871C-34R-2-27	
42	Pacific Ocean guyot	Authigenic oxides		871C-34R-1-46	
43	Pacific Ocean guyot	Glauconite/celadonite?		877A-20R-3-42	
44	Pacific Ocean guyot	Peat		877A-20R-2-115	
45	Tyrrenhian Sea	Mediterranean flood (reworked soil?)		652A-20R-6-56	
46	Escanaba Trough, Pacific Ocean	Clastic sulfides		1035A-14X-3-66	
47	Juan de fuca Ridge, Pacific Ocean	Authigenic carbonate		858B-2H-2-37	Clay T2
48	Pacific Ocean off Peru	Authigenic carbonate		991A-6H-1-58	
49	Mars and Ursa basins Gulf of Mexico	Clay rims on grains		1320A-17X-2-28	
50	Mars and Ursa basins Gulf of Mexico	Fe-stained quartz		1324B-54X-4-73	

Smear Slide Reference Set for Phase II: Biogenic Components Jan-18-2015

(note lithology names are from shipboard descriptions)

51	Japan Deep Sea Terrace	Siliceous ooze	Early Pliocene	438A-13-3-64	
52	Little Bahama Bank, Western Atlantic	Impure calcareous ooze with tunicate spicules	Pliocene	628A-2H-1-47	
53	Little Bahama Bank, Western Atlantic	Calcareous ooze	Late Miocene to Plioc.	628A-4H-3-95	
54	Little Bahama Bank, Western Atlantic	Spiculitic calcareous ooze	Middle Miocene	628A-15H-2-52	
55	Little Bahama Bank, Western Atlantic	Spiculitic foram-nanno chalk	Late Oligocene	628A-17H-3-52	
56	Little Bahama Bank, Western Atlantic	Nannofossil ooze	Early Olig. to latest Eoc.	628A-29X-1-52	
57	Western Galicia Margin, North Atalantic	Foram-nannofossil ooze	Early Pleistocene	637A-7R-2-79	
58	Eastern Tropical Atlantic	Mixed bioclastic sediment	Pleistocene	657A-4H-1-34	
59	Eastern Tropical Atlantic	Bioclastic calcareous silt	Late Pliocene	657A-9H-3-21	
60	Weddel Sea Antartica	Diatom ooze	Early Pliocene	690A-1H-6-105	
61	Weddel Sea Antartica	Mixed diatom/calcareous ooze	Late Pliocene	690A-1H-1-110	
62	Weddel Sea Antartica	Silicoflagellate-diatom ooze	Early Pliocene	690B-3H-3-50	4- Silieceous Ooze
63	Weddel Sea Antartica	Diatom-nannofossil ooze	Middle Miocene	690B-5H-2-57	1- Mixed Ooze
64	Weddel Sea Antartica	Siliceous/calcareous ooze	Lower Oligocene	690B-10H-6-120	
65	Weddel Sea Antartica	Foram-nannofossil ooze	Early Eoc. to late Paleoc.	690B-15H-4-35	
66	Exmouth Plateau Eastern Indian Ocean	Siliceous/calcareous ooze	Quaternary	763A-1H-2-79	
67	Exmouth Plateau Eastern Indian Ocean	Foram-nannofossil ooze	Late Pliocene	763A-6H-1-41	
68	Exmouth Plateau Eastern Indian Ocean	Nannofossil-foram chalk	Early Miocene	763A-17H-5-22	
69	Exmouth Plateau Eastern Indian Ocean	Foram-nannofossil ooze/chalk	Late Oligocene	763A-18H-5-80	
70	Exmouth Plateau Eastern Indian Ocean	Nannofossil-foram chalk	Late Campanian	763B-9X-5-40	
71	Exmouth Plateau Eastern Indian Ocean	Nannofossil-foram chalk	Middle Eocene	763B-6X-4-31	
72	Japan Sea	Siliceous/organic mixed sediment	Quaternary	799A-3H-1-125	
73	Ontong Java Plateau, West Central Pacific	Foram-nannofossil ooze	Pleistocene	807A-1H-2-93	2- Calcareous Ooze
74	Ontong Java Plateau, West Central Pacific	Foram-nannofossil ooze	Late Miocene	807A-21H-3-80	
75	Ontong Java Plateau, West Central Pacific	Nannofossil-foram chalk	Late Eocene	807C-24R-2-35	
76	Ontong Java Plateau, West Central Pacific	Limestone	Early Paleocene	807C-53R-3-5	
77	Ontong Java Plateau, West Central Pacific	Limestone	Maastrichtiaan	807C-57R-2-70	
78	Ontong Java Plateau, West Central Pacific	Radiolarian claystone	Albian-Cenomanian	807C-71R-6-95	
79	Eastern Equatorial Pacific	Radiolarian clay	Pleistocene	845A-1H-1-66	
80	Eastern Equatorial Pacific	Mixed diatom-radiolarian ooze with forams	Pleistocene	845A-2H-6-120	6- Siliceous Ooze
81	Eastern Equatorial Pacific	Mixed siliceouso ooze	Late Miocene	845A-15H-2-10	
82	Eastern Equatorial Pacific	Mixed nannofossil-siliceous ooze	Middle Miocene	845A-17H-2-20	
83	California Margin, Eastern Pacific	Micritic sediment	Late Pliocene	1014A-25X-2-60	
84	Northwest Atlantic Sediment Drifts	Bioclastic calcareous silt	Late Pliocene	1062A-16H-6-73	
85	Southwestern Pacific, New Zealand	Tuffaceous nannofossil-foram ooze	Quaternary?	1124C-2H-4-15	
86	Southwestern Pacific, New Zealand	Nannofossil ooze	Late Pliocene	1124C-8X-5-12	
87	Southwestern Pacific, New Zealand	Nannofossil chalk	Late Oligocene	1124C-42X-3-105	
88	Southwestern Pacific, New Zealand	Nannofossil chalk	Eocene	1124C-45X-3-105	
89	Tasman Plateau, Tasman Sea	Mixed siliceous-nannofossil chalk	Oligocene	1172A-38X-5-78	3- Mixed Ooze
90	Shatsky Rise, Northwest Pacific	Nannofossil ooze	Pleistocene	1210B-1H-4-50	
91	Shatsky Rise, Northwest Pacific	Nannofossil ooze	Miocene	1210B-11H-3-20	
92	Shatsky Rise, Northwest Pacific	Nannofossil ooze	Oligocene	1210B-13H-2-60	
93	Shatsky Rise, Northwest Pacific	Nannofossil ooze	Eocene	1210B-16H-3-120	
94	Shatsky Rise, Northwest Pacific	Nannofossil ooze	Paleocene	1210B-21H-4-15	
95	Shatsky Rise, Northwest Pacific	Nannofossil-foram ooze	Cretaceous	1210B-28H-2-30	
96	Equatorial Pacific	Calcite needles	Late Oligocene to early Miocene	1219A-6H-2-6	
97	Equatorial Pacific	Radiolarian ooze	Middle Eocene	1219A-20H-2-18	
98	Peru Margin, East-central Pacific	Siliceous ooze with authigenic carbonate	Pleistocene	1229A-2H-6-26	5- Siliceous Ooze
99	Walvis Ridge, Angola Basin, South Atlantic	Nannofossil ooze	Paleocene?	1267A-23H-1-60	
100	Walvis Ridge, Angola Basin, South Atlantic	Nannofossil chalk	Maastrichtian	1267A-33X-1-30	

Table with information on smear-slide reference sets for Part I (Marsaglia et al., 2013) and Part II (this volume). These reference sets are available on IODP drill ships and at the IODP core repositories.